The Handbook of Environmental Chemistry 82
Series Editors: Damià Barceló · Andrey G. Kostianoy

Alexander P. Lisitsyn
Liudmila L. Demina *Editors*

Sedimentation Processes in the White Sea

The White Sea Environment Part II

Springer

The Handbook of Environmental Chemistry

Founding Editor: Otto Hutzinger

Editors-in-Chief: Damià Barceló • Andrey G. Kostianoy

Volume 82

More information about this series at http://www.springer.com/series/698

Sedimentation Processes in the White Sea

The White Sea Environment Part II

Volume Editors: Alexander P. Lisitsyn · Liudmila L. Demina

With contributions by

T. N. Alexceeva · D. F. Budko · O. M. Dara · L. L. Demina · I. V. Dotsenko · Y. A. Fedorov · A. A. Klyuvitkin · A. I. Kochenkova · M. D. Kravchishina · A. P. Lisitsyn · I. A. Nemirovskaya · Y. A. Novichkova · A. N. Novigatsky · A. E. Ovsepyan · N. V. Politova · Y. I. Polyakova · A. E. Rybalko · V. A. Savitskiy · L. R. Semyonova · V. P. Shevchenko · M. Y. Tokarev · A. Yu. Lein · V. A. Zhuravlyov · A. A. Zimovets

Springer

Editors
Alexander P. Lisitsyn
Shirshov Inst. of Oceanology
Russian Academy of Sciences
Moscow, Russia

Liudmila L. Demina
Shirshov Inst. of Oceanology
Russian Academy of Sciences
Moscow, Russia

ISSN 1867-979X ISSN 1616-864X (electronic)
The Handbook of Environmental Chemistry
ISBN 978-3-030-05110-5 ISBN 978-3-030-05111-2 (eBook)
https://doi.org/10.1007/978-3-030-05111-2

Library of Congress Control Number: 2018964918

This Springer imprint is published by the registered company Springer Nature Switzerland AG
The registered company address is: Gewerbestrasse 11, 6330 Cham, Switzerland

The Handbook of Environmental Chemistry Also Available Electronically

The Handbook of Environmental Chemistry is included in Springer's eBook package *Earth and Environmental Science*. If a library does not opt for the whole package, the book series may be bought on a subscription basis.

For all customers who have a standing order to the print version of *The Handbook of Environmental Chemistry*, we offer free access to the electronic volumes of the Series published in the current year via SpringerLink. If you do not have access, you can still view the table of contents of each volume and the abstract of each article on SpringerLink (www.springerlink.com/content/110354/).

You will find information about the

– Editorial Board
– Aims and Scope
– Instructions for Authors
– Sample Contribution

at springer.com (www.springer.com/series/698).

All figures submitted in color are published in full color in the electronic version on SpringerLink.

Aims and Scope

Since 1980, *The Handbook of Environmental Chemistry* has provided sound and solid knowledge about environmental topics from a chemical perspective. Presenting a wide spectrum of viewpoints and approaches, the series now covers topics such as local and global changes of natural environment and climate; anthropogenic impact on the environment; water, air and soil pollution; remediation and waste characterization; environmental contaminants; biogeochemistry; geoecology; chemical reactions and processes; chemical and biological transformations as well as physical transport of chemicals in the environment; or environmental modeling. A particular focus of the series lies on methodological advances in environmental analytical chemistry.

Series Preface

With remarkable vision, Prof. Otto Hutzinger initiated *The Handbook of Environmental Chemistry* in 1980 and became the founding Editor-in-Chief. At that time, environmental chemistry was an emerging field, aiming at a complete description of the Earth's environment, encompassing the physical, chemical, biological, and geological transformations of chemical substances occurring on a local as well as a global scale. Environmental chemistry was intended to provide an account of the impact of man's activities on the natural environment by describing observed changes.

While a considerable amount of knowledge has been accumulated over the last three decades, as reflected in the more than 70 volumes of *The Handbook of Environmental Chemistry*, there are still many scientific and policy challenges ahead due to the complexity and interdisciplinary nature of the field. The series will therefore continue to provide compilations of current knowledge. Contributions are written by leading experts with practical experience in their fields. *The Handbook of Environmental Chemistry* grows with the increases in our scientific understanding, and provides a valuable source not only for scientists but also for environmental managers and decision-makers. Today, the series covers a broad range of environmental topics from a chemical perspective, including methodological advances in environmental analytical chemistry.

In recent years, there has been a growing tendency to include subject matter of societal relevance in the broad view of environmental chemistry. Topics include life cycle analysis, environmental management, sustainable development, and socio-economic, legal and even political problems, among others. While these topics are of great importance for the development and acceptance of *The Handbook of Environmental Chemistry*, the publisher and Editors-in-Chief have decided to keep the handbook essentially a source of information on "hard sciences" with a particular emphasis on chemistry, but also covering biology, geology, hydrology and engineering as applied to environmental sciences.

The volumes of the series are written at an advanced level, addressing the needs of both researchers and graduate students, as well as of people outside the field of

"pure" chemistry, including those in industry, business, government, research establishments, and public interest groups. It would be very satisfying to see these volumes used as a basis for graduate courses in environmental chemistry. With its high standards of scientific quality and clarity, *The Handbook of Environmental Chemistry* provides a solid basis from which scientists can share their knowledge on the different aspects of environmental problems, presenting a wide spectrum of viewpoints and approaches.

The Handbook of Environmental Chemistry is available both in print and online via www.springerlink.com/content/110354/. Articles are published online as soon as they have been approved for publication. Authors, Volume Editors and Editors-in-Chief are rewarded by the broad acceptance of *The Handbook of Environmental Chemistry* by the scientific community, from whom suggestions for new topics to the Editors-in-Chief are always very welcome.

Damià Barceló
Andrey G. Kostianoy
Editors-in-Chief

Preface

The book *The White Sea Environment* in the series "The Handbook of Environment Chemistry" contains the most important results of multiannual investigations conducted by the Shirshov Institute of Oceanology of the Russian Academy of Sciences over 2001–2016. Part II of this book aims to join results of the multidisciplinary researches of sedimentation processes in the White Sea. The long-term investigations in a small Arctic sea, as the White Sea is, have revealed new regularities of sedimentation processes which are characteristic of the sub-Arctic zones.

In Part II, for the first time, the in situ sedimentation processes in the White Sea were studied with the automatic deep-water observatories of sedimentation (AGOS). This led us to estimate contribution of sedimentary matter over different timescales: months, seasons, and years. The mineral, grain-size, isotopic, and elemental composition, including certain biogeochemical proxies, have been studied in both dispersed (suspended particulate matter and vertical fluxes of settling particles) and consolidated (bottom sediments) forms of sedimentary matter. It allowed us to estimate the biogeochemical processes of transformation, which take place within the water column in such key areas of the White Sea as the riverine–seawater interface.

The development history in Holocene and a three-member structure of the Quaternary cover have been revealed. Environmental conditions versus abundance and species composition of microalgae associations have been studied in bottom sediments, which improved our knowledge about relationships between different ecosystem components. The mineral phases of sedimentary matter at different stages of sediment formation have been documented. A specific character of the early diagenesis was revealed, as well as regularities of heavy metal accumulation, including the most toxic mercury, as well as aliphatic and polycyclic aromatic hydrocarbons in bottom sediments of different areas of the sub-Arctic White Sea.

This book is addressed to the specialists working in various fields of environmental problems, especially in marine geology, ecology, and biogeochemistry.

Collection and processing of sedimentary matter were performed in the framework of the state assignment of FASO Russia (theme No 0149-2018-0016). Analysis, interpretation of the data obtained, as well as preparation of materials for publication were supported by Russian Science Foundation grant (project No 14-27-00114-P).

Moscow, Russia Alexander P. Lisitsyn
Moscow, Russia Liudmila L. Demina

Contents

Introduction

Alexander P. Lisitsyn and Liudmila L. Demina

Contents

Abstract Within the framework of the scientific program "The White Sea System," many multidisciplinary expeditions have been held by the Shirshov Institute of Oceanology of Russian Academy of Sciences over 15 years (2000–2015). As a result, a large amount of various materials (bottom sediments, marine and river suspended particulate matter, sediment-laden snow and ice, aerosols of the near-water layer, biota) has been collected from the different geospheres. During such long-term investigations, the White Sea was considered as a natural range of environmental conditions of the Arctic and subarctic regions. In Part II of "The White Sea Environment," both the dispersed sedimentary matter (aerosols and suspended particulate matter) and the consolidated one (the bottom sediments) have been under considerations of researches of different specialization. Based on seismic and lithostratigraphic data, the major stages of the White Sea basin development were identified. Its history began about 14,000 years ago after the onset of the terrain deglaciation, while change of the sedimentation regime occurred about 11,000 years ago. Distribution pattern of marine diatoms and dinoflagellate cysts was used to characterize relationships between environmental parameters and water productivity at different areas of the sea. It was necessary to study the initial stage of SPM formation in water column, namely, changes in the amount and composition of the SPM in time (day-night, decades, months, seasons, and interannual changes). In the White Sea, we have introduced the sedimentation observatories equipped with automatic sediment traps to measure vertical fluxes of settling particles (mg m^{-2} day^{-1}) at different depths from the surface water to the seafloor. At the seafloor, an independent determination of fluxes into the bottom sediments has been carried out by the use of different methods of sediment age dating (biological, isotopic, and other methods).

A. P. Lisitsyn (✉) and L. L. Demina
Shirshov Institute of Oceanology of Russian Academy of Sciences, Moscow, Russia
e-mail: lisitzin@ocean.ru; l_demina@mail.ru

A. P. Lisitsyn and L. L. Demina (eds.), *Sedimentation Processes in the White Sea: The White Sea Environment Part II*, Hdb Env Chem (2018) 82: 1–12,
DOI 10.1007/698_2018_356, © Springer International Publishing AG, part of Springer Nature 2018,
Published online: 15 July 2018

Results of study of mineral, chemical (including toxic heavy metals, particularly mercury, as well as hydrocarbons), and isotope composition of bottom sediments are presented.

This book is addressed to the specialists working in various fields of environmental problems, especially in marine geology, ecology, and biogeochemistry.

Keywords Biogeochemistry, Bottom sediments, History, Particle fluxes, Suspended particulate matter, White Sea

In the first cruise of the research vessel "Vityaz" (1949), specialists in different fields of oceanography (hydrologists, biologists, geologists, chemists) have participated. They have performed a multidisciplinary research throughout the water column of the northwestern Pacific, including maximum depth equal to 11,040 m in the Mariana Trench [1, 2]. Since that time, marine geologists from different countries have exploited the marine bottom sediments as a natural record of the environment and the climate of the geological past ([3–10], etc).

There was a possibility of validation of this approach, primarily based on the study of modern sedimentation processes in different environmental and climate conditions, existing now in the World Ocean. In the early stages, it seemed that it was enough to make reliable maps of bottom sediments and compare them with modern environmental parameters of marine sedimentation. However, it turned out that the processes of modern sedimentation happen in different ways than it seemed; moreover, they are practically not studied, while the theoretical lithology argued that the ocean bottom sediments in all climatic zones at all latitudes as if correspond to the sediments of the humid zone, that there is no climatic zones in the oceans [11, 12].

In their constructions, theoretical lithologists issued that that the modern sedimentation process is well studied and clear, although in the USSR, in the years before the cruise of RV "Vityaz," there were no samples of ocean bottom sediments taken from depths of more than 2 km. Moreover, at that time, the level of study of the marine sediments in Russia was quite insufficient, most often it was a formal description of sediments without the necessary analytical definitions. The very processes that determine the quantitative sediment distribution (sedimentation rates, absolute mass, and thickness of sedimentary bodies), their grain-size, mineral, and chemical composition, as well as microfossils' assemblage, remained poorly understood, and the sedimentation processes were largely misinterpreted.

Over 10 years after the first cruise of RV "Vityaz," new possibilities for studying the marine sedimentation processes arose. These studies covered the long-term transects which began from the catchments areas' weathering cover on the continents and finished in the bottom sediments of the pelagic zone of seas and oceans, including the stages of preparation, transportation, and deposition of sedimentary matter. Even the classification and nomenclature of marine geologists working in the sea were different from that adopted by sedimentary theoretical geologists. At those years, the features of the modern sedimentary process were studied by the use of new

expedition ships equipped with new devices, instruments, and methods, based on new research approaches.

One of the new approaches is a study of micro- and nanoparticles dispersed in natural environment (in seawater, atmosphere, snow, and ice), which in a result of sinking in water column give a rise to consolidated forms of dispersed particles, namely, bottom sediments. These dispersed particles in seawater are at the stage of extremely dilution; they have a maximal specific surface area and are therefore particularly sensitive to the environmental changes.

Their major part is of pelitic grain-size (<0.01 mm), and their average content in seawater varies in limits of 0.1–1 mg L^{-1}. This value of suspended particulate matter's concentration was recorded for the first time in the cruise of RV "Vityaz" and then in other expeditions. Collection of this dispersed substance is associated with great difficulties: it is necessary to have a clean sampling technique, as well as reliable and high sensitive methods of treatment and analyses for many lithological and geochemical components. Currently, the main parameters of the dispersed sedimentary matter can be determined by several independent methods. It was possible to obtain hundreds and thousands of samples of suspended particulate matter (SPM) from all parts of the oceans and seas, from different depths, at different distances from the shore, and in different climate conditions of environment in the modern World Ocean [13–15]. Particular attention was paid to areas nearby the river mouths and rivers itself, since rivers were considered as the main sources of sediment that seemed was evidenced [16, 17].

The average dispersed sedimentary matter's content (in the form of SPM) for the World's rivers has been estimated as 490 mg L^{-1} [14], which is hundreds of times higher than that in the pelagic ocean water and in the shelf water. However, in the course of studies conducted at the transects between the river estuaries and the open sea located in different climatic zones, we have found that as a result of mixing processes of the river and seawater, about 90% of the SPM and about 40% of the dissolved fractions of the river water are precipitated in a limited area nearby the mouth. This phenomenon got a term an avalanche sedimentation [16]. Based on the direct data obtained, contribution of the riverine runoff as the main source of sedimentary material into the pelagic ocean was estimated to be almost ten times less. There is a phenomenon of marginal filter, which has never been studied by lithologists before [17].

Simultaneously with the study of the SPM in rivers, as well as in the sea and ocean water column, the study of dispersed forms of sedimentary matter started in the atmosphere (near-water layer), snow cover, sea ice, and icebergs, which serve as carriers of sedimentary matter in the Arctic [18].

The dispersed sedimentary matter has proved to exist in the atmosphere sometimes in large quantities (dust storms). Aeolian material (aerosols) is transported for a very long distance from its source; thus, it can be supplied from the northern hemisphere into the southern one. One of the features of this type of sedimentary substances' transport is frequent dust storms when visibility is less than 1 km. In arid zones, the frequency of dust storms reaches up to 60% throughout the year. A comparison of aerosol contents with that in the ocean water column shows that the

aerosol material rather than the solid river discharge dominates in the arid regions [13, 14, 19, 20].

Thus, modern studies of the sedimentation process involving new data on the quantitative distribution and composition of the dispersed sedimentary matter in different geospheres have shown that climatic zoning become apparent in the ocean. It is supplemented by the vertical, circum-continental, and tectonic types of zoning, i.e., the law of sedimentation zoning in the seas and oceans by Bezrukov et al. [21]. Studies of the terrigenous (continental) component of the dispersed sedimentary matter in comparison with the bottom sediments showed that at all stages of sedimentation (preparation, transportation, and deposition), they both are subjected to the laws of zoning – climatic, vertical, and circum-continental.

Biogenic (carbonate or siliceous) sedimentary material is an important component of sedimentary matter in the seas. Its content in bottom sediments reaches not 3–9.2%, as it previously was thought, but 40–50%. Biota is of great importance for transformation of all types of sedimentary material from its dispersed forms into pellets during biofiltration by plankton and benthic organisms. According to the new data, the whole water volume of the World Ocean is filtered by organisms in 0.5–1 year. The primary production of phytoplankton uses dissolved forms of biogenic elements and solar energy during photosynthesis; phytoplankton synthesizes autochthonous organic matter which is the basic trophic chain for all living organisms in the sea [22]. This process takes place in the upper photic zone of the World Ocean, i.e., it is closely related to both climatic zoning and seasonal processes. Circum-continental and vertical types of zoning are also clearly identified in the biota, its quantitative distribution, and qualitative composition of living organisms and their residues [23].

Thus, the sedimentary matter formed on the continents by many ways through interaction of different geospheres enters the seas and oceans – in the surface water layer. There, both the suspended and dissolved forms of sedimentary matter are processed by the biosphere.

Biosynthesis involves the selective extraction of nutrients from seawater (osmotic membranes) – this process is called a biofilter-1. This is followed by filtration of phytoplankton together with SPM by zooplankton in surface water (a biofilter-2). Zooplankton organisms perform a packing of organic matter into pellets which have a protective capsule. For this kind of micro-containers unlike fine-grained particles, a fast sink to the depths is characteristic. Such is a mechanism of the major biological pathway of SPM involved in the “living ocean”; this is different from the simple particles’ deposition in accordance with Stokes law [23].

These general regularities established for the oceans and seas have been complemented by specific data on a detailed comparative study of sediment formation in the seas of different climatic zones. One of these seas is the White Sea which belongs to the subarctic zone; it is covered with ice for a larger part of the year. The latter is one of the important factors which determines largely the sedimentation processes [24–26].

Our investigations were performed not only in the White Sea proper but also in its catchment areas [27]. As a result, it was possible to obtain, for the first time, the

direct data on the amount, composition, and properties of both dispersed forms of suspended particulate matter and dissolved forms of elements due to operation at the stations in the White Sea. These data allowed us to establish the regularities of migration of micro- and nanoparticles, i.e., the dispersed sedimentary matter within the White Sea water mass.

Part II of "The White Sea Environment" is devoted to both the dispersed sedimentary matter and the consolidated one, i.e., the bottom sediments, which differ in its physical properties from the dispersed ones. It is necessary to study the initial stage of SPM formation in water column, namely, changes in the amount and composition of the SPM in time (day-night, decades, months, seasons, and interannual changes).

To solve this problem, special approaches, devices, and especially the management of investigation, beginning from the regular short-term discrete to continuous long-term observations, were also required. In the White Sea, we have introduced the sedimentation observatories equipped with automatic sediment traps to measure vertical fluxes of settling particles (mg m^{-2} day^{-1}) at different depths from the surface water to the seafloor. At the seafloor, an independent determination of fluxes into the bottom sediments has been carried out by the use of different methods of sediment age dating (biological, isotopic, and other methods).

Application of these two methods of studying processes allowed to judge the dynamics of sedimentary process in time – by changing the settling particle flux values. For short-term investigations, using the current meters, it is also possible to study the real vectors of water dynamics by data of the four-dimensional oceanology [28].

Within the framework of the program "The White Sea System," many multidisciplinary expeditions have been held by the Shirshov Institute of Oceanology of Russian Academy of Sciences over 15 years (2000–2015). During such long-term investigations, the White Sea was considered as a natural range of environmental conditions of the Arctic and subarctic regions. As a result, a large amount of various materials (bottom sediments, marine and river suspended particulate matter, sediment-laden snow and ice, aerosols of the near-water layer, biota) has been collected from the different geospheres. The obtained datasets were analyzed and published in the four monographies [27, 29–31]. A new system of observations in space and time was elaborated which included the following:

1. Satellite observations with verification for the surface layer of water spatial changes and changes in time (decadal, monthly, seasonal, and interannual).
2. Observation at stations in expedition cruises – a continuous vertical sounding using a Rosette system equipped with different oceanographic sensors accompanied by water sampling by bathometers to subsequently study suspended and dissolved forms of chemical elements. At the same time, a measurement of horizontal currents by the ADCP system.
3. Operations while running of research vessel with sampling of surface water for verification of satellite data and collection of aerosol samples (under favorable winds and weather conditions), as well as filtration of water to collect SPM, measurement of the SPM grain-size composition by laser particle counters, etc.

4. Study of sedimentation processes in time by use of deep automatic sedimentary-geochemical deep-water observatories (AGOS) with automatic differential (once per month) and integral (throughout the year) sampling. The devices are placed along cable rope with the subsurface buoy at the key water column's horizons which were registered during vertical sounding.
5. Study of the upper sediment layer (interval of 0–1 cm) sampled with Multi-Corer and/or Neimisto tube for further determination of mineral and chemical composition, as well as sedimentation rate (mm year^{-1}) and absolute mass of bottom sediments (mg m^{-2} year^{-1}).

The major part of the White Sea research was carried out by staff of the laboratory of physical and geological researches of Shirshov Institute of Oceanology of Russian Academy of Sciences (IO RAS).

In total, the 22 interdisciplinary expedition cruises have been performed. In Fig. 1 the sampling stations are displayed. Researchers from the Institute of Oceanology and its branches, as well as Vinogradsky Institute of Microbiology RAS, Lomonosov Moscow State University, Saint Petersburg State University, and Institute of Water Problems of the Northern Karelian Scientific Centre, have participated in all the cruises.

This book contains 11 chapters including Introduction and Conclusions written by the volume editors.

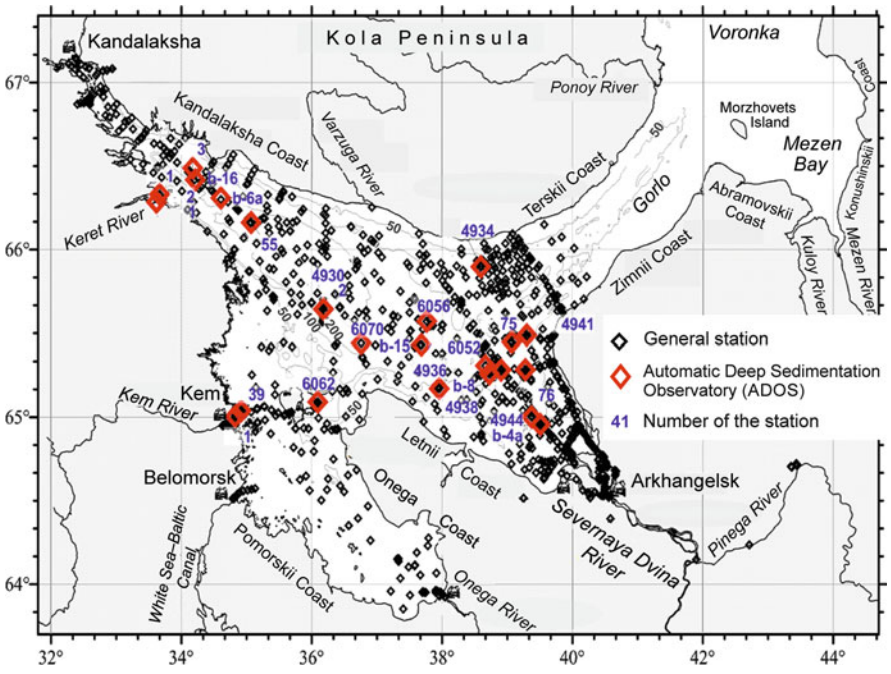

Fig. 1 Sampling stations of bottom sediments in the White Sea over 2000–2015

In Chap. 1 [32], concentration of suspended particulate matter (SPM), its composition and properties, as well as their changes due to environmental conditions have been described. In this chapter, the features in distribution pattern in the White Sea of the SPM concentration and its grain-size, mineral, isotope, and chemical (Al, Si, P, C_{org}, Chl-a) composition are discussed. It is highlighted that a dispersed system of the White Sea forms a giant reservoir of micro- and nanoparticles that serves as source of sedimentary material.

Chapter 2 [33] contains the research results of dispersed sedimentary matter captured by sediment traps deployed in the White Sea water column. The results of long-term investigations of spatial and temporal distribution of the vertical fluxes served as a basis for revealing new regularity characteristic of the sedimentary process in the subarctic and Arctic zones. The monthly, seasonal, and interannual dynamics of the main components of dispersed sedimentary matter were estimated, and the major stages of marine sedimentation were recognized. The contribution of main biogenic and lithogenic constituents per m^2 of the bottom area of the White Sea has been calculated.

In Chap. 3 [34], a development history of the modern White Sea Basin is under consideration. The Late Pleistocene and Holocene deposits are a key to study the paleogeography of Northwestern Russia. Methods of a seismic-acoustic profiling and lithostratigraphic analysis of selected cores were applied to characterize the Quaternary sedimentary cover. As a result, it was possible to identify its three-member structure composed of the glacial, glacial-marine, and marine facies.

Chapter 4 [35] is focused on studies of diatom and palynomorph assemblages from the White Sea sediments. It is shown that species composition of the marine plankton in bottom sediments reflects the features of the high-latitude position of the White Sea, as well as the Arctic and North Atlantic water masses' influence on hydrological regime of the White Sea. The characteristic property of the diatom and dinoflagellate cyst assemblages was found to be a presence (in high concentrations) of relatively warm-water species typical for the Atlantic water masses.

In Chap. 5 [36], the main aim was to study the mineral phases in fine-grained fraction (from 10 μm to less than 1 μm) both in dispersed sedimentary matter and consolidated one (bottom sediments) of the White Sea. By use of the X-ray difractometry and scanning electron microscopy, the clastic, clay, and carbonate minerals were analyzed in aerosols, river and marine suspended particulate matter, sediment-laden snow-ice cover, as well as in surface bottom sediments.

Chapter 6 [37] describes biogeochemical processes of early diagenetic processes in the White Sea bottom sediments based on changes in chemical, isotope, and mineral composition of dispersed sedimentary matter and bottom sediments. A special attention is paid to process of transformation of organic components in seawater, SPM, and pore waters. Rates of microbial biogeochemical processes with a tracer technique (^{14}C and ^{35}S), as well as analysis of isotopic composition of carbon compounds in suspended particulate matter (SPM) and in bottom sediments, were also under consideration.

In Chap. 7 [38], a detailed study of mercury – the most toxic heavy metal – has been performed in bottom sediments of the White Sea and the rivers of its basin. For the Northern Dvina River, concentration of methyl Hg in the bottom sediments was calculated based on data of field studies, physicochemical and lithological properties of sediments. Bottom sediments of the White Sea and river estuaries of its basin have been considered by levels of Hg content. The background level of Hg content in bottom sediments was established. Based on the spatial distribution of Hg in the surface bottom sediments, levels of Hg accumulation in the White Sea areas influenced by anthropogenic pollution were revealed.

Chapter 8 [39] is focused on the physical-chemical occurrence forms of aluminum, iron, manganese, and number of heavy metals (Cd, Co, Cr, Cu, Ni, Pb) and metalloid As in the bottom sediments of the White Sea. The pattern of chemical element partitioning among the different occurrence forms (adsorbed, bound to authigenic Fe-Mn oxyhydroxides and organic matter, as well as fixed in clastic and clay mineral structures) reflects principal processes of their accumulation in the modern bottom sediments of the White Sea. A spatial distribution of the occurrence forms of these elements in the surface sediments was estimated, while their analysis in high-resolution (1 cm scale) sediment core let us to study the metal behavior in the processes of early diagenesis.

In Chap. 9 [40], results of determination of oil compounds in bottom sediments were shown. Content and composition of aliphatic and polycyclic aromatic hydrocarbons in bottom sediments of different areas of the White Sea were studied during low and high waters to determine the influence of oil components. Relationships between hydrocarbon distribution and hydrological conditions in the riverine-seawater mixing zone were identified by the example of the Northern Dvina River – Dvina Bay boundary – where the precipitation of major part of pollutants takes place.

The book ends with our conclusions, where the abovementioned aspects have been generalized.

The book is addressed to specialists working in different fields of marine environmental sciences, including ecologists, geologists, geochemists, biologists, and microbiologists. New data on the Arctic environment by the example of the White Sea can also be of interest for a larger community. Graduate and undergraduate students in marine and environmental sciences will find this book as a valuable resource of knowledge, information, and references.

Acknowledgments The authors are thankful to Prof. Andrey Kostianoy – one of the series editors of *The Handbook of Environmental Chemistry* – for the idea to publish this book. We are grateful to the crews of research vessel "Ecolog," "Professor Shtokman," "Akademik Mstislav Keldysh," and our colleagues who contributed to the chapters, as well as to those who helped in the processing of the obtained materials. The research results of Part II were obtained in the framework of the *state assignment* of *FASO* Russia (theme No. № 0149-2018-0016). Proceeding of data obtained earlier were summarized with support of the Russian Scientific Foundation, project No. 14-27-00114-P.

References

1. Lisitsyn AP (1955) Some data on distribution of suspended particulate matter in waters of Kuril-Kamchatka depression. .Proc Inst Ocean USSR Acad Sci 5–11 (in Russian)
2. Lisitsyn AP (1955) Atmospheric and water particulate matter as source of marine sediments formation. Proc Inst Ocean USSR Acad Sci 13:16–22 (in Russian)
3. Biscaye PE (1965) Mineralogy and sedimentation of recent deep-sea clay in the Atlantic Ocean and adjacent seas and oceans. Geol Soc Am Bull 76:803–832
4. Bodungen B, Antia A, Bauerfiend E, Haupt O, Koeve W, Machado E, Peeken I, Reinert R, Reitmeier S, Thomsen C, Voss M, Wunsch M, Zeller U, Zeitzschel B (1995) Pelagic processes and vertical flux of particles: an overview of a long-term comparative study of the Norwegian Sea and Greenland Sea. Geol Rundsch 84:11–27
5. Fahl K, Nöthig E-M (2007) Lithogenic and biogenic particle fluxes on the Lomonosov ridge (Central Arctic Ocean) and their relevance for sediment accumulation: vertical vs lateral transport. Deep-Sea Res I 54:1256–1272
6. Honjo S (1980) Material fluxes and modes of sedimentation in the mesopelagic and bathypelagic zones. J Mar Res 38:53–97
7. Honjo S (1990) Particle fluxes and modern sedimentation in the polar oceans. In: Smith WO (ed) Polar Ocean part B: chemistry, biology and geology. Academic Press, San Diego, pp 687–739
8. Saukel C, Stein R, Vogy C, Shevchenko VP (2010) Clay-minerals and grain-size distributions in surface sediments of the White Sea (Arctic Ocean): indicators of sediment sources and transport processes. Geo-Mar Let 30:605–616
9. Stein R (2008) Ocean sedimentation processes, proxies, and paleoenvironment. Springer, Amsterdam, 592 pp
10. Stein R, Dittmers K, Fahl K, Kraus M, Mattiessen J, Niessen F, Pirrung M, Polyakova Y, Schoster F, Steinke T, Fűtterer DK (2004) Arctic (paleo) river discharge and environmental change: evidence from the Holocene Kara Sea sedimentary record. Quat Sci Rev 23(11–13):1487–1511
11. Strakhov NM (1947) Towards the knowledge of regularities and mechanisms of marine sedimentation. Black Sea. Izves Acad Sci USSR Geol Ser 2:113–148 (in Russian)
12. Strakhov NM (1956) Types of sedimentation and formations of sedimentary rocks. Izves Acad Sci USSR Geol Ser 5:8–39 (in Russian)
13. Lisitsyn AP (1972) Sedimentation in World Ocean. Banta Press, Tulsa, 218 pp
14. Lisitsyn AP (1996) Oceanic sedimentation: lithology and geochemistry. American Geophysical Union, Washington, 390 pp
15. Lisitzin AP (2002) Sea-ice and iceberg sedimentation in the ocean: recent and past. Springer, Berlin, 543 pp
16. Lisitsyn AP (1988) Avalanche sedimentation and interruptions in sediment formation in seas and oceans. Nauka, Moscow, 309 pp (in Russian)
17. Lisitsyn AP (1994) The marginal filter of the ocean. Oceanology 34(5):671–682
18. Lisitsyn AP (2010) Marine ice-rafting as a new type of sediment formation in the Arctic and novel approaches to study sedimentary processes. Rus Geol Geophys 51(1):12–47
19. Lisitsyn AP (1974) Sedimentation in the oceans. Nauka, Moscow, 438 pp (in Russian)
20. Lisitsyn AP (2014) Modern conceptions of sediment formation in the oceans and seas. Ocean as a natural recorder of geospheres' interaction. In: Lobkovsky LI, Nigmatulin RI (eds) World Ocean: physics, chemistry and biology of the ocean, vol 2. Scientific World, Moscow, pp 331–571 (in Russian)
21. Bezrukov PL, Lisitsyn AP, Petelin VP (1970) Map of bottom sediments' types in the Pacific Ocean. Nauka, Moscow, 176 pp (in Russian)
22. Lisitsyn AP, Monin AS (eds) (1983) Biogeochemistry of the ocean. Nauka, Moscow, 368 pp (in Russian)

23. Vinogradov ME, Lisitzyn AP (1981) Global patterns of living matter distribution in the ocean and their reflection in the bottom sediments' composition. Regularities of plankton and benthos distribution in the ocean. Izves Acad Sci USSR 3:279–328 (in Russian)
24. Shevchenko VP (2003) The influence of aerosols on the oceanic sedimentation and environmental conditions in the Arctic. Berichte zur Polar- und Meeresfor 464:1–149
25. Shevchenko VP, Lisitzin AP, Belyaev NA (2004) Seasonality of suspended particulate matter distribution in the White Sea. Berichte zur Polar- und Meeresfor 482:142–149
26. Shevchenko VP, Rat'kova TN, Bairamov IT, Boyarinov PV, Lorentzen C, Mitrokhov AD, Naumov AD, Notig E-M, Savvichev AS, Sergeeva OM, Svertilov AA (2002) Multidisciplinary studies in the Chupa Bay, White Sea in winter time. In: Abstr of 5th workshop on land-ocean interaction in Russian Arctic, Moscow, 12–15 Nov 2002, pp 119–121
27. Lisitsyn AP (2010) Processes in the White Sea catchment area: preparation, transportation and deposition of sedimentary material, the concept of a "living catchment". In: Lisitsyn AP, Nemirovskaya IA (eds) The White Sea System. Vol I The natural environment of the White Sea catchment area. Scientific World, Moscow, pp 353–446 (in Russian)
28. Lisitsyn AP (2013) System-defined four-dimensional studies of dispersed sedimentary matter in the water column of the White Sea, interaction between the catchment geospheres and the water. In: Lisitsyn AP, Nemirovskaya IA (eds) The White Sea System. Vol III Dispersed sedimentary hydrosphere material, microbial processes and pollution. Scientific World, Moscow, pp 25–38 (in Russian)
29. Lisitsyn AP, Nemirovskaya IA (eds) (2012) The White Sea System. Vol II Water column and interacting with it atmosphere, cryosphere, river runoff and biosphere. Scientific World, Moscow, 783 pp (in Russian)
30. Lisitsyn AP, Nemirovskaya IA (eds) (2013) The White Sea System. Vol III Dispersed sedimentary matter in hydrosphere, microbial processes and water pollution. Scientific World, Moscow, 665 pp (in Russian)
31. Lisitsyn AP, Nemirovskaya IA (eds) (2017) The White Sea System. Vol IV The processes of sedimentation, geology and history. Scientific World, Moscow, 1028 pp (in Russian)
32. Kravchishina MD, Lisitsyn AP, Klyuvitkin AA, Novigatsky AN, Politova NV, Shevchenko VP (2018) Suspended particulate matter as a main source and proxy of the sedimentation processes. In: Lisitsyn AP, Demina LL (eds) The White Sea environment part II. Handook of environmental chemistry. Springer, Berlin
33. Novigatsky AN, Klyuvitkin AA, Lisitsyn AP (2018) Vertical fluxes of dispersed sedimentary matter, absolute masses of the bottom sediments, and rates of modern sedimentation. In: Lisitsyn AP, Demina LL (eds) The White Sea environment part II. Handook of environmental chemistry. Springer, Berlin. https://doi.org/10.1007/698_2018_278
34. Rybalko AE, Zhuravlyov VA, Semyonova LR, Tokarev MY (2018) Development history and quaternary deposits of the White Sea Basin. In: Lisitsyn AP, Demina LL (eds) The White Sea environment part II. Handook of environmental chemistry. Springer, Berlin
35. Polyakova YI, Novichkova YA (2018) Diatoms and aquatic palynomorphs in the White Sea sediments as indicators of sedimentation processes and paleoceanography. In: Lisitsyn AP, Demina LL (eds) The White Sea environment part II. Handook of environmental chemistry. Springer, Berlin
36. Dara OM (2018) Mineral composition of pelitic fraction of dispersed and consolidated sedimentary matter in the White Sea. In: Lisitsyn AP, Demina LL (eds) The White Sea environment part II. Handook of environmental chemistry. Springer, Berlin
37. Lein AY, Lisitsyn AP (2018) Processes of early diagenesis in the Arctic seas (on the example of the White Sea). In: Lisitsyn AP, Demina LL (eds) The White Sea environment part II. Handook of environmental chemistry. Springer, Berlin
38. Fedorov Yu A, Ovsepyan AE, Zimovets AA, Savitskiy VA, Lisitsyn AP, Shevchenko VP, Novigatsky AN, Dotsenko IV (2018) Mercury distribution in bottom sediments of the White Sea and the rivers of its basin. In: Lisitsyn AP, Demina LL (eds) The White Sea environment part II. Handook of environmental chemistry. Springer, Berlin

39. Demina LL, Budko DF, Novigatsky AN, Alexceeva TN, Kochenkova AI (2018) Occurence forms of heavy metals in the bottom sediments of the White Sea. In: Lisitsyn AP, Demina LL (eds) The White Sea environment part II. Handook of environmental chemistry. Springer, Berlin
40. Nemirovskaya IA (2018) Oil compounds in the bottom sediments of the White Sea. In: Lisitsyn AP, Demina LL (eds) The White Sea environment part II. Handook of environmental chemistry. Springer, Berlin

Suspended Particulate Matter as a Main Source and Proxy of the Sedimentation Processes

Marina D. Kravchishina, Alexander P. Lisitsyn, Alexey A. Klyuvitkin, Alexander N. Novigatsky, Nadezhda V. Politova, and Vladimir P. Shevchenko

Contents

Abstract The material for our study was collected in the White Sea during 22 interdisciplinary expeditions organized by the Shirshov Institute of Oceanology, Russian Academy of Sciences (IO RAS), in 2000–2014. The researches were carried out mostly in June–August; however we have some samples for autumn–winter and early spring seasons. Here, we report the concentration of suspended particulate matter (SPM), its composition and properties, as well as their changes due to natural zoning and local conditions. This paper discusses the features in the distribution of

M. D. Kravchishina (✉), A. P. Lisitsyn, A. A. Klyuvitkin, A. N. Novigatsky, N. V. Politova, and V. P. Shevchenko
Shirshov Institute of Oceanology, Russian Academy of Sciences (IO RAS), Moscow, Russia
e-mail: kravchishina@ocean.ru

A. P. Lisitsyn and L. L. Demina (eds.), *Sedimentation Processes in the White Sea: The White Sea Environment Part II*, Hdb Env Chem (2018) 82: 13–48,
DOI 10.1007/698_2018_353, © Springer International Publishing AG, part of Springer Nature 2018,
Published online: 7 July 2018

SPM concentration, grain-size, mineral, and major phase composition. As far as possible, we involved our own and other published data on hydrology, bottom morphology, and particulate and dissolved river runoff from the catchment area, abundance and composition of marine phyto- and bacterioplankton. This new knowledge has been used to describe particles dispersion system of the White Sea, which forms a giant reservoir of micro- and nanoparticles, using terms adopted in sedimentology and oceanography.

Keywords Arctic, Chlorophyll "*a*", Grain-size, Major phase composition, Recent sedimentation, Suspended particulate matter

1 Introduction

The collection of samples and study of suspended particulate matter (SPM) for understanding some basic problems in sedimentology was first carried out by Lisitsyn in the Bering Sea in 1951 [1]. Studies of SPM in the White Sea, Russia, were initiated by Medvedev and Krivonosova in 1966, using a method developed by Lisitsyn [2]. Important quantitative characteristics were obtained for the distribution of SPM mass concentrations (in mg/L) and supplying of terrigenous particles. Subsequently, these studies were conducted by Aibulatov [3] and then by Lukashin and Dolotov [4–6] in the White Sea.

The study of SPM as a dispersed system requires an integrated approach, namely, combining the biological, hydrological, optical, geochemical, and geological parameters of marine environment. Integrated researches in the White Sea started in 2000 in the frame of the project "The White Sea System" [7].

Water sampling for the SPM study was preceded by a profiling instrument package measuring hydrooptical (beam attenuation coefficient, light scattering – proxies for particle concentration), hydrophysical (conductivity, temperature, depth), and biogeochemistry (fluorometer – proxy for phytoplankton, oxygen, pH, Eh) parameters of the water column and was accompanied by sampling for nutrients; bacterio-, phyto-, and zooplankton; and other special biogeochemical researches (methane concentration, rates of biogeochemical processes, etc.). Satellite ocean color data were used to show the areal distribution of SPM, chlorophyll, temperature, and other bio-optical parameters in the surface layer of the White Sea on many time scales [8–10].

The study of marine SPM provides knowledge on the cause-effect relationships of the recent sedimentation process (from the source of matter to bottom sediments deposition) and is a reliable basis for quantitative assessments of this process. For geochemists and sedimentologists, the SPM is a matter of interest not only as a material for the formation of bottom sediments but also as one of the occurrence forms of chemical elements and phases in seawater [11–13]. The marine SPM is one of the most powerful adsorbents on the Earth.

The SPM is a heterogeneous material and normally includes abiotic (mineral) and biotic (phytoplankton, detritus, partially bacterioplankton, spores) particles. The SPM participates in biogeochemical processes as a primary reacting substance or catalyst, and it is utilized by zooplankton and benthos during feeding via biofiltration. Marine particles participate in phase-to-phase transitions; their surface charge can change followed by alteration of their aggregative stability or coagulation and flocculation. SPM can exhibit the properties of some colloids and at the same time obeys the Stokes law [14].

There are many other reasons to be interested in SPM concentration and composition. Particles in the sea have a different grain-size and density; they scatter light and sound differently, have different specific surface areas, and, consequently, have different physicochemical ability and sedimentation rates. Bacteria, as well as SPM, are a dispersed phase, and they can affect the optical and other properties of seawater [15].

One of the main components of SPM in seas is a particulate organic matter (POM): terrigenous (allochthonous "humic") and biogenic (autochthonous "sapropelic"). Chlorophyll "a" (Chl-a) is the most important component of the primary organic matter, is present in almost all microalgae, and acts as a marker of phytoplanktonic material in SPM. Chl-a and its derivatives can be regarded as a proxy of the labile form of organic carbon [16]. In water column and bottom sediments, they characterize the contribution of only phytoplankton, and no other sources of organic matter.

In the Russian Arctic and Subarctic seas, to which the White Sea belongs, the SPM concentration and composition are still poorly understood. The new data will allow us to expand our knowledge of the recent sedimentation in the Arctic shelf seas, which are under the influence of climate change [17]. This is an important issue for the planned expansion of operations and investigations in the Arctic.

The Arctic seas, such as the White Sea, are subjected to a powerful river runoff and coastal abrasion, so terrigenous (allochthonous) material is an important and often predominant fraction of the total SPM [18–20]. The biogenic (autochthonous) component of the SPM usually has a secondary significance, the share of which depends on the primary production. Production and destruction of organic matter, river runoff, supply of biogenic elements, and many other processes in the White Sea have pronounced seasonal features [18, 21, 22].

The aim of this chapter is to present the results of long-term (2000–2012) interdisciplinary researches of the SPM (concentration and major phase composition) in the White Sea for understanding of the recent processes operating in the shelf seas and their role in the Arctic Ocean. Here, we report the SPM data in euphotic zone and on full-depth sections. This paper discusses the main features in the distribution of SPM concentration and bacterioplankton abundance, grain-size, major constituents content (POC, particulate inorganic carbon (PIC), Chl-a, lithogenic particles, etc.), and mineral composition. It allowed us to reveal the sources of the SPM and the features of the spatial and temporal variability of its concentration and composition in the White Sea.

2 Materials and Methods

The materials for our study were collected in the 22 interdisciplinary expeditions organized by IO RAS (28 expeditions, including works in the river–sea interface) (Fig. 1). Our research is based on SPM samples collected in the White Sea over 2000–2014.

Full sea depth sampling occurred on the basis of the hydrooptical (transmissometers, IO RAS) and hydrophysical (CTD Idronaut Ocean 316, Sea&Sun 90M, and SBE 25 plus) sounding profiles. The effect of hydrological conditions on the formation of extremes of suspended matter concentration was estimated. The paper [23, 24] reports on the hydrology and currents in the White Sea. Chemical composition of particulate and dissolved river runoff is presented in the paper [25], phytoplankton researches in [26], and biogeochemical processes in [22]. Water samples were taken using Niskin bottles and Rosette devices.

The SPM mass concentration was determined by the standard technique of vacuum filtration at 400 mbar using membrane filters (diameter 47 mm, pore diameter 0.45 μm) [1, 27, 28]. Each sample (~5 L) was simultaneously filtered through three or more membrane filters. The concentration was determined by

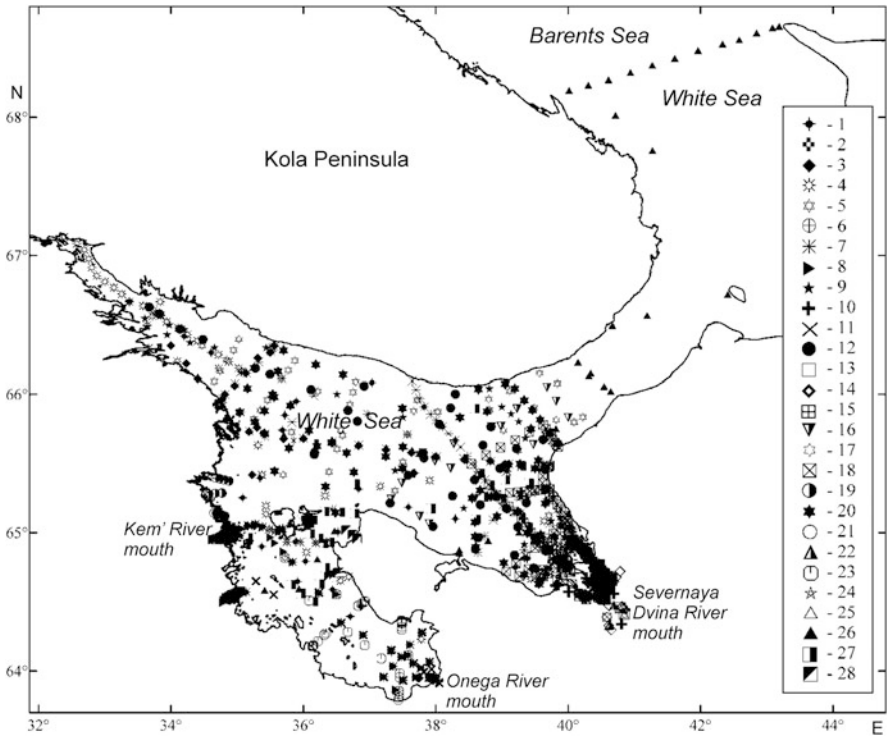

Fig. 1 The study sites of SPM in the White Sea during 28 expeditions of IO RAS, 2000–2014

weighing the filters within accuracy ±0.01 mg, correlating with the volume of filtered water. Total number of samples is 3,500.

The Multisizer™ 3 modification of a Coulter counter®, Beckman Coulter, USA (~2,000 samples), was used to determine the concentration by volume and grain-size (in the range of 2–60 μm) of the SPM [14, 29]. The device was calibrated on board the vessel using a standard latex suspension with a nominal particle size of 5 μm (Coulter® CC Size Standard L5).

SPM grain-size (1.22–118 μm) measurement in fresh river waters was carried out using a Malvern 3600Ec, UK, laser diffraction analyzer (15 samples).

For the total count of the microorganisms, water samples were filtered through Millipore ISOPORE black polycarbonate filters 25 mm in diameter with a pore size of 0.2 μm (246 samples). For more details see [30, 31].

The concentration of Chl-a and pheophytin "a" (Pheo-a) was determined in the samples with fluorometry (with extraction in 90% acetone) on a Trilogy 1.1 fluorometer, Turner Designs, USA, according to the approach described in [32]. The fluorometer was calibrated using the standard powder Chl-a, C6144–IMG Sigma, Austria. The share of Pheo-a (%) was calculated from the sum of Chl-a and Pheo-a.

Before determination of the Chl-a concentration, POC, PIC, and its isotopic composition ($\delta^{13}C_{POC}$), water samples were filtered under a vacuum of 200 mbar through Whatman GF/F glass fiber filters (diameter 47 mm, nominal pore size of 0.7 μm) precombusted at 450°C for 4 h.

The POC and bulk particulate carbon were determined by the automatic coulometric method on an AN 7560 carbon analyzer, Russia. Then, the PIC was determined as the difference between these two values. For a concentration of 30–100 μg C/L, the accuracy was ±15%, and the measurement range was 5–500 μg C/L. The POM content was determined as POC × 2 [33].

Values of $\delta^{13}C_{POC}$ were determined after conventional preparation of samples on a Delta Plus mass spectrometer, Germany, using the PDB standard with an accuracy of ±0.2‰ [18, 22, 31].

The Si, Al, and P content in the SPM were determined by the photometric method in line with the procedure [34] and modified for small weighed portions at the filter by Isaeva and Lukashin, IO RAS [35]. The accuracy of this method is ±15%. We use Al as a tracer of lithogenic particles. We use the upper continental crust Al content of 8.04% to calculate lithogenic phase of SPM [36].

The composition and morphology of the individual particles of the SPM were studied by use of the VEGA-3sem TESCAN scanning electron microscope, Czechia, equipped with the X-ray spectral microprobe Oxford INCA Energy 350, Great Britain.

X-ray powder diffractometry was used to study the mineral composition of the SPM: DRON-2.0 X-ray diffractometer, Russia, and Bruker D8 Advance system, Germany [37].

Data obtained with a MODIS-Aqua satellite ocean color scanner (http://oceancolor.gsfc.nasa.gov/) were used to analyze the areal distribution of water temperature, Chl-a, and SPM, in the surface water layer. Images of the distribution

patterns of these parameters were compiled, using regional algorithms developed at the Laboratory of Ocean Optics, IO RAS, from our original field measurements [8, 10, 38].

For the White Sea, estimation of bio-optical parameters by the satellite data is not an easy procedure, since several factors deteriorate correct calculation, including the low Sun position above the horizon (this increases the number of errors in calculating the atmospheric corrections), high clouds, and intensive riverine discharge with high content of colored dissolved organic matter (CDOM) [10, 38]. Development of algorithms that may be applied in local and seasonal aspects in the shelf seas is essential for reliable assessment of the satellite data; and this can be done only when referring to the field data.

3 Characteristic of Sedimentation Area

Compared to the other Russian Arctic shelf seas, the White Sea is a distinctive basin because it is semi-enclosed. It has quite small dimensions (area about 90,000 km^2, a volume of 5,375 km^3, an average depth about 67 m, the maximum one of 350 m), has a strongly partitioned shape, and receives a fluvial input from a relatively large catchment area of 715,000 km^2 [17, 39]. River runoff makes a dominant contribution to the freshwater budget (a total annual discharge of about 225–231 km^3) and little influence of sea ice formation or melt [40]. There are major rivers Severnaya Dvina (112 km^3/year), Mezen (24 km^3/year), and Onega (18 km^3/year) in the eastern part of the sea and many small rivers in the western part (Fig. 2). The bulk of the terrigenous matter is supplied to the White Sea with riverine runoff during spring flood which exceeds its supply during the summer mean water in two or more times [41]. The SPM concentrations varied usually from 2.0 to 11.6 mg/L in the delta of the Severnaya Dvina River in summer [9]. Despite the fact that the turbidity of river waters is not so significant, the total amount of particulate river runoff may be quite appreciable due to abundant annual runoff.

River waters are enriched in different forms of DOM including humates of iron and manganese [47]. Mean concentration of dissolved organic carbon (DOC) in the Severnaya Dvina River is 18 $\pm$ 2 mg/L [42]. Values of absorption by CDOM at 350 nm and DOC in surface waters of the White Sea basin are higher compared to other river-influenced coastal Arctic domains [40]. In this regard, the waters of the White Sea are characterized by the strongest absorption of solar radiation in comparison with the Kara Sea (subjected to huge river runoff) and especially the Barents Sea (with a small river runoff). Almost all the solar radiation entering the water is absorbed already in the upper 10–15-m layer [43].

The White Sea is characterized by a short vegetation period (210–123 days/year in different parts of the sea) [39]. Significant temporal and spatial variability in

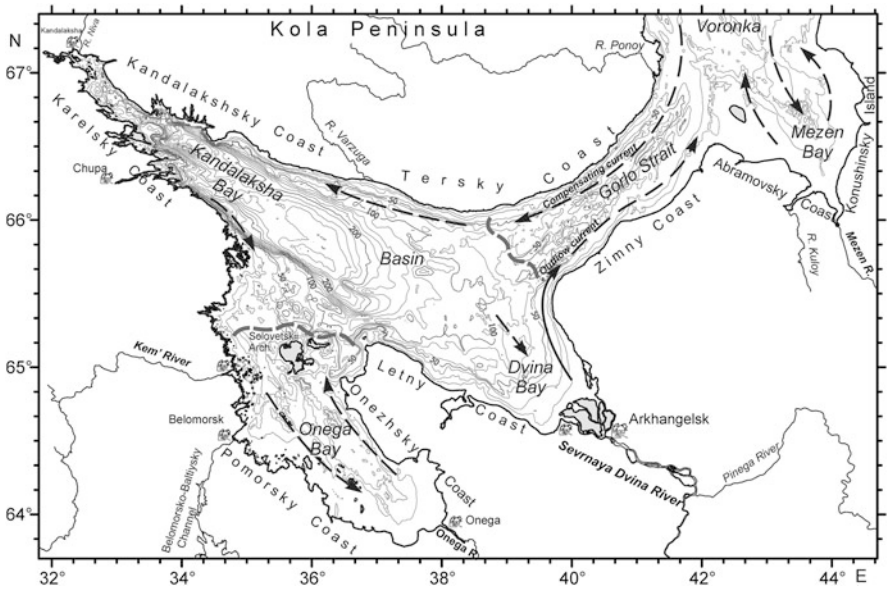

Fig. 2 The map of the White Sea, its bathymetry (based on IO RAS and GEBCO bathymetry), major currents shown by black arrows, and hydrological fronts shown by gray-dashed line (data from [23, 24])

euphotic zone primary productivity obviously causes variations in particle concentrations in the upper water layer [26].

The surface salinities are 24–28 and about 30 psu near the bottom [23]. Interaction between water masses of the White and Barents Seas is controlled by strong tidal mixing in the narrow and the relatively shallow Gorlo Strait, where current velocities of up to 2.5 m/s have been reported [17]. Tides flow into the White Sea from the Barents Sea as regular semidiurnal waves [14]. A water residence time is 5–6 years which is longer than that in neighboring Arctic shelf seas (1–2 years for the Kara Sea). Water masses from the Barents Sea have the Atlantic origin. They are characterized by a consistently high salinity of 34–35 psu and a relatively high temperature for the Arctic seas varying by seasons within about 3–8°C [23] (Fig. 3).

Waters with a quasi-homogeneous vertical distribution pattern of thermohaline characteristics are confined to the Gorlo and Onega Bay (due to tidal mixing) and stratified waters – to the Basin, Dvina, and Kandalaksha Bays. Nearby the large river inlets (such as the Severnaya Dvina, Onega, and Mezen) as well as between Gorlo and Basin, and between Onega Bay and Basin, the distinct hydrographic fronts are commonly found [24, 44].

It was revealed the climate warming in the Arctic Region has caused a reduction in freshwater inflow into the White Sea and an increase in evaporation [17] that may influence the SPM sources into the sea.

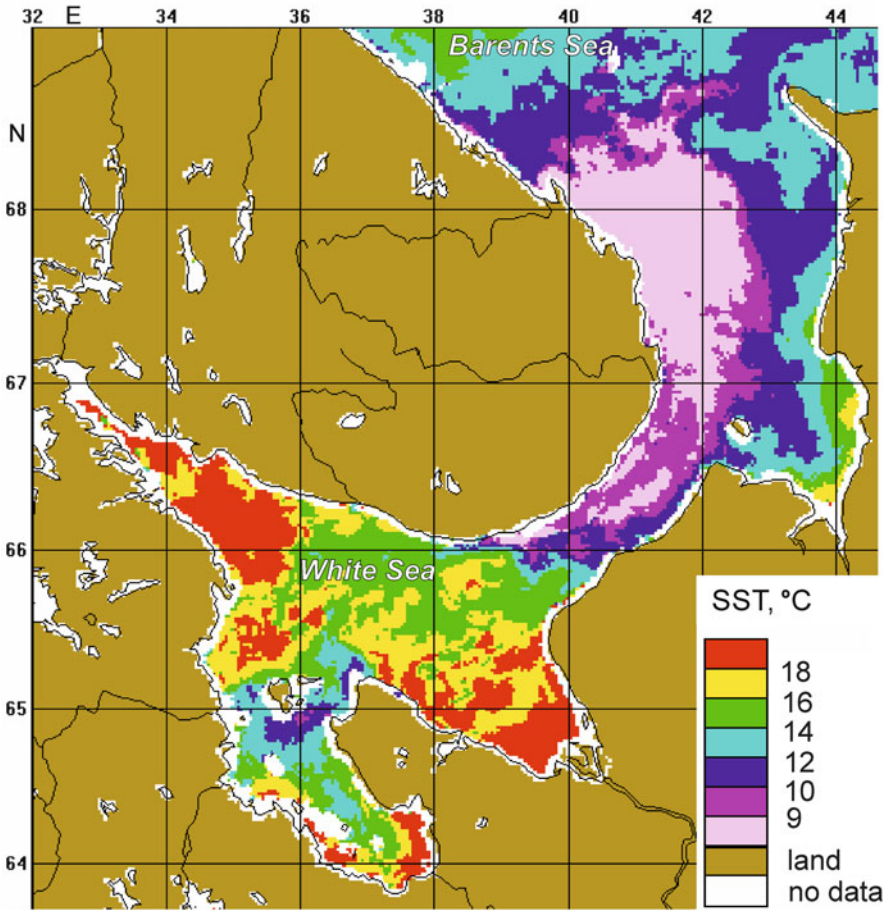

Fig. 3 Sea surface temperature (SST) distribution in the White Sea derived from MODIS-Aqua data. Image was composited over August 1–28, 2003, and provided by IO RAS, Ocean Optic Laboratory

4 SPM Sources

The distribution and dynamics (seasonal and interannual variations in the amount and composition) of SPM are determined by the sources of SPM. The main sources are allochtonous material (mostly transported by large rivers) and autochtonous (biogenic) matter. Allochtonous matter is supplied primarily by the Severnaya Dvina River (the peak is during flood in May). The distribution pattern of autochtonous material is determined by primary production.

In the beginning of the hydrological spring, the main SPM sources are cryosols and algal flora which are supplied during the sea- and river-ice melting. Mean concentration of particulate matter in sea-ice is about 5 mg/L [20]. This is a substantially lower

value than that for Siberian shelf seas. The sediment laden sea-ice is composed of mostly biogenic matter (diatoms, as a rule) [45]. The beginning of the biological spring is observed in the first decade of April.

Phytoplankton abundant in the White Sea is characterized by two maxima: in April–May and in June–July with domination of diatoms. In the end of summer (sometimes in July) in addition to diatoms, dinoflagellates dominated too [46]. Autumn phytoplankton blooms are usually weakly expressed.

Coastal abrasion material makes a significant contribution to the SPM concentration in the Mezen Bay and Voronka, on their eastern coasts [2]. The main part of material (first of all, the sandy–silty fraction) accumulates in the shallow tidal zone and in the zone of alongshore currents. In shallow Onega and Mezen Bays, resuspension processes caused by tidal currents and storm effects, at small depths, play a significant role.

Aerosols are one of the SPM sources. The concentration of insoluble aerosol particles above the sea is about 0.17 $\mu g/m^3$. This value is close to the average concentration for the Russian Arctic seas. The flux of aerosols to the water surface of the White Sea amounts 54,000 tons/year.

Evaluation of aerosol and coastal abrasion matter's fluxes is much lower than particulate river runoff. The total particulate runoff of three largest rivers (Northern Dvina, Mezen, and Onega rivers) is 5 million tons per year [19, 47]. If we take into account that about 70–80% (for different rivers) of the river particulate matter is deposited in the area of marginal filters [28], then approximately 250,000 tons/year of this material enters to the sea, which is about five times higher than the contribution of aerosols. Nevertheless, the supply of aerosols to the White Sea areas far from the large river mouths may be significant for some trace elements [48].

5 SPM Concentration by Mass and Volume in Surface Water Layer

The spatial and temporal variations in SPM concentration in the White Sea are caused by direct input of mineral particles from the catchment areas and river runoff, first of all the Severnaya Dvina River. Besides, there is an indirect SPM input resulted from diatom blooms which are controlled by supply of nutrients and quite narrow euphotic layer because of CDOM high content.

5.1 Mass Concentration of the SPM in Surface Layer

The typical SPM distribution pattern in the White Sea is presented in Fig. 4. Isoline positions can change significantly in the coastal zones, in areas of river marginal filters, and in frontal areas.

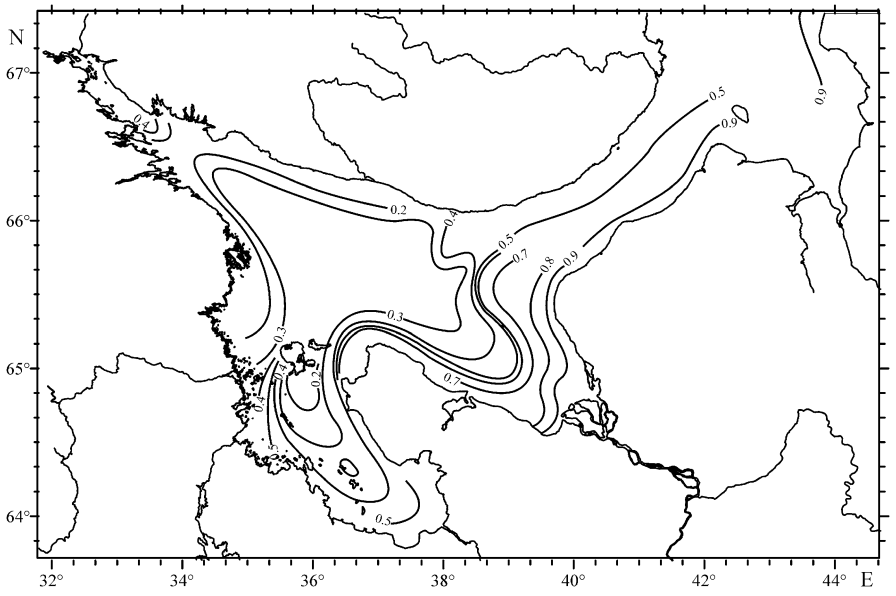

Fig. 4 The principle schematic map of the SPM distribution in the White Sea in summer, mg/L. Values of SPM concentrations are marked on isolines

The average SPM mass concentration beyond the river mouths was detected to be ~1.0–1.4 mg/L in the White Sea (June–September, 2000–2014). This value appeared to be close to the corresponding value in the Kara Sea (~1.2–1.3 mg/L on average for 2007 and 2011) and Laptev Sea (~1.7 mg/L on average for 2003, 2004, 2007, and 2008) [49]. Such a similarity is explained by the fact that these Arctic seas are subjected to strong influence of the river runoff, which controls the formation and spatial distribution of marine SPM. On the contrary, these values exceed the same parameter by 3–4 times in the Barents Sea where concentration usually varied from 0.2 to 0.5 mg/L, rarely to 1 mg/L, in summer 2017 [unpublished data] and autumn 1997-1998 [50].

Higher values of SPM concentration (>1 mg/L) were usually detected in the river mouth's area and located in a narrow (up to 20 km wide) coastal zone. Here, the complex structure of lateral fluxes of SPM is formed. This pattern is also evident in the other Arctic shelf seas [3, 49, 50]. Isolines of the higher SPM concentration generally run in parallel to the coastline (Fig. 3). The values of the SPM concentration decrease by a factor of 5–10 with distance off the coast. This phenomenon is characteristic for many shelf seas and coastal areas of the World Ocean [1].

SPM concentration may be changeable due to wind stress and tide phase. After the storm of July 2010 (intensity was up to 4 on the Beaufort scale), the water turbidity in the surface layer increased in 1.5–2 times (Fig. 5). Using the ADCP, the SPM dynamics dependence on the tidal cycle was studied at the diurnal stations: (a) the SPM concentration decrease in the high tide period, while it increases at low tide; and (b) variations in the SPM concentration within the whole water column

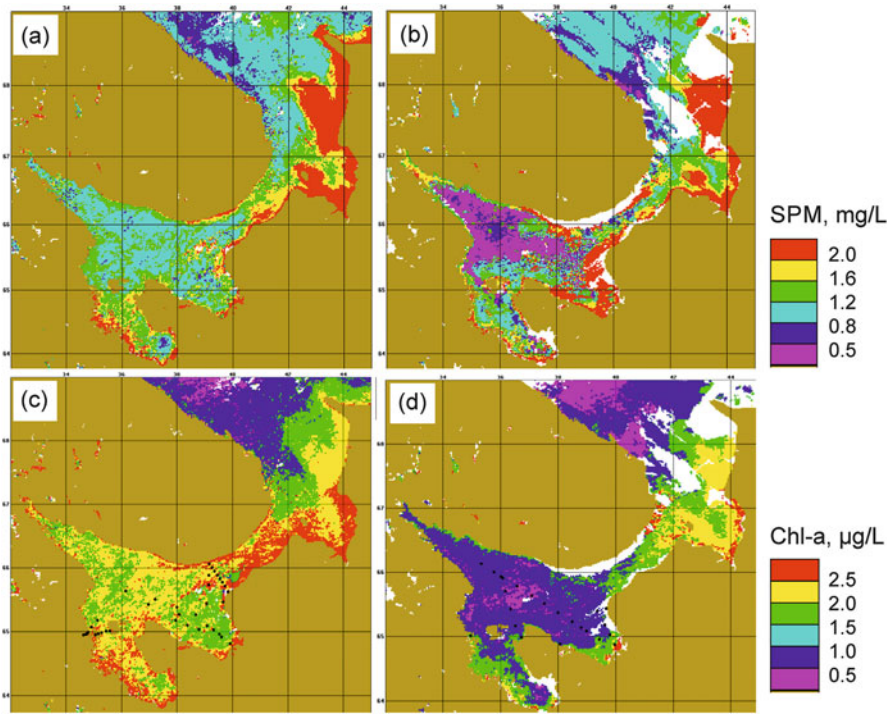

Fig. 5 The SPM and Chl-a concentration in the surface water layer of the White Sea before and after storm in July 2010. The SPM concentration (**a**) before storm, images were composited over July 20–24, (**b**) after storm, images were composited over July 25–29; Chl-a concentration (**c**) before storm and (**d**) after storm

reached 1.5-fold or even more (depending on the sea depth), both in the coastal and in distant zones (arbitrarily, down to the isobaths of 100 m) [10].

Despite the fact that the freshwater input of the Severnaya Dvina River is significantly higher than that of the Onega and Mezen Rrivers, the water turbidity is much larger in adjacent to the mouth areas of the latter. It's connected with powerful tidal mixing and resuspension processes in the Onega and Mezen Bays according to Dvina Bay.

In the central part of the White Sea (so-called Basin), SPM concentration varied from 0.3 to 0.8 mg/L, up to 1 mg/L locally. The likely reason for this is the anticyclonic water circulation in the White Sea, which transports the SPM along the coasts and prevents its inflow to the open sea areas. Excess water of low density (transformed water river) enters the Voronka and Barents Sea through the Gorlo Strait from the sea itself, where a constant outflow current (with SPM concentration about 1–2 mg/L) is directed along the eastern coast of the Dvina Bay and Gorlo Strait (Zimny Coast) (Fig. 2).

The Barents Sea waters enter the Basin through the Gorlo Strait mainly along the western Tersky Coast, compensating current (Fig. 3). The SPM concentration in these waters is noticeably lower (about 0.4 mg/L) than that along the eastern coast in

the outflow current. SPM concentration varied from 0.2 till 1 mg/L in the Voronka region. The trace of the White Sea own water was revealed near the northern boundary of the sea close to eastern coast [3].

Besides the anticyclonic circulation, hydrological fronts (tidal mixing fronts, local upwelling, currents, river marginal filters, etc.) distort the pattern of gradual decreasing of the SPM concentration in the off-the-coast direction. In these areas, gradient zones are formed (SPM fronts and biogeochemical barriers), and their positions can change seasonally.

The water salinity is the main factor that controls the changes in the SPM distribution in the marginal filter of the rivers [28, 51]. The SPM concentration decreases exponentially by up to 79% as salinity grows in the marginal filter area of the Severnaya Dvina River. So, close to the mouth area, concentration reached 6–3 mg/L in June and August, respectively.

A quasi-constant zone of low-temperature anomaly, located southeast of the Solovetsky Archipelago, is characterized by low SPM concentration (up to 0.2 mg/L) (Fig. 3). Primary production here is minimal due to wind stress at small depths that, however, promotes increase in the photic layer thickness [52].

In the Basin and Kandalaksha Bay, increased SPM concentration (>1 mg/L) was usually related to local phytoplankton growth, under the condition of sufficient nutrient supply [26]. Usually SPM concentration in Kandalaksha Bay (0.3–0.6 mg/L) was close to that in the Basin because of low particulate river runoff [4, 5].

5.1.1 Seasonal Variability

Broadly, we revealed seasonal variability is most expressed in the Dvina and Onega Bays (influenced by river runoff) and least expressed in the Kandalaksha Bay and in the Basin [10]. Low SPM concentrations were reported for July–August, while high ones were observed for May and often for September. The width outflow current in the Dvina Bay (where transformed river water is traced by SPM, temperature, Chl-a, and dissolved organic matter on the images of MODIS-Aqua) is characterized by seasonal and interannual variability, and this is verified by the data from paper [21]. In the Onega Bay, the highest SPM concentration is observed most often in September and likely caused by strengthening from storm-induced mixing [9].

In general, the spatial and temporal variations in the SPM concentration in the White Sea are directly (mineral particles from the catchment area) or indirectly (diatoms blooming due to supply of biogenic elements) caused by river runoff.

The SPM concentration in the Mezen Bay (May–September) is usually high (about 2 mg/L and higher), which is mainly caused by coastal and bottom abrasion and the most powerful tidal mixing (flow velocity up to 250 cm/s, tide height up to 9.8 m) at shallow depths (<10–50 m) and partly by the influence of the Mezen River runoff.

The data on the SPM concentration in winter (under the ice) was quite poor. At the end of hydrological winter (e.g., in the end of April 2003), it varies from 0.2 to 1.6 mg/L. The highest concentrations were reported in the Basin, as a result of enrichment surface water by biogenic particles (usually diatoms).

5.1.2 Interannual Variations

The greatest amplitude of the average annual variability in the SPM concentration was revealed in the Dvina, Onega, and Mezen Bays and in the eastern part of Gorlo–Voronka area affected by river runoff. However, the greatest relative difference between the average annual values for different years was 18% (the significance value is 0.05; confidence probability is 95%) [10]. The differences between the maximal and minimal average annual concentrations were statistically significant only for the Kandalaksha and Mezen Bays. The minimal average annual SPM concentration in the entire sea was observed in 2007, the year of the lowest sea-ice extent in the Arctic marginal ice area. Changes in ice conditions in the Barents–Kara Sea region appeared to be primarily forced by ocean heat fluxes during winter [53].

Based on the satellite data, the interannual linear trends of sea surface temperature, SPM concentration, Chl-a content, and CDOM absorption have been estimated; these estimates have shown no significant trend for the discussed period of 2003–2010 [38].

A significant correlation has been revealed between the average annual SPM concentrations in the White Sea as a whole, the eastern part of the Gorlo–Voronka region, and the Dvina Bay ($r = 0.7$, $n = 8$). This correlation indicates the determining role of the Severnaya Dvina River inflow in SPM dynamics of the White Sea. Additionally, a relationship has been found between the average annual values of SPM concentration in the western and eastern parts of the Gorlo–Voronka region ($r = 0.75$, $n = 8$); this relationship is caused by intensive turbulent mixing and lateral suspended particulate transport in this region [24].

Finally, we would like to conclude that the SPM concentration in the White Sea's surface active layer is about 1 mg/L, on average. The main sources of SPM in the White Sea have been found: mineral particles of river runoff origin and marine phytoplankton. First of all, they are particles supplied from the catchment areas with the river runoff (the most intensive flow is in May) and only partially supplied from melted ice cover (usually in April). Abundance of phytoplankton is caused by a combination of many abiotic factors, including the supply of nutrients with river runoff and melted ice. The local hydrological conditions promote the formation of high spatial variations of the SPM distribution.

We found out a relationship between the dynamics of the average annual SPM concentration in the White Sea as a whole and in the constant outflow current which transports water of the Severnaya Dvina River along the Dvina Bay to Gorlo Strait coast. We can suppose that seasonal and annual variability in the SPM concentration could decrease during climatic warming in the Arctic.

5.2 SPM Concentration by Volume in Surface Layer

The SPM study in the White Sea with the Multisizer 3 (Coulter counter) device demonstrated a good consistency with the data obtained by the traditional vacuum filtration method and optical measurements (Fig. 6).

The SPM concentration by volume in the White Sea varied from 0.2 to 5 mm^3/L and approximately 1.0 mm^3/L in average. The highest concentration was influenced by the river runoff area. SPM concentration by volume was about 5 mm^3/L in adjacent to the Severnaya Dvina River mouth (Table 1). The lowest one was observed in the upwelling nearby the Solovetsky Archipelago where the low primary production and phytoplankton abundance were detected.

The distribution of SPM concentrations by volume in the White Sea corresponds to the main features in the distribution of mass concentrations. However, SPM concentrations by volume are a reliable proxy for biogenic (phytoplanktonic) particles, whose sizes vary from 2 till 200 μm commonly. In addition, there are different approaches to measurement procedures.

We have made a comparison of the SPM concentration by volume (0.5–5 mm^3/L) and the phytoplankton abundance (0.1–3.7 mm^3/L) [52]. According to our calculations, percentage of phytoplankton in total SPM varied in the different regions of the White Sea: 27% in the Dvina Bay nearby the Severnaya Dvina River mouth, 40% in the Basin, and 65% in the Kandalaksha Bay. The content of terrigenous particles decreased with distance from the river mouths, although remains quite high (till 40%) in the open water areas.

In the coastal waters, we observed significant variations in SPM concentrations (from 1 to 5 mm^3/L in the marginal filter area of the Severnaya Dvina River). These variations depend on the river runoff volume, the tidal phases, and the water salinity. The position of the marginal filter is limited to isohalines of about 0.2 and 24 psu [28].

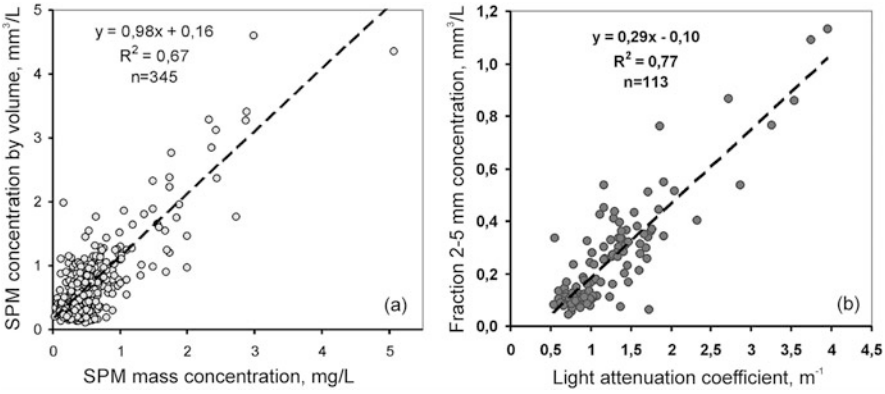

Fig. 6 The relationship between SPM concentration by mass and volume (**a**) and between light attenuation coefficient and fine fraction of the SPM (**b**) in the White Sea

Table 1 The SPM concentration in the surface layer of the White Sea after spring flood in June 2003

	SPM concentration by volume, mm^3/L	SPM mass concentration, mg/L	Total number of bacterioplankton, th. cells/mL
The inlet part of the Dvina Bay			
Variations	3.1–4.6	2.1–6.5	430–588
Mean	3.8	4.6	487
Sample number	4	5	3
Dvina Bay			
Variations	0.7–2.9	0.4–3.4	55–219
Mean	1.4	1.3	138
Sample number	29	28	16
Area of Solovetsky Archipelago			
Variations	0.4–0.9	0.4–1.2	64–96
Mean	0.6	0.8	81
Sample number	12	12	4
Kandalaksha Bay			
Variations	0.6–1.3	0.3–0.9	110–160
Mean	0.9	0.5	138
Sample number	9	9	4
Basin			
Variations	0.5–2.0	0.3–1.2	49–240
Mean	1.0	0.7	158
Sample number	22	22	8
Mean for the sea proper (excluding the inlet part of the Dvina Bay)			
Variations	0.4–2.9	0.3–3.4	49–240
Mean	1.0	0.9	134
Sample number	72	71	36

The SPM concentration in the Severnaya Dvina delta reached 5.8 mm^3/L where the water salinity was about 5 psu (coagulation and adsorption stage of the marginal filter). As the water salinity increased to 20 psu, a decrease in the SPM concentration was observed. It is remarkable that, in the mouth areas of the large Siberian rivers (Lena, Yenisei, Ob, Pur, Taz), high gradients in the SPM concentration decrease were established, which is approximately similar to the marginal filter of the Severnaya Dvina River within the hydrological front under salinity of 20 psu [54]. The sharp increase in the SPM concentration by volume was revealed in waters with salinity exceeding 23–24 psu in the area located immediately beyond the boundary of the saline front due to an increase in phytoplankton share in total SPM [28].

6 SPM Concentration by Mass and Volume in Water Column

The vertical distribution of SPM in the deep part of the White Sea, as well as the hydrological structure, has a three-layered structure. There are two maxima of the SPM concentrations at the surface (the surface active layer above the pycnocline) and at the near-bottom layer (nepheloid layer) separated by intermediate more clear water. Vertical stratification depends on heating intensity and freshwater input mostly in summer and salinity distribution basically in spring [23].

The temperature and density stratification of the water column and, as a consequence, SPM stratification are most pronounced in the deep part of the sea in summer. Density deformation of the vertical structure of the water column in summer forms a so-called liquid bottom, where a significant part of samples for SPM study was collected (usually at the layer of 5–20 m). The pycnocline (thermocline) depth usually ranges from 11 to 22 m. Subsurface pycnocline (close to water surface of 5–10 m) is formed more rarely near the surface of the sea. Beneath the pycnocline the SPM concentration decreases by 3–4 times (Fig. 7).

In summer, the intermediate more clear layer (deeper than 40 m) consists of warm and cold waters of advective origin [23]. The SPM concentration reached 0.2–0.3 mg/L in this layer that is close to the same concentration in the Barents Sea [50].

In spring (April 2003), the thickness of the upper (winter convective) layer came to 20–50 m (it is the boundary of the cold intermediate layer). The SPM concentration in water column varied 0.5–0.6 mg/L (deep sea areas) and increased till 0.8–1 mg/L just in the thin near-surface layer (spring phytoplankton bloom). The particles accumulated above and within the pycnocline during summer (when the strong seasonal stratification observed) begin to float and spread within the winter convective layer. The SPM didn't sink, since this is prevented not by pycnocline (like in summer) but by a gradual increase in water density with a depth below the thermocline [24].

A weak stratification or even a homogenous vertical distribution of SPM, temperature, and density was revealed in the Onega and Mezen Bays.

The thickness of the near-bottom nepheloid layers in the White Sea ranged from a few meters to a few tens of meters (10–20 m, on average). The SPM concentration in the nepheloid layer of the White Sea (up to 5 mg/L in the shallow area) is close to values in the nepheloid layer of the Barents Sea. However, the turbidity and thickness of these layers are usually much lower than in the Kara, Laptev, and East Siberian Seas [49, 50].

We revealed a powerful bottom nepheloid layer nearby the eastern coast of the Dvina Bay (outflow current) with SPM concentration till 5 mg/L in summer. The next one is located in the Gorlo Strait where the SPM concentration of the bottom nepheloid layer was always high (till 3 mg/L) in any tidal phase.

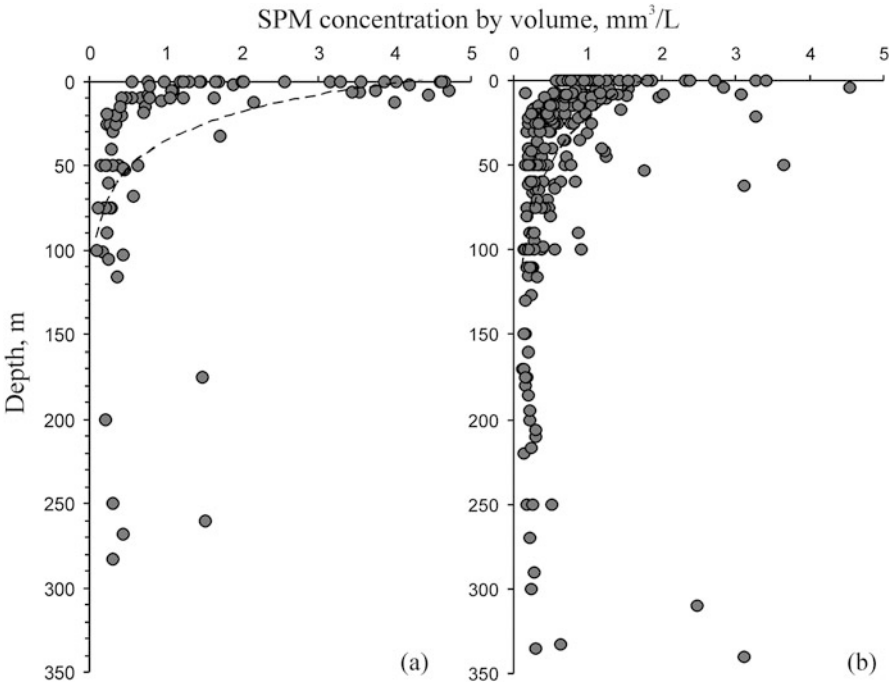

Fig. 7 The distribution of SPM concentration by volume according to the White Sea depth in June, 75 samples (**a**) and August, 398 samples (**b**)

Since a relatively clarity of the Barents Sea waters inflow along the Tersky Coast to the White Sea, the SPM stratification there differs from the other regions. Here, the presence of powerful temperature inversions (up to 2°C) and turbidity fluctuations with depth were observed.

Waters with the similar T^o–S indices were found in the deepwater part of the Basin in June 2003 and in the Gorlo Strait at the end of the hydrological winter, April 2003 [24]. The near-bottom water's hydrophysical characteristics in June fully coincided with the winter observations. The SPM concentration in the near-bottom layer (250–280 m) of the Basin in June corresponded to its values detected in this water mass in the Gorlo Strait in April (0.7–0.9 mg/L and 0.3 mm^3/L). These concentrations were slightly higher than that one in the intermediate water mass, where they did not exceed 0.3 mg/L or 0.1–0.2 mm^3/L. It may be caused by the phenomenon of cascading. It is assumed that the cascading has an advective and gravitational origin [4].

Some full-depth vertical transects are displayed in Figs. 8 and 9. SPM distribution is characterized by vertical stratification with maximal concentration in the upper active layer (10–15 m) according to the density and temperature structure.

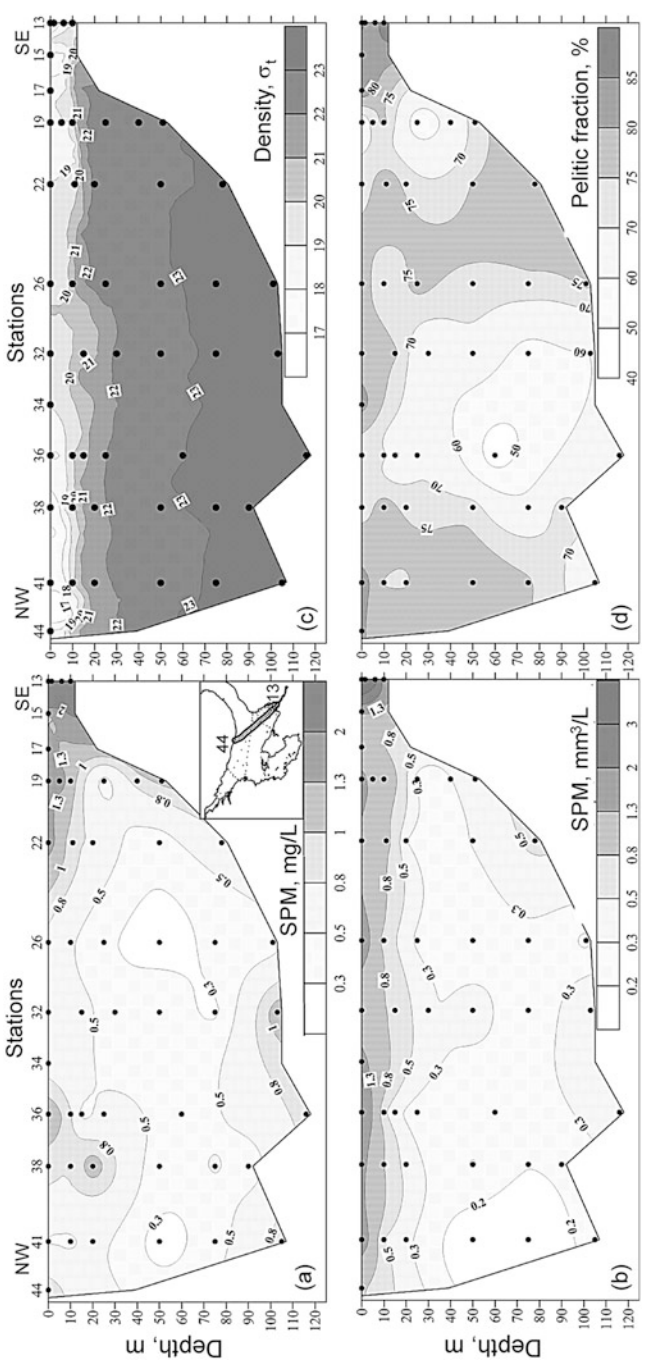

Fig. 8 The full-depth cross section from the Severnaya Dvina River mouth till the Tersky Coast in June 2003: (**a**) SPM concentration by mass and (**b**) volume, (**c**) water density, (**d**) pelitic fraction content

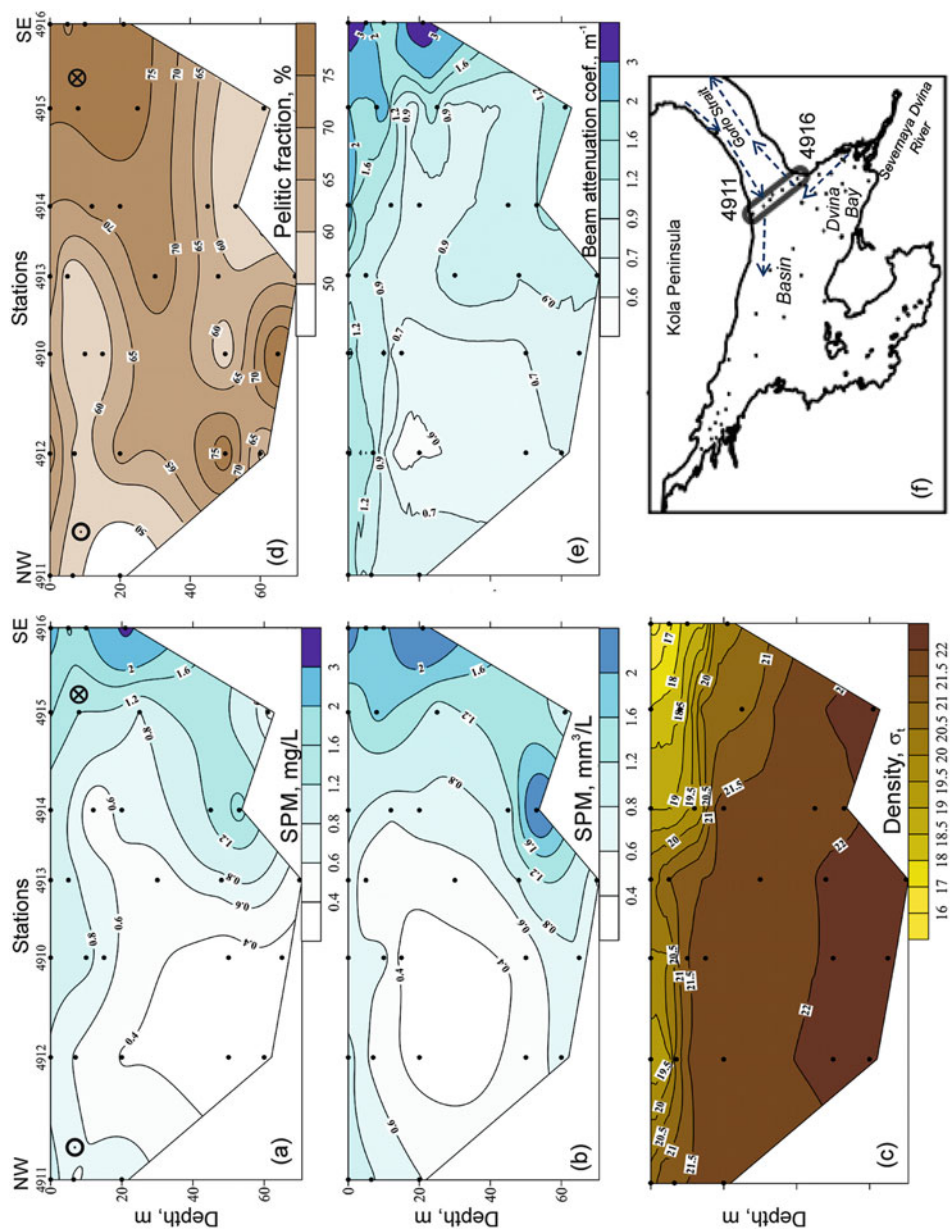

Fig. 9 The full-depth cross section in the southern part of the Gorlo Strait, August 2003: SPM concentration (**a**) by mass and (**b**) by volume, (**c**) water density, (**d**) pelitic fraction content, and (**e**) beam attenuation coefficient. Section location and major currents are shown in (**f**)

For isolines of SPM concentration and density, a quasi-horizontal distribution pattern is typical, reflecting a sharp thermocline with an axis on the 15 m depth and a coexisting halocline (Fig. 8).

Sometimes we observed subsurface lenses of turbidity waters in the areas close to hydrological fronts. Some kind of the turbid lenses were observed in the Kandalaksha Bay at the layer of 50–150 m in August and June. This is a consequence of the widespread phenomenon in the White Sea of interlayer transport, a related process to the so-called cascading – the sliding down of water off the slope in winter and the movement of water from the surface to a layer of 20–60 m in summer [4, 24].

Turbid waters nearby the Tersky Coast obviously resulted from some physical processes such as a tidal mixing and coastal upwelling.

One of the most interesting transects crossed the Gorlo Strait is shown at Fig. 9. One can clearly see the transport of transformed river water enriched in SPM and relatively clear water inflowed from the Barents Sea.

7 Chlorophyll "a" Concentration

The average concentration of Chl-a in the photic layer usually exceeds 1 μg/L (reaching 9 μg/L, and sometimes 21 μg/L, in the shallow inlets of the bays), i.e., the threshold for characterizing the waters as eutrophic ones. The thickness of photic layer in the White Sea is 10–15 m on average. In summer, the maximal concentration was observed in the surface water layer (about 0–12 m), sometimes in the subsurface layer of 0–5 m. The maximal annual variability of Chl-a concentration in the photic layer was observed in the Dvina Bay [55].

According to the optical measurements both in situ and by satellite scanners, the depth of 1% of PAR varies from 7.0 to 8.8 m, and 0.1% of PAR was found at 11.2–14.5 m, respectively [43]. The water masses of the White Sea are characterized by high solar light absorption comparing to the Barents Sea and the Kara Sea. This difference is primarily preconditioned by the content and composition of both the SPM and CDOM; the concentration of the latter is extremely high in the White Sea. The maximal photosynthetic activity in the White Sea was observed in the quite narrow surface water layer. Our data allowed us to conclude that photic layer in the White Sea is approximately less than 15 m depth; it varied from 2–5 m (Dvina Bay) to 20–25 m (deep part of the White Sea).

The average concentration of Chl-a in photic layer in June exceeded the values of July nearly twofold and more than twofold in August. In most of areas of the White Sea, in the late summer, the phytoplankton biomass was lower compared to spring and early summer. The studies of primary production in late August of 2001–2007 [31, 52] also support this observation. The results evidenced the oligotrophic status of the water masses in the central White Sea and the open part of the Kandalaksha Bay. The water masses of the Dvina and Onega Bays may be characterized as oligotrophic–mesotrophic in August. The minimal concentrations of Chl-a in the

White Sea are referred to the start and the end of the productive season, i.e., April and October, respectively.

When the water column is stratified well (deepwater area of the sea), a maxima of Chl-a concentration was observed above pycnocline, which usually coincided with the halocline; this refers to the pattern of the phytoplankton vertical profile.

Seventy percent of the phytoplankton biomass and Chl-a was concentrated in the photic layer (July 2009) [26]. Subsurface Chl-a maximum (3–5 m) was observed in the open water area of the Dvina Bay. There was surface Chl-a maximum in the area subjecting the Severnaya Dvina River flow (0–1 m) and in the Onega Bay and the Basin (0–3 m).

Subsurface Chl-a maximum was often detected in the photic layer; there was a tendency to increase the nitrate concentration as it approached the upper boundary of the thermocline (July–August 2014) (Fig. 10). The highest concentrations of nitrates were confined to the under thermocline water layer (up to 9 μg-at N/L).

The subsurface Chl-a maximum was observed in the 3–12 m water layer in August 2013 at most sites of the White Sea [56].

The highest biomass of phytoplankton and, accordingly, the concentration of Chl-a were usually recorded in weakly stratified waters, where nutrient supply is a result of tidal mixing. In the sharply stratified waters of the sea during the summer season, the supply of nutrients to the photic layer is limited, and the abundance of phytoplankton was low. Probably one of the significant factors determining the spatial heterogeneity of phytoplankton can be the penetration of freshwater lenses from the Dvina Bay to the Basin of the sea [26].

Below the pycnocline, the concentration of Chl-a decreased greatly with the sea depth increased. A decrease in the Chl-a concentration down to 0.5 μg/L and lower was observed in the intermediate water masses (depth range of 20–60 m, on average 50 m) and near-bottom water masses originating from the Barents Sea.

The concentration of Chl-a may reach extremely high values of 1–2 μg/L in the intermediate and near-bottom water masses (depths of 30–90 m) in the area of the structural hydrological front in the southern part of the Gorlo Strait. The phytoplankton biomass here was also high, which refers to the summer phytoplankton bloom [26].

Generally, the concentration of Chl-a in June–July varies from 0.05 μg/L (near-bottom water layer) up to 2.5 μg/L (surface-mixed photic layer), reaching 9 μg/L (and sometimes 21 μg/L) in the shallow inlets of the bays. The spatial distribution of Pheo-a was also patchy, as is observed for Chl-a. The content of Pheo-a varied from 0.6 to 100%. Alongside with that, a high share of Pheo-a (more than 50%) was usually observed in the intermediate and near-bottom water masses and also in the upper water layer of the river runoff and in the area of the salinity fronts.

So, the concentration of phytoplankton varies greatly in different areas of the White Sea during summer [26]. It was found that the distribution of Chl-a was also not uniform. The riverine inflow and hydrodynamics of the sea (hydrological fronts and increasing of the vertical gradients of water density) have the most pronounced effect, while water heating has a less effect.

The assessment of the monthly average of Chl-a concentrations in the different areas of the White Sea obtained by satellite observations evidences the similarity of

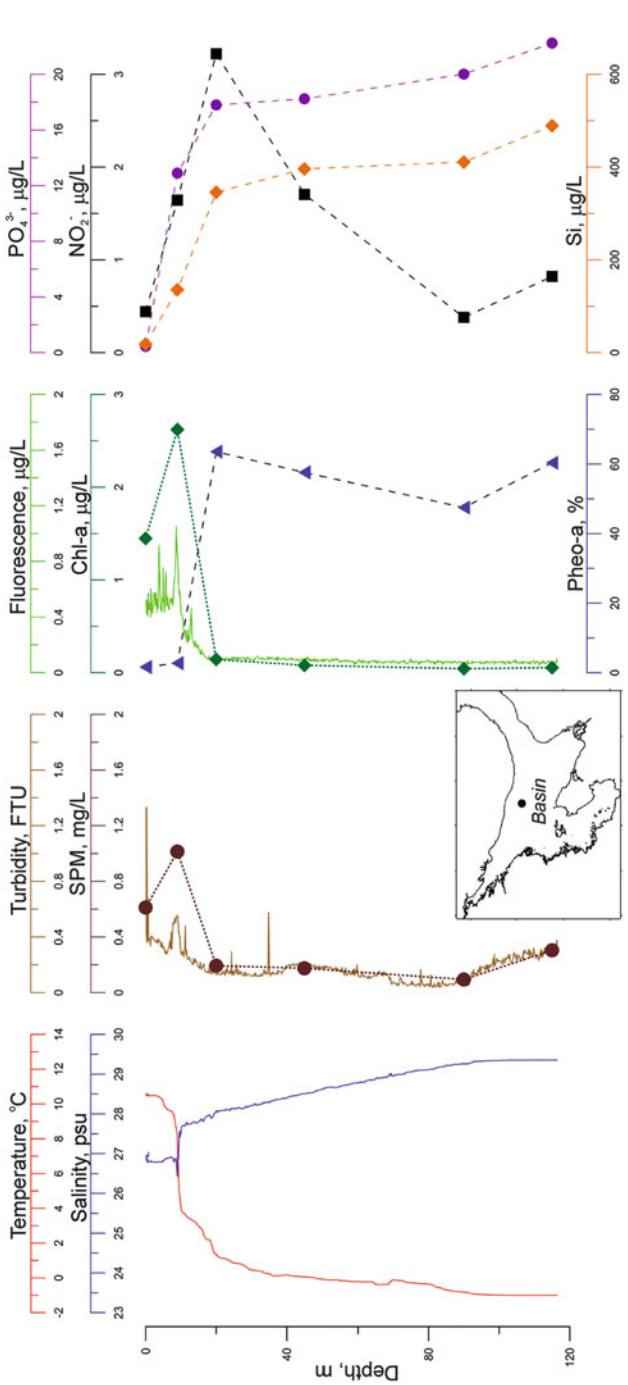

Fig. 10 The vertical distribution pattern of temperature, salinity, turbidity, SPM, and Chl-a concentration, Pheo-a content, and nutrients concentration in deep part of the White Sea, the northern area of the Basin. The sea depth is 120 m

the dynamics of Chl-a concentration and the SPM concentration [55]. However, the Chl-a dynamics is smoother. On the one hand, the concentration of Chl-a and SPM in the photic layer is controlled by the entrance of allochtonous matter with riverine discharge, which predetermined their similarity. On the other hand, the concentration of Chl-a (proxy of autochthonous matter) depends on the primary production intensity. The PAR depth and enrichment of the surface water layers in nutrients due to the mineralization of POM in the pycnocline smooth the seasonal variability of the Chl-a concentration during summer low-water in the catchment area.

The highest Chl-a concentrations are in the Onega, Dvina, and Mezen Bays, which are preconditioned by the riverine supply of nutrients.

The influence of the wind stress on the vertical distribution of Chl-a concentration was well pronounced in the photic layer. After the storm (up to 4 on the Beaufort scale, with a wind speed up to 16 m/s, July 2010), the average concentration of Chl-a in the upper layer in the Dvina Bay decreased by approximately 1.5 times. The SPM and Pheo-a concentration were correspondingly (by the same amount) [55]. According to the satellite images, the wind stress had a significant effect on the Chl-a distributional pattern for the most area of the White Sea (Fig. 5).

The concentration of Chl-a in the White Sea is significantly higher compared to the Barents Sea and the Pechora Sea and is quite similar to the Kara Sea, which is also affected strongly by intensive riverine discharge.

Despite the fact that Chl-a constitutes an insignificant part of the SPM (0.1–1.0% of dry weight), a positive correlation was found between these parameters, which becomes stronger in the areas affected by riverine discharge ($r = 0.8$ in the marginal filter of the Dvina Bay, $n = 13$). The correlation coefficient may vary and even reach zero depending on the phenological season.

A well-pronounced direct correlation between Chl-a and POM concentration was found for the different water masses of the White Sea [55].

These relationships are primarily predetermined by the same factor, i.e., by the riverine discharge, which carries both SPM and nutrients to the White Sea.

The typical full-depth vertical distribution of Chl-a are displayed in Fig. 11. The effect of the outflow current from the Dvina Bay was clearly shown. The high concentrations of Chl-a in a thin photic layer related the current were well illustrated (Fig. 11).

Finally, we would like to conclude that variability of monthly averages of Chl-a concentration, as calculated by the satellite data, evidences the similarity of seasonal dynamics of Chl-a and the SPM concentrations.

The maximal concentration of Chl-a (3–9 μg/L) was registered during the summer period at depths usually of 0–5 m and at deeper layers till 10–12 m. Most of the POM was synthesized by the phytoplankton during photosynthetic processes in a relatively narrow surface water layer of about 0–12 m, i.e., in one of the most biochemical active water layers.

Subsurface Chl-a maximum (3–12 m) was observed in well-stratified waters in summer. Surface Chl-a maximum was registered at the hydrological fronts, in the tidal mixing areas with low sea depth and in the river lenses (enriched with nutrients)

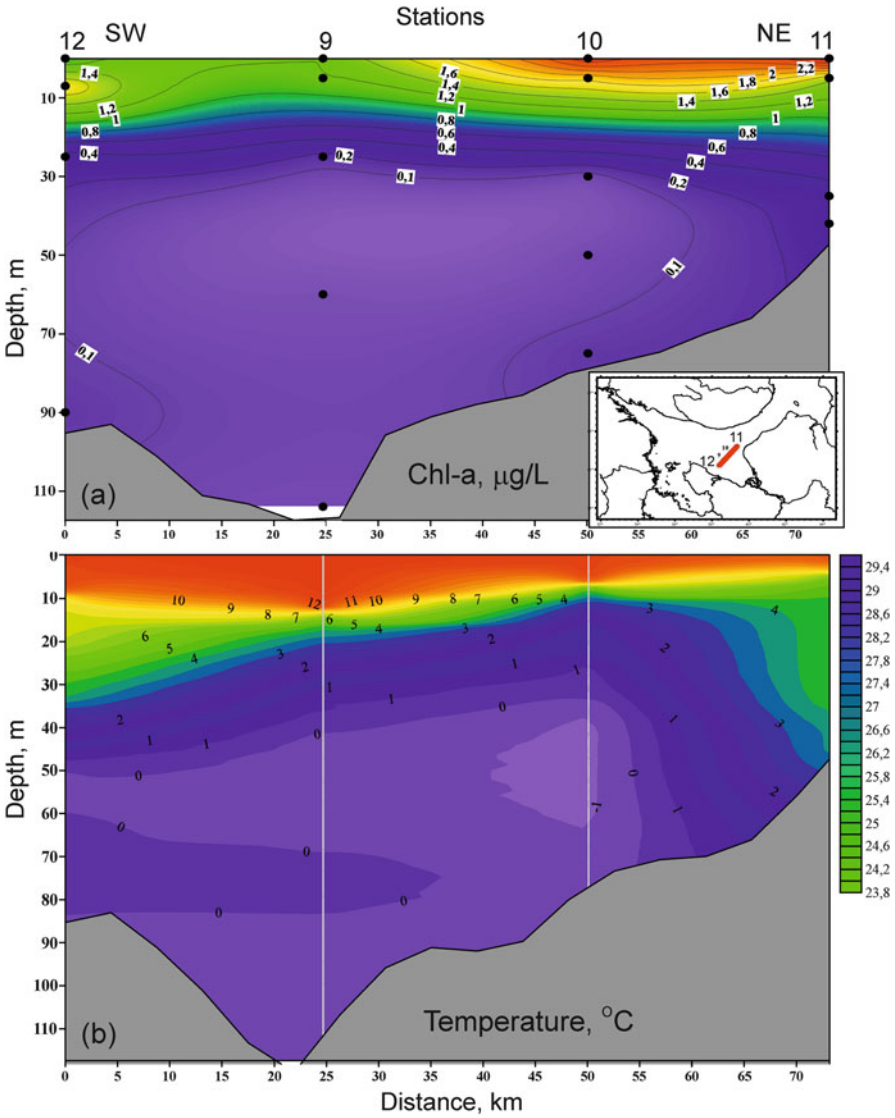

Fig. 11 The full-depth cross section of Chl-a concentration (**a**) and temperature (**b**) in the outer part of the Dvina Bay in July 2012

penetrated to the open water area as a result of wind stress. We generally found that both increased pigment per cell and cell numbers of phytoplankton in the White Sea.

8 SPM Grain-Size Distribution

The SPM, as a rule, has micron and submicron sizes. The SPM mostly consist two fractions: (1) 0.4–10 μm, pelitic, and (2) >10 μm, fine and coarse silty [57]. The most abundant particles in seawater are till 20 μm in size [58]. Sandy fraction (separate particles of detritus, secondary particles – coarse aggregates) is less common in the sea. This fraction is unstable in terms of sedimentation, and it forms the basis of vertical fluxes of sedimentary matter. The fractions here and further are distinguished according to the classification of Bezrukov and Lisitsyn [59] for marine bottom sediments, accepted in IO RAS, and underlying all maps of bottom sediments in the *Atlas of the Oceans* published in 1974–1980, USSR.

The SPM grain-size of the White Sea is formed under two main sources – lithogenic and biogenic ones – which are in complicated interactions in space and time. In this connection, the grain-size diversity of the SPM is due, first of all, to the different contributions of phytoplankton and riverine mineral particles. There are 12–25 million particles/L in the White Sea and 5–6 million particles/L in the open Atlantic Ocean.

The most common type of the SPM is silty–pelitic polydispersity, since the content of each fractions is rarely exceeds 50% (by volume).

The SPM of the White Sea was characterized by medium sorting as a rule. Median diameter (Md) of the SPM varied from 3 to 11 μm. Similar values were obtained for other seas of the Arctic as well. Due to the fact that the SPM is usually polydispersity, Md can deviate significantly from the modal diameter.

In the Arctic shelf seas such as White, Kara, and Laptev, the increased content of pelitic fraction (≥50%) is a proxy of the transformed river particulate flow (Figs. 8 and 9). The content of lithogenic particles and the content of pelitic fraction decreased with the distance from the river mouths.

The high content of pelitic fraction tends to the regions of river water discharge in the White Sea. Thus, the content of fine particles <5 μm usually exceeded 50%, and their Md was less than 5 μm. The sorption capacity of the SPM was maximal in the area of the Severnaya Dvina River marginal filter and decreased in the direction to the central parts of the sea. It is well known that the high dispersity of the SPM increases the sorption activity of the particles and may promote the development of bacteria. We showed that, in the White Sea, more than 60% of the total number of bacterioplankton (TNB) consisted of cells attached to detrital particles (Table 1) [30]. Each of these particles, as a rule, is saturated with bacteria, mostly in the form of rods and cocci.

The grain-size transformation of the SPM in the marginal filter of the Severnaya Dvina River was studied in August 2005 [30]. At the first stage, in the earliest steps of mixing river and seawater (salinity of water from 0.2 to 2 psu), the sandy and silty fractions were deposited. The decreasing of SPM concentration was accompanied by a twofold decrease in TNB (from 360 to 170 th. cells/mL).

Coagulation and sorption stage of the marginal filter were revealed between isohalines of 2–15 psu. Here, the principal sorbents are iron hydroxides, organic

matter, clay minerals, and siliceous and calcareous organism remains. At this stage, the greatest specific surface area of the SPM, according to the data of the laser analyzer, corresponded to its lowest Md and the maximal value of the TNB (520 th. cells/mL). Bacteria settled over the newly formed aggregates. In addition, at water salinity of 2–15 psu, the extinction of both freshwater and marine plankton occurs; as a result, DOM is released to provide the development of bacteria.

At the third (so-called biological) stage (water salinity 15–24 psu), the silty fraction prevailed in SPM due to phytoplankton development. It is shown that phytoplankton bloom is usually observed along the outer boundary of the marginal filter, where water salinity reached to 23–24 psu. The decline of the TAM (till 150 th. cells/mL) is caused by decrease in the amount of detritus (to which the development of bacterial cells is strongly related) and by the intensive formation of alive organic matter, which limits their development by the food and competitive interrelations.

So, we established that the water salinity is the main factor that controls the changes in the grain-size distribution and composition of the SPM in the marginal filter. The concentration by volume of fine particles (2–5 μm) and water salinity demonstrated negative correlation between each other ($R^2 = 0.86$, $n = 24$).

The largest variations in the SPM grain-size composition were found in the photic layer of the White Sea (about 0–15 m). The pelitic fraction (2–10 μm) prevailed in the surface water layer in June. The content by volume of the fraction reached 70–90%. During this period, the SPM can be called predominantly pelitic.

The content of pelitic fraction (40–70%) in surface layer was lower in August than in June. But maximal content of the fraction was always confined to the Severnaya Dvina River mouth. The Md of SPM in the outflow current was 5–7 μm which marked the trajectory of the current.

We revealed the influence of tidal phase on SPM grain-size composition. During the high tide, the content of the pelitic fraction decreased by almost twofold, while the silty fraction increased also by twofold in comparison with that during low tide in the Dvina Bay. The grain-size curve had bimodal distribution during high tide: 3 and 12 μm. The second peak connected with diatoms had been smoothed during low tide. The SPM of the transformed Barents Sea waters was characterized by a lesser sorting of particles than the river particulate matter during low tide.

The vertical zonality is reflected in SPM grain-size distribution and explained by stratification of the water column. In the surface layer (above pycno- and thermocline), the SPM grain-size is characterized by bimodal distribution: the first peak corresponds to the pelitic fraction, while the second peak coincides to the fine silt fraction. Under the pycnocline (~10 m), the content of silty fraction sharply reduced and the share of fine particles increased. Md was often several times reduced under the pycnocline layer in comparison with the surface water layer. This implies that the barrier effect of the pycnocline is reflected in the SPM grain-size according to hydraulic weigh, size, and composition. This layer, which is also referred to as "the liquid bottom," represents a trap for biogenic particles firstly (especially for plankton remains, which density is close to the density of the surface water). A bacteria growth is noted above the vertical density gradient. The abundance of

bacteria most often features a peak immediately beneath the SPM maximum, i.e., in the layer with the maximal content of detritus.

In the stratified water column, the content of pelitic fractions (2–10 μm) changed a little. This is so-called basic particles dispersion background of seawater.

Thus, extremes in the SPM distribution are governed by both the grain-size of primary material (sources) and trend of its transformation in water body.

Particles disperse system in the seawater is unstable. Coagulation rate of submicron particles is several orders of magnitude higher because of the Brownian motion as compared with that of their coarser counterparts [14]. Precisely this difference in coagulation rates is likely responsible for the aggregation of submicron particles and appearance of peaks in the fraction of 3–6 μm in deep water layers.

The content of silty fraction increased (till 60%) in the near-bottom nepheloid layer (particles and aggregates). The TNB growth in the near-bottom layer was often related to the nepheloid layer. This phenomenon is caused by the increase in the contents of the products of the OM destruction at the bottom; its decay also proceeds in the surface layer of the bottom sediments.

There is no recent sediments deposition in the area with high content of silty fraction and large Md (>10 μm) of the SPM in the nepheloid layer. Thus, glacial marine sediments and ridges of glacial origin are spread along the eastern coast of the Dvina Bay in the area of the outflow current. The less content of silty fraction and small Md (~5 μm) of the SPM in the near-bottom layer occurred in the areas with marine Holocene sediments of nepheloid genesis [57].

9 General Properties Indicative of SPM Origin

The SPM is a fine multiphase and complex object for studying; it is represented by a mixture of biogenic particles (phytoplankton and detritus), single mineral grains, aggregates, and layered silicates.

9.1 Main Mineral Composition

The share of the clay minerals in the SPM was 40% and even more in the White Sea [60]. In other words, the crystallic phase of SPM in seawater was represented by 50% clay minerals. Illite kept the dominant position (35–57% of the sum of the clays in the fraction of <0.01 mm). The high content of illite was a characteristic of the fine particles (both the pelitic and submicrons fractions of the SPM).

Smectite was represented by relatively high content (8–30%); it is characterized by higher dispersity and is mostly found in the subcolloidal fraction (<1 μm). This mineral is supplied with the Severnaya Dvina River runoff and accumulated in the finest muds at depths of more than 100 m.

The content of chlorite and kaolinite varied from 15 to 27%. Mixed-layered minerals usually comprised an insignificant admixture in the SPM (from trace amounts to 5%).

The similar composition of the clay minerals of the SPM was a characteristic of other Arctic shelf seas (Kara Sea and Laptev Sea), which are affected by the large lowland rivers crossing several natural zones [61, 62].

The fine fraction of the clastic minerals is found in every sample, both in the open sea areas and in the coastal waters, and in a significant amount. Among them, quartz and feldspar provide basic background (up to 50%), and quartz usually dominates. The smallest debris of these minerals reached the open sea areas and enriched the pelitic fraction of muds during the sedimentation process. This evidences the partly mechanical separation of the SPM in the dynamic system of the White Sea.

9.2 Content of Particulate Si, Al, P, and Organic Carbon (POC)

The content of total particulate Si in the photic layer of the White Sea varied from 1.8 to 26%. High content of total particulate Si was observed in the areas close to the river mouths and coasts subjected to river inflow. The content of lithogenic particles in these areas was high (30–92%), while that of biogenic Si (SiO_{2am}) varied from 7 to 21%.

We revealed the regular decrease of Al content with the distance from the coast. It is mainly associated with feldspars and clay minerals. The content of Al in the surface water layer varied from 0.3 to 7.9% averaging 1.3%. The mean value was close to the mean Al content in the SPM of the Baltic Sea (0.5–1%) and much less than in the Kara Sea (4%) [49]. Al was mainly accumulated in the pelitic fraction of the SPM as a component of the clay minerals and fine debris of feldspar. Al accumulated mostly in the pelitic fraction of the SPM (Fig. 12); its content increased exponentially in accordance with increase of the lithogenic pelitic fraction (<10 μm) [28].

The Al content in SPM of about 1% or less is a typical value for the White Sea central part (the Basin) and open areas of the Kandalaksha Bay. Higher Al contents (till 3.3%) are typical values for the transitional river–marine type of SPM; these values characterize the rest areas of the sea.

The high content of total particulate Si, as a rule, corresponded to an increased content of Al. The SPM of the White Sea was characterized by a direct linear correlation between Si and Al (Fig. 12). The content of lithogenic particles reached 69% in the outflow current (the transformed Severnaya Dvina River waters). We obtained the maximal content of lithogenic material (87%) in the bottom nepheloid layer close to the eastern coast of the Dvina Bay.

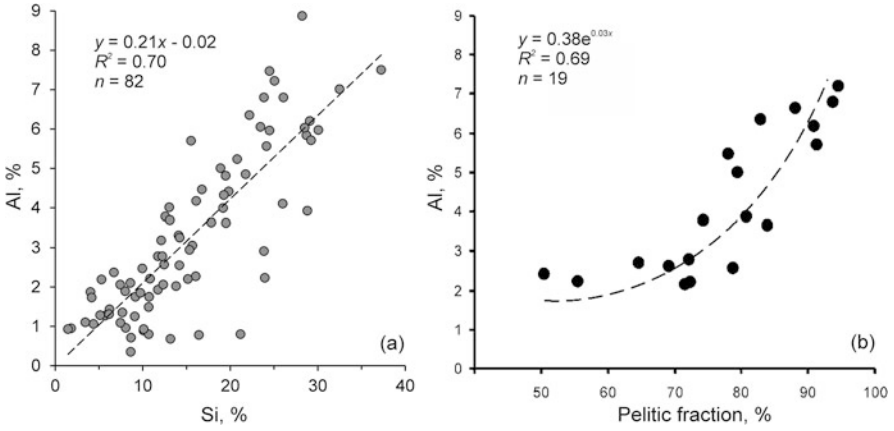

Fig. 12 The dependence of Al content in SPM from Si (**a**) and pelitic fraction (2–10 μm) (**b**) content in the White Sea in summer

The total Si/Al ratio in the SPM of the White Sea was close to that in the upper continental crust (3.3–3.8) in the regions subjected to the river inflow. This value was higher in the western part compared to the eastern ones.

The Severnaya Dvina River catchment area is located within the natural zones where a stage of the chemical denudation predominates over mechanical and acidic weathering stages. Among other components, Fe^{3+}, Al, and Ti are leached from the rocks [25]. At these conditions, the bulk of the particulate Si occurred not only as a component of clay minerals but also in the form of quartz. Because of this, the SPM and bottom sediments are enriched in Si in the White Sea.

High content of P (0.5–1%) was revealed in the Basin and Kandalaksha Bay. Nearby the sources of the lithogenic material supply, the P content decreases noticeably (to 0.1%).

The content of POC was 14% on average, varied usually from 5 to 30%. The average content of POC in the marine SPM was twofold higher than in the riverine SPM. The lowest content of POC (10%) was measured in the area of the Severnaya Dvina River mouth. We identified that POC content decreased logarithmically with increasing of the lithogenic material. We revealed the negative correlation between particulate Al and POC content.

So, POC in the White Sea had as a rule mostly autochthonous genesis rather than allochthonous. Its content depends on the composition and distribution of primary producers, i.e., phytoplankton. The content of POC in the plankton varied from 27 to 46% (35%, on average) [63]. The maximal content of POC was typical for the Kandalaksha Bay [21, 63].

In the liquid bottom layer of stratified waters, the separation of the major part of the biogenic elements (C, N, P, and others) from the solid (mineral) parts of organisms is accompanied by a growth in the bacteria abundance. It is established that the high bacterial production in the layer of the pycnocline resulted from the

formation of microzones enriched in nutrients around the decaying phytoplankton cells. A subsurface maximum of POC was caused by the accumulation of detritus, and bacterioplankton was often observed in the White Sea at depths of 10–20 m.

We found a positive correlation between the SPM mass concentration and the POC content, as well as between SPM concentration by volume and POC content. Then we studied the relationship between the POC concentration and the different SPM fractions. It turned out that the best correlation was characteristic for the finest of the studied pelitic fractions ($R^2 = 0.8$, $n = 54$). Consequently, the POC concentration in the water column of the White Sea is primarily related to the distribution of fine particles less than 10–8 μm.

The content of PIC was insignificant and represented mostly by dolomite (to 5%). Calcite and aragonite were of secondary importance; their content was about 1–2% or was beyond the detection limits.

9.3 Isotopic Composition of POC

Isotopically light POC [$\delta^{13}C_{POC}$ to −30.0‰ (PDB)] is transported to the White Sea from the coast mostly with river runoff. The Severnaya Dvina River water has a hydrocarbonate composition with the predominance of the sum of ions Ca^{2+} and Mg^{2+} over the sum of Na^+ and K^+. Isotopically heavy POC [$\delta^{13}C_{POC} = -18\ldots -22$‰ (PDB)] is a part of the phyto- and bacterioplankton biomass [18, 22, 31, 56].

Values of $\delta^{13}C_{POC}$ varied from −25.7 to −27.4‰ in the open water area of the Dvina Bay, and it was lighten to −28.1… –29.8‰ in the shallow costal area (July 2010). Allochtonous POC prevailed just on the sites close to the coast with sea depth of 12–26 m [56]. The value of $\delta^{13}C_{POC}$ (−23.1… –26.7‰) in the photic layer of the Dvina Bay in August 2014 were close to the data obtained in July 2010 [56]. These values indicate a mixed composition of POC for the larger part of the sea, which is evidenced by different proportion of autochthonous (phytoplanktonic) and allochthonous (lithogenic) material. It seems that the isotopically light POC was not supplied into the deep parts of the White Sea in July–August 2010 and in 2014. It should be noticed that isotopically light POC ($\delta^{13}C_{POC}$ = −28.1… –29.8‰) prevailed in the White Sea proper just at the end of August 2006 [31].

It was shown that concentration and composition of POC as well as DOC (including a colored dissolved organic matter) were subjected to the significant annual and seasonal variations [21, 28, 40, 41].

10 Concluding Remarks and Outlook to Future Researches

The SPM of the White Sea didn't pass the full mechanical and biological separation in the water body. The reason for this phenomenon would be the small volume of the sea (5,375 km^3) and the shallow sea depth (medium depth about 67 m) with the

significant annual volume of dissolved and particulate river runoff (230 km^3/year and 2,330 $\times$ 10^3 ton/year, respectively [25]).

The SPM concentration in the White Sea photic layer was about 1 mg/L (or about 1 mm^3/L), on average. The SPM concentration decreased exponentially in the area of the marginal filter. Only 30–20% of the river particulate matter pass through the marginal filter and enter the sea. The main factor which controls SPM concentration and composition in this area is water salinity.

Not surprisingly, the SPM concentration decreased in several times with the distance from the coast, i.e., outside the marginal filter area that is related to so-called circum-continental zonality, according to Lisitsyn [1]. The SPM distribution pattern was controlled by local factors such as the hydrological fronts (structural, salinity, estuary, etc.), tidal mixing, and wind stress.

We established that the SPM concentrations by volume are a reliable proxy for biogenic (phytoplanktonic) particles in the photic layer. According to our calculations, the share of phytoplanktonic particles in total SPM varied in the different regions of the White Sea from 27% in the inner part of the Dvina Bay (influenced by a huge river runoff) to 65% in the open part of the Kandalaksha Bay (small river runoff).

The primary sources of SPM in the sea have been identified. These were lithogenic particles of river origin and marine phytoplankton (as well as detritus). Aeolian, ice, and coastal abrasion particles were of a secondary importance. First of all, this is particulate material supplied from the Severnaya Dvina River watershed. The rock composition of the Severnaya Dvina River catchment area determines largely the lithogenic phase composition of the SPM. This is confirmed by smectite and quartz high content in the pelitic fraction, high particulate Al and Si content, and so on. This is a result of climatic zonality [1].

The Chl-a concentration (proxy for the phytoplanktonic particles) was preconditioned by the same factor as lithogenic phase, namely, by the riverine discharge, which transports not only solid load (suspended particulate matter) but also the dissolved nutrients. The huge content of colored dissolved organic matter (CDOM) in the river water and, as a consequence, high content of CDOM in the White Sea predetermined the quite narrow photic layer (about 10–15 m and not exceed 20–25 m in deep area). Most of the organic matter is synthesized by the phytoplankton during photosynthetic processes in a relatively narrow surface water layer of 0–10 m so-called particle production zone. The main biogeochemical transformation of the SPM composition took place within the narrow zone. POC content in the White Sea has mostly autochthonous (biogenic) genesis.

The SPM is a mixture of river lithogenic particles and marine biogenic particles. The proper marine SPM was found only in the deep part of the sea far from the sources of river runoff. The SPM grain-size composition and major constituents in the White Sea has been formed under influence of two main sources – lithogenic and biogenic – which are in complicated spatial and temporal interactions.

The spatial and temporal variations in SPM concentration in the photic layer of the White Sea were caused directly or indirectly by river runoff and, first of all, by the Severnaya Dvina River. Interannual variations in the SPM concentration based

on our multi-annual calculations for the White Sea were quite low; hence, they were statistically insignificant.

The vertical stratification (pycnocline which is confined by the halo- and thermocline) was the main factor that controlled the distribution of SPM in water column. We revealed three-layer vertical SPM distribution, so-called vertical zonality [1]: (1) the surface-mixed and photic layer, (2) the clear intermediate water layer, and (3) bottom nepheloid layer usually registered in the most of the near-bottom layer of the sea.

The most common grain-size type of the SPM was silty–pelitic polydispersity. The SPM was predominantly pelitic in June (after spring flood). In the stratified water column, the content of pelitic fractions changed little. This is so-called basic particles dispersion background of seawater. These fine particles reached the sea bottom just in a transformed form, i.e., captured by fecal pellets and aggregates of "marine snow," which form the vertical fluxes of dispersed sedimentary matter. These particles were studied with the help of other methods, and the results were presented in chapter [64]. Formation of the bottom sediments composition does not finish when SPM is deposited on the sea floor. The former SPM usually form a thin fluffy layer (about 0.5–1 cm) – a transition layer between two types of sedimentary bodies: a dispersed particulate matter (SPM) and consolidated particulate matter (bottom sediment). Fluffy layer consists mostly of organic and mineral aggregates; it lies over the relatively dense uppermost sediment layer saturated with water (till 90%) [22]. In this layer, the basic processes of SPM transformation into sediment occur, which later undergoes early diagenesis processes as well as bioturbation, resuspension, redeposition, etc.

Recent sedimentation processes in the White Sea are similar to that in the Arctic shelf seas subjected to a considerable impact of river runoff like the Kara and Laptev seas. However, the White Sea has some features which make this basin unique and perspective for further researches under the conditions of changing Arctic ecosystem.

Acknowledgments We would like to record our gratitude to many individuals who have provided inspiration, advice, and practical help, including Liudmila Demina, Alla Lein, Vyacheslav Lukashin, Inna Nemirovskaya, Alexander Filippov, Alexander Savvichev, Vladimir Burenkov, Oleg Kopelevich, Vladimir Artemiev, Vyacheslav Gordeev, Olga Dara, Nikolay Filatov, Vladimir Korobov, Alexey Tolstikov, Vadim Paka, Anna Chul'tsova, Elena Zolotyh, and Ludmila Gaivoronskaya. Our work would not have been possible without the professionalism and skills of the research vessel crews (*Professor Shtokman*, *Akademik Mstislav Keldysh*, *Ekolog*, *Ivan Petrov*), on which we continue to rely.

The processing of the SPM samples was funded by the Russian Science Foundation, project No. 14-27-00114-P. The researches were conducted in the frame of the state assignment Federal Agency for Scientific Organizations (FASO Russia), theme No. 0149-2018-0016.

References

1. Lisitsyn AP (1972) Sedimentation in the World Ocean. Society of Economic Paleontologists and Mineralogists, 218 pp
2. Nevesskii EN, Medvedev VS, Kalinenko VV (1977) The White Sea: sedimentogenesis and Holocene evolution. Nauka, Moscow, 236 pp, (in Russian)
3. Aibulatov NA, Matyushenko VA, Shevchenko VP, Politova NV, Potehina EM (1999) New data on the transverse structure of lateral flows of suspended particulate matter along the periphery of the Barents Sea. Geoecol Eng Geol Hydrogeol Geocryol 6:526–540 (in Russian)
4. Lukashin VN, Kosobokova KN, Shevchenko VP, Shapiro GI, Pantyulin AN, Pertzova NM, Deev MG, Klyuvitkin AA, Novigatsky AN, Solov'ev KA, Prego R, Latche L (2003) Results of multidisciplinary oceanographic studies in the White Sea in June 2000. Oceanology 43 (2):224–239
5. Cobelo-García A, Millward GE, Prego R, Lukashin VN (2006) Metal concentrations in Kandalaksha Bay, White Sea (Russia) following the spring snowmelt. Environ Pollut 143:89–99
6. Dolotov YS, Filatov NN, Shevchenko VP, Nemova NN, Rimskii-Korsakov NA, Denisenko NV, Kutcheva IP, Boyarinov PM, Petrov MP, Lifshitz VK, Platonov AV, Demina LL, Kukharev VI, Kovalenko VN, Zdorovennov RE, Rat'kova TN, Sergeeva OM, Novigatskii AN, Pautova LA, Filipieva KV, Nöthig E-M, Loronzen C (2005) Monitoring tidal conditions in estuaries of the Karelian coast of the White Sea. Water Res 32(6):611–628
7. Lisitsyn AP (2010) Marine ice-rafting as a new type of sedimentogenesis in the Arctic and novel approaches to studying sedimentary processes. Rus Geol Geophys 51(1):12–47
8. Kopelevich OV, Vazyulya SV, Saling IV, Sheberstov SV, Burenkov VI (2015) Electronic atlas "biooptical characteristics of the Russian seas from satellite ocean color data of 1998–2014". Mod Probl Rem Sens Earth Space 12(6):99–110 (in Russian)
9. Kravchishina M, Klyuvitkin A, Filippov A, Novigatsky A, Politova N, Shevchenko V, Lisitsyn A (2014) Suspended particulate matter in the White Sea: the results of long-term interdisciplinary research. Complex interfaces under change: sea–river–groundwater–lake, vol 365. IAHS, Oxford, pp 35–41
10. Lisitsyn AP, Kravchishina MD, Kopelevich OV, Burenkov VI, Shevchenko VP, Vazyulya SV, Klyuvitkin AA, Novigatskii AN, Politova NV, Filippov AS, Sheberstov SV (2013) Spatial and temporal variability in suspended particulate matter concentration within the active layer of the White Sea. Dokl Earth Sci 453(2):1228–1233
11. Boyd PW, Ellwood MJ, Tagliabue A, Twining BS (2017) Biotic and abiotic retention, recycling and remineralization of metals in the ocean. Nat Geosci 10:167–173
12. Demina LL, Lisitsyn AP (2013) Role of global biological filters in geochemical migration of trace elements in the ocean: comparative estimation. Dokl Earth Sci 449(2):469–473
13. Lam PJ, Lee J-M, Heller MI, Mehic S, Xiang Y (2018) Size-fractionated distributions of suspended particle concentration and major phase composition from the U.S. GEOTRACES Eastern Pacific Zonal Transect (GP16). Mar Chem 201:90–107
14. McCave IN (1983) Particulate size spectra, behavior, and origin of nepheloid layers over the Nova Scotian continental rise. J Geophys Res 88(C12):7647–7666
15. Kopelevich OV, Rodionov VV, Stupakova TP (1987) On the influence of bacteria on the optical characteristics of ocean waters. Oceanology 27(6):921–925
16. Stephens MP, Kadko DC, Smith CR, Latasa M (1997) Chlorophyll "a" and pheopigments as tracers of labile organic carbon at the central equatorial Pacific seafloor. Geochim Cosmochim Acta 61(21):4605–4619
17. Filatov N, Pozdnyakov D, Johannessen OM, Pettersson LH, Bobylev LP (2007) White Sea: its marine environment and ecosystem dynamics influenced by global change. Springer Science & Business Media, Dordrecht, 444 pp
18. Lein AY, Kravchishina MD, Politova NV, Ul'yanova NV, Shevchenko VP, Savvichev AS, Veslopolova EF, Mitskevich IN, Ivanov MV (2012) Transformation of particulate organic

matter at the water–bottom boundary in the Russian Arctic seas: evidence from isotope and radioisotope data. Lithol Miner Res 47(2):99–128
19. Rachold V, Eicken H, Gordeev VV, Grigoriev MN, Hubberten H-W, Lisitzin AP, Shevchenko VP, Schirrmeister L (2004) Modern terrigenous organic carbon input to the Arctic Ocean. In: Stein R, MacDonald RW (eds) The organic carbon cycle in the Arctic Ocean. Springer, Heidelberg, Berlin, pp 33–41
20. Shevchenko VP, Lisitsyn AP, Belyaev NA, Filippov AS, Golovnina EA, Ivanov AA, Klyuvitkin AA, Malinkovich SM, Novigutsky AN, Politova N, Rudakova VN, Rusakov VY, Slierbak SS (2004) Seasonality of suspended particulate matter distribution in the White Sea. Berichte zur Polar- und Meeresforschung 482:142–149
21. Agatova AI, Kirpichev KB (2000) Organic matter in the White Sea: interannual variability of organic matter distribution. Oceanology 40(6):791–795
22. Lein AY, Lisitsyn AP (2018) Processes of early diagenesis in Arctic seas (the White Sea for example). In: Lisitsyn AP (ed) The White Sea system. The recesses of sedimentation, geology and history, vol IV. Scientific World, Moscow, pp 512–576 (in Russian)
23. Pantyulin AN (2003) Hydrological system of the White Sea. Oceanology 43(1):S1–S25
24. Pantyulin AN (2012) The features of the White Sea physics – dynamics, structure and water masses. In: Lisitsyn AP, Nemirovskaya IA (eds) The White Sea system. Vol II water column and interacting with it atmosphere, cryosphere, river runoff and biosphere. Scientific World, Moscow, pp 309–378 (in Russian)
25. Gordeev VV, Filippov AS, Kravchishina MD, Novigatsky AN, Pokrovsky OS, Shevchenko VP, Dara OM (2012) Dispersed sedimentary substance of the continental part of the White Sea geosphere. In: Lisitsyn AP, Nemirovskaya IA (eds) The White Sea system. Vol II water column and interacting with it atmosphere, cryosphere, river runoff and biosphere. Scientific World, Moscow, pp 225–308 (in Russian)
26. Ilyash LV, Ratkova TN, Radchenko IG, Ghitina LS (2012) Phytoplankton of the White Sea. In: Lisitsyn AP, Nemirovskaya IA (eds) The White Sea system. Vol II water column and interacting with it atmosphere, cryosphere, river runoff and biosphere. Scientific World, Moscow, pp 605–639 (in Russian)
27. Cutter G, Andersson P, Codispoti L, Croot P, Francois R, Lohan M, Obata H, van der Loeff MR (2010) Sampling and sample-handling protocols for GEOTRACES cruises. Ver. 1.0. 144 pp. http://www.geotraces.org/libraries/documents/Intercalibration/Cookbook.pdf
28. Kravchishina MD, Lisitzin AP (2011) Grain-size composition of the suspended particulate matter in the marginal filter of the Severnaya Dvina River. Oceanology 51(1):89–104
29. Mercus HG (2009) Particle size measurements: fundamentals, practice, quality. Springer Science+Business Media BV, New York, 533 pp
30. Kravchishina MD, Mitzkevich IN, Veslopolova AF, Shevchenko VP, Lisitsyn AP (2008) Relationship between the suspended particulate matter and microorganisms in the White Sea waters. Oceanology 48(6):837–854
31. Savvichev AS, Rusanov II, Zakharova EE, Veslopolova AF, Mitskevich IN, Kravchishina MD, Lein AY, Ivanov MV (2008) Microbial processes in carbon and sulfur cycles in the White Sea. Microbiology 77(6):734–750
32. Arar EJ, Collins GB (1997) Method 445.0. *In vitro* determination of chlorophyll "a" and pheophytin "a" in marine and freshwater algae by fluorescence. Revision 1.2. U.S. Environmental Protection Agency, Cincinnati, 22 pp
33. Romankevich EA (1984) Geochemistry of organic matter in the ocean. Springer, New York 334 pp
34. Gel'man EM, Starobina IZ (1976) Photometric methods of determination of mineral-forming elements in ores, rocks, and minerals. Inst Geochemi Analyt Chem Acad Sci USSR. 69 pp (in Russian)
35. Lukashin VN, Lyutsarev SV, Shevchenko VP, Rusakov VY, Krasnyuk AD (2000) Suspended matter in estuaries of the Ob' and Yenisei rivers: data from the 28th cruise of R/V Akademik Boris Petrov. Geochem Int 38(12):1221–1236

36. Taylor SR, McLennan SM (1995) The geochemical evolution of the continental crust. Rev Geophys 33(2):241–265
37. Dara OM, Mamochkina AI (2017) Detrital and clay minerals of pelitic fractions in dispersed and consolidated sedimentary matter of the surface layer. In: Lisitsyn AP (ed) The White Sea system. The processes of sedimentation, geology and history, vol IV. Scientific World, Moscow, pp 301–336 (in Russian)
38. Burenkov VI, Vazyulya SV, Kopelevich OV, Shebertov SV (2011) Space-time variability of suspended matter in the White Sea derived from satellite ocean color data. Proceedings VI international conference current problems in optics of natural waters. Nauka, St. Petersburg, pp 143–146
39. Berger V, Dahle S, Galaktionov K Kosobokova X, Naumov A, Rat'kova T, Savinov VM, Savinova TN (eds) (2001) White Sea. Ecology and environment. Derzavets, St. Petersburg, 155 pp
40. Pavlov AK, Stedmon CA, Semushin AV, Martma T, Ivanov BV, Kowalczuk P, Granskog MA (2016) Linkages between the circulation and distribution of dissolved organic matter in the White Sea, Arctic Ocean. Cont Shelf Res 119:1–13
41. Kravchishina MD, Shevchenko VP, Filippov AS, Novigatsky AN, Dara OM, Alekseeva TN, Bobrov VA (2010) Composition of the suspended particulate matter at the Severnaya Dvina River mouth (White Sea) during the spring flood period. Oceanology 50(3):365–385
42. Pokrovsky OS, Viers J, Shirokova LS, Shevchenko VP, Filippov AS, Dupre B (2010) Dissolved, suspended and colloidal fluxes of organic carbon, major and trace elements in the Severnaya Dvina River and its tributary. Chem Geol 273:136–149
43. Vazyulya SV, Kopelevich OV (2011) Comparative estimates of the budget of photosynthetic available radiation (PAR) in the Barents, Black, Kara, and White seas derived from satellite and *in situ* data. Proceedings VI international conference current problems in optics of natural waters, Nauka, St. Petersburg, pp 124–128
44. Kostianoy AG, Nihoul JCJ, Rodionov VB (2004) Physical oceanography of frontal zones in the subarctic seas, vol 71. Elsevier Oceanography Series, Amsterdam, 316 pp
45. Rat'kova TN, Wassman P (2005) Sea ace algae in the White and Barents seas: composition and origin. Polar Res 24:95–110
46. Ilyash LV, Zhitina LS, Belevich TA, Shevchenko VP, Kravchishina MD, Pantyulin AN, Tolstikov AV, Chultsova AL (2016) Spatial distribution of the phytoplankton in the White Sea during atypical domination of Dinoflagellates (July 2009). Oceanology 56(3):372–381
47. Pokrovsky OS, Shirokova LS, Viers J, Gordeev VV, Shevchenko VP, Chupakov AV (2017) Dissolved organic carbon and organo-mineral colloids in the mixing zone of the largest European Arctic River. In: Pokrovsky OS, Shirokova LS (eds) Dissolved organic matter (DOM): properties, applications and behavior. Nova Science Publ, Inc, New York, pp 273–291
48. Starodymova DP, Vinogradova AA, Shevchenko VP, Zakharova EV, Sivonen VV, Sivonen VP (2018) Elemental composition of near-ground aerosol near the northwestern coast of Kandalaksha Bay of the White Sea. Atmosph Ocean Optics 31(2):181–186
49. Kravchishina MD, Lein AY, Sukhanova IN, Artem'ev VA, Novigatsky AN (2015) Genesis and spatial distribution of suspended particulate matter concentrations in the Kara Sea during maximum reduction of the Arctic ice sheet. Oceanology 55(4):623–643
50. Politova NV, Shevchenko VP, Kravchishina MD (2010) Suspended particulate matter in the Russian Arctic seas. Seabed morphology of Arctic Russian shelf. Series: oceanography and ocean engineering. Nova Science Publishers, Inc., New York, pp 73–85
51. Lisitsyn AP (1995) Marginal filter of oceans. Oceanology 34(5):735–747
52. Ilyash LV, Radchenko IG, Kuznetsov LL, Lisitzyn AP, Novigatskiy AN, Martynova DM, Chul'tsova AL (2011) Spatial variability of the species composition, abundance, and productivity of the phytoplankton in the White Sea in the late summer period. Oceanology 51(1):19–26
53. Barber DG, Hop H, Mundy CJ, Else B, Dmitrenko IA, Tremblay J-E, Ehn JK, Assmy P, Daase M, Candlish LM, Rysgaard S (2015) Selected physical, biological and biogeochemical implications of a rapidly changing Arctic marginal ice zone. Prog Oceanogr 139:122–150

54. Lisitsyn AP, Shevchenko VP, Burenkov VI (2000) Hydrooptics and suspended particulate matter of Arctic seas. Atmosph Ocean Optics 1(1):70–79
55. Kravchishina M, Burenkov VI, Kopelevich OV, Sheberstov SV, Vazyulya SV, Lisitsyn AP (2013) New data on the spatial and temporal variability of the chlorophyll *a* concentration in the White Sea. Dokl Earth Sci 448(1):120–125
56. Politova NV, Klyuvitkin AA, Novigatskii AN, Ul'yanova NV, Chul'tsova AL, Kravchishina MD, Pavlova GA, Lein AY (2016) Early diagenesis in recent bottom sediments of the Dvina Bay (White Sea). Oceanology 56(5):702–713
57. Kravchishina MD (2009) Suspended particulate matter of the White Sea and its grain-size. Scientific World, Moscow, 263 pp, (in Russian)
58. Honjo S (1980) Material fluxes and modes of sedimentation in the mesopelagic and bathypelagic zones. J Mar Res 38:53–97
59. Bezrukov PL, Lisitsyn AP (1960) Classification of bottom sediments in modern marine reservoirs. Proc Inst Oceanol 32:3–14 (in Russian)
60. Kravchishina MD, Dara OM (2014) Mineral composition of the suspended particulate matter in the White Sea. Oceanology 54(3):327–337
61. Müller C, Stein R (1999) Grain-size distribution and clay-mineral composition in surface sediments and suspended matter of the Ob and Yenisei rivers. Ber Polarforsch 300:179–187
62. Serova VV, Gorbunova ZN (1997) Mineral composition of soils, aerosols, suspended matter, and bottom sediments of the Lena River estuary and Laptev Sea. Oceanology 37(1):121–125
63. Demina LL, Nemirovskaya IA (2007) Spatial distribution of microelements in the Seston of the White Sea. Oceanology 47(3):360–372
64. Novigatsky AN, Klyuvitkin AA, Lisitsyn AP (2018) Vertical fluxes of dispersed sedimentary matter, absolute masses of the bottom sediments, and rates of modern sedimentation. In: Lisitsyn AP, Demina LL (eds) Sedimentation processes in the White Sea: the White Sea environment part II, handbook of environmental chemistry, Springer, Berlin. doi: https://doi.org/10.1007/698_2018_278

Vertical Fluxes of Dispersed Sedimentary Matter, Absolute Masses of the Bottom Sediments, and Rates of Modern Sedimentation

Alexander N. Novigatsky, Alexey A. Klyuvitkin, and Alexander P. Lisitsyn

Contents

Abstract A new approach using dispersed sedimentary matter of the water column captured by sediment traps in comparison with its consolidated form (surface layer of the bottom sediments) was applied to study sedimentation in the White Sea. The results of long-term investigations in a small sea of the Arctic Ocean served as a basis for revealing new regularities characteristic of the sedimentary process in the Subarctic and Arctic zones. The monthly, seasonal, and multiyear dynamics of the main components of dispersed sedimentary matter fluxes were analyzed by defining the marine sedimentation stage. It was shown that the biogenic constituents of the particle flux while its transition from the dispersed form to consolidated one decreased by an order of magnitude. The average values of the vertical flux were calculated including the total sedimentary flux and the contribution of main biogenic and lithogenic constituents per m^2 of the bottom area of the White Sea.

A. N. Novigatsky (✉), A. A. Klyuvitkin, and A. P. Lisitsyn
Shirshov Institute of Oceanology Russian Academy of Sciences (IO RAS), Moscow, Russia
e-mail: novigatsky@ocean.ru

A. P. Lisitsyn and L. L. Demina (eds.), *Sedimentation Processes in the White Sea: The White Sea Environment Part II*, Hdb Env Chem (2018) 82: 49–66,
DOI 10.1007/698_2018_278, © Springer International Publishing AG 2018,
Published online: 29 April 2018

Keywords Arctic Ocean, Bottom sediments, Sediment trap, Sedimentation, Suspended matter, Vertical flux, White Sea

1 Introduction

Dispersed matter is widespread in the environment. It occurs in all the Earth's geospheres: aerosol particles in the atmosphere and suspended particulate matter in the water column, ice, and snow. It is present in areas of deep-sea hydrothermal activity ("black smoker" plumes) and occurs as space dust in a small amount. An important role in the formation of dispersed sedimentary matter belongs to organisms-producers (diatoms, coccolithophores, etc.), which yield the biogenic suspension, and organisms-consumers (zooplankton and benthos), which feed on this fine suspension and small biogenic detritus [1]. The dispersed continental sedimentary matter is due to its origin from physical and chemical weathering of rocks and, to a significant degree, to the microorganisms, as well as plants (spores and pollen, plant debris). Many important peculiarities of the formation and transportation of the dispersed sedimentary matter remain still poorly studied in contrast to its consolidated form (bottom sediments of oceans, seas, and lakes). The suspended particulate matter (SPM) is one of the major sources of the bottom sediments' formation and the basic feeding source for marine organisms. The insignificant amount and very small size (1–100 μm) are the principal peculiarities of dispersed sedimentary material from all geospheres. Similar to bacteria (biogenic part of SPM), the dispersed sedimentary matter is invisible to the naked eye. Mobility, patterns of regional and global scales of distribution, and close relationship to environmental conditions and interaction and transportation are characteristic for dispersed sedimentary matter [1].

Dispersed sedimentary matter is a major source for pelagic bottom sediments. Fundamentally new data on sedimentation were obtained for direct determination of the vertical (and inclined) fluxes of dispersed sedimentary matter by use of sediment traps, rotators, isotopic methods, etc. [2, 3]. Sediment traps are the most interesting for sedimentology [4]. These are cones or cylinders with samplers, which capture the dispersed sedimentary material. The samplers are managed by the microprocessor, i.e., the trapping exposure may vary from 1 day up to months, seasons, or years. Typically, we sample the matter at different depths with an exposure of 1 month and change the stations one time per year.

Thus, we have obtained continuous temporal samples with monthly (differential fluxes) and annual (integral fluxes) exposures in the White Sea and in the Arctic and various oceanic zones. The reference stations equipped with traps, current gauges, transparency meters, and plotters mounted at different depths on a vertical cable with anchors are named the automatic deep-sea sedimentological observatories (AGOS) [5].

The Arctic Ocean is a basin with a strongly expressed seasonal variation in sedimentation. Parameters such as the area of marine ice spreading, dissolved and particulate river runoff, coastal abrasion, primary production, and the temperature of surface water masses and of the near-water layer of the atmosphere demonstrate a strongly marked seasonality. Over recent years we have studied in detail the interaction between dispersed and dissolved substances at the regional and local scales in

a typical water reservoir of the Arctic and Subarctic zones, which are in the White Sea. For most of the year, the sea is covered by drifting ice, and its bottom waters have a temperature of −1.4°C year-round; i.e., here the environment corresponds and conforms to the conditions of the ice sedimentation zones [6].

The rates of sedimentation in the bottom sediments of the World Ocean vary widely from less than 1 to 1,000 mm/year and more. The continental margins of the Arctic Ocean are characterized by values of ~10 mm/year (in deposition centers of river and oceanic water mixing zones, the Fram Strait, and some fjords). Zero and even negative values are typical of zones of bottom erosion (areas of the White, Barents, Kara, and other seas) at 0.01 mm/year – an average sedimentation rate in the pelagic zone of the Arctic Ocean of [7, 8].

Thus, the ocean represents the main trap for dispersed sedimentary matter (DSM) from all the geospheres of the Earth (both outer and inner ones); i.e., it serves as a global recorder of planetary geospheres (processes and events on continents and in oceanic water). Interaction between geospheres is particularly intensive at the two bathymetric levels: the surface layer for the outer geospheres and the bottom layer for the upper part of the sedimentary cover marked by interaction with sedimentary matter of the inner (deep) geospheres. In addition to these two types of sedimentary materials in seas and oceans, these basins themselves produce a biogenic dispersed matter: $\sum (CaCO_3 + SiO_{2am} + C_{org})$ [6, 9]. Mixing of sedimentary matter from all these geospheres (its dissolved and suspended forms) results in their transformation including repeated interaction and mixing during sedimentation. Owing to these processes, bottom sediments consist of sedimentary matter that was subjected to transformations on its way from the surface water of the ocean floor [2]. All these transformations are recorded in suspended particulate matter sampled through the water column: from the surface of the ocean to its floor and then in the bottom sediment section.

2 Material and Methods

For the first time for the White Sea, in the framework of the "System of the White Sea" program of Shirshov Institute of Oceanology, Russian Academy of Sciences (IO RAS), the sedimentary processes were continually studied both in the bottom sediments and in the water column. A complex of methods was applied including ultrafiltration of water and automatic deep-sea sedimentological observatories (AGOS) with monthly quantitative analysis of the vertical fluxes and constant sampling of the matter from various depths the whole year-round. This allows us to measure directly the quantitative content of SPM (mg/l), the rate of sedimentation (mm/year), and the vertical fluxes (g/m^2/year), i.e., the absolute masses of the dispersed sedimentary matter in the bottom water layer and the surface bottom sediments, as well as its changes in the course of surface-to-bottom precipitation; these data have consistently been obtained over 15 years of observations [10].

The sedimentological observations were combined with continuous satellite monitoring for the surface water layer and cruises aimed to perform oceanological and geological studies of the bottom sediments (sampling by multicorer) at stations (Fig. 1).

Such works based on the AGOS with continuous study of the dispersed matter in the water column (0–300 m) in comparison with bottom sediments were carried out in 2000–2014 in a megapolygon of the White Sea (Fig. 2).

Another independent method of the quantitative estimation of sedimentary matter in the water column (concentration, mg/l) is membrane ultrafiltration (capture of particles larger than 0.45 μm). It gives a simultaneous pattern of distribution of SPM only for the moment of study at the station. Commonly discrete sampling with bathometers follows continuous vertical sounding of the transparency and other water parameters, which opens the possibility of sampling not by horizons but in most important places. Annual satellite data (MODIS-Aqua satellite scanner) are used for the very upper layer (0–5 m) [11].

Thus, we combine the satellite and expedition observations of the SPM concentrations (mg/l), i.e., its continuous pattern of distribution for the surface layer, which was verified (controlled by direct discrete determinations with membrane filtration) and was further distributed for most of the year only by satellites both for the suspended sedimentary matter in general and for its biological part (by chlorophyll-*a*).

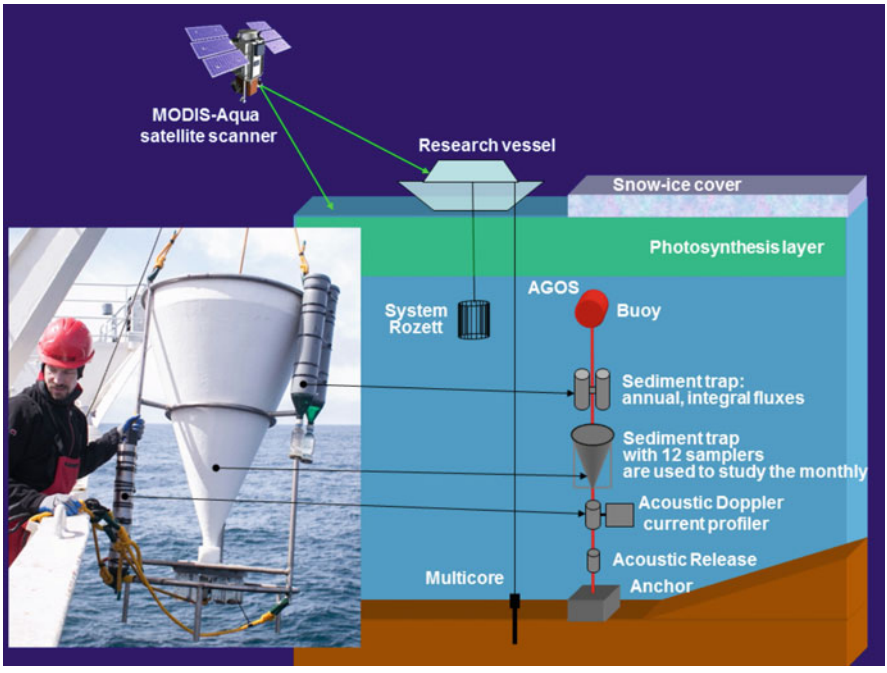

Fig. 1 Scheme of the automatic deep-sea sedimentological observatories (AGOS)

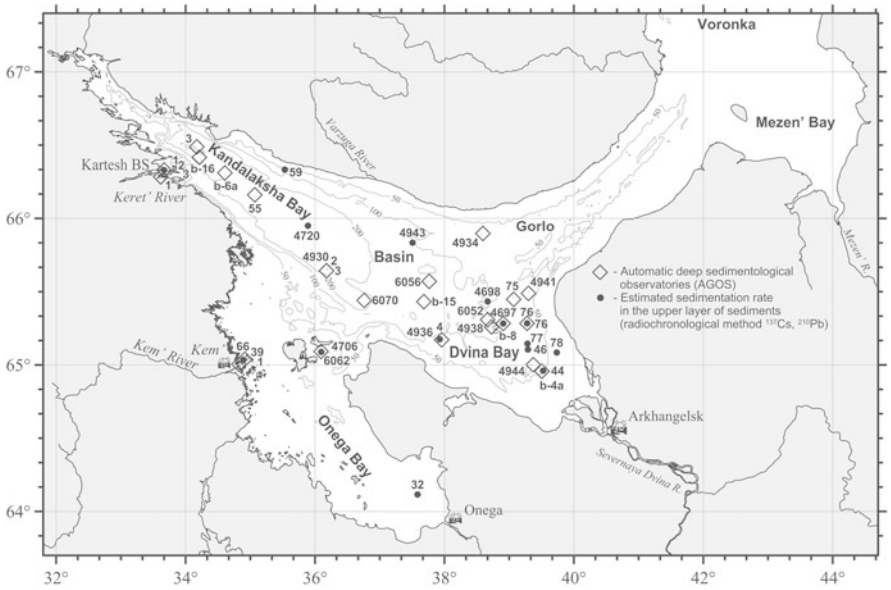

Fig. 2 Position of the AGOS with sedimentary traps and current meters and simultaneous studies of the suspended particulate matter and surface layer of bottom sediments and estimated sedimentation rate in the upper layer of bottom sediments (radiochronological method ^{137}Cs, ^{210}Pb)

The sinking dispersed sedimentary matter was largely composed of biogenic and lithogenic components. The biogenic components were represented by organic matter (OM), carbonate particles, and biogenic opal. The lithogenic components included clastic and clay minerals with subordinate quantity of volcanic ash. Indicators of these components for organic matter (OM) are C_{org} ($C_{org} \times 2 = OM$), for siliceous organic remains SiO_{2am}, and for carbonate organic remains $CaCO_3$, while Al and Si_{tot} are indicators of lithogenic particles [12]. The rates of modern sedimentation in the surface sediments (0–20 cm) of the White Sea were determined using the radionuclide dating analysis (^{137}Cs, ^{210}Pb) [13].

3 Results and Discussions

In this work, we discuss a new approach to the analysis of current sedimentation in seas and oceans using AGOS developed at the Institute of Oceanology. This method offers an opportunity to study dispersed sedimentary matter both in three dimensions as it is done traditionally in oceanology (latitude, longitude, depth) and in time (from months and seasons to decades). The method may also be used for analysis of the sedimentary matter at its transition from the dispersed (suspended particulate matter) to consolidated (bottom sediments) forms accompanied by drastic changes in rheology.

3.1 Seasonal Variation for the Monthly Values of the Fluxes of Sedimentary Matter and the Average Monthly Values of Suspended Particulate Matter Concentration

In spring, after the melting of ice and breakup on rivers, the main portions of sedimentary material begin to enter the Arctic rivers from the catchment areas [14, 15]. Along with this process in the ice-free water of the Arctic seas due to high solar activity combined with river-run input of dissolved nutrients and the melted marine ice that accumulates aerosols and other sedimentary materials throughout the winter, the spring bloom of phytoplankton [16] and rapid development of bacteria occur (the maximal amount of zooplankton is recorded a little later). As a result, the suspended particulate matter concentration exhibits an abrupt seasonal jump in the Arctic seas, as well as in the White Sea [11]. This is followed by a multiplied increase in the values of vertical fluxes of sedimentary matter from the surface to the sea floor (Fig. 3).

Figure 3 displays the plot of monthly values of the vertical fluxes that we have obtained since 2000. The sharp maxima of the fluxes are confined to the areas of estuaries and bays, where the continental runoff exerts a dominant influence on the delivery of sedimentary material [17, 18]. The sediment fluxes reach their maximal values in June, exceeding the value of 1,000 mg/m^2/day (station 3 is Kandalaksha Bay and station 75 is Dvina Bay).

The mean summer water level (the middle of July–August) in the White Sea is characterized by relatively low flux values, which did not exceed 200 mg/m^2/day (stations 75 and 76 are Dvina Bay; station 55 is Kandalaksha Bay; Fig. 3).

In late summer and early fall, the plankton community is restructured again; mesoplankton, euryphagous organisms, and large zooplankton grow rapidly [19]. The fall flood flows also contribute substantially to an increase in suspended particulate matter concentrations, which was directly reflected in the flux values and composition of sedimentary matter (Fig. 3). The estuarian areas, where the flux values of sedimentary matter reached 1,000 mg/m^2/day, respond to this first of all (Kem River, Kartesh Biological Station (Kartesh BS) on Fig. 3).

In early fall, the solar activity decreases, and the plankton communities migrate to greater depths (hibernation) [19]. The river runoff is restructured to the mean winter water level, and ice formation begins. The suspended particulate matter concentration is insignificant in the Arctic seas in this period; therefore, the fluxes of sedimentary matter are also very low (Fig. 3).

A relative increase in the fluxes of sedimentary matter could be observed in December (Fig. 3); it was likely attributed to change in the hydrological regime of the White Sea and consequently to a destruction of pycnocline. In accordance with data of M.D. Kravchishina [11], a jump in the density (pycnocline) promotes accumulation of a great amount of suspended particulate matter. When ice freeze, the brines are squeezed out and descend down; this phenomenon was manifested by a relatively high value of flux of sedimentary matter in December, which was described in detail [20]. Winter under the ice vertical fluxes of sedimentary matter

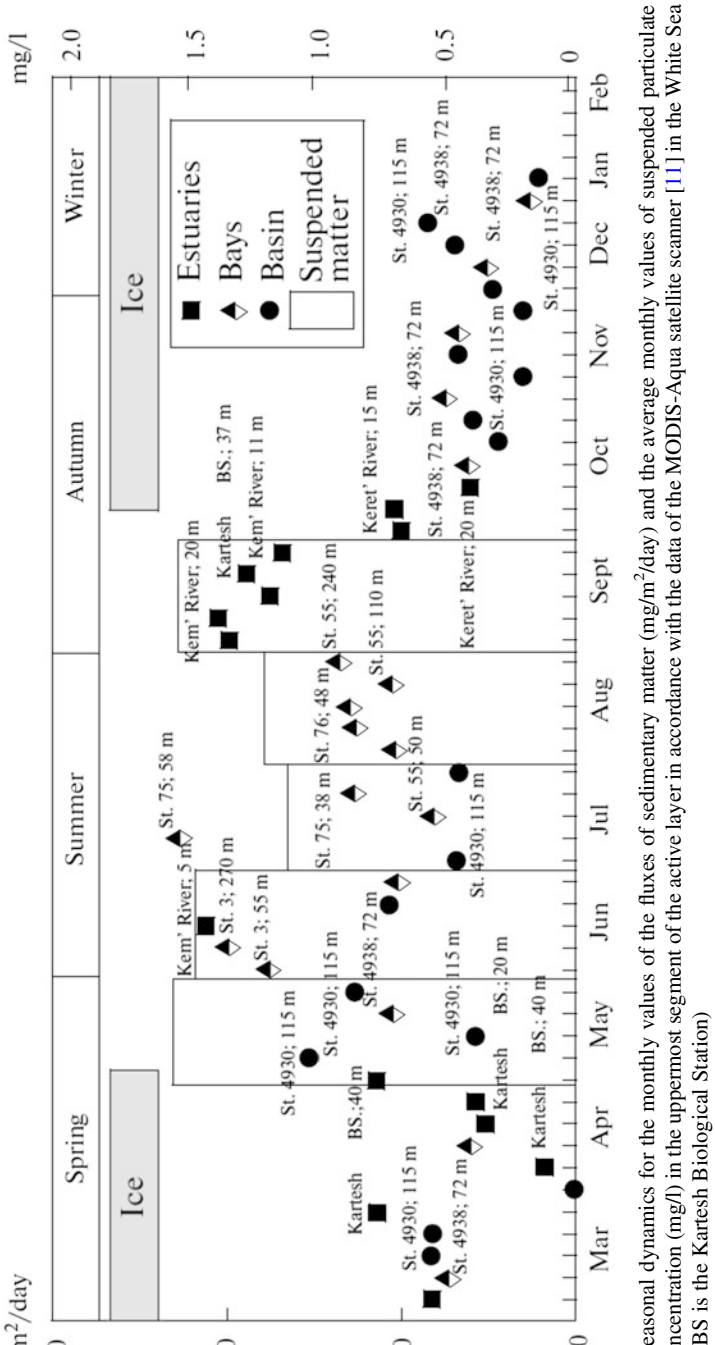

Fig. 3 Seasonal dynamics for the monthly values of the fluxes of sedimentary matter (mg/m^2/day) and the average monthly values of suspended particulate matter concentration (mg/l) in the uppermost segment of the active layer in accordance with the data of the MODIS-Aqua satellite scanner [11] in the White Sea (Kartesh BS is the Kartesh Biological Station)

were characterized by the lowest values, which did not exceed 70 mg/m^2/day (station 4,930 is the Basin; (Fig. 3). This is related to weakening of solar radiation and its total termination in the polar night.

Thus, there is a markedly expressed seasonal and even monthly variation in the fluxes of dispersed sedimentary matter in the White Sea; their quantity, composition, and properties change in the White Sea. The maximal values of the concentrations (mg/l) and the fluxes (mg/m^2/day) were typical of the ice-free spring-summer period; the minimal ones, for the winter period when the sea and the feeding catchment were under a snow-ice cover and the river and aeolian runoff was insignificant. When the hydrological and meteorological regime changes, the fluxes of dispersed sedimentary matter undergo seasonal changes, which recur annually: an increased content of fluxes in December, the ice unloading in April, and the bloom outburst of phytoplankton and flooded conditions in May.

The monthly, seasonal, and annual fluxes of dispersed sedimentary matter can differ from each other in many times, especially in spring, when the ice regime of the sea influences significantly on the flux values: solid mass discharge of snow and ice sedimentary matter, river runoff, abrasion, and phytoplankton bloom. The vertical fluxes of sedimentary matter to the sea floor depend directly on the interaction of matter coming from the outer geospheres.

3.2 Annual Integral Fluxes of the Dispersed Sedimentary Matter

As a result of our works, the two structural fronts were distinguished in the White Sea: (1) the northern front, where through the Gorlo water enters from the Barents Sea and comes off the White Sea, and (2) the southern front near the Solovetsky Islands [5]. In comparison with other parts of the sea, these zones are characterized by increased contents of SPM and sedimentary fluxes, high intensity of the tidal currents, and very high average annual flux values at three stations (6,062, 4,934, 4,941): from 1,814 to 4,082 g/m^2/year and 2,758 g/m^2/year, on average (area 1 on Fig. 4a).

The other parts of the White Sea (Basin, Dvina Bay, and Kandalaksha Bay) are characterized by lower tidal energy, low contents, and low fluxes of the dispersed sedimentary matter. The average value of sedimentary matter fluxes in the sea (excluding anomalies of two fronts) is 234 g/m^2/year; i.e., it is one order of magnitude lower than that in the frontal zones. The minimum fluxes (51 g/m^2/year) were found in the Basin (area 2 on Fig. 4a, station 4,930 in the central part of the sea), and the average long-term fluxes for the deep part of the White Sea amount to 213 g/m^2/year, which was similar to values for other Arctic seas [21, 22].

The sedimentary matter fluxes in the Dvina Bay and Kandalaksha Bay of the White Sea were found to be elevated in areas of their marginal filters (river-seawater mixing zones) [5, 20]. Thus, the average long-term flux value for Dvina Bay and

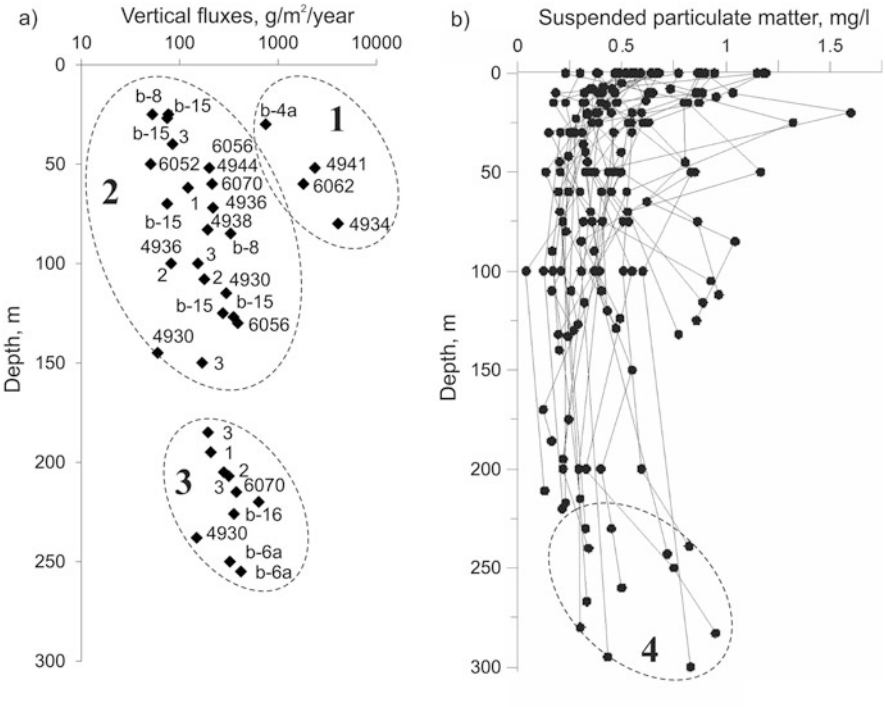

Fig. 4 Ratio of (**a**) integral vertical flux (g/m^2/year) and (**b**) suspended particulate matter (mg/l) in the White Sea with the depth (0–300 m): areas of the high and ultrahigh flux values (1), flux values under the pycnocline (2), bottom flux values (3), elevated values of SPM in the nepheloid layer (4) [23]

Kandalaksha Bay was equal to 243 and 367 g/m^2/year, respectively, for their open parts. Hence, our data suggest that the marginal filters are the second areas of increased values of sedimentary matter fluxes (Fig. 4a).

The third place of higher values of the fluxes and SPM content is the near-bottom areas, up to 100 m above the bottom, locally, more (area 3 on Fig. 4a). The near-bottom currents studied at some stations over several years were the most significant there. The semidiurnal tides with local deviations related to the configuration of the bottom and coasts are the most significant for water dynamics in the White Sea. The amplitude of the tidal currents increases with a decrease in depth. The velocities of the currents may be sufficient to erode the upper liquid sedimentary layer, which was directly confirmed by observations of the suspension concentration and transparency of waters of the bottom layer. The sounding and data on membrane filtration showed the appearance of layers and lenses of waters with higher turbidity (nepheloids) (Fig. 4b) [23].

The direct measurements of the bottom currents in the Basin showed a dominant eastern vector with reverse variations without rotation. The resulting currents vary from 2 to 20 cm/s (~1.5 cm/s, on average) [5]. The relation between the flux value

and the depth is also interesting (Fig. 4a). The high values registered above and on the pycnocline (area 1) decrease at the shelf (0–200 m) and increase at the slope (area 3 on Fig. 4a).

Thus, for the first time, the vertical sedimentary matter fluxes in the White Sea were studied by use of AGOS. New data on sedimentation in the water column from the surface to the bottom sediment layer have been obtained.

3.3 *The Rates of Modern Sedimentation and Absolute Masses*

Our data on the ^{210}Pb and ^{137}Cs isotope method for sediment dating estimated sedimentation rates for the entire White Sea ranging from 0.4 to 4.2 mm/year, which correspond to 93–1,260 g/m^2/year (310 g/m^2/year, on average) (Table 1). We have made a recalculation of the sedimentation rates to absolute masses of dry sediment (Table 1). The obtained data on absolute masses of dry sediment are in agreement with the sedimentation rates in the coastal areas of the Kandalaksha Bay of the White Sea (0.3–1.0 mm/year) [24], the Beaufort Sea (1.4 mm/year) [25], and

Table 1 Estimated sedimentation rate in the upper layer of sediments (radioactive ^{210}Pb and ^{137}Cs isotope method) [10]

Station	N	E	Depth, m	Sedimentation rate, mm/year	Absolute masses[a], g/m^2/year
4,697	65°17′	38°55′	96	0.40	120
4,698	65°25′	38°40′	107	0.79	237
4,706	65°05′	36°06′	66	0.85	255
4,720	65°57′	35°53′	290	2.2	660
32	64°07′	37°35′	16	2.7	810
78	65°05′	39°44′	32	4.2	1,260
66	65°02′	34°53′	21	0.82	246
76	65°17′	39°16′	68	0.91	273
77	65°08′	39°17′	76	0.31	93
59	66°20′	35°32′	81	0.62	186
3	66°20′	33°40′	62	0.51	153
4,943	65°50′	37°30′	116	0.69	207
44	64°58′	39°31′	54	2.6	780
46	65°06′	39°17′	73	1.1	330
4	65°10′	37°56′	88	1.7	510
Geometric mean				1.0	310
Minimum				0.40	93
Maximum				4.2	1,260
Standard deviation				1.1	332

[a]At an average density of dry sediment (0–20 cm) 0.3 g/cm^3

the other Arctic seas [7]. The direct quantification of the sedimentary matter fluxes in the bottom horizons of the White Sea, which have been made using sediment traps of the AGOS over 15 years, varied between 149 and 1,814 g/m^2/year (335 g/m^2/year, on average) (Table 2).

The lower values of the absolute masses of the surface bottom sediments in comparison with the bottom fluxes (in the same units g/m^2/year) were evidently due to destruction of organic matter (OM) in the fluffy layer. This is confirmed by the organic matter examination [26] that showed fuel consumption of organic carbon (C_{org}) by benthos and bacteria and partial dissolution of other components of the biogenic triad, such as $CaCO_3$ and SiO_2 amorphous, during the long residence time of particles in the uppermost sedimentary layer.

The highest values of sedimentation rates and near-bottom fluxes of dispersed sedimentary matter were revealed at the river-sea boundary (Severnaya Dvina, Onega, Kem Rivers), i.e., in the marginal filters of these rivers, as well as along the gravitational current of the Severnaya Dvina River in Dvina Bay (Fig. 2). High sedimentation rates were also found in the deep-sea areas of the Kandalaksha Bay and Dvina Bay and in the areas of the bottom depressions (Kandalaksha graben and

Table 2 Bottom integral (annual) fluxes of dispersed sedimentary matter

Station	N	E	Depth, m	Horizon, m	Value of the bottom flux, g/m^2/year
b-16	66°34′	33°47′	236	226	357
b-4a	64°57′	39°31′	50	30	752
b-8	64°35′	39°01′	96	85	330
b-15	65°26′	37°40′	132	125	276
b-15	65°26′	37°40′	132	127	354
b-6a	66°09′	35°03′	267	250	325
b-6a	66°09′	35°03′	267	255	421
6,056	65°34′	37°45′	139	130	390
6,062	65°05′	36°05′	70	60	1,814
6,070	65°26′	36°45′	229	220	639
4,930	65°38′	36°10′	255	238	149
2 (4,930)	65°38′	36°09′	249	207	317
3 (4,930)	65°38′	36°07′	255	185	195
3 (4,930)	65°38′	36°07′	255	195	208
3 (4,930)	65°38′	36°07′	255	205	282
3 (4,930)	65°38′	36°07′	255	215	378
4,944	65°00′	39°22′	67	52	201
4,938	65°15′	38°43′	117	72	219
4,936	65°10′	37°57′	97	83	193
Geometric mean					335
Minimum					149
Maximum					1,814
Standard deviation					372

others); they are related to the complex slope processes (mud flows, gravity, etc.) on the sea floor.

Higher values were found at station 6,062 (between Bolshoy Solovetsky and Anzer Islands): they strongly exceed the sedimentation rates in this area. This region is subjected to intense hydrodynamic activity (semidiurnal tidal cycles of the White Sea), which is expressed in the domination of lateral vector of sedimentary matter's transport over the usual vertical one. The total resulting annual velocity vector of the lateral movement of the near-bottom water masses of the White Sea is low enough (1.5 cm/s, on average) that provides no significant barriers to precipitation under gravity [5]. In addition, some areas were characterized by fast and ultrafast sedimentation rates, and they are the mouth (station b-4a) and slope (stations 6,070 and 3) areas.

Thus, we applied a new approach to study marine sedimentation using dispersed sedimentary matter collected in the water column by sediment traps in comparison with the surface layer of bottom sediments. This approach provides an opportunity to study in situ (by fluxes of sedimentary matter in the water column) the modern sedimentation in the surface layers of the bottom sediments and to observe changes in the environment and climate at a new technological level.

3.4 Dynamics of the Main Components of Fluxes of Sedimentary Matter

Figure 5 illustrates the monthly and seasonal changes in the basic components of the dispersed sedimentary matter (DSM) flux in the White Sea. The curve exhibits a predominance of lithogenic components over the year, which was characteristic of the inland seas. In addition, the lithogenic constituents of the flux prevailed also during the winter season, when the sea is covered by ice and snow, that suppress photosynthesis significantly and, correspondingly, reduce the biogenic components of the sedimentary flux.

A significant portion of the biogenic components in the vertical sedimentary flux was represented by planktonic algae, which constitute up to 90% of the total value [16]. The basic features of the White Sea that negatively affect development of carbonate organisms are absence of the warm water currents, weak water exchange with the ocean, a long ice-covered period, a large influx of freshwater, and low primary production of phytoplankton. The diatom assemblage in the White Sea is dominated by marine species with siliceous frustules (up to 70%); freshwater forms of these organisms are in a minor amount and inhabit only in bays influenced by the river runoff [27]. The maximum concentrations of biogenic components in the sedimentary flux were registered during the ice-free spring-summer-autumn period (Fig. 5). However, high values of organic matter concentrations were also recorded during winter months that could be explained by both the inflow of the Barents Sea

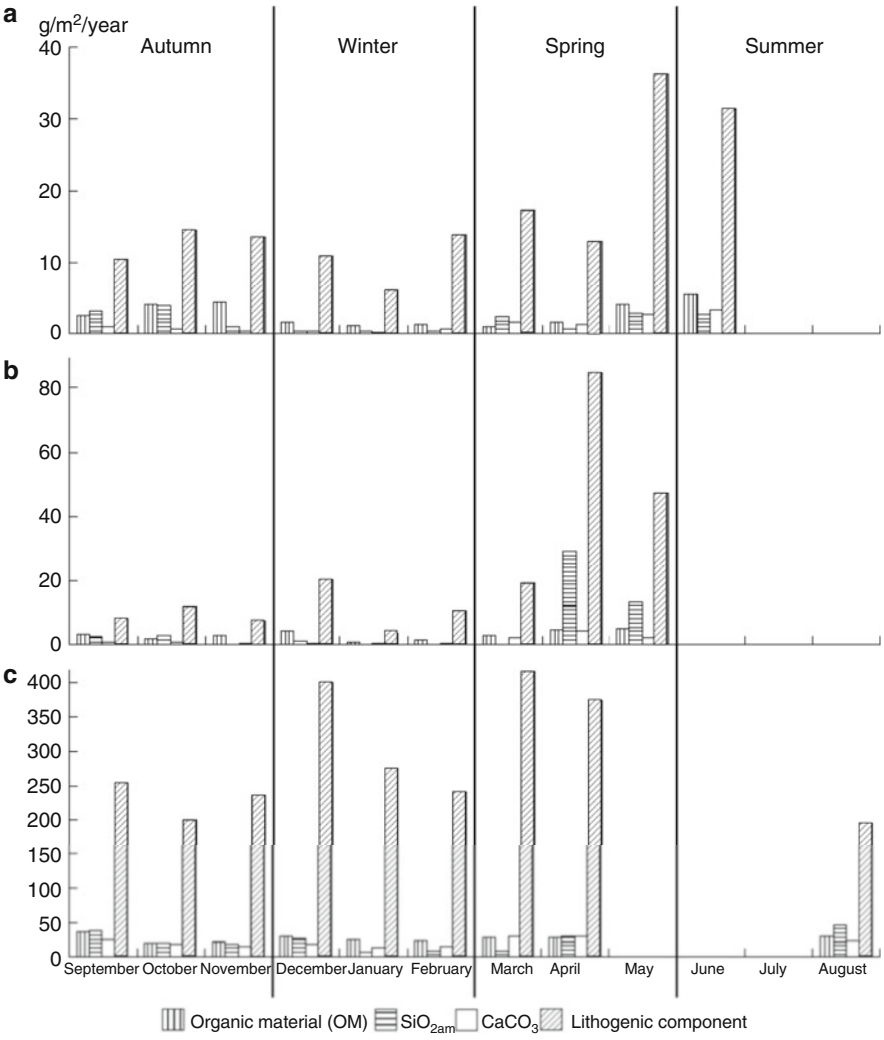

Fig. 5 Monthly and seasonal changes in the basic components of vertical fluxes (g/m^2/year) in the water column of the White Sea obtained in different areas using sediment traps of the AGOS system: (**a**) Dvina Bay (station 4,938, water depth 117 m, sampling depth 72 m), (**b**) Basin (station 4,930, water depth 255 m, sampling depth 145 m), (**c**) Kandalaksha Bay (station b-16, water depth 236 m, sampling depth 226 m). For the AGOS position, see Fig. 1

waters enriched with nutrients and winter migration of zooplankton to the seabed [19].

Noteworthy are the avalanche sedimentation rates during the spring-summer season (Fig. 5a, b). This phenomenon is typical of Arctic seas being determined by combination of sedimentary matter fluxes from several sources: melted snow-ice cover, intense phytoplankton bloom, and a powerful river flood [20].

Figure 6 displays the marine stage in sedimentation of the basic dispersed sedimentary matter components and their variations in time. Sedimentary matter with sampling time exposure (T_{exp}) of a month-long (SPM) was obtained during onboard works, sedimentary matter with a year-long T_{exp} was trapped by the AGOS system, while sedimentary matter with multiyear T_{exp} was taken by high-resolution sampling of bottom sediments with a multicorer sampler [28]. The portion of the biogenic constituents in the material with the year-long exposure was several times lower as compared to the month-long exposure. Contribution of biogenic constituents in material with the multiyear exposure was one order of magnitude less. So, the more T_{exp} was, the less portion of biogenic constituents was. It can be explained by the exhausted energy for biochemical processes during the transformation from dispersed forms of sedimentary matter to consolidated ones that was provided by organic matter of SPM and reduced compounds entered from sediments [26]. In addition, microbes and bacteria, which are responsible for transformation of organic matter in marine suspended particulate matter, contribute much to these complex biochemical processes, particularly at the initial stage of sediment formation [3].

From our data on the long-term AGOS investigations, we have calculated the flux and average contents of the basic components of the dispersed sedimentary matter in the White Sea (Table 3). Previously, there were attempts to estimate carbon fluxes

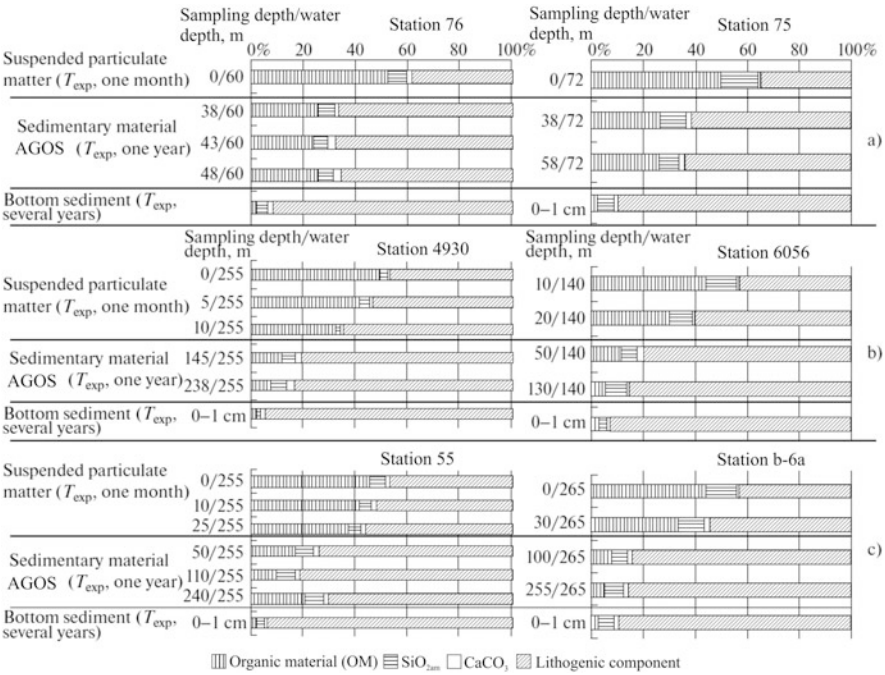

Fig. 6 Marine stage in accumulation of the main DSM components (%) with temporal changes obtained by the AGOS method: (**a**) Dvina Bay, (**b**) Basin, (**c**) Kandalaksha Bay. For the AGOS position, see Fig. 1

Table 3 Average values of the vertical sedimentary matter flux: total and basic biogenic (organic matter, $CaCO_3$, and SiO_{2am}) and lithogenic components per 1 m^2 of the bottom (g/m^2/year) and whole deep part of the White Sea (106 t/year)

	Vertical flux per 1 m^2 of the bottom surface (g/m^2/year)					Vertical flux on the entire deep part of the sea (S = 50,100 km^2) (10^6 t/year)				
Sampling depth, m	Total flux	OM	SiO_{2am}	$CaCO_3$	Lithogenic component	Total flux	OM	SiO_{2am}	$CaCO_3$	Lithogenic component
50–300	183	19	10	5	147	9	1	0.5	0.2	7.3

With the average content of components in the flux, %: OM = 11; $CaCO_3$ = 3; SiO_{2am} = 6; lithogenic component = 80

using the data on primary production [29] and satellite observations [30]. At the same time, no direct measurements at different levels of the water column over the entire sea have been conducted up to date.

Thus, it is shown that the biogenic contribution of the vertical flux decreases by an order of magnitude during the transformation from the dispersed forms to consolidated ones. The average values of the vertical flux have been calculated including the total sedimentary matter flux and the contribution of the basic biogenic and lithogenic components per m^2 of the bottom and the entire deep area of the White Sea.

4 Conclusions

For the first time, in situ investigations of sediment deposition processes in the White Sea, including vertical sedimentary matter fluxes, were studied with the automatic deep-sea sedimentological observatories (AGOS). New data on sedimentation through the water column starting from the surface layer to the uppermost bottom sediments have been obtained. This method provided a new possibilities for oceanology, sedimentology, geochemistry, and biology, namely, continuous observations in different terms: from days to decades.

There is a markedly expressed seasonal and even monthly variation in the vertical fluxes of the dispersed sedimentary matter (DSM) in the White Sea: their quantity, composition, and properties change in the White Sea. The maximal values of the SPM concentrations (mg/l) and vertical fluxes (mg/m^2/day) are typical of the ice-free spring-summer period, while the minimal ones for the winter period when the sea and the feeding catchment are capped by a snow-ice cover and the river and aeolian runoff is insignificant. When the hydrometeorological regime changes, the fluxes of dispersed sedimentary matter undergo seasonal changes, which recur annually: an increased content of fluxes in December, the melted ice discharge in April, as well as phytoplankton bloom and flooded conditions in May.

The monthly seasonal and annual fluxes of DSM can differ from each other by many times, especially in spring, when the ice regime of the sea exerts a significant influence on the flux values: the snow-ice cover provides discharge of sedimentary matter, river runoff, abrasion, and phytoplankton bloom.

The vertical fluxes of sedimentary matter down to the seafloor depend directly on the interaction of matter coming from the outer geospheres.

Thus, long-term investigations in a small Arctic sea, as the White Sea is, have revealed new regularities in sediment deposition processes in the Subarctic and Arctic zones. The monthly, seasonal, and multiyear dynamics of the basic DSM flux components was analyzed by the distinguishing marine stage in their accumulation and variations through time.

It was shown that the biogenic constituents of the vertical flux decreased by an order of magnitude during the transformation from the dispersed forms to concentrated ones. The average values of the vertical flux were calculated including the total

sedimentary matter and the contribution of the basic biogenic and lithogenic components per m^2 of the bottom and the entire deep area of the White Sea.

Thus, we applied a new approach in study of marine sedimentation by comparing the vertical fluxes of dispersed sedimentary matter in the water column with the surface layer of the bottom sediments. This approach provided an opportunity to study in situ the modern sedimentation in the surface layers of the bottom sediments and to reveal changes in the environment and climate.

Acknowledgments We would like to thank the Russian Scientific Foundation (Project No. 14-27-00114-П) for financial support of this research over the period of preparation of this chapter and also within the framework of the state task of the Academy of Sciences of the Russian Academy of Sciences for 2017–2018 on topic ?. 0149-2018-0016.

References

1. Lisitsyn AP (2004) Sediment fluxes, natural filtration, and sedimentary systems of a "living ocean". Rus Geol Geoph 45(1):15–48
2. Lisitsyn AP (2010) Marine ice-rafting as a new type of sedimentogenesis in the Arctic and novel approaches to studying sedimentary processes. Rus Geol Geoph 51(1):12–47
3. Lein AY, Kravchishina MD, Politova NV, Savvichev AS, Veslopolova EF, Mitskevich IN, Ul'yanova NV, Shevchenko VP, Ivanov MV (2012) Transformation of particulate organic matter at the water-bottom boundary in the Russian Arctic seas: evidence from isotope and radioisotope data. Lithol Min Res 47(2):99–128
4. Lukashin VN, Klyuvitkin AA, Lisitsyn AP, Novigatsky AN (2011) The MSL-110 small sediment trap. Oceanology 51(4):699–703
5. Lisitsyn AP, Novigatsky AN, Shevchenko VP, Klyuvitkin AA, Kravchishina MD, Filippov AS, Politova NV (2014) Dispersed organic matter and its fluxes in oceans and seas from the example of the White Sea: results of a 12-year study. Dokl Earth Sci 456(1):635–639
6. Lisitsyn AP (2002) Sea-ice and iceberg sedimentation in the ocean: recent and past. Springer, Berlin, 563 pp
7. Stein R (2008) Arctic Ocean sediments: processes, proxies, and paleoenvironment. Elsevier, II 592 pp
8. Rachold V, Eicken H, Gordeev VV, Grigoriev MN, Hubberten HW, Lisitsyn AP, Shevchenko VP, Schirrmeister L (2004) Modern terrigenous organic carbon input to the Arctic Ocean. Springer, Berlin, pp 33–41
9. Wassmann P, Bauerfeind E, Fortier M, Fukuchi M, Hargrave B, Moran B, Noji T, Nöthig E-M, Olli K, Peinert R, Sasaki H, Shevchenko V (2004) Particulate organic carbon flux to the Arctic Ocean sea floor. In: The organic carbon cycle in the Arctic Ocean. Springer, Berlin, pp 101–138
10. Lisitsyn AP, Novigatsky AN, Aliev RA, Shevchenko VP, Klyuvitkin AA, Kravchishina MD (2015) Comparative study of vertical suspension fluxes from the water column, rates of sedimentation, and absolute masses of the bottom sediments in the White Sea basin of the Arctic Ocean. Dokl Earth Sci 465(2):1253–1256
11. Kravchishina M, Klyuvitkin A, Filippov A, Novigatsky A, Politova N, Shevchenko V, Lisitsyn A (2015) Suspended particulate matter in the White Sea: the results of long-term interdisciplinary research. Proc Int Assoc Hydrol Sci 365:35–41
12. Lukashin VN, Isaeva AB, Rat'kova TN, Prego R (2003) Particulate matter and vertical particle fluxes in the White Sea. Oceanology 43:S159–S172

13. Aliev R, Bobrov V, Kalmykov S, Melgunov M, Vlasova I, Shevchenko V, Novigatsky A, Lisitsyn A (2007) Natural and artificial radionuclides as a tool for sedimentation studies in the Arctic region. J Radioanal Nucl Chem 274(2):315–321
14. Gordeev VV (2006) Fluvial sediment flux to the Arctic Ocean. Geomorphology 80(1):94–104
15. Kravchishina MD, Shevchenko VP, Filippov AS, Novigatsky AN, Dara OM, Alekseeva TN, Bobrov VA (2010) Composition of the suspended particulate matter at the Severnaya Dvina River mouth (White Sea) during the spring flood period. Oceanology 50(3):365–385
16. Ilyash LV, Radchenko IG, Novigatsky AN, Lisitsyn AP, Shevchenko VP (2013) Vertical flux of phytoplankton and particulate matter in the White Sea according to the long-term exposure of sediment traps. Oceanology 53(2):192–199
17. Shevchenko VR, Dolotov YS, Filatov NN, Alexeeva TN, Filippov AS, Nöthig E-M, Novigatsky AN, Pautova LA, Platonov AV, Politova NV, Rat'kova TN, Stein R (2005) Biogeochemistry of the Kem' River estuary, White Sea (Russia). Hydrol Earth Syst Sci 9 (1/2):57–66
18. Shevchenko VP, Pokrovsky OS, Filippov AS, Lisitsyn AP, Bobrov VA, Bogunov AY, Zavernina NN, Zolotykh EO, Isaeva AB, Kokryatskaya NM, Korobov VB, Kravchishina MD, Novigatsky AN, Politova NV (2010) On the elemental composition of suspended matter of the Severnaya Dvina River (White Sea Region). Dokl Earth Sci 430(2):228–234
19. Pertzova NM, Kosobokova KN (2000) Zooplankton of the White Sea. History of investigations and the present state of knowledge – a review. Berichte zur Polarforschung 359:23–29
20. Lisitsyn AP, Novigatsky AN, Klyuvitkin AA (2015) Seasonal variation of fluxes of dispersed sedimentary matter in the White Sea (Arctic ocean basin). Dokl Earth Sci 465(1):1182–1186
21. Lalande C, Nöthig E-M, Somavilla R, Bauerfeind E, Shevchenko V, Okolodkov Y (2014) Variability in under-ice export fluxes of biogenic matter in the Arctic Ocean. Global Biogeochem Cycles 28(5):571–583
22. Fahl K, Nöthig E-M (2007) Lithogenic and biogenic particle fluxes on the Lomonosov Ridge (central Arctic Ocean) and their relevance for sediment accumulation: vertical vs. lateral transport. Deep Sea Res I 54(8):1256–127222
23. Lukashin VN, Kosobokova KN, Shevchenko VP, Shapiro GI, Pantyulin AN, Pertzova NM, Deev MG, Klyuvitkin AA, Novigatsky AN, Solov'ev KA, Prego R, Latche L (2003) Results of multidisciplinary oceanographic studies in the White Sea in June 2000. Oceanology 43 (2):224–239
24. Mityaev MV, Gerasimova MV, Druzhkova EI (2012) Vertical particle fluxes in the coastal areas of the Barents and White Seas. Oceanology 52(1):112–121
25. Bringué M, Rochon A (2012) Late Holocene paleoceanography and climate variability over the Mackenzie slope (Beaufort sea, Canadian Arctic). Mar Geol 291:83–96
26. Politova NV, Klyuvitkin AA, Novigatsky AN, Ul'yanova NV, Chul'tsova AL, Kravchishina MD, Pavlova GA, Lein AY (2016) Early diagenesis in recent bottom sediments of the Dvina Bay (White Sea). Oceanology 56(5):702–713
27. Ilyash LV, Radchenko IG, Shevchenko VP, Lisitsyn AP, Burenkov VI, Novigatsky AN, Paka VT, Chul'tsova AL, Pantyulin AN (2011) Spatial distribution of phytoplankton in the White Sea in the late summer period with regard to the water structure and dynamics. Oceanology 51 (6):993–1003
28. Lisitsyn AP, Novigatsky AN, Shevchenko VP, Klyuvitkin AA, Kravchishina MD, Politova NV (2017) Dynamics of the main components of fluxes of sedimentary matter in the White Sea. Dokl Earth Sci 472(2):252–255
29. Berger VY, Primakov IM (2007) Assessment of primary production in the White Sea. Rus J Mar Biol 33(1):49–53
30. Vetrov AA, Romankevich EA (2014) Primary production and fluxes of organic carbon to the seabed in the Eurasian arctic seas, 2003-2012. Dokl Earth Sci 454(1):44–46

Diatoms and Aquatic Palynomorphs in the White Sea Sediments as Indicators of Sedimentation Processes and Paleoceanography

Yelena I. Polyakova and Yekaterina A. Novichkova

Contents

Abstract Comprehensive studies of diatoms and palynomorphs from the White Sea sediments revealed the following features of the composition of their assemblages. The species composition of the marine plankton diatoms and dinoflagellate cysts in the sediments reflects the features of the high-latitude position of the sea and the impact of the Arctic and North Atlantic water masses on hydrological regime of the White Sea. The spatial distribution of plankton species in the surface sediments (both diatoms and dinoflagellate cysts) matches the distribution of the main types of water masses in the White Sea. The characteristic property of the diatom and dinoflagellate cyst assemblages is the presence, in high concentrations, of relatively warmwater

Y. I. Polyakova (✉)
Geographical Faculty, Lomonosov Moscow State University (MSU), Moscow, Russia
e-mail: ye.polyakova@mail.ru

Y. A. Novichkova
Shirshov Institute of Oceanology Russian Academy of Sciences (IO RAS), Moscow, Russia

A. P. Lisitsyn and L. L. Demina (eds.), *Sedimentation Processes in the White Sea: The White Sea Environment Part II*, Hdb Env Chem (2018) 82: 67–104,
DOI 10.1007/698_2018_346, © Springer International Publishing AG, part of Springer Nature 2018,
Published online: 8 August 2018

species typical for the Atlantic water masses. Diatom algae, aquatic palynomorphs, and the grain size of surface sediments from bays of the White Sea were investigated in a program dedicated to the study of marginal filters (MF) in the Northern Dvina, the Onega, and the Kem' Rivers.

Three microalgae assemblages are established in surface sediments, which replace each other successively with the distance from river mouths, and are characterized by a gradual decrease in a share of freshwater species of diatoms and *Chlorophyceae* algae, significantly varying concentrations of marine diatoms and dinocysts due to changes in water salinity, grain-size composition of sediments, quantitative distribution of suspended particulate matter (SPM), and water productivity at different marginal filter's zones.

Keywords Diatoms, Dinoflagellate cyst, Green algae, Marginal filter sedimentation, The White Sea

1 Introduction

Diatoms and aquatic palynomorphs are among the most promising micropaleontological groups in paleoceanological studies Arctic, since they allow to solve a wide range of issues, such as reconstruction of water masses' paleocirculation, including the intensity of advection of the Atlantic and Pacific waters; changes in river flow to the Arctic shelf seas; the distribution limits and duration of the seasonal sea-ice cover, the origin of the ice and the ways of their drift; changes in paleotemperatures, paleosalinity, and paleoproductivity of water; etc. [1–13]. In addition, marine diatoms and organic-walled cysts of marine dinoflagellates are widely used in biostratigraphy and interregional correlations of sediments and paleo-events since the formation of the Arctic Ocean and throughout its development in the Cretaceous and Cenozoic.

Studies of diatoms in the sediments of the White Sea for the purposes of paleoceanological and paleogeographic reconstructions begun in the first half of the last century [14]. Systematic studies of diatoms from the bottom sediments of the White Sea, carried out by Dzhinoridze in the 1980s on the basis of changes in the species composition of diatom associations [15–17], revealed the main regularities in the formation of diatom associations in surface sediments, as well as the evolution of paleogeographic environments in the Holocene in various regions of the sea.

Particular attention in subsequent studies of diatom association from the surface sediments of the White Sea was paid to the distinct regularities in the formation of diatom associations in the bays of the White Sea. Dependence of their species composition and abundance in sediments on hydrochemical, hydrobiological, and sedimentation environments of marginal filter of the largest rivers in the White Sea basin were also under consideration [18–20].

Over the past decades, the White Sea has become a unique object for detailed studies of aquatic palynomorphs, primarily dinoflagellate cysts, in sediments. We have improved this new micropaleontological method due to complex multidisciplinary studies conducted in the White Sea [19, 21–23].

2 Materials and Methods

The 61 surface sediment samples used in this study were taken during expeditions of the RV "Professor Shtokman," "Ekolog," and "Ivan Petrov" in 2001–2006 by scientists from the Laboratory of Physical Geology Researches of the Shirshov Institute of Oceanology RAS. We also used published data of diatom analyses, which was carried out by Dzhinoridze and Polyakova [15–17, 19]. The surface samples cover the central deep-sea Basin, the Kandalaksha, the Onega and the Dvina Bays, the Kemskaya Guba Bay, and the Voronka Strait from the water depth of 10–250 m (Fig. 1).

Samples from the uppermost bottom layer (1–2 cm of each box cores) were put into plastic boxes and stored cool (<5°C) until further processing. Initially, sediment samples were freeze-dried. For diatom analysis approximately 2–3 g of each dried samples was treated with H_2O_2 (30%). Diatom valves were concentrated by decantation using distilled water. Slide preparation was carried out following Battarbee [24]. The residues were mounted on glass slides with the Naphrax mountant, which

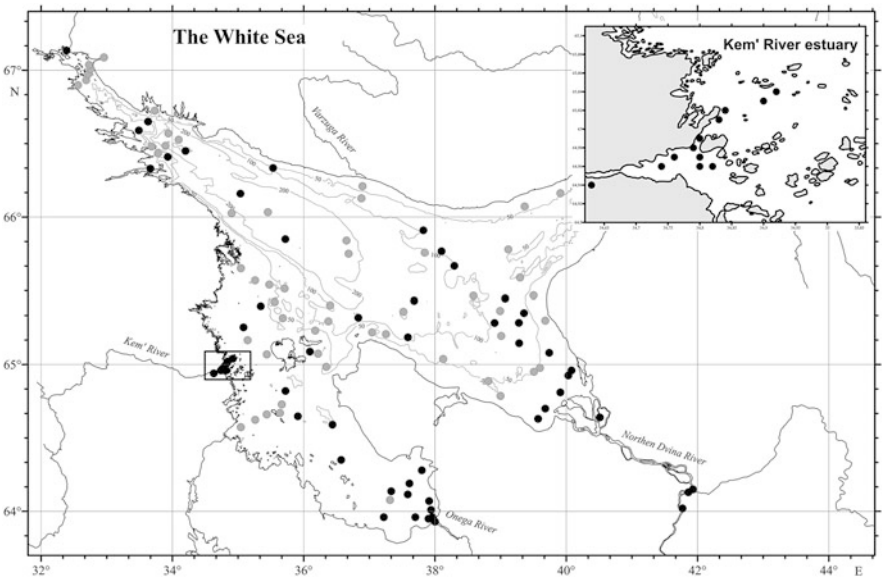

Fig. 1 Location of studied samples from the White Sea surface sediments: (1) modern study (diatoms and aquatic palynomorphs); (2) samples studied by Dzhinoridze (diatoms) [15]

has a refraction index of 1.73. The diatom valves were examined under an Axioskop 40 (Zeiss) optical microscope at 1,000× magnification. Generally, about 300–400 specimens were counted in each sample. The results were then calculated to census data and number of valves per gram of dry sediment (concentrations) and proportions of main ecological groups (marine, sea-ice, and freshwater species).

Samples for analysis of aquatic palynomorphs were treated as normal palynological technique. *Lycopodium clavatum* spores were added in order to calculate the absolute concentrations (cyst/g dry sediment) [25]. Sediment samples were treated with cold 10% HCl for 5 min in order to remove carbonates and then rinsing with distilled water. Additions of cold 48% HF for up to 5 days removed the siliceous particles. The residue was rinsed twice with distilled water and sonicated for between 0.2 and 0.8 min. The samples were sieved through 15 μm mesh sieves to eliminate fine material. The final fraction was collected on 15 μm mesh sieves and transferred to plastic tubes. Samples were centrifuged after each step of the described technique. No oxidation was applied in order to prevent loss of the more fragile *Protoperidinoid* cysts [26–28]. To estimate river runoff, the CD criteria [10, 11], which represents a ratio between freshwater *Chlorophyceae* algae and cysts of marine dinoflagellates in assemblages of aquatic palynomorphs, was used in addition to concentrations of freshwater species in diatom assemblages [7, 29]. The AH criteria (the ratio of cysts of autotrophic and heterotrophic species in assemblages of aquatic palynomorphs), which is used in the arctic seas as an indicator of the influx of North Atlantic water [11, 30], was also applied. The data on microalgae correlated with the mean interannual surface water summer salinity and temperature [31] (http://www.nodc.noaa.gov/OC5/woa13/), water depths of the basin, and the distance from river mouths. In constructing sections based on different parameters of microalgae assemblages, some data obtained at similar distances from river mouths were omitted from consideration. The grain size of bottom sediments was determined at the Analytical Laboratory of IO RAS in accordance with the standard method [32] (analysts A.N. Rudakova and T.N. Alexeeva). The total organic carbon (TOC) concentrations were measured by V.P. Shevchenko at the Alfred Wegener Institute for Polar and Marine Research (Bremerhaven, Germany). Organic carbon (C_{org}) was determined by coulometric titration of carbon dioxide released during high-temperature combustion ($t = 800°C$) of samples, which were preliminarily deprived of inorganic carbon of carbonates using 3 M HCl, in an oxygen flow. The organic carbon content was measured by an LECO CS 125 device [33].

3 Modern Sea-Ice and Hydrological Conditions

The White Sea is almost entirely located southward off the polar circle. It belongs to the basin of the Arctic Ocean and is the most isolated sea from it. It is connected with the Barents Sea via the shallow-water (<50 m water depth) Gorlo Strait. This small marginal arctic sea basin is approximately of 91,000 km^2, and it is characterized by significant water depth drops [16, 34]. The average seawater depth equals about

67 m; the maximal depths are recorded in the central depression named the Basin (down to 350 m water depth). With respect to the structure and geomorphology, the following major structural elements are distinguished, the Voronka, the Gorlo, and the Basin, and four major bays, the Onega, the Dvina, the Mezen', and the Kandalaksha Bays. They differ in the regimes of the freshwater supply, influence of tides, salinity gradients, sea-ice conditions, and biota [35–38].

Presently, within the framework of modern concepts, the White Sea is regarded to represent as "estuarine" system. The upper level of the hierarchy is the entire sea, within which two water masses occur (the White Sea water mass with salinity of 25–30 psu and the Barents Sea mass with salinity of 34–35 psu). When changing the scale of the consideration, the sea becomes a system of four-bay estuaries rather than a single estuary [39–41].

The present-day hydrological conditions of the White Sea are mostly formed under the influence of the fresh riverine runoff and the water exchange with the Barents Sea. To a significant extent, the abundant riverine runoff (~225 km^3/year) defines the regularities and particular features of the biogeochemical processes within its area. The particularity of the continental runoff lies, first of all, in the fact that all the largest rivers fall into the Dvina, the Onega, and the Mezen' Bays, i.e., isolated sea areas, that cause the strongly irregular distribution of the surface seawaters' salinity (Fig. 1). Herewith, the maximal runoff values, as well as those of the supply of suspended matter and nutrients, are observed in the spring flood period in May [42].

The suspended matter is one of the principal forms of the sedimentary matter transfer [35–37], and its elevated or reduced content in the water directly influences the ecological balance in the aquatic area. Phytoplankton, being an important constituent of the suspended matter, is part of a long food chain, and its mineral particles (at their high contents) attenuate the solar flux to the deeper layers and retard the development of living organisms [35, 43].

The water exchange with the Barents Sea is implemented via a narrow shallow-water strait – the Gorlo of the White Sea (Fig. 1). The permanent gravitational current of the freshened surface waters to the Barents Sea (with a discharge of ~2,200 km^3/year) runs along the Zimnii Coast of the White Sea. A reverse flow of heavy normally saline oceanic waters (~2,000 km^3/year) is directed from the Barents Sea via the Gorlo; this way, approximately two-thirds of the deep White Sea water is annually renewed [34, 44].

The most important features of the White Sea hydrological regime are tides, which reach their maximal heights (up to 10 m) in the Mezen' Bay. The intensive tidal movements provide strong vertical mixing of the waters; therefore, in the regions with relatively small sea depths (e.g., the Gorlo, the Onega, and Mezen' Bays), there is virtually no vertical stratification [34, 41].

The surface summer water temperatures in the White Sea range from +7 to +15°C, and in the winter the temperatures fall down to −1.6°C in the north and to −1.7°C in the south. The river waters, which freshened mainly the southeastern part of the sea, provide additional favorable conditions for the formation of sea-ice cover. Since November to May, the sea is covered with seasonal sea ice; in the bights near

river mouths, fast ice is formed. Due to this reason, the White Sea is characterized by more severe sea-ice conditions that are characteristics of the corresponding latitudes that affect the dynamics of the biological productivity of phytocenoses [45–47]. In addition to the local impacts, due to the exchange currents between the Barents and the White Seas, the sea ice formed in the inner basin is supplied to the Arctic Ocean, where it participates in the global thermohaline circulation [48].

Ice formation starts in the White Sea in apices of bays at the beginning of November. In the winter time, the entire sea is covered with ice of different types during 1–3 months. The strong winds of different intensity and duration, prevailing in the White Sea basin, ensure sea-ice removal through the Gorlo Strait to the Barents Sea. The White Sea becomes free from ice completely during April and May; herewith, ice removal through the strait prevails (50–80% of seasonal sea-ice cover) over its melting in this sea [40] that governs the species composition and productivity of sea-ice communities and spring phytoplankton.

The spatial inhomogeneity in the halocline parameters is determined by the horizontal advection, the contacts between water masses of different origins, the riverine runoff distribution, and the intensity of the biochemical processes [47, 49, 50]. The horizontal circulation is the principal mechanism of the redistribution of elements over the sea area. The mean annual productivity of phytoplankton of the White Sea varies from 13 to 95 g C/m^2 and features two seasonal peaks related to the spring and summer [47, 50–54]. In so doing, the peak of the dinoflagellate development follows the summer time peak of the development of diatoms.

4 Diatoms and Aquatic Palynomorphs in the Surface Sediments

4.1 Modern Sea-Ice and Phytoplankton Communities

During the more than hundred-year investigations of the White Sea, the extensive data relating phytoplankton, benthic, and sea-ice microalgae communities were collected. The pioneering set of information about the species composition and seasonal development of the White Sea phytoplankton including diatoms and dinoflagellates as the dominant groups was summarized by I.A. Kiselev [55, 56]. These data are based on his own materials composed of his studies and analysis of data published by that time [57–59 and others]. In the 1980s, on the basis of new achievements in the fields of taxonomy and electronic microscopy, researchers revised the taxonomic composition of the White Sea plankton flora. Likewise, the list of species – above all, diatoms and dinoflagellates – was revised from the standpoint of their environmental and phytogeographical characteristics [60]. These data showed that the White Sea flora is an impoverished population of the Barents Sea algae flora [61, 62]. The decreased salinity of the White Sea waters prevents the development of selected stenohaline species typical of the Barents Sea.

In addition, a number of cold-water arctic-boreal species characteristic for the arctic seas are absent.

Stationary observations of spring phytoplankton development and biocoenosis inhabiting the sea ice, in selected coastal areas of the sea, have allowed to discover the seasonal dynamics of phytoplankton and, in addition, a group of specific sea-ice species [45, 46, 63, 64]. In the frame of the scientific program "The White Sea System" (2001–2018 years), the satellite measurements of chlorophyll "a" were one of the major methods of receiving persistent annual data according to distribution of suspended matter and phytoplankton productivity [37, 65, 66].

Diatoms Diatoms are the most taxonomically diverse group of microalgae in the White Sea phytoplankton [50, 52, 60] that is typical for the arctic seas [55, 67]. According to the latest assessment [52], 262 species of marine and brackishwater-marine diatoms were recorded in the White Sea plankton. However, the authors included in this list along with true planktonic and sea-ice species, the so-called accidentally planktonic species, namely, epibenthic and epiphytic species, the latest inhabited submerged plants, stones, etc. These diatoms enter the water column due to intensive tidal and wave currents. Among true planktonic diatom species, the following genera are the most taxonomically diverse: *Chaetoceros* (46 taxa), *Thalassiosira* (18 taxa), and *Coscinodiscus* (12 taxa) [50, 60].

More than 30 identified taxa from the White Sea are the sea-ice-associated species, which develop under the influence of ice melt waters [50, 68–70]. The part of the life cycle of these species related to the sea ice, and they continue their development in the adjacent sea surface waters, determining the short-term (2 weeks) spring phytoplankton bloom in arctic seas [71–77], including the White Sea [60, 68, 78–81]. The mean annual contribution of sea-ice assemblages to the primary production in the arctic seas puts together 20–25% [82, 83]. In the central regions of the White Sea, outside the bays, sea-ice algae, primarily diatoms (up to 99%), produce more than 95% of total biomass [68].

In accordance with phytogeographical characteristics of the diatom species [15, 60, 84, 85], the planktonic flora of the White Sea is affiliated with the arctic-boreal region, and it is characterized by the prominence of the cold-water arctic-boreal and bipolar species in the composition of the diatom flora (more than 50%). A distinctive feature of the species composition of phytoplankton in this region is the high diversity of the arctic-boreal-tropical species and cosmopolitans (>40%), as well as the considerable participation of relatively warmwater species, which distribution in the Arctic Ocean is limited by the Atlantic and the Bering Sea water masses [5].

The epibenthic and epiphytic diatom flora of the White Sea is exceedingly diverse, and their total number is more than 750 taxa [86] that is caused by the diversity of environmental conditions within the wide littoral and sublittoral zones in the bays, high seasonal and daily variations of water salinity, temperatures and bioproductivity, and diversity of biotopes.

Dinoflagellates Dinoflagellates along with diatoms represent the leading group of phytoplankton (139 taxa) and the principal biological producers of the White Sea [45, 46, 50, 52, 56, 60, 87]. According to the type of metabolism, these dinoflagellates are represented by photoautotrophic, mixotrophic, and heterotrophic species as well as in the other arctic seas. Group of heterotrophic species is dominated by *Protoperidinium* genus (28 taxa).

A revision of the taxonomic composition of the White Sea dinoflagellates [11, 45, 46, 50, 60, 88] showed that, with respect to the species number, the phytoplankton of the White Sea is rich as that of the Barents Sea. Meanwhile, the reduced salinity of the White Sea waters hampers the development of selected stenohaline species typical of the Barents Sea, while the high seasonal temperature gradients result in the absence of a series of cold-water arctic-boreal species. The flora of the White Sea contains no less than 50% of the Barents Sea species [62]. According to the phytogeographical characteristics of the species, the planktonic flora of the White Sea belongs to the arctic-boreal domain; meanwhile, the proportion of arctic-boreal species (15%) in the dinoflagellate composition is lower compared to diatoms. The group of dinoflagellates, in contrast to the other phytoplankton components, features the highest proportion of boreal species (13%). Along with this, the intensive water exchange with the Barents Sea provides a high species diversity of the arctic-boreal-tropical (14% in the composition of Dinophyta algae) and cosmopolitan (up to 28%) species, several of which are never or rarely encountered in the Siberian seas of Eurasia [5, 11, 20, 89].

As distinct from diatoms, dinoflagellates have never been abundant in the sea ice, notwithstanding their frequent occurrence in ice of the arctic seas that is caused by cells icebound during the sea-ice formation [72, 73, 90]. Ice-associated dinoflagellates from the early spring phytoplankton of the White Sea are represented by scanty photoautotrophic, mixotrophic, and heterotrophic species from *Gymnodinium*, *Gyrodinium*, *Amphidinium*, and *Protoperidinium* genera, which develop close to the melting sea ice. However, until now only one species *Polarella glacialis* is regarded as true cyst-forming sea-ice dinoflagellate [91–94].

Cells of the living forms of dinoflagellates are subjected to rapid damage and are not preserved in marine bottom sediments. Meanwhile, only one-fifth of species form cysts that can be conserved in the sediments [11, 95]. These organic-walled dinoflagellate cysts are one of the major objects of our study in the White Sea.

In the White Sea, two maxima of phytoplankton biomass were observed during the vegetation period – spring and summer [50, 52]. The spring peak (April to May) is formed by the sea-ice diatoms and the cold-water ice-associated planktonic species as well as in the other arctic seas. In the summer (July) phytoplankton is characterized by the maximal taxonomical diversity of the planktonic centric diatoms (*Chaetoceros*, *Thalassiosira*, *Coscinodiscus*, *Skeletonema*, *Leptocylindrus* genera). The increase in abundances of dinoflagellates usually starts in July, and in August dinoflagellates predominate in the phytoplankton; however, the total biomass is less than in April to May or in July.

Up to the present, the obtained data give evidence that after the spring bloom, when the photic layer of the White Sea is impoverished of nutrients, in June to July, the maximal intensity of productive processes takes place at the frontal zone and dynamically active sea areas, where the vertical cyclonic motion governs upwelling [41, 47].

The maximal value of primary production coincides with the frontal zone of the Dvina Bay [2.2–2.7 g C/(m^2 day)], which separates the marine and brackishwater-marine waters of this bay. The Kandalaksha Bay is characterized by the high water transparency and thickness of the photic layer (12–14 m), where primary production is relatively high [1.2–1.4 g C/(m^2 day)]. The lowest value of primary production was recorded in the Onega Bay [0.6–0.8 g C/(m^2 day)] that was caused by the low-water transparency. This is due to abundant discharge of humic matter and intensive tidal movement. In the central part of the White Sea, the Basin, the water productivity is similar to that in the Dvina Bay.

4.2 Species and Quantitative Compositions of Microalgae Assemblages in the Surface Sediments

4.2.1 Diatom Assemblages in the Surface Sediments

In the studied surface sediments of the White Sea, more than 300 species and varieties of diatoms have been identified [15, 17]. Of them, 150 species are typical marine and brackishwater-marine species, with a taxonomically diverse group (>60 species) of euryhaline polyhalobous and mesohalobous diatoms according to the classification by Simonsen (1962) [96] and Pankow (1990) [97]. Among marine diatoms, the so-called "sea-ice" species are widely represented (>20 taxa). Part of their life cycle is associated with the sea ice [72, 73, 76, 77]. These species, after being washed away from ice floes, continue to grow in the surface layer of the sea waters, between the melting blocks of ice and in polynyas. This is primarily responsible for the "spring maximum" in the phytoplankton development of the arctic seas; the White Sea is among them [56, 60]. In the surface bottom sediments, among the "sea-ice" diatoms, the most abundant species are *Fossula arctica*, *Fragilariopsis oceanica*, *F. cylindrus*, *Nitzschia frigida*, *Navicula vanhoeffenii*, *Melosira arctica*, *Psedogomorphonema arcticum*, *P. groenlandicum*, *Attheya septentrionalis*, and *Pauliella taeniata.* The total abundances of the "sea-ice" diatoms reach 4×10^6 valves/g, while their percentage in the diatom assemblages get together >40%, remaining persistently high in the areas of distribution of the seasonal sea ice. In the group of marine and brackishwater-marine diatoms, the planktonic neritic and panthalassic species (approximately 50 taxons) are the taxonomically diverse. These are the most characteristic species of the neritic and oceanic plankton in the arctic and subarctic waters. In their composition, the dominant species are those of the *Thalassiosira*, *Chaetoceros* (spores), and *Coscinodiscus* genera. Concentrations of the planktonic diatoms reach the highest

values ($>10^6$ valves/g) in the Basin and in the Kandalaksha Bay, where their total abundances comprise 70–90% of diatoms in assemblages (Fig. 2a, b).

Meroplanktonic species (16 taxa), associated in their development with the sublittoral macroflora, are the most abundant in the sediments of the offshore areas of the White Sea. In the diatom assemblages from the surface sediments, the widespread euryhaline epiphytic species *Paralia sulcata* is predominant. The abundance of its valves may reach 7×10^6 valves/g in the shallow-water Onega Bay. Moreover, the high abundances of this species were observed in the central deep-water area of the sea; this may be related to the structure of the coarse-armored valves of *Paralia sulcata* and to the possibility of their transportation across long distances.

Species such as *Hyalodiscus obsoletus*, *H. scoticus*, *Odontella aurita*, *Melosira moniliformis*, and *M. nummuloides* are the subdominant species of the meroplanktonic sublittoral flora, and they are the typical inhabitants of the offshore freshened waters of the arctic and subarctic seas [5]. An analysis of the phytogeographical properties of the planktonic diatom species recorded in the surface sediments of the White Sea shows that the diatom assemblages reflect the features of the composition of present-day phytoplankton, as well as the distribution of the main types of water masses. In the species composition of the planktonic flora, the cold-water arctic-boreal and bipolar species predominate (approximately 60% of taxonomic diversity). Among them, the species of the *Thalassiosira* genus (*T. gravida*, *T. antarctica*, and *T. nordenskioeldii*) and *Chaetoceros* genus (*C. diadema*, *C. furcellatus*, *C. mitra*) are the most abundant. However, it should be noted that only part of *Chaetoceros* species forms the silicified spores, which were preserved in the sediments. In the White Sea identification of *Chaetoceros* spores on the species level was able only for 7 of the 33 species recorded in the phytoplankton, taken into consideration that part of them do not form spores.

More than 30% of the species found in the sediments are cosmopolitans and arctic-boreal-tropical species, notably species having the wide adaptive flexibility. In the composition of this group, *Thalassionema nitzschioides*, *Coscinodiscus radiatus*, *C. asteromphalus*, *Thalassiosira oestrupii*, and *Proboscia alata* are abundant in the sediments. It should be noted that each of these species, with the exception of *Thalassionema nitzschioides*, are considered as indicators of the advection of the North Atlantic and the Bering Sea waters into the arctic seas [5]. Their high abundances in the sediments are recorded only in the southwestern areas of the Barents Sea [15]. The presence in the sediments of a few boreal-tropical diatoms, such as *Hemidiscus cuneiformis*, *Psammodiction panduriforme*, *Rhizosolenia styliformis*, and others (6% of the taxonomic diversity), which were transported to the White Sea along with the system of currents from the main oceanic circulations of the North Atlantic, is a distinctive property of the White Sea's diatom assemblages.

Due to the shallow-water character of the majority of the White Sea water area, taxonomic diversity of the benthic and epiphytic marine and brackishwater-marine diatoms is high (more than 100 taxa) in diatom assemblages from the surface sediments of sea. Their total abundances in the Onega and the Dvina Bays are

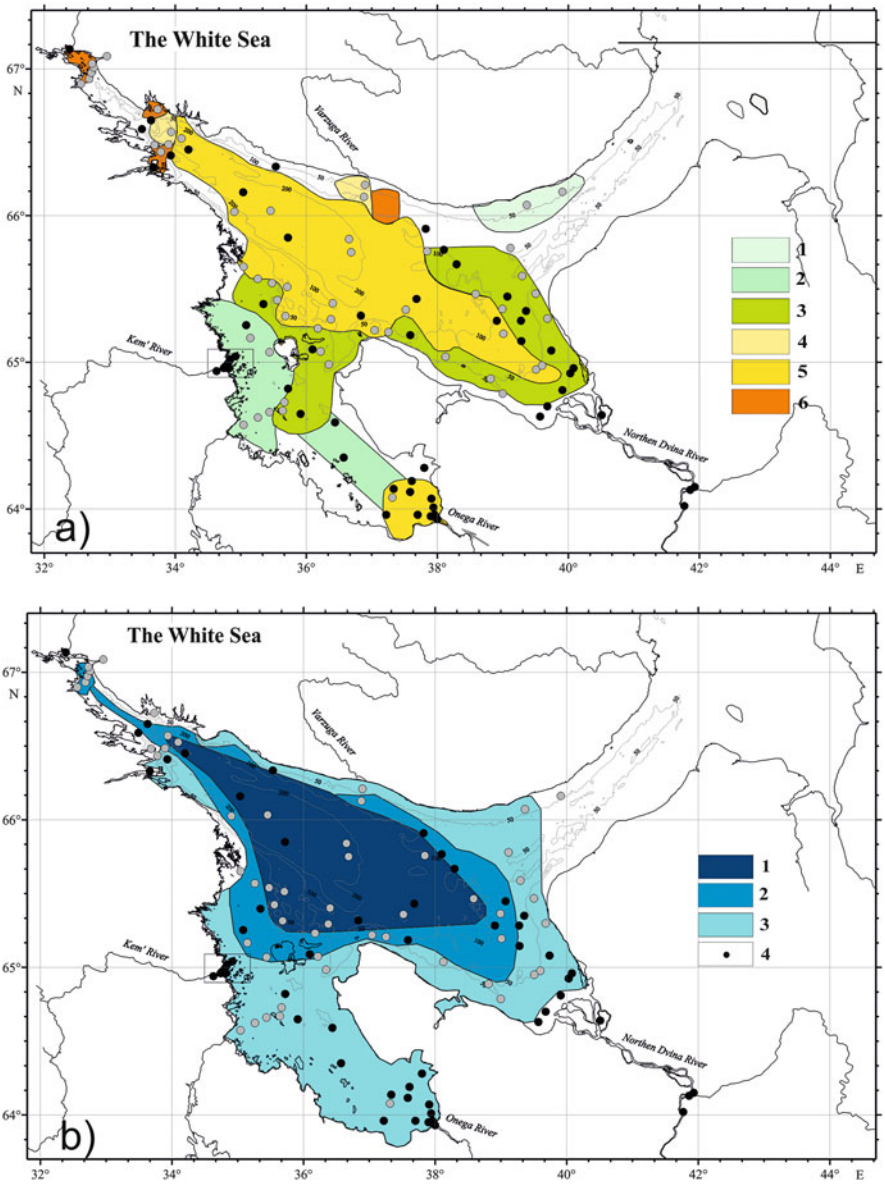

Fig. 2 Distribution of (**a**) total concentrations of diatoms the surface sediments of the White Sea (in 10^6 valves/g dry sediment): (1) diatoms are absent; (2) 0.1–1.0; (3) 1–5; (4) 5–10; (5) 10–15; (6) 15–25; (7) sampling stations; (**b**) neritic and panthalassic plankton species and sublittoral species of diatoms (in %) in diatom assemblages from the surface sediments of the White Sea. The main types of the diatom assemblages: (1) Zone I (neritic); (2) Zone II (sublittoral-neritic); (3) Zone III (sublittoral)

more than 70% (Fig. 2). The characteristic features of the White Sea benthic and epiphytic diatom flora are the prevalence of cosmopolitans (50%) and species with a wide geographical distribution along with the high abundances of the relatively warmwater species (*Auliscus coelatus*, *Diploneis bombus*, *Isthmia nervosa*, and others), which do not live in the arctic seas.

With respect to the composition of diatom assemblages, the bottom sediments of the White Sea are divided into three zones (Fig. 2b) [15, 17], namely, (1) Zone I, which is characterized by the prevalence of the neritic and panthalassic plankton species, as well as the sea-ice species (70–90%), and occupies the deepwater part of the sea; (2) Zone II, which represents a sublittoral, neritic zone, where sublittoral and neritic species are almost equal in proportion; and (3) the sublittoral Zone III, where sublittoral species prevail (70–75%).

An analysis of the species composition of the diatom assemblages from the White Sea surface sediments indicates the significant regional peculiarities related to the features of the sea-ice, hydrological, and geomorphological conditions of selected areas.

The Onega Bay is the most shallow-water bay; in the summertime, its waters are warmed to the greatest extent, practically down to the bottom. The high degree of hydrodynamic activity and water mixing create a homothermal and homohaline regime. Diatom assemblages from the surface sediments of this bay are dominated by the widespread euryhaline meroplanktonic species *Paralia sulcata*, along with taxonomically diverse sublittoral benthic and epiphytic *Rhabdonema arcuatum*, *Navicula distans*, *Delphineis surirella*, *Isthmia nervosa*, and others. The total abundances of true plankton species do not exceed 20%. They are represented by the cosmopolitan, relatively warmwater species such as *Coscinodiscus radiatus*, *C. asteromphalus*, *Actinoptychus senarius*, *Thalassionema nitzschioides*, and *T. latimarginata* and by the cold-water species *Thalassiosira gravida*, *T. antarctica*, and *T. nordenskioeldii.*

The Dvina Bay located in the eastern part of the White Sea is characterized by the high salinity gradients of its surface waters in the summer that is caused by the large runoff from the Northern Dvina River. The permanent surface current, going along the eastern coast of the bay, is directed toward the Gorlo Strait. In the Dvina Bay, the so-called hydrological cold pole is located, which is related to the upwelling of the deep waters, and governs the negative temperatures observed at the water depths of about 12 m [16, 41].

Diatom assemblages from the surface sediments of this "hydrological cold zone" are characterized by the highest abundances of cold-water marine planktonic and sea-ice diatoms in the White Sea (*Melosira arctica*, *Thalassiosira hyaline*, *T. antarctica*, *T gravida*, *T. baltica*, *Chaetoceros mitra*, *C. diadema*, *Coscinodiscus oculus-iridis*, *Detonula confervaceae*, *Nitzschia frigida*, and others). The total abundances of relatively warmwater species for the arctic seas, such as *Thalassiosira latimarginata*, *T. angulata*, *Coscinodiscus radiatus*, *Proboscia alata*, and others, do not exceed 5–10%. The total abundances of diatoms in the surface sediments vary from 1 to 15 $\times$ 10^6 valves/g.

The Kandalaksha Bay is the most deepwater bay in the White Sea, and it is characterized by the relatively quiet hydrodynamic regime, with steady water stratification during the summer period. The high phytoplankton productivity (see above) is reflected in the high abundances of marine diatoms in the sediments (up to 20–25 $\times$ 10^6 valves/g) in this bay. The diatom assemblages are dominated by the marine planktonic arctic-boreal and bipolar species *Thalassiosira gravida*, *T. antarctica*, and the species typical for the North Atlantic current *T. latimarginata*. The total relative abundances of marine benthic diatoms are less than 20%.

The White Sea Basin occupies the central area of the sea with water depths of 100–300 m. This deep part is filled up with the transformed Barents Sea waters. This is reflected in species composition of diatom assemblages from the surface sediments. The following species, which are indicators of Atlantic waters in the Arctic Ocean, are the most abundant: *Thalassiosira latimarginata* (30%), *Coscinodiscus radiatus* (15%), and *C. asteromphalus* (10%). The surface sediments of the Basin are characterized by the persistently high concentrations of diatoms (5–15 $\times$ 10^6 valves/g), with the maximum content of the true plankton species of diatoms.

In the surface sediments off the Terskii Coast, along which the current runs from the Barents Sea, the total abundances of diatoms vary from 5 to 10 $\times$ 10^6 valves/g. The characteristic feature of diatom assemblages from this region is the maximum concentrations of sea-ice diatoms (*Fossula arctica*, *Fragilariopsis oceanica*, *F. cylindrus*, *Nitzschia frigida*, and others), reflecting the presence of seasonal sea ice.

4.2.2 Dinoflagellate Cysts in the Surface Sediments

The studied surface sediments of the White Sea are characterized by a relatively high diversity of the grain-size composition: from fine-grained sands to silty clays. The sizes of dinoflagellate cysts range from 32 to 100 μm, which corresponds to the coarse-grained silty fraction of the White Sea sediments. The maximal dinocyst concentrations (up to 22 $\times$ 10^3 cyst/g dry sediment) were recorded in the silty fractions of the surface sediments (Fig. 3a).

The minimal concentrations (<100 cyst/g) were recorded in the fine-grained sands, which are usually perfectly washed. In the sands with various admixtures of silty and clayey matter, the concentrations of dinoflagellate cysts amounted from a few tens to 9.5 $\times$ 10^3 cyst/g of dry sediment. From this fact, it is possible to conclude that the increased dinocyst concentrations in the Central Basin and their reduced values in bays may be related to the grain-size composition of the White Sea sediments. Another factor that restricts the dinocyst contents in the sediments is the salinity of the surface seawater. Dinoflagellate cysts, as derivatives of marine phytoplankton, were recorded in the samples from the White Sea within the salinity interval from 15 to 25 psu.

Sixteen dinocyst species were identified in the surface sediments of the White Sea (Table 1, Appendices 1 and 2); this comprises approximately one-eighth of the

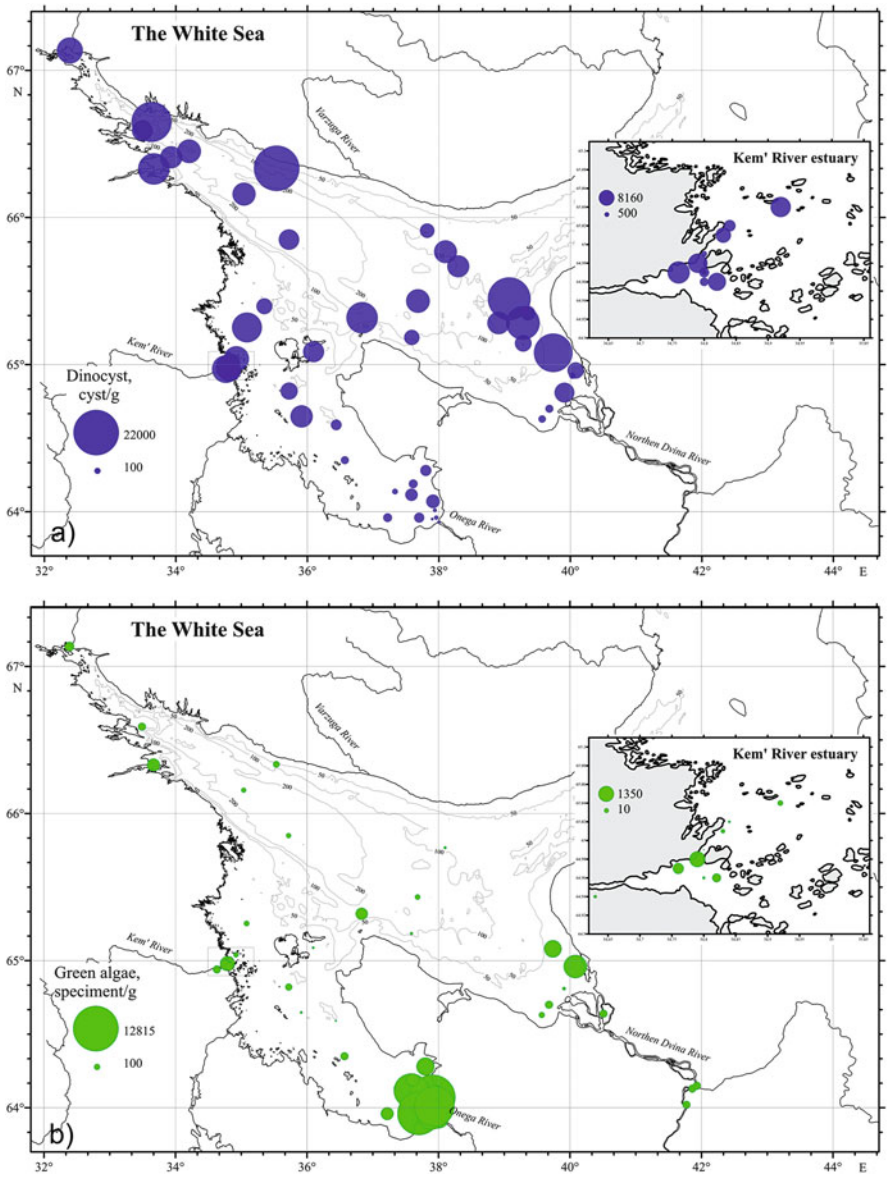

Fig. 3 The concentrations: (**a**) the marine dinoflagellate cysts, (**b**) freshwater green algae in the White Sea surface sediments

dinoflagellate species ever recorded in the plankton of this sea (see above). The dominant *Operculodinium centrocarpum* (Fig. 3) is a widespread cosmopolitan species that is confirmed by the ecology of living form of this dinocyst (biological taxon *Protoceratium reticulatum*). This species is a neritic dinoflagellate, which is

Table 1 List of currently known cyst-forming dinoflagellates in the plankton of the Arctic Ocean and dinoflagellate cysts in recent sediments from the Arctic Ocean according to [11, 99], which was identified in the White Sea surface sediments (see Appendices 1 and 2)

Biological taxon	Cyst-based taxon	Plankton	Sediments	Autotrophic	Heterotrophic
	Brigantedinium spp.		X		X
?*Gonyaulax alaskensis* KOFOID	Spiniferites sp.	X		X	
Gonyaulax digitale (POUCHET) KOFOID	*Bitectatodinium tepikiense* WILSON	X	X	X	
Gonyaulax elongate (REID) ELLEGAARD, DAUGBJERG, ROCHON, and LEWIS	*Spiniferites elongates* REID		X	X	
Gonyaulax cf. *spinifera* (CLAPAREDE & LACHMANN) DIESING	*Spiniferites ramosus* (EHRENBERG) MANTELL		X	X	
Unknown, probably *Gonyaulax spinifera* complex	*Nematoshaeropsis labyrinthus* (OSTENFELD) REID		X	X	
Unknown, probably *Gonyaulax* sp.	*Impagidinium pallidum* BUJAK		X	X	
Pentapharsodinium dalei IDELICATO & LOEBLICH III	Cyst of *Pentapharsodinium dalei* INDELICATO & LOEBLICH III		X	X	
Protoceratium reticulatum (CLAPAREDE & LACHMANN) BUTSCHLI	*Operculodinium centrocarpum* sensu WALL & DALE 1966	X	X	X	
Protoperidinium avellanum (MEUNIER) BALECH	*Brigantedinium cariacoense* (WALL) LENTIN & WILLIAMS		X		X
Protoperidinium conicoides (PAULSEN) BALECH	*Brigantedinium simplex* (WALL) ex LENTIN & WILLIAMS	X	X		X
Protoperidinium conicum (GRAN) BALECH	*Selenopemphis quanta* (BRADFORD) MATSUOKA	X	X		X
Unknown, probably Protoperidiniaceae	*Echinidinium karaense* HEAD, HARLAND & MATTHIESSEN		X		X
Unknown, probably Protoperidiniaceae	*Islandinium minutum* HEAD, HARLAND & MATTHIESSEN		X		X
Unknown, probably Protoperidiniaceae	*Islandinium? cezare* HEAD, HARLAND & MATTHIESSEN		X		X
	Cyst of *Polykrikos* sp. sensu KUNZ-PIRRUNG		X		

widespread in the boreal zone of the World Ocean [9, 88]. The other dominant dinocyst *Pentapharsodinium dalei* belongs to the *Gonualax* sp. group and is also a cosmopolite which is mostly distributed in the Northern Hemisphere [98, 99]. Cysts of these species dominate (up to 76% of dinocysts assemblages) in the northern and central areas of the White Sea. The species *Spiniferites ramosus* is also cosmopolitan and is most abundant in mixing layers of the surface waters [11, 99, 100]. In the White Sea, this species is most abundant (up to 51%) in the unstratified waters of the Onega Bay.

The heterotrophic marine dinocyst species, typical of polar and subpolar regions, such as *Islandinium minutum* and similar morphotypes (*I. cezare* and *Echinidinium karaense*), inhabit in the wide temperature and salinity ranges. They are capable of dwelling over 8–12 months under the conditions of sea-ice cover [8, 98, 99, 101] and are most abundant (up to 33%) in the central and southern parts of the White Sea. The cysts of the neritic species *Brigantedinium cariacoense* and *Brigantedinium simplex*, which belong to heterotrophic planktonic dinoflagellate of the *Protoperidinium* genus, are widely spread in cold waters. In the White Sea, these species are characteristics of dinocyst assemblages from the northern and central regions, where their total abundances reach 42%. The highest abundances (up to 18%) of the species *Selenopemphix quanta*, which is highly tolerant to the salinity and temperature of the surface waters, recorded in dinocyst assemblages of the Dvina Bay. In plankton, cells of this species are prevalent in cold, temperate, and warm waters [98, 99].

The total content of the other dinocysts species never exceeds 10% in the White Sea sediment assemblages. Meanwhile, their ecological and phytogeographical characteristics may provide additional information on the hydrological environments. Cysts of *Polykrikos* sp. Arctic morphotype are characteristics (up to 2%) of the Kandalaksha and the Dvina Bays. Cysts of *Bitectatodinium tepikiense*, which also belong to widespread tropical-boreal species [98, 99], are relatively abundant in the northern parts of the Basin and in the Dvina Bay (up to 5–10%). Species of the *Nematosphaeropsis* genus are cosmopolites and, at their living stage, refer to the *Gonyaulax spinifera* species as well as species of the *Spiniferites* genus. In the sediments of the White Sea, they occur occasionally (up to 1%), primarily in the central parts of the sea.

The Dvina Bay with the maximal freshwater input via the Northern Dvina River runoff is characterized by the gradual increase of dinocyst concentrations in surface sediments from 400 to 5×10^3 cyst/g with increase of surface water salinity. The maximal concentrations (up to 20×10^3 cyst/g of dry sediment) were recorded at the exit from the bay toward the Gorlo Strait, where active water exchange with the Barents Sea occurs. Here, the dinocyst assemblages are dominated by the autotrophic species *Operculodinium centrocarpum.* In the bay apex, in the region of the operation of the marginal filter [35, 102], an enhanced concentration (up to 40%) of dinocysts of the heterotrophic species *Islandinium minutum* and *Echinidinium karaense*, whose presence was related to the high water turbidity, and a decrease in the number of autotrophic species were noted.

The Onega Bay is one of the most shallow-water bays of the sea. Its waters are formed under the influence of an intensive Onega River runoff and of the waters of the Basin that penetrate into the most deepwater northern part of the bay via the Zapadnaya Solovetskaya Salma Strait. The waters of the northern part are characterized by a higher salinity (25–26 psu) and a lower temperature. Onega Bay is an estuary with the most complicated mosaic structure of the bottom topography, islands, and water stratification [39, 41]. In this region, the composition of the dinocysts in the surface sediments is completely dominated by the autotrophic cosmopolitan species *Operculodinium centrocarpum*, *Pentapharsodinium dalei*, and *Spiniferites* spp. (up to 50%) at high contents of heterotrophic species such as *Islandinium minutum* and *Polykrikos* sp. Arctic morphotype [23]. The highest concentrations of *Operculodinium centrocarpum* and *Pentapharsodinium dalei* were up to 1,700 cysts/g of dry sediment, and total relative abundances in the sediment associations reached 37%. The concentration of *Spiniferites* species (40–50%) ranged from 0.38×10^3 to 1.4×10^3 cyst/g toward the Solovetsky Islands. The prevalence of autotrophic species in the dinocyst associations of the Onega Bay surface sediments is related to the composition of the phytoplankton and the temperature conditions favorable for the development of dinoflagellates during the vegetative season. Along with this, the raised percentages of the heterotrophic species *Islandinium minutum* and related morphotypes (*I. cezare*, *Echinidinium caraense*) are probably caused by the enhanced concentrations of suspended matter in the frontal river–sea zone, whose surface waters are characterized by high productivity during the vegetative season (see above; [35]).

The Kandalaksha Bay is the most deepwater bay of the White Sea, which is characterized by a relatively calm hydrological regime and a steady water stratification in the summertime [39, 41]. This bay is prominent by the most indented coastline and irregular riverine runoff in different parts. In its water structure, three types of water masses are distinguished, namely, the surface, intermediate, and bottom waters [39, 41]. The dinocyst concentrations in the sediments of the central part of this bay reach 17.1×10^3 cyst/g and increase up to 22×10^3 cyst/g toward the central depression. Photoautotrophic species such as *Operculodinium centrocarpum* and others dominate (up to 76%) in the dinocyst associations from the surface sediments (high AH-ratio), and their total concentrations reach 3×10^3 cyst/g in the sediments from the bay apex and increase up to 13×10^3 cyst/g in the middle, most open part. Heterotrophic species such as *Islandinium minutum* and related morphotypes are also present (up to 18%) in the dinocyst assemblages with the total concentrations up to 2.5×10^3 cyst/g. Cysts of the tropical-boreal species *Polykrikos* sp. Arctic morphotype comprise 1–2%. On the whole, the cysts of heterotrophic species are mainly confined to the shallow-water regions of the bay, in contrast to the cysts of autotrophic species, which are spreading in the open parts of the sea characterized by a higher transparency (low AH-ratio). This is also confirmed by a presence of the *Spiniferites* species (with a total content up to 32% in the dinocyst assemblages) confined to the areas with the minimal suspended matter's concentrations nearby the Solovetsky Islands. This agrees with both satellite and expeditionary data [35]. In the apex of the Kandalaksha Bay, the

heterotrophic *Selenopemphix quanta* occur with relative abundances up to 10% in dinocyst assemblages.

The Basin of the White Sea occupies the central part of the sea with water depths of 100–300 m. The surface sediments of the Basin are characterized by constantly high dinocyst concentrations (>7,000 cyst/g of dry sediment) (Fig. 3a). The photoautotrophic species *Operculodinium centrocarpum*, *Pentapharsodinium dalei*, and others (up to 65% in dinocyst assemblages) and species of the *Spiniferites* genus (up to 40%) dominate marking the zones with the lowest concentrations of suspended matter. In the central part of the Basin, autotrophic *Nematosphaeropsis labyrinthus*, preferred the high water depth [101], generally occur at the highest water depth of the Basin [23].

The principal types of dinocyst assemblages in the surface sediments of the White Sea. An analysis of the species composition of the dinoflagellate cysts and their abundances in the associations of the surface sediments of the White Sea allowed us to distinguish the following principal types of associations, whose spatial distribution is controlled, primarily, by the feeding type and species composition of living dinoflagellates that produce their cysts in the photic layer of the White Sea waters [45, 46].

The autotrophic association includes species of the *Gonyaulacaceae* genus (*Operculodinium centrocarpum*, *Pentapharsodinium dalei, Spiniferites* group, and others), which dominates almost all over the White Sea surface sediments. Their highest relative abundances revealed in the central part of the sea (up to 95%) and in the region adjacent to the Solovetsky Islands (70%), where the minimal concentrations of suspended matter in water were recorded and, therefore, there are the most favorable conditions for photosynthesis.

The heterotrophic association is mainly represented by cysts of the *Protoperidinium* genus: *Islandinium minutum*, *I. cezare*, *Echinidinium karaense*, *Brigantedinium cariacoense*, and *Brigantedinium simplex*. Their highest abundances in the dinocyst associations (up to 47%) are rather clearly confined to the inner parts of bays with shallow unstratified waters and with high water turbidity, first of all, in the regions nearby the Onega and the Northern Dvina Rivers.

4.3 Peculiarities of Microalgae Accumulation under the Marginal Filter Conditions

A recent approach to studying bottom sediments in the White Sea is based on comprehensive analysis of the drainage area – sea system – which has been successfully used in practice by scientists from the Laboratory of Physical Geology Researches of IO RAS since 2000 [36, 37, 103]. The data obtained during this period demonstrate that the transformation of particulate and dissolved matter transported

from drainage basins occurs in the mouth areas of rivers and in bays, which serve as typical marginal filters (MFs) [33, 35–37, 42, 51, 53, 54, 102, 104–110]. These MFs represent a natural system of gravitational, physicochemical (coagulation–adsorption), and biological stages, which successively replace each other with distance from river mouths. One of the main components of suspended matter (SPM) in MFs of the arctic seas is represented by riverine and marine phytoplankton, the accumulation of which, as well as biological water productivity, is controlled by physicochemical processes in the river–sea water mixing zone [7, 18–20, 35, 43, 102, 111, 112, 113].

In this chapter, we present results of a detailed study of microalgae (diatoms and aquatic palynomorphs) distribution in surface bottom sediments of the largest bays of the White Sea and the formation of their assemblages at different MF stages. Diatoms and aquatic palynomorphs (cysts of marine dinoflagellate species and freshwater *Chlorophyceae* algae), which represent reliable indicators of the sea-ice and hydrological regime and depositional environments in the White Sea [7, 17, 19, 23], were the objects of this study.

The examined samples were obtained in bays with different hydrology and physicogeographical conditions (Table 2, Fig. 1), located away from river mouths seaward to 110 km (the Dvina Bay), 160 km (the Onega Bay), and 18 km (the Kemskaya Guba Bay), where water depths attained 75.8, 36.1, and 20.8 m, respectively. The mean interannual summer (April–September) surface water salinity varies from 0 to 26.3 psu, from 0 to 23.4 psu, and from 0 to 26.7 psu in the Dvina and the Onega Bays and the Kemskaya Guba Bay [31, 44], and mean interannual surface summer water temperatures are 2.9–7.6°C, 6.6–11.8°C, and 2.9–7.7°C.

Analysis of the quantitative distribution of diatoms and aquatic palynomorphs in surface sediments of the Dvina and the Onega Bays, and the Kemskaya Guba Bay, and the river estuaries revealed a regular increase in microalgae concentrations in fine-grained sediments (Fig. 4) that was primarily caused by the sizes of dominant diatom (10–100 μm) and dinocysts (32–100 μm) species.

In sediments with content of silty-clay fraction <35–40%, the total abundance of diatoms usually below 0.2×10^6 valves/g dry sediment is sharply increasing by nearly an order of magnitude with growth of the latter up to >40%. Maximum concentrations of diatoms and aquatic palynomorphs (up to 8.6×10^6 valves/g and 19.5×10^3 specimens/g, respectively) were confined to sediments with content of the silty-clay fraction up to 80–100%. The following regional features of diatom and aquatic palynomorph assemblage formation were established in the studied bays.

The Dvina Bay The Dvina Bay annually receives over half the total river runoff into the White Sea mostly due to the Northern Dvina River discharge [110]. The amplitude of tidal changes in sea level in this basin is 0.5–1.2 m. Diatom assemblages in surface sediments of the Northern Dvina River Delta branches under water salinity of ~0 psu are largely represented by freshwater diatoms dominated by planktonic (*Aulacoseira italica*, *A. subarctica*, *A. granulata*) and taxonomically diverse periphytic and benthic (*Staurosira construens*, *Fragilaria capucina*, *Tabellaria flocculosa*, *Amphora ovalis*) species typical of northern rivers

Table 2 Geographic position of analyzed samples of bottom sediments in the Dvina, the Onega, and the Kemskaya Guba Bays of the White Sea, abundances of aquatic palynomorphs (specimens/g dry sediment) and diatoms (valves/g dry sediment), average annual salinity and temperature in surface water layer [31], and grain-size composition of sediments

Station number	Northern latitude, degree	Eastern longitude, degree	Cruise	Abundance of aquatic palynomorphs, specimens/g	Abundance of diatoms, 10^3 valves/g	Water depth, m	Summer *T*, °C	Summer *S*, psu	Sand, %	Silt, %	Clay, %
1	65.04	34.92	EK01	7950.2	3513.5	7.8	6.61	26.647	7.89	36.48	54.85
5	65.01	34.83	EK01	4087.0	3603.4	8.6	6.61	22	29.15	35.93	27.53
9	64.64	40.51	DV08	0.0	972.7	River	–	0	33.12	30.91	28.98
24	65.02	34.84	EK02–1	2434.7	3799.1	8.7	6.61	24	60.57	9.94	25.92
15	64.99	34.8	EK01	583.8	221.2	11	6.61	20	86.19	2.64	8.05
16	64.97	34.8	EK02–1	1619.8	3523.8	5	6.61	20	11.45	8.1	79.17
18	63.96	37.22	EK04	2401.3	82.0	9.5	7.595	24.0405	65.73	1.43	5.05
19	64.13	41.86	DV08	0.0	4475.8	River	–	0	99.35	0.1	0.55
22	64.28	37.8	EK04	4205.8	2039.5	7	7.97	23.254	31.26	15.35	51.09
23	64.07	37.91	EK04	15354.7	4939.0	7.8	8.07	22.9955	17.18	15.36	60.35
25	64.15	41.93	DV08	0.0	4.4	River	–	0	–	–	–
29	64.02	41.77	DV08	0.0	4.0	River	–	0	–	–	–
32	64.12	37.58	EK02–2	9780.2	2031.2	15.8	7.87	23.385	9.11	21.3	67.98
33.1	63.96	37.7	EK02–2	12728.2	182.6	9	8.07	22.9955	86.8	8.74	3.48
40	65.03	34.9	EK02–1	5192.4	2415.5	20.8	6.61	25	17.92	37.44	36.31
43	64.19	37.61	EK02–2	2401.3	3733.3	15.03	7.87	23.385	–	–	–
62	64.82	35.72	EK02–2	7700.9	–	20	6.62	26.3545	39.16	20.29	19.23
75	65.45	39.07	EK02–2	19473.5	4680.8	75.8	6.99	23.815	6.03	16.83	76.61
76	65.28	39.28	EK02–2	12001.2	1706.6	66.2	6.965	23.5215	4.87	3.29	91.45
77	65.14	39.28	EK02–2	2936.7	1185.0	75	7.39	22.706	29.82	16.22	51.3
78	65.08	39.74	EK02–2	17887.3	581.4	31.8	7.375	22.3375	1.51	6.18	92.18
88	64.92	40.03	EK02–2	605.1	750.7	12.7	7.85	20.561	23.47	54.19	22.09
98	63.93	38	EK04	2776.5	305.8	4.2	11.836	12.089	–	–	–

100	63.96	37.96	EK04	3203.7	389.5	3.9	8.215	21.484	–	–	–
101	63.95	37.93	EK04	436.9	74.4	2.7	8.215	21.484	67.36	15.87	8.62
103	63.95	37.9	EK04	5269.4	146.9	4	8.07	22.9955	61.93	9.91	3.44
104	64.01	37.94	EK04	10101.8	2197.1	4.6	8.07	22.9955	13.97	14.71	70.57
105	64.98	34.79	EK04	8270.9	7931.1	3	2.92	17	32.44	25.39	35.82
106	64.96	34.74	EK04	0.0	1647.6	1.1	2.92	8	13.8	3.17	80.47
107	64.97	34.76	EK04	8808.9	8585.3	0.8	2.92	12	3.23	21.11	72.13
108	64.96	34.8	EK04	1315.0	981.5	3.4	2.92	20	38.75	7.09	43.86
109	64.97	34.8	EK04	386.9	1672.5	3.9	2.92	20	44.62	13.83	28.49
4,685	64.7	39.68	PSH01	–	363.4	10	8.275	20.6025	10.45	53.74	35.81
4,694	64.81	39.91	PSH01	4232.8	–	10	7.865	21.089	3.75	17.88	78.38
4,697	65.28	38.91	PSH01	5339.5	1396.5	87	7.015	24.103	3.97	2.14	93.89
4,709	64.59	36.44	PSH01	1368.2	–	56.3	6.945	25.8855	49.56	5.79	32.39
4,712	64.14	37.33	PSH01	596.7	–	36.1	7.685	23.7905	66.38	7.15	23.84
4,713	64.35	36.57	PSH01	–	–	26.7	7.155	25.412	67.57	5.35	21.64
4,714	64.65	35.91	PSH01	5903.8	–	51.9	6.675	26.2825	16.95	16.48	39.44
4,728	65.35	39.36	PSH01	2208.8	795.0	56.5	6.965	23.5215	30.17	25.04	44.4
4,923	64.96	40.08	PSH55	6154.1	4162.6	12	7.85	20.561	2.36	2.85	93.81
4,926	64.63	39.57	PSH55	897.4	361.0	15	8.275	20.6025	–	–	–
108-A	64.96	34.82	EK04	6159.0	3125.8	0.3	2.92	20	10.97	15.84	69.54
25a	64.94	34.63	EK01	–	138.2	2.7	–	0	92.08	1.3	5.9

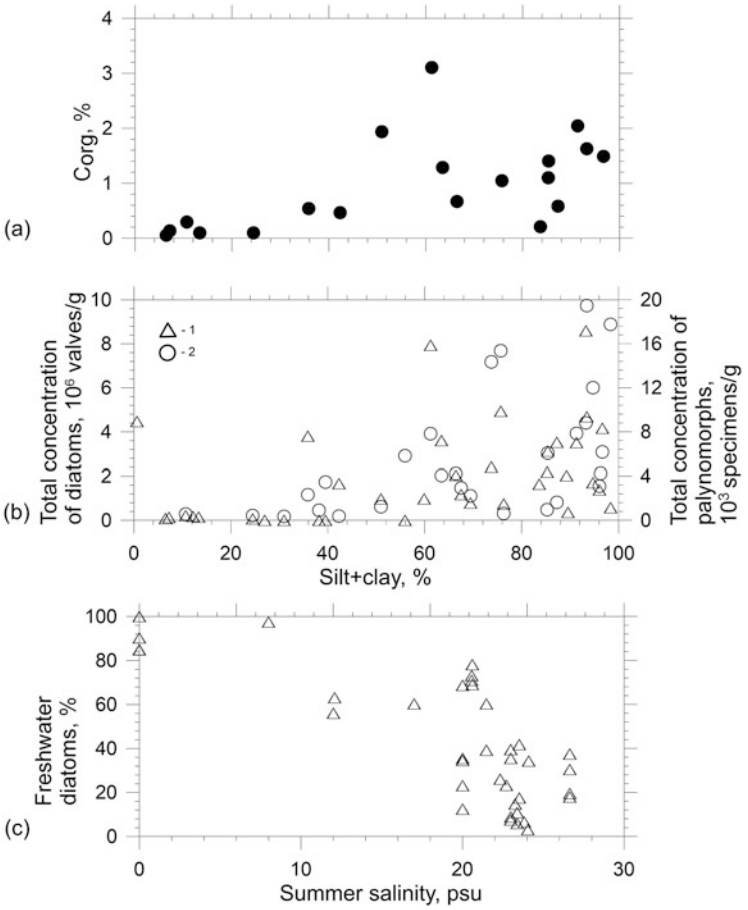

Fig. 4 Correlation of total silt and clay fractions (in %) with (**a**) C_{org} content (%), (**b**) total concentrations of diatoms (1; in 10^6 valves/g sediment) and aquatic palynomorphs (2, in 10^3 specimens/g sediment), (**c**) correlation between average annual summer surface water salinity and content of freshwater diatoms (%) in assemblages from bottom sediments of the Dvina, the Onega, and the Kemskaya Guba Bays

accompanied by single valves of marine taxa. Extremely high concentrations of diatoms (up to 4.4×10^6 valves/g) have been recorded in a bend of the Northern Dvina River (Figs. 4 and 5), likely corresponding to the first (gravitational) MF stage I, which is characterized by slow water flow and avalanche-like accumulation of the terrigenous component of SPM including particulate organic carbon (POC) [102, 114]. This assumption is confirmed by the high content of the sandy fraction (99.4%) in the studied samples.

In the river–sea barrier zone, 15–20 km away from the river mouth, at the water depth of approximately 5 m, the average annual summer water salinity in the surface

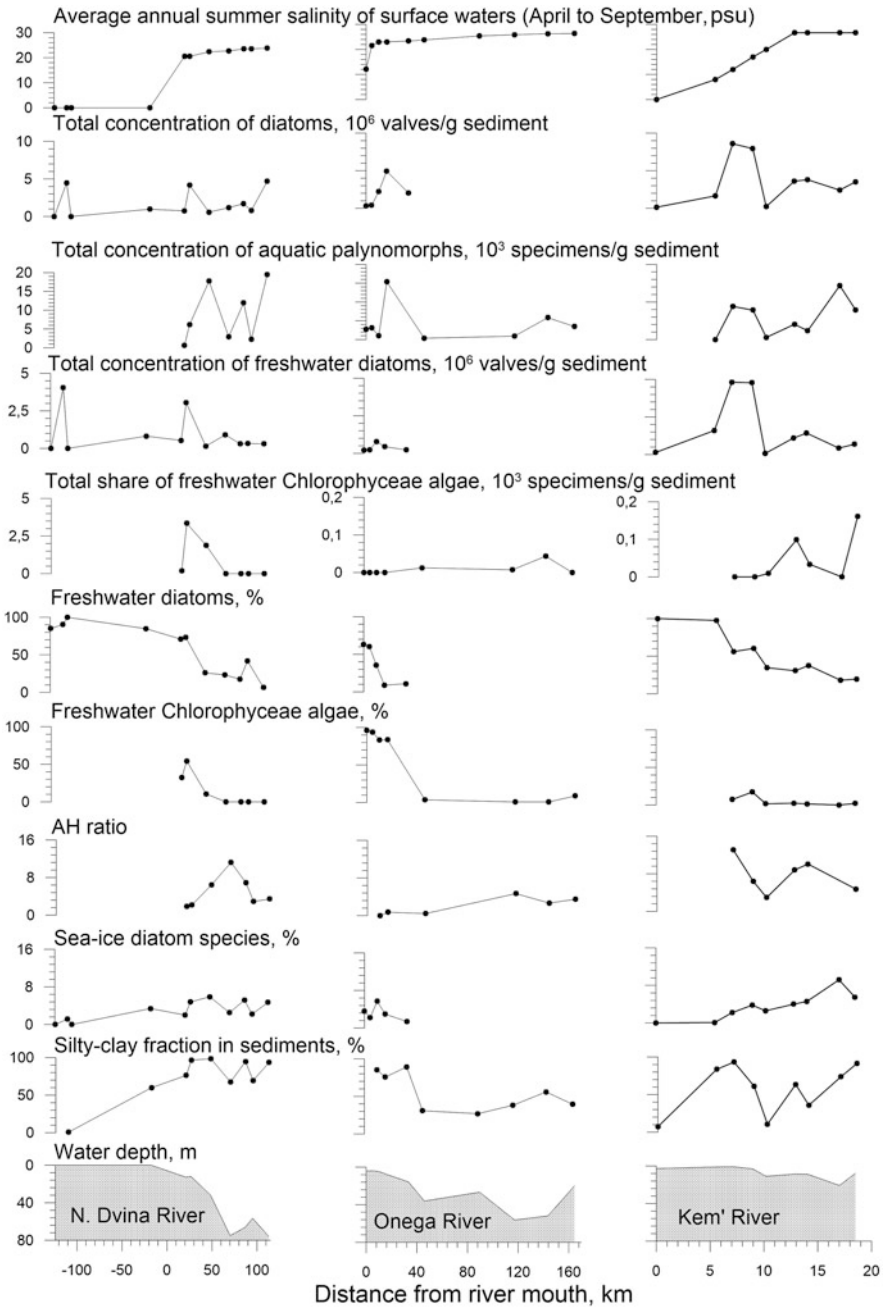

Fig. 5 Correlation between different parameters of microalgae assemblages in bottom sediments of the Dvina, the Onega, and the Kemskaya Guba Bays along land-sea profile

layer increases rapidly up to 18–20 psu. This is accompanied by a sharp decrease in concentration of SPM, which corresponds to the next, physicochemical (or coagulation–adsorption) MF stages II and III [35, 54, 102]. The microalgae assemblages in surface sediments of this area were characterized by low concentrations of diatoms ($<0.75 \times 10^6$ valves/g) and aquatic palynomorphs (<100 specimens/g), which are consistent with their grain size and relatively low content of the silty-clay fraction (50–60%). The diatom assemblages are dominated by freshwater, mostly planktonic riverine species of *Aulacoseira* genus (71–78%, Fig. 5) along with taxonomically diverse benthic forms. The influence of riverine runoff is also reflected in the high relative abundances of freshwater *Chlorophyceae* algae in aquatic palynomorphs assemblages (up to 54%) and CD-ratio (up to 1.2). Marine diatoms are represented mostly by planktonic species of the *Thalassiosira* genus (*T. gravida*, *T. nordenskioeldii*, *T. hyperborea*, *T. lineata*). The total amount of sea-ice diatoms (*Fragilariopsis oceanica*, *Fossula arctica*, *Nitzschia frigida*) has never exceeded 1.5–2.0% (Fig. 5). Aquatic palynomorphs assemblages were dominated by cysts of marine euryhaline heterotrophic dinoflagellate species (*Islandinium minutum*, *Echinidinium karaense*). The AH-ratio values have never exceeded 2.

The most significant changes in concentrations of SPM and composition of microfossil assemblages in bottom sediments have been revealed approximately 26 km from the mouth of the Northern Dvina River, at water depth of 10–15 m. This area, which was characterized over the summer low-water seasons of 2001–2005 by salinity ranging from 19 to 25 psu, exhibits a distinct ($R^2 = 0.80$ for $n = 12$) inverse linear correlation between the volume concentration of SPM and water salinity and a four- to fivefold decrease of the former [54]. SPM was deposited due to coagulation and the biofiltration system of plankton (MF, biological stage IV) [35, 43, 54, 102]. Bottom sediments of this region were characterized by an extremely high content of the silty-clay fraction (up to 96.7%) and the total concentrations of diatoms (up to 4.16×10^6 valves/g) and aquatic palynomorphs (up to 6.15×10^3 specimens/g). It should be noted that microfossil assemblages in the area under consideration exhibit the second maximum of abundances of freshwater diatoms and freshwater green algae, which total concentrations reached 3.04×10^6 valves/g and 3.5×10^3 specimens/g, respectively (Fig. 5).

Seaward of the Northern Dvina mouth, beyond of the coagulation–adsorption MF stages II–III, the surface water salinity varies over a small range (from 22.3 to 23.8 psu) with maximum values in the outer part of the bay. In this salinity range, the SPM concentration increased mostly due to relatively high phytoplankton productivity (MF, biological stages IV–V) [43, 54, 103]. In surface sediments of this region, the content of the silty-clay fraction was usually high (up to 93.4%). The total concentration of marine diatoms, represented predominately by planktonic species (*Thalassiosira antarctica*, *T. baltica*, *T. angulata*, *T. oestrupii*, *Thalassionema nitzschioides*, spores of the *Chaetoceros* genus), reached 4.38×10^6 valves/g sediment, and relative abundances of sea-ice species (*Fragilariopsis cylindrus*, *F. oceanica*, and others) in diatom assemblages composed

4–6%. It should be noted that freshwater diatoms occurred in almost all studied surface sediment samples from this part of the bay that indicates an influx of the Northern Dvina River during the spring flood [35, 54]. The total amount of freshwater diatoms in diatom assemblages did not exceed 6.6%. However, freshwater *Chlorophyceae* algae eliminated almost completely from the surface sediments of this area, and CD-ratio was approximately 0.1–0.5. Concentrations of dinocysts increased up to 19.5×10^3 cysts/g. The values of AH-ratio could be as high as 8–10, reflecting the predominance of cysts of autotrophic dinoflagellate species (*Operculodinium centrocarpum*, *Pentapharsodinium dalei*, *Spiniferites ramosus*).

The Onega Bay The Onega Bay is the largest and shallowest among the others and receives approximately one-third of the entire river runoff into the White Sea. It is characterized by maximum hydrodynamic activity due to tides with an amplitude up to 2.7 m, which results in drainage of a significant part of it during low tide phase [51, 110]. In surface sediments of the Onega River branches, which are active during the low tides, and the adjacent sea shoals, under salinities from 0 to 11.8 psu (Table 2, Fig. 5) [51, 110], the concentrations of aquatic palynomorphs and diatoms were of the lowest values: $<2–3 \times 10^3$ specimens/g and $<0.4 \times 10^6$ valves/g, respectively. The microalgae assemblages are strongly dominated by taxonomically diverse freshwater diatoms (*Aulacoseira italica*, *Fragilaria capucina*, *F. construens*, up to 63%) and *Chlorophyceae* algae (up to 100%) that is a characteristic of the coagulation–adsorption MF stages II–III in the White Sea. The values of CD-ratio are very high – up to 18–20 (Fig. 6).

With increasing distance from the Onega River mouth (about 40 km distance, 10–15 m depth) at the river–sea barrier zone, where the surface water salinity increases up to 21–23 psu, the major part of SPM was deposited, and its concentrations sharply decreased in 10–15 times (coagulation–adsorption stages II-III of MF) [35, 51, 115]. The major bulk of freshwater diatoms and green algae, transported by the river, was deposited within these MF stages. It was realized in sharp decrease of proportions of freshwater algae in the assemblages from surface sediments (down to 8–15% and 20–30%, respectively) and maximum values of the CD-ratio (up to 60). However, unlike the other arctic seas [7], the abundance of freshwater algae in sediments of coagulation–adsorption MF stages in the Onega Bay remains extremely low that is caused most likely by the high intensity of tidal currents.

Moving seaward off the Onega River mouth (up to 160 km) in the study area of the bay with the water depths varied from approximately 20 m in the underwater river channel during low-water period and never exceeded 2.7 m in coastal areas. The mean interannual surface summer water salinity in this area was characterized by insignificant variations (from 21.5 to 23.5 psu), while the total content of the silty-clay fraction in bottom sediments is highly variable, ranging from 13.4 to 89.3%. The maximum concentrations of diatoms (up to 3.7×10^6 valves/g sediment) and aquatic palynomorphs (up to 2.4×10^3 specimens/g) are confined to sediments with the highest content of the silty-clay fraction (up to 75.7%). As opposed to the Dvina Bay, the dominant species in the group of marine diatoms in the headwaters of the Onega Bay was represented by meroplanktonic euryhaline species *Paralia sulcata*

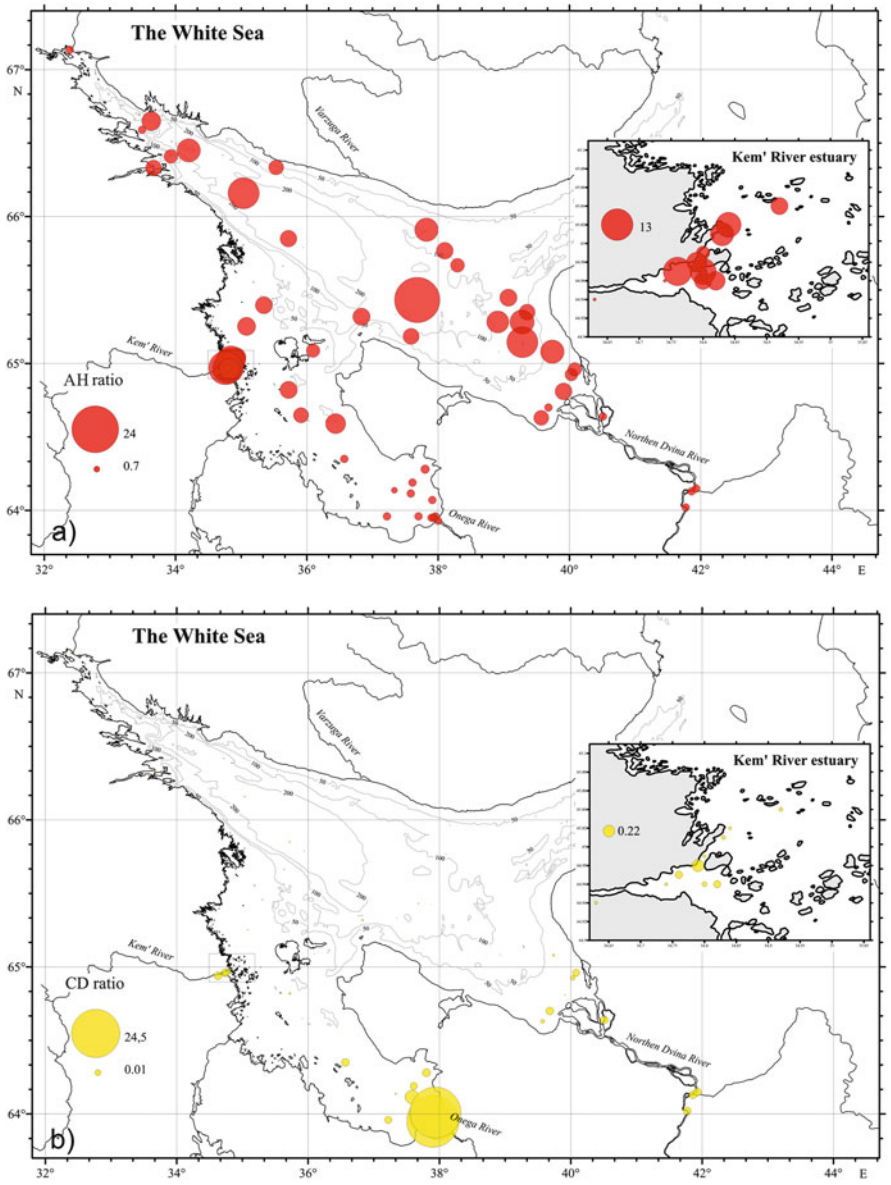

Fig. 6 Distribution of the AH (**a**) and CD (**b**) ratios in aquatic palynomorph assemblages from the White Sea surface sediments

that was caused by high summer heating of the waters (up to 20–22°C) in the shallow Onega Bay [51]. In the outer part of the Onega Bay (up to 160 km away from the mouth, water depths up 36.1 m), microalgae assemblages in bottom sediments

were dominated by cysts of marine dinoflagellates (up to 80%) represented mostly by autotrophic species (up to 4×10^3 cysts/g, AH-ratio 4–5; Fig. 6) *Operculodinium centrocarpum*, *Pentapharsodinium dalei*, and *Spiniferites ramosus.*

The Kemskaya Guba Bay The Kemskaya Guba Bay represented a typical estuary characterized by successive deepening away from the mouth (to 11 m in study area) and mean interannual summer surface water salinity up to 26.7 psu (Fig. 5) [108, 109, 115]. In the mouth of the Kem' River, sandy sediments (sandy fraction up to 92.1%; MF stage I, gravitational) yielded only freshwater periphyton diatoms with total concentrations never exceeding 140×10^3 valves/g (*Tabellaria flocculosa*, *Eunotia pectinalis*, *E. faba*, *Fragilaria capucina*; Fig. 4). In the outer part of the estuary at the river–sea barrier zone, where salinity increased up to 18–22 psu, concentrations of SPM sharply decreased down to <1 mg/l, which corresponded to the coagulation–adsorption stages II–III of the MF [35, 109]. The bottom sediments with content of the silty-clay fraction up to 93.2% were characterized by maximum abundances of diatoms (up to 8.6×10^6 valves/g) and aquatic palynomorphs (to 8.8×10^3 specimens/g). The relative abundances of freshwater species in diatom assemblages decreased gradually from 69 to 13%, as does that of *Chlorophyceae* species. The dinocysts mostly represented by autotrophic species *Operculodinium centrocarpum*, *Pentapharsodinium dalei*, and *Spiniferites ramosus* (AH-ratio up to 11.2–13.0). The marine group of diatom assemblages was dominated by the sublittoral meroplanktonic *Paralia sulcata*, planktonic species of the *Thalassiosira* genus, and relatively abundant (up to 10.3%) sea-ice species *Fossula arctica*, *Fragilariopsis cylindrus*, *Nitzschia frigida*, and *Navicula vanhoeffenii*.

Beyond the estuary (up to 10 km, water depth 5–6 m) in the adjacent part of the sea under surface summer water salinity of 22–27 psu, a general decrease in SPM concentrations was accompanied by a successive increase in the share of POC in its composition (19.0–52.6%) [109], which was characteristic of the MF biological stage IV. The major part of POC was likely composed of marine phytoplankton (diatoms, dinoflagellates), which was evident from the significant increase in their abundance in bottom sediments (up to 3.6×10^6 valves/g and 6.7×10^3 cysts/g, respectively; Figs. 5 and 7).

The assemblages of marine diatoms were dominated (up to 2.8×10^6 valves/g) by planktonic species belonging to the genera *Thalassiosira* (*T. gravida*, *T. nordenskioeldii*, *T. angulata*, *T. oestrupii*, *T. constricta*) and *Coscinodiscus* (*C. oculus-iridis*, *C. radiatus*, *C. asteromphalus*). A notable part of these assemblages was represented by sea-ice species (up to 12%). The dinoflagellate cysts assemblages were characterized by high concentrations of the autotrophic species *Operculodinium centrocarpum* (AH-ratio up to 14).

5 Conclusions

The main results of the study of diatoms and aquatic palynomorphs in surface bottom sediments from various areas of the White Sea are as follows.

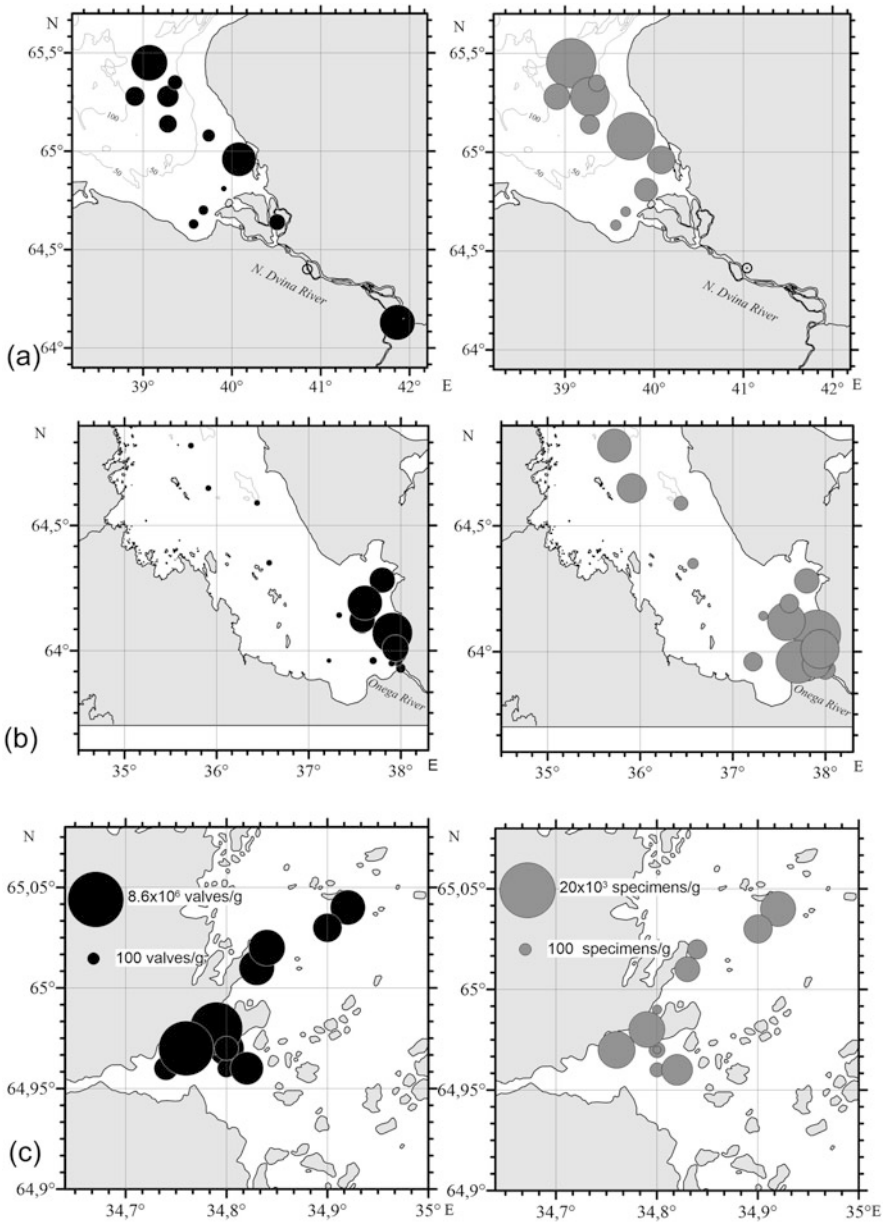

Fig. 7 Distribution of abundance of diatoms (left) and aquatic palynomorphs (right) in bottom sediments of bays in the White Sea: (**a**) Dvina, (**b**) Onega, (**c**) Kemskaya Guba

Data obtained on the distribution of diatoms and aquatic palynomorphs in surface sediments of the bays of the White Sea reflect a consistent mix of sedimentary and biological processes in the bays as they are removed from the mouths of rivers, while an increase in the water salinity has specific regional features. However, despite the existing differences in the quantitative and species composition of the microalgae associations due to the volume of rivers inflow, the depths of the bays and the intensity of the tidal currents, an identical sequence of their changes, are established at different stages of the marginal filter (MF) of rivers.

At the MF gravitational stage I, which is installed in the mouth area rivers, almost exclusively freshwater species of diatoms were encountered, the number of which in individual samples (the Northern Dvina River) reached several million valves/g of dry sediment.

At the MF coagulation–adsorption stage II and III, a sharp decrease in the number and percentage of freshwater diatoms and green algae entering the sea from river flow was observed in the bush area of the bays.

The total diatom content in the surface sediments from these areas in the Dvina and the Onega Bays varies widely, remaining mainly low. It resulted from the high turbidity of water, which prevents vegetation of algae, and the intensity of tidal currents. In the species composition of the group of marine diatoms in the assemblages from the surface sediments, euryhaline species are the most diverse. The dinocyst assemblages are dominated by heterotrophic species. The maximum concentrations of microalgae are confined to sediments with a content of silty-clay fraction >70–80%.

At the MF stage IV, a normal vegetation of marine plankton species proceeds, which is reflected in the composition of microalgae tanatocenoses from bottom sediments.

Acknowledgments We would like to thank the Russian Scientific Foundation (Project No 14-27-00114-P) for the financial support of this research over the period of preparation of this chapter. The micropaleontological investigations were made in the framework of the state assignment of FASO Russia (theme No. 0149-2018-0016), supported in part by basic research program of the RAS Presidium (project by Novichkova Ye.A.). The authors are grateful to Academician A.P. Lisitzin for general leadership; scientists from the Laboratory of Physical Geology Researches of the P.P. Shirshov Institute of Oceanology RAS for different advices; the crew of the R/V "Ecolog," R/V "Professor Stokman," and R/V "Ivan Petrov"; and all participants of the voyages for cooperation.

Appendix 1

Photomicrographs of *Operculodinium centrocarpum* (a–c) from the White Sea (st. 6062; central body maximum diameter 45 μm); *Operculodinium centrocarpum* short process (d, e; st. 6050; central body maximum diameter 45 μm); cyst of *Pentapharsodinium dalei* (f; st. 6050; central body maximum diameter 30 μm);

Echinidinium karaense (g–i; st. 6050; central body maximum diameter 31 μm); *Spiniferites ramosus* (j–l; st. 6050; central body length 40 μm).

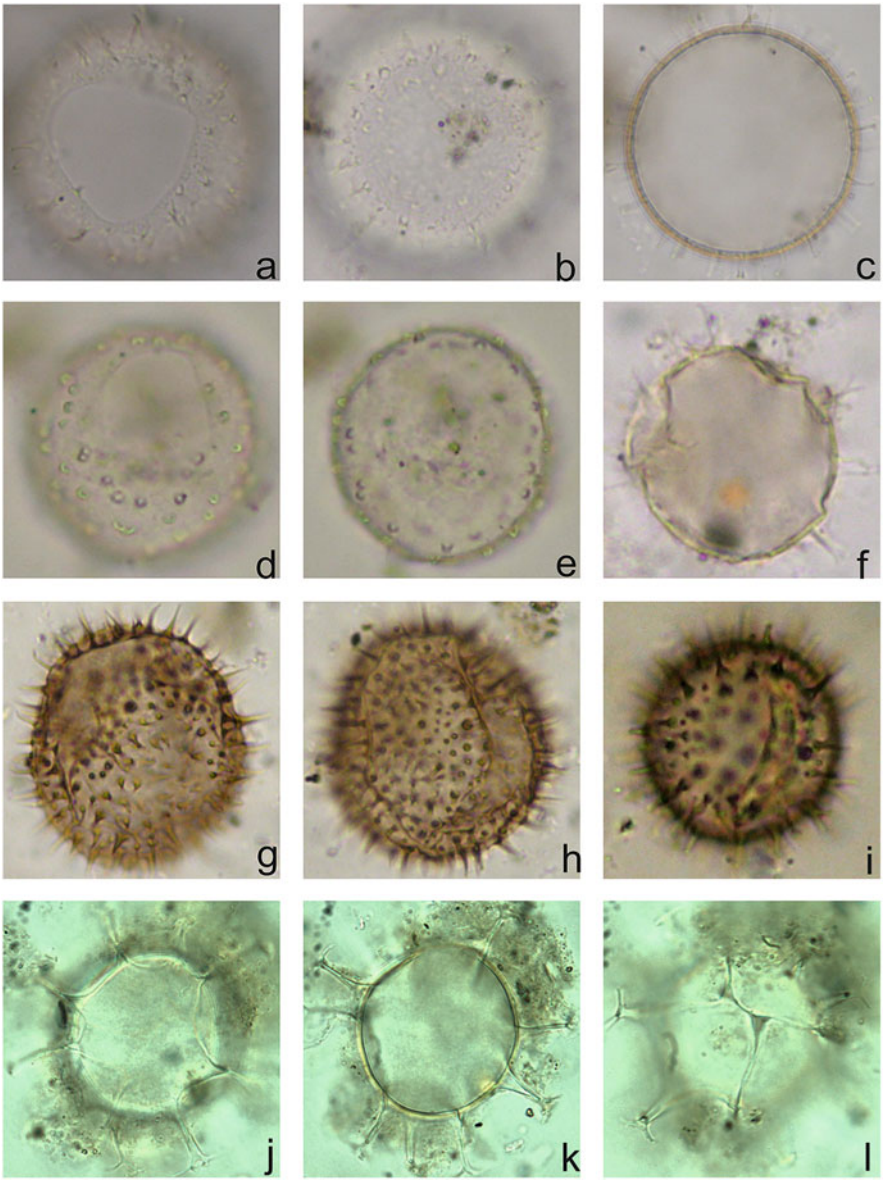

Appendix 2

Photomicrographs of *Bitectatodinium tepikiense* (a, b; st. 6062; central body maximum diameter 45 μm); *Selenopemphis quanta* (c; st. 6050; central body width 82 μm); *Operculodinium centrocarpum* Arctic morphotype (d; st. 6050; central body maximum diameter 35 μm); *Brigantedinium simplex* (e; st. 6050; central body diameter 45 μm); *Brigantedinium cariacoense* (f; st. 6050; diameter 53 μm); *Spiniferites elongates* (g–i; st. 6050; central body length 62 μm); *Pediastrum kawraiskyi* (j); *Pediastrum boryanum* (k), remains of foraminifer linings (l); *Botryococcus* cf. *braunii* (m).

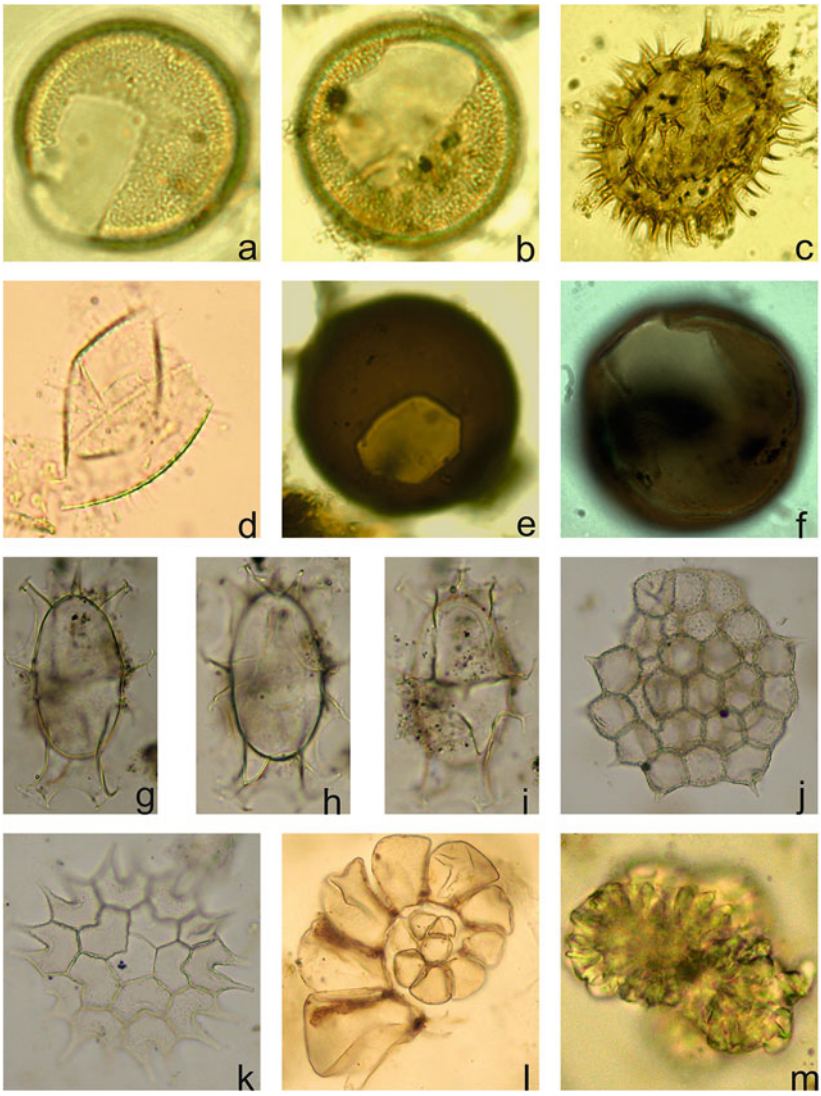

References

1. Crosta X, Koç N (2010) Diatoms: from micropaleontology to isotope geochemistry. In: Hillaire-Marcel C, de Vernal A (eds) Proxies in late Cenozoic paleoceanography. Elsevier, Amsterdam, pp 327–370
2. de Vernal A, Marret F (2010) Organic-walled dinoflagellate cysts: tracers of sea-surface conditions. In: Hillaire-Marcel C, de Vernal A (eds) Proxies in late Cenozoic paleoceanography. Elsevier, Amsterdam, pp 371–408
3. Polyakova YI (2010) Diatom analysis. In: Kaplin PA, Yanina TA (eds) Methods of paleogeographic reconstructions. Geographical Faculty of MSU, Moscow, pp 126–160 (in Russian)
4. Polyakova YI, Novichkova YA, Klyuvitkina TS (2010) Analysis of aquatic palynomorphs. In: Kaplin PA, Yanina TA (eds) Methods of paleogeographic reconstructions. Geographical Faculty of MSU, Moscow, pp 103–125 (in Russian)
5. Polyakova YI (1997) The Eurasian Arctic seas during the late Cenozoic. Scientific World, Moscow, 146 pp (in Russian)
6. Polyakova YI (2001) Late Cenozoic evolution of Northern Eurasian marginal seas based on diatom records. Polarforschung 69:211–220
7. Polyakova YI (2003) Diatom assemblages in the surface sediments of the Kara Sea (Siberian Arctic) and their relationship to oceanological conditions. In: Stein R, Fahl K, Fütterer DK, Galimov EM, Stepanets OV (eds) Siberian river run-off in the Kara Sea: characterization, quantification, variability, and environmental significance. Proceedings in marine sciences. Elsevier, Amsterdam, pp 375–400
8. de Vernal A, Henry M, Matthiessen J, Mudie PJ, Rochon A, Boessenkool KP, Eynaud F, Grosfjeld K, Guiot J, Hamel D, Harland R, Head MJ, Kunz-Pirrung M, Levac E, Loucheur V, Peyron O, Pospelova V, Radi T, Turon JL, Voronina E (2001) Dinoflagellate cyst assemblages as tracers of sea-surface conditions in the northern North Atlantic, Arctic and sub-Arctic seas: the new n=677 data base and its application for quantitative palaeoceanographic reconstruction. J Quaternary Sci 16:681–698
9. de Vernal A, Rochon A, Fréchette B, Henry M, Radi T, Solignac S (2013) Reconstructing past sea ice cover of the northern hemisphere from dinocyst assemblages: status of the approach. Quat Sci Rev 79:122–134
10. Matthiessen J, Kunz-Pirrung M, Mudie PJ (2000) Freshwater chlorophycean algae in recent marine sediments of the Beaufort, Laptev and Kara seas (Arctic Ocean) as indicators of river runoff. Int J Earth Sci 89:470–485
11. Matthiessen J, de Vernal A, Head M, Okolodkov Yu, Zonneveld K, Harland R (2005) Modern organic-walled dinoflagellate cysts in Arctic marine environments and their paleoenvironmental significance. Palaeontol Zietsch 79(1):3–51
12. Armand LK, Leventer A (2010) Palaeo sea ice distribution and reconstruction derived from the geological records. Chapter 13. In: Thomas DN, Dieckmann GS GS (eds) Sea ice. 2nd edn. Wiley-Blackwell, Oxford, pp 469–530
13. Stein R, Fahl K, Müller J (2012) Proxy reconstruction of Cenozoic Arctic Ocean sea-ice history – from IRD to IP25. Polarforschung 82(1):37–71
14. Zabelina MM (1939) Diatoms from the bottom of the White Sea in the region of the small Pir'yu-Guba. Proc State Hydrol Inst 8(17):183–200 (in Russian)
15. Dzhinoridze RN (1972) Diatoms in the surface sediments of the White Sea. Dokl Earth Sci 204 (1):207–209 (in Russian)
16. Nevesskii EN, Medvedev VS, Kalinenko VV (1977) The White Sea. Sedimentogenesis and history of development in Holocene. Nauka, Moscow 236 pp (in Russian)
17. Polyakova YI, Dzhinoridze RN, Novichkova TS, Golovnina EA (2003) Diatoms and palynomorphs in the White Sea sediments as indicators of ice and hydrological conditions. Oceanology 43(Suppl):144–158

18. Novichkova EA, Polyakova YI (2013) Associations of microalgae in bottom sediments of marginal filters areas (White Sea bays). Dokl Earth Sci 449(2):413–417
19. Polyakova YI, Novichkova YA, Lisitzin AP, Shevchenko VP, Kravchishina MD (2016) Diatoms and aquatic palynomorphs in surface sediments of the White Sea bays as indicators of sedimentation in marginal filters of rivers. Oceanology 56(2):289–300
20. Polyakova YI, Novichkova YA, Klyuvitkina TS (2017) Diatoms and palynomorphs in surface sediments of the Arctic seas and their significance for paleoceanological studies at high latitudes In: Lisitsyn AP, Shevchenko VP, Vorontsova VG (eds) The White Sea system. Vol IV the processes of sedimentation, geology and history. Scientific World, Moscow, pp 796–859 (in Russian)
21. Novichkova EA (2008) Postglacial history of the White Sea based on aquatic and terrestrial palynomorph investigations. PhD thesis. MSU, 262 pp
22. Golovnina EA, Polyakova EI (2005) Dinoflagellate cysts in the bottom sediments of the White Sea (western Arctic). Dokl Eath Sci 400(1):136–139 (in Russian)
23. Novichkova EA, Polyakova YI (2007) Dinoflagellate cysts in the surface sediments of the White Sea. Oceanology 47(5):660–670
24. Battarbee RW (1973) A new method for estimation of absolute microfossil numbers, with reference especially to diatoms. Limnol Oceanogr 18(4):647–653
25. Stockmarr J (1971) Tablets with spores used in absolute pollen analysis. Pollen Spores 13 (4):616–621
26. Dale B (1976) Cyst formation, sedimentation, and preservation: factors affecting dinoflagellate assemblages in recent sediments from Trondheimsfjord, Norway. Rev Palaeobot Palynol 22:39–60
27. Pospelova V, Esenkulova S, Johannessen SC, O'Brien MC, Macdonald RW (2010) Organic-walled dinoflagellate cyst production, composition and flux from 1996 to 1998 in the central strait of Georgia (BC, Canada): a sediment trap study. Mar Micropaleontol 75:17–37
28. Zonneveld KAF (1997) Dinoflagellate cyst distribution in surface sediments from the Arabian Sea (northwestern Indian Ocean) in relation to temperature and salinity gradients in the upper water column. Deep Res Part II Top Stud Oceanogr 44:1411–1443
29. Bauch HA, Polyakova YI (2003) Diatom-inferred salinity records from the Arctic Siberian margin: implications for fluvial runoff patterns during the Holocene. Paleoceanography 18:1–10
30. Klyuvitkina TS, Bauch HA (2006) Hydrological changes in the Laptev Sea during the Holocene inferred from the studies of aquatic palynomorphs. Oceanology 46(6):859–868
31. World Ocean Atlas (2013) In: Boyer T (ed) Mishonov A, Technical Ed., Product documentation. 14 pp
32. Petelin VP (1967) Grain-size analysis of sea bottom sediments. Nauka, Moscow 128 p. (in Russian)
33. Demina LL, Filip'eva KV, Shevchenko VP, Novigatskii AN, Filippov AS (2005) Geochemistry of the bottom sediments in the mixing zone of the Kem' River with the White Sea. Oceanology 45(6):805–818
34. Berger VY, Naumov AD (2000) General features of the White Sea. Morphology, sediments, hydrology, oxygen conditions, nutrients and organic matter. Berichte zur Polarfoschung 359:3–9
35. Lisitzin AP, Shevchenko VP, Burenkov VI, Kopelevich OV, Vasil'ev LY (2003) Suspended matter and hydrooptics of the White Sea: new patterns of quantitative distribution and grain-size analysis. In: Laverov NP (ed) Actual problems of oceanology, pp 554–608 (in Russian)
36. Lisitsyn AP (2010) The processes in the White Sea catchment area: preparation, transfer and sedimentation of matter, flows of matter, and the concept of "living watershed". In: Lisitsyn AP, Nemirovskaia IA (eds) The White Sea system. Vol I natural environment of the catchment area of the White Sea. Scientific World, Moscow, pp 353–445 (in Russian)
37. Lisitsyn AP (2012) Dispersed sedimentary substance in the earth geospheres and in the White Sea system. In: Lisitsyn AP, Nemirovskaya IA (eds) The White Sea system. Vol II water

column and interacting with it atmosphere, cryosphere, river runoff and biosphere. Scientific World, Moscow, pp 19–48 (in Russian)
38. Gordeev VV (2004) Rivers of Russian Arctic: flows of sediments from continent to the ocean. New ideas in oceanology. Vol II. Nauka, Moscow, pp 113–166 (in Russian)
39. Pantyulin AN (2003) Hydrological system of the White Sea. Oceanology 43(Suppl):1–14
40. Pantyulin AN (2012) Ice cover and ice of the White Sea after the observation data. In: Lisitsyn AP, Nemirovskaya IA (eds) The White Sea system. Vol II water column and interacting with it atmosphere, cryosphere, river runoff and biosphere. Scientific World, Moscow, pp 120–132 (in Russian)
41. Pantyulin AN (2012) The features of the White Sea physics – dynamics, structure and water masses. In: Lisitsyn AP, Nemirovskaya IA (eds) (2012) The White Sea system. Vol II water column and interacting with it atmosphere, cryosphere, river runoff and biosphere. Scientific World, Moscow, pp 309–378 (in Russian)
42. Lisitsyn AP, Nemirovskaya IA (eds) (2012) The White Sea system. Vol II water column and interacting with it atmosphere, cryosphere, river runoff and biosphere. Scientific World, Moscow, 783 pp (in Russian)
43. Lisitzin AP (2009) Biofilters of the Arctic Ocean and processes of sedimentation. In: Kassens H, Lisitzin AP, Thiede J, Polyakova YeI, Timokhov LA, Frolov IE (eds) System of the Laptev Sea and the adjacent Arctic seas: modern and past environments. Moscow University Press, Moscow, pp 71–121 (in Russian)
44. Hydrometeorology and Hydrochemistry of the USSR Seas (1991) The White Sea: hydrometeorological conditions. Gidrometeoizdat, Leningrad, 240 pp (in Russian)
45. Rat'kova TN (2000) The White Sea basin phytoplankton – a review. Berichte zur Polarforschung 359:3–29
46. Rat'kova TN (2000) Phytoplankton composition in the White Sea basin in summer-autumn 1998 and 1999. Berichte zur Polarforschung 359:97–100
47. Sapojhnikov VV, Arjhanova NO, Mordasova NV (2012) Hydrochemical features of bioproductivity and production-destructive processes in the White Sea. In: Lisitsyn AP, Nemirovskaya IA (eds) The White Sea system. Vol II water column and interacting with it atmosphere, cryosphere, the river runoff and the biosphere. Scientific World, Moscow, pp 433–472 (in Russian)
48. Aagaard K, Carmack EC (1994) The Arctic Ocean and climate: a perspective. The polar oceans and the role in shaping the global environmental: the Nansen centennial volume. Geophys Monogr Am Geophys Union 85:5–20
49. Maksimova MP (2004) Comparative hydrochemistry of seas. New ideas in oceanology, vol I. Nauka, Moscow, pp 168–189 (in Russian)
50. Il'yash LV, Zhitina LS, Fedorov VD (2003) Phytoplankton of the White Sea. Yanus-K, Moscow 168 pp (in Russian)
51. Dolotov YS, Filatov NN, Shevchenko VP, Petrov MP, Tolstikov AV, Zdorovennov RE, Platonov AV, Filippov AS, Bushuev KL, Kutcheva IP, Denisenko NV, Stein R, Saukel C (2008) Multidisciplinary studies in Onega Bay of the White Sea and the estuary of the Onega River during the summer period. Oceanology 48:255–267
52. Il'yash LV, Rat'kova TN, Radchenko IG, Zhitina LS (2012) Phytoplankton of the White Sea. In: Lisitsyn AP, Nemirovskaia IA (eds) The White Sea system. Vol II water column and interacting with the atmosphere, cryosphere, the river runoff and the biosphere. Scientific World, Moscow, pp 605–640 (in Russian)
53. Kravchishina MD, Shevchenko VP, Filippov AS, Novigatskii AN, Dara OM, Alekseeva TN, Bobrov VA (2010) Composition of the suspended particulate matter at the Severnaya Dvina River mouth (White Sea) during the spring flood period. Oceanology 50(3):396–416
54. Kravchishina MD, Lisitzin AP (2011) Grain-size composition of the suspended particulate matter in the marginal filter of the Severnaya Dvina River. Oceanology 51(1):89–104

55. Kiselev IA (1925) The phytoplankton of the White Sea. Proc RGI 105(2):1–38 (in Russian)
56. Kiselev IA (1950) Dinoflagellates of the USSR seas and freshwater basins. Nauka, Moscow 280 p (in Russian)
57. Merezhkovsky KS (1878) Diatoms of the White Sea. Proc St Petersburg Soc Nat 425–446 (in Russian)
58. Reingard L (1882) Zur Kenntnis der Bacillariaceen des Weissen meres. Bulletin de la Societe Imperial des Naturalists 5(57):297–304
59. Levander KM (1916) Zur Kenntnis des Kustenplanktons im Weissen Meere Meddelanden af Societans pro Fauna Fennica 42:150–158
60. Semina GI, Sergeeva OM (1983) Planktonic flora and biogeographical characteristics of the White Sea phytoplankton. Plankton 1:3–17 (in Russian)
61. Matishov GG (1997) Plankton of the sea of the western Arctic. Kola Science Centre RAS, Apatity, 352 pp (in Russian)
62. Kuznetsov LL, Shoshina EV (2003) Phytocenoses of the Barents Sea (physiological and structural characteristics). Kola Scientific Center RAS, Apatity, 308 pp (in Russian)
63. Zhitina LS, Mikhailovsky GE (1990) Ice and planktonic flora of the White Sea as an object of monitoring. Biological monitoring of the coastal waters of the White Sea. Nauka, Moscow, pp 37–41 (in Russian)
64. Mikhailovsky GE, Zhitina LS (1989) Cryoplankton flora of the White Sea and its seasonal dynamics, revealed by the methods of correlation analysis. Oceanology 29(5):796–803 (in Russian)
65. Kravchishina MD, Burenkov VI, Kopelevich OV, Sheberstov SV, Vazyulya SV, Politova NV, Novigatsky AN, Filippov AS, Shevchenko OV (2011) Spatial and temporal variability of chlorophyll "a" in the White Sea in 2003-2010 from satellite and ship data. Proceedings of the VI international conference "Current problems in optics of natural waters". Nauka, St Petersburg, pp 82–85
66. Kravchishina MD, Lisitzin AP (2013) Pigments of phytoplankton as an indicator of the biogenic part of the dispersed sedimentary matter. In: Lisitsyn AP, Nemirovskaya IA (eds) The White Sea system. Vol III dispersed sedimentary matter in hydrosphere, microbial processes and water pollution. Scientific World, Moscow, pp 169–170
67. Poulin M, Daugbjerg N, Gradinger R, Ilyash L, Ratkova T, von Quillfeldt C (2011) The pan-Arctic biodiversity of marine pelagic and sea-ice unicellular eukaryotes: a first-attempt assessment. Mar Biodivers 41(1):13–28. https://doi.org/10.1007/s12526-010-0058-8
68. Sajin AF, Rat'kova TN (2012) Inhabitants of the White Sea seasonal ice In: Lisitsyn AP, Nemirovskaya IA (eds) The White Sea system. Vol II water column and interacting with it the atmosphere, cryosphere, the river runoff and the biosphere. Scientific World, Moscow, pp 201–224 (in Russian)
69. Zhitina LS, Il'yash LV (2010) Species composition of ice diatoms of the seas of the Russian Arctic. Arctic Antarctic 7(41):115–149 (in Russian)
70. Rat'kova TN, Wassmann P (2005) Sea-ice algae in the White Sea and the Barents Sea: composition and origin. Polar Res 24:95–110
71. Usachev PI (1949) Microflora of polar ice. Proc Inst Oceanol USSR Acad Sci 3:216–259 (in Russian)
72. Melnikov IA (1997) The Arctic Sea ice ecosystem. Gordon and Breach Science Publishers, Amsterdam, 204 pp
73. Horner R (1989) Arctic Sea-ice biota. In: Herman Y (ed) The Arctic seas. Climatology, oceanography. geology, and biology. Van Nostrand Reinhold Company, New York, pp 123–146
74. Horner R (1990) Ice-associated ecosystems. In: Medlin LK, Priddle J (eds) Polar marine diatoms. British Antarctic Survey, Cambridge, pp 19–23

75. Syvertsen EE (1991) Ice algae in the Barents Sea: types of assemblages, origin, fate and role in the ice-edge phytoplankton bloom. Polar Res 10(1):277–287
76. Von Quillfeldt CH (1997) Distribution of diatoms in the northeast water polynya, Greenland. J Mar Syst 10:211–240
77. Okolodkov YB (1992) Cryopelagic flora of the Chukchi, East Siberian and Laptev Seas. Polar Biol 5:28–43
78. Gogorev RM (1998) Diatom algae from the late spring sea ice of the White Sea. Bull Systemat Inferior Plants 32:8–13
79. Melnikov IA, Zhitina LS, Kolosova EG, Shanin CS (2003) Dynamics of ecological-biochemical characteristics of sea ice in the coastal zone of the White Sea. Izv Akad Nauk Ser Biol 3:235–242 (in Russian)
80. Melnikov IA, Dikarev SN, Egorov VG, Kolosova EG, Zhitina LS (2005) Structure of the coastal ice ecosystem in the zone of sea-river interactions. Oceanology 45(4):511–519
81. Shevchenko VP, Filippov AS, Novigatsky AN, Gordeev VV, Gorynova NV, Demina LL (2012) In: Dispersed sedimentary substance of freshwater and sea ices In, Lisitsyn AP, Nemirovskaya IA (eds) The White Sea system. Vol II. Water column and interacting with it the atmosphere, cryosphere, the river runoff and the biosphere. Scientific World, Moscow, pp 169–200 (in Russian)
82. Legendre L, Ackley SF, Dieckmann GS, Gulliksen B, Horner R, Hoshiai T, Melnikov IA, Reeburgh WS, Spindler M, Sullivan CW (1992) Ecology of sea ice biota. Global significance. Polar Biol 12:429–444
83. Lalande C, Nöthig E-M, Somavilla R, Bauerfeind E, Shevchenko V, Okolodkov Y (2014) Variability in under-ice export fluxes of biogenic matter in the Arctic Ocean. Global Biogeochem Cycles 28:1–13
84. Beklemishev KB, Semina GI (1986) Geography of plankton diatoms of high and moderate latitudes of the world ocean. Proc All-Union Hydrobiol Soc 27:7–23 (in Russian)
85. Semina HI (1997) An outline of the geographical distribution of oceanic phytoplankton. Adv Mar Biol 32:527–563
86. Bondarchuk LL, Zernova VV, Koltsova TI (1985) Diatoms of some Arctic shelf regions: ecology of fauna and flora of coastal ocean zones. Nauka, Moscow, pp 74–93 (in Russian)
87. Sergeeva OM (1991) Distribution of phytoplankton in the basin of the White Sea in July 1972 and in August 1973. Phytoplankton research in the monitoring system of the Baltic Sea and other seas of the USSR. Gidrometeoizdat, Moscow, pp 82–94 (in Russian)
88. Okolodkov YB, Dodge JD (1996) Biodiversity and biogeography of planktonic dinoflagellates in the Arctic Ocean. J Exp Mar Biol 202:19–27
89. Okolodkov YB (2000) Dinoflagellate (Dinophyceae) of the seas of the Eurasian Arctic. Abstract of Disser. Dr. Biol. Scie. Komarov Botanical Institute RAS. St Petersburg, 50 pp (in Russian)
90. Tuschling K, Juterzenka von K, Okolodkov Y, Anoshkin A (2000) Composition and distribution of the pelagic and sympagic algal assemblages in the Laptev Sea during autumnal freeze-up. J Plankton Res 22(5):843–864
91. Okolodkov YB (1999) An ice-bound planktonic dinoflagellate *Peridiniella catenata* (Levander) Balech: morphology, ecology and distribution. Bot Mar 42:333–341
92. Bérard-Therriault L, Poulin M, Bossé L (1999) Guide d'identification du phytoplankton marin de l'estuaire et du golfe du Saint-Laurent incluant également certains protozoaires. Can Spec Publ Fish Aquat Sci 128:387
93. Montresor M, Lovejoy C, Orsini L, Procaccini G, Roy S (2003) Bipolar distribution of the cyst-forming dinoflagellate *Polarella glacialis*. Polar Biol 26:186–194
94. Montresor M, Procaccini G, Stoecker DK (1999) *Polarella glacialis*, Gen. Nov., Sp. Nov. (*Dinophyceae*): Suessiaceae are still alive! J Phycol 35:186–197
95. Fensome RA, Taylor FJR, Norris G, Sarjeant WAS, Wharton DI, Williams GL (1993) A classification of living and fossil dinoflagellates. Micropaleon Spec Publ 7:1–315

96. Simonsen R (1962) Untersuchungen zur Systematik und Ökologie der Bodendiatomeen der westlichen Ostsee. International der Gesamten Hydrobiologie. Systematische Beihefte 1:9–148
97. Pankow H (1990) Ostsee-Algenflora. Gustav Fischer Verlag, Jena 648 pp
98. Konovalova GV (1998) The Dinoflagellates (Dinophyta) of the eastern seas of Russia and adjacent seas of the Pacific Ocean. Dalnauka, Vladivostok, 300 pp (in Russian)
99. Zonneveld KAF, Marret F, Versteegh GJM, Bogus K, Bonnet S, Bouimetarhan I, Crouch E, de Vernal A, Elshanawany R, Edwards L, Esper O, Forke S, Grøsfjeld K, Henry M, Holzwarth U, Kielt JF, Kim SY, Ladouceur S, Ledu D, Chen L, Limoges A, Londeix L, Lu SH, Mahmoud MS, Marino G, Matsouka K, Matthiessen J, Mildenhal DC, Mudie P, Neil HL, Pospelova V, Qi Y, Radi T, Richerol T, Rochon A, Sangiorgi F, Solignac S, Turon JL, Verleye T, Wang Y, Wang Z, Young M (2013) Atlas of modern dinoflagellate cyst distribution based on 2405 data points. Rev Palaeobot Palynol 191:1–197
100. Rochon A, de Vernal A, Turon J-L, Matthiessen J, Head MJ (1999) Distribution of dinoflagellate cysts in surface sediments from the North Atlantic Ocean and adjacent basins and quantitative reconstruction of sea-surface parameters. Am Assoc Stratigraphic Palynologists Contrib Series 35, 146 p
101. Marret F, Zonneveld KAF (2003) Atlas of modern organic-walled dinoflagellate cyst distribution. Rev Palaeobot Palynol 125:1–200
102. Lisitzin AP (1995) Marginal filter in the oceans. Oceanology 34(5):671–682
103. Lisitzin AP (2014) Modern concept about sedimentation in the oceans and seas. An ocean as the natural chronicle of geosphere interaction in the earth. In: Lobkovskii LI, Lisitzin AP (eds) The World Ocean physics, chemistry, and biology of an ocean. Sedimentation in the ocean and interaction of geospheres of the earth. Scientific World, Moscow, pp 331–548 (in Russian)
104. Lisitsyn AP, Nemirivskaya IA (eds) (2010) The White Sea system. Vol I natural environment of the catchment area of the White Sea. Scientific World, Moscow, 480 pp (in Russian)
105. Lisitsyn AP, Nemirovskaya IA (eds) (2013) The White Sea System. Vol III dispersed sedimentary hydrosphere material, microbial processes and pollution. Scientific World, Moscow, 668 pp (in Russian)
106. Lisitsyn AP, Shevchenko VP, Vorontsova VG (eds) (2017) The White Sea system. Vol IV the processes of sedimentation, geology and history, Scientific World, Moscow, 1030 pp (in Russian)
107. Kravchishina MD, Shevchenko VP (2005) First determinations of the grain-size composition of suspended particulate matter in the White Sea. Dokl Earth Sci 400(1):140–144
108. Shevchenko VP, Lisitzin AP, Belyaev NA, Filippov AS, Golovnina EA, Ivanov AA, Klyuvitkin AA, Malinkovich SM, Novigatsky AN, Politova NV, Rudakova VN, Sherbak SS (2004) Seasonality of suspended particulate matter distribution in the White Sea. Berichte zur Polar-und Meeresforschung 482:142
109. Shevchenko VP, Dolotov YuS, Filatov NN, Alexseeva TN, Nöthig E-M, Filippov AS, Novigatsky AN, Pautova LA, Platonov AV, Politova NV, Rat'kova TN, Stein R (2005) Biogeochemistry of Kem' estuarine zone, White Sea (Russia). Hydrol Earth Syst Sci 9:57–66
110. Shevchenko VP, Filippov AS, Lisitsyn AP, Zolotykh EO, Isaeva AB, Kravchishina MD, Novigatsky AN, Politova NV, Pokrovsky OS, Bobrov VA, Bogunov AY, Kokryatskaya NM, Zavernina NN, Korobov VB (2010) On the elemental composition of suspended matter of the Severnaia Dvina River (White Sea region). Dokl Earth Sci 430(2):228–234
111. Polyakova YeI, Kassens H, Stein R, Bauch H (2009) Diatoms in the Siberian Arctic seas as indicators of postglacial changes of the riverine discharge, ice-hydrological regime, and sedimentary environments on the shelf. In: Kassens H, Lisitzin AP, Thiede J, Polyakova YeI, Timokhov LA, Frolov EI (eds) System of the Laptev Sea and the adjacent Arctic seas. Modern and past environments. Moscow University Press, Moscow, pp 427–447 (in Russian)
112. Stein R, Dittmers K, Fahl K, Kraus M, Matthiessen J, Niessen F, Pirrung M, Polyakova YeI, Schoster F, Steinke T, Fütterer DK (2004) Arctic (palaeo) river discharge and environmental change: evidence from the Holocene Kara Sea sedimentary record. Quat Sci Rev 23:1485–1511

113. Stein R (2008) Arctic ocean sediments processes, proxies and paleoenvironment. Elsevier, Amsterdam, 592 pp
114. Romankevich EA, Vetrov AA (2001) The carbon cycle in the Arctic seas of Russia. Nauka, Moscow, 301 pp (in Russian)
115. Dolotov YS, Rimskii-Korsakov NA, Telikovskii AA, Pronin AA, Novigatskii AN, Filippov AS, Petrov MP, Tolstikov AV, Dunchevskii AS (2005) Bottom topography, bottom sediments, and structure of the sedimentary sequence in different zones of the Kem' River Estuary (White Sea). Oceanology 45(6):877–884

Mineral Composition of Pelitic Fraction of Dispersed and Consolidated Sedimentary Matter in the White Sea

Olga M. Dara

Contents

Abstract Investigation of sedimentation processes led to an understanding of the relationship between consolidated bottom sediments and dispersed sedimentary matter supplied by the different geospheres: atmosphere, cryosphere, hydrosphere, and biosphere. The long-term research work of the Shirshov Institute of Oceanology RAS in the Russian Arctic seas, including the White Sea, enabled to collect aeolian (atmogenic) material, marine and river suspended particulate matter, ice and snow solids, as well as bottom sediments, for a comprehensive study of the sedimentation process. The bulk of sedimentary matter from these environments is composed of dispersed sedimentary matter with micro- and nano-sized particles. The aim of this chapter was to study the dispersed and consolidated mineral phases of fine-grained fraction (from 10 μm to less than 1 μm) in different geospheres of the White Sea.

O. M. Dara (✉)
Shirshov Institute of Oceanology, Russian Academy of Sciences (IO RAS), Moscow, Russia
e-mail: olgadara@mail.ru

A. P. Lisitsyn and L. L. Demina (eds.), *Sedimentation Processes in the White Sea: The White Sea Environment Part II*, Hdb Env Chem (2018) 82: 105–134,
DOI 10.1007/698_2018_351, © Springer International Publishing AG, part of Springer Nature 2018,
Published online: 7 July 2018

They are as follows: aerosols, river and marine suspended particulate matter, solids carried by snow and ice, as well as surface bottom sediments. The X-ray diffractometry (XRD) and scanning electron microscopy (SEM) were the main instruments of the study.

It is established that about half of the finely dispersed mineral phases was composed of clay minerals. The rest of the sedimentary matter was presented by a fine-grained clastic terrigenous material which characterizes the feeding provinces. When passing through the water column to seabed, mineral phases are transformed in different ways.

Keywords Aerosols, Bottom sediments, Dispersed sedimentary matter, Fine-dispersed fraction, Scanning electron microscopy, Suspended particulate matter, White Sea, X-ray diffractometry

1 Introduction

In accordance with modern concepts, the process of sedimentation should be considered taking into account the transport of sedimentary matter by natural environments (atmosphere, hydrosphere, snow, ice). Thanks to a multidisciplinary investigation over recent years [1–3], it became obvious that the atmosphere, cryosphere, hydrosphere, and biosphere contribute to the processes of sedimentation. These geospheres bear the dispersed sedimentary matter mostly in the form of micro- and nanoparticles (from 10 μm to less than 1 μm). In the course of interaction of sedimentary matter from different geospheres, their dispersed forms entering the sea are transferred into a consolidated form of bottom marine sediments [4, 5]. The first attempts to obtain dispersed sedimentary matter from seawater have been undertaken by A.P. Lisitsyn in the middle of the last century [6, 7]. Further, the study of the fine-grained sedimentary matter was continued by many researchers [8–13]. Numerous expeditions, the modern tools, sampling techniques, and recent analytical methods allowed to obtain data on the dispersed sedimentary matter and to extend our understanding of modern sedimentary processes [5, 14].

2 Materials and Methods

Within the framework of the program “The White Sea System,” many multidisciplinary expeditions have been held by the Shirshov Institute of Oceanology of Russian Academy of Sciences. As a result, large amount of various materials (bottom sediments, marine and river suspended matter, snow, ice, aerosols of the near-water layer, biota) has been collected from the different geospheres. Dispersed sedimentary matter of all the seven geospheres of the White Sea was extracted for analysis by X-ray diffractometry (XRD) and scanning electron microscopy (SEM). For collection of bottom sediments, sampling by gravity tube of the large diameter as

well as Neimisto tubes and multicorers was used. Figure 1 a displays sampling stations of the surface bottom sediments in the White Sea. At the same stations, the aerosol material was taken by the net method and the suspended particulate matter – by methods of vacuum filtration of seawater and decantation of the river one [4, 5].

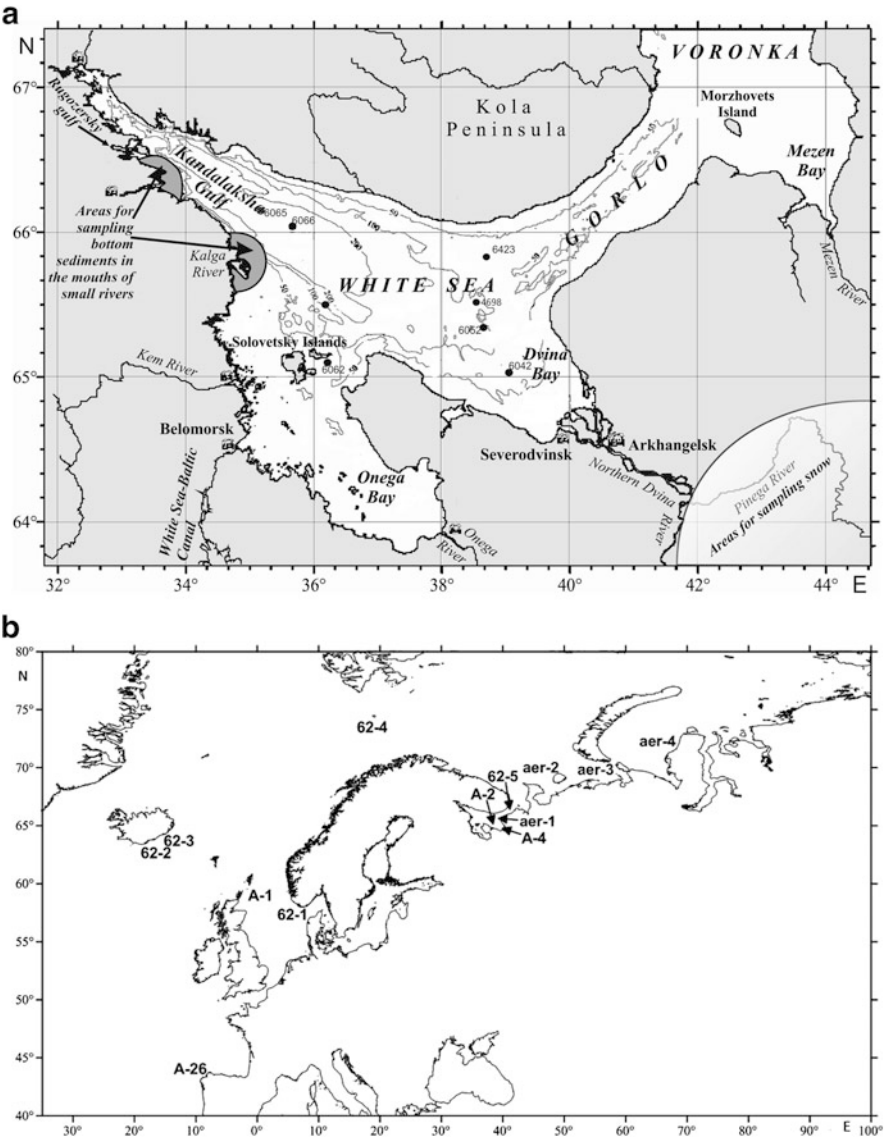

Fig. 1 Map scheme of sampling stations of suspended particulate matter (dispersed forms of sedimentary matter) and bottom sediments (consolidated forms of sedimentary matter) (**a**) and aerosol material (**b**) in the White Sea

Currently, the X-ray powder diffractometry is the most informative method for studying the fine-grained substances (size from 10 μm to <1 μm), aerosols, marine and river suspended matter, and the ice and snow solids, which finally sank to the bottom and formed a consolidated bottom sediments of the seas and oceans.

This method allows to determine different mineral phases and their content in the solid sample based on the analysis of the diffraction pattern. The diffraction image is the result of the interaction of X-ray beams with a powder of solid sample. As the distance between atoms is commensurate with the wavelength of the secondary coherent radiation, the crystal can serve as a diffraction grating for it.

It is possible to consider a diffracted beam as result of reflection from one of the crystal planes of an atomic lattice and obtain information about the d-spacing in the crystal. The value of d-spacing together with the crystallographic Miller indices (hkl) of these planes and the intensities of the diffraction reflections for each substance are strictly individual; therefore the X-ray diffraction pattern unambiguously characterizes the mineral composition of the examined substance. The method provides information directly both on the substance's structure and its composition without destruction of the sample. Measurements do not require a large amount of substance, and, finally, they allow to quantify the content of individual mineral phases (minerals) in the sample. The X-ray powder diffractometry (XRD) is characterized by the high sensitivity, reliability, less time-consuming for analysis, as well as small mass of samples (a few mg). To study small substance amounts, low-background cells are used. Such cells are made of a single silicon crystal, and their working surface does not have diffraction reflections in the investigated angular range.

The investigations were carried out on the X-ray diffractometers DRON-2.0 (Bourevestnik Inc.) and D8 ADVANCE (Bruker AXC), Cu-Kα, with Ni 0.02-filter, 40 kV, 40 mA, with linear detector LYNXEYE and samples scanning in discrete mode in steps of 0.02°Θ, exposure 8 s/step in the range 2.0–70° 2Θ, with and without rotation (for oriented clay preparations). For primary processing, interpretation of spectra, and calculation, the programs DIFFRAC.EVA and DIFFRAC.TOPAS were used.

For the analysis of a fine-grained (both dispersed and consolidated) substances, the standard methods commonly used in XRD diffractometry were applied [15, 16], and corundum numbers from the ICDD database were used for the calculation. The study of clay minerals (as part of marine suspended matter, aeolian material, and bottom sediments) as the most labile, with a wide range of crystallic chemical characteristics, has a great importance. Variable composition, structural defectiveness, and the possibility of mutual transitions provide information on the nature of geological processes. Micro- and nanoscale clay particles and, as a consequence, a large electric charge of their surface contribute to their cohesion and the formation of microaggregates consisting of several minerals. The identification of clay minerals and the determination of their quantitative relationships are now being studied by many researchers [15, 17–19]. The methods proposed by these authors were applied in the study of aeolian material, marine and river suspended particulate matter, as well as a fine-grained fraction of the bottom sediments of the White Sea. The identification of clay minerals was carried out on oriented air-dried mount prepared from a suspension of a clay fraction separated from the sample in distilled water.

Then the preparations were saturated with ethylene glycol (for the diagnosis minerals of the smectite group, as well as mixed-layered clay minerals with swelling layers) and heated at 550°C (for diagnostics kaolinite and chlorite). Another method of studying micro- and nanoparticles was the scanning electron microscopy. Electron microscopic studies were performed using the SEM Vega 3 Tescan (Czech Republic); the elemental microanalysis of the particles was performed by X-ray spectral microanalyzer INCA Energy 350 (Oxford Instruments, Great Britain).

3 Mineralogy of Dispersed Sedimentary Matter

3.1 Aerosols from the Above-Water Layer

As it was mentioned above, substances carried by the air masses make a significant contribution to bottom sediments and expand the spectrum of minerals involved in the formation of bottom sediments [20]. To collect an essential mass of aerosols' sample, the nylon nets (with total area about 10 m^2) were used which were installed in the nostrum deck of the ship at height of 4–9 m above the deck [2, 21]. A countercurrent of air mass causes the occurrence of an electrostatic charge, which attracts aerosol particles. After the exposure (usually 1 day), the nets were rinsed with distilled water (to remove the particle charge), followed by this water filtration through a Nuclepore filter (pore size of 0.45 μm). The aerosol samples obtained in such a way are free of sea salt; however, the water-soluble aerosol substances are lost during this procedure. To prevent contamination of samples from the side of the vessel, aerosols were sampled only during the movement of the vessel in a headwind.

Samples of aerosol material were collected in cruises 53 and 59 of R/V "Akademik Mstislav Keldysh" (White and Kara Seas, 2007, 2011) and cruise 80 of R/V "Professor Shtokman" in the White Sea (2006) (Fig. 1b). Mineral phases in all the samples collected were studied by X-ray powder diffractometry (XRD) and SEM.

Table 1 displays the mineral composition of the aerosol material collected in the above-water layer of the White and Kara Seas, as well as in the adjacent parts of the North Atlantic and the Arctic Ocean.

Atmospheric transport is also a contributor of the biogenic substances from the continent; these are the spores, pollen, plant fibers, and other organic particles. Figures 2, 3, and 4 show photomicrographs of aeolian material transferred by air masses to the above-water layer of the White Sea and the North Atlantic.

A wide range of minerals is transported by atmospheric particles which were defined: quartz (2–35%), microcline (9–33%), and amphibole (3–5%). The aerosol material of the above-water layer of the Kara, White, Barents, and North Seas contains an albite in the amount of 16–20%. In the North Atlantic aerosols, andesine and anorthite in combination with clinopyroxenes were mostly recorded. This was obviously due to the active volcanism of the Iceland.

Table 1 Mineral composition (%) of the aerosol material of the layer above water of the White and Kara Seas, the North Atlantic, and the Arctic[a]

	White Sea		Kara Sea				North Atlantic and Arctic						
Date	August 2006, PSh-80	August 2001, PSh-49	September 2011, AMK-59				Spring 2015,AI-47	Summer 2015,AI-49	July–August 2015, AMK-62				
Station	A-2	A-4	aer-1	aer-2	aer3	aer-4	A-26	A-1	62-1	62-2	62-3	62-4	62-5
Coordinates (beginning and end of an exposition)	65°45.41 N 39°26.58 E/64°42.65 N 40°30.43 E	64°56.41 N 39°58.58 E./ 64°45.65 N 39°42.43 E	65°11.16 N 39°46.05 E/ 68°34.51 N 42°39.37 E	68°46.98 N 43°20.54 E/ 69°12.97 N 45°35.91 E	69°39.47 N 47°57.08 E/ 70°00.30 N 57°02.51 E	70°00.30 N 57°02.51 E/72°12.98 N 65°26.14 E	41°37.30 N 12°56.50 W	57°57.20 N 01°57.20 E	59°00.00 N 9°00.00 E/ 60°00.00 N 0°00.00 E	63°00.00 N 15°00.00 E/65°00.00 N 22°00.00 E			66°00.00 с.ш. °00.00 в.д.
Fine-grained clastic minerals													
Quartz	25	22	Occur	28	30	35	32	13	10	2	5	7	3
Anorthite	–	–	–	–	–	–	12	23	–	48	29	23	6
Albite	24	23	Occur	21	16	20	–	–	17	–	–	–	8
Microcline	15	14	Occur	8	7	9	9	10	17	–	–	20	22
Amphibole	3	5	Occur	3	3	4	–	4	4	–	–	4	5
Augite	1	–	–	2	–	3	3	–	–	16	18	3	–
Calcite	–	–	–	–	2	–	–	8	1	–	–	–	–
Clay minerals													
Smectite	–	–	–	–	–	–	–	–	–	–	8	–	–
Illite	9	11	Occur	13	21	14	16	25	20	9	–	34	31
Chlorite	7	7	Occur	13	7	8	12	11	10	4	12	9	9
Kaolinite	7	9	–	5	5	6	14	1	14	5	9	–	7
Other minerals													
Gypsum	–	–	–	–	–	–	–	–	–	–	–	–	–
Talc	3	9	–	–	–	–	–	–	7	–	–	–	9
Hematite	–	–	–	–	1	1	1	–	–	–	–	–	–
Analcime	–	–	–	–	–	–	–	–	–	7	2	–	–
Geylandite	–	–	–	5	4	–	–	–	–	9	16	–	–
Dolomite	5	–	–	2	1	–	–	–	–	–	–	–	–
Cristobalite	1	–	–	–	3	–	–	–	–	–	–	–	–
Magnetite	–	–	–	–	–	–	–	1	–	–	–	–	–

"–" Beyond a detection limit

[a]Aerosol material obtained by A.N. Navigatsky expeditions of the IO RAS (White Sea R/V "Professor Shtokman," Kara Sea R/V "Academician Mstislav Keldysh," North Atlantic R/V "Akademik Ioffe," and R/V "Academician Mstislav Keldysh")

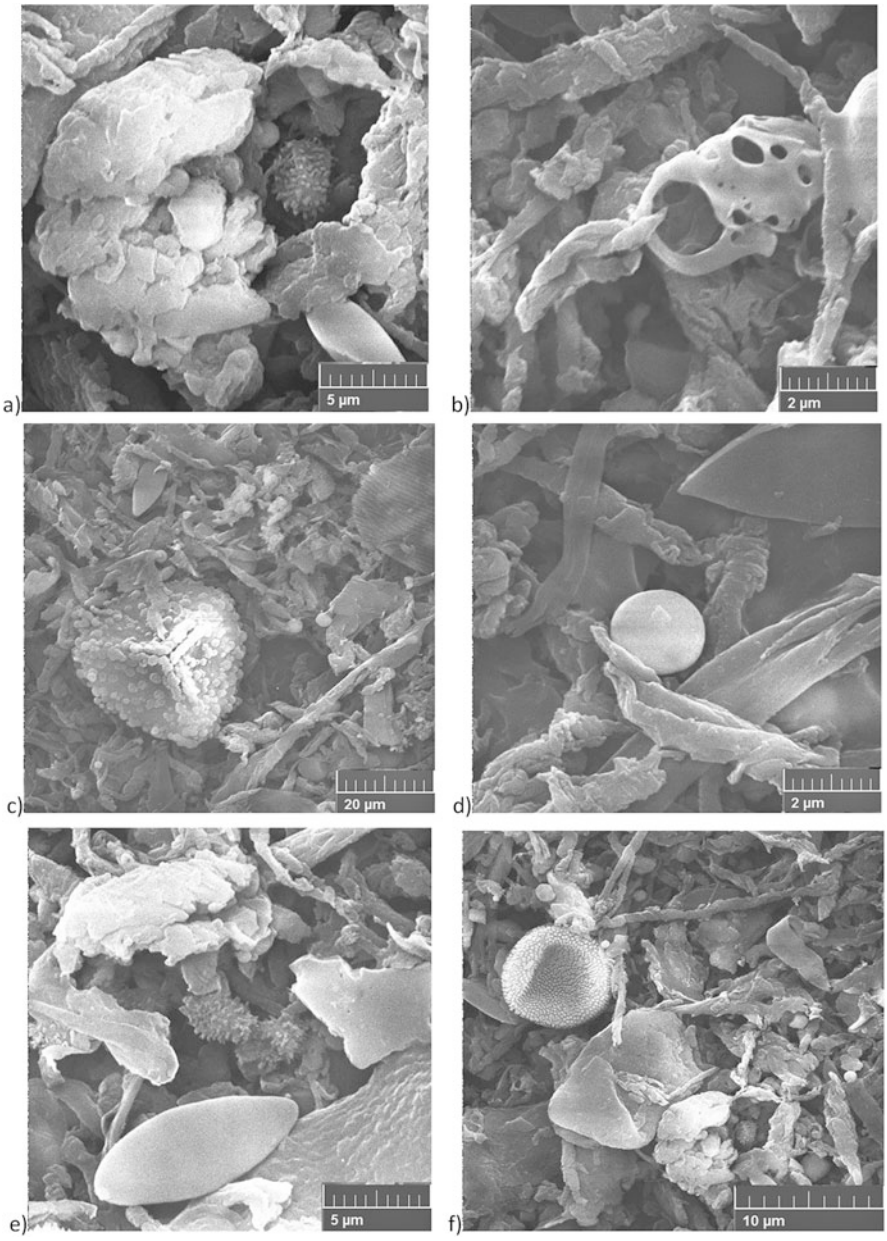

Fig. 2 Microphotographs of the aerosol material collected in the White Sea (cruise 80 of R/V "Professor Shtokman," August 2006; see coordinates in Table 1): mineral aggregates (**a**); volatile ash (**b**); pollen (**c**); plant residues, mineral aggregates (**d**); mineral aggregates, pollen, plant residues (**e**); spores, pollen, mineral aggregates, plant residues (**f**)

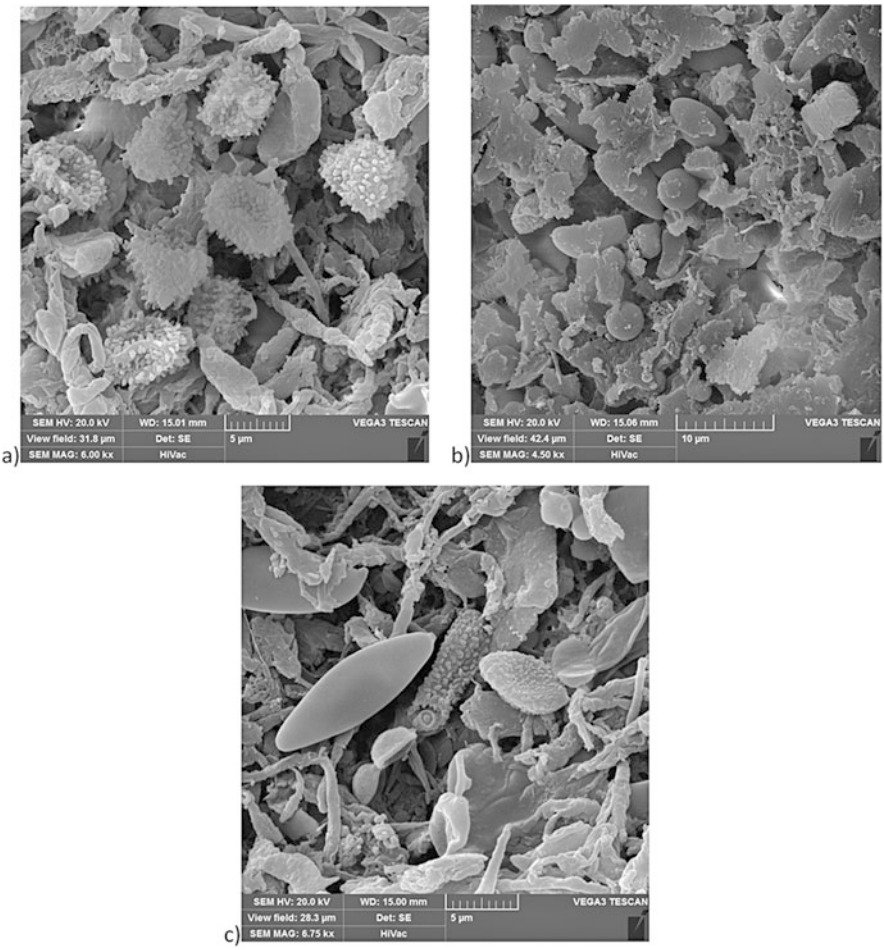

Fig. 3 Microphotographs of the aerosol material collected in the North Atlantic (cruise 62 of the R/V "Akademik Mstislav Keldysh," July 2015; see coordinates in Table 1): spores, pollen, plant residues, aggregates of clay minerals, clastic minerals (**a**, **b**, **c**)

Carbonates in the White Sea aerosol material were mostly presented by dolomite.

Clay minerals were found everywhere: chlorite (2–12%), illite (9–25%), kaolinite (1–14%), and rarely smectite. In the aerosols of the Kara Sea, regular hydrobiotite (vermiculite-illite), i.e., a weathering product of soils, and zeolites-geilandite and 16-Å K-zeolite have been detected. In general, amount of clay minerals in aerosol material did not exceed 45%. Thus, the fine-grained (within the range of 1–10 μm) clastic minerals in the aerosols of the above-water layer were predominated by quantity over the remaining components of the aeolian material.

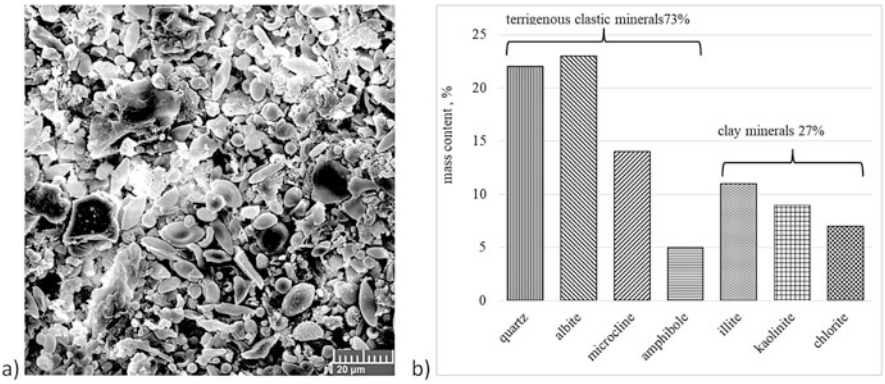

Fig. 4 The mineral composition (%) of the aerosol material collected in the White Sea (cruise 49 of RV "Professor Shtokman," August 2001; see coordinates in Table 1): microphotographs of aerosol samples – spores, pollen, plant residues, aggregates of clay minerals, clastic minerals (**a**); mineral composition of aerosols from the X-ray phase analysis data (**b**)

The aerosol material involved in the formation of the surface layer of bottom sediments in the White Sea, according to our data, is essentially composed of the fine-grained matter transported by wind from the land surface (terrigenous aeolian material). This is suggested by presence of pollen, spores, microorganisms, remnants of plant fibers, combustion spheres, and mineral dust in terrigenous material. The dimensions of aerosol particles did not exceed 100 μm; they are mostly of submicron fractions, i.e., they are an invisible dispersed sedimentary material [2]. Analysis of aeolian material revealed that the atmospheric source contributes significantly to the fine-grained fraction of the bottom sediments of the White Sea.

3.2 Sediment-Laden Sea Ice and Snow Particles

Atmospheric precipitation is of importance in the mobilization and concentration of dust carried by the air masses. To obtain information on the mineral composition of this dust captured by fallen wet snow (wet leaching), in a number of the Arkhangelsk district, the Komi Republic, and the Nenets Autonomous District, a suspension of melted snow material was also investigated.

Based on the results of the XRD phase analysis, quartz (45–52%) and clay minerals (25–35%) predominated in the crystalline material extracted from the melted snow. The quartz/feldspars ratio, one of the important characteristics of the mineral composition of aerosols, varies from 3.4 to 8.7. The value of this ratio depends on the intensity of weathering processes when destruction of feldspars

primarily took place, while quartz was preserved, and this ratio is an important characteristic of the feeding provinces. In clayey shales that are the main sedimentary rocks of continents, value of quartz/feldspar ratio is close to 2. An increased value of this ratio indicates a more intensive destruction of feldspars during the weathering. The content of goethite in samples, from XRD phase analysis, varied from 5 to 12% (Table 2).

Similar results were obtained using SEM with an energy-dispersive attachment. Here, the iron minerals were detected in quantity of the average 5–7% by weight, and they were represented mainly by goethite, while hematite and limonite were found as an admixture. These minerals provide the brownish-yellow color of the samples studied. Occasionally goethite generated thin brownish films over quartz grains.

Among the clay minerals in the samples, illite prevailed, and its content varied from 39.3 to 57% (on average, 48.2% of the sum of clay minerals). Illite is the most abundant clay mineral in the continental crust (except for the equatorial zone where the content of kaolinite and montmorillonite is increased).

All samples contained a large amount of biogenic matter – pollen and spores [22]. In general, the mineral composition of the dust identified these to have a soil source, transported by the wind over long distances.

During the snow and ice melting period in the catchment areas, the accumulated aerosol material is transferring with meltwater into the rivers, followed by their entering the White Sea. Then this material, as well as the material accumulated in the ice cover of the sea, sinks down the floor contributing to the fine-dispersed component of the bottom sediments.

Table 2 Mineral composition (%) of the suspended particulate matter extracted from snow cover of the Russian northern areas (March 25–26, 2008)

Minerals	s. Zachachie 63°25′ N 41°48′ E	s. Emets 63°29′ N 41°48′ E	s. Brin-Navolok 63°44′ N 41°25′ E	s. Kapachevo 63°58′ N 41°42′ E	s. Pinega 64°42′ N 43°23′ E
Quartz	50	45	48	48	52
Albite	5	6	7	5	3
Microcline	3	6	5	3	3
Diopside	1	3	1	1	–
Amphibole	1	3	1	–	–
Calcite	–	1	–	0	5
Goethe	5	10	8	12	10
Clays	35	25	30	25	25
Proportion of clay minerals					
Illite	42	39	47	57	54
Smectite	10	17	5	нет	6
Kaolinite	34	33	37	32	29
Chlorite	13	10	9	9	9

"–" Beyond a detection limit

3.3 Mineral Composition of Fine-Dispersed Fraction (<1 μm) of the Bottom Sediments of Small Rivers in the Catchment Area of the Northwestern White Sea

Analysis of the fine-dispersed material (<1 μm) in the surface layer of bottom sediments of the lower stream and the Kalga River marginal filter (Table 3) has revealed a high content of terrigenous quartz, albite, and microcline (in sum more than 70%) with a minimum contribution of clay minerals (~15%).

In addition, the Kalga River contributes to pelitic fraction of the surface sediment layer in the White Sea with minerals as follows: amphibole, pyroxene, epidote, calcite, aragonite, phlogopite, vermiculite (Fig. 5), goethite and hematite. Minerals of the amphiboles group were represented by hornblende and tremolite; augite (the pyroxenes group) was the most frequently detected.

The soil covering the catchment area was identified by the presence of illite, vermiculite, and phlogopite. These minerals of the fine-dispersed fraction emphasize the interrelationship of the White Sea bottom sediments with their source areas of the Karelian coast.

The process of the Holocene sedimentation in the Kandalaksha Bay was closely related to the development of the coastline. The sediment stratification on the bedrock substrate due to fall of the World Ocean level was also reflected in the composition of the fine-grained fraction of bottom sediments in the northwestern White Sea. The histogram of average mineral's composition of the surface bottom sediments of Rugozerskaya Bay (fraction <1 μm) is shown in Fig. 6.

Table 4 displays the XRD results of fine-dispersed fraction (<1 μm) of the bottom sediments of the surface layer of the Rugozerskaya Bay. The abundance of clastic minerals was estimated to be 63%, on average, while that of clay −35%.

The spectrum of minerals, determined in the fine-grained fraction of surface bottom sediments of the White Sea, indicates that source of their supply is obviously the river runoff, as well as coastal abrasion.

3.4 Mineral Composition of Fine-Grained Fractions of Marine Suspended Matter

The mineral composition of a fine-dispersed fraction of suspended particulate matter from the White Sea and the Northern Dvina River is of great interest when determining the origin and source of suspended particles; this problem has been a subject of our research [5].

The White Sea suspended particulate matter is a complex object for identification of the mineral composition. This is caused by the low concentration of suspended matter (that is typical for the Arctic seas), the seasonal variability in abundance of biogenic components that are not distinguished by XRD method, the intensity of fluvial supply by the rivers, ice and snow cover of the sea, and

Table 3 Mineral composition (%) of the Kalga River surface bottom sediments (fraction <1 μm) in the lower stream and marginal filter, Karelian coast of the White Sea, summer 2009 (see Fig. 1)[a]

Sample no.	Coordinates	Fine-grained clastic minerals										Clay minerals			Other minerals	
		Quartz	Albite	Microcline	Amphibole	Pyroxene	Epidote	Phlogopite	Calcite	Aragonite	Vermiculite	Illite	Kaolinite	Chlorite	Goethite	Hematite
2	65° 45′ 04” N 34° 02′ 54″ E	22	30	9	7	1	–	5	–	1	8	4	3	6	2	1
3	65° 46′ 19″ N 34° 09′ 56″E	27	30	14	8	2	2	5	–	1	4	4	1	2	–	–
6	65° 46′ 21″ N 34° 38′ 13″ E	22	22	10	8	3	6	–	–	–	–	18	4	4	2	1
8	56° 45′ 04″ N 34° 42′ 52″E	28	26	12	10	3	5	–	1	3	–	6	3	3	–	–

“–“ Beyond a detection limit

[a]Material was collected in expeditions of the Northwestern Branch of the IO RAS

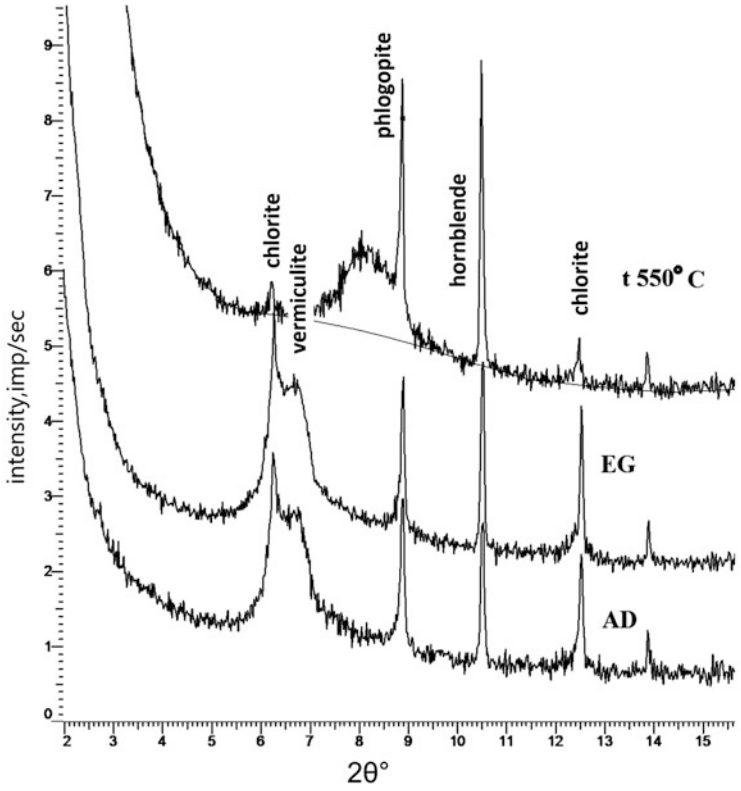

Fig. 5 Vermiculite in the fine-grained fraction of bottom sediments of the marginal filter of the Kalga River (Karelian coast of the White Sea, summer 2009, sampling sites; see Fig. 1). *AD* air-dried preparation, *EG* saturated with ethylene glycol, *t 550°C* sample heated at the indicated temperature

catchment area. A preliminary electron microscopic study of our samples showed that material was represented by a biogenic XRD amorphous mass (biogenic detritus, pollen and spores, phyto- and zooplankton) with individual grains of detrital minerals, mineral aggregates, and scaly formations of layered silicates. Samples were collected by both the vacuum filtration and decantation of suspended matter from water collected in plastic tanks in the marginal filter's areas and mouth of the Northern Dvina River [23]. The mineral substance collected on the filters mainly consisted of particles of pelitic fraction. Its content depends on the water depth and sampling location. The substance was studied by the XRD method using a low-background cell.

Mineral composition and its distribution in the water column were studied in marine suspended particulate matter (collected by the vacuum filtration in August–September 2007 in cruise 53 of R/V "Akademic Mstislav Keldysh"). The three areas

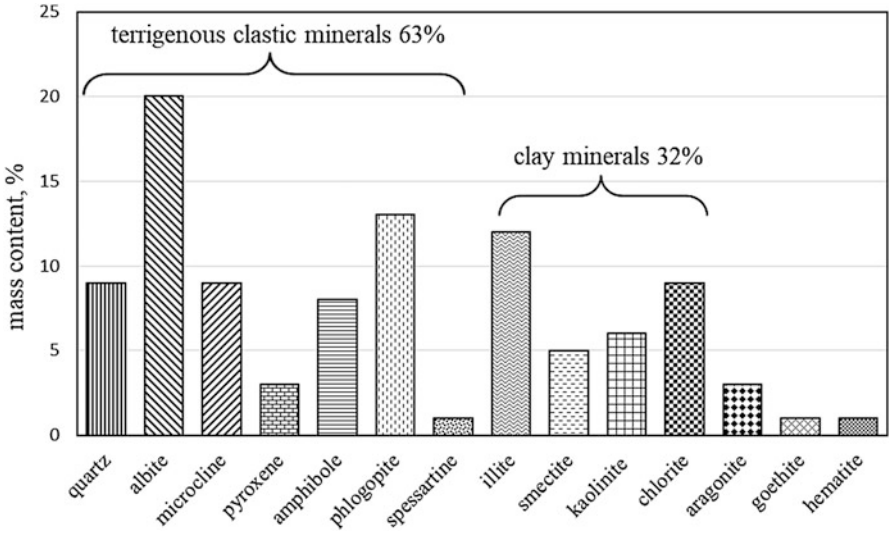

Fig. 6 Mineral composition (%) of the fine-grained fraction bottom sediments of Rugozerskaya Bay

of the White Sea were examined: the marginal filter of the Northern Dvina River, the Gorlo, and the Voronka of the White Sea (Fig. 7).

The total mineral composition of suspended particulate matter in these three regions collected at different horizons of the water column was rather monotonous, which was probably due to the high hydrodynamic activity of these regions. The bulk clay minerals transported by the Northern Dvina River were found in bottom sediments of the mixing zone of river freshwater with the saline one. About 90% of the riverine suspended load is deposited there [24, 25] as a result of avalanche sedimentation. In water of the Dvina Bay, the suspended matter contained more clay minerals; there, the smectite content reached the maximum values. Proportion of clay minerals in the fine-grained fraction of the Dvina Bay particulate matter is shown in Fig. 8.

In general, in the samples from three different areas, the clay mineral total content in the White Sea suspended matter did not exceed 15%, with the predominance of illite.

Among the carbonate minerals, aragonite was identified only in the suspended particulate matter from the Northern Dvina River marginal filter. Calcite and dolomite were found in all the samples studied. The majority of aragonite and calcite in the White Sea suspended particulate is of a biogenic origin. The shells were examined by XRD method layer by layer. External skeletal formation of the studied shells (ostracum) consisted of calcite while the inner thin pearl layer (gipostracum) – of aragonite. It is supposed that source of dolomite in suspended matter was the pre-Quaternary sedimentary rocks of the northern part of the Russian plate.

Table 4 Mineral composition (%) of the Rugozerskaya Bay surface bottom sediments (fraction <1 μm) in the vicinity of the Moscow State University Biological Station in June 2010 (for location, see Fig. 1)[a]

No	Sample no.	Fine-grained clastic minerals						Clay minerals				Other minerals			
		Quartz	Albite	Microcline	Amphibole	Pyroxene	Phlogopite	Illite	Smectite	Kaolinite	Chlorite	Goethite	Hematite	Spessartite	Aragonite
1	1-5	10	25	13	8	3	11	11	4	5	7	–	–	–	–
2	2-5	9	19	10	7	2	15	13	5	6	9	1	1	1	–
3	3-3	9	21	11	8	3	13	11	6	7	10	–	–	–	–
4	3-4	10	21	12	7	2	14	12	5	6	9	1	–	–	–
5	4-1	9	19	11	8	3	13	12	6	7	10	–	–	–	–
6	4-2	11	22	12	8	2	12	11	5	6	8	1	1	–	–
7	5-3	9	19	11	7	3	13	12	6	6	10	1	1	–	3
8	7-3	10	22	11	8	3	12	12	5	6	9	1	–	–	–
9	9-3	9	23	12	8	2	12	11	5	6	9	–	–	–	–

" – " Beyond a detection limit

[a]Samples were obtained from V.P. Shevchenko

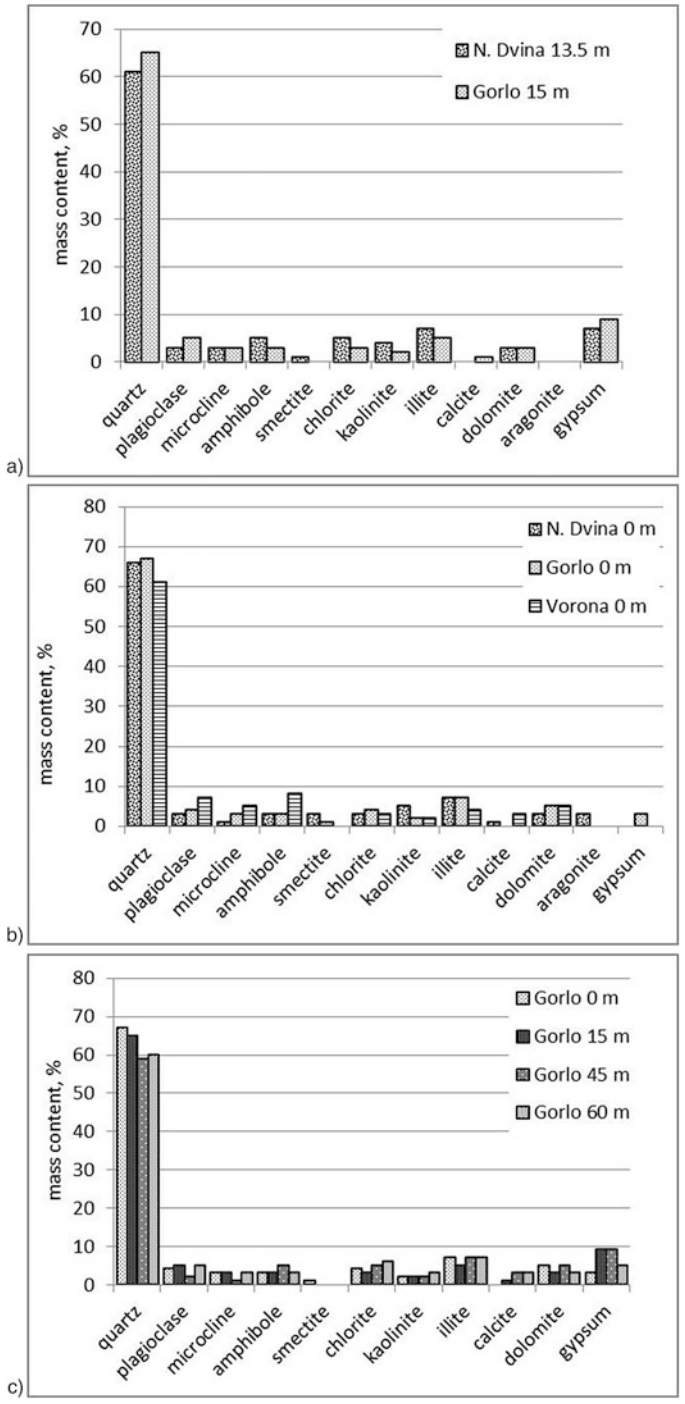

Fig. 7 Comparison of mineral composition of the suspended particulate matter (SPM) from the three areas of the White Sea (the mouth of the Severnaya Dvina, Gorlo, Voronka), sampled by

The fine-dispersed quartz dominated, and it was evenly distributed in the White Sea suspended matter. The amount of terrigenous clastic minerals of the amphibole group (hornblende, tremolite), microcline, and albite was of subordinate importance. A relatively higher content of these minerals was determined in the surface sediments of the Voronka of White Sea, from which clay particles are carried away by currents.

The concentration of suspended matter in fresh river water was much higher compared to marine water, and this allowed to use a decantation method successfully for its collection. The study of decantation matter let us see the spectrum of minerals typical for freshwater of the Northern Dvina River (Table 5).

In addition to the minerals that are present in the marine suspended matter, the riverine suspension contains the mixed-layered minerals (montmorillonite-chlorite), minerals of the serpentine group, as well as vermiculite, mica, gypsum, and bassanite $[CaSO_4] \bullet 0.5H_2O$.

The marginal filter of the Northern Dvina River is characterized by a change in the alkaline-earth type of montmorillonite ($Na^+ + K^+/Ca^{2+} + Mg^{2+}$) <0.5, $d_{001} \sim 14$ Å in alkaline ($Na^+ + K^+/Ca^{2+} + Mg^{2+}$) >1, $d_{001} \sim 12$ Å. The interlayer exchange of Ca^{2+} and Mg^{2+} cations of smectite from freshwaters of the Northern Dvina River, in the saline waters of the Dvina Bay, is replaced by Na^+ and K^+ of seawater. The free from overlay reflection of montmorillonite with $d_{001} \sim 12$ Å makes it possible to diagnose it as alkaline.

The 14-Å peak of alkaline-earth montmorillonite is hidden under the basal reflection of 001 chlorite (Fig. 9); saturation of the sample with ethylene glycol leads to its transfer to the 17A region, which provides reliable diagnostics of this species.

3.5 The Role of Biota in the Formation of Bottom Sediments

One of the mechanisms of supplying fine-dispersed mineral suspensions to bottom sediments is a sedimentation by biological transport. Zooplanktonic that filters suspended micro- and nanoparticles plays a key role in this process. Phyto- and zooplanktonic organisms realize several biogeochemical functions, such as transforming of dissolved elements' species into suspended particles, biogenic triad ($CaCO_3 + SiO_2 +$ Corg); consuming organic constituents of suspended matter as food; concentrating mineral particles; and packaging them into cover (peritrophic membrane) with subsequent accelerated vertical transport to the bottom in the form of pellets.

Fig. 7 (continued) filtration from several horizons of the water column in August–September 2007. SPM from the 13.5 m and 15 m horizons (**a**); SPM from the upper (0 m) horizon (**b**); SPM from 0, 15, 45, and 60 m horizons of the Gorlo area (**c**)

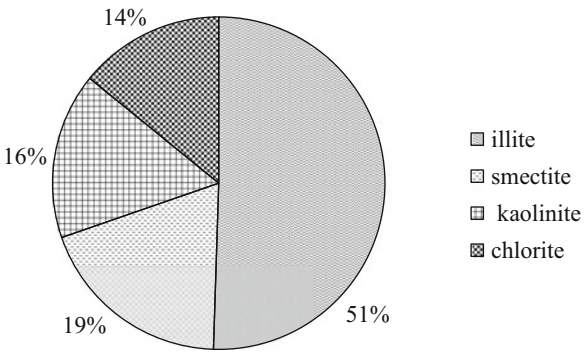

Fig. 8 The average percentage of clay minerals in the SPM of the Dvinsky Bay (July 2012)

Table 5 Mineral composition of (%) suspended particulate matter from the Northern Dvina River in June and August 2015

	Dates and sites of samples collection				
	12.05.2015	16.06.2015	22.06.2015	18.08.2015	21.08.2015
Mineral	Dock	Port "economy"	Dock	Dock	Port "economy"
Quartz	20	16	13	18	22
Albite	18	23	20	18	20
Microcline	12	12	12	14	11
Virgin	2	4	3	1	1
Amphibole	5	5	7	6	6
Smectite	12	9	12	9	9
Illite	13	14	11	13	11
Chlorite	8	7	6	5	6
Kaolinite	6	5	5	5	6
Calcite	–	–	1	3	–
Dolomite	4	3	2	3	3
Bassanite	–	–	–	5	3
Gypsum	–	–	–	–	2
Serpentine	–	–	8	–	–
Sso mr[a]	–	Trace	–	–	–

"–" Beyond a detection limit

[a]Mixed-layered formation of the montmorillonite-chlorite type

Copepods of the genus *Calanus* contribute to precipitation of marine suspended matter in the White Sea, as well as in the entire Arctic basin. The mechanisms of biological sedimentation were studied in the White, Caspian, and Kara Seas [1, 26, 27].

Comparative XRD analysis of marine suspended matter and pellets, produced by copepods of the genus *Calanus*, showed the following. The crystalline part of marine suspended matter consists of three main components. The predominant component

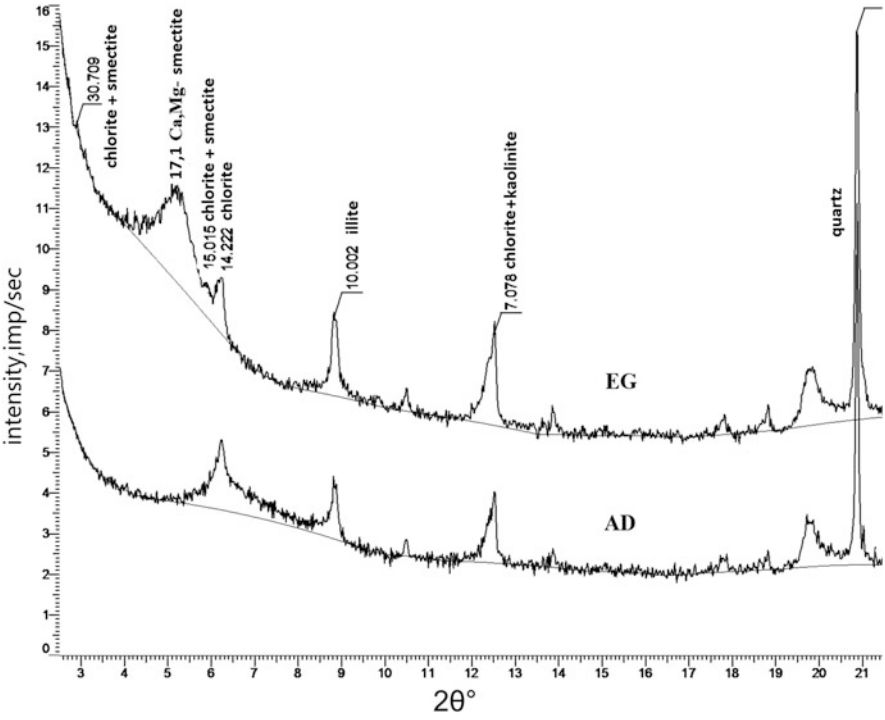

Fig. 9 Diffractogram of the clay fraction of the SPM collected by the decantation method at the port Ekonomiya of Arkhangelsk in June 2015. *AD* air-dry sample, *EG* the same sample saturated with ethylene glycol

of lithogenous fine-grained clastic minerals composed of quartz, feldspars, and pyroxene group, amounted from 35 to 60%. The second important component was the clay group's minerals: layered silicates (chlorite, kaolinite, illite, muscovite) that also make a significant contribution (30–48%) to the mineral composition of suspended matter. The third group was carbonate minerals (dolomite, calcite, aragonite) in the amount of <10%. In addition, in particulate matter, a biogenic opal SiO_2 was present (<10%) which was detected by optical microscopy and chemical analysis. In general, such a composition and quantitative proportions of minerals were characteristics of the marine suspended matter of the White, Kara, and other seas of the Russian Arctic.

Our XRD analysis of mineral particles packed in fecal pellets of *C. glacialis* showed that their composition was almost identical to the mineral composition of the marine particulate matter.

We observed a selectivity of copepods in consumption of mineral suspensions with the preference for the fine-grained fractions compared to coarser particles. Particularly noticeable was a relative decrease in quartz content (Fig. 10) from 32% in marine suspension to 15% in pellets. Quartz is known to be a resistant

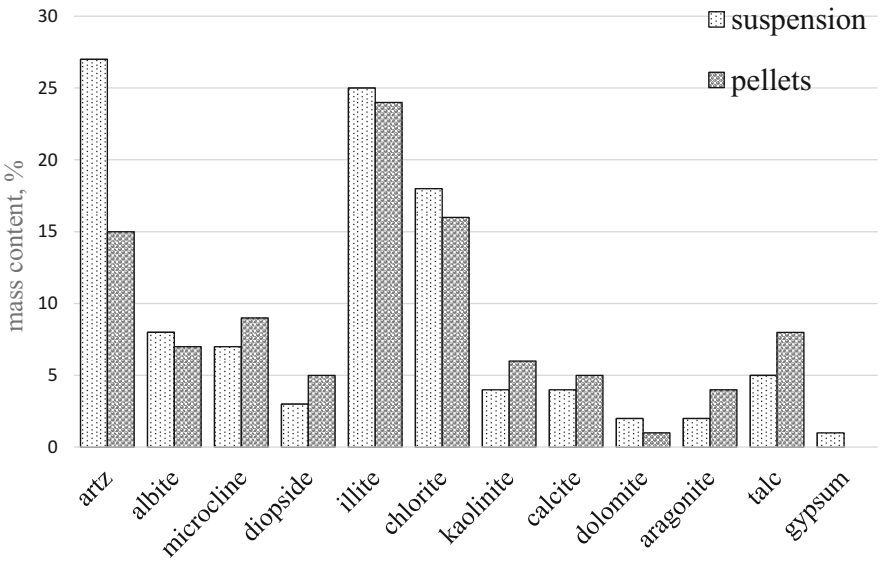

Fig. 10 Comparison of the mineral composition (%) of marine SPM and fecal pellets of *Calanus glacialis* sampled at the same station from the same horizon

mineral to mechanical breakage. In general, the mineral proportion of clastic and clay minerals in suspended matter and in pellets did not differ significantly.

Apparently, this is due to the greater adaptability of the crustaceans' filtration apparatus to consumption of particles of a certain size, depending on their own size. Copepods' feeding a suspension promotes the movement of detrital fine-grained pelitic material into bottom sediments. Thus, this mechanism promotes the transformation of dispersed forms of sedimentary matter into the bound ones (pellets). It is an important stage in the formation of a consolidated form of sedimentary matter, namely, the bottom sediments.

4 Mineral Composition of Pelitic Fractions of the White Sea Bottom Sediments

Traditionally it is considered that the main constituents of pelitic fraction (<1 μm) of bottom sediments are the clay group minerals. However, from results of the XRD analysis of samples of bottom sediments in the southern part of the Basin, Dvinsky, and Onega Bays, we have discovered that the pelitic fraction of the White Sea sediments is a three-component one. It is composed of fine-grained clastic, clayey, and biogenic minerals. The other minerals are of subordinate importance and have a local distribution.

Comparison of mineral content in fractions <1 and <10 μm shows that the fraction <10 μm was enriched in quartz in all samples; besides, only in this fraction, almandine (mineral of garnet group) was identified. Other clastic minerals have no clear relation with one of the two grain-size fractions. The content of clay minerals was somewhat higher in the fraction <1 μm (Fig. 11).

From our data it follows that predominant group was the lithogenic clastic minerals resulted from weathering of rocks on land and supplied into the sea due to the river runoff, ice and snow melting, and aeolian transport. Lithogenous clastic minerals include mineral components of the light and heavy subfractions, such as quartz, feldspars, carbonates, minerals of the epidote, pyroxene, amphibole, garnet, and mica groups. The group of clay minerals (smectite, illite, kaolinite, chlorite) in the fractions under study rarely exceeds 50%, and generally they have a quantitative subordination. The third group was planktonic and benthic biogenic calcareous and siliceous minerals, whose contribution to the bottom sediments of the White Sea was relatively small.

The total content of clastic minerals in the fine-grained fraction of surface sediments varied, according to our data, from 43.6 to 89.5%. In Fig. 12, a diffraction pattern of the surface bottom sediments of the White Sea collected by gravity tube of the large diameter and histogram with quantitative analysis results is shown. The pelitic fraction in this sample contains 62% of clastic minerals, 35% of clay, and 2% of aragonite.

Clastic minerals are represented by quartz, albite, anorthite, microcline, hornblende, and augite and clay minerals with alkali dioctahedral smectite, magnesia-ferruginous chlorite, kaolinite, and illite. In addition, the sample contains aragonite and trace amounts of epidote.

Variations in the percentage of major clastic minerals in the fine-grained fraction in surface bottom sediments along the axial section of the White Sea are small.

The presence of carbonate minerals in the fine-grained fraction and high concentrations of feldspars (albite and microcline) makes it possible to consider that both strongly weathered material from the northern Russian Plate and the fresh material from the Karelian coast were mobilized in the White Sea sediments.

Clayey component of surface sediments of the White Sea, as in the case of the entire Arctic basin generally, was dominated by illite and chlorite. The highest levels of smectite were observed in the areas of the Dvina Bay.

Transformation of dispersed sedimentary matter in water column (suspended particulate matter) into sediments depends on the various chemical, physical, and biological factors that accompany the particle flux in the sea. This transformation is most active at the water-bottom boundary [28]. This zone consists of three subzones: near-bottom water, fluffy layer, and surface sediments. In Fig. 13 the schematic map is shown of sampling by use of Neimisto tube.

The use of the Neimisto tube as well as multicorer allowed us to collect undisturbed sediment core and to perform detailed investigation of mineral composition of sedimentary material deposited in a contact zone between near-bottom water and the uppermost sediment layer. The clastic minerals are represented by quartz (19–34%), albite (15–35%), microcline (7–12%), minerals of amphibole

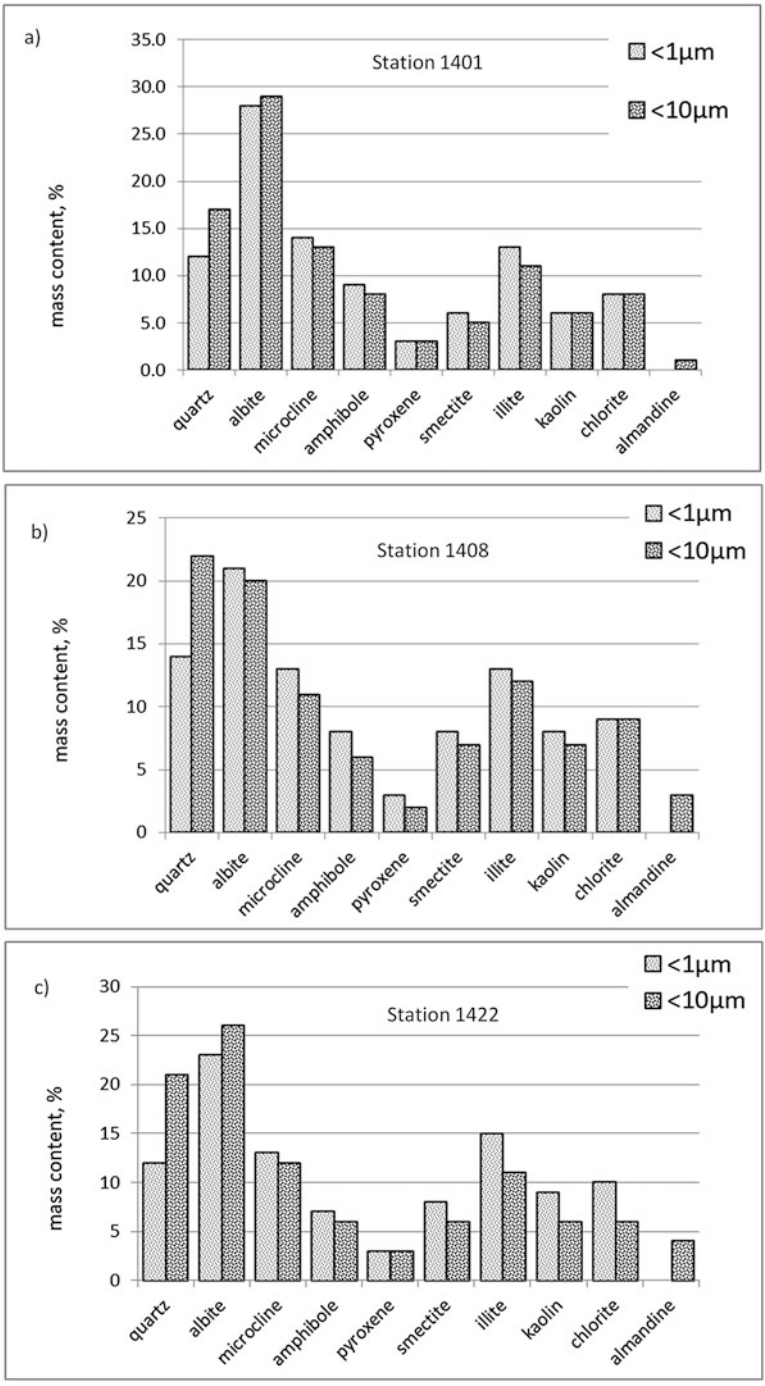

Fig. 11 Comparative characteristics of accumulation of terrigenous clastic minerals and clay minerals in two fractions (<1 and <10 μm) of bottom sediments by the example of three (**a**–**c**) sampling points (White Sea, August 2014, RV Ecolog, stations 1401, 1408, and 1422, 153 m depth)

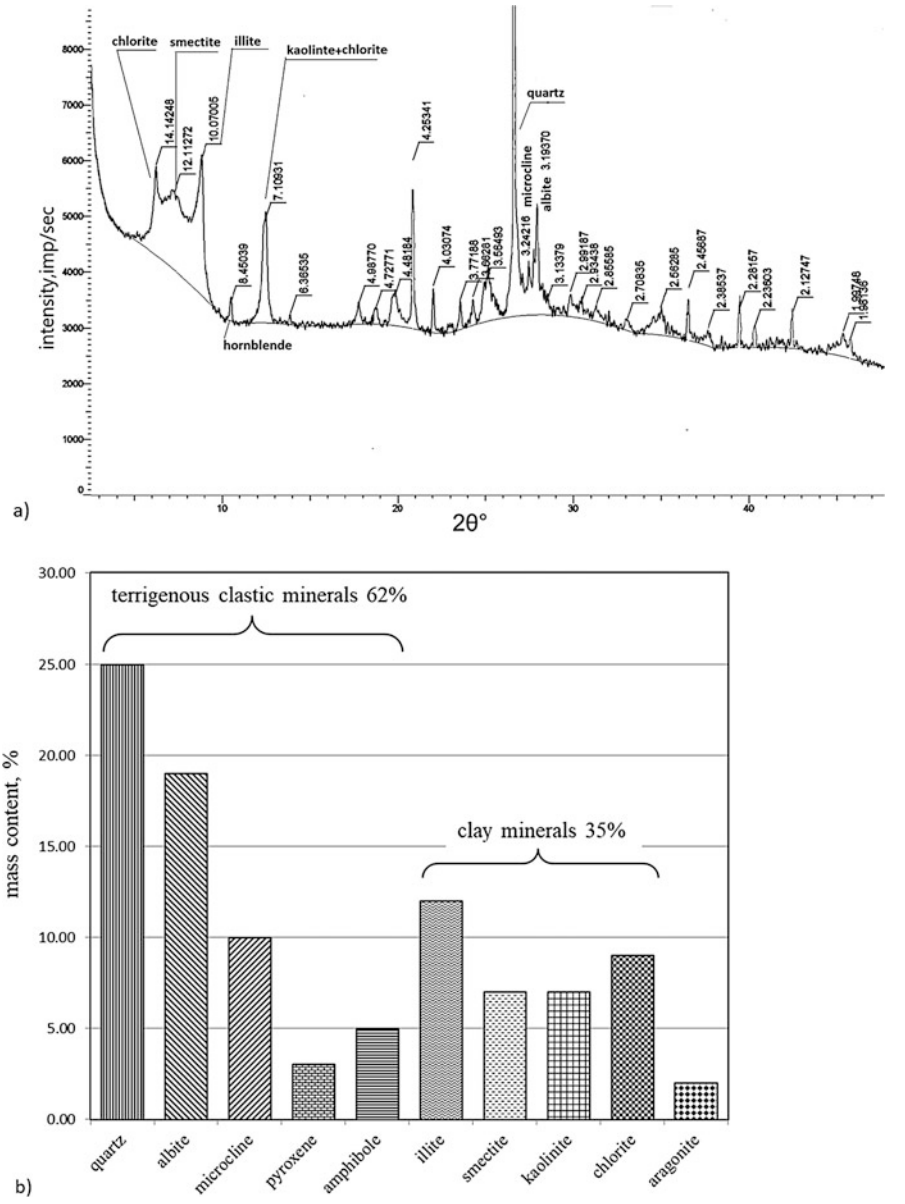

Fig. 12 Mineral composition of the fine-grained (<1 μm) fraction of the White Sea bottom sediments of (cruise 64 of RV "Professor Shtokman," August 2004, station 6423, 65°46′00″N, 38°50′00″E, depth of 65 m: the diffraction pattern of the sample (**a**), proportion (%) of minerals (**b**)

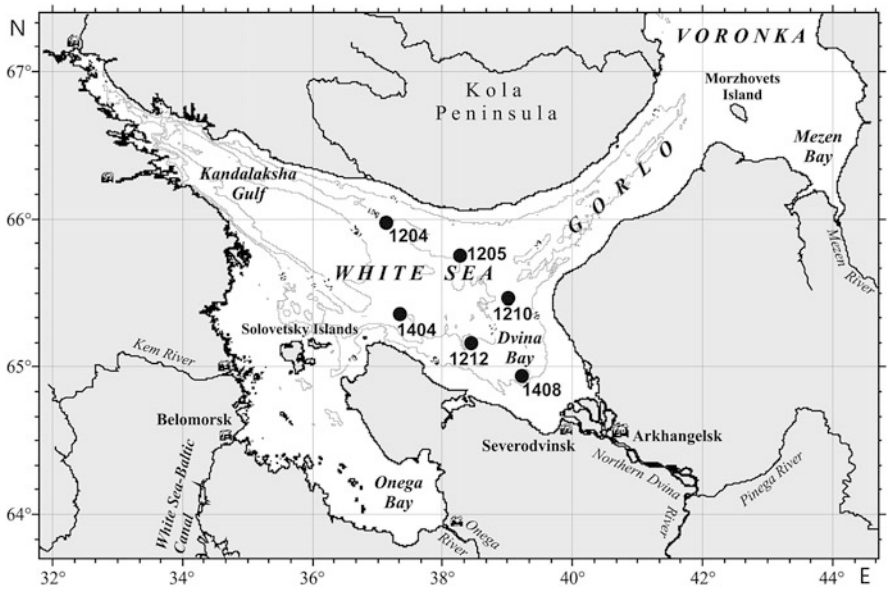

Fig. 13 Sampling stations of bottom sediments taken with Neimisto tube (July 2012, 2014)

groups (hornblende and tremolite, 2–6%), and pyroxene (diopside, augite, 0–3%). The carbonate group is represented by ubiquitous dolomite (2–3%), calcite (0–2%), Mg-calcite (~2%), and aragonite (1–2%). In addition, the samples contain iron hydroxides (goethite), as well as epidote, garnet (up to 3%), and mica (muscovite and phlogopite, 5–21%). In the clay mineral group, illite (6–10%), smectite (0–5%), kaolinite (0–6%), and chlorite (2–11%) were registered. As a whole, the mineral composition of sediments at four stations inherits, with minor variations, a mineral complex which has been identified in dispersed sedimentary matter of the water column (Fig. 14).

Dioctahedral smectites (montmorillonite is a member of this group) are formed by triple-layered tetrahedron-octahedral-tetrahedron packets and the hydrated exchange cations Na^+, K^+, Mg^{2+}, and Ca^{2+} between them. They regulate the degree of intercrystalline swelling of smectites. This, in turn, is reflected in their diffraction pattern: the basal reflection of 001 montmorillonite with the exchange cations Na^+ and K^+ corresponds to an interplanar spacing d ~ 12.4 Å. Substitution of these cations for Mg^{2+} and Ca^{2+} leads to increase in d to 15.5 Å.

It was found that the two groups were distinguished in the bottom sediments of the White Sea. Montmorillonites from the brackish water sediments of river mouths have a packet height d ~ 14.4 Å, for montmorillonites from marine sediments d ~ 12.6 Å. In marine suspended particulate matter and fluffy layer, the exchange cations have a mixed composition. The montmorillonite content was mainly increased with depth in water column. The relative content of montmorillonite in surface sediment layer varied from the detection limits in the hydrodynamically

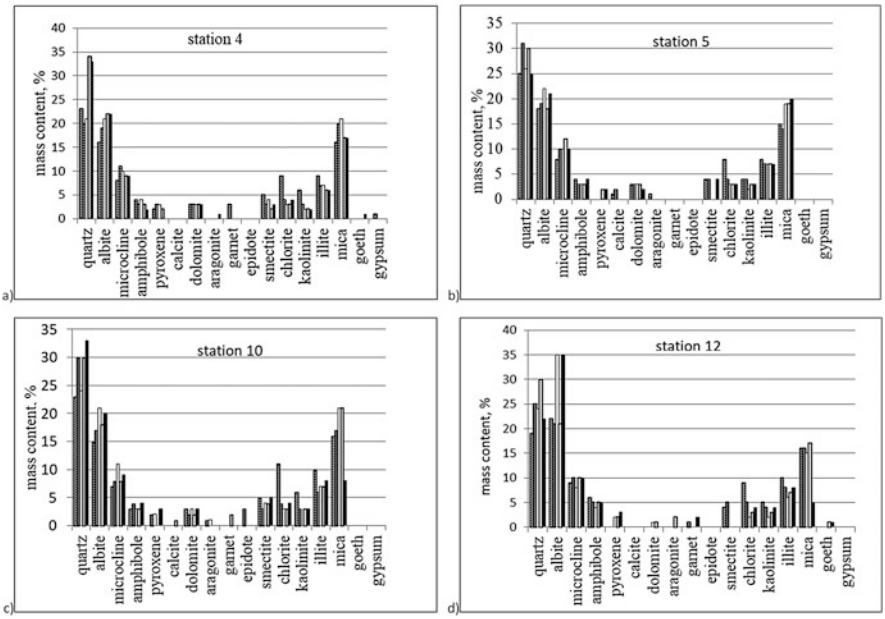

Fig. 14 Mineral composition (%) of the White Sea sediments in the near-water-seabed barrier zone [July, 2012, stations 4, 5, 10, 12 (**a**–**d**) – sampler – Neimisto tube]

active areas of the White Sea to 15% in the marginal filter of the Northern Dvina River.

Chlorite with a different proportion of Fe and Mg was detected in the White Sea bottom sediments everywhere, and its content varied from 6 to 17%. Kaolinite of different degrees of crystallization accounted for 3 to 10%. The most common mineral of the clay group is illite; its content varied from 49 to 87% (of the total clay minerals).

In order to identify post-sedimentation zoning in sedimentary complexes, the Kübler Index (KI), the crystallinity index of illite, is widely used. High amounts of illite in the White Sea made it possible to determine this index for bottom sediments at several stations. The material was obtained by the Neimisto tube in July 2012. The Kübler Index is experimentally determined by measuring the width of the basal XRD diffraction reflection 001 illite at half of its height (full width at half maximum – FWHM). This value indirectly characterizes the thickness of the illite packet (the coherent scattering area), which can indicate a grade of early diagenetic changes. From Fig. 15, one may see that at this stage of sediment formation, thickness of the illite packet decreases from suspended matter to the fluffy layer and further to surface sediments.

In this case, we observe transformation in the row of mica-illite-smectite. One of the key phenomena here, perhaps, is the substitution of inter-pack potassium mica

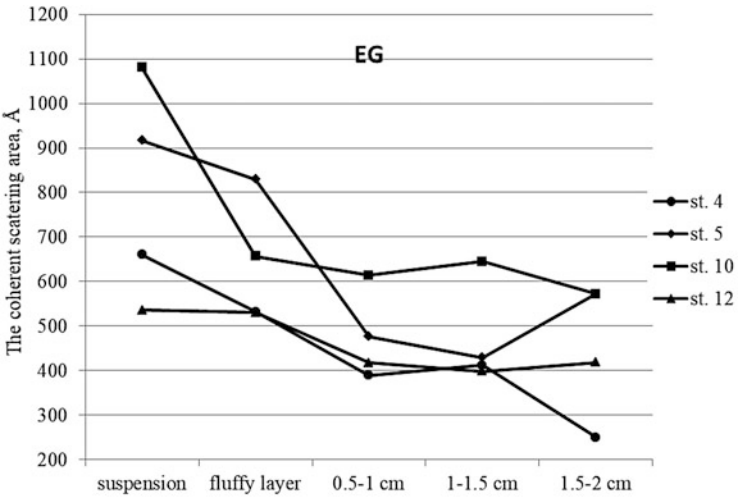

Fig. 15 Early diagenetic changes in the crystallinity of illite (July 2012, stations 4, 5, 10, 12, Neimisto tube sampler)

for the hydrated cations of the surrounding aquatic environment. This is also confirmed by a slight relative increase in the smectite content.

In Fig. 16, distribution of percentage of fine-grained clastic (terrigenous) minerals at sites where surface bottom sediments were collected is displayed. One can see an evident dominance (up to 89%) of fine-grained clastic minerals in all the samples studied. A group of clay minerals accounted for 44–90%.

The clastic terrigenous group is represented by a wide spectrum of minerals carried by both air masses and as a result of snow melting, coastal abrasion, and fluvial supply. This includes the mineral components of light and heavy subfractions, such as quartz, feldspars (albite, anorthite, microcline), minerals of the epidote, pyroxene (diopside, augite), amphibole (tremolite, hornblende), garnet (spessartine, almandine), and mica (muscovite, phlogopite) groups.

A group of carbonates consists of a widespread terrigenous dolomite, authigenic Mg-calcite, as well as the biogenous calcite and aragonite of planktonic and benthic origin. Their contribution to the fine-grained fraction of bottom sediments was minimal.

Clay minerals (smectite, illite, kaolinite, chlorite) occupy the second place in terms of prevalence and have a different genesis. The distribution and composition of clay minerals in the White Sea surface sediments as a whole do not differ from those in the Arctic basin, where illite and chlorite also dominate. In the composition of the fraction studied, the sum of clay minerals rarely exceeded 50% and generally had a subordinate value. It was revealed that the layered silicates' transformation proceeds in a row: mica → illite → illite-smectite → smectite in sedimentary matter at the water-bottom interface, as well as in the early diagenesis stage. The data obtained can serve a basis for further study of sedimentation processes.

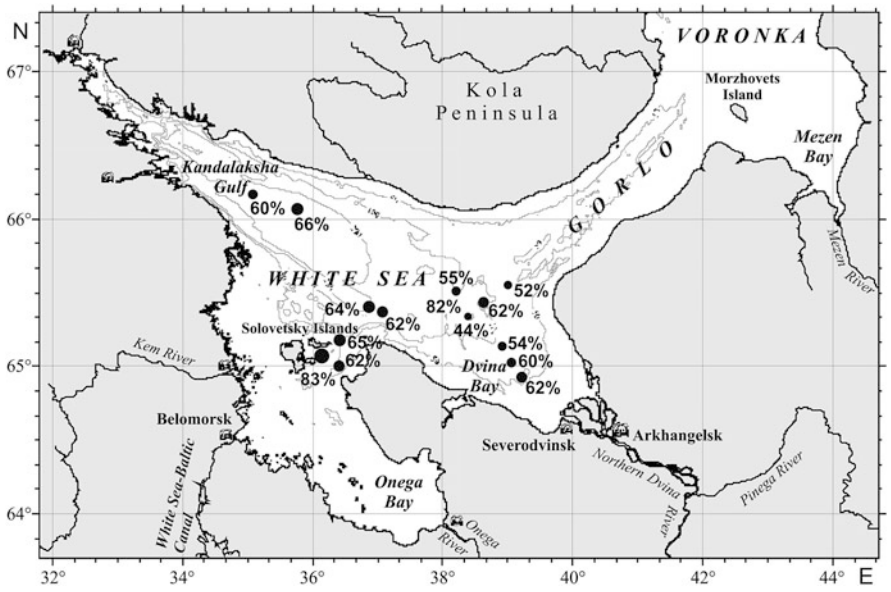

Fig. 16 The content of clastic minerals (%) in the fine-grained fraction (<1 μm) of the surface (0–5 cm) bottom sediments of the White Sea

5 Conclusions

1. The mineral composition of fine-grained (<10 and <1 μm), dispersed (aerosols, cryosols, riverine, and marine suspended matter), and consolidated (bottom sediments) sedimentary matter of the White Sea was studied.
2. It was revealed that opposed to traditional views, the fine-grained pelitic fraction of the White Sea bottom sediments consists not only of *clay* minerals, whose content rarely exceeds 50%, but mostly of fine-grained *clastic* terrigenous minerals.
3. Quartz and feldspars (albite, anorthite, andesine, microcline, orthoclase) dominate among the fine-grained minerals. Dark-colored minerals are represented by a group of amphiboles (hornblende, tremolite) and pyroxenes (augite, diopside). Mica (muscovite, phlogopite) is of subordinate importance.
4. It was defined that albite and microcline could be used as markers of eolian material supply to the eastern Arctic seas, while anorthite, andesine, and orthoclase are indicative of the North Atlantic source, where they are characteristics of aeolian material.
5. The most common clay minerals in the White Sea are illite and chlorite, and this is true for many areas of the Arctic basin. Montmorillonite is the main mineral of the smectite group in the bottom sediments of the White Sea. The alkaline-earth

species of montmorillonite is replaced with the alkaline one in the barrier mixing zone of river and sea water.
6. One of the main mechanisms for settling of fine-grained suspended particulate matter beyond the marginal filter is biosedimentation; the size of the precipitated particles depends on size of the zooplankton filtration apparatus.

Acknowledgments This research was performed in the framework of the state assignment of FASO Russia (theme No. 0149-2018-0016), and analytical data were processed within framework of the RSF grant (project No 14-27-00114-p).

References

1. Lisitsyn AP (2014) Modern conceptions of sediment formation in the oceans and seas. Ocean as a natural recorder of geospheres's interaction. In: Lobkovsky LI, Nigmatulin RI (eds) World ocean physics, chemistry and biology of the ocean, vol 2. Scientific World, Moscow, pp 331–571 (in Russian)
2. Klyuvitkin AA (2009) Formation a suspended sediment in the surface waters of the Atlantic Ocean. PhD dissertation, IO RAS, Moscow, 281 pp. (in Russian)
3. Shevchenko VP (2003) The influence of aerosols on the oceanic sedimentation and environmental conditions in the Arctic. Berichte zur Polar- und Meeresfor 464:1–149
4. Lisitsyn AP (2012) Scattered sediment in the geospheres of the earth and in the White Sea system. In: Lisitsyn AP, Nemirovskaya IA (eds) The White Sea system. Vol II water column and interacting with it atmosphere, cryosphere, river runoff and biosphere. Scientific World, Moscow, pp 19–48 (in Russian)
5. Lisitsyn AP (2013) Systemic four-dimensional studies of dispersed sedimentary matter in the water column of the White Sea, interaction between the catchment geospheres and the water. In: Lisitsyn AP, Nemirovskaya IA (eds) The White Sea system. Vol III dispersed sedimentary hydrosphere material, microbial processes and pollution. Scientific World, Moscow, pp 25–38 (in Russian)
6. Lisitsyn AP (1955) Atmospheric and aqueous suspended particulate matter as a source of formation of marine sediments. Proc Shirshov Ocean Ins 13:16–22 (in Russian)
7. Lisitsyn AP (1974) Sedimentation in the oceans. Nauka, Moscow, p 438 (in Russian)
8. Lisitsyn AP (2010) Marine ice-rafting as a new type of sediment formation in the Arctic and novel approaches to study sedimentary processes. Rus Geol Geoph 51(1):12–47
9. Lisitsyn AP (2010) Processes in the White Sea catchment area: preparation, transportation and deposition of sedimentary material, the concept of a "living catchment". In: Lisitsyn AP, Nemirovskaya IA (eds) The White Sea system. Vol I the natural environment of the White Sea catchment area. Scientific World, Moscow, pp 353–446 (in Russian)
10. Krivonosova NM, Medvedev VS, Rateev MA, Kheirov MB (1974) Clay minerals in suspended matter of the White Sea coastal zone. Izv Vys Uch Zav Geol Raz 3:52–60 (in Russian)
11. Kalinenko V, Rateev M, Kheirov M, Shevchenko A (1974) Clay materials in sediments of the White Sea. Lith Min Res 4:10–23 (in Russian)
12. Rateev MA, Rasskazov AA, Shabrova VP (2001) Global patterns of distribution and formation of clay minerals in modern and ancient seas and in the World Ocean and geological factors. Proc IPhE RAS, 199 pp. (in Russian)
13. Rateev MA, Sadchikova TA, Shabrova VP (2008) Clay mineral in recent sediments of the world ocean and their relation to types of lithogenesis. Lith Min Res 43(2):125–135 (in Russian)
14. Lisitsyn AP, Novigatsky AN, Shevchenko VP, Klyuvitkin AA, Kravchishina MD, Filippov AS, Politova NV (2014) Dispersed organic matter and its fluxes in oceans and seas on the example of the White Sea: results of a 12-year study. Doklady Earth Sci 456(4):635–639 (in Russian)

15. Moore DM, Reynolds RC (1997) X-ray diffraction and the identification and analysis of clay minerals, 2nd edn. Oxford University Press, Oxford, NY, 378 pp
16. Frank-Kamenetsky VA (ed) (1983) X-ray analysis of the main types of rock-forming minerals. Nedra, Leningrad, p 360 (in Russian)
17. Biscaye PE (1965) Mineralogy and sedimentation of recent deep-sea clay in the Atlantic Ocean and adjacent seas and oceans. Geol Soc Am Bull 76:803–832
18. Shlykov VG (2006) X-ray analysis of the mineral composition of dispersed soils. GEOS, Moscow, p 176 (in Russian)
19. Brown G (ed) (1965) The X-ray identification and crystal structures of clay minerals. Mir, Moscow, p 600 (in Russian)
20. Lisitsyn AP (1978) Processes of ocean sedimentation. Lithology and geochemistry. Nauka, Moscow, p 392 (in Russian)
21. Shevchenko VP, Grieken RV, Malderen HV, Lisitsyn AP, Kuptsov VM, Serova VV (1999) Composition of individual aerosol particles in marine boundary layer over the seas of western Russian Arctic. Doklady Earth Sci 366(2):242–247
22. Shevchenko VP, Filippov AS, Lisitsyn AP, Zolotykh EO, Isaeva AB, Kravchishina MD, Novigatsky AN, Politova NV, Pokrovsky OS, Bobrov VA, Bogunov AY, Kokryatskaya NM, Zavernina NN, Korobov VB (2010) On the elemental composition of suspended matter of the Severnaya Dvina River (White Sea region). Doklady Earth Sci 430(5):686–692
23. Kravchishina MD, Dara OM (2014) Mineral composition of the suspended particulate matter in the White Sea. Oceanology 54(3):327–337
24. Lisitsyn AP (1991) The processes of terrigenous sedimentation in the seas and oceans. Nauka, Moscow, p 271 (in Russian)
25. Lisitsyn AP (1995) The marginal filter of the ocean. Oceanology 34(5):671–682
26. Nikishina AB, Dara OM, Drits AV, Gordeev VV, Sergeeva VM, Soloviev KA, Stupnikova AN (2015) The role of zooplankton in the sedimentation of suspended matter by the example of the Wellbeing Bay. In: Flint MV (ed) Ecosystems of the Kara Sea: new data from expeditionary research. Shirshov Institute of Oceanology RAS, Moscow, pp 142–146 (in Russian)
27. Drits AV, Kravchishina MD, Pasternak AF, Novigatsky AN, Dara OM, Flint MV (2017) Role of zooplankton in the vertical flux in the Kara and Laptev Sea in Autumn. Oceanology 577 (6):934–948
28. Lein AY, Kravchishina MD, Politova NV, Ul'anova NV, Shevchenko VP, Savvichev AS, Veslopolova EF, Mittskevich IN, Ivanov MV (2012) Transformation of particulate organic matter at the water-bottom boundary in the Russian Arctic Seas: evidence from isotope data. Lith Min Res 47(2):99–128

Development History and Quaternary Deposits of the White Sea Basin

Aleksander E. Rybalko, Vitaliy A. Zhuravlyov, Lyudmila R. Semyonova, and Mikhail Yu. Tokarev

Contents

Abstract The Late Pleistocene and Holocene history of the White Sea Basin is a key to the paleogeography of Northwestern Russia. The chapter describes successively the history of the study of Quaternary sediments in the White Sea, the existing views on the time, and features of the development of the modern sea basin. A seismic-acoustic profiling and lithostratigraphic analysis of selected cores were used to divide the Quaternary cover. Geophysical data made it possible to characterize its three-member structure: glacial, glacial-marine, and marine facies. Lithological and micropaleontological data were used to justify the age of seismic-acoustic units, as well as to characterize facies of the seabed deposits. Analysis of seismic and lithostratigraphic data characterized the major stages of the White Sea Basin history, which began about 14,000 years ago after the onset of the terrain deglaciation. The change of the

A. E. Rybalko (✉)
Institute of Earth Sciences of St. Petersburg State University, St. Petersburg, Russia
e-mail: alek-rybalko@yandex.ru

V. A. Zhuravlyov
Marine Arctic Geological Expedition (MAGE), Murmansk, Russia

L. R. Semyonova
Geological Institute (VSEGEI), St. Petersburg, Russia

M. Y. Tokarev
Lomonosov State University, Moscow, Russia

A. P. Lisitsyn and L. L. Demina (eds.), *Sedimentation Processes in the White Sea: The White Sea Environment Part II*, Hdb Env Chem (2018) 82: 135–164,
DOI 10.1007/698_2018_318,
Published online: 15 August 2018

sedimentation regime occurred about 11,000 years ago. As a result of the penetration of seawater through the Gorlo Strait, glacial-marine basins appeared in the White Sea Basin. In the boreal time of the Holocene (about 9,000 years ago), the marine regime was finally established in all White Sea. A schematic of the Late Pleistocene glacial flow distribution is attached to the chapter. We assume that the Late Pleistocene glaciers did not come in stages from the west but also from the northeast over Kanin Peninsula. New data add details to the Holocene sedimentation history and establish the onset of marine environment on Kola Peninsula, in Karelia, and in the Arkhangelsk region. Recent seismic-acoustic surveys and multichannel high-frequency tools expanded our knowledge of geological bodies and their stratigraphic position in the inner glacial basin. New dating of drill cores and recent geophysical data added quantitative criteria to the Quaternary history.

Keywords Glacial history, Glaciation, Holocene, Quaternary deposits, Seabed sediments, Seismic profiling, White Sea

1 Introduction

The Late Pleistocene and Holocene history of the White Sea Basin is a key to the paleogeography of Northwestern Russia. Many studies of this area were carried out by the Kola and Karelian branches of the Russian Academy of Sciences, some results of which have been published [1–4].

The Pleistocene, more precisely, Late Pleistocene sediments were deposited in the White Sea Basin, so the main features of the basin history should be sought on the seafloor. This study was based on the following aims:

- Analysis of geological surveys performed by A.P. Karpinsky Russian Geological Research Institute (VSEGEI) in the middle of the twentieth century
- Review of the Quaternary studies on Kola Peninsula supplemented by original data, including description of key sections studied by VSEGEI during geological mapping covering all the area of the White Sea and a coastal land at 2003–2005
- Interpretation of new seismic-acoustic lines surveyed by Marine Arctic Geological expedition (MAGE) in 2003–2007 in the White Sea and the analysis made during preparation to publishing of the State Geological Maps
- Geological data obtained by Sevmorgeo in cooperation with the Institute of Oceanology of the Russian Academy of Sciences while completing the *World Ocean* and *White Sea* programs (2004–2007)
- The latest seismic-acoustic data obtained by SIC and Sevmorgeo in the northwestern White Sea

The authors are members of the named institutions, and the materials presented here make up a version of Quaternary geology of this most interesting region.

2 Milestones of the White Sea Quaternary Studies

The first information on the White Sea floor sediments was obtained during hydrobiological studies carried out in the nineteenth century. The greatest contribution to the seabed description was made by outstanding Russian hydrobiologist K. M. Deryugin. He was the first who established deepwater sands, sandstones with concretions, and other evidence of slow sedimentation in the White Sea deepwater environment [5].

A detailed study of the White Sea sediments was undertaken by the Boat-Based Marine Institute (Plavmornin), which was established in 1923 in Murmansk on the *Perseus* vessel. The *Perseus* lifted the first columns of seabed sediments and obtained detailed information on the distribution and composition (including chemical composition) of the sediments, provided a detailed description of concretions. The first description of the lithostratigraphic column of the White Sea was published by I. K. Avilov [6], who discovered that the Holocene seabed sediments have glacial formations at the base, which then have been overlaid by glacial-lacustrine and marine-glacial deposits.

The second phase of the lithologic-stratigraphic works in the White Sea was performed by the Belomorskaya Expedition of the Institute of Oceanology in 1957. These works made a significant contribution to understanding of the White Sea history and to stratigraphy of the Late Pleistocene deposits [7–9]. The current Quaternary stratigraphic column includes glacial, glacial-lacustrine, glacial-marine, and marine sediments, as well as transitional strata between the last two types.

The next lithologic-stratigraphic stage of research was an offshore mapping. The mapping was initiated by VSEGEI in 1971, and it included sampling of seabed sediments using ground pipes and drags. The mapping first included geophysical surveys. In 1972, VSEGEI together with Lomonosov State University, Moscow, completed a seismic-acoustic survey [10]. It discovered that the Quaternary sediments make up an almost continuously cover over the White Sea floor, but they are missing on separate basement highs [11]. The sampled deposits primarily represented the latest glaciation–sedimentation cycle, i.e., the Ostashkovian moraine and the late postglacial sediments [9, 12, 13].

The pilot mapping was supported by biostratigraphic studies based on palynological (Ye. A. Spiridonova, L.V. Kalugina, N. A. Gey, et al.), diatom (R. N. Ginoridze), and micropaleontological (Ye. A. Kirienko) determinations. In total, more than 43 columns from various locations were studied. The results were described in many publications [14–17]. The studies discovered deposits older than those of the latest glaciation–sedimentation cycle. These deposits occur locally in small topographic lows on the basement surface [18]. Such lows were found on the northern slope of the central deepwater trough, north of the Solovets Islands.

In the eastern White Sea (the southern and southeastern parts of Dvina Bay and the southeastern part of the Gorlo Strait), new data on Quaternary sediments were obtained in 1981–1990 by the Novodvinsk expedition and the Moscow Geological Exploration Institute. They first added offshore drilling to the geological survey, and drilled a 10-m-thick member of clayey sands with shell remains, occurring in a sink

on the bedrock seabed in the Gorlo Strait [18, 19]. The sand was subjected to the thermic-luminescent analysis and dated back to the Mikulino (Eemian) interglacial (110–160 kyr). These data agree with the materials of VSEGEI of 1975, according to which a unit of gray soft silty clays was penetrated by drilling abeam the village of Chapoma. The spore and pollen analysis (by Ye. A. Spiridonova) suggested that clays were deposited in the interstadial of the Moscovian glaciation [15]. The Onega Bay deposits were also subjected to palynological and paleomagnetic analyses and dated back to the Middle Valdaian interstadial [2, 20].

Finally, in the late 1980s, a lithostratigraphic scale was supported by seismic-acoustic and biostratigraphic data. The scale included (1) marine deposits of the Mikulino interglacial, (2) lacustrine-marine (lacustrine-glacial) deposits of the Middle Valdaian interstadial, (3) the Late Valdaian moraine, (4) glacial-lacustrine and glacial-marine sediments (from the Younger Dryas to the Boreal inclusive), and (5) marine deposits (from the Atlantic to the Subatlantic) [11].

The survey data of VSEGEI and of the Novodvinsk expedition of Arkhangelskgeologiya made up a basis for geological maps at a scale of 1:1,000,000, quadrangles Q-35, Q-36, and Q-37 (new series) [21].

New Quaternary stratigraphic data were obtained during sedimentological studies in the White Sea under the *World Ocean* research program supervised by Acad. A. P. Lisitsin [22]. The peak of the sampling program, performed by the *Professor Stockman* and the *Academic Keldysh* research vessels, was in 2003–2007. In 2003–2006, MAGE was engaged in a geological survey for updating the state geological map (scale 1:1,000,000) of the White Sea and adjacent land. Cartographic works with participation of VSEGEI and Sevmorgeo were carried out in 2008–2011 [23–25].

3 White Sea Quaternary Deposits

3.1 Seismic Stratigraphy

Seismic-acoustic data play a decisive role in shaping the views on the White Sea unconsolidated sediments. General stratigraphy is shown on the regional seismic-geological section based on a seismic profiling by MAGE (Fig. 1). The almost entire seafloor is covered by Quaternary deposits unconformably overlying the Archaean-Proterozoic and Riphean basement. In the northern part of the White Sea Voronka, the basement consists of Paleozoic sedimentary rocks belonging to a platform cover of the Russian Plate (Fig. 2).

A thickness of the Quaternary deposits sharply changes from 0 to 200 m, averaging to 30–40 m [12, 26, 27]. The thickest Quaternary occurs in older incised tectonic-erosional lows. The longest and deepest low runs along the southwestern steep side of the Kandalaksha Graben. A base of the Quaternary was identified by CMP at a depth of 480 m below sea level (b.s.l.) (Fig. 1). The Quaternary has its maximum thickness of 200 m in the center of the basin. A high thickness (100 m and more) is also known from the glacier ridges running along the southern coast of Kola

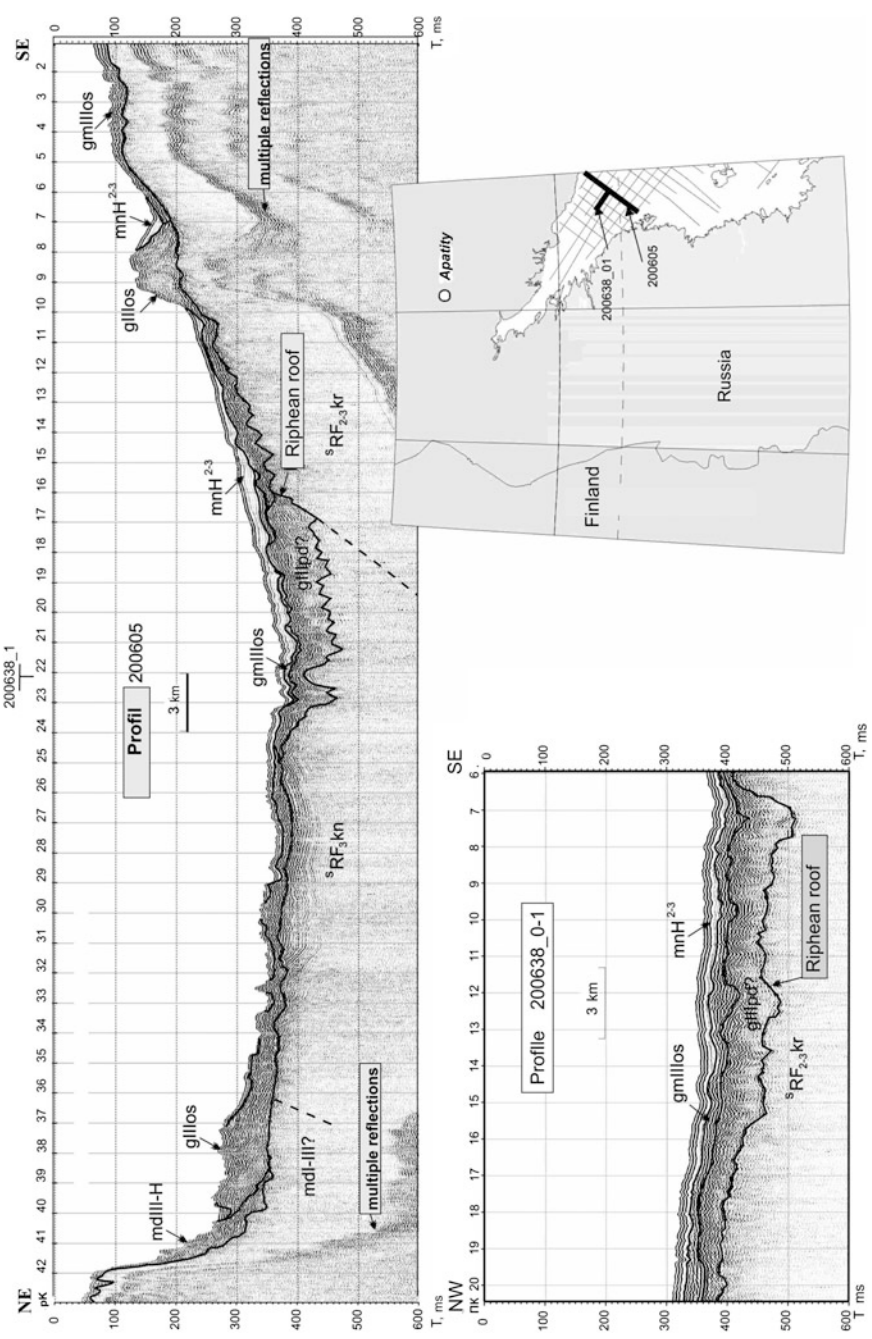

Fig. 1 Seismic-geological section across the central part of the White Sea Basin illustrating the occurrence and relationships of main lithostratigraphic units. The lower panel shows a two-member structure of the glacial sequence. Conventions: $^{s}RF_{2-3\ kr}$ seismic complex, corresponding to the Middle-Upper Riphean,

Fig. 1 (continued) $^{s}RF_{3\ kn}$ seismic complex, corresponding to the Upper Riphean, Quaternary deposits: *mdI-III* gravity deposits, Lower-Upper Pleistocene, *gIIIpd* glacial deposits of Upper Pleistocene, Podporozhsky strata, *gIIIos* glacial deposits of Upper Pleistocene, Ostashkovsky strata, *gmIIIos* glacial-marine deposits of Upper Pleistocene, Ostashkovsky strata, *mdIII-H* gravity deposits, Upper Pleistocene–Holocene, mnH^{2-3} marine nepheloid deposits of Middle and Upper Holocene (Courtesy of MAGE, 2009)

Peninsula and clearly seen in Fig. 1. The least thickness Quaternary cover revealed by seismic-acoustic profiling is on the plateau located north of the Solovets Islands and in the Gorlo Strait.

The seismic-geological units are sedimentary units which are considered as the stratigraphic units consisting of conformable sequences of genetically allied deposits separated by base and top unconformities or corresponding conformable surfaces. The stratigraphic units consist of genetically allied deposits accumulated during a certain period. They may be considered as chronostratigraphic units providing an ideal opportunity for stratigraphic analysis.

In the White Sea – a typical shelf basin – the Quaternary deposits often have a spot occurrence in the internal sea areas and are not laterally continuous (Fig. 3).

At the same time, the seabed glacial, fluvial-glacial, and fluvial deposits demonstrate a specific recorded wave field and compose the bodies with inherent geometry which may guide geological and facies interpretation [1, 28, 29].

The oldest Pleistocene deposits fill two deep incised lows in the northwestern and central parts of the White Sea. The both lows are confined to the tectonic zones trending SE–NW and deeply carved by two lobes of a glacier (Fig. 4).

The base of the unconsolidated sedimentary cover was identified by CMP at a depth of 480 m b.s.l., and here the maximum thickness of the sediments reached 200 m. The seismic-acoustic profiling penetrated only the upper part of this unit and produced an "irregular record" with scarce internal reflections. Such a record indicates an unsorted fill of the lows. The detachment surfaces which mark a multistage land sliding were also revealed by seismic-acoustic profiling (Fig. 5).

Unit SSUIII (Table 1) consists of the Mikulino marine deposits locally occurring along the southeastern coast of Kola Peninsula and in the Gorlo Strait. The features of the unit are extensive separated bright reflections. Near the mouth of the Varzuga River, the deposits have a thickness of 10–15 m. In the southern Gorlo Strait, the deposits are as thick as 7 m, as drilling data suggest [18]. The seismic-acoustic records show that the Mikulino deposits are overlaid by glacial-marine and moraine deposits. On the Zimniy Coast, at the mouth of the Ruchi River, the Mikulino deposits are as thick as 70 m [24] (Fig. 6).

Unit SSUII, the second seismic-stratigraphic unit, is widely developed in the White Sea. It consists of glacial deposits of various types that were mapped by VSEGEI together with Lomonosov Moscow University [11, 23]. On a seismogram, the glacial deposits produce chaotic reflections, occasionally with variously oriented layering, tile-like wave patterns, and diffraction axes (Fig. 7).

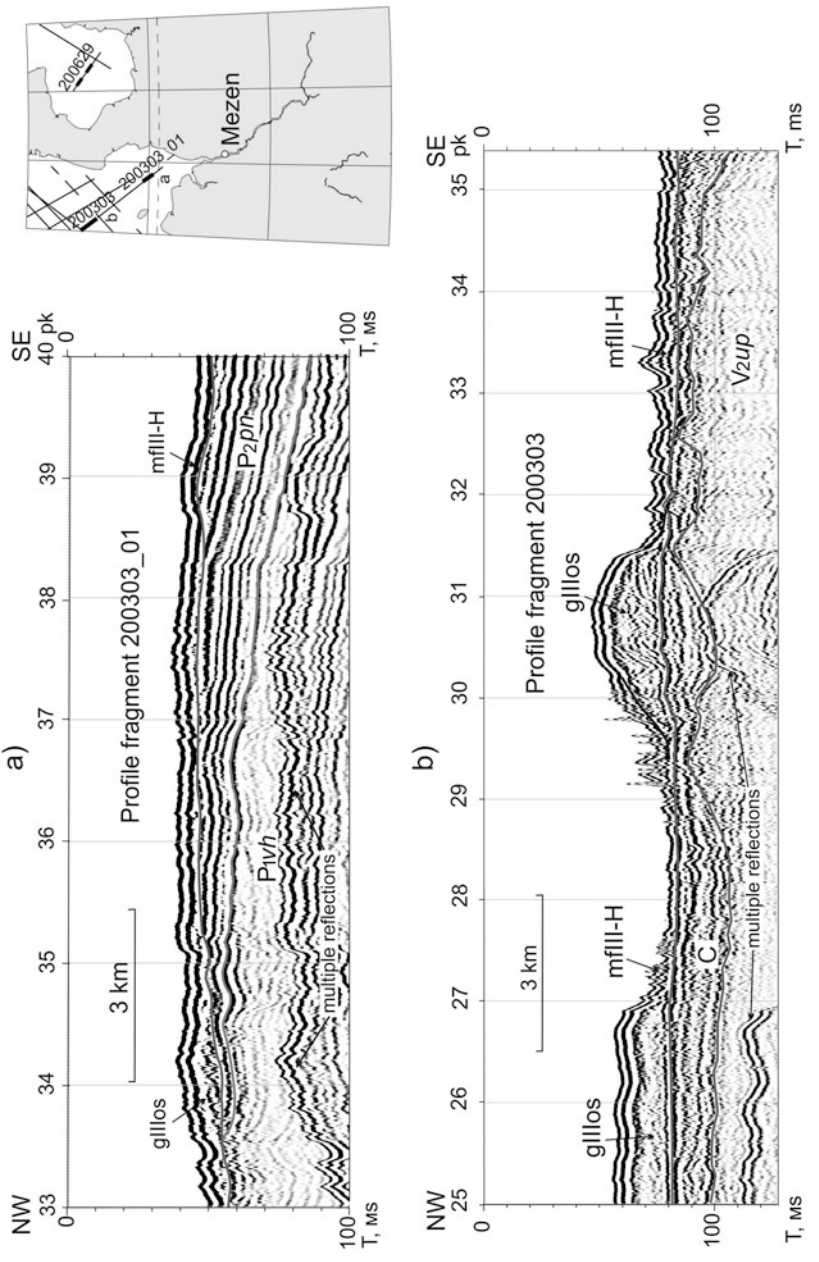

Fig. 2 The wave field and structure of Paleozoic series in Mezen Bay: (**a**) the Vikhtovo and Pinega groups, (**b**) the undifferentiated Carboniferous overlain by Quaternary moraine and marine fluvial deposits. After V. A. Zhuravlyov and S. I. Shkarubo (State ..., 2009). Conventions: $V_{2\,up}$ Vendian deposits, Ust-Pinega suite, *C* carboniferous deposits, P_1 *vh* Lower Permian deposits, P_2*pn* Upper Permian sediments, quaternary deposits: *gIIIos* glacial deposits of Upper Pleistocene, Ostashkovsky strata, *mfHIII-H* marine fluvial deposits of the Upper Pleistocene–Holocene

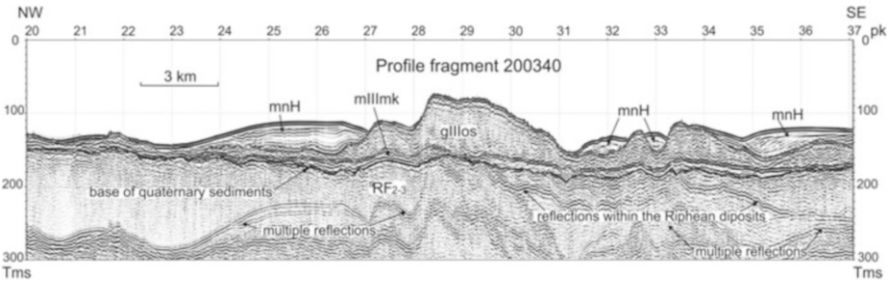

Fig. 3 Spot occurrence of marine deposits on the erosional surface of glacial deposits (Courtesy of MAGE). Conventions: $RF_{2–3}$ Middle-Upper Riphean deposits; quaternary deposits: *mIIImk* marine Upper Pleistocene (Mikulin) sediments, *mnH* marine nepheloid deposits of Holocene

Fig. 4 Isolines of the base of the Quaternary in the White Sea. After V. A. Zhuravlyov (State. . ., 2012a)

Subunit SSUIIa consists of the oldest glacial deposits occurring in a short and wide low, which is incised into the basement to 120 m. This low is located in the north-central part of the Kandalaksha Graben (Fig. 1). The seismic-acoustic record suggests that here we see the lowest glacial sequence. The overlying glacial deposits were eroded, and a younger moraine, fluvial-glacial, and marine sediments lay directly upon the lower glacial strata. This subunit is the lowest glacial deposit of the Podporozhye (Early Valdaian) phase of glaciation.

Subunit *SSUIIb* is widely known from the entire White Sea. It consists of a main ablation moraine that lies as a drape over older deposits (Fig. 1) but occasionally may build hummocks (Figs. 4 and 7). In Kandalaksha Bay, the maximum thickness of the

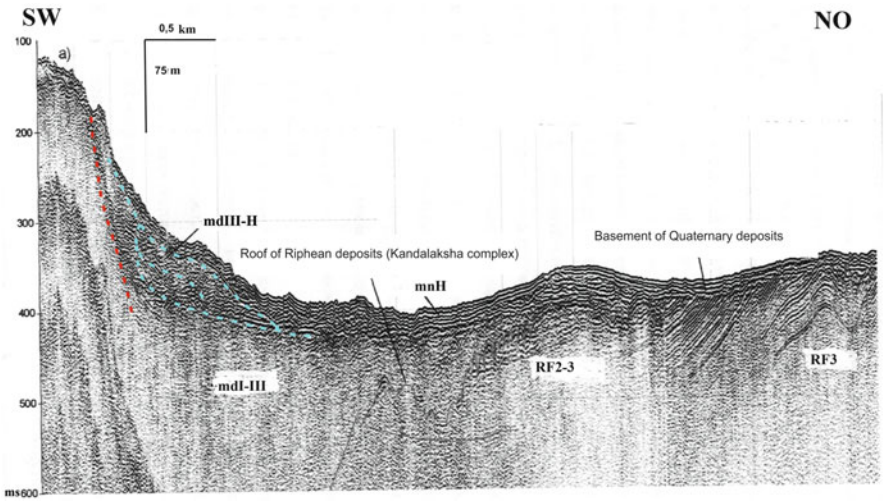

Fig. 5 A seismogram from the southern part of Kandalaksha Bay (Oleny Island). The red dashed line depicts a fault, and the green one is a landslide detachment surface. Conventions: RF_{2-3} seismic complex, corresponding to the Middle-Upper Riphean, RF_3 seismic complex, corresponding to the Upper Riphean; quaternary deposits: *mdI-III* gravity deposits, Lower-Upper Pleistocene, *mdIII-H* gravity deposits, Upper Pleistocene–Holocene, *mnH* marine nepheloid deposits Holocene (Courtesy of MAGE)

Table 1 Scheme of comparison of seismostratigraphic and stratigraphic units

SSU		Indexes Stratigraphic subdivisions that are part of this SSU						
Epoch/Age	Horizon	SSUI						
Holocene	Upper				mnH, mH, mpH, amH	$mnH^{2, 3}$	mdI-II-H, mfII-I-H	mvH^3, mfH^3
	Middle							
	Lower					mnH^1		
Pleistocene	Ostashkovsky	SSUIV	SSUII	SSUIIb, SSUIIc	mdI-III (?)	gIIIos, fIIIos, lgIIIos, gmIIIos		mfIII
	Graghdansky							
	Podporoghsky			SSUIIa		gIIIpd		
	Mikulinsky		SSUIII			mIIImk		
	Babushkinsky							
	Oksky							

? the existing uncertainty in determining the age without drilling data

subunit (120 m) was recorded in the two-layered terminal moraine near the Ostrye Ludy Islands. The main moraine has a spot occurrence in the central part of the basin, where glacial exaration reached its maximum, but it exists also in Onega Bay, where its thickness increases. Here, the moraine lies on bedrock, fills deep paleo-valleys, and flattens the erosional-tectonic topography of the older seafloor.

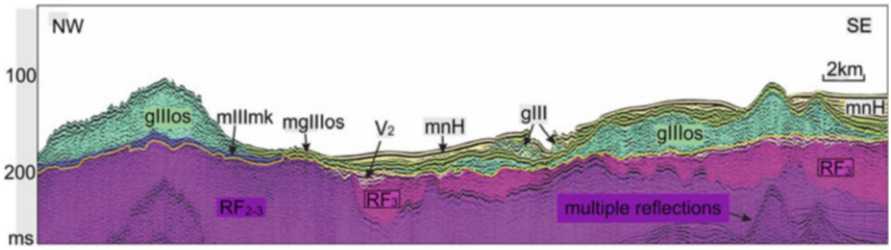

Fig. 6 Relationships of seismic-stratigraphic units and subunits SSUIII (*mIIImk*), SSUIIb (*gIIIos*), SSUII (*mgIIIos*), and SSUI (*mnH*) in the northern White Sea. Bedrock: RF_{2-3} seismic complex, corresponding to the Middle-Upper Riphean, RF_3 seismic complex, corresponding to the Upper Riphean, *V* Vendian deposits. Part of seismic profile AR-3 (Courtesy of Sevmorgeo and MAGE)

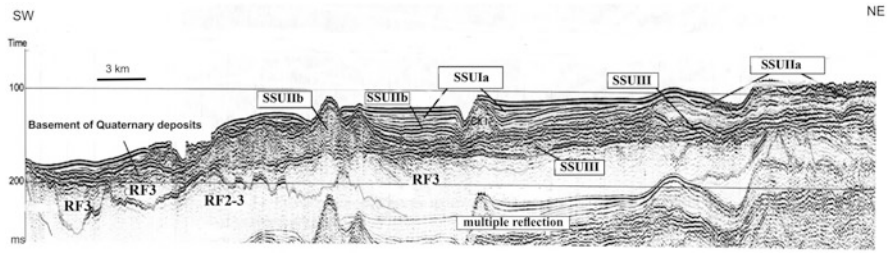

Fig. 7 An intricate combination of glacial and supraglacial deposits in a glacier-marginal moraine on the southern coast of Kola Peninsula. Conventions: RF_{2-3} seismic complex, corresponding to the Middle-Upper Riphean, RF_3 seismic complex, corresponding to the Upper Riphean, Quaternary deposits: *SSUIII* marine Upper Pleistocene (Mikulin) sediments, *SSUIIb* till, Ostashkovsky horizon, *SSUIIa* till + fluvioglacial deposits, Ostashkovsky horizon, *SSUIb* marine-glacial deposits, Lower Holocene, *SSUIa* marine nepheloid deposits Holocene

Thick, occasionally multilayered, moraines, submarine landslides, and gravity deposits occur along the steep southwestern side of the Kandalaksha Graben. Glacier-marginal moraines make up two ridges and trend from Kola Peninsula along the Terskiy Coast between the mouth of the Olenitsa River and the Gorlo Strait (Figs. 3 and 7). The thickness of glacial deposits in those ridges reaches 60 m. Moraine formations in the Gorlo Strait are largely eroded and are oriented along the sea current; they may represent glacier-marginal ridges. In the White Sea Voronka, the moraine lies on the erosional bedrock surface. Under the impact of tidal currents, the moraine transfers into ridges of the NNW–SSE trend. A thickness of glacial deposits occasionally reaches 50 m and averages to approx. 20 m. The largest ridges extend off the shore to Morzhovets Island.

Subunit SSUIIc consists of convex bodies leaning against the steep side of the Kandalaksha graben and existing in the Great Salma Strait. The chaotic seismic-acoustic record occasionally shows long reflections as an evidence of the multiphase deposition. These are also submarine gravity deposits of the Late Pleistocene–

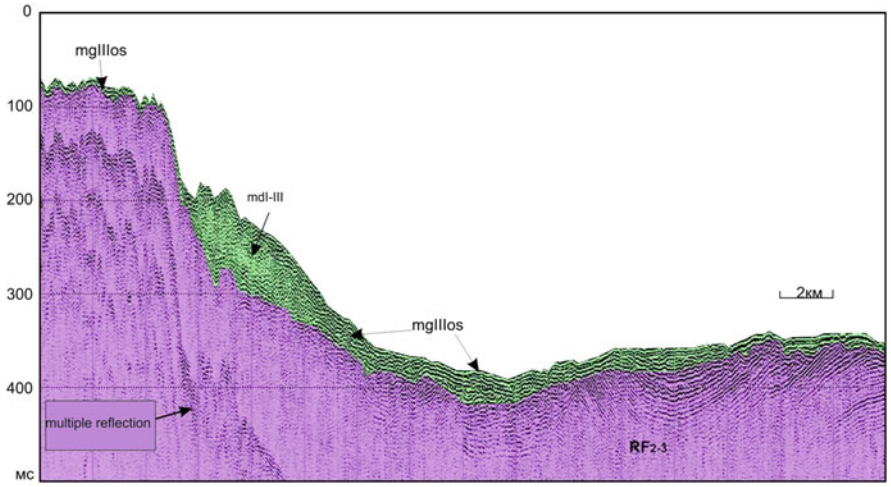

Fig. 8 A composite land slide consisting of a series of slid slabs of glacial deposits. Seismic-acoustic line 200606-1. Conventional symbols see Fig. 1 (Courtesy of MAGE)

Holocene consisting of imbricate series of glacial and interglacial deposits, the formation of which is associated with younger geodynamic movements (Fig. 8).

The recent seismic-acoustic studies have shown that the role of submarine gravity deposits is underestimated. Thus, the subsea slopes of the Velikaya Salma Strait between Velikiy Island and the mainland have a steplike profile. The water depth here ranges from 0 to 120 m. The steps are 100–120 m wide and 20 m (occasionally 30 m) high. A lack of depth correlation, sharp angular unconformities, transition from layered to diffuser structures, and, finally, occasional fine corrugated folding at the base of the steps indicate a gravitational origin (Fig. 9).

In the Velikaya Salma Strait, it is clearly seen that these landslide bodies are closely related to a blocky structure of primary slopes. Shaping of the blocks presumably took place in the Holocene time, and it was associated with glacial isostatic and tectonic rise of shores.

More information on the landslide zones was obtained by a profilograph. It is clearly seen from geo-echograms that all flat steps have a thick (up to 10 m and more) layer of postglacial (mostly Holocene) sediments. The features of sediments suggest that they were deposited after the shaping and flattening of the step surfaces and presumably originated from a turbid suspension agitated by land sliding. Actually, in the lowest part of the trough, there is practically no Holocene sediments, and the seabed is underlain by older rugged sediments. Thus, the seabed in the foothill areas of the basin is almost entirely underlain by submarine gravity sediments, and a genesis of so large landslide masses is closely related to Holocene tectonic movements.

The Quaternary is topped by the first (upper) seismic-stratigraphic unit (SSUI), which consists of sedimentary bodies divided by an angular unconformity from older formations and characterized by a layered transparent wavefield record with rare reflectors. The deposits form a wide range of the late glacial and postglacial

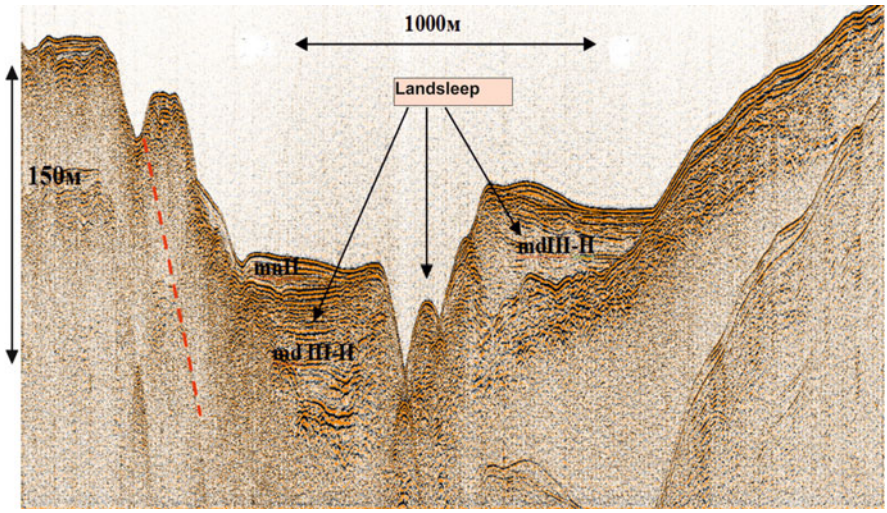

Fig. 9 Landslide gravitational steps in the Velikaya Salma Strait. The red dashed line is a tectonic fault. Conventions: *mdIII-H* gravity deposits, Upper Pleistocene–Holocene, *mnH* marine nepheloid deposits Holocene

buildups of glacial-lacustrine, glacial-marine, fluvial-glacial, and marine origin. Their age is Late Pleistocene–Holocene, i.e., they were deposited after deglaciation of the terrain. The features of the record allow for recognition of several subunits in this seismic-stratigraphic unit. They are as follows:

Subunit SSUIa has a seismic-acoustic record with bright reflections from nearly flat discontinuous layers or ripples of geological bodies which are not homogeneous; they often have inner unconformities indicating erosion. This is proved by pollen analysis that showed mass redeposition of pollen [17] and a glacial-turbidite origin of the layered Late Pleistocene sediments. These sediments occur almost everywhere. The contact of the SSUIa bodies with an underlying moraine is sharp and clear, with distinct erosion. The upper boundary is not always clear, but it is usually characterized by an angular unconformity. The subunit consists of several genetic types: fluvial-glacial, lacustrine-glacial, and marine-glacial deposits accumulated, mainly, in the end of the Ostashkovian time. In terms of their age, the sediments are similar to those of SSUII (Table 1), and this makes the interpretation of seismic-acoustic data ambiguous and shows a lack of geological information for reliable seismogram interpretation (Fig. 10).

Subunit SSUIb is seen on the seismic-acoustic record of the uppermost sedimentary sequence. Occasionally it has a translucent wavefield record, often without clear internal reflections – these are Holocene marine nepheloid sediments filling seabed lows and sinks. The SSUIb in general composes a drape over older deposits (Figs. 6 and 11). On a high-frequency acoustic record, marine sediments produce a transparent weakly layered wavefield pattern, while the underlying glacial-marine and glacial-lacustrine sediments have a distinctly layered pattern. Moreover, even at shallow depths in closed bays, where the sediment accumulation is was quicker, rather large tracts of the seabed

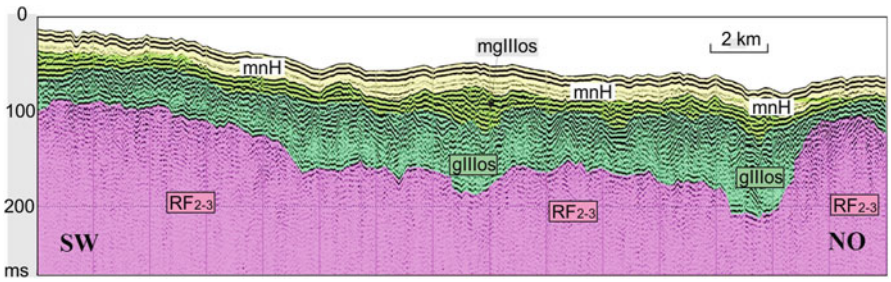

Fig. 10 Conformable occurrence of main seismic-stratigraphic units in the north of the White Sea. The supraglacial sedimentary deposits are easily stratified. Conventional symbols see Fig. 6 (Courtesy of MAGE)

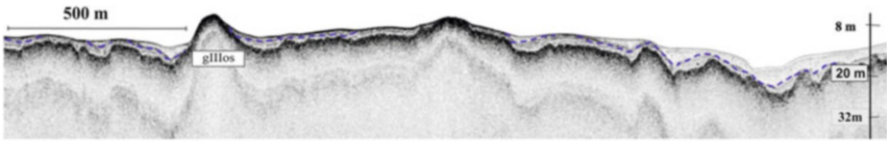

Fig. 11 Geo-echogram (high-resolution seismic-acoustic profiling) from Rugozero Guba Bay of the White Sea. Distribution of Holocene marine deposits (a blue dashed line marks the base), glacial and glacial-marine deposits (the base is marked by an intense black reflection)

are underlain by glacial-marine deposits topped with a thin layer of sand-pebble marine perluvium.

A rugged seabed, often associated with higher velocity of the sea current in shallow waters (<100 m), leads to a spotty occurrence of nepheloid marine deposits. So, these deposits generally are missing on the moraine ridges, which run along the southern coast of Kola Peninsula and make up the northern slope of the Kandalaksha Graben. Here, the hummocky surface may indicate that the seabed is underlain by glacial-marine sediments partly eroded during the transgressive-regressive Late Pleistocene–Holocene history of the basin (Fig. 12).

The seismic-acoustic survey revealed two previously unknown facies of Holocene marine sediments. The first facies include thick bodies of layered sediments in the rear of glacier-marginal ridges in the southeastern Kola Peninsula and off the Onega Peninsula coast (Figs. 1 and 7). On the seismic-acoustic record, they form translucent lenticular wavefield patterns with unclear stratification and a (Fig. 13) progradational sequence. A total thickness is higher than 15 m. The sediments were deposited either within glacier ridges, or on their rear side, where the products of glacier melting accumulated in ridge-dam pools.

In 1985, these sediments were mapped as a separate seismic facies of Quaternary deposits [23]. The sediments are most clearly recognized on high-resolution seismic-acoustic profiling among glacier-marginal formations occurring close to Zhizhigin Island (Fig. 13). The local thick nepheloid sediments were deposited here by both

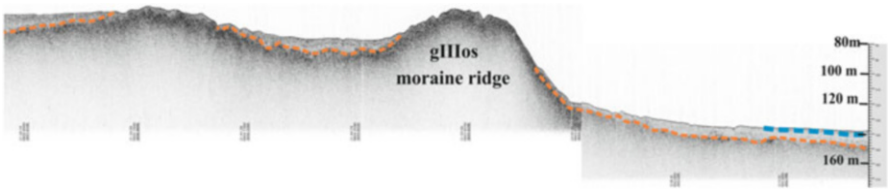

Fig. 12 Geo-echogram from inner and outer slopes of the moraine ridge. In the rear of the ridge, marine Holocene sediments (a blue dashed line marks the base) occur above 80 m b.s.l., and on a seaward slope of the glacier ridge, Holocene silts occur below 140 m b.s.l. In the interval between 80 and 140 m, the seabed is underlain by glacial-marine and glacial deposits (a orange dashed line marks the base glacial-marine deposits)

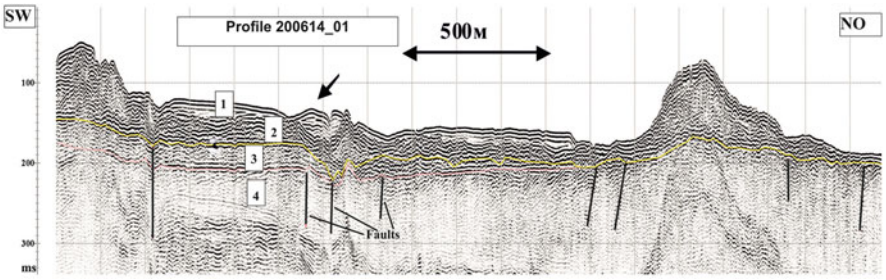

Fig. 13 Thick late glacier and postglacier sediments in the vicinity of Zhizhigin Island. (1) Holocene silts, (2) glacial, (3) Vendian platform cover, (4) Riphean. The arrow points to the zone of abnormally thick Holocene silts.Yellow line is base of Quaternary deposits. Red line—base of the sand-argillaceous deposits of Vendian age. Black line is fault (Courtesy of MAGE)

sediment influx from the shore and erosion of thick glacial-lacustrine clays deposited on the periphery of glacier-marginal buildups at the early time of glacier melting.

Subunit SSUId is another subunit mapped at the transition from the Gorlo Strait to the interior basin, i.e., in the zone of divergence and slowdown of sea currents [24]. In a seismogram, it is shaped like a convex body with a layered gentle-wavy structure. The lowest sediments fill and flatten the older topographic lows; their top was eroded, crop out to the seabed, or overlain by a thin drape of nepheloid deposits. The wedge-like profiles of the sedimentary bodies with gradual thinning out toward the high sea are common. These deposits consist of fine materials transported through the Gorlo Strait and forming the detrital cone composed of fine-grained sediments (fan). Geophysical data of MAGE were proved by sampling performed by the Institute of Oceanology and Sevmorgeo in 2005. In column 06/313 (6059), the sediments consisted of light-gray soft-plastic clays with abundant very small lenticular stringers of sand (Fig. 14).

Subunit SSCIe consists of a special type of Holocene seabed sediments occurring in the White Sea Voronka and the Gorlo Strait. On seismograms, the subunit looks like a pattern of sand ridges, waves, and ripples and corresponds to wave and tidal

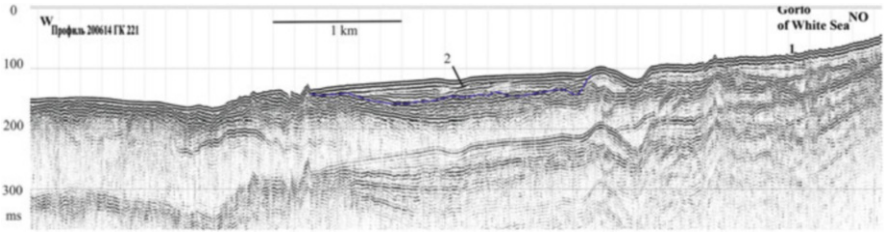

Fig. 14 Subsea fan deposits at the exit from the Gorlo Strait (Courtesy of MAGE). 1—Sand ripples in the zone of underwater currents, 2—progradation bedding in a sandy-silt fans. Blue line of the base of a fanny deposits

Table 2 Dynamic seabed forms in the Gorlo Strait

Seabed form	Height (m)	Length (m)	Width (m)	Crest shape
Longitudinal forms				
Sand strip	*n* 1	500–1,000	*n* 1	Composed of mesoforms
Sand ribbon	Same	200–300	Same	Same
Sand stream	Same	*n* 100	5–10	Same
Transversal forms				
Composite sand wave	4–10	200–300	500	Straight
Major asymmetrical sand wave	4–8	150–200	500	Straight
Sand wave	2–6	50–180	200–400	Straight
Minor sand wave	1–3	50–150	100–200	Straight
Subsea dune	1–2	60–80	50–100	Crescent
Megaripple	1–2	30–70	200	Crescent
Microforms				
Ripple	0.01–0.05	0.1–0.2	0.1–0.2	Crescent

sediments of the Late Holocene. Quantitative parameters of these sediments and their seabed forms are given in Table 2.

The dynamic seabed forms are associated with current velocity and abundance of a clastic load. At a high current velocity, a seabed erosion prevails, and the seabed is underlain by a sand-pebble perluvium protecting it from further destruction. With a higher clastic load and current slowdown, longitudinal accumulative seabed forms, such as sand strips, ribbons, and streams, began to form (Figs. 15 and 16).

The seismogram from the central part of the Gorlo Strait shows that here the Quaternary cover is thin (often not more than 10 m). The seabed forms are large ridge-shaped remnants with their surface sculptured by microridges. Thus, the use of a multi-tool seismic-acoustic profiling made it possible not only to construct a stratigraphic scale of the unconsolidated seabed sediments but to estimate their thickness and identify seismic facies related to sedimentation environments.

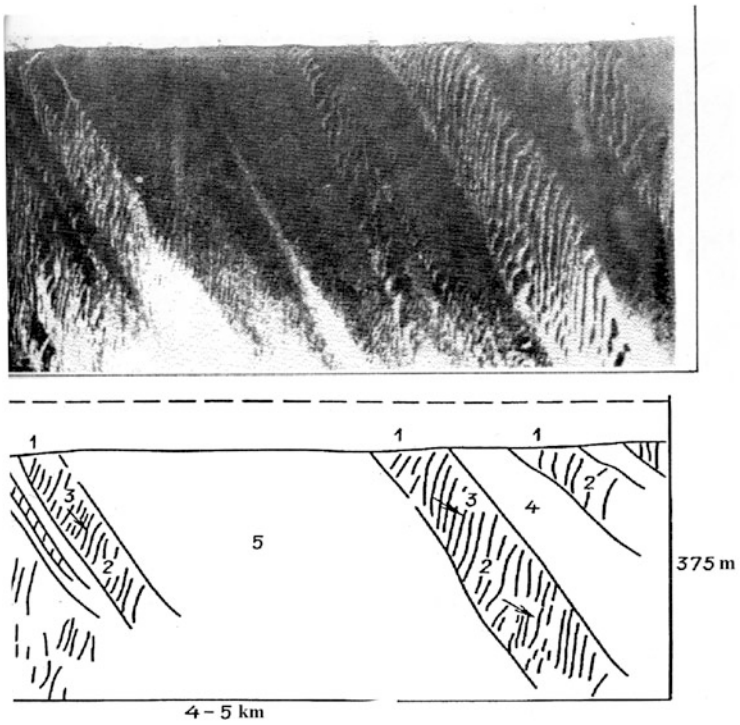

Fig. 15 Dynamic seabed forms in the Gorlo Strait: (1) sand ribbons, (2) sand waves >1 m high, (3) sand waves <1 m high, (4) erosional seabed underlain by perluvium sand, (5) erosional seabed underlain by a boulder-pebble material. The arrow indicates a trend of sand migration. Sonogram

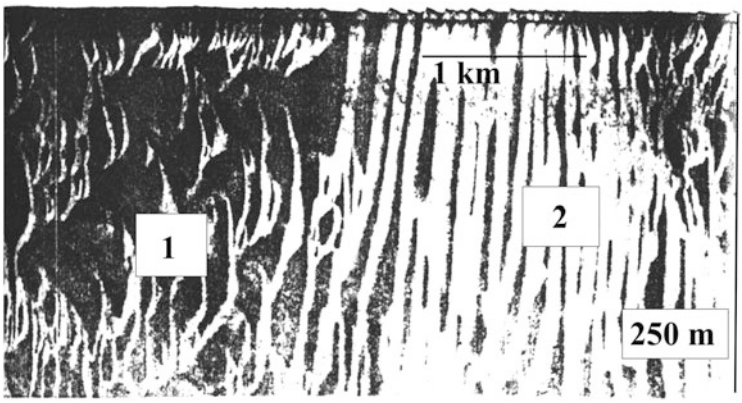

Fig. 16 Types of seabed sand forms on sonograms (see Table 2 for explanations)

3.2 Lithostratigraphy

The seismic-acoustic profiling of the 1970–1990s showed that unconsolidated Quaternary deposits have their basal beds consisting of main, lateral, and ablation moraines [11, 30]. In the 2000th, new seismic-acoustic tools established that the sediments included interglacial and glacial deposits of various phases of the Late Pleistocene glaciation (Fig. 3).

The Novodvinsk expedition drilled Middle-Late Pleistocene marine deposits, which correspond to the European Eemian transgression and are analogs of the Mikulino deposits discovered earlier by drilling in the Gorlo Strait near the mouth of the Verkhnyaya Zolotitsa River [18]. The deposits are 10 m thick and consist of clayey sands with abundant shell remains. The age of sands according to thermic-luminescent analysis is 110–160 kyr [18, 19]. The stratigraphic position of these sediments belongs to the lower Mikulino deposits cropping out at the shore cliffs of the Zimniy Coast. Their thickness in individual lows may reach 100 m, but usually does not exceed 10–30 m.

3.2.1 Late Pleistocene Deposits

In the Quaternary stratigraphic scale of Northwestern Russia, Late Pleistocene deposits belong to the Valdaian (Wurm) suprahorizon. It includes the Podporozhye, Leningrad, and Ostashkovian horizons (Old Wurm, Middle Wurm, and Late Wurm).

The oldest layers of these sediments belong to the Podporozhye and consist of moraines and other deposits left by a continental ice sheet and mountain glaciers, glacial-lacustrine and fluvial-glacial deposits [31]. On the shores of Kola Peninsula, they include sediments of the glacial paragenetic series in the lower reaches of the Chavanga, Kamenka, and Bolshaya Kumzhevaya rivers. In the opinion of F. A. Kaplyanskaya and V. D. Tarnogradskiy [32], these strata may be attributed to the Podporozhye glacial horizon, which is associated with the growth of the Kara glacier in the Early Valdaian time (IKS 4). The recent data suggest that the Strelna sediments [33], widely known from the southern coast of Kola Bay, were also deposited in the Early Valdaian time (IKS 5) [34]. The Late Pleistocene continental glaciation lasted for a short time, which was deduced from the low thickness and limited occurrence of correlative deposits. On the White Sea floor, according to a seismic-acoustic profiling, these sediments arbitrary include the lower unit of glacial deposits, separated by an unconformity, and old glacial deposits found in Kandalaksha Bay, in the southwest of Turiy Peninsula, and in deep lows incised into the Riphean basement (Fig. 1).

The Leningrad horizon, deposited during the Middle Valdaian interstadial on Kola and Onega peninsulas, consists of lacustrine, lacustrine-fluvial, undivided lacustrine, and palludal sediments. Reliable data on the Leningrad marine sediments are lacking. The Podporozhye and Ostashkovian moraines are divided from each other by an erosion unconformity, and no sediments are found between them. However, the columns from Onega Bay show dense brown clays with an unclear almost horizontal

banding, and these clays are overlain by a thin layer of Holocene clay sediments laying on an erosional surface. A characteristic feature of these clays is a high content of kaolinite, nowhere else found [20]. Palynological characteristics of the clays (by E. A. Spiridonova, L. V. Kalugina) are in good agreement with palynological spectra hosted by sandy clays' deposits of the Leningrad interstadial deposits in the western coast of Onega Peninsula [24]. The age is inferred from the paleomagnetic study of column 56–84, in which the Kargopol geomagnetic excursion was identified (39–41 kyr) [2]. However, the unclear geological position and unknown top and base prevent from the final age decision.

3.2.2 Late Valdaian (Ostashkovian) Deposits

The Late Valdaian consists of continental ice sheet deposits and other sediments of the glacial-lacustrine, fluvial-glacial, and glacial-marine genetic types. These deposits build seabed forms in the White Sea, compose terminal glacier ridges of glacial lobes, and infill most of small and medium lows on a bedrock and glacial surface.

The seismic-acoustic data suggest that the deposits of the main regularly layered moraine occur in the basal part of the unconsolidated sequence (Figs. 1, 3, and 7). The glacial deposits are as thick as 10–50 m. The deposits were penetrated by vibration drilling in northern Kandalaksha Bay, where they consist of clayey sands with abundant boulders and fragments of crystalline rocks. The glacial deposits are very dense, have a specific cake-like structure, and host little of highly deformed pollen. Similar characteristics were obtained by vibration drilling in 1974 [9].

Among the most noticeable seabed forms on the today's White Sea floor, there are lateral-moraine ridges. Most clear are the two ridges running along the Tersky Coast (Figs. 2 and 7) of Kola Peninsula from the mouth of the Olenitsa River to the Gorlo Strait. The ridges are as high as 60 m. The lateral moraine unit, according to the seismic-acoustic profiling, occurs along the Zimniy Coast in Dvina Bay and near the northwestern cape of Onega Peninsula. The ridges are asymmetric with steep northern and gentler southern slopes. Inside the moraines, there are long reflectors that may be stratigraphic boundaries. Their age is deduced from the stratigraphic position, relations with the glacier-marginal units on land, and the age of overlying deposits. Sampling shows that the moraines consist of clayey sands and sandy clays with abundant fragments of crystalline rocks. They have a high density (up to 2.3 g/cm^3) and a cake-like structure.

The fluvial-glacial deposits were identified in several boreholes drilled by the Novodvinsk expedition in the 1990s off the Zimniy Coast. They consist of sand, medium, occasionally loamy, gray with a brownish hue, hosting gravel and pebbles (up to 40%) of crystalline rocks.

In the White Sea, the glacial-lacustrine sediments were found only in Onega Bay, where they were confined to the unit of glacier-marginal deposits of the Neva age. They consist of typical banded clays, which grade upward to monotonous brown clays. E. A. Spiridonova and N. A. Gey extracted from laminated clays a palynological spectrum dominated by birch pollen of both woody and shrub species; the

Fig. 17 Sand-pebble perluvial deposits of Kandalaksha Bay at a water depth of 30–40 m. Sand grains are characteristically brown because of ferruginous coatings and manganese-ferruginous rims around clasts of crystalline rocks. A thickness is 20 cm

herbaceous pollen is dominated by Artemisia. The sediments are arbitrary attributed to the Okhta interstadial (13–14 kyr) [20]. The age of the clays also refers to the Göteborg paleomagnetic excursion dated back to 12–14 kyr [2].

The glacial-marine deposits widely occur on the White Sea shelf. They compose a continuous drape over the preglacial formations and, at a depth more than 50–60 m, are overlain by Holocene sediments. At a depth less than 50–60 m, they crop out to the seafloor. In the high sea, they are only covered by thin (50 cm or less) perluvium (Fig. 17).

Glacial-lacustrine sediments occur in Onega Bay; they consist of clayey sands resting upon the moraine and grading upward to brown dense banded clays. North of the Solovets Islands, the sediments consist of monotonous ash-gray sandy clays laterally grading into laminated clays and silts with a small admixture of gravel and pebbles. All studied profiles have a transgressive type with an upward grading of layered clays into homogenous clays with a low sand and silt content. In the northern White Sea, near the Kola Bay coast, glacial-lacustrine deposits consist of laminated clays and clayey silts of brownish-gray color; near the Varzuga River mouth, they grade into brown fine-elutriated clays, and toward the Gorlo Strait, they grade into brownish-gray laminated clays with minor sand and gravel.

Biostratigraphic dividing is mainly based on pollen determinations. In the northern White Sea, E. A. Spiridonova found sediments of the Allerød oscillation and Younger Dryas interstadials [14]. The top of these sediments is metachronous – in the Gorlo Strait, the accumulation of brownish-gray clays ceased in the Late Allerød oscillation, while deposition of their glacier-marginal analogs in the east continued until the end of the Younger Dryas.

In Onega Bay, the age of glacial-marine sediments also was defined as the Allerød oscillation – Younger Dryas. According to R. N. Dzhinoridze, the Allerød oscillation deposits host a rather poor community of freshwater diatoms *Aulacoseira ambigua*, *Stephanodiscus dubius* var. *arcticus*, and other species, and this points to the lacustrine-glacial environment. In the Younger Dryas, a sublittoral Arctic Boreal brackish water

community of diatoms *Coscinodiscus lacustris* var. *septentrionalis* and *Chaetoceros holsaticus* indicates a glacial-marine environment proved by E. A. Kirienko's findings of foraminifers *Retroelphidium clavatum*, *Elphidium* sp., *Nonionellina labradorica*, *Bucella frigida*, and other species [15]. These species indicate that seawater began to encroach Onega Bay in the Younger Dryas.

North of the Solovets Islands, in the basal gray-layered clays, the pollen spectrum was dominated by herbaceous plants and spores of the Middle Dryas. The following palynological spectrum, compared with that of the Allerød oscillation, was dominated by pollen of woody species (60–70%), among which pines prevail, and pollen of woody birches prevail over birch shrubs. Sediments of the Younger Dryas host a small amount of organic remains such as sponge spicules and charred wood debris. In the general composition of the pollen spectra, the leading role belongs to non-wood species – herbaceous pollen and spores [17].

Holocene marine deposits are quite diverse, and the widest facies diversity was a characteristic of the Early Holocene. In Kandalaksha Bay, these deposits occur only in full sections making up thin members (not more than 0.5 m) of fine-elutriated brown clays with small authigenic concretions of sulfides. In Onega Bay, these deposits consist of homogeneous gray clays and silts, with occasional greenish hue, that grade into unconsolidated water-saturated clays and silty clays with xenomorphic layer-bound hydrotroilite concretions. The sediments host shells and shell debris of sea mollusks. North of the Solovets Islands, Early Holocene marine nepheloids consist of brownish liquid-plastic clays with xenomorphic concretions of hydrotroilite and organic matter. A thickness of the Early Holocene deposits is 0.5–5 m.

Along the Kola Peninsula shoreline, these deposits consist of soft clays and silty clays, brownish-gray, variegated, with spots of black organic matter and hydrotroilite. These spots may include authigenic yellowish sulfides. The sediments are very fine-grained and thus correspond to the maximum of the postglacial transgression. A thickness of the sediments was established by high-resolution seismic-acoustic profiling as 5–8 m, i.e., the maximum in the White Sea. The age is determined by a palynological spectrum that falls into two parts. The lower spectrum is dominated by tree pollen with abundant pollen of *Betula nana* added with herbaceous pollen and spores. The upper spectrum is dominated by spores (30–77%), among which *Lycopodium* prevail. The pollen of woody and herbaceous plants is suppressed. This spectrum corresponds to the Pre-Boreal and Boreal times [30]. In the sediments of the Pre-Boreal time, brackish water, North Boreal, nearly littoral species of diatoms are ubiquitous, especially *Hyalodiscus scoticus*. Diatoms *Thalassionema nitzschioides*, *Thalassiosira gravida*, and *Porosira glacialis* indicate a marine environment on the Solovets shelf in the Pre-Boreal time [20]. A transit from the Pre-Boreal to Boreal is marked by the development of a shallow-water Arctic-North Boreal diatom community.

In Onega Bay, a palynological spectrum from the described horizon was dominated by pollen of trees. In the basal layers, the periglacial floral elements play a leading role, but they gradually vanished upward, while pine pollen became more abundant. This observation classifies the hosting sediments to the Holocene Pre-Boreal and Boreal times [14]. The Early Holocene age was also confirmed by the paleomagnetic dating of clays [2].

The Middle and Late Holocene marine clastic and clastic-biogenic sediments occur locally in lows of the glacial topography between Bolshoy Solovetsky and Anzer islands. They consist of sandy and clayey silts with shells of marine mollusks abundant in individual beds. These sediments differ from the lower Boreal ones by a rise of $CaCO_3$ to 18%. According to L. V. Polyak, the lower beds are full of *Astarte elliptica* and *A. montagui*, while the upper beds host *Hiatella arctica*. A general abundance of shells decreased upward.

The oxygen isotopic analysis of shells and the Ca/Mg ratio determination show that during the deposition of mollusk shells (7,500 years) the summer temperature of surface waters was 1.5–2°C higher than today, then it dropped (6,500 years), and after that it increased by 1°C [35]. According to palynological data collected south of the Anzer Islands, the flowering period of mollusks was established to be in the Atlantic time. This was confirmed by the ^{14}C radiologic dating performed by the Institute of Oceanology in 1974 (three ages between 7,600 and 6,200 years) [9] and by the latest data obtained by the Belomorskaya expedition [36].

The diatom analysis showed that in the sediments of Atlantic age were dominated by South Boreal marine diatoms (up to 18% of total), which indicate a stable connection between the White and Barents seas.

This assumption is confirmed by the fact that concentration of dinoflagellate cysts in Atlantic sediments reaches 500,000 pcs/g predominantly warmwater cosmopolitan and Boreal pollen forms [37]. The subsequent pollen, diatom, and foraminifer studies suggest that the overlying strata were deposited in the Subatlantic and Subboreal times of the Holocene.

Middle-Late Holocene marine deposits top the Holocene sequence and cover about 50% of the seabed. They are localized in depressions of the glacial topography, owing to which their thickness is extremely variable from 1–2 to 10–12 m, with an average of 5–6 m. In the high sea, the deposition starts from a depth of 50 to 60 m and in bays from 5 to 10 m. The sediments consist of soft greenish-gray clays and silty clays with a characteristic spotted appearance caused by black accumulations of organic matter and hydrotroilite.

Marine nepheloid deposits conformably overlay the Early Holocene and compose a transitional zone between glacial-marine and marine sediments. Coastward and on shoals, the sequence of the Middle-Late Holocene sediments was reduced and included sand layers. The topmost layers were enriched with sand and contain some gravel and pebbles.

The upper horizon contains abundant pollen and diatoms and as scarce fragments of small shells of marine mollusks. A palynological spectrum demonstrates the predominance of woody species, and the change of dominants distinguishes the Atlantic, Subboreal, and Subatlantic times of the Holocene [9, 20]. In the reduced sections, the full horizons with a specific palynological spectrum are missing due to the intermittent sedimentation. Diatom species are mainly Arctic Boreal. Close to mouths of large rivers, brackish and freshwater species appear [17].

Marine fluvial sediments occur locally in the eastern part of the delta, between Mudyug Island and the coast, as well as in the Western and Eastern Solovets Salma Straits, and in the Gorlo Strait (Figs. 15 and 16). The sediments were deposited by

river and tidal currents. The seabed sediments consist of sands, medium and fine, rarely silty when deposited in still waters.

Marine wave sediments occur along the Kola Peninsula coasts to a depth of 10 m; near the mouths of the Varzuga, Chapoma, and Strelna rivers, they expand more widely. Almost a continuous zone of wave deposits runs along the Onega Peninsula coast and along the Zimniy Coast. The sediments consist of fine to medium well-sorted pure sands with a high content of heavy minerals. The wave sands always have a rippled surface. Their thickness by geophysical data is 10 m or less. On the seaward side, the wave deposits have poor sorting, admixture of coarse materials, and quartz and feldspar grains stained with iron hydroxides.

Alluvial-marine sediments occur mostly in the Severnaya Dvina delta. The prodelta consists of sands with interbeds of lagoon clayey silts. In the opinion of E. N. Nevesskiy, the delta began to grow in the Boreal, then the shoreline changed its position, and the delta continued its expansion in the Subatlantic [9]. Our studies near Severodvinsk show that now the outer delta is subjected to an active destruction which is caused by an anthropogenic impact to the environment leading to a reduced sediment runoff and water shortage in the North Dvina River [38].

Drilling data show that on the islands the thickness of the alluvial-marine sediments exceeds 15 m; however, on bedrock highs it is only 1–3 m. A. P. Lisitsyn considers that the sedimentation in the outer delta belongs to three facies zones: the first zone is associated with a sharp slowdown of current velocity (a mechanical or gravitational barrier), the second zone is governed by transformation of dissolved substances into suspended matter and accumulation of heavy metals, and the third zone is associated with hydrobiological processes with almost no mechanical sedimentation [39]. The effectiveness of the barrier zone is so high that there is practically no pollution in Dvina Bay, while in the deltaic channels both the sediments and waters are contaminated. Other rivers have almost no deltas (the Onega River only has a small delta), and fluvial-marine sediments form mouth bars at places where the flow velocity drops sharply.

Marine perluvium is one of the most common genetic types of marine sediments. It covers the older formations everywhere. The perluvium occurs to the water depth of 50–60 m; however, a high-frequency profiling shows that it may occur at 100–150 m b.s.l. (Fig. 13). The sediments consist of silty sand-gravel sediments with pebbles, small boulders, and mollusk shell debris. The sediments have a sharp disparity of the grain size vs. hydrodynamic activity, fractional composition, small thickness (from 10–20 cm to 0.5–1.0 m), sharp, often ferruginous contact with underlying bedrocks. The deposits contain iron-manganese crusts and concretions, particularly at the exit from the Gorlo Strait [40], which indicate a very low sedimentation rate.

4 History of Geological Development of the White Sea Basin in the Late Pleistocene–Holocene

These data clarify some issues of the Late Pleistocene–Holocene history of the White Sea Basin, especially of the latest glacial sedimentation cycle. The basin itself is very old, and its initiation was associated with the Riphean tectonic faults cutting the sedimentary cover of the Russian Plate. At that time the Kandalaksha and Onega grabens were formed and filled with clastic deposits. The today's basin is thought to be shaped at the Pliocene-Quaternary border. Later its outlines were considerably modeled by the Scandinavian glacier, which repeatedly invaded the White Sea Basin and, probably, filled it completely.

The oldest Mikulino deposits, which were drilled in the Gorlo Strait, proved the conclusion that in the warm periods the White Sea Basin was a single or multiple marine basin. At that time, the shoreline in the Arkhangelsk region was 100–110 m higher, and in the Kola region, it was 60–150 m higher than today [24].

In the Leningrad time (the Valdaian interstadial), cold-water glacial desalinated basins existed in Onega Bay and, probably, in Dvina Bay. It is important that glaciers were advancing not only from the northwest but from other directions, as the mineral assemblage of clays (the higher kaolinite content) suggested.

The most important and debatable issue is a character of the Quaternary glaciation in both the White Sea and the Barents Sea. There are alternative visions not only of the existence of glaciation but also about the specifics of its history. Most of the researchers follow G. G. Matishov [41] and believe that the glaciation centers existed on the today's land, and the glaciers descended to the marine shelf from the Scandinavian mountains. At the same time, the White Sea periodically ceased to exist as a water body, and at the glaciation maximums, it was completely filled with ice.

Another point of view was first published by M. G. Grosswald and supported by many, especially Norwegian, geologists [42, 43]. This point suggests the existence of the Pan-Barents ice sheet, which was advancing on land, in particular, on Kola Peninsula up to the Khibiny Mountains.

Integrated geological and geophysical studies based on a seismic-acoustic profiling and sediment sampling facilitated building of a composite lithostratigraphic column. It consists of glacial and glacial-lacustrine (continental), glacial-marine, and marine deposits, which differ in physical, mechanical, structural, mineralogical, and grain size properties.

Geomorphological aspects of the glaciation and, first of all, a spatial position of the glacier-marginal ridges are clearly seen on seismograms (Figs. 1 and 3). They facilitate the reconstruction of phases of the glacier retreat in the White Sea Basin. To build this scale for the eastern part, between the White Sea and Chyosha Guba Bay, we used VSEGEI land surveys of 2003–2005 (Fig. 18).

On Kola Peninsula and along the White Sea shores, the cold events were marked in the glacier retreat process. During the active glacier growth, the general direction of ice advancement was maintained, and different directions were governed by local orographic features. By now, when the boundaries of phases and oscillations are

Fig. 18 Boundaries of the Late Valdaian glaciers and of some Scandinavian glacier oscillations in the White Sea Basin scale 1:5,000,000 (after L.R. Semyonova, A. Ye. Rybalko, V. A. Zhuravlyov)

known, their age seems to be a problematic in many cases. The boundaries of the maximum expansion of the Scandinavian glacier, Neva and Salpausselka-I stages, are established with a high degree of reliability (Fig. 18). The ages of other stages recognized on Kola Peninsula and in the White Sea Basin are conventional, especially knowing that many glacier-marginal deposits belong to different phases. For a long time, the ice-marginal units on the White Sea shores and their seismic-acoustic analogs remained uncorrelated, and the glacial reconstructions were problematic.

Within its eastern sector, the Scandinavian glacier repeatedly interacted with the glaciers advancing from the Novaya Zemlya Islands across the Pechora Sea, i.e., from the northeast. Before the Scandinavian glacier reached its maximum, the Novaya Zemlya glacier probably reached the Gorlo Strait and even Kola Peninsula. Later, the Scandinavian glacier overlapped the western edge of the Novaya Zemlya glacier, what is clearly seen from the structure of the glacier-marginal units on Kanin Peninsula. Later, after the retreat of the Scandinavian glacier, the ice again invaded from the Chyosha Guba Bay direction and left its marginal deposits as the Konosha hills on the western coast of Kanin Peninsula (Fig. 18).

The Late Pleistocene warm period dated from the graphs of climatic changes [44–46] left no clear traces on Kola Peninsula. Probably, during this period, the thickness of the Kuloy Ice Sheet in the Arkhangelsk region decreased. During the subsequent Early Dryas cold event (the Luga stage) (14.7–13.0 kyr), the two lobes of the

Scandinavian Ice Sheet overlapped the Ponoy Ice Sheet and flowed around the most elevated parts of the Kuloy glacier. On Kola Peninsula, the Keiva I ridge was formed by this process. On the western coast of the White Sea, the glacier-marginal deposits appeared on the Kuloy Plateau and in the Pinega valley.

During the Bölling warm interstadial (from 13.4–13.0 to 12.2–12.3 kyr) the glacier degradation continued; the melting of the Ponoy and Kuloy small glaciers could come to the end at that time. Note that in some locations the melting of dead ice massifs took a long time – till the Holocene. At that time, glacial lakes already existed within today's Onega Bay.

The Middle Dryas cold event (from 12.2–12.3 to 11.8–12.0 kyr) caused a new twofold advance of the ice (early and late substages of the Neva phase), but an unclear expression of the glacier-marginal formations (including the Keiva II ridge) suggests that the stabilization of the glacier edge at the coldest time was short. On Kola Peninsula, in mouth of the Olenitsa River and west of it, the glacier-marginal formations of the Neva stage were not differentiated. East of the Olenitsa River, the glacier-marginal formations of the early sub-phase of the Neva phase built the Keiva II ridge (south of the Keiva I ridge) and expanded to the shoreline. At that time, large ridges of 60–80-m-thick glacial deposits could be formed in the White Sea, between Voronov Cape and Morzhovets Island.

Along foots of the White Sea – Kuloy Plateau – in the Mezen valley and on Onega Peninsula, the early sub-phase glacier boundary was traced based on the genetic types of glacial deposits and the boundaries of glacier-dam lakes. The south ice boundary crossed southern Onega Bay and terminated at the Zimniye Mountains. At that time, most of Onega Peninsula was covered with reticulated ice.

The ice-marginal deposits of the late Neva sub-phase were distinguished by the seismic-acoustic profiling. These are two oscillatory ridges, which extend to the mouth of the Olenitsa River, where they pass into a N–S trending set of ridges, and then run to the Lovozero tundra. A thickness of the glacial deposits in these ridges reaches 60–80 m. The ridges have an asymmetric profile with steep northern and gentle southern slopes. There are long reflectors inside the ridges that may be boundaries of the different age moraines.

At the same time, thick glacial deposits on the Solovets Islands were formed. The southern boundary of the glacier of the late substage of the Neva stage crossed southern Onega Bay (the Lyamyts glacier-marginal unit) and run along the eastern shore of Dvina Bay. We also conventionally attribute to this sub-phase a set of glacier ridges on Zhizhigin Island, where the deglaciation was very rapid and was accompanied by the quick filling of inter-ridge lows with a 35-m-thick late glacial and postglacial deposits.

The last major ice advance was in the Younger Dryas (from 11.3–11.2 to 10 kyr). On Kola Peninsula, it has three stages: Salpausselkja I, II, and III. The Salpausselkja I glacier ridges exist in the southwest of Kola Peninsula, in the White Sea, and in Karelia. The ridges left by other stages are known only on land. In the north of Kola Peninsula, the Tromsø-Lyngen ridge has the same history. In the White Sea, apart from the main glacier-marginal Salpausselkja I deposits, two oscillatory ridges were distinguished in Poroy Bay and on the northwestern Stolbovy Ludy Islands. Here a

thickness of glacial deposits reaches 100 m. Evidently, radial glacier ridges in the ice-gathering funnel of Kandalaksha Bay are also associated with this time. When glacial ridges occurred on the crystalline basement (the today's Kandalaksha skerries), their thickness did not exceed a few tens of meters.

The principal novelty in this scale is the Novaya Zemlya glaciation (Late Valdaian), which advanced right up to the White Sea Voronka. These data largely contradict the negation of the Barents glaciation in the Late Valdaian time. However, the presence of a young glacier moving from Chyosha Guba Bay in the southwest direction is known from field observations on the Chyosha-Mezen watershed [21].

Recent data show that the penetration of the Barents Sea water to the White Sea Basin began at the end of the Allerød oscillation. The development of a sea basin near the Solovets Islands began in the Late Dryas. This opinion does not agree with the idea of the Pan-Barents glacier existence till the beginning of the Holocene.

5 Conclusions

As a result of the geological mapping, new seismic-acoustic surveys of 2005–2006, recent high-frequency multichannel survey, and sediment sampling under the *World Ocean* program in 2004–2007, a map of Quaternary deposits was built at a scale of 1:1,000,000. This map shows not only the intricate occurrence of lithostratigraphic units of the latest glaciation–sedimentation cycle, but it also shows buried landforms and the role of neotectonic movements in the distribution of mapped units.

Here we first showed a wide occurrence of gravity deposits and their relations to neotectonic movements. A complex combination of Quaternary units predetermines an alternation of lithotypes of sediments. Based on the seismic profiling, the two new Holocene lithofacies were discovered: they are nepheloid sediments deposited in a ridge-dam environment and silt fans in the south Gorlo Strait.

The new data make it possible to detail the sedimentation process in the Holocene and to determine the onset of marine sedimentation on Kola Peninsula, in Karelia, and in the Arkhangelsk region. The main conclusion is the predominance of land rise, at least within the Baltic crystalline shield, which implies to the White Sea the features of a regressive basin. This is extremely important for predicting placers in shoreface sediments of the White Sea. During the entire Holocene, these sediments were washed with the gradual enrichment in heavy minerals, including commercial ore minerals.

The latest seismic-acoustic surveys and multichannel high-frequency tools expanded our knowledge of geological bodies and their stratigraphic positions in the inner glacial basin. The new core sample dating added with geophysical data allows for quantitative criteria for the Quaternary geological history.

Acknowledgments We consider it our duty to thank our colleagues who took part in the fieldwork and the processing of the materials that served as the basis for this article: from VSEGEI (S.F. Manuilov, V.A. Zhamoyda, P.E. Moskalenko) and from Sevmorgeo (N.K. Fedorova, K.A. Nikonov, M.A. Nikitin) and micropaleontologists, who made it possible to create a stratigraphic scheme, E.A. Spiridonova and

R.N. Ginoridze. The authors thank the Acad. A.P. Lisitsyn, under whose leadership the program on the White Sea was carried out, and the world's only four-volume monograph on various aspects of the oceanology of this sea was published. We are grateful to the Doctor of Engineering Sciences, General Director of JSC MAGE, G.S. Kazanin, for the support and kindly presented results of seismic-acoustic surveys. The authors are particularly grateful to I. V. Yegorov, who not only translated this article but also made a great contribution to the editing of its text, which allows us to consider him our co-author. The work was carried out with the financial support of the Rosnedra Agency (State Contracts No. 09/03/12-23, 2006 and F3227, 2008) and support of grants from St. Petersburg State University No. 18.42.1258.2014, 18.42.1488.2015, and 0.42.956.2016 (for expedition studies) and RFBR grant No. 18-05-00303.

References

1. Evzerov VY (2010) Glaciations in the Wight Sea basin. A system of the White Sea. Environments of the White Sea catchment area, vol 1. Nauchny Mir, Moscow, pp 76–93 (in Russian)
2. Kochegura VV, Rusinov BS (1987) Paleomagnetic dividing and correlation of Pleistocene and Holocene sediments of Onega Bay. Integral marine G&G studies in the glacial shelf interior seas. VSEGEI, Leningrad, pp 63–71 (in Russian)
3. Demidov IN (2010) Geology and dynamics of the newest period of the White Sea development. A system of the White Sea. Environments of the White Sea catchment area, vol 1. Nauchny Mir, Moscow, pp 58–75 (in Russian)
4. Strelkov SA, Evzerov VY, Koshechkin BI, Rubinraut GS, Afanasjev AP, Lebedeva RM, Kagan LY (1976) History of landforms and unconsolidated deposits of the northeastern Baltic Schield. Nauka, Leningrad, 164 pp (in Russian)
5. Deryugin KM (1928) The White Sea fauna and its habitat. State Hydrol. Institute, Leningrad, 511 pp (in Russian)
6. Avilov IK (1956) Thickness of contemporary sediments and the post-glacial history of the White Sea. Pros Oceanogr Inst 3:45–47 (in Russian)
7. Govberg LB, Medvedev VS, Nevesskiy YN (1974) A problem of biostratigraphic dividing of the White Sea sedimentary formations and major stages of the Holocene basin history. Bull MOIP Geol 49(2):23–34 (in Russian)
8. Malyasova YS (1976) Palynology of the White Sea sediments. LGU, Leningrad, 119 pp (in Russian)
9. Nevesskiy YN, Medvedev VS, Kalinenko VV (1977) The White Sea: sedimentation and Holocene geological history. Nauka, Moscow, 235 pp (in Russian)
10. Kalinin AV, Kalinin VV, Pivovarov BL (1983) Seismic-acoustic surveying of water areas. Nedra, Moscow, 204 pp (in Russian)
11. Spiridonov MA, Devdariani NA, Kalinin AV, Kropatchev YP, Manoulov SF, Rybalko AY, Spiridonova YA (1980) Geology of the White Sea. Soviet Geol 4:46–56 (in Russian)
12. Rybalko AY, Lisitsin AP, Shevchenko VP, Zhuravlyov VA, Varlamova AA, Nikitin MA (2009) New data on geology of the White Sea quaternary. Geology, geography, and ecology of the oceans. Publishing House of UNSC RAS, Rostov-on-Don 186 pp (in Russian)
13. Rybalko AY, Semyonova LR, Zhuravlyov VA (2007) Quaternary deposits of the White Sea. I: geology of the seas and oceans. Materials of the XVII Int. Scientific Conference, vol 2. GEOS, Moscow, pp 256–260 (in Russian)
14. Dzhinoridze RN, Kirienko EA, Kalugina LV, Rybalko AY, Spiridonov MA, Spiridonova YA (1979) Stratigraphy of upper quaternary deposits in the northern White Sea. Late quaternary history and sedimentation in marginal and interior seas. Nauka, Moscow, pp 34–39 (in Russian)
15. Kalugina LV, Rybalko AY, Spiridonova YA, Spiridonov MA (1979) Palinological studies in the northern White Sea as a basis for stratigraphy. Vestnik LGU 7(12):63–71 (in Russian)
16. Kirienko YA (1977) Foraminifer community in the White Sea seabed deposits. Quaternary stratigraphy and paleogeography of the north of the European USSR. Publishing House of Karelian Branch of the USSR AS, Petrozavodsk, pp 40–47 (in Russian)

17. Manuylov SF, Rybalko AY, Spiridonov MA, Dzhinoridze RN, Kalugina LV, Kirienko YA, Spiridonova YA (1981) Stratotype of late Pleistocene and Holocene deposits of the Solovets Islands shelf in the Wight Sea. Palynology of the Pleistocene and Holocene. LGU, Leningrad, pp 116–134 (in Russian)
18. Sobolev VM, Aleshinskaya ZV, Polyakova YI (1995) New data on paleogeography of the White Sea in the late Pleistocene and Holocene. Correlation of paleogeographic events: continent – shelf – ocean. MSU, Moscow, pp 120–129 (in Russian)
19. Sobolev VM (2009) Stratigraphy and composition of quaternary deposits of the White Sea Gorlo Strait. Fundamental problems of the quaternary: summary of the completed studies and main trends for the future. Mater. of the VI Quaternary Conference, Novosibirsk, pp 554–556 (in Russian)
20. Rybalko AY, Spiridonov MA, Spiridonova YA, Moskalenko PE (1987) Quarternary deposits of Onega Bay and main features of its paleogeography in the Pleistocene and Holocene. Integral marine G&G studies in the glacial shelf interior seas. Publishing House of VSEGEI, Leningrad, pp 38–52 (in Russian)
21. State Geological Map of the Russian Federation. 1:1,000,000 (New series) (2004) Quadr. Q-35, 37 (Kirovsk). Explanatory note. Factory on Printing of Maps (Kartfabrica) of VSEGEI, Saint Petersburg 268 pp (in Russian)
22. Lisitsin AP (2010) Environmental studies of the White Sea catchment area. System of the Wight Sea, vol I. Nauchny Mir, Moscow, pp 353–445 (in Russian)
23. State Geological Map of the Russian Federation 1:1,000,000 (Third generation) (2012) Baltic series, Quadr. Q-35, 36 (Apatity). Factory on Printing of Maps (Kartfabrica) of VSEGEI, Saint Petersburg, p 436 (in Russian)
24. State Geological Map of the Russian Federation. 1:1,000,000 (Third generation) (2012) Baltic series, Quadr. Q-37 (Arkhangelsk). Factory on Printing of Maps (Kartfabrica) of VSEGEI, Saint Petersburg, p 302 (in Russian)
25. State Geological Map of the Russian Federation. 1:1,000,000 (Third generation) (2009) Mezen series. Quadr. Q-38 (Mezen). Factory on Printing of Maps (Kartfabrica) of VSEGEI, Saint Petersburg, p 338 (in Russian)
26. Malakhovskiy DB, Amantov AV (1991) Geological and geomorphological anomalies in northern Europe. Geomorphology 1:85–95 (in Russian)
27. Tarasov GA, Shlykova VV (2006) Distribution of quaternary deposits and main features of the pre-Valdaian seabed of the Wight Sea. Rep RAS 411(2):226–230 (in Russian)
28. Kalinin AV, Kalinin VV, Kovalskaya IY, Pivovarov BL, Spiridonov MA, Rybalko AY (1976) Structure of the Kandalaksha Bay deposits. Rep Acad Sci USSR 229(5):345–349 (in Russian)
29. Shalayeva NV, Starovoytov AV (2010) Basics of acoustic studies in shallow waters. MSU, Moscow, 256 pp (in Russian)
30. Rybalko AYe (1998) Late quaternary sedimentation in the interior seas on a glacial shelf of NW Russia. Doctor of Science thesis. Saint Petersburg, 48 pp (in Russian)
31. Legkova VG, Semyonova LR, Moskalenko PY (2004) Quaternary system. State geological map of the Russian Federation. 1:1,000,000. Quad. Q-35, 37 (Kirovsk). Factory on Printing of Maps (Kartfabrica) of VSEGEI, St. Petersburg, pp 32–51 (in Russian)
32. Kaplyanskaya FA, Tarnogradskiy VD (1993) Glacial geology. Guidebook to glacier deposits. SPb, Nedra, 327 pp (in Russian)
33. Gudina VI, Evzerov VY (1973) Stratigraphy and foraminifers of the upper Pleistocene of Kola Peninsula. Nauka, Novosibirsk, 146 pp (in Russian)
34. Korsakova OP, Zozulya DR, Kolka VV (2004) Selected data on the Kara glacier penetration to Kola Peninsula. Geology and mineral resources of European NE Russia. Materials of the XIV Geological Congress of the Komi Republic-Syktyvkar, vol II. Geoprint-Press, Syktyvkar, pp 19–20 (in Russian)
35. Dorofeyeva LA, Prilutskiy RY, Rybalko AY, Badinova VP (1991) Methodology of determination of the oxygen isotopes in paleo-waters (an example of the Wight Sea in the Atlantic time). Methods of isotope geology. Publishing House of VSEGEI, Saint Petersburg, pp 57–58 (in Russian)

36. Novichkova YA, Polyakova YI, Bauch HA (2008) Post-glacial history of the White Sea based on aquatic palynology. News of paleontology and stratigraphy. Supplement to geology and geophysics, vol 49(10–11). Siberian Branch, Russian Academy, Novosibirsk, pp 447–449 (in Russian)
37. Novichkova YA, Bauch HA (2007) Post-glacial history of the Wight Sea based on dinoflagellate cists. Geology of the seas and oceans. Materials of the XVII Int. Scientific Conference, vol 1. GEOS, Moscow, pp 252–254 (in Russian)
38. Rybalko AY, Fyodorova NK, Nikonov KA, Klimov AI (2007) Current state and evolution of the shoreface of Yagry Island (in the Severnaya Dvina delta) in connection with the shoreline reinforcement. Geology of the seas and oceans. Materials of the XVII Int. Scientific Conference, vol 2. GEOS, Moscow, pp 282–283 (in Russian)
39. Gordeev VV (2013) A global role of the marginal oceanic filter. Pros. of the VII Russian lithologic conference. Novosibirsk, pp 242–244 (in Russian)
40. Sternberg LY, Lavrushin YA, Sivtsov AV, Golubev AI, Spiridonov MA (1985) Iron-manganese concretions from the Wight Sea Gorlo Strait. Lithol Econ Miner 5:66–75 (in Russian)
41. Matishov GG (1984) Ocean floor in the glacial age. Nauka, Leningrad, 176 pp (in Russian)
42. Forman S, Lubinski D, Miller GH, Snyder J, Matishov G, Korsun S, Myslivets V (1995) Postglacial emergence and distribution of late Weichselian ice-sheet loads in the northern Barents and Kara seas, Russia. Geology 23(2):113–116
43. Grosswald MG (1983) Glaciation of continental shelves. Resumes of science and technics. Ser. paleogeography. VINITI, Moscow, 165 pp (in Russian)
44. Evzerov VY, Nikolayeva SB (2000) A belts of glacier-marginal buildups on Kola Peninsula. Geomorphology 1:61–73 (in Russian)
45. Alm T, Vorren K-D (1993) Climate and plants during the last ice age. Plant life. University of Tromsø; Tromsø Museum, Tromsø, pp 4–7
46. Lehman SJ, Keigwin LD (1992) Deep circulation revisited. Nature 358:197–198

Processes of Early Diagenesis in the Arctic Seas (on the Example of the White Sea)

Alla Yu. Lein and Alexander P. Lisitsyn

Contents

Abstract During an early diagenetic stage of sedimentation, a continuous exchange between bottom water and pore solution happens. Throughout the diagenetic stage, an oxygen, SO_4^{2-}, Ca^{2+}, and Mg^{2+} diffuse into pore solution from near-bottom water, but the gases generated within sediments (CO_2, NH_3, H_2S, CH_4, etc.), and other pore waters' components (Fe^{2+}, Mn^{2+}) are transferring from surface sediments into near-bottom water. At the same time, as a result of some ions' oversaturation, a precipitation from pore water of a number of chemical compounds takes place followed by formation of authigenic minerals. Their composition depends on oxidation-reduction conditions within sediments. In oxidizing conditions (in upper sediment layers), ferromanganese mineral associations, as well as glauconite, phosphates, etc., are formed. As the environment becomes reducible after loss of free oxygen due to diagenetic processes, mainly, metal sulfides and carbonate minerals

A. Yu. Lein (✉) and A. P. Lisitsyn
Shirshov Institute of Oceanology Russian Academy of Sciences (IO RAS), Moscow, Russia
e-mail: lein@ocean.ru; lisitzin@ocean.ru

A. P. Lisitsyn and L. L. Demina (eds.), *Sedimentation Processes in the White Sea: The White Sea Environment Part II*, Hdb Env Chem (2018) 82: 165–206,
DOI 10.1007/698_2018_345, © Springer International Publishing AG, part of Springer Nature 2018,
Published online: 7 July 2018

are formed. Such is an idealized scheme of transformation of seawater into pore waters in a humid zone.

Keywords Arctic Ocean, Bacteria, Early diagenesis, Radioisotopes, Stable isotopes, White Sea

1 Introduction

The White Sea was formed in the early Holocene approximately 11–12,000 years ago, on the site of glacial lake. The composition of water mass of the sea was formed due to mixture of fresh river waters and saline water inflowing from the Barents Sea. River waters enter mainly in the shallow Dvina and Onega Bays. Respectively, a number of biogeochemical processes proceeding in water column and in sediments of the White Sea are influenced by composition of organic matter of river waters. Other important feature of the White Sea ecosystem, the characteristic of all Arctic seas, is the pronounced seasonality of all biogenic processes. The vastness of the coastal zone of the White Sea, as well as the activity of the littoral, determines the scale of the arrival and transformation of organic matter, the main agent of early diagenetic processes in sediments. Another important feature of the Arctic seas is the significant participation of terrigenous material, carried down from the land in the composition of river suspension.

The podzolic soil weathering profile on the White Sea catchment facilitates the entry of a large number of dissolved iron and manganese compounds with the river runoff, which distinguishes the northern part of the humid zone from other climatic zones [1, 2].

The White Sea is characterized by a complex system of currents; very significant interannual, interseasonal, and even daytime variations in the chemical composition of the water column; and content and composition of suspended particulate matter (SPM), including organic matter (OM).

The diversity of spatial seasonal structure of the White Sea ecosystem explains an absence of unified ideas about its trophicity [3]. Detailed characteristic of the biogeochemical processes within the water column was given in the monograph [4].

2 Material and Methods

This chapter is based on research results of the biogeochemical processes at a stage of early diagenesis of bottom sediments in polar regions on the example of the White Sea. Materials were collected during cruises R/V “Ekolog” in 2014. Sampling stations are shown in Fig. 1.

The study of processes of early diagenesis of sediments of the White Sea includes a complex of various methods such as determination of total number of microorganisms, rates of microbial biogeochemical processes with a tracer technique

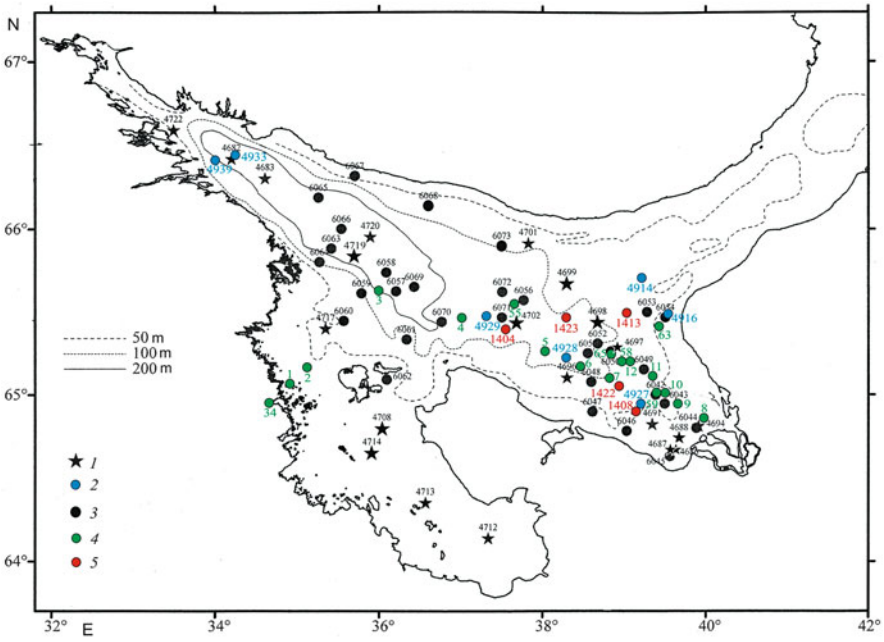

Fig. 1 Location of sampling stations in the White Sea, cruise of R/V "Ecolog," 2014. 1, CTD + ADV probing; 2, complex stations; 3, collection of sediments by Neimisto tube; 4, sampling by a box corer; 5, buoy stations

(^{14}C and ^{35}S), as well as analysis of isotopic composition of carbon compounds in suspended particulate matter (SPM) and in bottom sediments. Radioactive isotopes of carbon in sediments of the White Sea have not been studied before our research. The methods of sampling and preparation of samples for analysis, as well as methods of analysis, were described in details in [5–7].

3 Results and Discussions

3.1 Characteristic of the White Sea Water Column

Estimates of primary production of a photosynthesis in the White Sea, which were carried out in expeditions over 1999–2002, vary from 45 to 100 mg C m^{-2} day^{-1} in its open part, from 45 to 270 mg C m^{-2} day^{-1} in the Dvina Bay, and from 50 to 360 mg C m^{-2} day^{-1} in the open part of the Kandalaksha Bay. According to these data, the White Sea belongs to mesotrophic reservoirs with intermediate level of primary production [8].

The main C_{org} form in water column of the Arctic seas is the dissolved carbon (DOC). Distribution of dissolved C_{org} concentrations in August 2006 and July 2003

varied in dependence on values of primary production of the White Sea. In the Dvina Bay, a slightly elevated mean values were detected in August 2006 (3.5–8.0 mg C l^{-1}) compared to that in the Basin (4.0–6.0 mg C l^{-1}) [9] (Fig. 2). The content of particulate C_{org} (POC) in the White Sea ranged from 0.05 to 0.25 mg l^{-1}.

The presence of a methane in water column and finds of pyrite framboids in the floating diatom tests prove the existence of the organic matter (OM) destruction processes already at the stage of a sedimentation. In the mineralization of organic matter in the water column of the White Sea, not only aerobic but also anaerobic microorganisms take part. The number of microorganisms increases at the boundary of the water-sediment. Low total number of microorganisms (TNM, 50–100 × 10^3 cells ml^{-1}) was recorded in the western and central parts of the Basin. In the surface water of the Basin for 5 years of measurements, TNM varied from 50 × 10^3 to 200 × 10^3 cells ml^{-1} [6, 8].

The biogeochemical and microbiological characteristics of the surface water are listed in Table 1.

Values of $\delta^{13}C$-C_{org} in the SPM varied in the surface layers of water column in August 2006 (cruise 80 of R/V "Professor Shtokman") from −29.3‰ in the Dvina Bay up to −28.6‰ in the deepwater part of the White Sea, having remained approximately the same isotope light in the near-bottom water l (−28.0 ÷ −30.5‰). In water layer above sediments collected with the Neimisto tube, content of ^{13}C isotope in SPM and values of $\delta^{13}C$-C_{org} were within the limits of −27.3 ÷ −28.4‰, i.e., C_{org} content of planktonic origin ($\delta^{13}C_{aver.}$ from −20 to −22‰) has decreased (Table 2).

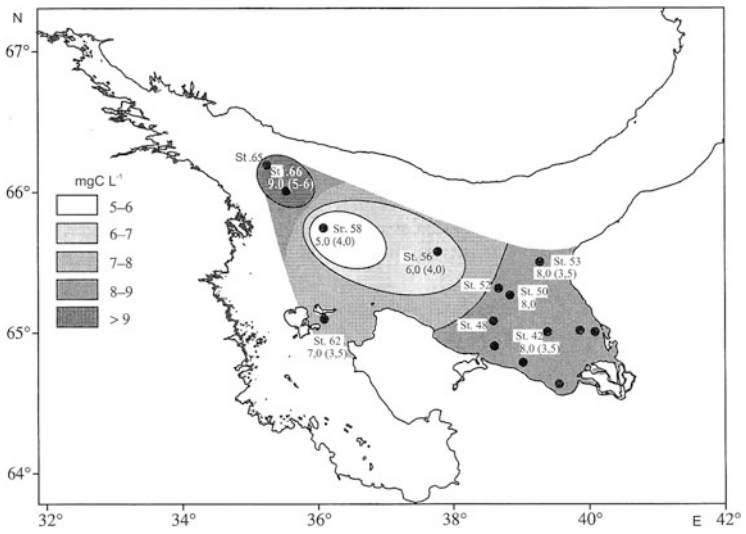

Fig. 2 Distribution of dissolved C_{org} (mg C l^{-1}) at different stations in the surface water layer of the White Sea in August 2006 and in June 2003 (values in brackets)

Table 1 Microbiological and biogeochemical parameters of the surface water layer in the White Sea [8]

Depth, m	T, °C	PP, mgC m^{-2} day^{-1}	TNM, 10^3 cell ml^{-1}	PB, mkgC l^{-1} day^{-1}	CH_4, nM	MO, 10^{-3} nM l^{-1} day^{-1}
Basin, throat, and open part of the Kandalaksha Bay						
54–30	0.5–11	$\frac{45-100}{55}$	$\frac{150-750}{280}$	$\frac{0.7-15}{4.2}$	$\frac{1.8-7.1}{3.3}$	$\frac{1.8-85}{18}$
Dvinsky and Onega Bays						
8–55	4.5–15	$\frac{45-270}{105}$	$\frac{150-950}{390}$	$\frac{0.5-28}{7.8}$	$\frac{1.8-19}{8.1}$	$\frac{3.6-240}{65}$
Kandalaksha Bay (nearshore)						
4–23	5.0–14	$\frac{50-360}{105}$	$\frac{170-520}{290}$	$\frac{0.5-35}{11}$	$\frac{1.8-25}{12}$	$\frac{3.6-410}{110}$

In the numerator, the limits of values; in the denominator, an average
PP primary production, *TNM* total number of microorganisms, *PB* production of bacterial plankton, *CH_4* concentration of methane, *MO* oxidation rate of methane

Table 2 The content of particulate C_{org} and values of $\delta^{13}C$-C_{org} in the particulate matter of the surface water, near-bottom water (sampled by Rozette and Multicorer), and upper (0–15 cm) sediment layer of the White Sea

Station number	Depth, m	Surface water layer		Near-bottom water (Rozette sampler)[a]		Near-bottom water (Multicorer sampler)[b]		Upper layer of sediments	
		C_{org}, %	$\delta^{13}C$-C_{org}, ‰	C_{org}, %	$\delta^{13}C$-C_{org}, ‰	C_{org}, %	$\delta^{13}C$-C_{org}, ‰	C_{org}, %	$\delta^{13}C$-C_{org}, ‰
6042	61	–	−29.3	0.372	−29.0	1.272	−27.7	1.646	−26.6
6048	80	0.488	−29.2	0.436	−28.0	1.900	−27.7	1.784	−25.8
6056	133	0.652	−28.6	0.188	−29.0	–	−27.4	1.601	−25.4
6058	300	–	−28.6	–	−30.5	1.076	−28.4	1.734	−25.8
6066	264	–	–	–	–	2.840	−27.3	1.692	−25.8

[a]Sampled at 3–5 m horizon above the bottom
[b]Sampled at 3–5 cm above the bottom

The total C_{org} distribution in surface water over the three summer seasons (July 2006, August 2010, and July–August 2014) varied noticeably at stations located at different depths (Fig. 3). It let us to conclude that influence of terrigenous runoff of the Northern Dvina River was insignificant even over the main production period (in summer) in the White Sea. In water column deeper than 15–60 m, the values of particulate $\delta^{13}C$-C_{org} decreased with depth, i.e., isotope composition was lightened, which means a decrease in contribution of C_{org} of a plankton origin in July–August (Table 3).

At all the stations studied, low concentrations of methane of microbial origin (1.8–25 nM) were detected in water samples. Methane was formed in the anaerobic microniches inside slurry aggregates and was oxidized by activity of microorganisms at a rate (1.8–410) $\times$ 10^{-3} nM day^{-1} (Table 1).

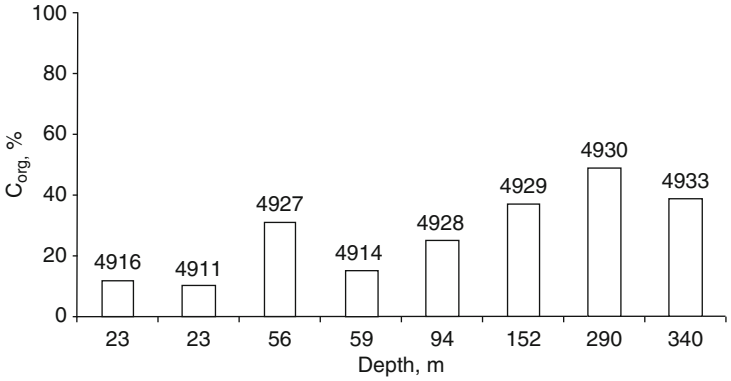

Fig. 3 Particulate C_{org} concentrations (% dry weight) in the surface water layer of the White Sea in August 2003

The SPM of the White Sea is formed generally from the river suspended particulate matter, aerosols, coastal abrasion (lithogenous source), as well as from phytoplankton and a bacterial plankton (biogenic source). The SPM during different seasons has different substantial, grain-size, and chemical composition, different proportion of biogenic and lithogenous components, and different content and composition of organic matter.

The first stage of the SPM transformation begins with the moment of its entering to the marine environment. The SPM chemical composition changes resulted from its partial dissolution, and proportion of fine-grained clay minerals changes also. The SPM sinking to seabed is mainly composed of various aggregated fecal pellets, "marine snow," and others. On boundary of near-bottom water and bottom sediments, there is the second stage of the SPM transformation, at first into a fluffy layer and then into sediments where process of a sedimentation comes to an end and process of early diagenesis begins. The analysis of the available data on biogeochemistry of water column leads to the following conclusions:

The White Sea is characterized by the complex system of currents; very essential interannual, interseasonal, and even daytime variations of chemical composition of water column; and contents and composition of the SPM and particulate organic matter (POM). The water column of the White Sea is formed due to mixing with the Barents Sea waters and the riverine inflow, whose bulk is composed of the Northern Dvina River.

The average content of particulate C_{org} was estimated as 27.25%, varying from 4.0 to 49%, while the highest concentrations of particulate C_{org} were detected in the surface water where active biogeochemical processes took place. In the near-bottom water, an average particulate C_{org} content was equal to 10.2%; it means that throughout the water column, particulate C_{org} decreased due to transformation of organic compounds during biogeochemical processes.

Table 3 Isotope composition of particulate C_{org} in water of the Dvina Bay (R/V "Ekolog" July–August 2014)

Station number	Sea depth, m	Horizon, m	$\delta^{13}C_{org}$
1404, Rozette sampler	153	0	−23.15
		10	−24.35
		30	−27.77
		50	−25.45
		70	−24.36
		150	−24.72
Neimisto tube sampler		153	−22.43
1408	53	0	−24.10
		7	−24.25
		20	−25.78
		40	−25.87
		49	−24.93
Neimisto tube sampler		53	−23.72
1413	83	0	−26.73
		10	−24.38
		22	−27.94
		55	−26.10
		80	−25.84
Neimisto tube sampler		83	−23.99
1422	105	0	−25.67
		7	−24.88
		15	−26.61
		25	−26.28
		45	−26.37
		99	−26.63
		Water	−24.16
1423	110	0	−23.26
		6	−23.11
		15	−22.79
		30	−27.44
		60	−27.35
		107	−24.85

3.2 Geochemical Barrier at the Water-Sediment Interface

The main transformation of energy and substance proceeds in a boundary zones of the marine Basins. One of them is a geochemical barrier zone between the seawater and sediments. Organic matter in sinking particles and anaerobic compounds entering from sediments serve as energy sources for biogeochemical processes at border zone between near-bottom water and surface sediment layers [10, 11].

In a vertical profile of this border zone, the following layers could be defined: (1) a near-bottom water layer, 5–30 cm above seafloor; (2) a fluffy layer (with very high turbidity) above the consolidated sediments, whose thickness varied from decimal units to a few centimeters; and (3) a surface sediment layer (Figs. 4 and 5).

In near-bottom water samples, abundance of microorganisms and bacterial mucilage was so great (110–259) $\times$ 10^6 cells ml^{-1} that their account was complicated. Therefore, for some samples from fluffy layer and surface sediment layer, we have to use a conditional value of ONM – more than 1×10^3 ml C l^{-1}. Along with increase in ONM, rates of biogeochemical processes with participation of microorganisms sharply increase in near-bottom water and in surface sediment layer. The integral characteristic of these processes is a value of dark $^{14}CO_2$ assimilation which is quantitatively determined with the use of $NaH^{14}CO_3$ [12]. This value in the surface sediment layer is three orders of magnitude higher than that in the water column (Table 1).

While studying border zone water-sediments, we have revealed high rate of the CO_2 assimilation that reached 170 μg C dm^{-3} day^{-1} in a layer of 0.0–0.5 cm

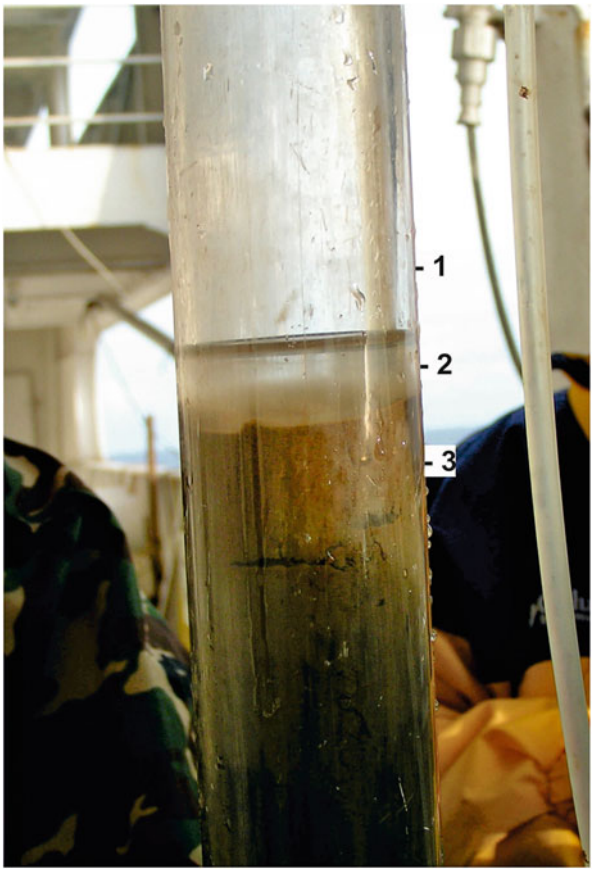

Fig. 4 A view of the water-sediment interface in Neimisto tube collected in the Dvina Bay in August 2006. (1) 5–30 cm above the bottom; (2) fluffy layer enriched in particulate matter above the sediment; (3) surface layer of bottom sediments

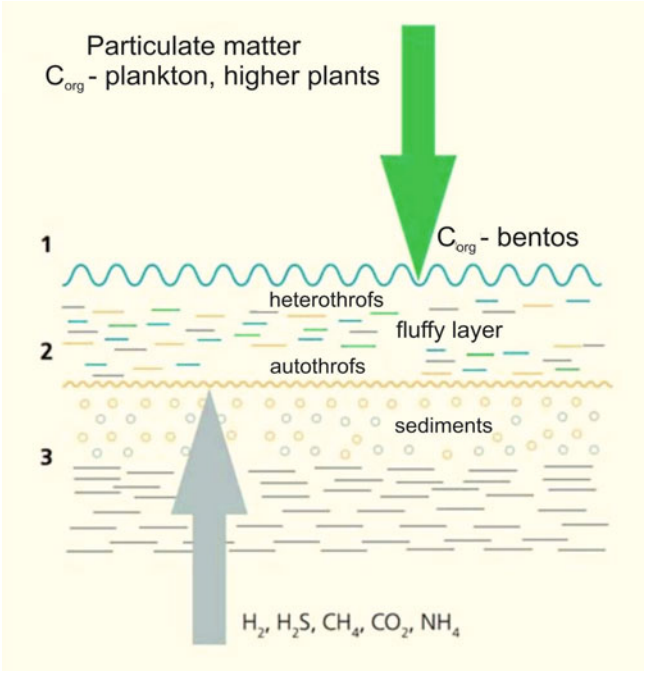

Fig. 5 Scheme of the C_{org} sources at the water-sediment contact zone

(Table 3). Besides, essential rates of a sulfate reduction, methane generation, and methane consumption were determined experimentally that proved an input to seafloor of reduced gasses such as H_2S, CO_2, and CH_4 which are products of early diagenetic transformation of organic matter. Therefore, in a boundary layer, not only heterotrophic but autotrophic microbial processes of CO_2 assimilation and synthesis of the "de novo" microbial biomass.

In near-bottom water, content of isotope ^{13}C in particulate C_{org} increased. Enrichment in isotope ^{13}C of organic carbon in the surface sediment layer was more expressed: for 2.0‰, on average. A mean value of $\delta^{13}C\text{-}C_{org}$ for 12 samples of surface sediments was equal to −23.81‰ (Table 4). The similar isotope composition of C_{org} was characteristic for the whole marine Holocene sediments [13]. The results obtained showed that process of C_{org} isotope weighting in sediments, compared to that in particulate matter, is localized in a fluffy layer, i.e., at the water-sediment interface.

An additional source of C_{org} in sediments is a biomass of microorganisms formed at the water-sediment boundary. The C_{org} of the newly formed biomass of microorganisms is enriched in isotope ^{13}C ($\delta\ ^{13}C$ varied from −20.0 to −22‰, on average) that promoted a shift of the value $\delta^{13}C\text{-}C_{org}$ toward enrichment in heavy isotopes in sediments. Calculation of the substantial isotopic balance equation has revealed that from 26.6 to 50.5% of total C_{org} in the surface (0.0–0.5 cm) sediments was produced by microbial biomass, which was formed at the water-sediments interface (Table 4).

Table 4 The concentration of suspended particulate matter (SPM), C_{org}, and C_{total} in particulate matter and the isotopic composition of particulate organic carbon in water samples from the water column and from the water-sediment interface (R/V "Ekolog," July 2010)

Station number/ depth, m	Location		Horizon, m	C_{org}, μg l^{-1}	Suspended particulate matter, mg l^{-1}	C_{org}, % of total particulate matter	C_{total}, μg l^{-1}	C_{carb}, μg l^{-1}	C_{carb}, % of total particulate matter	Particulate $\delta^{13}C$-C_{org}, ‰
	N	E								
Kem River Basin										
34/2	64°56.964′	34°37.881′	0	155	4.61	3.36	272	118	2.54	−28.2
1/21	64°04.501′	34°55.034′	0	60	1.07	5.65	109	48	4.57	−23.9
2/50	65°10.692′	35°08.395′	0	89	0.77	11.54	128	39	5.14	−23.6
Dvinsky Bay Basin										
8/12	64°48.870′	39°55.304′	0	85	2.18	3.91	125	22	1.81	−27.4
9/26	64°55.062′	39°36.583′	0	257	1.28	20.09	315	57	4.51	−25.7
63/48	65°23.986′	39°22.055′	0	–	–	–	–	–	–	–
			48	58	1.27	4.58	74.2	16.0	–	−23.7
			NT water 0–30 cm	1,610	72	2.22	2,375	765	1.06	−22.2
			NT water >30 cm	72	27	0.27	88	16.0	0.06	−22.4
			NT fluffy layer 0–0.5 cm	145,400[a]	–	–	297,667[a]	152,266[a]	–	−21.2
			NT fluffy layer 0–0.5 cm	111,267[a]	–	–	213,067[a]	101,800[a]	–	−21.8
10/53	64°57.948′	39°31.717′	0	183	0.62	29.48	266	84	13.51	−23.6
			3	245	0.64	38.33	295	50	7.78	−24.1
			15	37	0.39	9.40	103	67	17.1	−24.8
			50	130	0.71	18.37	408	277	39.09	−23.8

			NT water 0–10 cm	920	128	0.72	3,300	2,380	1.86	−23.2
			TN fluffy layer 0–0.5 cm	183,600.0	–	–	305,933[a]	122,333[a]	–	−22.4
59/59	64°57.604′	39°26.159′	0	–	–	–	–	–	–	–
			57	10.5	0.99	1.06	71	60.9	6.16	−24.1
			NT water 0–7 cm	5,170	162.57	3.18	6,670	5,007	0.92	−23.3
			NT fluffy layer 0–0.5 cm	245,333[a]	–	–	229,933[a]	–	15.4	−24.1
7/62	65°02.069′	38°47.642′	0	215	0.72	29.9	370	154	21.47	−24.2
11/68	65°01.662′	39°19.124′	0	229.	0.75	30.6	304	74.2	9.89	−25.0
12/68	65°05.504′	39°05.332′	0	81	0.93	8.7	194	114	12.25	−24.0
5/82	65°10.625′	37°58.369′	0	306	1.06	28.9	381	75.0	7.07	−20.9
58/83	65°05.308′	38°59.586′	80	23.2	0.57	0.72	23.2	19.1	3.35	−24.2
6/94	65°06.116′	38°22.476′	0	160	0.57	28.07	146	–	–	−23.5
65/111	65°23.986′	39°22.055′	109	25.2	0.39	6.5	48.0	22.2	5.85	−24.8
			NT water 0–40 cm	8.0	11.22	0.07	0.0	–	–	−23.2
			TN water >40 cm	952.0	54.57	1.74	1,668	716	1.3	−25.4
			NT fluffy layer 0–0.5 cm	173,533[a]	–	–	–	47.5[a]	–	−23.2

(continued)

Table 4 (continued)

Station number/ depth, m	Location		Horizon, m	C_{org}, μg l^{-1}	Suspended particulate matter, mg l^{-1}	C_{org}, % of total particulate matter	C_{total}, μg l^{-1}	C_{carb}, μg l^{-1}	C_{carb}, % of total particulate matter	Particulate $\delta^{13}C$-C_{org}, ‰
	N	E								
Basin										
55/141	65°30.881′	37°31.179′	0	0.9	0.54	0.16	4.9	4.0	0.75	–
4/200	65°25.732′	36°58.585′	0	111	0.66	16.79	216.4	105.6	16.0	−23.6
3/220	65°38.442′	36°09.329′	0	90	0.62	14.52	275.6	185.6	29.93	−23.3

NT Neimisto tube, which was used to collect samples from the water-sediment interface

[a]The C_{org} data are converted to the volume of filtered water

A presence of microbial biomass in the surface layer of sediment is confirmed by both increase in percentage of the C_{12}–C_{17} homologues and existence of *n*-alkanes with chain length of C_{12}–C_{14} (Table 5).

The peculiar microbial filter which is formed at border water-sediments, on the one hand, prevents from input of OM decomposition's products from sediments mass into near-bottom water, and, on the other hand, microbial filter reduces C_{org} input from water column during sedimentation. We have shown for the first time experimentally that biogeochemical processes with the participation of microorganisms tare responsible for transformation of particulate C_{org} into sedimentary C_{org} in the initial stage of sedimentation.

3.3 Chemical Composition of the White Sea Modern Sediments

From data of the X-ray fluorescent analysis (Table 6), the SiO_2 and Al_2O_3 dominated in sediments of the White Sea. In the Dvina Bay, these compounds were the main part of aluminosilicates – clay minerals. Proportion of SiO_2 and Al_2O_3 let us to account the Si/Al ratio to be equal to ~3.05. This value is similar to the Si/Al ratio in the clay minerals assemblage of the Russian platform deposits, which are known to be the main supplier of sedimentary material by the rivers inflowing the eastern part of the White Sea. Toward the northwestern coast, a contribution of crystalline rock deposits framing the Kandalaksha Bay increased. The Si/Al ratio considerably exceeded 3.05 due to high content of silicon minerals, mostly quartz (Fig. 6).

Among sedimentary mineral components, the kaolinite, chlorite, montmorillonite, quartz, albite, and potassium feldspars prevailed. Content of carbonate minerals varied from trace quantities in sediments of the Dvina Bay up to 10.8% in sediments of the western depression (Table 7). Authigenic minerals in the oxidized sediments were presented by iron and manganese oxides, often X-ray amorphous.

The majority of carbonate minerals in the White Sea sediments resulted from sedimentation processes; however, there were found also 2–3% of authigenic carbonates formed from carbonic acid. Our calculations showed that their origin was associated with the organic matter's decomposition (Table 8). Values of $\delta^{13}C$-C_{org} and percentage of terrigenous C_{org} in sediment cores of the White Sea are listed in Table 9. As one can see, the terrigenous C_{org} input varied from 35 up to 100%.

Glendonites ("White Sea rogulki") are an exotic authigenic carbonate minerals in sediments of the White Sea. Their finds are characteristic for the Tersky Coast (area of the Olenitsa River). Separate finds of glendonite are known in the Holocene deposits of the Arctic Shelf. Recently glendonite was supposed to be a pseudomorph of a calcite on the ikaite metastable authigenic mineral which was formed in marine sediments at low temperatures, around freezing (up to −1°C). At temperature above +6°C, crystals of the ikaite are destroyed and lose water, thereafter transferring into "a calcite meal." Glendonite serve as authigenic mineral – indicator of cold climate

Table 5 The content of the suspended particulate matter (SPM), particulate C_{org}, the C/N ratio, and content of *n*-alkanes in the SPM and in the surface (0–3 cm) sediment layer in the White Sea (55 cruise R/V "Professor Shtokman," August 2003) [10]

Station number / Depth, m	Water horizon, m	SPM, mg/l	Particulate C_{org}, mg/l	C/N	C_{org}, % mass	*n*-Alkanes, ng/l	*n*-Alkanes, % of total alkanes		
							Σ(C_{12-} C_{17})	C_{12}	C_{13}
Dvinsky Bay									
4927/56	0	0.63	0.198	5.5	31	172	13.4	0.14	0.19
	50	0.96	0.048	7.4	5	129	11.7	0	0.13
	sediment			10.8	1.5	2.77[a]	16.2	0.65	1.18
4928/94	0	0.71	0.182	5.8	25	319	11.8	0	0.1
	90	0.26	0.33	–	13	193	11.8	0.11	0.07
	sediment			8.2	1.7	4.98	35.5	1.62	2.88
Basin									
4928/152	0	0.60	0.224	6.8	37	249	15.9	0	0.3
	145	0.38	0.045	6.6	12	63.3	16.2	0.16	0.28
	sediment			8.6	1.7	3.87	18.0	0.62	1.3
4930/290	0	0.48	0.231	5.9	49	267	9.4	0.11	0.2
	290	0.43	0.106	4.4	25	390	13.9	0	0.19
	sediment			9.2	1.7	13.5	69.0	5.4	7.8
Gorlo									
4911/23	0	0.89	0.093	7.7	10	111	13.7	0	0
	23	0.61	0.076	7.7	13	93	11.1	0	0.12
	sediment			10.3	0.06	0.25	38.1	1.1	2.0
4914/59	0	0.91	0.134	–	15	79	9.8	0	0
	53	2.73	0.170	8.9	6	127	25.4	0	0
	sediment			6.1	0.04	0.34	33.1	1.1	2.7
4916/23	0	2.44	0.283	7.8	12	374	14.4	0	0.15
	21	2.87	0.129	7.5	4	175	15.6	0	0
	sediment				0.22	1.92	38.7	2.4	4.2

Kandalaksha Bay									
$\frac{4933}{340}$	0	0.45	0.178	5.9	39	194	8.1	0.06	0.16
	333	0.53	0.038	8.1	7	99.1	13.9	0	0.14
	осадок			8.7	2.1	3.77	14.4	1.1	1.6

[a]The content of *n*-alkanes is given in mg/g in sediments; dash (here in after) – no definitions

Table 6 Chemical composition of the sediments of the White Sea (from the X-ray fluorescence analysis)

Station	Horizon, cm	SiO_2	Al_2O_3	Fe_2O_3	MgO	CaO	K_2O	TiO_2	MnO	Loss on ignition
6042	0–5	52.46	15.18	8.08	3.56	1.52	3.03	0.86	0.09	11.7
	5–10	53.89	15.6	8.02	3.69	1.53	3.15	0.89	0.077	9.63
	10–15	53.28	15.78	8.42	3.6	1.53	3.23	0.93	0.089	9.64
	15–27	54.03	15.7	7.72	3.8	1.57	3.15	0.9	0.081	9.55
	40–48	54.84	14.83	7.93	3.91	1.58	2.99	0.82	0.082	9.51
	48–55	53.66	15.67	7.69	4.17	1.53	3.08	0.87	0.083	9.74
6052	0–5	46.86	13.6	7.08	3.38	1.45	2.77	0.79	6.14	14.39
	5–21	49.97	14.32	8.07	3.59	1.44	3.03	0.8	2.63	12.65
	21–40	50.43	15.04	8.60	4.14	1.36	3.18	0.85	0.59	11.97
	40–50	49.39	15.06	9.48	3.92	1.56	3.20	0.90	1.49	11.49
	55–63	52.26	14.94	8.68	3.91	1.44	3.17	0.82	1.22	10.62
6062	2–5	66.79	13.6	3.99	3.03	2.5	2.44	0.54	0.065	3.53
	10–21	71.35	12.2	3.21	2.46	2.28	2.03	0.41	0.046	2.48
6065	5–10	51.03	14.24	8.86	3.67	1.78	2.94	0.86	0.64	12.47
	10–25	51.76	14.79	9.18	3.38	1.7	3.09	0.91	0.42	11.26
	25–40	52.18	14.81	8.74	3.76	1.61	3.07	0.89	0.35	11.08
	40–51	52.81	14.72	8.83	3.2	1.63	3.05	0.89	0.38	10.99
6066	5–10	45.76	13.2	6.03	3.18	1.38	2.69	0.76	9.15	14.3
	10–20	49.33	14.01	7.76	3.94	1.63	2.91	0.78	2.95	13.8
	20–37	52.27	14.6	8.34	3.64	1.42	3.13	0.82	0.46	11.82
	32–52	52.84	14.65	8.82	3.74	1.39	3.11	0.82	0.43	10.73
	52–62	51.32	14.67	9.19	4.06	1.44	3.05	0.86	0.54	11.36

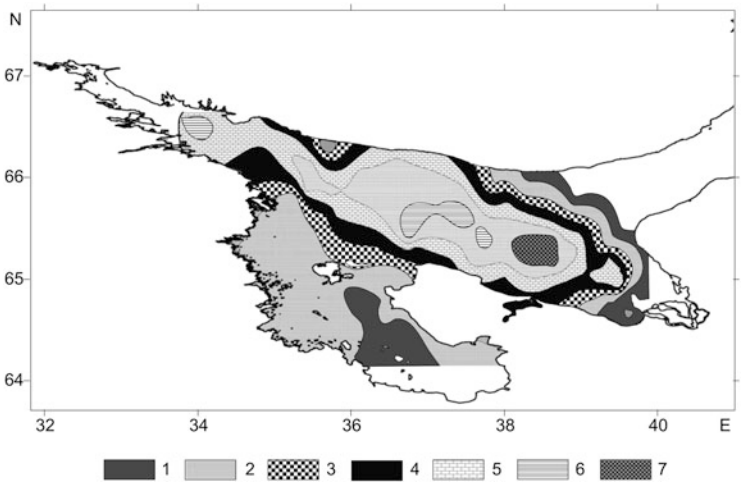

Fig. 6 Distribution of grain-size fractions in the White Sea surface (0–2 cm) sediments [17]. Fractions: 1, sand; 2, silt mud (pelite 60%); 3, aleurite-pelite (pelite 45%); 4, aleurite-pelitic (pelite 60%); 5, pelitic silt (pelite 32%); 6, pelitic silt (pelite 94%); 7, pelitic (pelite ~100%)

Table 7 Mineral composition of the surface layer of bottom sediments of the White Sea (XRD semiquantitative phase analysis results)

No	Station number	Sediment horison, cm	Mineral composition, %								
			Clays[a]	Quartz	Albite	Microcline	Calcite	Dolomite	Pyroxenes	Amphiboles	Others
1	6042	5–10	40.5	24.4	11.7	3.9	3.6	3.1	2.6	5.2	Tridymite
2	6052	0–5	56.4	12.9	11.7	5.3	Trace	Trace	Trace	8.7	Tridymite, rhodochrosite
3	6052	5–21	51.2	16.6	14	3.8	–	–	4.2	5.1	Tridymite
4	6052	21–40	42.8	13.9	12.2	7.6	5.7	3.8	4.1	4.8	Phyllosilicates
5	6052	40–50	44	17	14.5	6.2	–	3	4.2	5.9	Rhodochrosite, hydrotroilite
6	6052	55–63	31.5	16.7	20.7	7.4	5.8	3	5.8	4.1	Rhodochrosite
7	6062	2–5	10.5	23.9	39.9	10.3	Trace	Trace	–	10.4	Hydrotroilite
8	6062	10–21	9.6	24.6	33.5	20.3	Trace	Trace	Trace	7.2	Rhodochrosite
9	6065	5–10	39.9	13.7	11.3	9.8	2.7	7.1	9.5	1	Hydrotroilite
10	6065	10–25	39.3	22.7	11.8	6.5	–	4.5	5.2	5.2	Hydrotroilite, zeolites
11	6065	25–40	41.4	18.7	14	5.7	–	7.4	7.8	Trace	Hydrotroilite
12	6065	40–51	47.4	18.6	10.3	3.5	4	5.3	2.9	2.9	Tridymite
13	6066	5–10	33.8	22	20.4	8.6	–	Trace	5.8	4.4	Phyllosilicates
14	6066	10–20	30.8	19	18.3	10.7	4.7	2.8	5.6	3.3	Zeolites, rhodochrosite
15	6066	20–37	36	16.2	17.8	10.1	5.8	2.1	Trace	6.9	Zeolites, hydrotroilite
16	6066	32–52	36	14.4	12.3	11.7	4.2	3.5	6.9	5.9	Phyllosilicates
17	6066	52–62	43.3	12.9	11.6	3	5.8	5	7.5	5.8	Palygorskite, hydrotroilite

– no data

[a]Sum of the montmorillonite, kaolinite, chlorite, and illite. Data of Dr. O.M. Dara, IO RAS

Table 8 The isotopic composition of C_{org} in the 0.0–0.5 cm sediment layer and percentage of the newly formed C_{org} from the total C_{org}

Sampling date	White Sea area	Station number depth, m	Coordinates		$\delta^{13}C\text{-}C_{org}$, ‰	$\delta^{13}C\text{-}C_{carb}$, ‰	Percentage of C_{org}[a] newly formed from total C_{org}
			N	E			
15.08.06	Dvina Bay	$\frac{6042}{61}$	64°59′946″	39°22′981″	−26.60	−15.02	26.6
20.08.06	Basin	$\frac{6056}{133}$	65°34′230″	37°46′155″	−25.40	−11.14	40.0
21.08.06	Basin	$\frac{6058}{300}$	65°44′259″	36°04′61″	−25.81	−11.20	35.4
	Dvina Bay	$\frac{6062}{71}$	65°05′505″	36°05′475″	–	−14.80	–
	Basin	$\frac{6063}{270}$	65°52′977″	35°23′935″	−24.78	−11.0	46.9
23.08.06	Kandalaksha Bay	$\frac{6065}{245}$	66°11′265″	35°15′615″	−25.03	−2.58	44.1
	Kandalaksha Bay	$\frac{6066}{265}$	65°59′786″	35°32′287″	−24.51	−11.91	49.9
	Basin – Gorlo	$\frac{6068}{108}$	66°08′455″	36°36′519″	−25.11	−2.03	43.2
	Basin	$\frac{6069}{285}$	65°39′381″	36°25′769″	−24.48	−15.17	50.22
	Basin	$\frac{6070}{228}$	65°26′456″	36°45′941″	−24.45	−15.10	50.5
24.08.06	Basin	$\frac{6071}{143}$	65°27′900″	37°29′635″	−24.53	−16.9	49.7
		$\frac{6072}{138}$	65°37′100″	37°29′897″	−24.52	−10.12	

[a]Calculation from the equation of substantial isotope balance: $100 \cdot A = Bx + (100-x)C$, where (A) δ13C-$C_{org}$ in sediment; B, $\delta^{13}C\text{-}C_{org}$, in biomass of microorganisms (−20‰); C, $\delta^{13}C\text{-}C_{org}$ suspended particulate matter (−29‰); x, percentage of C_{org}, newly formed from total C_{org}, %

Table 9 Values of $\delta^{13}C\text{-}C_{org}$ and content of terrigenous C_{org} in sediment cores of the White Sea

Station number	Horizon, cm	$\delta^{13}C\text{-}C_{org}$, %	Number of samples	Average, $\delta^{13}C\text{-}C_{org}$, %	Terrigenous C_{org} [a], %
Dvina Bay					
6042	0–80	−25.20 ... −26.54	6	−26.26	78
	80–190	−24.78 ... −25.58	5	−25.00	62
	190–290	−26.20 ... −26.46	2	−26.33	79
	290–460	−27.50 ... −29.36	9	−28.43	100
6050	16	−24.06	1	−24.06	51
	30	−23.76	1	−23.76	47
	70	−25.6	1	−25.6	70
	100–150	−23.5 ... −24.1	2	−23.80	47
	210–252	−23.69 ... −23.97	2	−23.83	48
	278–308	−26.12 ... −26.50	3	−26.33	79
	320–335	−27.15	1	−27.15	89
Basin					
6058	0–55	−25.33 ... −26.53	8	−26.15	77
	55–66	−23.17 ... −25.62	2	−25.76	72
	66–270	−22.35 ... −23.17	8	−22.89	36
6066	0–65	−25.62 ... −26.00	6	−25.82	73
	65–112	−22.68 ... −22.85	3	−22.78	35
	112–130	−24.26 ... −24.31	2	−24.28	53
	130–160	−22.95 ... −23.95	3	−23.41	43
	160–242	−24.41 ... −24.57	4	−24.19	56
Solovki Islands					
6062	0–25	−24.93 ... −25.15	2	−25.04	53
	25–55	−25.20	1	−25.20	65
	55–90	−25.61	1	−25.61	70
	90–188	−26.52	1	−26.52	81.5

(continued)

Table 9 (continued)

Station number	Horizon, cm	$\delta^{13}C\text{-}C_{org}$, ‰	Number of samples	Average, $\delta^{13}C\text{-}C_{org}$, ‰	Terrigenous C_{org} [a], %
	188–200	−29.23	1	−29.23	100
	200–250	−30.66 . . . −30.91	3	−30.79	100
	330–338	−29.41	1	−29.41	100

[a]Calculation by the equation of material-isotope balance: $A \cdot 100 = Bx + (100–x)C$, where x, terrigenous C_{org} in the test samples; A, values of $\delta^{13}C\text{-}C_{org}$ of test samples; B, average value of $\delta^{13}C\text{-}C_{org}$ removed from the land; C, average value of $\delta^{13}C\text{-}C_{org}$ of White Sea phytoplankton

[14]. Ikaite particles, unlike glendonite, do not include terrigenous material. They are formed at the surface or in the uppermost sediment layer. The isotopic composition of carbonate carbon of the White Sea glendonites varied from −14 to −22.4‰, on average, −16.65‰ (7 samples) [14]. Similar values of $\delta^{13}C\text{-}CO_2$ were characteristic for diagenetic carbonates which have been formed due to microbial decomposition of organic matter.

Distribution of the Mn occurrence forms is one of the indicators of early diagenetic transformations in the White Sea sediments [1, 15–17]. Along the axial transect, the content of MnO in the surface sediments varied from the hundredth parts of percent up to 5.73% [17]. Formation of manganese (and ferromanganese) micro-concretions in the surface sediments of the White Sea takes place at the first stage of physical chemical equilibration of the watered sediments. These sediments are enriched in the labile organic matter (OM) of phytoplankton genesis and microbial biomass, along with the terrigenous OM.

At this stage, during the early diagenesis, free oxygen is exhausted almost completely in pore water, and vigorous dissolution of Mn^{4+} ("manganese respiration," by Yudovich and Ketris [18]) starts, causing a rise of already transformed Mn^{2+} to the surface bottom sediments where Mn^{2+} can partly diffuse to near-bottom water. However, major part of Mn is fixed in the oxidized zone of surface sediments in the authigenic mineral forms, giving to these sediments a black-brown color and changing a grain-size distribution from pelitic to aleurite-pelitic "with sandy admixtures" in shape of micro-concretions. Reduction of Mn^{4+} is followed by a reduction of Fe^{3+}. The surface horizons of sediment core enriched in Mn are underlain by sediments with higher content of Fe, according to a difference of their redox potentials.

Appearance of authigenic sulfide minerals (hydrotroilite and pyrite) in sediments, along with change of the Eh, testifies a change in oxidizing conditions on oxidation-reduction and the reduction ones. Finds of hydrotroilite in the open part of the Dvina Bay were detected already at the horizon of 3–8 cm. This horizon operates as a transferring zone of Fe^{3+} reduction into Fe^{2+} comparing with the horizon of 2–3 cm (Table 7). In the Basin sediments, the similar border of sharp transition of Fe^{3+} goes down the horizon of 10–11 cm (St. 6056) and even below (up to 18 cm) in the western depression (St. 6058).

Thus, in the oxidized upper sediment layer (0–5–10 cm, St. 6056, 6058), the ferric Fe^{3+} prevailed, while reactive ferrous Fe^{2+} is practically absent; however, deeper 10 cm in sediments of the Basin, Fe^{2+} prevailed which is mainly a part of silicates (leptokhlorite) and FeS_{n-1} monosulfides (hydrotroilite). Amount of reduced compounds (derivatives of microbial H_2S in sediments) did not exceed 0.5%. In the surface-oxidized sediments, sulfur speciation was presented by an elemental and organic sulfur. Below oxidized zone, H_2S derivatives were found in sediments, mainly, in the form of the "hydrotroilite" (FeS_{n-1}) of diagenetic origin. These black fine-grained crystals of pyrite ($FeS_{2)}$ were oxidized fast under air condition and were detected as X-ray amorphous minerals. The first data on sulfur isotope composition ($S\text{-}SO_4^{2-}$) of the ocean water (17.0‰) and pore water (1.8‰) from the surface sediment horizon in the Ermolyevsky Bay of the White Sea were provided in work [19]. The same work contains data on isotopic composition of SO_4^{2-} in the Great Salma ($\delta^{34}S = 19.4‰$) water that is close to water of the open ocean.

Values of organic $\delta^{34}S$ in plants practically were very close to isotopic composition of sulfate ion (from 14.0 to 19.5‰) in both blooming plants and algae (red, brown, green). The values of $\delta^{34}S$ included in OM of animals ranged from 13 to 14‰, since the biomass of animals was studied in places of significant inflow of fresh water having values of $\delta^{34}S\text{–}SO_4$ around 13–15‰. Our long-term researches of sulfur compounds in sediments of different marine Basins let us to reveal the main regularities of the isotopic composition of oxidized S (SO_4^{2-} of pore waters) and reduced S (FeS_{n-1}, FeS_2, HS, S_{org}, S_{elem}) species in marine and ocean sediments [20]. Beginning with the work [21], it is known that isotopic composition of $S\text{-}SO_4^{2-}$ is enriched in heavy isotope ^{34}S down the core, while the reduced sulfur species, on the contrary, have the negative values of $\delta^{34}S$. Such a distribution of $\delta^{34}S$ values for $S\text{-}SO_4^{2-}$ and reduced S species is given for the White Sea sediments [22]. Values of $\delta^{34}S$-reduced S species (FeS_{n-1} and FeS_2) varied from -18 to $-46‰$. The difference in isotopic composition of $S\text{-}SO_4^{2-}$ and S-pyrite can reach more than 70‰ in the Holocene sediments, which is characteristic for processes with very slow rates when microbial fractionation of sulfur isotopes was the maximal ones, respectively.

It should be noted that the amount, composition, and distribution of the Mn- and Fe-containing reduced sulfur compounds in sediments of the White Sea resemble a distribution which we observed in the pelagic oceanic sediments where high degree of a reduction was not reached due to low concentration of labile forms of organic matter and its exhaust by reduction of Mn^{4+} and Fe^{3+} in the surface layer. For example, such situation happened in the Norwegian Sea at depths ~1,000 m nearby the Haakon Mosbi mud volcano [23] and in the pelagic sediments of the Pacific Ocean nearby the Marcus-Necker islands [24].

In case of the White Sea sedimentation, it is necessary to recognize that terrigenous OM whose amount is higher compared to hydrogenous OM is not a good substratum for developing the anaerobic diagenetic processes.

3.4 Methane in Sediments of the White Sea

Concentration of CH_4 which is the second (after H_2S) important diagenetic gas generated in sediments, varied in the oxidized layer (0–1 cm) from 2.3 μl dm^{-3} (at 133 m depth, St. 6056) up to 3.5 in the oxidized layer (0–1 cm) μl dm^{-3} (at 300 m depth, St. 6058). Concentration of CH_4 (7.98 μl dm^{-3}) was measured in the 0–1 cm layer in an open part of the Dvina Bay (St. 6042). In shallow water in the Dvina Bay, concentration of CH_4 varied from 6.4 to 12.5 μl dm^{-3} (St. 6048, 6046, 6045). Concentration of methane in the surface layer (0–1 cm) of all studied sediments was as much as ten times higher than in near-bottom water. This fact is an evidence of active methane diffusion caused by a concentration gradient from sediments into water column. The highest methane concentrations were recorded in different sites of the Kandalaksha Bay littoral (15,000–25,000 μl dm^{-3}) [8, 25].

Thus, the irregular distribution of CH_4 concentrations in the surface sediment layers is probably caused first of all, by input of particulate C_{org} that define physical and chemical conditions in sediments of the White Sea. Down the core, CH_4 concentration increased, which was noticed already at the 5 cm horizon and continued till the horizon of 200–250 cm. We have calculated the methane bulk amount under 1 m^2 of seafloor throughout the 55 cm thickness of sediment core (collected by Neimisto tube) for different parts of the White Sea [9]. The maximal CH_4 amount (6.3 ml m^{-2}) was calculated in deepwater sediments of the Basin where the most sorted fine-grained sediments with high content of autochthonic C_{org} are located. At given sedimentation rate in the White Sea, which varied from 0.1 to 0.17 mm/year [26, 27], the methane pool over the surface 55 cm sediment core at the constant sedimentation rate will be approximately 4×10^5 m^3 of CH_4 for the last 500 years.

3.5 Organic Matter in the White Sea Sediments: Content, Distribution, Carbon Isotope Composition, n-Alkanes, and Genesis

The study of organic matter of the White Sea sediments began in the first third of the twentieth century [28]. The greatest contribution to dataset on the C_{org} content and its distribution in sediments was made by Nevessky with coauthors [1].

In our study, the main emphasis is placed on the organic matter's genesis based on results of the C_{org} isotope analysis of suspended particulate matter (SPM) and sediments. For the White Sea, we were the first who obtained these data. The 30 samples of surface sediments from the Basin, Kandalaksha Bay, and Dvina Bay have been analyzed. The surface sediments (0–2 cm) from the open part of the Dvina Bay contain C_{org}, on average, 1.65%, from the western depression of the Basin and Kandalaksha Bay 2.0%, and from area nearby the Solovetsky Islands 0.65% (Fig. 7). Down the sediment core, the C_{org} content decreased gradually that testified a rather small C_{org} consumption during oxidizing and reduction diagenetic

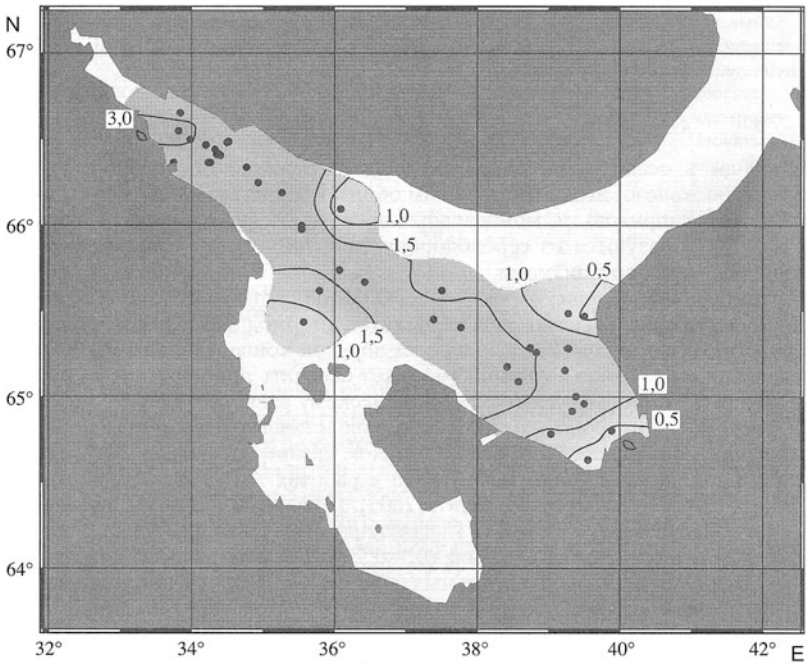

Fig. 7 Distribution of C_{org} (% dry weight) in the surface (0–2 cm) sediment layer of the White Sea

processes in the surface 50 cm sediment thickness studied: 0.5% in the Dvina Bay and 0.05–0.65% in the Basin.

The major part of OM in the studied sediments is composed of insoluble (residual) components of the mixed hydrogenous and terrigenous genesis which relate, in accordance with Danushevskaya classification [29], to the II OM sediment type. The terrigenous components of OM are presented of heavily mineralized compounds of humus origin. According to Gorshkova [28], content of the humus substances in the White Sea sediments can reach 48–85%. The White Sea is characterized by a mosaic distribution of the C_{org} content, controlled primarily by the complex hydrological regime and controlled by, as a rule, the grain-size composition of sediments. A maximal C_{org} content was found in pelitic silts of the central part; in sands, a minimal; and in silty-pelitic, an intermediate ones.

The C/N ratio usually is used as an indicator of OM origin in SPM and sediments. For hydrogenous OM, values of C/N $\leq$ 7 and for terrigenous OM C/N $>$ 7 are characteristic [10]. The C/N ratios in deposits of the Dvina Bay were particularly high (9.5, on average). In the Basin sediments, on the contrary, C/N values were minimal, which proves a higher OM content of plankton genesis there. In surface sediments sampled at 61 m depth in 2006 in the Dvina Bay, an average value of $\delta^{13}C\text{-}C_{org}$ was 26.6‰ (Table 8). While in 2010, a rather variable isotopic composition of C_{org} in the surface sediments of the Dvina Bay was recorded: from −27.4‰ at 12 m depth to −20.9% at a 82 m depth.

It should be noticed that the $\delta^{13}C\text{-}C_{org}$ values less than $-18 \div -22‰$ testify, as a rule, a presence in sediments of terrigenous OM that was supplied from the land or as a result of coastal abrasion. So, in the studied samples from the Dvina Bay at the water depths of 12 m and 26 m, there was mainly terrigenous OM (Table 3). On the contrary, in sediments at St. 5 and St. 63 at depths of 82 and 48 m, respectively, because of hydrologic features and seafloor's morphology, there was practically no terrigenous OM that was reflected in isotopic composition of C_{org} ($\delta^{13}C\text{-}C_{org} = -21.5 \div -20.9‰$). So, at most stations in the Dvina Bay, according to isotopic data, a participation of allochthonous (or hydrogenous) sedimentary matter, with an average value of $\delta^{13}C\text{-}C_{org} = -23.83‰$, was recorded. The sediment age at the 0–5 cm horizon by ^{210}Pb distribution [27] varied from 12 years at shallow stations to 50 years at depths of 50–100 m. Over this time, the OM of mixed origin has been accumulated at the bottom of the Dvina Bay; at one site there was a dominance of autochthonic (hydrogenous) OM while in others of allochthonous (hydrogenous) OM. Sediments of the whole White Sea contain up to 78–80% of terrigenous organic matter presented by carbon compounds that are heavily assimilated by microorganisms [10, 11, 13].

In surface sediments nearby the Basin and Kandalaksha Bay, isotopic composition of C_{org} ($\delta^{13}C\text{-}C_{org}$) varied in narrow limits: from -24.45 to $-25.81‰$, $-24.91‰$ on average for 11 samples (Table 8). That is an evidence of presence in sediments of C_{org} having both a terrestrial and marine origin. A calculation of terrigenous C_{org} contribution based on equation of material-isotope balance (Table 8) also corresponds to results of stratigraphic analysis of sedimentary thickness (Fig. 8), beginning with freshwater deposits of the Allered and ending with the modern ones of marine stage [13].

A contribution of OM having plankton genesis to surface sediments could be estimated from short-chain (C_{12}–C_{17}) *n*-alkanes' contents. Maximal content of these *n*-alkanes which characterizes a plankton genesis was detected in deepwater sediments of the Basin (69% of *n*-alkanes in sum) [30]. The least quantity of *n*-alkanes that corresponds to terrigenous origin was revealed in surface sediments of the Dvina Bay; similar data were obtained by other methods.

As soon as microorganisms are the main agents of diagenetic processes, the activity of microorganisms is hampered in sediments of the White Sea due to the high content of terrigenous OM. Thus, it was assumed a priori that the rates of diagenetic processes should be lower than those in other seas of the humid zone.

3.6 Chemical Composition of Pore Waters

Pore waters proved a valuable information on scales and direction of biogeochemical processes in bottom sediments. We studied pore waters of the upper 40–50 cm of sediments which were collected in the Dvina Bay, in the Basin, and in the western deepwater depression of the White Sea nearby the Kandalaksha Bay (Fig. 9). A

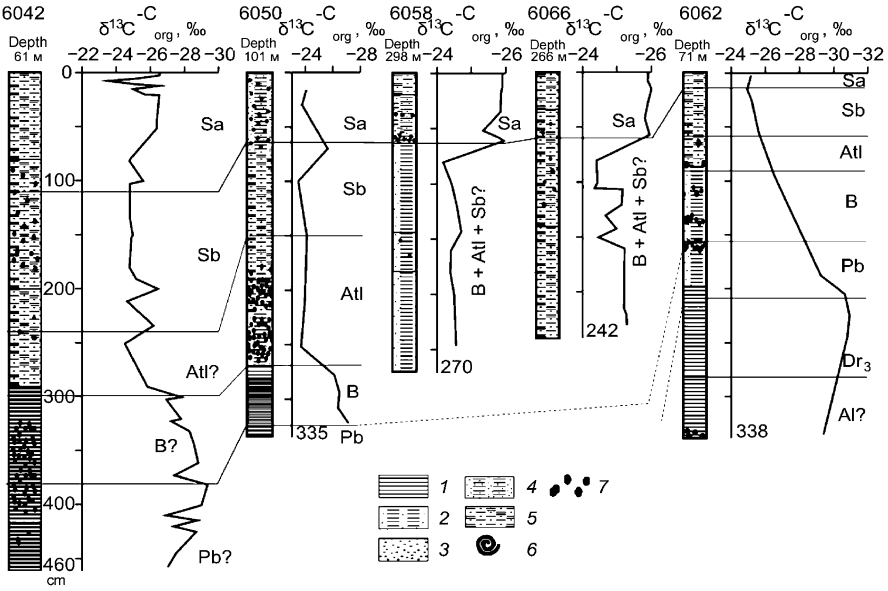

Fig. 8 Distribution of the $\delta^{13}C$-C_{org} values in the White Sea Holocene sediments over the climatic periods (from the core bottom upward). Late glacial: Al, Allred; Dr., Upper Driassic. Postglacial: Pb, Abortion; B, Boreal; ATL-SB, Atlantic-Subboreal, SA, Subatlantic. Numbers from 1 to 5 mean grain-size fractions: 1, clay; 2, aleurite-pelitic; 3, sand; 4, pelites; 5, clayey silts; 6, bivalve debris; 7, hydrotroilite

chemical composition of near-bottom water from bathometers and water from Neimisto tube from water-sediment contact zone was also analyzed (Table 10).

Along the axial transect from south-east to north-west, a salinity of near-bottom and pore waters increases, which was traced by change in Cl-ion concentration from 440 mM in the Dvina Bay up to 472 mM in the western depression of the White Sea. Thus an existence of two main sources of water of the White Sea is confirmed – a fresh input from the continent and saline water inflowing from the Barents Sea. For a reference Eh point of the Barents Sea near-bottom water, a value Eh = 445 mV could be taken. This water contains 27.0 mM of SO_4^{2-}, and a value of water alkalinity (Alk) varies from 2.1 to 2.2 mg eqv l^{-1}.

Near-bottom waters in the Dvina Bay considerably differ from that of the Barents Sea in less concentration of SO_4^{2-} ion (24.6 ÷ 25.7 mM), while Alk values (2.03 mg eqv l^{-1}) are similar (Table 10). In sulfate ion's distribution in near-bottom water, a small increase in concentration of SO_4^{2-} ion was detected along the transect from the shallow station 1408 (24.6 mM) to the deepwater station 1404 (25.1 mM).

Values of pH in pore water, by results of potential metric measurements, were characterized by decreased pH (6.8–7.8) and Eh (up to −90 mV) values in comparison with near-bottom waters where pH = 7.5–8.3 and Eh = 225 ÷ 470 mV. Decrease of Eh values is caused by diagenetic processes of OM destruction, as

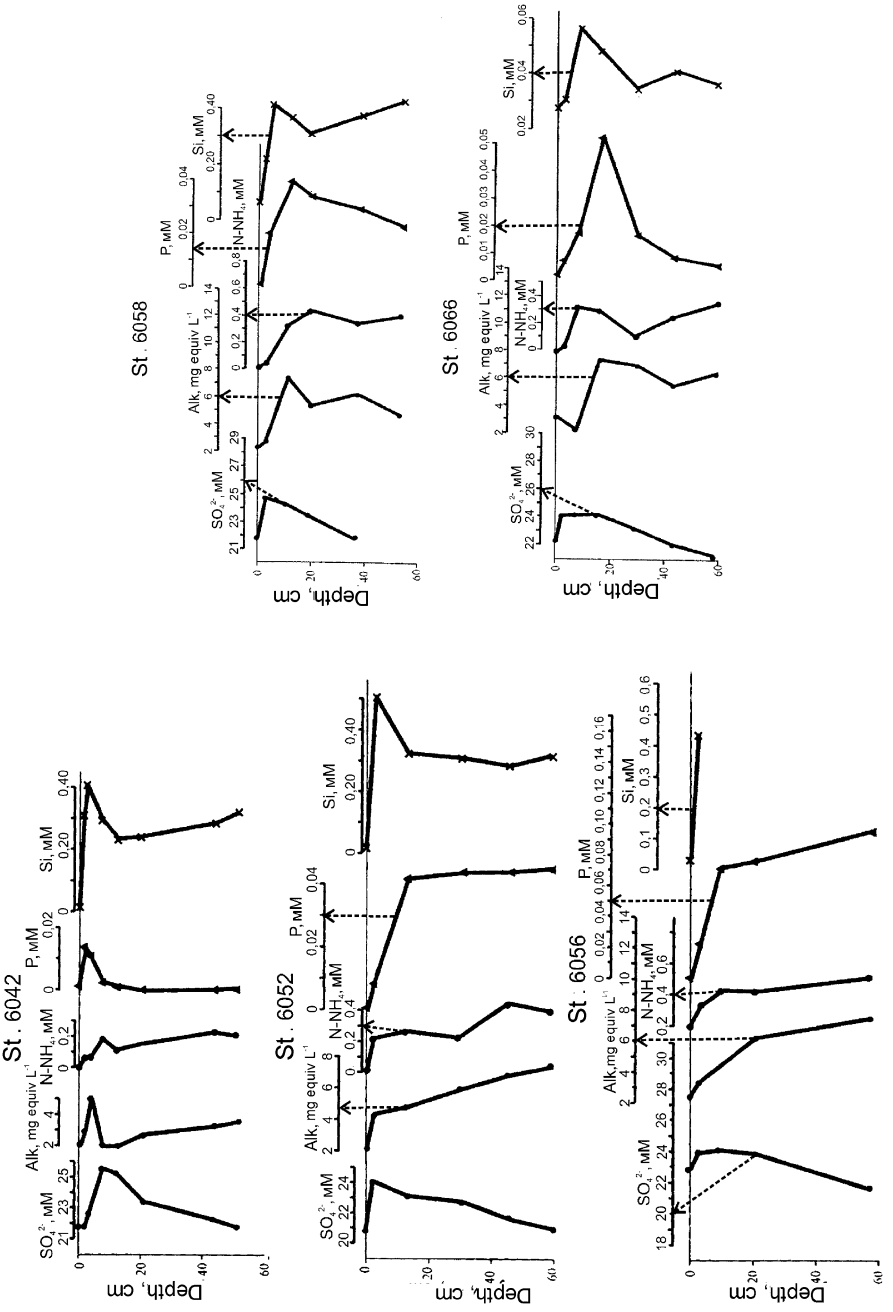

Fig. 9 Chemical composition of the pore waters in the White Sea typical sedimentary profile

Table 10 Chemical composition of the White Sea sediments

Station number, coordinates N, E; depth	Horizon, cm	Humidity, %	*Alk*, mg equl^{-1}	SO_4^{2-}, mM	N, mM	P, mM	Si, mM	CH_4, нм дм$^{-3}$	Cl, mM	C_{org}, %
80 R/V "Professor Shtokman," 2006										
6042	Bottom									
TN	water	–	–	–	–	–	–	6.85	–	–
Dvina Bay 64°59.6946	0–0.1	–	–	–	–	–	–	162.01	–	–
39°22.981	0–1	84.69	–	–	–	–	–	231.57	–	–
61 m	1–2	–	–	–	–	–	–	315.90	–	–
Gravity core	2–5	66.86	2.10	21.8	<0.001	0.026	0.354	312.35	440	–
	5–10	–	–	–	0.052	–	–	330.85	–	–
	10–15	62.60	3.0	21.56	–	0.007	0.296	356.47	–	1.646
	15–27	61.45	3.0	21.5	0.068	0.013	0.310	375.17	–	–
	30–32	–	5.0	25.64	0.071	0.011	0.411	241.60	–	–
	40–48	–	2.00	25.50	0.179	0.002	0.290	321.83	451	1.287
	48–55	65.37	2.03	25.28	0.113	<0.001	0.228	467.70	442	1.175
	53–55	–	2.74	23.57	0.151	<0.001	0.242	328.21	432	1.213
	90–95	–	–	–	–	–	–	351.91	–	–
	150–160	61.00	3.27	22.14	0.225	<0.001	0.278	551.58	458	1.223
	210–220	59.14	3.58	21.86	0.200	<0.001	0.323	413.00	424	1.162
	280–290	53.70	–	–	–	–	–	1,003.78	–	–
	330–340	44.46	–	–	–	–	–	729.36	–	–
	390–400	46.33	–	–	–	–	–	611.75	–	–
	450–460	40.58	–	–	–	–	–	485.93	–	–
6052	Bottom									
TN	water	–	2.15	21.00	<0.001	0.001	0.022	5.77	451	–
Dvina Bay 65°17.205	0–5	–	4.50	24.00	0.210	0.009	0.511	24.63	478	2.029
38°44.814	5–21	–	4.79	23.15	3.62	0.041	0.324	–	445	1.611
126 m	21–40	–	5.87	22.72	3.12	0.038	0.312	153.10	452	1.188
	40–50	–	6.79	21.64	6.00	0.030	0.281	–	449	1.298
	55–63	–	7.32	21.00	5.40	0.025	0.309	260.47	442	1.340

(continued)

Table 10 (continued)

Station number, coordinates N, E; depth	Horizon, cm	Humidity, %	*Alk*, mg equl^{-1}	SO_4^{2-}, mM	N, mM	P, mM	Si, mM	CH_4, нм дм$^{-3}$	Cl, mM	C_{org}, %
6056	Bottom									
TN	water	–	2.40	22.93	<0.001	0.001	0.039	1.88	–	–
Basin	0–6	82.43	3.25	22.50	0.143	0.023	0.445	9.10	–	–
65°24.230	6–13	–	5.03	22.14	0.232	0.061	–	208.24	465	–
37°46.155	13–30	67.78	6.25	21.81	0.220	0.076	–	121.98	482	–
133 m	30–31	–	–	–	–	–	–	186.21	456	–
Gravity core	45–70	71.87	7.50	21.64	0.298	0.095	–	288.07	464	–
	50–55	66.57	9.00	23.28	0.456	0.123	0.559	296.33	–	–
	100–110	64.02	12.00	23.27	0.618	0.171	0.632	411.04	467	–
	140–145	60.69	12.50	18.61	0.675	0.158	0.619	382.60	–	–
	170–180	60.36	13.00	19.72	0.742	0.169	0.598	667.08	–	–
6058	Bottom									
TN	water	–	2.23	22.50	<0.001	0.001	0.067	4.70	–	–
Basin	0–6	–	–	–	–	–	–	–	457	–
65°44.259	7–16	–	2.20	22.29	<0.001	<0.001	0.031	–	–	–
36°04.061	16–21	80.67	2.66	22.29	0.029	0.019	0.414	154.80	–	2.039
300 m	26–46	–	7.31	21.40	0.307	0.039	0.370	271.68	472	1.597
Gravity core	46–58	70.60	5.18	20.86	0.411	0.035	0.316	–	–	1.567
	21–39	–	6.14	18.75	0.343	0.029	0.387	–	–	1.391
	52–56	–	4.62	18.56	0.401	0.022	0.429	–	–	1.548
	30–35	72.93	–	–	–	–	–	364.82	–	–
	45–55	74.19	10.50	20.95	0.850	0.001	0.400	579.40	–	–
	90–100	–	–	–	–	–	–	623.23	–	–
	110–120	70.93	–	–	–	–	–	671.63	–	–
	160–180	–	–	–	–	–	–	704.50	–	–
	230–260	67.03	12.90	20.83	0.696	0.012	0.310	883.47	–	–
	–	61.81	13.50	19.69	0.765	0.344	0.344	**1,329.08**	–	–
	–	59.46	13.50	18.57	0.646	0.423	0.423	1,126.37	–	–

6062	Bottom									
TN	water	–	2.10	23.15	<0.001	<0.001	0.025	5.38	–	–
Solovki Islands,	2–4	–	2.80	25.07	0.226	0.007	0.356	170.32	–	0.648
71 m	10–21	–	1.68	27.81	0.064	<0.001	0.284	–	–	0.353
Gravity core	10–21	–	1.68	28.29	0.064	<0.001	0.284	389.47	–	–
	20–30	–	2.09	28.07	0.066	<0.001	0.267	400.43	–	0.516
	40–45	–	–	–	–	–	–	395.87	–	–
	50–60	–	2.88	27.81	0.110	<0.001	0.317	723.68	454	0.403
	90–100	–	3.59	26.57	0.223	<0.001	0.278	509.09	–	0.576
	140–150	–	4.61	25.50	0.275	<0.001	0.261	973.87	–	0.613
	185–195	–	5.09	22.24	0.430	0.004	0.302	1,992.01	–	0.485
	200–210	–	5.35	21.98	0.353	0.004	0.264	–	–	0.418
	220–230	–	5.48	21.56	0.294	0.002	0.233	2,220.29	–	0.321
	240–250	–	5.40	20.73	0.375	<0.001	0.257	2,528.93	–	0.236
	270–271	–	–	–	–	–	–	1,607.58	–	–
	330–340	–	2.14	21.78	0.375	<0.001	0.146	751.07	–	0.495
6065	Bottom									
TN	water	–	2.18	23.57	<0.001	<0.001	0.045	–	–	–
Kandalaksha Bay	0–5	76.68	3.63	27.43	0.028	0.019	0.360	–	–	–
66°11.265	5–10	66.98	4.01	24.00	0.161	0.022	0.361	4.83	470	2.071
35°15.615	10–25	67.62	4.39	23.36	0.111	0.021	0.380	–	469	1.699
245 m	25–40	65.42	4.97	24.65	0.263	0.010	0.388	–	–	1.353
	40–51	63.12	6.15	23.15	0.439	0.008	0.333	–	–	1.420
R/V “Ecolog,” 2014										
1413	Bottom									
83 m	water	–	2.03	25.0	–	0.001	0.02	–	–	–
	Fluffy layer	–	2.19	25.8	–	0.004	0.19	–	461	1.274
	2–4	69.4	(up to	25.6	–	0.007	0.26	–	459	1.46
	4–6	66.0	6 cm)	25.6	–	0.015	0.25	–	460	1.447
	6–8	66.0	–	25.5	–	0.054	0.27	–	448	1.539
	8–10	63.5	2.53	25.5	–	0.10	0.25	–	442	1.443
	10–12	63.3	(up to	25.5	–	0.004	0.27	–	449	1.367

(continued)

Table 10 (continued)

Station number, coordinates N, E; depth	Horizon, cm	Humidity, %	*Alk*, mg equl^{-1}	SO_4^{2-}, mM	N, mM	P, mM	Si, mM	CH_4, нм дм$^{-3}$	Cl, mM	C_{org}, %
	12–14	62.5	22 cm)	25.4	–	0.038	0.28	–	446	1.271
	14–16	61.8	–	25.3	–	0.025	0.28	–	449	1.044
	16–18	62.5	–	25.3	–	0.239	0.21	–	452	1.141
	18–20	61.3	–	25.1	–	0.038	0.31	–	454	1.178
	20–22	55.7	–	25.1	–	0.014	0.37	–	461	1.209
	22–24	58.1	–	25.1	–	0.008	0.30	–	461	1.015
	24–26	60.8	–	25.0	–	0.043	0.31	–	453	0.987
	26–28	61.2	2.95	25.0	–	0.030	0.39	–	454	0.924
	28–30	59.5	(up to	24.7	–	0.015	0.34	–	450	0.953
	30–32	57.6	40 cm)	24.7	–	0.013	0.38	–	459	0.988
	32–34	56.8	–	24.6	–	0.236	0.47	–	456	1.045
	34–36	58.0	–	24.6	–	0.012	0.42	–	456	0.972
	36–38	58.0	–	24.6	–	0.012	0.39	–	456	1.040
	38–40	58.7	–	24.5	–	0.014	0.44	–	465	1.049
	–	–	–	–	–	–	–	–	–	0.957
	–	–	–	–	–	–	–	–	–	1.045
	–	–	–	–	–	–	–	–	–	0.988

Notation: – no data
Bold values represents detachment number of station

well as acidifying of pore waters (fall of pH) – with generation of CO_2. In pore water from a fluffy layer, SO_4^{2-} ion concentration changed from 23.8 to 25.5 mM, generally repeating a tendency of the latitudinal distribution of SO_4^{2-} in near-bottom water. In the upper sediment horizons, a concentration of SO_4^{2-} ion in pore water at the shallow station 1408 decreases, obviously due to the most intensive microbial processes. At other stations, concentration of SO_4^{2-} ion in pore water practically did not differ from that in water from a fluffy layer, averaging 24.68 mM at the 2–4 cm horizon.

In pore waters from the Dvina Bay sediment cores (about 40 cm long), collected by Neimisto tube in 2014, decrease of SO_4^{2-} ion concentration from top to the bottom of the core occurs rather regularly. This corresponds to the fact that from sediment horizon of 6–8 cm (at St. 1408) and 12–14 cm (at St. 1413), hydrotroilite was detected and its amount increased with a depth. A weak decrease in Eh and pH values exhibits a low activity of sulfate reduction processes, although Alk values (to 5.5–7.5 mg eqv l^{-1}), concentration of N-NH_4 (to 0.44 mM) and P (to 0.95 mM), and especially decrease of sulfate ion's concentrations are caused by sulfate reduction processes. Concentration of Si is low but ten times more, on average, than that in near-bottom water. In pore waters from sediments of two deepwater stations (St. 6065 and St. 6066), high concentrations of dissolved Mn (up to 792 mM) were measured.

Results of chemical analysis of the pore waters, and the presence of hydrotroilite (and pyrite) in sediments and methane in pore water, suggested that in the modern White Sea sediments, along with aerobic (oxidizing) biogeochemical processes, an anaerobic destruction of OM proceeds. Among these processes, the most considerable is a microbial sulfate reduction and methane generation. In shallow water of the Dvina Bay, these processes take place already in the upper 10 cm of sediments. They are followed by decrease of concentration of a SO_4 ion, characteristic of anaerobic diagenesis, from top to down the core, and by increase of Alk, CH_4, and biogenic elements down the core. Judging by a composition of pore waters, the diagenetic changes in sediments of the White Sea are of a considerably weaker scale comparing to that of modern sediments in other marine Basins of the humid of zones [31].

3.7 Microorganisms and Rates of Microbial Processes in Sediments of the White Sea

At the White Sea floor, negative temperatures (−1.4°C) were recorded, both in near-bottom water and in surface sediments [32]. Negative temperatures are a distinctive feature of the polar seas. The question was, how diagenetic processes proceed with the participation of microorganisms, in the first microbiological studies in the Arctic latitudes and, in particular, in the Arctic seas [33–35].

Studies of the last decades proved that microorganisms are capable to survive at low temperatures and that they are "an important terrestrial colonialists," possessing "the unknown strategy of maintaining viability" [36].

Microorganisms in ground sediments of the Arctic seas are involved in the modern biogeochemical cycles. They influence upon speed of processes of transformation of OM and gases (CO_2, H_2S, CH_4, H_2, NH_4, etc.) production. At a stable mode of negative temperatures, as it takes place at the White Sea bottom, one can assume that microorganisms has developed adaptation mechanisms of viability for a long time, as it was proved for permafrost of the Arctic land [36]. The modern soils of the Arctic region at depth of 1.0 cm account for, on average 2.0×10^7 cells of methane generation and 2.0×10^2 of sulfate reduction microorganisms.

Majority of microorganisms functioning in the Arctic region are psychrophiles which can grow at temperature within an interval from −10°C to +20°C. Psychrophiles are steady against the low-temperature stress, for example, due to ability to form a special structures (cysts and spores) or due to extraction of sugars and proteins [37].

The initial stage of organic compounds' transformation in the surface lithosphere, as a rule, is an aerobic processes which are performed by various classes of microorganisms. Aerobic destruction of organic matter is described by the schematic equation $C_6H_{12}O_6 + 6O_2 = 6CO_2 + 6H_2O$ + biomass of microorganisms. The most important geochemical consequence of aerobic destruction of organic matter is a consumption of molecular oxygen that leads to replace of oxidizing environment with the reducing one and is followed by development of an anaerobic destruction of organic matter. In anaerobic destruction of organic matter, the two stages are distinguished. At the first stage, a heterogeneous group of microorganisms, so-called primary anaerobe bacteria, subject the main classes of organic compounds (proteins, lipids, and polysaccharides) to enzymatic hydrolysis and fermentation followed by formation of low fatty acids, alcohols, aldehydes, ketones, CO_2, and H_2. At the second stage of an anaerobic destruction, these metabolites serve as substrata for "secondary anaerobe bacteria" – the sulfate reductors and methane-generating microorganisms (Fig. 10) [38].

It is necessary to emphasize that in anaerobic environment, in the course of the organic matter's destruction, there is a continuous formation and consumption of low-molecular organic compounds. The interior C_1–C_6 fatty acids are constantly present there. In our works of last years, on the example of sediments of the trans-Pacific profile and other marine Basins, it was shown that microorganisms which function as sulfate reductors and methane generators are widely spread [39]. Measurements of rates of sulfate reduction and methane generation by a tracer techniques have revealed that more than hundreds μg of H_2S in 1 kg of wet sediments can be formed per day in marine ecosystems [20]. Generation of methane is as a rule performed by bacterial reduction of CO_2 by H_2.

Processes of microbial generation of H_2S and CH_4 are followed by the energy consumption arising at anaerobic oxidation of low-molecular organic compounds or molecular H_2. Total number of microorganisms in the surface layer (0.1–5.0 cm) of sediments of the White Sea in all tests exceeded 1 million cells ml^{-1} that it is slightly

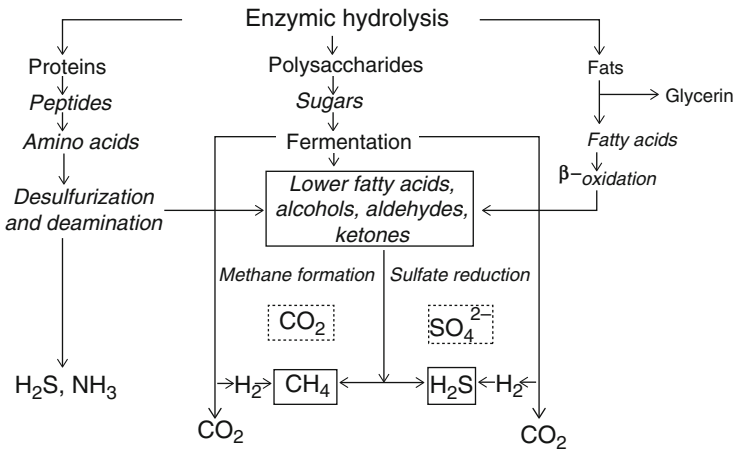

Fig. 10 Scheme of the organic matter's decomposition [38]

less than in a fluffy layer where TNM reaches (110–259) $\times$ 10^6 cells ml^{-1}. Similar values of TNM (170–630) $\times$ 10^6 of cells ml^{-1} were obtained for surface sediments (1–2 cm) of the Barents Sea at depths of 150–790 m [10]. Down the sediment core, TNM considerably decreases.

In typical samples of the White Sea sediments at stations of the axial transect, radioactive isotope determination of rates of sulfate reduction, methane generation, and methane oxidation processes, as well as integral rates of microbial processes (CO_2 assimilation), was performed for the first time.

The surface horizons are characterized by oxidizing conditions: Eh values were positive and varied from 175 mV in Onega Bay, 250 mV in the Dvina Bay, and up to 300–320 mV in deepwater sediments of the Basin. Oxidizing conditions were very quickly replaced with oxidation-reduction and further by reduction ones where the basic diagenetic process of OM destruction is sulfate reduction process. Rate of a sulfate reduction processes in the surface-oxidized sediments (0–1 cm) ranged from 9 to 170 μg S dm^{-3} day^{-1}. Reduced compounds of sulfur in surface-oxidized layers do not form mineral phases; they diffuse into a fluffy layer and near-bottom water where they become a substratum for bacteria (chemoautotrophs) at water-sediment border. The CO_2 assimilation rates (ranged from 22 to 170 μg C dm^{-3} day^{-1}) in the surface sediments probably confirm a noticeable participation of chemoautotrophs in formation of microbial biomass at water-sediment border. The rate of a microbial sulfate reduction was determined in sediments at eight typical stations along the axial transect. The maximal rates were determined in the upper 50 cm sediment thickness in the central part of the Basin at St. 4702 (180–800 μg S dm^{-3} day^{-1}). In the Dvina and Onega Bays in the upper 50 cm, rates of sulfate reduction fluctuated within the limits of 5–120 μg S dm^{-3} day^{-1} (St. 4686 and 4712), increasing to 342.5 mkg of S dm^{-3} day^{-1} in sediments of central part of the Dvina Bay (St. 6042). At St. 6058, in a deepwater part of Kandalaksha Bay, rate of sulfate reduction reached

135.1 μg S dm^{-3} day^{-1} already in the upper 6 cm of sediments, and down the core, it considerably decreased (up to 30 μg S dm^{-3} day^{-1} at the horizon of 26–46 cm). In sediments of the central part of the Basin (St. 6056), rate of sulfate reduction fluctuated from 9.0 to 47.7 μg S dm^{-3} day^{-1} that was lower comparing to close located St. 4702.

Thus, radioisotope experiments with sediments along the axial transect of the White Sea, exhibited that maximal rates of sulfate reduction process were characteristic for terrigenous sediments with homogeneous grain-size composition. Such sediments are located in the central part of the Dvina Bay and in the Basin. The minimal rates were typical for coarse-grained sediments within the delta of Northern Dvina and Onega Rivers where rates of sulfate reduction seldom exceeded 100 μg S dm^{-3} day^{-1} (Table 11).

Heterotrophic sulfate-reducing microorganisms in the upper sediment horizons utilize, first of all, the dissolved organic matter (DOM), whose concentration always exceeds content of organic matter in a solid phase of sediments. Consumption of C_{org} in the course of sulfate reduction fluctuates differently at different stations: from 3.8 μg S dm^{-3} day^{-1} (St. 4686, the Dvina Bay) up to 601.5 μg S dm^{-3} day^{-1} (St. 4702, the central part of the Basin) (Table 11).

Comparison of the data obtained in the White Sea sediments with sediments of the humid zone seas (Table 12) let us to conclude that in polar seas, rates of sulfate reduction process are much slower than that in other midland seas. For example, in the Baltic Sea, this rate averages 1,380 μg S dm^{-3} day^{-1} [39], whereas in the White Sea, even a maximal measured rate of sulfate reduction accounted for 800 μg S dm^{-3} day^{-1} rates, i.e., it was 1.7 times less than average value in the Baltic Sea.

A maximal rate of the dark microbial CO_2 assimilation process was found in the surface layer (0–1 cm) in sediments of the Dvina Bay (170 μg C dm^{-3} day^{-1}). From top to bottom of the sediment core, a rate of CO_2 assimilation decreased, indicating a decrease of total bacterial activity in sediments below 50 cm. Minimal rate of CO_2 assimilation characterizes surface sediments (22.5 μg C dm^{-3} day^{-1}) and sediments of the whole section of St. 6056. In deepwater sediments of the western depression, microbial activity was recorded throughout the whole 50 cm core (St. 6058). In surface layer of the Basin, sediment rate of a methane generation (MG) varied from 23.7 to 32.1 nl dm^{-3} $day^{-1}$and increased to 71 nl dm^{-3} day^{-1} in open part of the Dvina Bay sediments.

A process of methane generation was found in all the sediment samples studied, starting from surface-oxidized layer and downward. Process rate as a rule was minimal in the surface layer (24–71 nl CH_4 dm^{-3} day^{-1}), then increased at the 10–15 cm horizon, and further changed slightly down the core. A rather high MG rates (to 126–144 nl CH_4 dm^{-3} day^{-1}) were measured in sediments of the Dvina Bay. In the Basin sediments, MG rate did not exceed 78 nl CH_4 dm^{-3} day^{-1}. Higher MG rates were found in microlandscapes of the Kandalaksha Bay littoral, where methane was formed in amount to 69,600 nl CH_4 dm^{-3} day^{-1} [8, 25]. From these data, taking into account a methane consumption rate, methane flux from littoral sediments accounted for 192–300 CH_4 l km^{-2} day^{-1}.

The ability to function in a wide temperature interval explains a global distribution of methane-generating bacteria (Archean) inhabiting all known anaerobic

Table 11 The rates of biogeochemical processes in the sediments of the White Sea (August 2001, cruise 49 of R/V "Professor Shtokman")

Station / Depth, m	Sediment horizon, cm	Eh, mV	Methane generation, nl CH_4 dm^{-3} day^{-1}	Methane oxidation, nl CH_4 dm^{-3} day^{-1}	Sulfate reduction, μg C dm^{-3} day^{-1}	Consumption of C_{org} for sulfate reduction, μg C dm^{-3} day^{-1}
4686 / 8.2	0–1	250	900	0.75	30.0	22.5
	5–6	200	40	0.75	5.0	3.8
	8–10	50	130	0.60	78.0	58.6
4698 / 101.0	0–1	300	–	1.0	25.0	18.8
	90–100	270	–	1.0	65.0	48.9
	150–160	270	–	2.0	40.0	30.0
	170–175	50	–	–	–	–
	220–225	−30	–	0.75	62.0	46.6
	260–275	50	–	1.25	50.0	37.6
4702 / 107.0	0–1	320	250	4.3	250	188.0
	1–5	175	550	3.8	800	601.5
	10–15	50	500	–	180	135.3
	30–40	100	750	–	800	601.5
	40–50	150	250	4.0	200	150.4
	90–100	0	1,200	4.1	800	601.5
	190–200	50	300	5.0	150	112.8
	270–275	75	200	4.5	25	18.8
4712 / 34.8	0–1	175	400	0.5	15	11.3
	1–5	110	1,000	0.75	120	90.2
	80–100	80	300	0.20	20	15.0
	140–150	60	2,500	0.80	180	135.3
	240–260	−20	1,600	0.85	370	278.2
	270–280	–	–	1.20	30	22.5
4719 / 288	0–1	200	–	0.2	15	11.3
	1–5	200	–	1.7	15	11.3
	5–25	125	–	3.3	30	22.5
	50–60	100	–	0.7	15	11.3
	100–120	125	–	1.1	55	41.3
	130–140	125	–	2.0	15	11.3
	210–225	25	–	0.3	60	45.1
	250–275	−50	–	1.6	55	41.3

ecosystems of our planet, including the polar Basins [9]. Methanotrophic bacteria are the second major participant of methane cycle in the biosphere since under its thermodynamic conditions, a chemical methane oxidation cannot happen, and representatives of obligate methanotrophs held this process in a wide temperature, salinity, and pH interval [12]. Methanotrophs prevent input of greenhouse methane gas into atmosphere; and anywhere these microorganisms are in abundance, and they produce a noticeable amounts of organic matter which is utilized by heterotrophs [12, 40]. The determination method of rates of methane microbial oxidation is set out in the monograph by V.F. Galchenko [12]. Rate of methane oxidation process in the

Table 12 The rates of the sulfate reduction process in the present sediments of the White Sea and other intercontinental seas (mean values) [39]

Sea, its area (or season)	Sulfate reduction rate, μg C dm^{-3} day^{-1}
White Sea	
Basin, central part	48–800
Basin, deepwater part	15–135
Dvina Bay	30–340
Onega Bay	15
Baltic Sea	
Shallow water	1,380
Central part	1,100
Black Sea	
Shelf	1,600
Deepwater part	480
Azov Sea	
(Winter	660
Summer)	7,550
Caspian Sea	
(Shallow water part)	1,180

surface horizons of the White Sea sediments varied from 13.51 nl CH_4 dm^{-3} day^{-1} in deepwater depression of the Basin to 6.4 nl CH_4 dm^{-3} day^{-1} in the central part of the Basin (St. 6058, 6056). In the Dvina Bay sediments, the maximal rate of methane oxidation accounted to 6.30 nl CH_4 dm^{-3} day^{-1} (St. 6042) and changed around 0.75 nl CH_4 dm^{-3} day^{-1} (St. 4686, 4698). Down the sediment core, the rate of methane oxidation increased up to 18–35 nl CH_4 dm^{-3} day^{-1}, evidently due to activity of the Archean anaerobic methanotrophs in consortium with sulfate-reducing bacteria [41].

Results of determination of a methane generation's rates allowed us to calculate microbial production of a diagenetic methane in sediments. So in the Dvina Bay over 500 years, 8.98 l of CH_4 under bottom area of 1 m^2 could be formed. In the Basin at a depth of 133 m, this value was equal to 5.52 l m^{-2} and in a deepwater western part of the Basin 4.29l m^{-2}. Daily rates of methane oxidation in the White Sea sediments, on average, are less than methane generation's rates. In the oxidized surface sediments (0–5 cm), consumption of CH_4 by microorganisms happens with greater rates than in slightly reduced subsurface sediments.

Simple calculations show that a minimal CH_4 amount (8.9%) was oxidized in more reduced pelitic sediments at 300 m depth (St. 6058) over 500 years. Meanwhile in more oxidized coarse-grained sediments at 133 m depth, 22% of the total methane generated was oxidized. At the same time, in the course of a methane generation, not less than 2% of C_{org} buried in the sediments studied has been utilized.

Comparison of production of CH_4 values in surface sediments of the White Sea with that of the Kara and Chukchi Seas exhibits a similarity of White Sea microbial production of CH_4 (0.3–1.1 μM m^{-2} day^{-1}) with the delta sediments of the Yenisei River (which have a low CH_4 production about 1.4 μM m^{-2} day^{-1}) and with

sediments nearby the Alaska sediments (0.6 μM m^{-2} day^{-1}). In the latter areas, the minimal rates of anaerobic microbial processes for these two seas were observed in oxidized surface sediments that are close in physicochemical properties to the White Sea Basin sediments [24, 42, 43].

The whole data obtained, namely, low concentration of biogenic elements, low total number of microorganisms, and low speed of microbial processes in the water column and in sediments, indicate a low value of primary products in August 2006.

Over ~500 years of the Holocene, the modern White Sea conditions last out. Calculation of CH_4 production, without microbial CH_4 consumption, showed that in Basin sediments, i.e., approximately on 2/3 areas, during 500 years, microorganisms could generate 4 l of CH_4 under 1 m^2 and as twice as more in sediments of the Dvina Bay open area.

Comparison of CH_4 production with CH_4 concentration under 1 m^2 of sedimentary thickness of 50 cm showed that nearly 99% of methane diffuse from sediments into water column which holds 0.4×10^6 m^3 CH_4. Therefore, it should not to expect some significant accumulation of diagenetic methane in well-aerated subpolar internal shallow Basin like the White Sea is. At the same time, by our estimates, CH_4 emission into atmosphere from littoral sediments of similar Basins in summer months can reach 300 l CH_4 km^{-2} day^{-1} [8, 25].

There are several approaches to calculation of C_{org} consumption in processes of an anaerobic OM destruction. The first one is based on accounting preservation of C_{org} (or N_{org}) in lower horizons of sediment thickness in comparison with C_{org} content in surface horizon which is considered as initial content of C_{org} [44]. Similar approach, first, does not consider possible changes in sediment formation affecting initial concentration $C_{org.}$ Secondly, as an initial C_{org} is accepted a residual one, since intensive OM destruction happens at the water-sediment interface.

Another approach, which is widely accepted in Russian researches, is based on calculation of C_{org} consumption for formation of the Mn-, Fe-, and S-reduced compounds by the balance formulas of Uspensky and Strakhov [45]. This second approach allows to estimate C_{org} consumption per the solid-phase content compounds. In essence, only C_{org} consumption for formation of stable Fe sulfides (pyrite), since C_{org} consumption for reduction of Fe^{3+}, Mn^{4+}, and other oxidized components so insignificant that they are, as a rule, neglected. Strakhov, who offered this estimation method of primary (or initial) C_{org} preservation, wrote about approximation of such estimates, since organic matter has been decomposed during other types of its transformations, for example, due to eliminating of COOH, CH_4, NH_3, etc. [46, p. 214]. Biogeochemical researches give a reason to account that in a solid sediment phase, not the whole hydrogen sulfide formed in situ resulted from bacterial sulfate reduction is fixed. As an evidence of migration and partial oxidation of H_2S within reduced sediments where it occurs in a free state [47, 48], data on chemical analyses could be used. From these data, in pore waters, the subsurface maximum of SO_4 ion, enriched in light ^{32}S isotope in comparison with SO_4 ion isotopic composition in near-bottom water, was detected ($\delta^{34}S = -18.8 \div -15.6‰$). The latter circumstance can be considered as the unique evidence of a subsurface sulfate maximum resulted from oxidation of light isotope of metabolic hydrogen sulfide. Data on all sulfur forms in gaseous, dissolved, and solid phase of reduced

sediments in Limfyord, Denmark, showed that only 10% (0.7 mM) of a metabolic H_2S in the forms of sulfides were buried in sediments. The rest 90% of a newly formed H_2S diffused partially from shallow sediments into near-bottom water and/or were oxidized followed by internal sulfur circulation in sediments.

Considering the above mentioned, we proposed a different approach to estimating the OM amount mineralized during anaerobic destruction. This approach is based on an experimental study of the rate of biogeochemical processes under conditions that are very similar to natural ones by use of sulfur and carbon radioisotopes [47, 49, 50].

It was established that 90–95% of C_{org} involved in anaerobic biogeochemical reactions are consumed during bacterial sulfate reduction [38, 50]. Therefore, to estimate amount of C_{org} consumption during anaerobic diagenesis, it should to apply a rate of bacterial sulfate reduction in sediments. A simple calculation of equation of the following sulfate reduction reaction

$$\underset{24}{SO_4^{2-}} + 2C_{org} + \text{sulphate reducing microorganisms} \rightarrow \underset{32}{S^{2-}} + 2CO_2$$

allows us to quantify a rate of C_{org} mineralization proceeded from aerobic OM decomposition by sulfate-reducing bacteria.

A value of anaerobic OM destruction by methane-generating bacteria is calculated, for example, according to the equation [38]

$$\underset{48}{4HCOOH} + 4H_2 + 4CO_2 + \text{methane generating microorganisms} \rightarrow \underset{12}{CH_4} + 2H_2O + 3CO_2$$

Comparison of intensity of bacterial sulfate reduction in the marine sediments estimated by different researchers, using both calculation methods (a modeling) and experimental radioisotopes' results, showed a similarity of data obtained. This let us to apply experimental data on bacterial processes' rate in the upper 50 cm layer which has been congregated up to date, for assessment of C_{org} consumption under conditions of early diagenesis in the reduced sediments. The offered approach seems to be more correct compared to earlier ones since it allows to consider C_{org} consumption for formation not only the solid phase but also dissolved products of metabolism of the microbial processes that took place during early diagenesis in the White Sea sediments [49].

4 Conclusions

Features of the early diagenesis in sediments of the Arctic waters is considered by the example of the White Sea. In the humid zones, diagenesis is a process of sediment formation under unsteady physical and chemical conditions, when sediments are saturated with water and relatively enriched in organic matter, including biomass of

living benthos and microbial population. At the earliest stage of diagenesis, microorganisms and benthic animals assimilate the free oxygen from followed by reduction of the Mn^{4+} and Fe^{3+} oxy-hydroxides. After that, an oxygen of sulfate ion in pore water is involved in chemical reactions. As a result, an oxidized ecosystem turns into the reducing one. Solid biogenic compounds, such as SiO_2, $CaCO_3$, and $MgCO_3$ which remained in an undersaturated state for a long time in the pore waters, transfer into the dissolve form gradually till the complete pore water's saturation with them. In the same time, there is an exchange between the cations which are in the absorbed state on clay mineral micelles and cations of the pore water.

Organic matter during the destruction transfers into reduced gases (CO_2, NH_3, H_2S, CH_4, etc.), as well as into water-soluble compounds and more stable solid compounds, which were preserved in a solid phase of sediments, while oxygen disappears. As a result, the pore waters of sediments change their composition. The amount of sulfates in pore waters gradually decreases down the sediment core, value of total alkalinity grows, and sediments enrich in Fe^{2+}, Mn^{2+}, and SiO_2.

The dataset obtained provides an evidence that the basic substrate (composed of the White Sea OM) is not very suitable for the anaerobic microflora's functioning. As a result of this, the early diagenetic processes, firstly, need more time and, secondly, are far from completion. This is confirmed by composition of authigenic sulfides (FeS_{n-1}) represented by X-ray amorphous "hydrotroilite," as well as by the absence of authigenic carbonates.

One of the important diagenetic processes, revealed over the last decades in the Arctic Sea sediments, is an anaerobic oxidation of methane which enters to young sediments from any sources. Within the sediments, CH_4 is partially oxidized under anaerobic conditions followed by a fresh organic matter (OM) formation in the form of biomass of microorganisms and products of their metabolism. This fresh OM formation strengthens the diagenetic processes which have been weakened by this time, as it was shown for the Black Sea sediments [9].

A dominance in the Arctic Basins of terrigenous OM is confirmed by data on the C/N and on the *n*-alkanes' composition, as well as results of the pore waters analysis which displayed a very sluggish slight decrease of sulfate ion and insignificant of Alk in the pore waters down the sediment core. Experiments with radioisotopes aimed to evaluate rates of the basic microbial diagenetic processes confirm the decreased sulfate reduction rates in the White Sea sediments in comparison with sediments of midland seas of the humid and humid-arid zones.

In polar reservoirs, similar processes were observed only in caldera of Haakon Mosbi mud volcano so far [23]. In general, delay of diagenesis rates in the polar seas could be explained by the low value of primary production, while terrigenous organic matter's inflow into the sea from the continent was very high. Low temperatures of the microorganisms' habitat have a secondary importance.

Acknowledgments We would like to thank the Russian Scientific Foundation (Project No 14-27-00114-П) for financial support of this research over the period of preparation of this chapter and also within the framework of the state task of the Academy of Sciences of the Russian Academy of Sciences for 2017-2018, theme No. 0149-2018-0016.

References

1. Nevessky EN, Medvedev VS, Kalinenko VV (1977) The White Sea: sedimentogenesis and holocene development. Nauka, Moscow., 184 pp (in Russian)
2. Strakhov NM, Shterenberg LE, Kalinenko VV, Tikhomirova ES (1968) Geochemistry of manganese ore process. Proc Geol Ins Acad Sci USSR:216 (in Russian)
3. Berger VY, Primakov IM (2007) Estimation of primary production in the White Sea. Biologiya Morya 33(1):54–58 (in Russian)
4. Lisitsyn AP, Nemirovskaya IA (eds) (2013) The White Sea system. Vol III dispersed sedimentary matter in hydrosphere, microbial processes and water pollution. Scientific World, Moscow, p 665 (in Russian)
5. Lein AY, Rusanov II, Savvichev AS, Pimenov NV, Miller YM, Pavlova GA, Ivanov MV (1996) Biogeochemical processes of sulfur and carbon cycles in the Kara Sea. Geochem Int 34 (11):925–941
6. Savvichev AS, Rusanov II, Zakharova EE, Veslopolova EF, Mitskevich IN, Kravchishina MD, Ivanov MV (2008) Microbial processes of the carbon and sulfur cycles in the White Sea. Microbiology 77(6):734–750
7. Kravchishina MD (2009) Suspended matter of the White Sea and its grain-size composition. Scientific World, Moscow, 288 pp. (in Russian)
8. Savvichev AS, Rusanov II, Yusupov SK, Pimenov NV, Lein AY (2005) Microbial processes of the organic matter transformation in the White Sea. Oceanology 45(5):689–702
9. Lein AY, Ivanov MV (2009) Biogeochemical cycle of methane in the ocean. Nauka, Moscow, p 464 (in Russian)
10. Lein AY, Belyaev NA, Kravchishina MD, Savvichev AS, Ivanov MV, Lisitsyn AP (2011) Isotopic markers of organic matter transformation at the water-sediment geochemical boundary. Dokl Ear Sci 436(1):83–87
11. Lein AY, Kravchishina MD, Politova NV, Savvichev AS, Veslopolova EF, Mitskevich IN, Ivanov MV (2012) Transformation of particulate organic matter at the water-bottom boundary in the Russian Arctic seas: evidence from isotope and radioisotope data. Lithol Miner Res 47 (2):99–128
12. Galchenko VF (2001) Methanotrophic bacteria. GEOS, Moscow, p 500 (in Russian)
13. Lein AY, Novichkova YA, Rybalko AY, Ivanov MV (2013) Carbon isotope composition of organic matter in Holocene sediments of the White Sea as one of the indicators of sedimentation conditions. Dokl Eart Sci 452(2):1056–1061
14. Geptner AP (1994) Local carbonatization sediments of the White Sea (the concept of microbiological formation). Lithol Miner Res 5:3–22 (in Russian)
15. Strekopytov SV, Uspenskaya TY, Vinogradova EL, Dubinin AV (2005) Geochemistry of early diagenesis of sediments of Kandalaksha Bay of the White Sea. Geochem Int 43(2):117–130
16. Rozanov AG, Volkov II, Kokryatskaya NM, Yudin MV (2006) Manganese and iron in the White Sea: sedimentation and diagenesis. Lithol Miner Res 41(5):483–501
17. Kuzmina TG, AYu L, Lutchsheva LV, Murdmaa IO, Novigatsky AN, Shevchenko VP (2009) Chemical composition of the White Sea sediments. Lithol Miner Res 2:115–132
18. Yudovich YE, Ketris MP (2013) Factors controlling the geochemistry of manganese in marine sediments. Bull Geol Inst Komi Sci Center Ural Branch Russ Acad Sci 11(227):11–15 (in Russian)
19. Pankina RG (1978) Geochemistry of Sulphur isotopes, oil and organic matter. Nedra, Moscow, p 246 (in Russian)
20. Lein AY (1985) The isotopic mass balance of sulphur in oceanic sediments (the Pacific Ocean as an example). Mar Chem 16(3):249–257
21. Hartmann M, Nielsen H (1969) ^{34}S-werte in rezenten meeresse-dimenten ind ihre deutung am Beispiel einiger sedimentprofile aus der westlichen ostsee. Geol Rundsch 58:621–655
22. Volkov II, Kokryatskaya NM (2004) Compounds of reduced inorganic sulfur in the waters of the White Sea and the Northern Dvina Mouth. Water Resour 31(4):423–430

23. Lein AY, Vogt P, Crane K, Egorov AV, Pimenov NV, Savvichev AS, Ivanov MV (1998) Geochemical features of gas-bearing (CH_4) deposits of a submarine mud volcano in the Norwegian Sea. Geochem Int 36(3):190–208
24. Lein AY, Kudryavtseva AI, Matrosov AG (1976) Isotopic composition of sulfur compounds in sediments of the Pacific. Biochemistry of diagenesis of ocean sediments. Nauka, Moscow, pp 179–185 (in Russian)
25. Savvichev AS, Rusanov II, Yusupov SK, Pimenov NV, Lein AY, Ivanov MV (2004) The biogeochemical cycle of methane in the coastal zone and littoral of the Kandalaksha Bay of the White Sea. Microbiol 73(4):457–468
26. Sapozhnikov RB, Chenborisova RZ, Berzin RG (2003) Effect of the CDP seismics in the study of geology of the Mezen syncline. Razvedka i Okhrana Nedr 5:32–35 (in Russian)
27. Aliev R, Bobrov V, Kalmykov S, Melgunov M, Vlasova I, Shevchenko V, Novigatsky A, Lisitzin A (2007) Natural and artificial radionuclides as a tool for sedimentation studies in the Arctic region. J Radioanal Nucl Chem 274(2):315–321
28. Gorshkova TI (1975) Organic matter of modern shelf sediments of the northern seas of the USSR. Nauka, Moscow, p 66 (in Russian)
29. Danyushevskaya AI, Petrova VI, Belyaeva AN (1990) Evolution of organic matter in the sedimentary strata of the Eurasian continental margins of the World Ocean. Izv AN SSSR, pp 95–103 (in Russian)
30. Lein AY, Belyaev NA, Kravchishina MD, Savvichev AS, Ivanov MV, Lisitsyn AP (2011) Isotopic markers of organic matter transformation at the water-sediment geochemical barrier. Dokl Ear Sci 436(2):228–232
31. Lein AY (1983) Consumption of Corg during the processes of mineralization of organic matter in modern oceanic sediments. Geochem 11:1634–1639 (in Russian)
32. Dobrovolsky AD, Zalogin BS (1992) Regional oceanology. MSU, Moscow, p 382 (in Russian)
33. Isachenko BL (1914) Study of bacteria in the Arctic Ocean. Tr Murman Nauchno-Promysl Ekspeditsii 1906–1914 gg
34. Kriss AE (1945) Microorganisms of the Eastern Arctic Ocean. Microbiology 14(4):268–276 (in Russian)
35. Kriss AE (1959) Marine microbiology: deep water. Publishing House of the Academy of Sciences of the USSR, p 186 (in Russian)
36. Gilichinsky DA (2002) Cryobiosphere of the late Cenozoic: permafrost as a medium for the conservation of viable microorganisms. Tyumen, 326 pp. (in Russian)
37. Melnikov VP, Rogov VV, Kurchatova AN, Brushkov AV, Griva GI (2011) Distribution of microorganizms in frozen ground. Earth Cryosph 15(4):86–90
38. Belyaev SS, Lein AY, Ivanov MV (1981) The role of methane generating and sulfate reducing bacteria over destruction of organic matter. Geochem Int 3:437–445
39. Lein AY, Ivanov MV (1983) The global biogeochemical cycle of sulfur and its impact on the human activity. Nauka, Moscow, p 162 (in Russian)
40. Lein AY, Pimenov NV, Rusanov II, Miller Y, Ivanov MV (1997) Geochemical consequences of microbiological processes on the Northwestern Black Sea shelf. Geochem Int 35 (10):865–883
41. Boetius A, Ravenschlag K, Schubert CJ, Rickert D, Widdel F, Gieseke A, Pfannkuche O (2000) A marine microbial consortium apparently mediating anaerobic oxidation of methane. Nature 407(6804):623
42. Savvichev AS, Rusanov II, Pimenov NV, Zakharova EE, Veslopolova EF, Lein AY, Ivanov MV (2007) Microbial processes of the carbon and sulfur cycles in the Chukchi Sea. Microbiology 76(5):603–613
43. Savvichev AS, Zakharova EE, Veslopolova EF, Rusanov II, Lein AY, Ivanov MV (2010) Microbial processes of the carbon and sulfur cycles in the Kara Sea. Oceanology 50(6):893–908
44. Emery KO, Rittenberg SC (1952) Early diagenesis of California Basin sediments in relation to origin of oil. AAPG Bull 36(5):735–806

45. Bordovsky OK (1964) Accumulation and transformation of organic matter in marine sediments: a study on the problem of the origin of oil. Nedra, Moscow, p 188 (in Russian)
46. Strakhov NM (1976) Problems of geochemistry of modern oceanic lithogenesis. Proc Geol Ins Acad Sci USSR, 228 pp. (in Russian)
47. Ivanov MV, Lein AY (1980) Distribution of microorganisms and their role in the processes of diagenetic minerals' formation. Geochemistry of diagenesis of precipitation of the Pacific Ocean (Pacific profile). Nauka, Moscow, p 117 (in Russian)
48. Lein AY, Grinenko VA, Matrosov AG, Tokarev VG, Bondar VA (1981) Fractionation of sulfur and carbon isotopes in recent sediments with different rate of process of bacterial sulphate reduction. Nauka, Pushchino, pp 134–166 (in Russian)
49. Lein AY (1984) Anaerobic consumption of organic matter in modern marine sediments. Nature 312(5990):148–150
50. Belyaev SS, Lein AY, Ivanov MV (1980) Role of methane producing and sulfate reducing bacteria in the destruction of organic matter. Biogeochemistry of the past and present. Springer, Berlin, pp 235–242

Mercury Distribution in Bottom Sediments of the White Sea and the Rivers of Its Basin

Yury A. Fedorov, Asya E. Ovsepyan, Alina A. Zimovets, Vyacheslav A. Savitskiy, Alexander P. Lisitsyn, Vladimir P. Shevchenko, Alexander N. Novigatsky, and Irina V. Dotsenko

Contents

Abstract Interest in the study of subarctic areas of the Earth increases year by year, due to the accelerating pace of development of high latitudes and increasing anthropogenic pressure. In parallel with these processes, there is a growing need to study the behavior of substances of the first class of danger in the natural objects of the region. This article summarizes and analyzes data on Hg content in bottom sediments of the White Sea and rivers of its basin. The influence of the river flow of the Northern Dvina, Kyanda, and Kem Rivers on the formation of Hg concentrations in the bottom sediments of the White Sea, Dvinsky, and Onega bays has been studied.

The spatial distribution of Hg in the bottom sediments was investigated; the levels of Hg accumulation in areas affected by anthropogenic activity were shown. Bottom sediments of the White Sea and estuaries of its basin have been zoned by levels of Hg content. For the Northern Dvina River, the amount of methyl-Hg formed in the

Y. A. Fedorov (✉), A. E. Ovsepyan, A. A. Zimovets, V. A. Savitskiy, and I. V. Dotsenko
Southern Federal University, Rostov-on-Don, Russia
e-mail: fed29@mail.ru

A. P. Lisitsyn, V. P. Shevchenko, and A. N. Novigatsky
Shirshov Institute of Oceanology Russian Academy of Sciences (IO RAS), Moscow, Russia

A. P. Lisitsyn and L. L. Demina (eds.), *Sedimentation Processes in the White Sea: The White Sea Environment Part II*, Hdb Env Chem (2018) 82: 207–240,
DOI 10.1007/698_2018_319, © Springer International Publishing AG, part of Springer Nature 2018,
Published online: 8 June 2018

bottom sediments was calculated based on the data of field studies, physicochemical and mineralogical properties of the bottom sediments, and their pollution level.

The river-sea sections were studied, and action of marginal filters of the rivers of the White Sea basin has been shown. The background level of Hg content in bottom sediments was established. Comparative analysis of Hg content in bottom sediments of different water basins which are exposed to different anthropogenic influence has been carried out.

Keywords Bottom sediments, Mercury, Spatial distribution, The White Sea basin

1 Introduction

Mercury its compounds are highly toxic substances. The potential toxicity of Hg for humans and other living organisms varies widely depending on the chemical form and the exposure pathways, amount, and vulnerability of the target. The relevance of the topic is confirmed by its recognition at the international level. Thus, on January 19, 2013, after 4 years of negotiations, the UN participants agreed a new international document on the problem of Hg pollution. The purpose of this document is to reduce the Hg use in industry, as well as the elimination of accumulated Hg-containing waste [1]. The Arctic Monitoring and Assessment Programme (AMAP) notes: "Hg, lead and cadmium are the most dangerous heavy metals whose contamination of the Arctic environment poses a serious threat." The greatest influence on the organisms is rendered by Hg, carried by the rivers flowing into the Arctic Ocean. High watering of the Arctic rivers provides concentrations that are significantly lower than the global average. Nevertheless, the total Hg runoff by the Eurasian rivers is about 10 tons per year [2].

Mercury is an ever-present heavy metal. Its content in the Earth's crust, according to various estimates, ranges from 0.03 to 0.08 μg g^{-1} dry weight. Hg belongs to the most labile components of the ore-forming process and is a "through" element that is fixed in the products of all stages of ore formation [3, 4]. The most probable forms of Hg transfer from the mantle substance with a high content of this element to the upper parts of the Earth's crust are gas, vapor-gas, and dissolved ones. The migration of these forms is carried out mainly through deep fault zones, where most of the Hg deposits are concentrated [4, 5]. One of the main natural sources of Hg released into the environment is the so-called Hg breath of the Earth (mantle degassing during the tectonic process). The global Hg emission into environment as a result of volcanic activity is 20–90 tons per year according to modern reports [6]. The global exogenous sources of Hg are rock minerals, the ocean, underground and surface waters, forest fires, and the biosphere as a whole. About 0.1% of the Hg received from the mantle is in the oceans in dissolved form [7]. According to others [8], the total amount of Hg in the World Ocean is 206 million tons. As the oceans contain 97% of the surface water of the Earth, they are the largest accumulators of dissolved Hg. There are about 2,000 Hg deposits in the world, in which no more than 0.02% of the total Hg scattered in the earth's crust is concentrated [5].

The presence of Hg reserves in the Russian Arctic is of particular interest in the aspect of this study. The least remote from the study area deposits were discovered on the Taimyr Peninsula (Izvilistoye, Uboyninskoye, and Tareiskoye), but its main reserves are concentrated in the Chaun (more than 90% of the total reserves of the region) and Anadyr fields of the Yana-Chukotka province. The Tamvatneyskoye field is explored in detail. These deposits contain tungsten, arsenic, and antimony as associated components. The largest field – Zapadno-Polyanskoye located 160 km from Pevek – is a stockwork with two lenticular deposits in sandstones [9]. Thus, the literature review allows us to draw a conclusion that according to the currently available data the lithogenous (natural) base of the study area does not belong to the Hg-containing planetary zones or anomalies and cannot be the reason of the increased concentrations of Hg in components of environment of the White Sea basin. Only volcanoes outside the subarctic territory can be attributed to external natural sources of Hg.

Currently, Russian and foreign scientists are actively engaged in studying the behavior of Hg in various environments. Concerning scientific research devoted to this problem in the announced region, it should be noted that they are conducted, but in most cases, they are single and unsystematic. Regular comprehensive studies designed to clarify the features of Hg accumulation in the mouth area of the Northern Dvina River were conducted by employees of the Southern Federal University since 2004. During this time, Hg concentrations in soils, water, bottom sediments, marine biota, rainfalls, and snow cover in relatively "clean" and impact areas of the White Sea basin were determined [10–29].

The peculiarity of bottom sediments is their ability to deposit Hg and its compounds and under changing physical, chemical, or hydrodynamic conditions return them partially to the water column. This causes "secondary pollution" of water, which can go on for many years. Generally, the most toxic forms of Hg released from the bottom sediments. Such phenomena formulate environmental problems, because there are explosions of extremely high concentrations of Hg and its compounds against the backdrop of a seemingly generally favorable state of the aquatic environment and the absence of visible pollution sources [16].

Information on global, regional, and local events that can affect the space and temporal distribution of Hg in bottom sediments is used to explain the chronology of its input into the White Sea basin. Humans have used Hg since the ancient times. However, it is generally accepted that Hg usage has increased since the beginning of the industrial period, which according to various estimates began 250–300 (an average of 270) years ago [30]. The industrial revolution as a global phenomenon started from the middle of the eighteenth century. During this period, Hg began to be widely used in gold mining, medicine, the manufacture of lighting, agriculture (for seed treatment of grain crops), and military (Hg (II) fulminate-Hg $(ONC)_2$ was used to make fuses and primers for cartridges and shells). Emission of Hg increased especially during the periods of two world wars, when its extraction, production, and usage increased greatly. Hg production in the world increased until the late 1960s, after which it fell in developed countries due to toughening of environmental legislation.

We have considered the complete marginal filter in full in its classical sense [31] only for the Northern Dvina River, while for the Kem and Kyanda Rivers its individual sections or zones have been studied. Therefore, when describing the river-sea systems, we used the term "river mouth area" (according to [32]) or the "marginal filter section," while the White Sea was described separately.

2 Materials and Methods

During the research, a modified procedure of sampling, sample preparation, and determination of Hg content was employed. This technique previously had been tested on different water objects of Russia [11, 13, 14, 19, 26, 33]. The main array of Hg determinations was made by the method of atomic absorption in a cold vapor in the certified laboratory of the Southern Federal University by analytical chemist Anikanov A.M. The repeatability of the results obtained was monitored at the Federal State Unitary Enterprise "Yuzhgeologiya." The error of determination amounted to 10–15%. In bottom sediments, pH and Eh were also measured, and in parallel, methane and organic carbon contents were determined.

Before the bottom sediments sampling, the chemical vessels were treated with nitric acid, washed, and twice rinsed with bidistilled water. The 10–15 g mass of material from each sedimentary layer was placed in the polyethylene bags. Bottom sediments stored at a low temperature in the refrigerator.

Bottom sediments in the Northern Dvina River mouth area were sampled aboard the R/V "Iceberg-2" using the Petersen bottom grab, as well as in the channels – at the shore – with a special tube (50 mm in diameter, 500 mm long). At some stations, the sampling was impossible or difficult because of submerged logs, which accumulated here as a result of long-term traditional practice of molten wood from the harvesting area to sawmills. Our research includes data obtained by the staff of the Department of Physical Geography, Ecology, and Nature Protection of the Institute of Earth Sciences of the Southern Federal University in the course of long-term observations conducted during ten expeditions in this area since 2004 [10–29, 33]. More than 150 samples of bottom sediments at 18 stations in the mouth area were collected and analyzed. Studies in the estuary area of the Kyanda River were carried out by the staff of the North-West Division of the RAS Shirshov Institute of Oceanology and the Institute of Earth Sciences of the Southern Federal University in August 2014 [34]. The length of the bottom sediment core reached up to 20 cm. Bottom sediments in the White Sea were sampled by the staff of Laboratory of Physico-geological Studies, Shirshov Institute of Oceanology RAS aboard the R/V "Professor Shtokman" led by A.P. Lisitsyn (64th cruise, August 2004) using a Neimisto ground tube [35–37]. Further processing of samples was carried out at the Institute of Earth Sciences of Southern Federal University. The total number of Hg determinations in the bottom sediments in the White Sea amounts 177.

In this chapter, we compare our results with that for the bottom sediments of the Kem River [38]; sampling was performed in the estuary of the Kem River and the adjacent part of the Onega Bay of the White Sea by use of Van Veen grab (0.1 m^2).

3 Mercury in the Bottom Sediments of Water Bodies of the Globe

The authors carried out generalization of the world data on total Hg content in the bottom sediments on a global scale (Table 1) in order to compare with those observed in the White Sea and its basin's water bodies.

From Table 1, it follows that Hg content in the bottom sediments of the water bodies of our planet is distributed very heterogeneously, that is due to the fact that sediments are under influence of both the natural and man-made factors and processes. Concentrations of Hg and its compounds increase significantly in bottom sediments exposed to the direct effects of enterprises for which Hg is a characteristic pollutant. Study of bottom sediments in the areas nearby gold mining enterprises in Russia and Brazil showed that the degree of Hg contamination of bottom sediments depends on the duration and intensity of the metallic Hg usage, as well as on the technology of its treatment of mining placer by the draft method [63, 65, 66]. The difference between the Hg content in the bottom sediments of water bodies located near the mines of the gold extraction or the bottom of the tailings pond and those in the bottom sediments of the background areas is 90–500 times [40, 62, 63]. Mercury contents are comparatively lower in the bottom sediments of water bodies, at whose drainage basins the deposits of Hg and hydrocarbons are located. There Hg contents are approximately at the same level as in areas affected by runoff from urban agglomerations, shipping, and some other anthropogenic pressure. At the same time, bottom sediments of these water reservoirs contain as much as 5–20 times more Hg compared to the background areas [39, 43, 44, 47, 60, 61, 64, 67, 74–76].

Commonly, the Hg contents in the bottom sediments of relatively uncontaminated water bodies of the Arctic Basin do not exceed 0.03–0.06 μg g^{-1} d.w., while in other regions they are higher and can reach the integer values of μg g^{-1} d.w. For example, according to Novikov and Zhilin [72], the content of total Hg in the upper layer of the bottom sediments of the Barents Sea varies from 0.15 to 0.8 μg g^{-1} d.w. The most of the Hg measurements was made in the Murmansk bank area seaward the Eastern Kola Peninsula coast. These concentrations were close to those observed by us [24] in the bottom sediments of the Northern Dvina River, confined to the agglomeration of Arkhangelsk. The authors of [72] did not comment this phenomenon. Notwithstanding, from the above analysis of the increased contents of other heavy metals in the bottom sediments of this area of the Barents Sea,

Table 1 The mercury content in the upper layer of the bottom sediments of the Earth's water bodies

Water object	Hg, μg g^{-1} d.w.	Source of information
Don River, Russia	0.06–0.18/0.13	[39]
Taganrog Bay of the Azov Sea, Russia	0.01–5.0/0.3	[39]
Atamanskoe Lake, Rostov region, Russia	0.2–13.6	[40]
Sornoe Lake, Rostov region, Russia	5.5	[40]
Sornoe Lake, Rostov region, Russia (soft-plastic and hard plastic silt)	0.06–0.08	[40]
Rostov region, man-made muds (sludge accumulators), Russia	9.0–15.0	[40]
Danube River, Ukraine	0.03–1.67/0.50	[41]
Mouth area of Danube River, Ukraine	0.085–0.86	[41]
Danube River, former-Yugoslavia	0.20–0.50	[42]
Katun River, Russia	0.04–0.66	[43, 44]
Rivers of Chukotka region, Russia	0.044–0.055	[45]
Kola River, Russia	0.009–0.2/0.11	[46]
Rivers of the Kola Peninsula, Russia	0.265	[45]
River sediments of the "Pechenganikel" area, Murmansk district, Russia	0.005–0.51/0.17	[46]
River sediments of the "Severonikel" area, Murmansk district, Russia	0.03–0.39/0.16	[46]
Kola Bay of the Barents Sea, surface layer, Russia	0.5	[47]
The same	0.04–0.011/0.03	[48]
The same, at individual sampling stations (Tuva Bay, Mishchakova Village, Salny Island)	0.50–2.25	[48]
The Barents Sea, the Shtokman gas condensate field, Russia	0.05–0.09	[47]
Estuary of the Kem River, Russia	0.006–0.07/0.016	[38]
Onega Bay of the White Sea, Russia	0.02	[49]
Dvina Bay of the White Sea, Russia	0.05–0.1	[49]
Anadyr Bay of the Bering Sea, Russia	0.02–0.063/0.039	[2]
The Bering Sea Basin, Russia	0.02–0.06/0.037	[2]
The Bering Sea, Russia	0.025	[2]
The Laptev sea, Russia	0.037	[50]
The Kara Sea, Russia	0.028	[50]
The East Siberian Sea, Russia	0.037	[50]
The Beaufort Sea, Northern America	0.017–0.074	[51, 52]
Faroe Islands	0.004–0.012	[53]
Port Valdez, Alaska, USA	0.01–0.06/0.04	[2]
The sea of Japan, Bay	0.036–0.529	[54]
Sea of Okhotsk, Russia	0.006–0.121	[54]
The rivers of the European territory of Russia	0.01–0.45/0.08	[55]
Rivers of Europe	0.01–11/0.09	[55]
Rivers of Asia	0.01–0.02/0.011	[55]
The rivers and lakes of Australia	0.13	[55]

(continued)

Table 1 (continued)

Water object	Hg, μg g^{-1} d.w.	Source of information
Rivers of North America	0.004–2.1/0.11	[55]
Lower Amur River Basin, Russia	0.1–0.79/0.23	[56]
Nura River (background value), Kazakhstan	0.031–0.083	[57]
Venetian lagoon, Italy	0.5–2.5	[58]
Mouth area of the Loire River (Bay of Biscay), France	0.006–0.073/0.026	[59]
Sochi-Tuapse sector of the Black Sea, Russia	0.037–0.4	[60, 61]
Novorossiysk-Arhipo-Osipovsky sector of the Black sea, Russia	0.096–0.196	[60, 61]
Technogenic silts of the Pregola River, Baltic Sea, Russia	0.213	[62]
Technogenic silts of the Karagaily River, Republic of Bashkortostan, Russia	2.44	[62]
Technogenic silts of the Ekateringofka River, Saint Petersburg, Russia	2.69	[62]
Technogenic silts of the Neva Bay, Russia	0.68	[62]
The bottom sediments surface layers of background freshwater bodies and watercourses, global data	0.01–0.030	[7]
Zabaykalsky Krai, Russia	0.01–54.2	[63]
The same, background watercourses	0.01–0.11	[63]
The same, bottom sediments on the territory of the "Lubov" Mine	0.43–54.2	[63]
The Hudson River Estuary, flowing through a region with a high concentration of industrial production, Canada	1.0	[64]
The gold mining regions of South America	1.60–2.05	[65]
Gold mining in the Madeira River Basin, Brazil	157.0	[66]
The tidal swamps of the San Francisco Bay (at 30 km downstream of the mercury mining area of New Almanden), USA	0.03–0.08	[67]
Lakes and canals of Bolshezemelskaya tundra, Russia	0.012–0.095	[68]
Lakes of Arkhangelsk and its surrounding area	0.002–0.052/0.012	[27]
Razdolnaya River of the Amur Bay of the Sea of Japan, Russia		
River	0.023–0.095/0.056	[69]
Bay	0.102–0.196/0.143	
The Chukchi Sea and the adjacent part of the Arctic Ocean, Russia	0.007–0.09/0.03	[70]
Basin of Deriugin of the Sea of Okhotsk	0.006–0.421/0.067	[70]
Amur Bay of the Sea of Japan	0.005–0.198/0.06	[70]
Svalbard Archipelago, Norway	0.01–0.08	[71]
The Barents Sea, seaward of the Eastern coast of the Kola Peninsula	0.15–0.80	[72]
The Gulf of Finland of the Baltic Sea, surface layer (0–1 cm)		
1992–1995	0.05–0.39/0.18	[73]
2001–2004	0.04–0.32/0.1	[74]
2012	0.04–0.1/0.07	[70]

(continued)

Table 1 (continued)

Water object	Hg, μg g^{-1} d.w.	Source of information
Poznań River, Poland	0.029–0.283/0.097	[75]
Marabasco River, and it's delta, Mexico	0.002–0.022/0.009	[76]
Navidad Lagoon, the Gulf of Mexico	0.002–0.032/0.015	[76]
Mouth area of the Ob River of the Kara sea, Russia	0.010–0.065/0.033	[77]

The numerator contains the mercury content range; the denominator is the average data

it can be assumed that it was due to atmospheric transport of Hg from areas of the Kola Mining and Metallurgical Company enterprises' (ASC "Kola MMC") operation. This assumption was indirectly confirmed by elevated Hg content in bottom sediments of the rivers of the Kola Peninsula and the Kola Bay of the Barents Sea (Table 1).

Bottom sediments of the rivers and canals with advanced navigation over a long time contain significant amounts of Hg which exceed the background by 80 times [58]. It should be noticed that the mouth area of the Northern Dvina River was used as a transport artery, where the main watercourse and its ducts were navigable channels.

4 Estuary of the Kem River

The rivers of the Onega Bay basin that are not subjected to direct anthropogenic impact represent a valuable source of information on the background Hg content and its behavior in the water of the marginal filter. The research work in the estuary of the Kem River and the adjacent part of the Onega Bay of the White Sea was carried out along three transects (Fig. 1). In the surface layer (0.0–3.0 cm) of bottom sediments, samples were collected in which the contents of macro- and trace elements, including Hg [38] were determined.

The total Hg content was determined in ten samples of bottom sediments collected in the transitional and marine parts of the estuary. It varied from 0.006 to 0.07 μg g^{-1} d.w. (average 0.016 μg g^{-1} d.w.). Here the catchment area of the White Sea is composed mainly of Archean and Proterozoic rocks [78]. According to [79], a poorly rounded sedimentary material fixed in the transition zone contains a mixture of pelite with untreated pebbles, gravel, and sand of various dimensions as evidence of an elementary stalling of material along a steep slope without its processing. In the marine part of the estuary (in the depressions), the bottom is composed of sediments of alluvial origin, rendered by strong tidal tides. At the same time, Demina et al. [38] noted the complexity of dividing the estuarine water area into zones. The distribution of Hg content along transects (Fig. 2) was not uniform and corresponded to peculiarities of accumulation and composition of bottom sediments in the transit area. In only one sample out of ten (station 125), the Hg content showed a significant

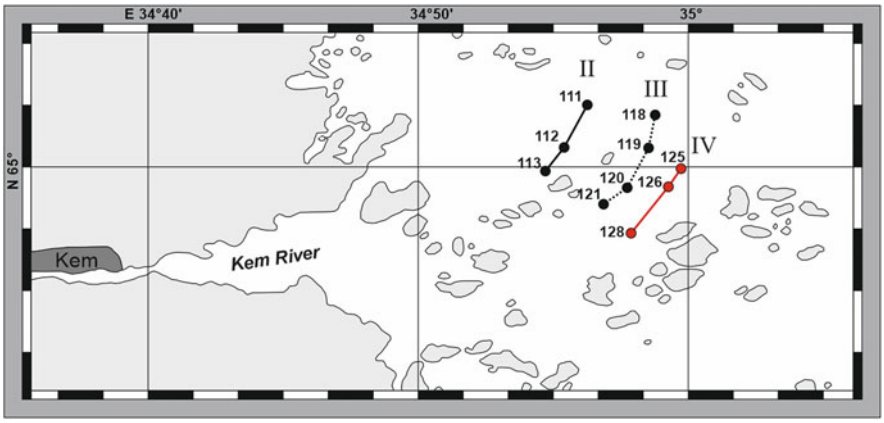

Fig. 1 Scheme of the location of sampling stations in the Kem River estuary (compiled by [38])

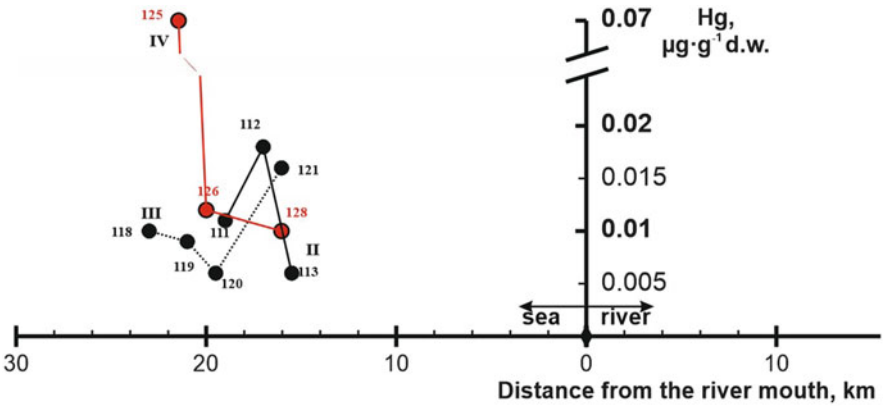

Fig. 2 Mercury content by sections (II–IV) in the Kem River estuary (compiled by [38])

excess over the background value established for the mouth area of the Northern Dvina River [17]. In general, we may conclude that the total Hg content corresponds to its natural distribution in the structure of minerals.

5 The Mouth Area of the Kyanda River (The Onega Bay and the Kyanda River Mouth)

The Kyanda River is one of the largest rivers flowing into the Onega Bay of the White Sea, its length is 49 km, and the stream gradient is 2.55‰. The source of the river is a swamp on the Onega Peninsula to the west of Lake Solozero (the source of Solza River). In its course, the river flows through the riverbed Lake Kyandozero

into the Onega Bay of the White Sea. The tributaries of the Kyanda River are Voya, Malojma, and Chiksha. The Kyanda River is located in the North of the Arkhangelsk region of Russia. According to [80], a characteristic feature of the Kyanda River is a presence in its coastal zone of a wide strip of wetlands (floodplain) overgrown with reeds. These sites are separated from the riverbed by a sandy riparian shaft (Fig. 3).

At the high tide level, the seawater percolates through sandy sediments. During the low tide, water accumulated in sandy sediments infiltrates gradually in river stock waters, thereby increasing their salinity. There are several watercourses flowing into the Kyanda River with exclusively local toponyms (Pine Creek, Black Stream) that are registered in the State Water Register [81]. The territory of the Kyanda river basin is composed of thick Proterozoic clays, sands, and siltstones, overlapped by the Quaternary sediments. This composition is determined by the position of the Onega Peninsula in the northern part of the Russian platform, at the junction of the Russian plate and the Baltic crystalline shield [82]. At low tide, width of the drying zone in some places reaches 2.5–3.0 km. If sandy and silty deposits predominate in the coastal section of the drying zone, stony ridges often occur in the marine part of shallow water, protruding into the low tide and flooded into high water period [80]. According to [83], for the sampling stations located in the drying belt, the main component of the bottom sediments is silt, and its percentage varies from 51 to 72%. In this zone, station OOB is located (Fig. 4). Bottom sediments within the Kyanda riverbed are composed mainly by aleuritic-clayey silt with sand-alluvial admixture usually wedging with depth.

Fig. 3 Sampling station 45NYA during low tide

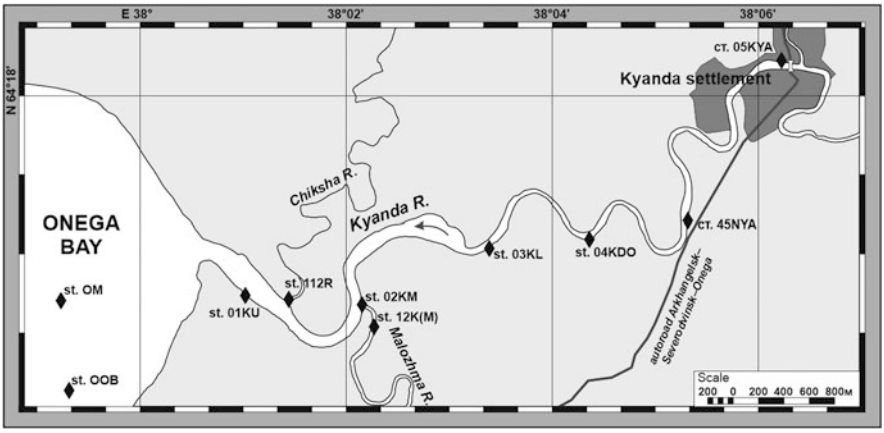

Fig. 4 Scheme of the location of sampling stations on the profile "the Kyanda River-Onega Bay of the White Sea"

Table 2 The total Hg content in bottom sediments of the Kyanda River

Sampling station	Distance from the river mouth, km	Coordinates of stations	Hg content, μg g^{-1} d.w.			Standard deviation μg g^{-1} d.w.
			Minimal	Maximal	Average	
OOB	−1.5	N 64°16′45.1″ E 37°59′19.7″	0.007	0.019	0.005	0.002
01KU	0.5	N 64°17′08.8″ E 38°01′01.8″	0.020	0.042	0.030	0.009
12KM	2.0	N 64°17′08.1″ E 38°01′26.5″	0.007	0.020	0.015	0.005
03KL	3.3	N 64°17′20.8″ E 38°03′23.6″	0.012	0.022	0.017	0.005
45NYA	5.8	N 64°17′28.4″ E 38°05′18.9″	0.012	0.020	0.015	0.003
01KU-b	0.8	N 64°17′07.8″ E 38°01′07.7″	0.024	0.075	0.036	0.019

Based on analysis of the entire data set including all sampling depths, it was established that the total Hg content in bottom sediments of the Kyanda River varied from 0.007 to 0.075 μg g^{-1} d.w. (0.022 μg g^{-1} d.w. on average) (Table 2).

The occurrence frequency of the various Hg contents in the bottom sediments is shown on Fig. 5. One can see that most of samples with the low values (<0.03 μg g^{-1} d.w.) were confined to layers deeper than 10 cm. For the surface layers (0–5 cm), a relatively uniform concentration distribution was typical for Hg contents from 0.01 to 0.02 μg g^{-1} d.w., and below the background content (0.03 μg g^{-1} d.w.) for the White Sea basin, there were 82% of determinations [84]. It should be noted that the remaining 18% were confined to two stations with a strong smell of hydrogen sulfide (H_2S) in sediments.

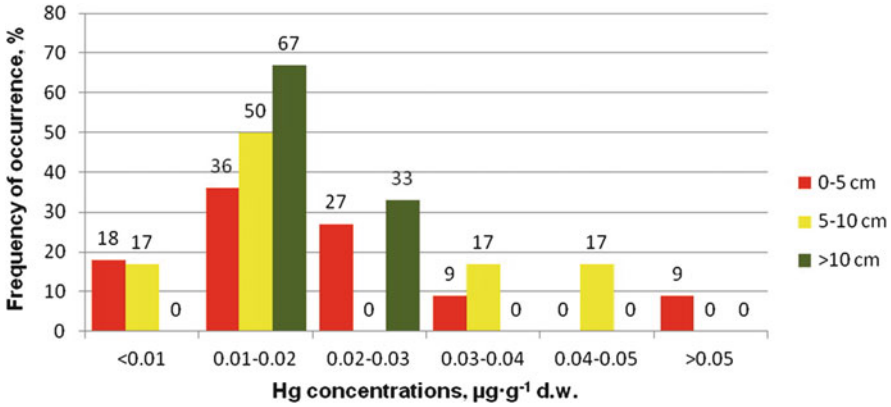

Fig. 5 Frequency of occurrence of mercury content values in the Kyanda River mouth area by the layers

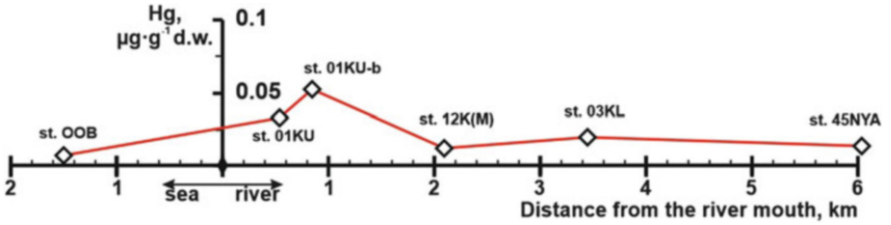

Fig. 6 Distribution of the mercury average concentrations in the surface layer of bottom sediments along the transect "the Kyanda River-Onega Bay of the White Sea"

Further, we consider the distribution of the total Hg content along the river profile. The lowest total Hg content was recorded for stations located outside its main channel, namely, station OOB, located within the Kyanda Bay, and station 12KM, confined to the place of the confluence of the Malozhma River in the Kyanda River and located 0.1 km from it (Figs. 4 and 6).

The Hg distribution in sediment core is uneven, with relatively low concentrations in the upper layer (0–5 cm), high concentrations in the middle of the columns, and further reduction in the lower layers. From the overall picture, station located at the river mouth on the border with Onega Bay (p. OOB) stands out, for which Hg content increased with depth (Fig. 7).

The highest Hg content was found at stations 01KU and 01KU-b, where bottom sediments were composed of the silty material with admixtures of plant residues smelled of hydrogen sulfide. Generally, the Hg content increased from the Kyanda River mouth to the seaward, i.e., the Onega Bay. It should be noted that the natural background total Hg concentrations in bottom sediments of the White Sea basin (0.03 μg g^{-1} d.w.) [20, 84] was exceeded in only two columns where a strong smell of hydrogen sulfide was detected. This indicates the probability of formation of mercury sulfides and its capture in the structure of iron sulfides.

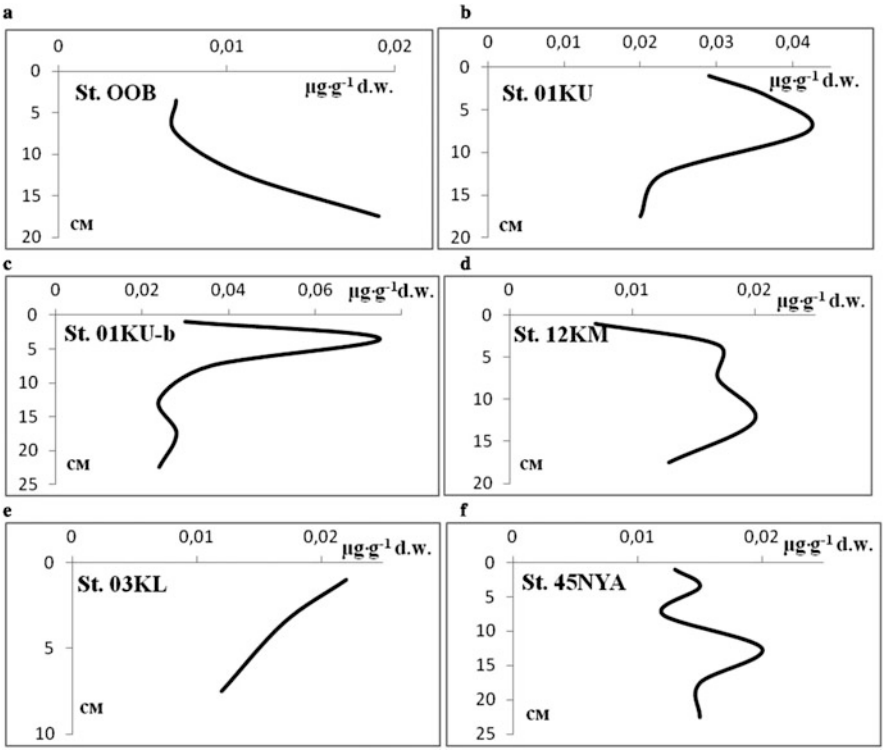

Fig. 7 Variations of the total mercury content in the bottom sediments of the Kyanda River mouth area (compiled by the authors based on the research materials, 2014)

6 The Mouth Area of the Northern Dvina River

The Hg content in the bottom sediments of the mouth area of the Northern Dvina River and Dvina Bay varied from 0.02 to 0.80 μg g^{-1} d.w., averaging 0.135 μg g^{-1} d.w. [16, 24]. An extremely high Hg content was found in bottom sediments of internal ducts crossing Arkhangelsk. These abnormal values were excluded when calculating average concentrations.

Distribution of Hg contents by frequency of occurrence in the general data set (Fig. 8) showed that in 76% of cases Hg concentration did not exceed 0.2 μg g^{-1} d.w. Elevated Hg concentrations (>0.4 μg g^{-1} d.w.) were found in single samples.

In the general dataset, 52.5% of Hg values exceeded 0.1 μg g^{-1} d.w. in the 0–5 cm layer – in 50%, in the 5–10 cm layer – in 56%. Thus, the percentage of high Hg values was more often observed in the 5–10 cm layer.

Based on the generalized results of long-term studies [24], a schematic map was constructed (Fig. 9) which reflected spatial distribution of Hg contents in the 0–5 cm layer of bottom sediments in the mouth area of the Northern Dvina River.

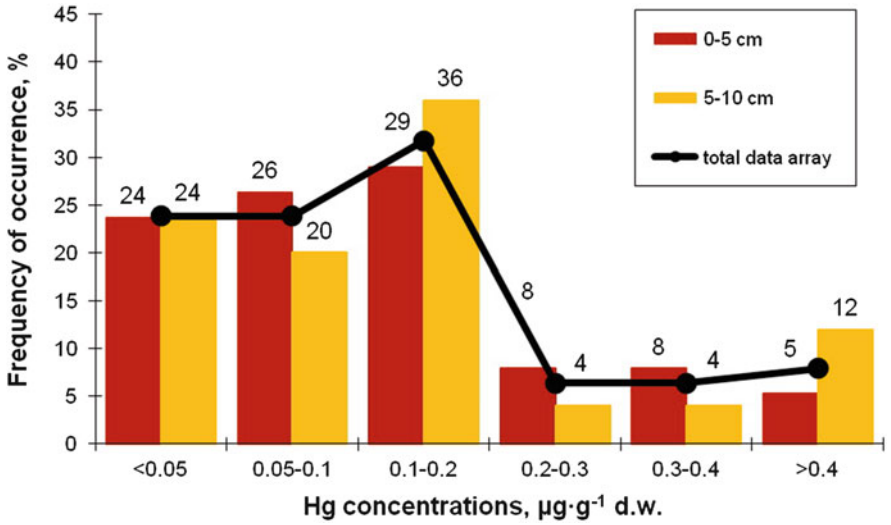

Fig. 8 Frequency of occurrence of mercury content values in the mouth area of the Northern Dvina River by the layers

The averaged data were used to construct a map scheme. As can be seen from Fig. 9, the bottom sediments of area influenced by Novodvinsk were the most polluted. In this area the largest in the region pulp and paper factories operates.

In Novodvinsk and the downstream Port of Bakaritsa, the Hg content in the bottom sediments varied from 0.2 to 0.3 μg g^{-1} d.w. In the Kuznechiha channel below the confluence of the Juras River and pier on the Solombala Island, Hg content exceeded 0.18 μg g^{-1} d.w. High Hg values were also determined in the bottom sediments of Maimaksa channel nearby the Port Economy and Lesozavod No 24.

The elevated Hg values in the bottom sediments were revealed in the geochemical barrier zone – the mixing zone of the river and sea waters (Fig. 9). When passing a geochemical barrier, an active removal of Hg happens from the aqueous solution due to its adsorption on the suspended matter followed by Hg sedimentation [12, 85, 86]. Mudyugsky Island acts as a mechanical barrier to the advancement of river waters. Here, the water flow rate decreases, and the finely dispersed suspended material is precipitated, which are the most enriched with Hg [11, 12, 24]. Such a behavior of Hg is well explained from the point of view of the theory of marginal filters [31], which includes the Northern Dvina Mouth. The considered site belongs to the area of salty waters where there were an intensive redistribution of migration forms and elevated Hg concentration in water [15, 19]. Such a mechanical barrier can also contribute to the Hg accumulation in the bottom sediments in the area of Novodvinsk where in the riverbed there are numerous islets and shoals. Thus, environmental conditions combined with human-induced factors contribute to the maximum values of Hg. The least polluted areas of the mouth region are located at the station “Ust-Pinega”, also at the upper part of Nikolsky and Murmansk arms of the

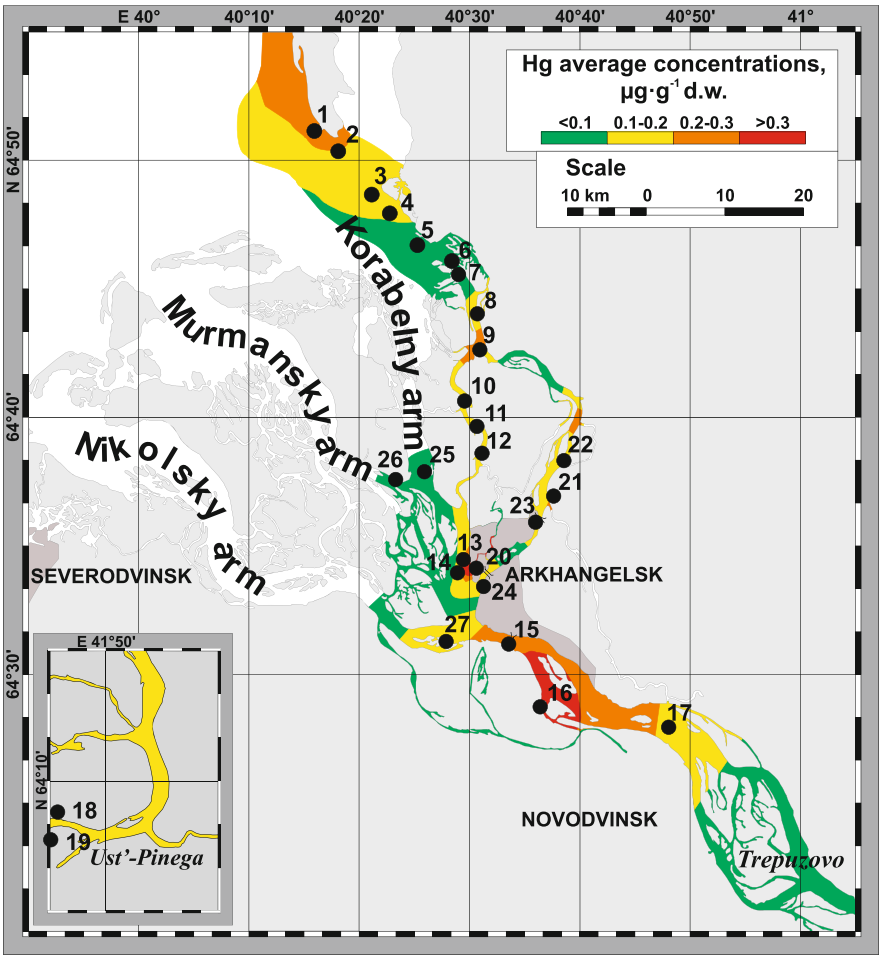

Fig. 9 Mercury distribution in the bottom sediments of the 0–5 cm layer of the Northern Dvina River mouth area [16, 24]. *Sampling stations*: 1, Mudyugsky Island; 2, Suhoe more; 3, Lebedyn Island; 4, Ustyanskie Povorotnie stvory; 5, Murovie povorotnie stvory; 6, Lapominka Village; 7, Chijovka Village; 8, Old Izhma River; 9, Port Economy; 10, Lesozavod No 24; 11, Nijnie Povrakul'skie stvory; 12, Hydrolysis factory; 13, Solombala Island; 14, Molodezhny Island; 15, Top of the Delta; 16, Port Of Bakaritsa; 17, Novodvinsk; 18, Ust'-Pinega; 19, the Mouth of the Pinega River; 20, Solombalka Channel; 21, Juras River; 22, Kuznechikha Channel; Lesozavod No 29; 23, Kuznechikha Channel, below pulp and paper mill; 24, Kuznechikha Channel, above pulp and paper mill; 25, Korabelny arm; 26, Murmansk arm; 27, Nikolsky arm

river. Areas of the bottom sediments with the average Hg content lower 0.1 μg g^{-1} d.w. were not exceed 30–35 % of total area investigated.

We have detected vertical variations in the Hg content in the sediment core. The average Hg content in the upper layer (0–5 cm) was 0.11 μg g^{-1} d.w. while in the 5–10 cm layer 0.16 μg g^{-1} d.w. These values are significantly higher than those in the Kem and Kyanda Rivers, as well as the background Hg content, in the bottom

sediments of the rivers entering the White Sea [17], and background world data for freshwater basins and rivers (Table 1). The range of total Hg contents for the Northern Dvina River is in good agreement with the values listed in Table 1 for rivers of the European territory of the Russian Federation, including rivers of the Kola Peninsula, Europe, Asia, Australia, North America, and the lower Amur basin.

The grain-size composition of bottom sediments is known to be one of the important factors that determine the Hg accumulation. Table 3 shows the characteristics of the main groups of the bottom sediments, the content of Hg and physical and chemical environmental parameters (Table 3).

From Table 3, it follows that the maximum Hg values were detected in silty and silty-sandy sediments. It should be noted that in 90% of the silty sediments, there was a smell of H_2S. In sandy fractions, relatively low Hg concentrations were detected. Clay fractions were 4–7 times enriched in Hg compared to sandy ones. We have revealed the Hg content variations in dependence of grain-size composition of sediments at station "Port Economy" (located in the main navigable channel of Maimaksa) over 2004–2006. In 2004 there were predominantly sandy sediments (Hg content 0.09 μg g^{-1} d.w.), in 2005 silty-sandy ones (Hg content 0.48 μg g^{-1} d.w.), and in 2006 sandy-silty ones enriched in organic matter (Hg content 0.11 μg g^{-1} d.w.). The Hg concentrations in bottom sediments are controlled by a pelitic fraction content, while the anthropogenic impact is related to pulp and paper production wastes. In sandy sediments with relatively high values of Eh and pH, low total Hg contents were typical. Earlier it was found that the methylation rate of bivalent Hg in aerobic conditions is higher than in anaerobic ones [87, 88]. However, at higher Eh values, when optimal conditions are created for the functioning of *Pseudomonas* demethylating bacteria, elemental Hg or dimethyl Hg may be formed. Since the Eh values in sandy bottom sediments (Table 3) do not exceed the values from −100 to +150 mV, the main most likely form of Hg is methyl-Hg. Reduction conditions prevail in bottom sediments that contain high concentrations of pelitic fraction, organic matter, hydrogen sulfide, and methane. It was found that methylating bacteria *Clostridia* predominate in anaerobic environment, whose highest productivity was observed at Eh about 0.0 mV [87–89]. Oxidation-reduction potential (ORP) in clayey-silty and silty sediments studied was usually much lower, so when ORP drops to −100, the process of methylation of Hg may be replaced with authigenic sulfides formation. While hydrogen sulfide and hydrosulfide concentrations grow, methyl-Hg is transformed into dimethyl-Hg. In sediments polluted by anthropogenic organic matter, methane can be generated synchronously with sulfate reduction. This is facilitated by bacteria-methanogens and other microorganisms whose enzyme systems contain methylcobalamin coenzyme, a methylated form of B-12 vitamin, which acts a donor of methyl groups [90–92].

Sedimentation in the mouth area of the Northern Dvina River is complicated by tidal activity. During tidal and especially storm conditions, desorption of Hg from resuspended uppermost sediments happens that resulted to its migration into the near-bottom water. Pore water of the bottom sediments also contain dissolved forms of Hg (methyl-Hg, Hg dichloride). However, the Hg content in the near-

Table 3 Variations in pH and Eh value, content of CH_4, C_{org} and Hg in the bottom sediments [16]

The bottom sediment description	Eh, mV	pH	CH_4, μg g^{-1} w.m.	Hg, μg g^{-1} d.w.	C_{org}, %	Methylmercury, ng g^{-1} d.w. (calculated value)
Sand of different grain sizes, washed, often with man-made material (glass, concrete, plastic, etc.)	−22.9...+73.0 +20	7.71–7.80 7.74	0.27–0.30 0.28	0.04–0.09 0.05	0.12–1.04 0.40	0.05–1.57
Sandy-silt, contaminated with waste paper and pulp production	−64.4...−107.2 −78	6.93–7.33 7.05	0.03–5.40 1.56	0.02–0.15 0.09	0.50–6.07 1.28	0.09–3.15
Sandy-silt, sandy ooze, as a rule, with the hydrogen sulfide smell	−92.8...−150 −110	6.71–7.17 6.90	0.11–21.00 6.90	0.21–0.37 0.29	3.78–27.95 5.20	0.87–23.20
Clayey silt, with the hydrogen sulfide smell	−96.5...−176 −130	6.58–7.56 6.90	2.03–45.50 14.80	0.10–0.80 0.35	11.10–40.30 14.20	1.05–28.00

The numerator is Hg content range; the denominator is the average value
w.m. wet mass

bottom water fluctuated slightly between periods of low tide and high tide [15, 19]. That suggested a low influence of tidal activity on Hg desorption from the upper sediment layer. A similar phenomenon was also noted for the Hudson River mouth area [64], i.e., the tidal processes did not cause bottom sediments erosion and Hg desorption.

Salinity in the near-bottom water of the barrier zone changes twice a day by 2‰ on average. In those parts of the river, where saline waters do not penetrate from the Dvina Bay and where the sulfate content remains low, methanogenesis prevails over sulfate reduction in bottom sediments and near-bottom water. According to [91] under such conditions, the bacteria-methanogens are activated, and, as a result, methane formation and methylation of Hg are intensified.

At sampling stations, where there was practically no influence of tidal activity, mineralization of water is low and does not change, as well as, respectively, the concentration of sulfate ions. Based on the above conditions and processes occurring in the mouth area of the Northern Dvina River [16, 93] a spatial zoning scheme was developed for the predominant forms of Hg in the upper sediment layer (Fig. 10).

Methylation reaction is one of the main processes of Hg compound transformation in the water basins. These processes mainly determine its back diffusion flow from bottom sediments [7]. According to the authors who studied equilibrium processes in the model systems "water-bottom sediment-fish," it follows that the methyl-Hg content in the aquatic environment should not exceed 10% of the total [87, 92]. For sandy sediments, it varies from 0.1 to 3.5% and for deposits enriched with organic matter, up to 8%. In general, for the bottom sediments, the methyl-

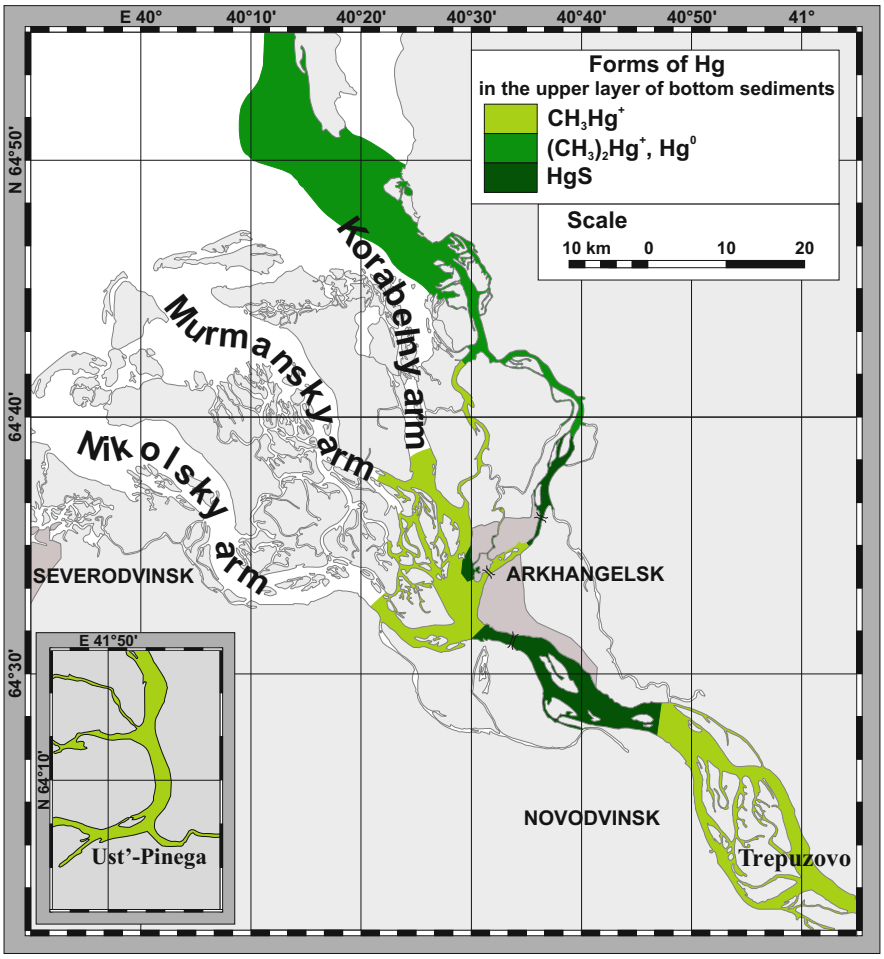

Fig. 10 Forms of mercury speciation, estimated for the surface layer of the Northern Dvina River mouth area bottom sediments [16, 24]

Hg percentage of total Hg content lies within 0.1–10% [58, 90]. For the Canadian and Japanese rivers, methyl-Hg accounts for 30% of the total Hg content (2.2–7.0 μg g^{-1} d.w.) in water [92].

The synchronous determinations of dissolved and suspended Hg in water, as well as methyl-Hg and total Hg in the bottom sediments of extremely polluted Temernik River [91, 94], showed a similarity with the calculated data. The variation intervals of methyl-Hg content [16, 24, 93] in the bottom sediments of the studied water area (Table 3) were calculated based on experimental data on Hg content in the bottom sediments combined with values of pH, Eh of sediments in the Northern Dvina mouth area, as well as on available published data on proportion of total Hg and methyl-Hg related to various physical and chemical environments.

Bottom sediments with high portion of pelitic fraction are believed to contain an increased content of methyl-Hg. However, for the pelitic sediments, the high H_2S content is characteristic, i.e., Hg methylation process is more likely to synchronize with the sulfate reduction process [93]. Increased levels of sulfidic sulfur and elemental sulfur were detected in the mouth area of the Northern Dvina River at sites located below points of the pulp and paper factories' sewage discharge [95]. For example, for the Kuznechikha Channel, the concentrations of sulfur compounds exceeded the values typical for the water areas located upstream of the river as much as nine times. In sediments with negative Eh where H_2S was detected, the sulfate reduction dominate over methylation. Here the methyl-Hg content does not reach the maximum possible for a given type of the bottom sediments (0.87–28.0 $ng \cdot g^{-1}$ d.w.). Sandy and sandy-silt sediments are characterized by relatively high values of Eh and high contamination by waste products of pulp and paper production. From the theoretical point of view, these conditions are favorable for methylation. However, taking into account the fact that the Hg content is relatively low here, we assume the methyl-Hg content in the sediments should not be also large. Based on our calculations, methyl-Hg content should lie within the range of 0.05–3.15 $ng \cdot g^{-1}$ d.w. [16, 24, 93]. Of particular interest is the Hg behavior in the bottom sediments formed at different salinity. According to some authors, in marine sediment, the intensity of methylation was only 40% from that of freshwater sediments, so high salinity contributes to Hg demethylation [96, 97].

The mouth area of the Northern Dvina River flowing into the White Sea is a part of the marginal filter where natural processes and anthropogenic ones operate immediately. The Hg content along with the technogenic radionuclides [98] in the bottom sediments can be considered as an indicator of anthropogenic influence. In this regard, the Hg behavior in bottom sediments was studied along a transect from the Northern Dvina River marginal filter to the White Sea deep areas [17]. This transect covered 520 km length and included 11 stations (Fig. 11, Table 4).

Overall, the Hg total content (μg g^{-1} d.w.) varied from 0.018 to 0.4 in the river-delta-sea section, from 0.04 to 0.4 (average 0.16) in the river-delta section (station 18–1), and from 0.02 to 0.4 (average 0.11) in the delta area (stations 9, 1, 34). At sea stations 27, 20, 04, and 08, the total Hg content varies between 0.018 and

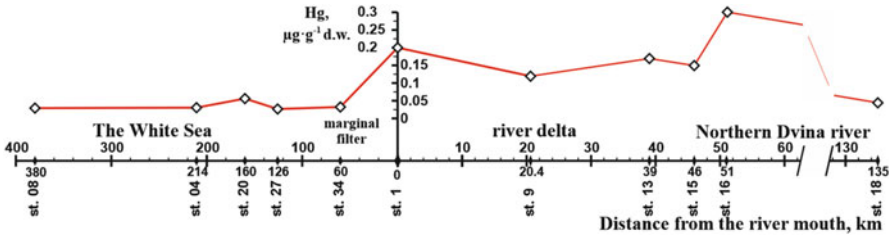

Fig. 11 Distribution of average mercury content values in the upper layer of the bottom sediments along the profile "Northern Dvina River-the White Sea"

Table 4 The mercury content in the surface layer of the bottom sediments of the marginal filter the Northern Dvina River–the White Sea

Sampling station	Distance from the river mouth, km	GPS	Mercury content, μg g^{-1} d.w.		
			Min	Max	Average
18 "Ust'-Pinega"	135	N 64°09.192′ E 41°54.608′	0.04	0.05	0.045
16 "Port Of Bakaritsa"	51	N 64°28.85′ E 40°36.514′	0.22	0.37	0.3
15 "Top of the Delta"	46	N 64°31.398′ E 40°33.182′	0.05	0.18	0.15
13 "Solombala Island"	39	N 64°34.575′ E 40°30.038′	0.13	0.21	0.17
9 "Port Economy"	20.4	N 64°40.737′ E 40°29.693′	0.05	0.4	0.12
1 "Mudyugsky island"	0	N 64°51.3′ E 40°15.0′	0.15	0.22	0.2
34 "Southern part of the Dvina Bay"	60	N 64°50.56′ E 39°10.23′	0.02	0.047	0.033
27 "North-Western part of the Dvina Bay"	126	N 65°02.45′ E 38°00.22′	0.018	0.035	0.028
20 "The White Sea Basin, Northern part"	160	N 65°54.20′ E 38°15.71′	0.03	0.095	0.057
04 "The White Sea Basin, Central part"	214	N 65°48.58′ E 36°45.90′	0.022	0.05	0.031
08 "Kandalaksha Gulf"	380	N 66°29.10′ E 34°06.16′	0.024	0.046	0.03

0.095 μg g^{-1} d.w. (average 0.038). So, there is a distinct decrease in the total Hg content in the seaward direction from the top of the delta to its marine edge.

Along the transect from the Port of Bakaritsa to the Mudyugsky Island, two peaks of total Hg content are clearly seen (Fig. 12). The first Hg peak (0.30 μg g^{-1} d.w.) was detected in the river part of the transect (station 16, Port of Bakaritsa), where a significant amount of the Hg coming from the Novodvinsk area was accumulated on the gravitational barrier in the silty bottom sediments. The second Hg peak (0.2 μg g^{-1} d.w.) was found at station 1, Mudyugsky Island (Fig. 12).

In accordance with the theory of marginal filters, stations 15–9 can be attributed to the gravitational barrier zone, where in the 1–15‰ salinity interval, a mixing zone of river and seawater is located. The heavy coarse-grained suspended particulate matter is precipitated here, which is accompanied by an active adsorption and co-precipitation of Hg with suspended matter on sinking particles. This process took place till station 34. Part of transect between stations 9 and 1 is characterized by the predominance of physical and chemical processes, primarily coagulation and

Fig. 12 Sampling station "Mudyugsky Island," mouth area of the Northern Dvina River (2006)

flocculation, over gravitational removal of suspended Hg from water. The bottom sediments are represented here with sandy ooze and muddy sands. Between stations 1 and 34 there is a change in the granulometric composition of bottom sediments: pelitic and sandy-silty fractions of the river estuary (Mudyugsky Island) replaced by pelite-silty and pelitic ooze in the Central part of the Dvina Bay. This part of the marginal filter can be attributed to biological zone with high content of biogenic elements. Here, bioaccumulation of Hg occurs along with desorption processes.

According to the data [15, 24], redistribution of the proportion of dissolved and suspended Hg was observed in the barrier zones described above. Up to 95% of suspended Hg and up to 90% of dissolved Hg are removed from the water. The sea part of the transect (stations from 27 to 8) was characterized by a relatively low and uniform distribution of the total Hg content in the surface bottom sediments. The exception was station 20 located in the central part of the sea near the border with the White Sea Throat, where the influence of the Barents Sea waters was noticed [99, 100].

It should be noted that the marginal filter of the Northern Dvina River contributes to the Hg co-precipitation with the suspended matter of the bulk of anthropogenic Hg and thus dramatically reduces the risk of Hg penetration into the White Sea and partly with the inflow into the Barents Sea.

7 Mercury in the Bottom Sediments of the White Sea

Based on the analysis of the entire data set, it was found that the Hg concentrations in the bottom sediments of the White Sea vary within 0.006–0.095, averaging 0.024 μg g^{-1} d.w. Distribution of the total Hg content in the White Sea was studied based on bottom sediments sampled at stations shown, in Fig. 13.

The frequency of various Hg concentrations' occurrence in the whole White Sea bottom sediments was analyzed using a histogram (Fig. 14). The calculated average content of the total Hg (0.024 μg g^{-1} d.w.) regardless of the sampling depth was plotted. It was found that in 65% of cases, the Hg content was below the average, and in 46% of cases, the Hg values ranged from 0.01 to 0.02 μg g^{-1} d.w. The highest percentage (41%) of Hg concentrations falls on the deeper layers (below 10 cm) of the bottom sediments.

For the upper 0–5 cm layer (Fig. 15), the highest percentage (41%) of Hg concentrations occurs within the range 0.01–0.02 μg g^{-1} d.w., 27% within the range 0.03–0.04, 2% within the range 0.04–0.05, and 15% more than 0.05 μg g^{-1} d.w. The Hg levels below 0.02 μg g^{-1} d.w. were detected in less than 4% of cases.

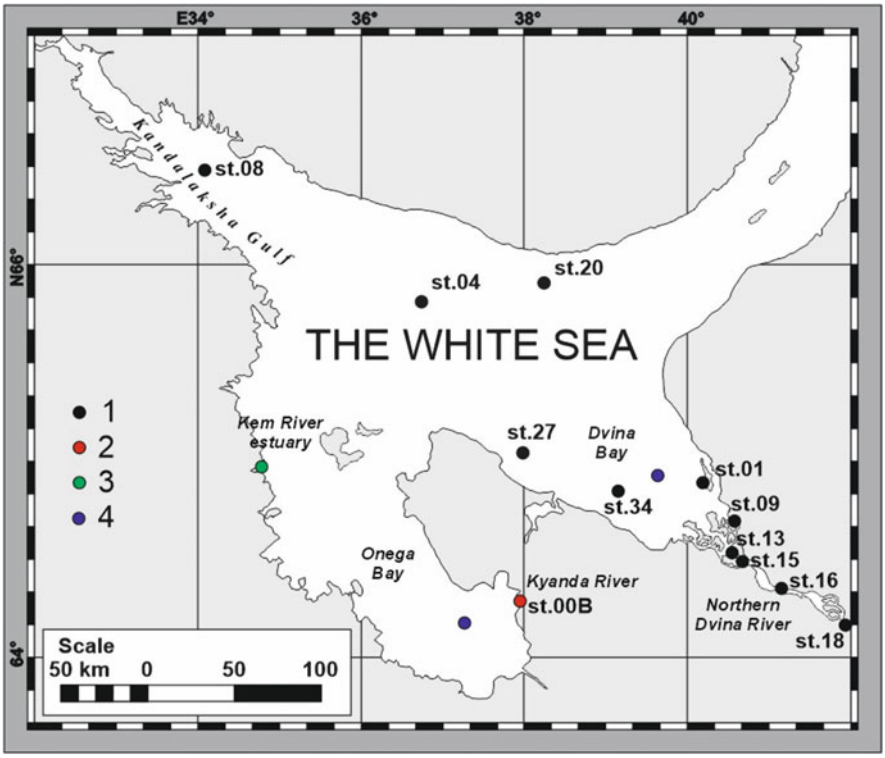

Fig. 13 Scheme of the location of sampling stations on the White Sea basin (1, compiled by [17]; 2, compiled by [23]; 3, compiled by [38], 2005; 4, compiled by [49])

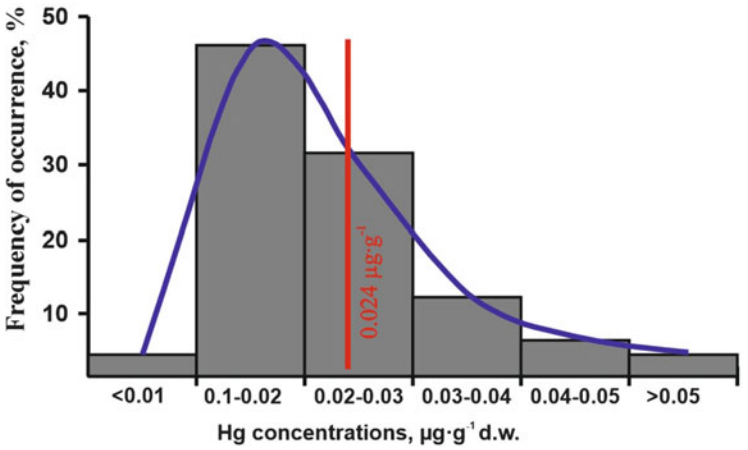

Fig. 14 Frequency of occurrence of mercury content values in the bottom sediments of the White Sea (whole array of data)

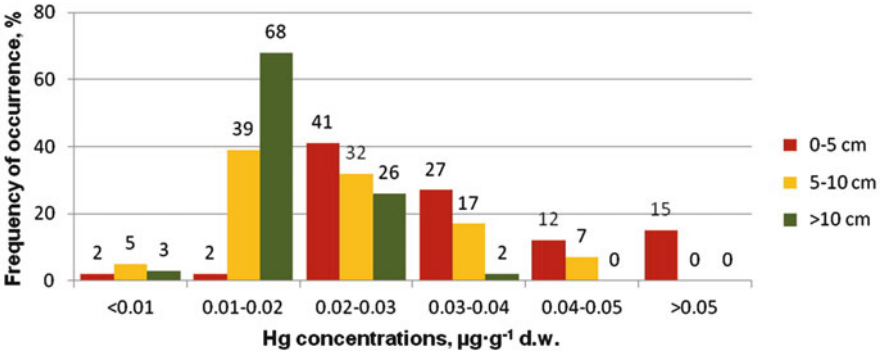

Fig. 15 Frequency of occurrence of mercury content values in the bottom sediments of the White Sea basin by the layers

For the layer 5–10 cm, the largest percentage of the Hg occurrence (39%) was within the range 0.01–0.02 μg g^{-1} d.w. and 32% for the range 0.02–0.03 μg g^{-1} d.w. In 7% of cases in this layer, Hg values exceeded 0.04 μg g^{-1} d.w. and were below 0.01 μg g^{-1} d.w. in 5%.

For the layer deeper than 10 cm, as for layers 5–10 cm, the largest percentage (68%) of Hg contents was in the range 0.01–0.02 μg g^{-1} d.w. and the smallest one (3%) for values less than 0.01 μg g^{-1} d.w. In this horizon, Hg contents greater than 0.04 μg g^{-1} d.w. were not found.

Generalized scheme of spatial Hg distribution in the upper layer of bottom sediments is displayed on Fig. 16. There is a tendency for Hg content to increase from the low values in the Onega Bay, where the minimum metal content was found at the mouths of the Kem and Kyanda Rivers, to higher ones in the central part of the White Sea. Elevated Hg concentrations were detected in the upper layer of the bottom sediments of the Dvina Bay and on the mouth of the Northern Dvina River.

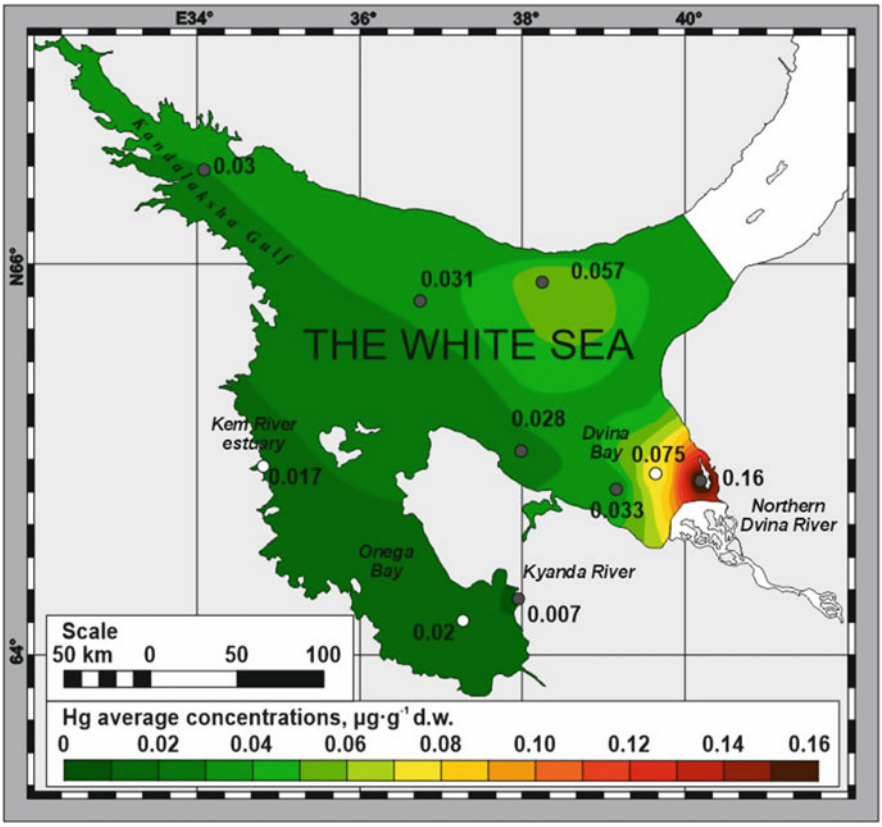

Fig. 16 Spatial mercury distribution in the bottom sediments of the White Sea (compiled by [17, 38, 49])

The distribution pattern of total Hg concentrations in the vertical section (0–15 cm horizons) of the White Sea bottom sediments is shown in Fig. 17. The whole White sea (except Kandalaksha Bay) is characterized by the abrupt changes in Hg concentrations with a general tendency to decrease with depth. The uppermost horizon (0.0–1.5 cm) is characterized by low Hg concentrations, this is more likely to be caused by erosion and oxidation processes at the water-sediment boundary. The maximum Hg concentrations were revealed in the horizon 1.5–3.0 cm, while the lower values (2.5 times less than in the upper horizon) were observed at horizons 7.5–10.0 cm. The latter was probably due to the increased content of iron sulfides here.

Describing the distribution of Hg content by layers of sediment cores, we will try to justify the peak concentrations. The first peak concentrations recorded at the 1.5–3.0 cm horizon may be attributed to period when an active phase of industrialization of the area and the development of pulp and paper production have begun. Meanwhile formation of the 1.5 cm layer corresponded to the period of industrial

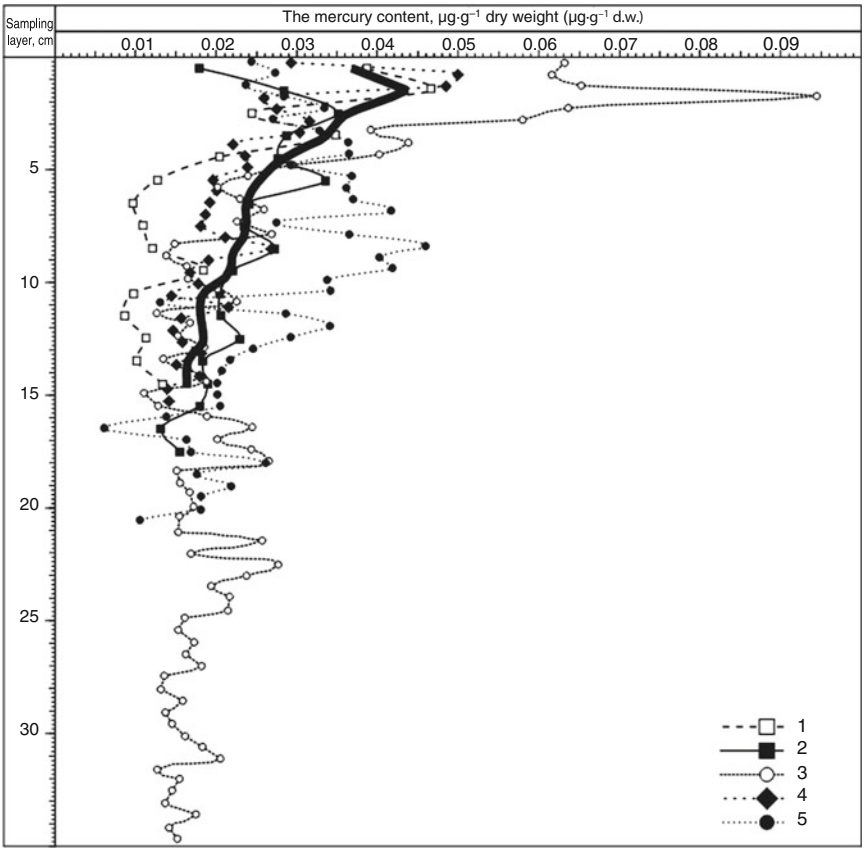

Fig. 17 Distribution of total mercury content in the vertical section of bottom sediments in the White Sea. *Sampling stations*: 1, station 34 "southern part of the Dvina Bay"; 2, station 27 "northwestern part of the Dvina Bay"; 3, station 20 "the White Sea basin, northern part"; 4, station 04 "the White Sea basin, central part"; 5, station 08 "Kandalaksha Gulf"
(the bold line indicates the average concentration in the sampling horizon)

boom, i.e., it covers the period up to the early 1990s of the last century. The formation of high Hg concentrations at this time can be explained by Hg input into the bottom sediments with the river runoff; besides, it could be also be due to the global Hg falling out from the atmosphere [6, 101]. At several stations, there was a peak at the 3.5–4.0 cm horizon (not so pronounced). Its formation could be related to the global air mass transfer of Hg to the Arctic regions which resulted from intensification of burning of coal, oil, and peat as well as during fighting on the fronts of the World War I and Civil War. One can see from Fig. 17 that the presence of bursts of Hg content in the underlying layers, in particular, at 7.0–10.0 cm horizon, often coincides with the presence of greenish-gray sandy, clay-sandy aleurite, hydrotroilite, or organic matter. It should also be noted that for all stations except Kandalaksha Bay, the Hg content at these horizons of the bottom sediments

did not exceed the background value determined for the White Sea as a whole. The observed fluctuations of the Hg content which are not beyond the background range should be regarded as resulted from the natural factors.

It is worth mentioning station 20 where the highest Hg concentration of 0.095 μg g^{-1} d.w. that was formed in 1970–1980 was detected in the 1.5–2.0 cm horizon. The Hg content ranged from 0.012 to 0.095 (Fig. 17), averaging 0.024 μg g^{-1} d.w. Station 20 (81 m depth) is located in the Northern part of the central part of the White Sea (Fig. 13). This area is most remote from both the direct impact of industrial companies and shipping, as well as from the river runoff transport paths. So we may suppose that the main source of Hg entering the Sea is atmospheric fluxes, whose Hg contents were related to the time of industrial activity [85, 101]. In addition, station 20 is located southwest to the White Sea Throat which is known to transfer more saline waters inflowing from the Barents Sea [99]. Thus, formation of the high Hg concentrations was probably due to its co-precipitation with suspended matter promoted by interactions of waters of different salinity at contact of the Barents and White Sea water. This version was indirectly confirmed by the data on elevated total Hg content in the bottom sediments of the Murmansk Bank located in the Barents Sea not far from the Throat of the White Sea [72]. Down the core, a monotonic decrease in the Hg content was observed. In general, the vertical distribution of Hg in sediment core at station 20 is rather uneven.

Station 08 located in the Kandalaksha Bay, the sediments we taken from a depth of 298 m (Fig. 13). The Hg content here varied from 0.006 to 0.046, averaging (0.029 ± 0.003) μg g^{-1} d.w. At this station, unlike the others, a monotonous increase in the Hg content from the upper layers to the 7.5–10.5 cm horizon was detected, where it reached a maximum (Fig. 17). Further, down the core, an abrupt decrease in Hg concentration was observed. We propose that such a type of Hg distribution down the core could be called an "inverted" one that could be formed due to the bottom sediments' redeposition. The reason for this may be both of the natural and anthropogenic origin. It is known that the Kandalaksha Bay belongs to the seismically active zone of the White Sea. The spatial-temporal distribution of the focuses of tangible earthquakes in the Kandalaksha Bay was given in [102]. Over the period from 1847 to 1995, three cycles of migration of the focuses were identified: (1) from 1847 to 1935, (2) from 1935 to 1970, and (3) from 1970 to 1990. It was noted that the predominant directions of migration of tangible earthquakes focuses were spatially close to tectonic faults. In opinions of these authors [102], the Kandalaksha Graben is a structure, within whose branches there was a cyclic migration of earthquake focuses, that resulted to formation of landslide processes. Landslides can also be caused by the freezing blows (frost cracking of the soil and ice in water bodies). When the ice was cracked, its impact on the Bay coasts took place which, in our opinion, could initiate landslide processes. According to studies [103], the station 08 is located in the zone of landslide processes.

In the Kandalaksha Bay, construction of the channel and extension of the tank farm were accompanied by the use of explosions. According to [104], this has led to a change in the current lithological situation. There was a replacement of bottom sediments, accompanied by deposition of the lower horizons over the upper ones. We believe that was caused by slide of more contaminated surface sediments into the deeper areas of the Bay. Now these more polluted layers are covered with less polluted layers of bottom sediments. The most polluted areas of the Kandalaksha Bay are its edge parts that were revealed by data analysis over the period of 1996–1999 [104]. In most cases, the decreased Hg concentrations in the 0–1.5 cm horizon were observed.

At all sampling stations, with the exception of station 08, there were areas influenced by bottom erosion resulted from storms. Besides, the Hg content might be caused by its desorption from the uppermost 0–1.5 cm sediment layer into the near-bottom water, where an oxidation conditions promoted the Hg precipitation. It is known that the Hg demethylation processes prevail at high positive Eh values, the products of these processes might be Hg^0, CH_4, or $Hg(CH_3)_2$. Further the low soluble dimethyl-Hg due to photo-oxidative degradation can be transformed into Hg^0. Below the redox barrier, there is a reducing condition, where formation of sulfides of Hg and Fe occurs. The Fe sulfides tend to capture Hg in their matrix. The next peak of Hg content recorded for all stations at the 7.5–10 cm horizon was possibly associated with an elevated concentration of Fe-sulfides, low values of ORP, and consequently binding of Hg in these layers.

The background value of the total Hg concentration for the White Sea basin was established as 0.03 μg g^{-1} d.w. [17, 20, 22, 84]. The correctness of this value is confirmed by the fact that about 80% of the bottom sediment samples contain Hg less than 0.03 μg g^{-1} d.w. This value is comparable to the average Hg content in the bottom sediments of the Arctic Seas and does not exceed the Hg content in the background areas of the globe [2, 24].

By use of the background Hg content, its percentage of anthropogenic origin in bottom sediments was calculated [22]. The highest percentage of anthropogenic Hg was recorded in the upper 0.0–5.0 cm horizon, where it varied on average from 4% at station 04 to 47% at the station 20. In the underlying layers, the share of anthropogenic Hg was very small, and only in the 0.5–10.0 cm horizon at station 08, it was about 20% on average. From our data, bottom sediments deeper than 10.0 cm horizon, excluding station 08, were not influenced by anthropogenic activity, and the Hg contents in these layers should be referred as the background ones. The portion of anthropogenic Hg was high at stations 1, 9, 13, 15, and 16 of the mouth area of the Northern Dvina River where it reached up to 85–94%. This is significantly higher than at station 34 located in the outer part of the Dvina Bay where the content of anthropogenic Hg was 36%. This fact speaks in favor of the efficiency of the marginal filter in the system of the Northern Dvina River – the White Sea.

8 Conclusions

The distribution of total mercury content in bottom sediments along the 500 km transect, including stations in the estuary area of the Northern Dvina River and deepwater areas of the White Sea and Kandalaksha Bay, has been studied. The background content of Hg was determined to be 0.03 μg g^{-1} d.w. Marginal filter "the Northern Dvina River-the White Sea" is a barrier for Hg transportation to the open part of the White Sea. The total Hg contents in the bottom sediments of the small Kem and Kyanda Rivers flowing into the Onega Bay were similar and corresponded to its natural distribution in the lithogenous matrix. An elevated Hg content in the upper layer of sediments was determined seaward the Kyanda River mouth. The background of Hg content here was exceed only in two cases, for bottom sediments with a strong smell of H_2S, which indicates the probability of formation of Hg-sulfides and its capture in the structure of Fe-sulfides.

Comparative analysis of Hg concentrations in the upper layer of bottom sediments showed that their greatest values were characteristic for the Northern Dvina River estuary. They were significantly higher than that in the Kem and Kyanda Rivers, the background Hg content in the bottom sediments of the rivers inflowing the White Sea, as well as the world data for background freshwater bodies and watercourses. At the same time, the range of total Hg concentrations in bottom sediments of the Northern Dvina River was comparable to that for rivers of the European territory of the Russian Federation; watercourses of the Kola Peninsula, Europe, Asia, Australia, and North America; and the lower Amur River basin located in areas of chronic anthropogenic impact. For the Northern Dvina River, the methyl-Hg content variations were calculated and spatial distribution pattern of the predominant Hg forms in the upper horizon of bottom sediments was developed. For the White Sea, the vertical distribution of Hg mercury in the sediment cores was shown; a tendency to decrease down the core has been revealed for the Hg content. The percentage of the anthropogenic Hg was calculated in the bottom sediments of the White Sea: the highest percentage was recorded in the 0.0–5.0 cm horizon, where it varied from 4% in the central part of the basin to 47% in its Northern part. The share of anthropogenic Hg was very high (85–94% from total content) in the Northern Dvina River estuary and delta stations. That was significantly higher than that in the outer part of the Dvina Bay, i.e., far from the Northern Dvina River mouth where its content was 36% on average. That is an additional argument for the efficiency of Hg removal over the marginal filter "the Northern Dvina River-the White Sea."

Acknowledgments This research was supported by grants of the Ministry of Education and Science of the Russian Federation "The Base Part of State Assignment" No 5.5795.2017/8.9 and No 5.5791.2017/6.7.

References

1. Minamata Convention on Hg. http://Hgconvention.org/Portals/11/documents/Booklets/Minamata_convention_Russian.pd. Accessed 24 Jan 2018
2. AMAP (2005) Heavy metals in the arctic. AMAP, Oslo, 265 pp
3. Fedorchuk VP (1998) Mineral raw materials. Hg. ZAO Geoinformmark, Moscow. 27 pp (in Russian)
4. Ozerova N (1986) Hg and endogenous ore formation. Nauka, Moscow. 230 pp (in Russian)
5. Jonasson IR, Boyle RW (1972) Geochemistry of Hg and origins of natural contamination of the environment. Can Min Metall Bull 1:8
6. Fitzgerald WF, Mason RP (1996) The global Hg cycle: oceanic and anthropogenic aspects. In: Baeyens W (ed) Global and regional Hg cycles: sources, fluxes and mass balance, vol 1. Kluwer, Dordrecht, pp 85–108
7. Moore GV, Ramamurthy S (1987) Heavy metals in natural waters. Mir, Moscow. 285 pp (in Russian)
8. Trahtenberg IM, Korshun MN (1988) Hg and its compounds. In: Filov VA (ed) Harmful chemicals. Inorganic compounds of elements of groups I-IV. Khimiya, Leningrad. 170–188 pp (in Russian)
9. Mineral resources of the Russian Arctic (2005) www.arctictoday.ru. Accessed 15 Jan 2018 (in Russian)
10. Fedorov YA, Garkusha DN, Ovsepyan AE (2005a) Hg in the aquatic ecosystems of the Northern part of ETR and its biogeochemical features of the distribution, migration and transformation. In: Proceedings of the II scientific-practical conference "Ecological problems. Look into the future", Rostov-on-Don, pp 121–124 (in Russian)
11. Fedorov YA, Garkusha DN, Ovsepyan AE et al (2005b) Main results of expeditionary research on the Northern Dvina and the Dvina Bay of the White Sea. University news. North-Caucasian region. Nat Sci Ser 3:95–100. (in Russian)
12. Fedorov YA, Ovsepyan AE (2006) Hg and it's connection with physicochemical water parameters (on the example of the rivers of the Northern ETR). University news. North-Caucasian region. Nat Sci Ser 2:82–89. (in Russian)
13. Fedorov YA, Ovsepyan AE, Dotsenko IV (2007) Hg in soils of the estuarine region of the Northern Dvina River. University news. North-Caucasian region. Nat Sci Ser 6:109–114. (in Russian)
14. Fedorov YA, Ovsepyan AE, Zimovets AA et al (2009) Integrated ecological-geochemical expedition at the mouth area of the Northern Dvina River at the winter season 2008. University news. North-Caucasian region. Nat Sci Ser 1:110–114. (in Russian)
15. Fedorov YA, Ovsepyan AE, Korobov VB (2010a) Pecularities of Hg distribution, migration, and transformation in the estuarine area of the Northern Dvina River. Russ Meteorol Hydrol 35(4):289–294. https://doi.org/10.3103/S1068373910040072
16. Fedorov YA, Ovsepyan AE, Korobov VB et al (2010b) Bottom sediments and their role in surface water pollution with Hg (with a special reference to the Northern Dvina River mouth and the Dvina Bay of the White Sea). Russ Meteorol Hydrol 35(9):611–618. https://doi.org/10.3103/S1068373910090050
17. Fedorov YA, Ovsepyan AE, Lisitzin AP et al (2011a) Patterns of Hg distribution in bottom sediments along the Severnaya Dvina–White Sea section. Dokl Earth Sci 436(1):51–54. https://doi.org/10.1134/S1028334X11010041
18. Fedorov YA, Zimovets AA, Ovsepyan AE et al (2011b) Physico-chemical conditions in the mouth region of the Northern Dvina River and their influence on the forms of occurrence and migration of Hg. University news. North-Caucasian region. Nat Sci Ser 2:86–89. (in Russian)
19. Fedorov YA, Ovsepyan AE (2013) Hg and its connection with physicochemical water parameters (case study of the rivers of the Northern European territory of Russia). In: Hg: sources, applications and health impacts. Nova Science, New York, pp 155–172

20. Fedorov YA, Ovsepyan AE, Savitskiy VA (2013) Distribution of Hg in bottom sediments of the White Sea. Living and bioinert ecosystems. http://www.jbks.ru/archive/issue-2/article-8/. (in Russian)
21. Fedorov YA, Ovsepyan AE, Savitskiy VA et al. (2016) Physical and chemical characteristics of water in the mixing zone: River Kyanda – Onega Bay of the White Sea. In: Conference proceedings of 16th international multidisciplinary scientific GeoConference, Bulgaria. Book 3, vol 1, pp 553–560. https://doi.org/10.5593/SGEM2016/B31/S12.072
22. Fedorov YA, Ovsepyan AE (2017) Hg in the bottom sediments of the mouth area of the Northern Dvina River and the White Sea. In: The White Sea system, vol 4, pp 712–720 (in Russian)
23. Fedorov YA, Savitskiy VA, Zimovets AA (2017) Distribution of Hg in bottom sediments on the profile of "River Kyanda–Onega Bay of the White Sea". In: Ecological problems. Looking to the future: a collection of works of VIII International scientific-practical conference, Publishing House of Southern Federal University, Rostov-on-Don, 462–465. (in Russian)
24. Ovsepyan AE, Fedorov YA (2011) Hg in the mouth area of the Northern Dvina River. ZAO Rostizdat, Rostov-on-Don/Moscow. 198 pp (in Russian)
25. Ovsepyan AE, Fedorov YA, Savitskiy VA (2014) Assessment of Hg in fish in the mouth of the Northern Dvina River and the Dvina Bay of the White Sea. In: Proceedings of 14th international multidisciplinary scientific geoconference and EXPO, SGEM 2014, Albena, Book 5, vol 1, pp 81–87
26. Ovsepyan AE, Fedorov YA, Zimovets AA et al. (2015a) Department of physical geography, ecology and nature conservation, Institute of Earth Sciences, SFU Research of the behavior of Hg under conditions of water bodies in the North of ETR. In: Proceedings of the VII international scientific-practical conference. Publishing Southern Federal University, Rostov-on-Don, 245–250 pp (in Russian)
27. Ovsepyan AE, Fedorov YA, Zimovets AA et al. (2015b) Features of accumulation of Hg in the bottom sediments of lakes in Arkhangelsk and its surrounding area. In: Proceedings of 15th international multidisciplinary scientific geoconference and EXPO, SGEM 2015, Albena, Book 5, vol 1, pp 353–360
28. Ovsepyan AE, Fedorov YA, Zimovets AA (2016) Diurnal dynamics of Hg in water objects of the North European part of Russia. In: Proceedings of 16th international multidisciplinary scientific geoconference and EXPO, SGEM 2016. Albena, vol 1, pp 243–250
29. Ovsepyan AE, Zimovets AA, Fedorov YA (2017) On the dynamics of Hg in the mouth area waters of the Northern Dvina River for a 10-year observation period. In: Ecology, economics, education and legislation conference proceedings, vol 17, issue 51, pp 713–720. https://doi.org/10.5593/sgem2017/51/S20.137
30. Schuster PF, Krabbenhoft DP, Naftz DL et al (2002) Atmospheric Hg deposition during the last 270 years: a glacial ice core record of natural and anthropogenic sources. Environ Sci Technol 36(11):2303–2310
31. Lisitsyn AP (1994) Marginal filter of the oceans. Oceanology 34(5):735–747. (in Russian)
32. Mikhailov VN (1997) Hydrological processes in estuaries. Moscow, GEOS. 171 pp (in Russian)
33. Zimovets AA, Fedorov YA, Ovsepyan AE et al. (2015) About the features of the Hg levels in precipitation formation of the Azov Sea and the White Sea. In: Proceedings of international multidisciplinary scientific geoconference surveying geology and mining ecology management, SGEM 15th, vol 3, pp 19–24
34. Leshchev AV, Korobov VB, Khomenko GD et al (2015) The first complex studies of Kyanda River (Onega Bay, The White Sea) and its marginal filter (July 22 to August 3, 2014). Oceanology 55(5):769–770. https://doi.org/10.1134/S0001437015050100
35. Leonova GA, Bobrov VA, Shevchenko VP et al (2006) Comparative analysis of the microelement composition of Seston and bottom sediments in the White Sea. Dokl Earth Sci 406(1):136–140. https://doi.org/10.1134/S1028334X06010338
36. Lisitsyn AP (2010) Processes in the catchment area of the White Sea: preparation, transportation and deposition of sediment, streams of substances, the concept of a "living watershed". The White Sea system, vol 1. Nauchniy Mir, Moscow, pp 353–446 (in Russian)

37. Shevchenko VP, Starodymova DP, Lisitzin AP et al (2013) Geochemistry of terricolous lichens in the White Sea catchment area. Dokl Earth Sci 450(1):514–520. https://doi.org/10.1134/S1028334X13050073
38. Demina LL, Shevchenko VP, Novigatskii AN et al (2005) Geochemistry of the bottom sediments in the mixing zone of the Kem' River with the White Sea. Oceanology 45 (6):805–818
39. Fedorov YA, Hkansivarova IM, Predeina LM (2003) Features of the distribution of Hg and lead in bottom sediments of Taganrog Bay and the South-Eastern part of the Azov sea. Vodnoe Hkozyaistvo 5(6):51–58. (in Russian)
40. Privalenko VV, Mazurenko VT, Panskov VI et al (2000) Environmental problems of the city of Kamensk-Shakhtinskiy. Publishing house ZAO "Tsvetnaya pechat", Rostov-on-Don. 152 pp (in Russian)
41. Kozlova SI (1989) Spatial and temporal variability of Hg distribution in the Kiliya Delta of the Danube. In: The Monitoring of background pollution of natural environments, vol 5. Gidrometeoizdat, Leningrad, pp 236–252. (in Russian)
42. Petrovich G (1982) Heavy metals in bottom sediments of the Danube in the area of the reservoir Xherdan. In: Proceedings of XX international conference for the study of the Danube. Naukova Dumka, Kiev, pp 39–42 (in Russian)
43. Roslyakov NA, Kuskovsky VS, Nesterenko GV et al (1992) Katun: ecogeochemistry of Hg. Russian Academy of Sciences, Siberian branch, United Institute of Geology, Geophysics and Mineralogy, Novosibirsk. 180 pp (in Russian)
44. Vasiliev OF, Sukhenko SA, Atavin AA et al (1992) Environmental aspects of the project of the Katun hydroelectric power station, due to the presence of Hg in the natural environment of the Altai mountains. Water Resour 6:107–123. (in Russian)
45. Melnikov SA (1991) Reports on heavy metals. The state of the Arctic environment reports, vol 2. Arctic center, University of Lapland, Rovaniemi, pp 82–153
46. Moiseenko TI, Dauvalter VA, Rodushkin IV (1998) The circulation mechanisms of natural and anthropogenic metals in surface waters of the Arctic basin. Water Resour 25:231–243. (in Russian)
47. Tsibulski V, Yatsenko-Khemelevskaya M, Gordeev V et al (2001) Summary of the Russian research for the AMAP II HM Report. In: International workshop on trends and effects of heavy metals in the Arctic, 85 pp
48. Pavlova LG (2001) The Geochemistry of pore waters in the conditions of Arctic ice-marine sedimentogenesis. Sedimentological processes and evolution of marine ecosystems in conditions of marine periglacial collection of scientific works. Kola Science Center RAS (Apatity), Murmansk, pp 101–111. (in Russian)
49. Sapozhnikov VV, Sokolova AS (1994) The distribution of pollutants in water and bottom sediments of the White Sea. In: Complex research of the ecosystem of the White Sea: collection of scientific works, Moscow, pp 104–108 (in Russian)
50. Esnough TE (1996) Trace metals in sediment of coastal Siberia. MS dissertation, Texas A&M University, College Station, 146 p
51. Naidu SA, Goering JJ, Kelley JJ (2001) Historical changes in trace metals and hydrocarbons in the inner shelf sediments, Beaufort Sea: Prior and subsequent to petroleum-related industrial developments. OCS Study MMS 2001–061, Final report, University of Alaska-Fairbanks, 80 p
52. Valette-Silver NJ, Hameedi MJ, Efund DW et al (1997) Contaminants in the sediments and biota of the western Beaufort Sea. National Oceanic and Atmospheric Administration. Natl Ocean Serv, USA, p 179
53. Olsen J, Hoydal K, Dam M (2003) AMAP Faroe Islands 1999–2001 Heavy metals. In: Hoydal K, Dam M (eds) AMAP Greenland and the Faroe Islands. The environment of the Faroe Islands, vol 3. AMAP, Oslo, p 265
54. Luchsheva LN (1995) Hg content in the ecosystem components of Alekseeva Bay (Peter the Great Bay, Sea of Japan). Biologiya Morya 21(6):412–415. (in Russian)
55. Petrukhin VA, Andrianov A, Burtseva LV et al. (1986) The Background content of lead, Hg, arsenic and cadmium in natural environments (in the world). Message 3. In: Monitoring of

background pollution of natural environments. Gidrometeoizdat, Leningrad, 3–27 pp (in Russian)
56. Kot FS (1993) Hg in the waters of the Lower Amur and the mixing zone. Biogeochemical examination of the state of the environment. Dalnauka, Vladivostok, pp 106–115. (in Russian)
57. Yanin EP (1989) Environmental and geochemical assessment of pollution of river Nura by Hg. IMGRE, Moscow. 43 pp (in Russian)
58. Bloom NS, Moretto LM, Scopece P et al (2004) Seasonal cycling of Hg and monomethyl-Hg in the Venice Lagoon (Italy). Mar Chem 91(1–4):85–99
59. Savitskiy V, Fedorov Yu, Zalouk-Vergnoux A et al. (2017) Les premières données sur la distribution du mercure dans les sédiments du fond selon le profil "La rivière de Loire – le Golfe de Gascogne". In: Problèmes écologiques. Un regard vers l'avenir: actes de la VIIIème Conférence scientifique et pratique internationale, Rostov-sur-le-Don, 363–368 pp
60. Shimkus KM, Komarov AV, Tikhomirov AA (1994) Pricelessly Pollution of the coastal zone of the Black Sea heavy toxic metals and pesticides. In: Comprehensive study of man-made pollution in the coastal zone of the Caucasian black sea shelf. Gelendjik, Roskomnedra, 100–127 pp (in Russian)
61. Shimkus KM, Komarov AV, Tikhomirov AA (1996) Features of the accumulation and concentration of pollutants in the process of sedimentogenesis. In: Technogenic pollution and natural processes of self-purification Pricelessly zone of the Black Sea. Moscow, Nedra, 415–432 pp (in Russian)
62. Opekunov AY (2005) Aqual Technosedimentogenesis. Trudy VNIIIOkeangeologii Ministerstva Prirodnykh Resursov R. Nauka, St. Petersburg. 278 pp (in Russian)
63. Laperdina TG (2000) Determination of Hg in natural waters. Nauka, Novosibirsk. 222 pp (in Russian)
64. Heyes A, Miller C, Mason R (2004) Hg and methyl-Hg in Hudson River sediment: impact of tidal resuspension on partitioning and methylation. Mar Chem 1(4):5–89
65. Pfeiffer WC, Lacerda LD, Malm O et al (1989) Hg concentrations in inland waters of gold-mining areas in Rodonia, Brasil. Sci Total Environ 87(88):233–240
66. Malm O, Pfeiffer WC, Souza CM, Reuther R (1990) Hg pollution due to gold mining in the Madeira River basin, Brazil. Ambio 19:11–15
67. Conaway CH, Watson EB, Flanders JR et al (2004) Hg deposition in a tidal marsh of South San Francisco Bay downstream of the historic New Almaden mining district, California. Mar Chem 90(1–4):175–184
68. Gordeev VV (2009) Trace elements in water, suspended matter and bottom sediments of the Gulf of Ob, Yenisei Bay and the Lena Delta and adjacent areas of the Kara Sea, and Laptev Sea. In: The System of the Laptev Sea and adjacent seas of the Arctic. Publishing house of Moscow University, Moscow, 202–224 pp (in Russian)
69. Polyakov DM, Aksentov KI, Ivanov MV (2008) Hg in the bottom sediments of the marginal filter of the Razdol'naya River. Amur Bay Geochem Int 46(6):614–621. https://doi.org/10.1134/S0016702908060074
70. Ivanov MV (2014) Hg in bottom sediments of marginal seas of northeast Asia. Russ J Pac Geol 8(4):288–299. https://doi.org/10.1134/S1819714014040046
71. Bełdowski J, Miotk M, Zaborska A et al (2015) Distribution of sedimentary Hg off Svalbard, European Arctic. Chemosphere 122:190–198
72. Novikov MA, Zhilin AY (2016) Distribution of heavy metals in bottom sediments of the Barents Sea based on the results from statistical analysis. Vestnik KRAUNC. Nauki o Zemle 1 (29):78–88. (in Russian)
73. Vallius H, Leivuori M (1999) The distribution of heavy metals and arsenic in recent sediments in the Gulf of Finland. Boreal Env Res 4:19–29
74. Vallius H (2009) Heavy metal distribution in the modern soft surface sediments off the Finnish coast of the Gulf of Finland. Baltica 22(2):65–76
75. Boszke L, Kowalski A (2006) Spatial distribution of Hg in bottom sediments and soils from Poznań. Pol J Environ Stud 2:211–218

76. Willerer AO, Kot M, Shumilin FS et al (2003) Hg in bottom sediments of the tropical Rio Marabasco, Its Estuary and Laguna de Navidad, Mexico. Bull Environ Contam Toxicol 70:1213–1219
77. Demina L, Gordeev V, Galkin S et al (2010) The biogeochemistry of some heavy metals and metalloids in the Ob River Estuary-Kara Sea section. Oceanology 50(5):729–742. https://doi.org/10.1134/S0001437010050103
78. Gubaidullin MG (2010) Basic data on the geological structure of the Eastern part of the watershed of the White Sea. In: The system of the White Sea. Natural environment of the watershed of the White Sea, vol 1. Nauchniy Mir, Moscow, pp 40–57. (in Russian)
79. Dolotov YS, Rimskii-Korsakov NA, Telikovskii AA et al (2005) Bottom topography, bottom sediments, and structure of the sedimentary sequence in different zones of the Kem' River Estuary (White Sea). Oceanology 45(6):877–884
80. Khomenko DG, Leshchev AV, Korobov VB (2013) The Peculiarities of the hydrological regime of river mouth areas of small rivers of the White sea (according to the forwarding observations 2010-2012). In: Proceedings of the twentieth international conference (School) on marine geology. Geology of seas and oceans, vol 3. GEOS, Moscow, pp 266–268. (in Russian)
81. Bednaruk SE (2008) Hydrographic zoning of the territory of the Russian Federation. Book 1. NIA-Priroda, Moscow 541 pp (in Russian)
82. Kaplin PA, Leontyev OK, Lukyanova SA et al (1991) The shore. MYSL, Moscow. 479 pp (in Russian)
83. Lukyanov SA, Shvartsman YG (2013) Grain-size composition of bottom sediments in the estuarine zones of the minor rivers of the White Sea Onega Bay. Arct Environ Res 2:28–34. (in Russian)
84. Fedorov YA, Ovsepyan AE, Dotsenko IV et al (2015) Chronology of modern marine sedimentogenesis and deposition of Hg in the White Sea. Hg in the Biosphere: ecological and geochemical aspects. INH SO RAS, Novosibirsk. 370–375 pp
85. Shevchenko VP (2006) The influence of aerosols on environment and marine sedimentation in the Arctic. Nauka, Moscow. 266 pp (in Russian)
86. Skibinskii LE (2005) The Role of geochemical barriers and geochemical barrier zones in forming of the hydrochemical regime of coastal waters of Arctic Seas. In: Proceedings of the XII congress of Russian Geographical Society, vol 5, pp 148–155. (in Russian)
87. Yamamoto J, Kaneda Y, Hikasa Y et al (1983) Translocation of inorganic/organic Hg in a model aquatic system. Water Res 17(4):435–440
88. Compeau G, Bartha R (1987) Effect of salinity on Hgmethylating activity of sulfate-reducing bacteria in estuarine sediments. Appl Environ Microbiol 53:261
89. Tonomura K, Furakawa K, Yamada M (1972) Microbial conversion of Hg compounds. In: Proc. IV JF.S. Ferment Technol. Today, 563–567 pp
90. Bartlett PD, Craig PL (1981) Total Hg and methyl Hg levels in British estuarine sediments. Water Res 15(1):37–47
91. Fedorov YA (2004) Characteristic features of Hg and methane formation and distribution in surface waters. In: Problems of hydrometeorology and geoecology. Izd. SKNTs VSh APSN, Rostov-on-Don, 57–62 pp (in Russian)
92. Kudo A, Nagase H, Ose Y (1982) Proportion of methyl-Hg to the total amount of Hg in river waters in Canada and Japan. Water Res 16(6):1011–1015
93. Ovsepyan AE, Fedorov YA (2006) On some peculiarities of Hg distribution in bottom sediments of the mouth area of the Northern Dvina River. In: Materials of the XVII youth scientific conference dedicated to the memory of K. O. Kratts. Karelian Research Center of RAS, Petrozavodsk, 233–236 pp (in Russian)
94. Fedorov YA, Berezan OA, Velichko ML, et al. (2002) Distribution and levels of Hg concentration in the atmosphere and water bodies of the Sea of Azov. In: Ecosystem research of the Sea of Azov and its coast. Izd. KNTs RAN, Apatity, 150–166 pp (in Russian)

95. Kokryatskaya NM, Volkov II, Demidova TP et al (2003) Sulfur compounds in bottom sediments of freshwater water bodies (the estuarine area of the Northern Dvina River and Rybinsk water reservoir). Litologiya I Poleznye Iskopaemye 6:647–659
96. Coquery M, Cossa D, Sanjuan J (1997) Speciation and sorption of Hg in two macrotidal estuaries. Mar Chem 58:213
97. Kongchum M, Devai I, DeLaune RD et al (2006) Total Hg and methyl-Hg in freshwater and salt marsh soils of the Mississippi river deltaic plain. Chemosphere 63:1300–1303. https://doi.org/10.1016/j.chemosphere.2005.09.024
98. Aliev RA, Bobrov VA, Kalmykov SN et al (2007) Natural and artificial radionuclides as a tool for sedimentation studies in the Arctic region. J Radioanal Nucl Chem 274(2):315–321. https://doi.org/10.1007/s10967-007-1117-x
99. Filatov NN, Terzhevik AY (2007) White Sea and its watershed under the influence of climatic and anthropogenic factors. Karelian Research Center of Russian Academy of Sciences, Petrozavodsk. 349 pp (in Russian)
100. Hydrometeorology and hydrochemistry of the USSR seas (1991) In: Glukhovski BH (ed) White Sea. V. 1. Hydrometeorological conditions. Gidrometeoizdat, Leningrad. 240 pp (in Russian)
101. Fitzgerald WF, Lamborg CH (2003) Treatise on geochemistry. The crust, vol 3. Elsevier, Amsterdam, pp 107–148
102. Yudakhin FN, Frantsuzov VI (2010) Seismicity of the White Sea and adjacent areas and regularities of its manifestation. In: The system of the White Sea. The natural environment of the watershed of the White Sea, vol 1. Nauchniy Mir, Moscow, pp 118–147. (in Russian)
103. Rybalko AE, Fedorova NT, Nikitin MA et al. (2013) Geodynamic processes in the Kandalaksha Bay of the White Sea, their role in the formation of the cover of recent sediments. In: Geology of seas and oceans: materials of XX international scientific conference (School) on marine geology, vol 3. GEOS, Moscow, pp 237–241. (in Russian)
104. Peresypkin VI, Romankevich EA (2010) Biogeochemistry of lignin. GEOS, Moscow. 340 pp (in Russian)

Occurrence Forms of Heavy Metals in the Bottom Sediments of the White Sea

Liudmila L. Demina, Dmitry F. Budko, Alexander N. Novigatsky, Tatiana N. Alexceeva, and Anastasia I. Kochenkova

Contents

Abstract The White Sea is an inner subarctic marine basin where sedimentation is known to be influenced by mostly terrigenous processes. In the catchment area of the White Sea, a lot of the mining, manufacture, and pulp and paper industry plants are located whose solid and liquid wastes contain heavy metals, including the toxic ones. Through the solid and dissolved river runoff, atmospheric fluxes, and coastal abrasion, heavy metals enter the seawater where they are involved in various biogeochemical processes before to be precipitated on the sea floor. Many studies of marine sedimentation concern total metal concentration; meanwhile, an assessment of contribution of different biogeochemical processes stays incomplete. In this chapter, we try to evaluate the partitioning among the different forms (speciation) of heavy metals that reflect principal processes of their accumulation in the modern bottom sediments of the White Sea. We study both the rock-forming (Al, Fe, Mn) and trace elements (Mo, Cr, Ni, Co, Cu, Pb, Cd, and As) by use of a modified method of selective sequential chemical leaching.

A spatial distribution of the occurrence forms of these elements in the surface sediments was estimated, while their analysis in high-resolution (1-cm-scale) sedimentary core lets us to study their behavior in the processes of early diagenesis.

L. L. Demina (✉), D. F. Budko, A. N. Novigatsky, T. N. Alexceeva, and A. I. Kochenkova
Shirshov Institute of Oceanology, Russian Academy of Sciences (IO RAS), Moscow, Russia
e-mail: l_demina@mail.ru

A. P. Lisitsyn and L. L. Demina (eds.), *Sedimentation Processes in the White Sea: The White Sea Environment Part II*, Hdb Env Chem (2018) 82: 241–270,
DOI 10.1007/698_2018_328,
Published online: 7 July 2018

Our data evidenced a correctness of using Al as element indicator of terrigenous deposition in the marine bottom sediments. In both oxidized surface sediments and high-resolution sedimentary core, geochemically inert lithogenic form of Al dominated absolutely (on average, 95% of total content). Predominance of lithogenic form of Fe, Cr, Ni, and As (68–85% for each of these metals, on average) suggested the major role of terrigenous processes in their accumulation. For Cu, Cd, Pb, and Co, the sum of the three labile forms (adsorbed on clays/carbonates, authigenic Fe-Mn oxyhydroxides, and organic matter) and the inert lithogenic form contributes approximately equal portions into accumulation of these metals in the White Sea bottom sediments. Mn and Mo were found to be the most labile metals: only till 10% in the lithogenic form in the upper 0–6 cm layer, while down the core portion of this form increased progressively.

A detailed record of Mn and Fe occurrence forms revealed that a ratio of Mn/Fe in the labile (absorbed/carbonate and authigenic Mn-Fe oxyhydroxides) forms has changed abruptly during early diagenesis. The Mn/Fe ratio was the highest in the 1–2 cm upper oxidized sedimentary layer, decreasing sharply at intervals 6–7 cm in the White Sea, staying constantly low in deeper sedimentary layers. From this we suppose Mn/Fe ratio to be applied as a proxy of the early diagenesis of the bottom sediments.

Keywords Bottom sediments, Diagenesis, Occurrence forms, Trace metals, White Sea

1 Introduction

Investigation of physicochemical occurrence forms of elements allows to quantify the contribution of various biogeochemical processes in their accumulation in bottom sediments. On the study of chemical element migration, it is important to distinguish among the two basically different occurrence forms: (1) geochemical labile ones providing exchange and mobilization processes and (2) geochemical inert ones or lithogenous when elements are fixed in crystalline lattices of clastic and clay minerals. The proportion of chemical elements' occurrence forms is controlled by such lithological-geochemical parameters as grain-size and mineral composition, moisture's content, organic carbon content, and redox potential. The study of physicochemical occurrence forms of trace elements in the sedimentation processes began about 40 years ago [1–5]. It was established that in the suspended particulate matter (SPM) in the surface water of the tropical Indian and Pacific Oceans, trace metal accumulation has resulted mostly (to 90%) from biogenic processes [6, 7]. This was evidenced by predominant contribution of the hydrogenous forms (absorbed and bound to organic matter) averaged about 70% for Fe, Mn, and Zn and about 90% of Cu in the total metal content in SPM. The contribution of the hydrogenic forms of Al, traditionally regarded as an indicator of terrigenous input, reached 55% in SPM of subtropical water of the Indian Ocean [6].

In surface bottom sediments of the pelagic zone of the Pacific, trace elements are accumulated mainly due to biogenic and hydrogenic processes and in all the types of pelagic sediments of the Pacific and Indian Oceans [5]. In the recent 20 years, investigation of global biogeochemical cycles of iron, which limits the phytoplankton growth thus affecting the climate change, was enforced. In some publications [8–10], to distinguish and evaluate the different geochemical processes (mobilization in the river flow, transformation in the river-sea mixing zones, sedimentation in the marine basins), analysis of the occurrence forms of heavy metals by the method of sequential chemical extraction was used.

In the Arctic seas, the river runoff, aerosols, melting sea ice, coastal abrasion, and urban activity are the basic sources of chemical elements [11, 12]; there, one could see a different proportion of the occurrence forms. In surface sediments of the Barents Sea and the Dvina Bay of the White Sea [13], as well as in the Kara Sea [14], a predominance (over 60% of total content) of geochemically inert forms of Fe, Zn, Co, Cr, Ni, and Pb has been found.

Sedimentation in the subarctic White Sea takes place under the prolonged ice-covered periods, low water temperatures, and high hydrodynamics, coupled with semidiurnal fluctuations in the sea level [15–18]. One of the characteristic features of the White Sea is a presence of cyclic tidal currents with velocities up to 100–200 cm/s that cause turbulent mixing of water at depths up to 70 m. Direct determinations of vertical fluxes of dispersed sedimentary matter, first made in the White Sea [19], have revealed a irregularity of input of sedimentary material to the bottom over this basin. Annually vertical fluxes of sedimentary material displayed a maximum value (2,758 g m^{-2} $year^{-1}$) in the frontal zones (Gorlo and Solovetsky Islands) and minimum one (51 g m^{-2} $year^{-1}$) in the central part of the White Sea [11, 17]. In the near-bottom water, the sedimentary matter collected by sediment traps was dominated by abiotic components: quartz (29%), clay minerals (30%), feldspars, and carbonates (15%); organic matter amounted to 26%, on average [18, 19].

Aluminum, as one of the major rock-forming elements, is often used as normalizer for other elements to estimate of aluminum silicates contribution in sediments. However, according to Yudovich and Ketris [20] in the case of a small portion of terrigenous material (Al content is $\leq$3–5%), this approach seems to be unacceptable. Terrigenous material plays a predominant role in composition of the bottom sediments of the White Sea [11, 16–18]. In this regard, it is of interest to quantify a contribution of terrigenous processes and to clarify the role of the diagenetic changes during accumulation of aluminum, iron, and trace elements in sediments as well. Quantification of physicochemical forms of Al, along with data on mineral carriers of trace metals and grain-size analysis of bottom sediments of the White Sea, was of paramount importance.

Reduction of ice cover and permafrost layer, which was recently observed in the Arctic basins, leads to increased river runoff and change in its chemical composition [12]. These factors obviously have impact on changes of migration forms of

chemical elements during sedimentation processes. However, an incomplete understanding of how various environmental factors of sedimentation in the Arctic affect the occurrence forms of heavy metals at different stages of sedimentation still remains.

The aim of this chapter is to obtain quantitative estimates of geochemical processes' contribution in the heavy metal accumulation in bottom sediments of the White Sea. An instrument for this investigation was the physicochemical speciation of Al, As, Fe, Cd, Cu, Co, Cr, Mn, Mo, Ni, and Pb in the bottom sediments of the surface layer and in the high-resolution sediment core.

2 Materials and Methods

In this work, we investigated surface sediments sampled by box corer "Ocean-0.25" ($n = 30$) along with the two transects: the axial transect 1 from the Dvina Bay to Kandalaksha Bay and the Onega transect 2 from the mouth of the Onega River to the Solovetsky Islands (Fig. 1). From these areas, the dry samples were taken for analysis, which were obtained during the expeditions of the IO RAS in different years. In addition, samples of natural moisture and undisturbed texture, as well as the pore waters, were collected from the high-resolution (1-cm-scale) sedimentary core

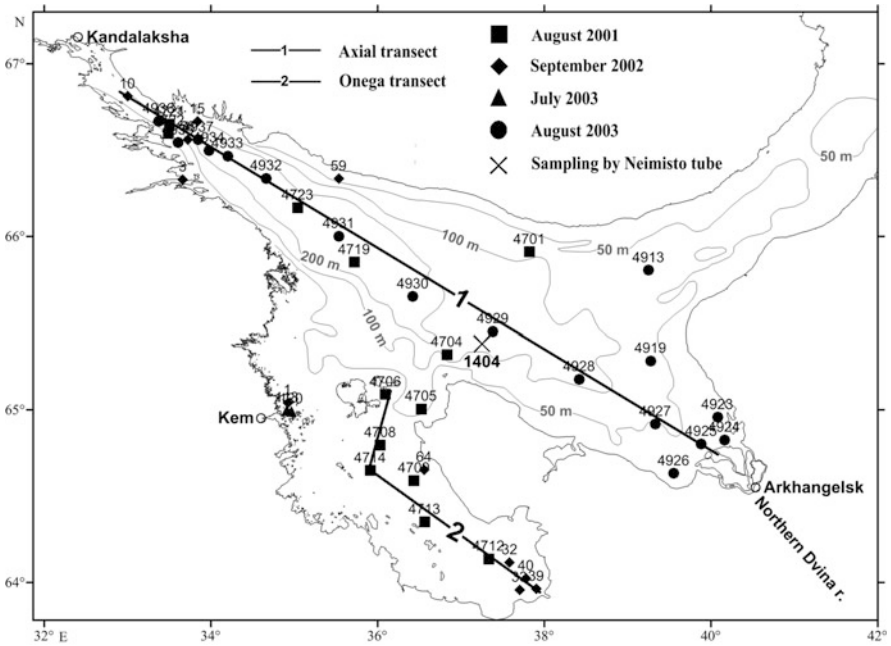

Fig. 1 Location of sampling stations of surface bottom sediments sampling, position of the axial (1) and Onega (2) transects, and core sediment Station 1404

($n = 37$). These samples were captured by the use of Neimisto tube (46 cm core length) in 2014 in the expedition of the research vessel "Ekolog" at Station 1404 (65°23,291′ N; 37°14,773′ E, water depth 150 m), located in the outer part of the Dvina Bay (Fig. 1).

Using plastic knife, undisturbed sediment core (44 cm length) was divided into 18 samples, each 1–1.5 cm thick. On board, samples of pore waters were separated from wet sediments by centrifugation (300 rpm), followed by filtration through the nuclepore filters. Samples of pore waters prior to analysis were acidified using ultrapure 65% HNO_3 to pH = 2. In stationary laboratory, samples of pore water were diluted 1:10 with deionized water before trace metal analysis. The sediment samples of natural moisture were placed in hermetically closed polymer bags, which were then kept in a fridge until the samples were analyzed. In stationary laboratory, sediment samples were analyzed for natural moisture content (by weighting method) and grain-size composition (by means of water-mechanical analysis) [21]. In addition the contents of organic (C_{org}) and carbonate carbon (C_{carb}) were measured in the dried samples on Express Analyzer, a 2970-n with accuracy of 0.1%.

Quantification of physicochemical forms of Al, Fe, Mn, Cu, Cr, Co, Mo, Ni, Pb, Cd, and As from the surface layer (0–5 cm) was made by the sequential leaching procedure from the dried samples (500 mg weight) of surface bottom sediments and from wet samples (1,000 mg weight) collected from 46 cm core length (discreteness 1–2 cm) at Station 1404. The chemical element occurrence forms (speciation) were distinguished as follows:

Form-1 – elements adsorbed on clay particles and associated with carbonates (reactant: mixture of 25% acetic acid and acetate buffer [22]).

Form-2 is amorphous Fe-Mn oxyhydroxides and associated trace metals (Chester reagent; [23]).

Form-3 – bound to organic matter (OM) and sulfides (reactant, 0.02M HNO_3 + 30% H_2O_2; [24]).

Form-4 or a lithogenous one is a residual solid that contains metals fixed in the crystal structures of detrital and/or clay minerals (complete decomposition with mixture of concentrated HNO_3 and HF).

The first three forms (1–3) contribute to assess the geochemically labile metals, whereas the form-4 is a geochemically inert one, containing metals in primary and secondary minerals.

Concentrations of heavy metals (Mn, Fe, Pb, Cd, Co, Cu, Cr, Mo, and Ni) in the obtained solutions and diluted pore waters have been analyzed by atomic absorption spectrometry on KVANT-2A (Kortek, Russia) and by inductively coupled plasma mass spectrometry (ICP-MS Agilent 7500a, United States). The accuracy of the analysis was controlled by replicate analyses of internationally certified standard samples of bottom sediments (NIST 2703 and GSD-2 and GSD-6). The differences between the tabulated and measured metal concentrations were within 5–18%.

3 Occurrence Forms of Chemical Elements in the Surface Layer of Bottom Sediments

The lithological and geochemical characteristics of the bottom sediments studied are listed in Table 1.

On the axial section from the Dvina Bay (13 m water depth) to the Kandalaksha Bay (340 m water depth), content of natural moisture in sediments was highly variable – from 18.2 to 61.0% depending on grain-size and mineral composition. The content of pelite fraction (<0.01 mm) varied also considerably from 20.2 to 89.0%, as well as the sand fraction did (from 2.6 to 75.2%). It should be noticed that these two contrary fractions changed in inverse proportion at every station. It is known that sediments with predominance of fine-grained clay fraction can adsorb larger quantities of metals due to their physicochemical properties (high specific area and cation exchange capacity), compared to sandy sediments. The C_{org} and C_{carb} contents varied within the limits of 0.37–3.41 and 0.9–11.2%, respectively; their elevated contents were detected usually in the fine-grained sediments. Recently, it was established that difference between C_{org} contents in sandy and pelitic sediments reached four- to sevenfold, while the Kandalaksha Bay sediments are enriched in C_{org} compared to average values for these types of sediments for the White Sea [25].

Mineral phases of sediments are known to be the main carrier of various chemical elements. According to data on the quantitative powder X-ray diffraction (Brucker Company, Germany), the dominant portion (63.3% on average) of the White Sea bottom sediments is composed by clastic minerals (quartz, feldspar, etc.) [26], rather than by clay minerals (montmorillonite, illite, kaolinite, etc.), as it was earlier considered [15].

3.1 Rock-Forming Elements

Aluminum and iron are important constituents of the mineral phases that form rocks of lithosphere. Our data suggest that portion of Al in lithogenous form Al-4 varied from 95 to 99% of total content Al (98% on average). It means that almost the whole Al is fixed in crystal structure of clastic or/and clay minerals. In the latter, Al serves as a principal structure element. These mineral forms are supplied into the White Sea primarily through to the river runoff, as well as by aerosol material, and as a result of coastal abrasion.

Based on small quantity of biogenic components BSi (opal), ranging from 0.5 to 6.3%, and low content of C_{org} (Table 1), one may suggest a terrigenous origin of these sediments. Let us test this by distribution of the Al and Fe occurrence forms.

Aluminum On the axial transect 1 from the Dvina Bay to Kandalaksha Bay, the total Al content ranges from 4.4 to 7.4, averaging 6.1% dry w. Lower Al contents (on average, 5.05% dry w.) were detected in coarse-grained (silty and sandy)

Table 1 Physical, lithological, and biogeochemical characteristics of surface sediments' samples collected in the White Sea

Station	Sampling area	Sea depth, m	Sampling horizon, cm	Moisture of sediment, %	Sandy fraction, %	Pelite fraction, %	$SiO_{2amorhous}$, %	$C_{organic}$, %	$C_{carbonate}$, %	CaCO3, %
4919	Dvina Bay	69	0–1	56.45	1.61	95.17	2.65	1.30	0.36	2.98
4923	Dvina Bay	12	0–1	43.68	2.36	93.81	0.38	2.40	0.93	7.76
4924	Dvina Bay	13	0–1	54.89	4.84	73.56	1.13	3.41	1.33	11.12
4925	Dvina Bay	13	0–1	ND	ND	ND	1.43	0.79	0.56	4.63
4926	Dvina Bay	15	0–1	ND	ND	ND	0.75	0.79	0.61	5.07
4927	Dvina Bay	56	0–1	58.53	2.28	93.52	2.99	1.05	0.47	3.88
4928	Dvina Bay	95	0–1	ND	ND	ND	3.62	1.45	0.41	3.41
4929	Бассейн	152	0–1	ND	ND	ND	4.92	1.12	0.26	2.18
4930	Бассейн	290	0–5	60.99	1.1	98.01	4.05	1.147	0.51	4.27
4931	Бассейн	273	0–1	ND	ND	ND	4.01	1.43	0.54	4.51
4913	Бассейн	73	0–3	14.76	68.47	16.35	0.48	0.18	0.18	1.50
4701	Бассейн	94	0–3	56	11.34	61.23	3.55	0.785	0.395	3.29
4704	Бассейн	134	0–5	65.68	1.11	96.45	6.89	ND	ND	ND
4719	Бассейн	281	0–5	68.03	1.97	96.95	4.39	1.36	0.31	2.60
4932	Kandalaksha Bay	256	1–2	60.12	2.64	85.09	4.01	1.56	0.54	4.53
4933	Kandalaksha Bay	340	0–1	ND	ND	ND	4.99	1.71	0.51	4.22
4934	Kandalaksha Bay	339	0–1	ND	ND	ND	4.50	1.76	0.56	4.68
4935	Kandalaksha Bay	178	0–5	55.91	3.16	88.96	5.57	0.37	0.12	0.99
4936	Kandalaksha Bay	67	1–2	51.03	8.02	31.86	1.25	1.57	0.49	4.04

(continued)

Table 1 (continued)

Station	Sampling area	Sea depth, m	Sampling horizon, cm	Moisture of sediment, %	Sandy fraction, %	Pelite fraction, %	$SiO_{2amorhous}$, %	$C_{organic}$, %	$C_{carbonate}$, %	CaCO3, %
4937	Kandalaksha Bay	156	0–5	49.07	3.6	90.89	4.88	1.28	0.66	5.50
4721	Kandalaksha Bay	181	0–5	18.28	75.16	20.20	0.76	0.14	ND	ND
4722	Kandalaksha Bay	132	0–5	34.65	28.11	20.22	6.28	0.55	ND	ND
4723	Kandalaksha Bay	226	0–5	73.37	51.53	0.72	6.1	1.55	0.44	3.63
10	Kandalaksha Bay	75	0–1	49.73	5.65	57.28	1.87	0.54	0.16	1.30
15	Kandalaksha Bay	89	0–2	21.14	19.33	12.24	3.34	0.29	0.13	1.07
16	Kandalaksha Bay	253	0–1	53.51	12.6	53.95	4.71	0.58	0.27	2.22
58	Kandalaksha Bay	86	0–3	25.54	6.7	6.89	4.20	0.35		
59	Kandalaksha Bay	80	0–2	52.14	13.02	65.6	5.45	0.598	0.14	1.17
1	Onega Bay	28	0–1	50.98	32.48	33.13	3.00	2.04	0.38	3.20
32	Onega Bay	16	0–3	40.99	9.11	67.98	6.00	0.112	0.03	0.25
33	Onega Bay	9	0–2	16.27	86.8	3.48	1.44	0.043	0.04	0.37
39	Onega Bay	6	0–2	29.26	68.96	10.24	0.49	0.12	0.5	0.18
40	Onega Bay	9	0–2	67.8	7.71	83.56	2.34	1.031	0.06	0.50
64	Onega Bay	49	0–3	25.24	51.79	25.97	3.73	0.307	−0.307	0.31
113	Onega Bay	17	0–3	36.42	3.31	72.56	3.13	1.66	0.33	2.75

120	Onega Bay	15	0–3	18.35	30.16	27.97	1.15	0.30	0.17	1.42
4705	Onega Bay	61	0–5	н/д	н/д	н/д	1.54	0.55	0.17	1.44
4706	Onega Bay	66	0–5	36.01	8.04	44.96	2.18	0.46	0.24	2.02
4708	Onega Bay	39	0–5	14.72	85.77	2.25	0.16	0.02	0.01	0.10
4709	Onega Bay	56	0–5	26.53	49.56	32.39	0.73	0.38	0.01	0.09
4712	Onega Bay	36	0–5	23.65	66.38	23.84	1.04	0.27	0.02	0.20
4713	Onega Bay	27	0–5	16.93	67.57	21.64	0.50	0.10	0.09	0.78
4714	Onega Bay	52	0–5	37.6	16.95	39.44	1.73	0.80	0.01	0.05

Notation: *ND* no data

sediments on the shallow transect 2 from the mouth of the Onega River to the Solovetsky Islands. In these sediments, with large portion of sandy material, 99% of the total Al content was fixed in lithogenous form (clastic and clay minerals). Thus, our data confirm the totally terrigenous origin of Al, as well as the well-known regularity that the coarse-grained marine sediments are commonly depleted in Al. The content of the form Al-2 (associated with Fe-Mn oxyhydroxides) was negligible (<0.5%), which allows us to conclude about the absence of Al adsorption on amorphous Fe-Mn oxyhydroxides.

Iron In sediments along the axial transect 1, the lithogenous form Fe-4 is the dominant; it amounts 79% on average of total Fe content. Similarly to Al, the total content of Fe is lower in shallow sediments (at depth <50 m) compared to deep stations of the central part and the Kandalaksha Bay (Fig. 2a). The maximum total Fe content (6.8%) was found at Station 4928. As can be seen from Fig. 2a, this was mostly provided by a large portion of the form Fe-2, i.e., amorphous oxyhydroxides, although for all samples the percentage of this form was 16% on average of the Fe total content. In shallow sediments of the Kandalaksha Bay, as well as along the Onega Bay transect 2, where content of the sand fraction reached 85%, the total Fe content was almost twice as less, while portion of the lithogenous form Fe-4 was much larger (Fig. 2b) than that in deep-sea sediments with a predominance of pelitic fraction. From this, it follows that increase in portion of fine-grained sediments leads to growth of the Fe labile fraction, i.e., authigenic amorphous Fe oxyhydroxides.

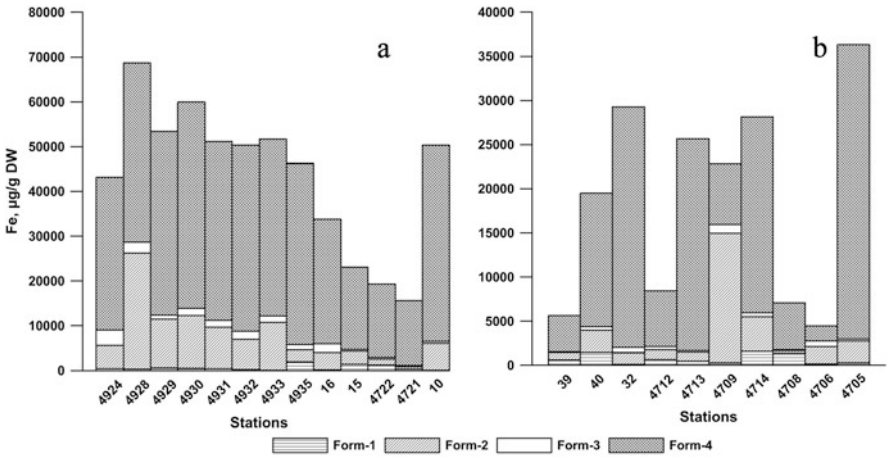

Fig. 2 Occurrence forms of Fe in surface bottom sediments at the axial transect from the Northern Dvina mouth to Kandalaksha Bay (**a**) and at the Onega transect from the Onega River estuary seaward (**b**). Legend: form-1 is metal adsorbed on clay particles and associated with carbonates; form-2 is amorphous Fe-Mn oxyhydroxides and associated heavy metals; form-3 is metal bound to organic matter; form-4 is a residual solid or lithogenous form that contains metals fixed in the crystal structures of detrital and/or clay minerals (complete decomposition with mixture of concentrated HNO_3 and HF)

In surface sediments of the Dvina Bay and the central part of the White Sea (Stations 4928–4931) with increased content of pelitic fraction, the portion of the Fe-2 form (amorphous Fe oxyhydroxides) was also increased till 40% on average. The main "supplier" of Fe in the White Sea basin is the Northern Dvina River runoff, where percentage of amorphous Fe oxyhydroxides accounted for about 20% on average [27]. So we may suppose that geochemical labile Fe forms in the river suspended particulate matter are not only "inherited" but also "multiplied" in the surface marine sediments due to the diagenetic processes, as it will be shown below.

Marine sediments of the continental margins contain around 50% of Fe in the lithogenous form; the geochemical labile Fe oxyhydroxides amount on average 27%, while the less labile Fe (magnetite, organic matter, sulfides) accounts for 23% of Fe total content [10]. These data are in rather good agreement with the results we have obtained.

Manganese The proportion of the Mn forms can be called the opposite ones to that of Al. Along the axial transect 1, 93% on average of Mn total content was represented by the sum of geochemical labile forms (Mn-1, Mn-2, and Mn-3) with a clearly predominant portion (75% on average) of the amorphous Mn oxyhydroxides (form Mn-2). Percentage of lithogenous form accounted for less than 10% on average. Along the transect 1, total Mn content varied from 0.5 to 4.7% dry w.; its increase resulted from growth of amorphous Mn oxyhydroxides. The lithogenous form (Mn-4) remained constantly low (<10%) along this transect 1. The increased Mn total contents (with maximum 4.7% dry w.) were found in the deep Kandalaksha Bay sediments, as well as in the central part of the White Sea. Here, the high C_{org} content (1.5–2%) and the predominance of pelitic fraction (up to 90–95%) in sediments was detected [25]. Both these factors are known to promote an intensive formation of the Mn oxyhydroxides. Our data does not confirm the asymmetry in the Mn distribution pattern along the axial profile: a maximum in the Kandalaksha Bay (0.7%), intermediate content (0.1–0.5%) in the central part, and a minimum (<0.05%) in the Dvina Bay, noted earlier [28].

The main process of Mn accumulation in shallow sediments along the Onega transect 2 has proved to be a formation of amorphous Mn oxyhydroxides (75% of Mn total content), while its total content (average 0.1% dry w.) was almost three times lower than that on the axial transect 1. This may be caused by predominance of the coarse-grained fraction in sediments. We could not notice any regularity in Mn forms' distribution. However, one can say only that in sediments of central deeper part of the Onega Bay, the total Mn content was higher compared with the coarse-grained nearshore areas, as well as near the Solovetsky Islands (Station 4705-1). In these areas, the percentage of lithogenous form Mn-4 was found to be a maximal (42% of total Mn).

3.2 Heavy Metals and Metalloid As

Heavy metals and As are known to occur in bottom sediments in the concentrations commonly less than 100–200 μg/g dry w.

Chromium Distribution of Cr occurrence forms is close to Al, namely, the distinct predominance of lithogenous form, averaging 79% of total Cr content. Remaining portion of Cr is in adsorbed form (Cr-2), mostly in association with Fe-Mn oxyhydroxides. The elevated and even high Cr concentrations (70–118 μg/g dry w.) were detected in the shallow sediments (Stations 4712 and 4713) of the central part of the Onega Bay, in nearshore part of the Kandalaksha Bay, as well as in estuary of the Northern Dvina River. That was obviously due to the fact that sandy-silty sediments of these hydrodynamics active environments contain an essential portion (to 10%) of heavy minerals fraction with a specific gravity of 2.9 g/cm^3; among these minerals, there are grenades or uvarovite which contains Cr as an accessory element [29]. On the other hand, totally sandy sediments of the shallow Onega Bay are characterized by low Cr content (<20 μg/g).

One important fact should be noted: at both transects, summary Cr content in labile forms (Cr-1, Cr-2, and Cr-3) is rather small (20% on average). Along both transects, it changes slightly, while an increase in Cr total content was more likely caused by increase in its lithogenous form.

Cobalt Our data suggest that Co is more labile in the White Sea bottom sediments compared to Cr and Ni: an average percentage of the Co lithogenous form (Co-4) accounts for 35% of its total content. A significant amount of Co (maximum 67%, and 50% on average) was accumulated in sediments of the both transects due to adsorption processes (the sum of the forms of Co-1 and Co-2); a significant contribution was also made by the organic form (Co-3): 15% of the total. The total Co content in sediments of the axial transect 1 was on average three times higher than that of the Onega transect, with the highest concentrations (0–12 μg/g) recorded in the sediments of the Dvinsky Bay and the central part of the White Sea (Fig. 3a). Here, against the background of the constancy of the Co lithogenous form (Co-4), change in the Co total content was determined by the form Co-2, i.e., adsorption processes onto amorphous Fe-Mn oxyhydroxides.

The Co content decreased two to three times in the nearshore part of the Kandalaksha Bay; here contribution of lithogenous form varied greatly. The same could be noted about the Onega Bay sediments (Fig. 3b). There, we have revealed a significant variation in both the total Co content (within five times) and the proportion of its lithogenous and hydrogenous forms that apparently reflected the unstable sedimentation conditions.

Nickel The Ni distribution pattern has a close resemblance with Co, differing in details. We may conclude that terrigenous material (mostly clastic minerals) was a main factor in the Ni accumulation in sediments. The maximum total Ni content (93 μg/g dry w.) was determined in the fine-grained sediments of outer part of the

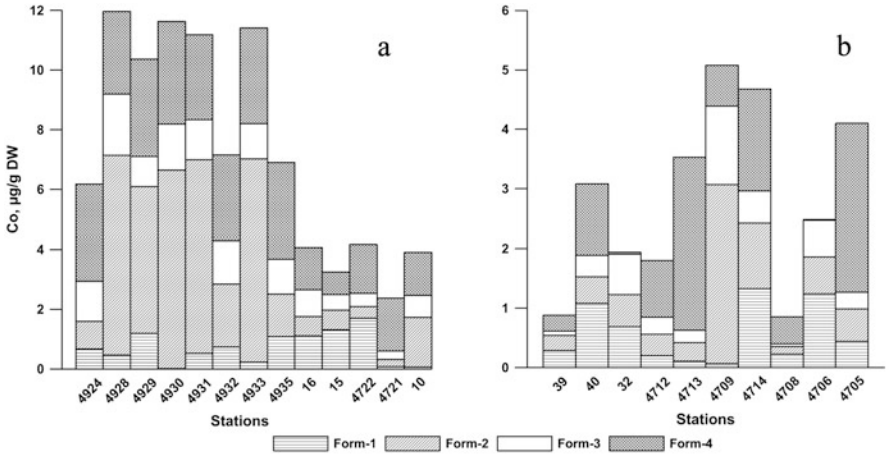

Fig. 3 Occurrence forms of Co in surface bottom sediments at the axial transect from the Northern Dvina mouth to Kandalaksha Bay (**a**) and at the Onega transect from the Onega River estuary seaward (**b**). Legend: see at Fig. 1

Onega Bay (Station 4713), where Ni occurred almost absolutely (up to 95% of its total content) in lithogenous form. In the White Sea as a whole, this form accounts 68% on average of the total Ni content, while the contribution of hydrogenous processes, firstly adsorption and biogenic processes (forms Ni-1, Ni-2, and Ni-3), constitutes 25% on average. It should be noted that the sum of these three labile forms reached up to 60% only at some stations of the central part of the Sea, as well as in the Kandalaksha and Onega Bays. Along with that, in the shallow coarse-grained sediments of the Onega Bay, the Ni total content (similar to that of Cr) was very low (about 10 µg/g dry w.) Fine-grained pelitic sediments at the axial transect contained more Ni (36 µg/g dry w. on average). In the same way, as for the Cr, the change in the Ni content on both transects was provided by lithogenous form's increasing or decreasing, which was probably connected with changes of grain-size composition of sediments which are under the control of hydrodynamic factors.

Cupper In the White Sea sediments, majority of Cu occurs in the labile geochemical forms (sum of Cu-1, Cu-2, and Cu-3) constituting from 55 to 88% of the total content (70% on average). The deeper sediments lay, the more percentage of the fine-grained fraction and the higher Cu content is in sediments. The Dvina Bay and the deep part of the Kandalaksha Bay displayed an almost constant distribution of Cu total – 10.5 µg/g dry w. on average (Fig. 4a). This value is significantly (two times) higher than that in the shallow Onega Bay (Fig. 4b).

Such a distribution pattern of Cu is similar to Fe and Co (see above). A distinctive feature of the Cu from other metals is that organic matter plays an essential role in its accumulation in the bottom sediments: the Cu-3 form accounted 35% of the total Cu content on average. The largest portion of Cu bound to organic matter (form Cu-3) was determined in fine-grained sediments of the Dvina Bay (Station 4924,

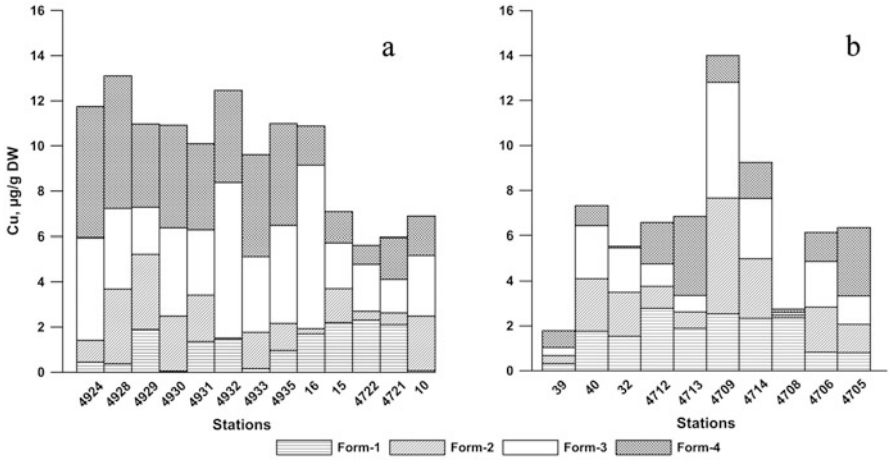

Fig. 4 Occurrence forms of Cu in surface bottom sediments at the axial transect from the Northern Dvina mouth to Kandalaksha Bay (**a**) and at the Onega transect from the Onega River estuary seaward (**b**). Legend: see at Fig. 1

Fig. 4a) and the Kandalaksha Bay (Station 4932), as well as in the silty-sandy sediments of the Onega Bay (Station 4709, Fig. 4b). The substantial formation of the Cu-organic complexes may be referred to a specific biogeochemical property of Cu that is characteristic not only for bottom sediments but also for marine and ocean suspended particulate matter enriched in biogenic (plankton) substance [7, 30]. The same proportion of Cu (35% of total content) was accumulated in sediments as a result of adsorption processes (sum of Cu-1 and Cu-2 forms). On the other side, the maximum Cu total content (10.8 μg/g dry w.) was recorded at the relatively "deep-sea" Station 4709 (56 m depth) (Fig. 4b). There, we found a high portion of organically bound Cu (50%), while the sandy fraction was also large (about 50% of sediment mass). So, it is rather difficult to discern any regularity in the Cu forms' change along this transect.

Lead The mean Pb concentration in the White Sea sediments was detected as 12.5 μg/g dry w.; this value is close to background values (14.2 μg/g dry w.) [31]. From our data, it follows that the main process of Pb accumulation in bottom sediments is adsorption on amorphous Fe-Mn oxyhydroxides (Pb-2 form) and on clay minerals (Pb-1 form) contributing, respectively, 60 and 18% of Pb total content on average. Percentage of lithogenous processes' contribution did not exceed 20% on average, and it has proved to be almost constant in sediments. The Pb distribution, both of its total content and forms, has proved to be different along the both transects. In fine-grained and enriched in C_{org} (up to 2.5%) sediments of the Kandalaksha Bay, the mean Pb total content (17 μg/g dry w.) was higher by a factor of three compared to that in the shallow coarse-grained sediments of the Onega Bay (Fig. 5a, b). However, in both cases, a growth of Pb total content resulted from the adsorption complex (Pb-1 and Pb-2 forms) whose contribution increased till 95% in sediments at some stations.

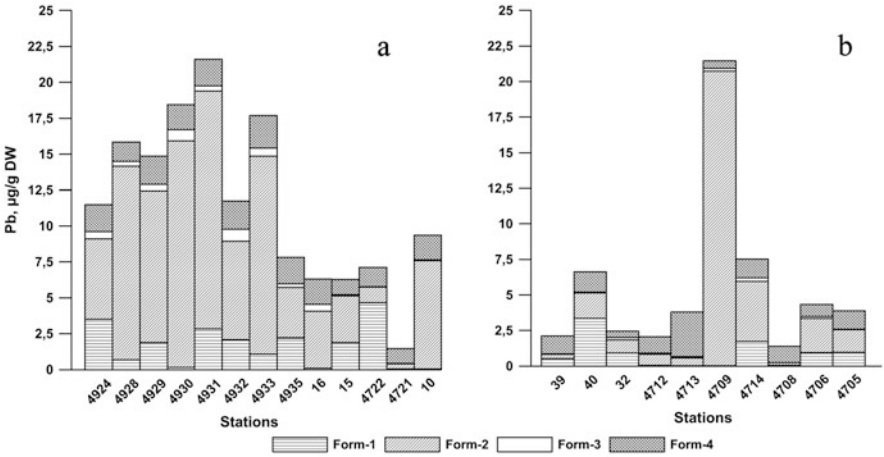

Fig. 5 Occurrence forms of Pb in surface bottom sediments at the axial transect from the Northern Dvina mouth to Kandalaksha Bay (**a**) and at the Onega transect from the Onega River estuary seaward (**b**). Legend: see at Fig. 1

Cadmium The total content of Cd in the sediments ranges from 0.06 to 0.18 (0.10 on average) µg/g dry w. That is slightly lower than background value for Arctic areas −0.14 µg/g dry w [31]. Similarly to Mn, distribution of the Cd forms was characterized by an absolute predominance of geochemical labile forms (Cd-1, Cd-2, and Cd-3), totaling from 73 to 90% (87% on average) of Cd total content for the whole White Sea. Adsorption processes on the clay particles (Cd-1 form) and amorphous Fe-Mn oxides (Cd-2 form), contribute 77% in sum. In organic matter (Cd-3 form), there were only 10%. From this it follows that increase in Cd total content was mainly caused by the labile forms in the White Sea sediments. The total Cd content at both transects was approximately the same, although the peak Cd content (0.18 µg/g dry w.) was recorded in shallow water (<40 m) sediments (Station 4712) at the Onega transect where the contribution of lithogenous form was also significantly higher (up to 50% of the total) than that at the axial transect 1.

Arsenicum According to AMAP [32], in the bottom sediments of the most polluted Mediterranean Sea ports, the As total content reached 99 µg/g dry w., with up to 35% of As being adsorbed on the Fe-Mn oxyhydroxides and about the same amount associated with organic matter and sulfides. Only 17% of the As total concentration was detected in lithogenous form. Meanwhile, in relatively uncontaminated Mediterranean Sea areas, very low As total content was detected (11 µg/g dry w.), of which about 30% were fixed in lithogenous form. Rather low As mean content (23 µg/g dry w.) was found in the silty-pelitic Baltic Sea bottom sediments nearby the burial place of chemical weapons [33].

According to our data, the average As total content 26.3 μg/g dry w. somewhat exceeded the background value (20 μg/g dry w.). Proportion of the As forms was characterized by a distinct predominance of lithogenous form: 75% of the As total content. Adsorption processes, mainly on amorphous Fe-Mn oxyhydroxides (form As-2), contribute only 20% As into sediments, while forms reflecting association with organic matter and adsorption on clay minerals As-1 almost have no significance (5% of As total content). An increased content of the As adsorbed form (up to 50% of total content) was determined in silty-pelitic sediments of the White Sea central part, as well as in the Kandalaksha Bay deep area, whereas the As lithogenous form dominated strongly (85–90% of the total As) in the shallow areas of the Kandalaksha and Onega Bays. In the latter, As total content was significantly less compared to deeper sediments of the axial transect 1.

Statistical processing of the whole dataset obtained by applying the R-factor analysis was performed. The type of factoring has been selected as the principle components with the varimax rotation. The aim was to evaluate contribution of biogeochemical processes (nine factors) to the trace metal accumulation in the surface bottom sediments of the White Sea. The variables of factor analysis included the physicochemical occurrence forms of trace elements and basic geochemical parameters (C_{org}, C_{carb}, BSi), as well as depth of the sampling station. As a result, nine factors accounting for 85.2% of the variability in the dataset were obtained (Fig. 6).

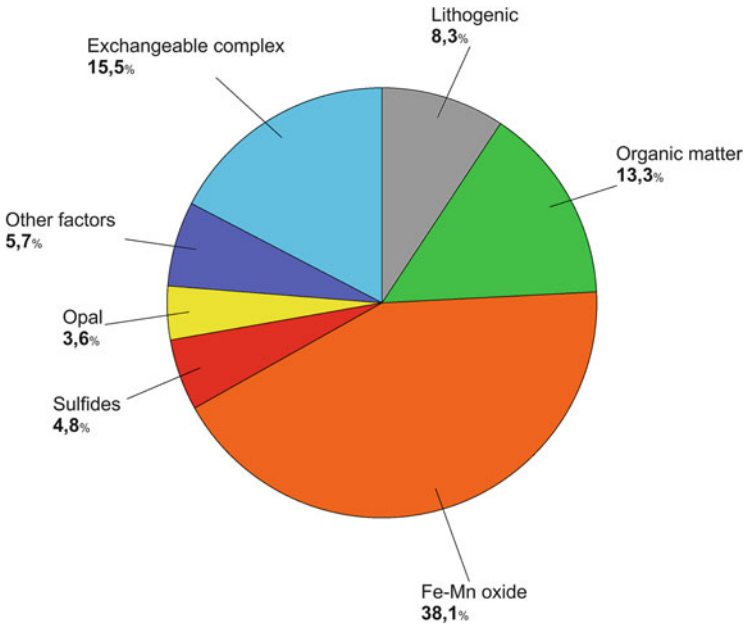

Fig. 6 Assessment of different factors that influence heavy metal accumulation in surface bottom sediments of the White Sea based on R-factor analysis, PCA type, varimax method

From Fig. 6, one can see that accumulation of trace metals in the surface sediments is influenced by adsorption processes on the Fe-Mn oxyhydroxides (38%) and exchangeable complex on clay minerals (15.5%) whose sum contribution accounts for about 54%.

Comparison of our average data on metal forms in surface layer of bottom sediments with similar data on suspended matter of the Northern Dvina River [27] let us to elucidate in the first approximation what changes undergo the metals in river suspended load during sedimentation in the White Sea. From Fig. 7, it can be seen that the partition of metal occurrence forms in the Northern Dvina River's particulate

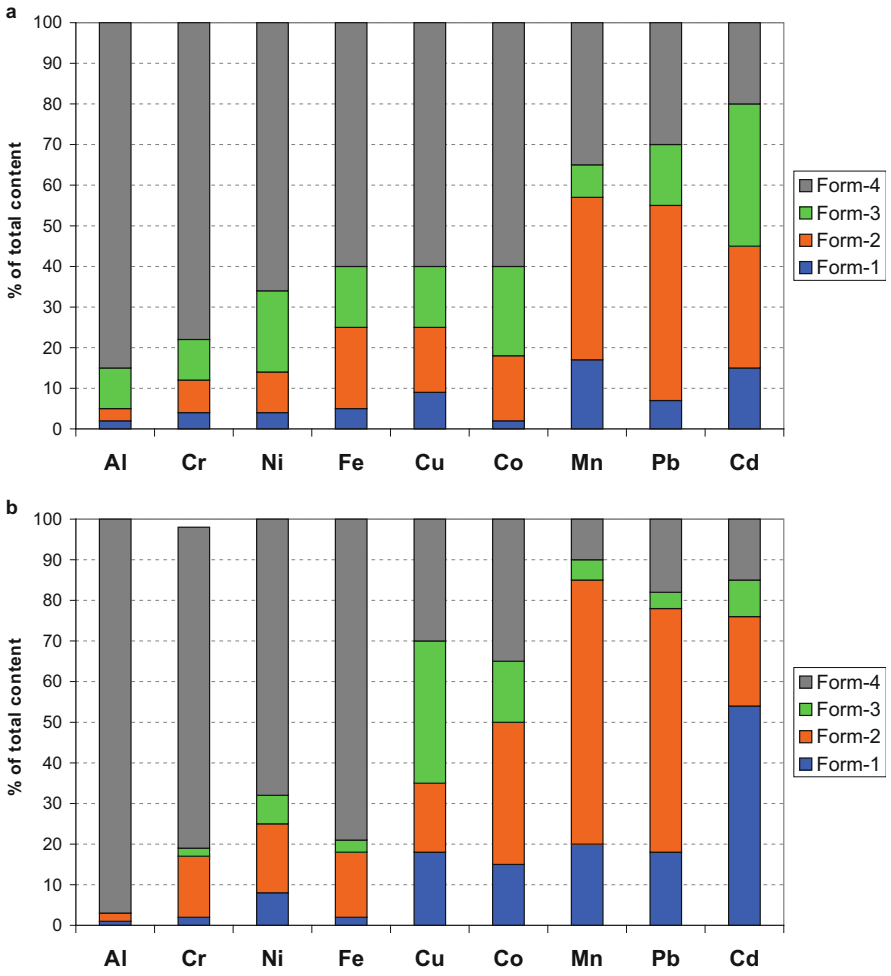

Fig. 7 Comparison of partition of occurrence forms of Al and heavy metals (% of total content) in suspended particulate matter of the Northern Dvina River (**a**) [27] and in surface bottom sediments of the White Sea (**b**). Legend: see at Fig. 1

matter (Fig. 7a) and surface bottom sediments (Fig. 7b) is generally similar. During the migration from the mouth of the Northern Dvina River in Dvinsky Bay and further seaward to the central part of the White Sea, partition of the Al, Fe, Cr, Co, and Ni forms exhibits the smallest change while that of Mn – the largest one. In the surface 0–5 cm layer of bottom sediments, Mn becomes the most mobile due to the reducing diagenesis, as it will be shown below. The Cd, Cu, and Pb content in geochemical labile form-1 and form-2 was noticeably higher in the surface sediments compared to river suspended particulate matter. Obviously these heavy metals were mobilized during precipitation of suspended particles when passing through the water column due to the adsorption on Mn-Fe hydroxides.

4 Occurrence Forms of Heavy Metals at the Early Diagenetic Stage

Diagenetic changes in bottom sediments begin immediately after the deposition of dispersed sedimentary matter, followed by the long-term transformation of sediment into sedimentary rocks, such as sediment consolidation and changes in the mineral and chemical composition. Early diagenesis starts on the bottom water-sediment contacting zone in the surface layers. Early diagenesis involves various processes, primarily redox processes, which accompany the transformation of organic matter (OM), as well as sediment consolidation due to decrease of its water content and transformations of its mineral and chemical composition [34].

In the uppermost sediment layer, the biogeochemical processes with the participation of heterotrophs and autotrophs are the most intense [35]. In the central part of the White Sea, diagenetic processes resulted in the organic matter oxidation that has led to a reducing environment in sediments [36]. The concentrations of geochemical reactive Fe and Mn occurrence forms strongly changed with depth [28, 37]. Species of the reduced sulfur, as derivatives of bacterial hydrogen sulfide, have a tendency to precipitate already in the upper sediment layers, and their contents increased with depth [38, 39].

By the use of a Neimisto tube, as well as Multicorers samplers, we have got a possibility to study diagenetic processes correctly due to sampling undisturbed sediment layers of high resolution (at scale of <1–2 cm). Site 1404 that we tested is situated at a terraced continental slope in the central part of the White Sea. The slope is covered with Holocene sediments, in which according to classification of [40], a pelitic fraction (particles <0.01 mm) dominated: the content of this fraction in the sediment core varied from 85.05 to 95.77% (Fig. 8a).

The uppermost layers (horizon 0–6 cm) composed of oxidized brown silt were enriched in water: the maximum water content was 77.34% in 0–1 cm layer. Below this, in the 2–5 cm layer, oxidized sediments become the grayish brown color and then the olive-gray ones. The lower portion of the examined core (from 6 to 44 cm) was fairly homogeneous, was more dense (the average density is 67.10%), and was

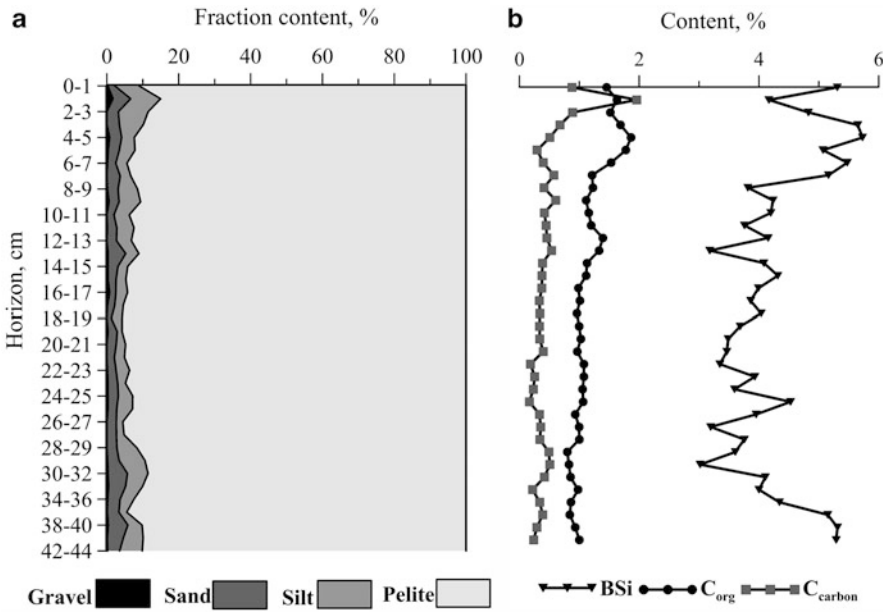

Fig. 8 Grain-size composition (**a**), concentrations of $C_{organic}$, $C_{carbonate}$, and SiO_{2bio} (**b**) in sedimentary core at Station 1404 (65°23,291′ N; 37°14,773′ E, water depth 150 m)

dominated by gray pelitic ooze (90–95%) with minor admixtures of sand and gravel (2.58 and 0.21% on average, respectively) (Fig. 8a). The sediment layers deeper than 6 cm contain nodules of amorphous Fe sulfides and were riddled with randomly oriented burrows filled with hydrotroilite ($FeS{\cdot}nH_2O$), which suggested the conditions were reduced. The bottom sediments contain relatively little C_{org} (<2%) and $CaCO_3$ (<1% on average) that are typical of Arctic shelf seas [41, 42]. The content of C_{org} gradually decreased with depth as much as twice (Fig. 8b). Given the insignificant variations in the pelitic fraction's content, this suggests that organic matter was oxidized down the core.

Concentrations' limits and average values of elements studied in the 44 cm sediment core are listed in Table 2, where one can see that variations in contents were rather different for different elements. The largest difference between the minimal and maximal contents could be seen for Mn (100-fold) and Mo (40-fold), while for the rest of elements, variations did not exceed fourfold. This evidently could testify by indirection a high geochemical lability of Mn and Mo.

Aluminum The geochemical inert lithogenous form of Al was absolutely prevailed throughout the core length constituting on average 97% of the total content (Fig. 9a).

This fact reflects the predominance of terrigenous material in the bottom sediments of the White Sea [18, 19], as well as it confirms the correctness of applying the Al as an indicator of terrigenous input to bottom sediments. The total Al content's

Table 2 Concentrations of Al, Fe (%), and trace elements (μg g^{-1} dry w.) in sedimentary core 1404 of the White Sea ($n = 37$)

	Al, %	Fe, %	Mn	Cd	Co	Cr	Ni	Cu	Mo	Pb	As
Min–max	2.08–6.64	4.25–6.66	523–53,038	0.065–0.25	13.3–27.8	78–157	40.9–77.4	19.5–42.5	0.67–25.4	9.2–25.5	20.3–38.7
Average	4.93	5.14	5,703	0.11	19.6	123	59.4	29.3	3.39	13.6	27.73

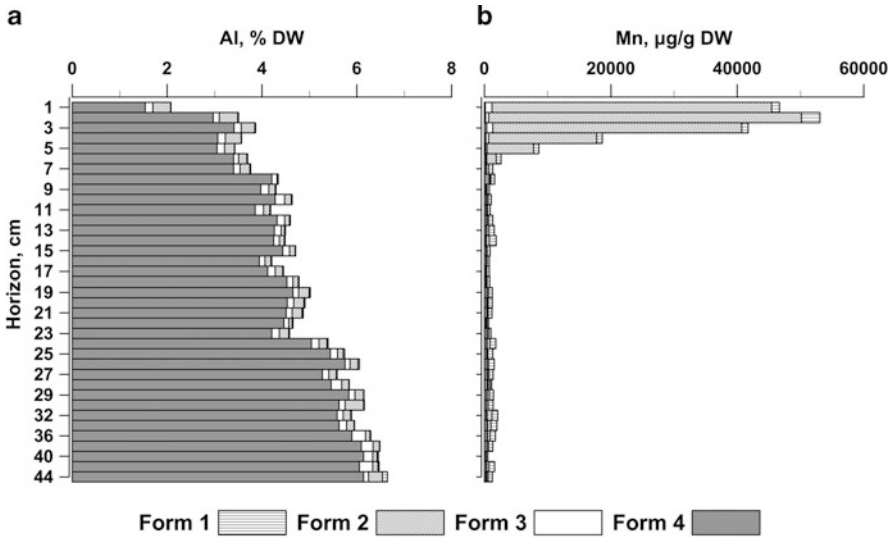

Fig. 9 Partition of the Al (**a**) and Mn (**b**) occurrence forms in sediment core at Station 1404. Legend: see at Fig. 1

distribution displayed a trend to increase down the core from its minimal value (2%) in upper layer to 5.5% at the core bottom. It could be explained by growth of the river runoff in the Russian Arctic which has increased over the past 80 years [42] and earlier, which led to the increased supply of terrigenous material.

Manganese Within the 0–6 cm layer Mn was almost completely (90–95% of its total content) constituted of amorphous oxyhydroxides (form-2). Total Mn concentration has drastically decreased within the 0–6 cm layer from 4.42 to 0.15% (Fig. 9b) by a factor of about 30, and the concentration gradient (grad Mn = $\Delta C/\Delta L$) was 4.42–0.15%/6 cm = 0.71%/cm. The redox potential Eh in the near-bottom water of the White Sea varied from +225 to +471 mV [36, 38]; however, in the upper 0–20 cm layer of bottom sediments, a negative Eh (−176 mV) was detected, which implies a presence of sulfate reduction. Under conditions of oxygen loss which was spent for organic matter oxidation, the diagenetic process became a reducing one when fast reduction of Mn(IV) to Mn(II) and migration of the latter into the pore water took place. This was suggested by drastically increased concentration of dissolved Mn in the vertical profile of the pore water – from 1.2 mg/l at 0–2 cm horizon to 18 mg/l at 6 cm horizon, these high values remained at greater depths (Fig. 10). The low Mn concentration in the pore waters in the upper 0–2 cm layer (1.2 mg/l) was more likely caused by the diffusion fluxes from sediments to near-bottom waters, as it was established earlier [28, 36, 38, 43, 44].

Deeper the 6 cm horizon, Mn occurred mostly in form-1 (Fig. 9b), which controls exchange processes between the pore water and sediments. Our data show that Mn-1 form and carbonate content are directly correlated ($R2 = 0.89$) varying

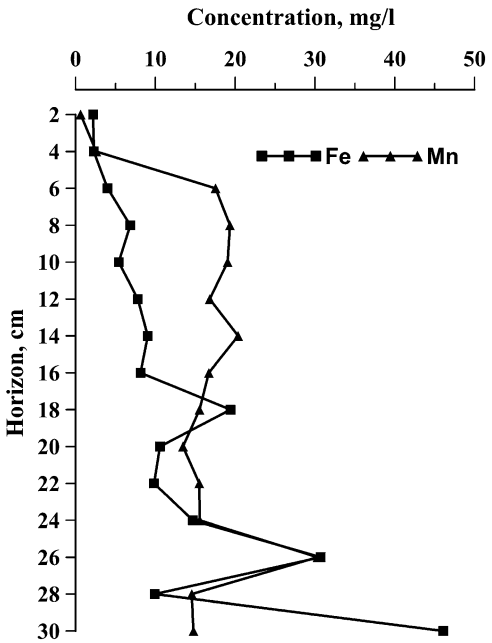

Fig. 10 Change in dissolved Fe and Mn concentrations (mg l^{-1}) in pore water of sediment core at Station 1404

synchronously down the core; it may suggests that Mn is mostly contained in carbonate minerals mostly in this form-1. The content of lithogenous form Mn-4 varied rather insignificantly.

Iron Unlike Mn, the dominant quantity of Fe (80% on average throughout the sediment core) was determined in lithogenous form (Fe-4), whose content rose downward. Only within the 0–6 cm layer, Fe was roughly equally distributed between amorphous oxyhydroxides (Fe-2 form) and lithogenous form (Fe-4). Deeper than 6 cm, the form-2 decreased noticeably, and lithogenous form was prevailing down the core. The Fe concentration in pore water increased from 2.1 mg/l at the 0–2 cm horizon to 6 mg/l at 6 cm (Fig. 10), so concentrations of Fe dissolved in pore water did not display such a sharp increase with depth as the Mn did. That could be explained by a different kinetic of the Fe and Mn redox processes, namely, Fe is oxidized faster than Mn in reducing environments, while Mn is reduced more fast than Fe. This apparently could result in low value of concentration gradient of the amorphous Fe oxyhydroxides (0.06%/cm), which was almost one order of magnitude smaller than that for the Mn oxyhydroxides (0.71%/cm).

The Mn/Fe ratio is conventionally used to estimate the oxygen paleodynamics [45] and, hence, the redox parameters of the sedimentation. A novelty of our approach is to show Mn/Fe ratio expressed not only as total content of Mn and Fe but as a ratio of their occurrence forms (Fig. 11).

So the high value of Mn/Fe ratio should reflect a predominance of the Mn geochemically labile forms over that of Fe. If to consider a Mn/Fe ratio's distribution

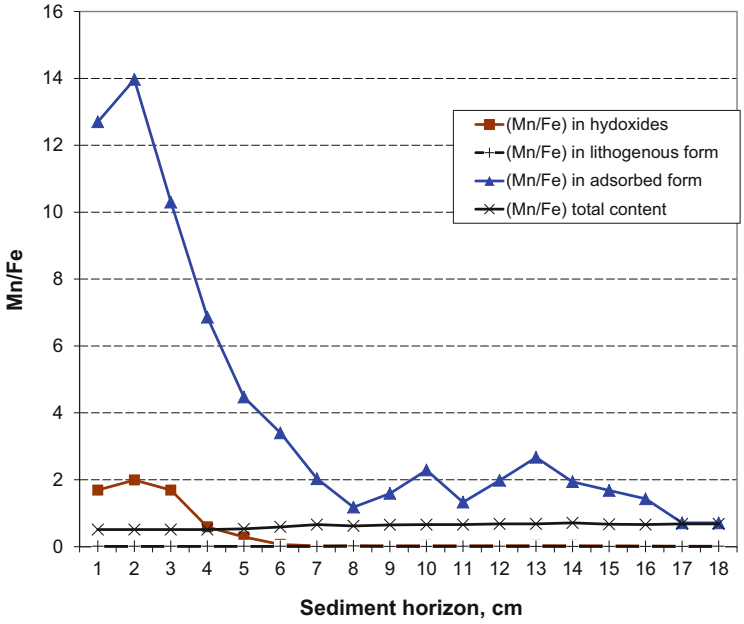

Fig. 11 Change in Mn/Fe ratio in geochemical labile forms along the sediment core at Station 1404

pattern along the core Station 1404, one may notice that after the peak of the ratio of the Mn/Fe labile forms (adsorbed form-1 and oxyhydroxides form-2) at horizon 1–2 cm layer, the Mn/Fe ratio sharply decreased at 6 cm horizon and remained constantly low down the core (Fig. 11). Such a sharp decrease in the Mn/Fe labile forms' ratio apparently was due by their desorption while pH decreased. During the oxidation of organic matter in the sediment core, value of pH commonly decreases; this phenomenon was firstly described by Yu Gursky [37]. From this one may suppose that below the 6 cm horizon, the early diagenetic processes in sediments started to stabilize. It should be noted that according to the lithological description in many layers, the hydrotroilite concretions were noticed, which can also serve as manifestation of reducing diagenesis.

Molybdenum Molybdenum, along with Mn, is one of the most sensitive metals to changes in redox conditions, both in the near-bottom water and in sediments. For Mo it is characteristic to be adsorbed or onto the amorphous Mn oxyhydroxides or to be associated with sulfidic minerals [46]. From our data, a distribution of Mo, especially of its labile forms, is similar to Mn: in the 0–2 cm layer, the Mo displayed the total concentration peak (24 μg/g dry w.) followed by a sharp downfall to 3.1 μg/g dry w. at 6 cm horizon (Fig. 12a).

From Fig. 12a, one can see that this abrupt drop was evidently caused by the Mo labile forms, associated with Mn oxyhydroxides (Mo-2 form), as well as adsorbed onto the clay minerals (Mo-1 form). Unlike Mn, a distinguishing feature of Mo was a relatively high Mo content in form-3 (bound to organic matter and/or sulfides).

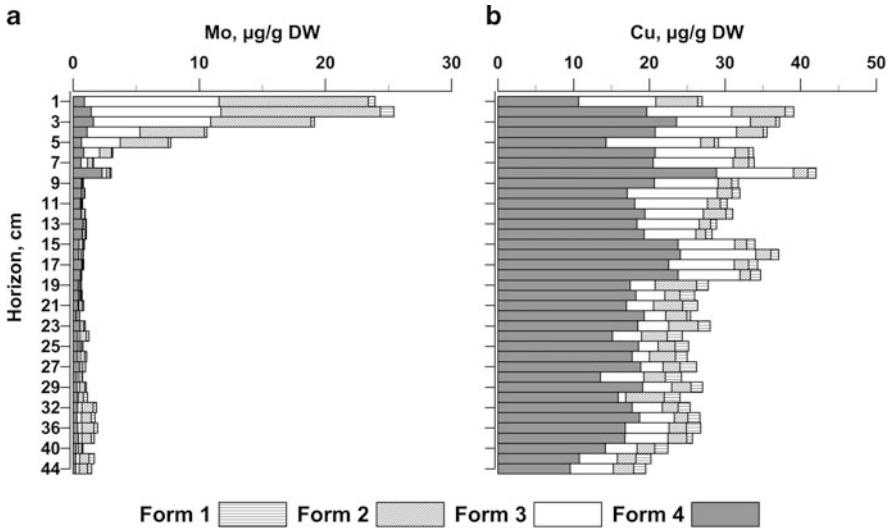

Fig. 12 Partition of the Mo (**a**) and Cu (**b**) occurrence forms in sediment core at Station 1404. Legend: see at Fig. 1

Percentage of the Mo-3 form content in the 0–6 cm layer was comparable with that in the Mo-2 form content −40% of the Mo total concentration on average. Below the 6 cm layer, the total Mo content was no higher than the Mo mean content in lithosphere (2 μg/g dry w.).

Chrome and Nickel Cr and Ni were closest to Al in terms of the lithogenous form's contribution: 90 and 75% on average, respectively, of total content. The minimum of Cr and Ni total content coincided with the lithogenous form's minimum was detected in the uppermost oxidized fluffy layer (0–1 cm). On the contrary, the peaks of lithogenous forms of Cr and Ni were found in the 8–16 cm layer with an increased proportion of silt and sand fractions. The contribution of lithogenous form seemed to be risen down the core, while proportion of their geochemically mobile form-1, form-2, and form-3 decreased. However, there was a difference between the Cr and Ni vertical distribution: the Cr lithogenous form absolutely dominated throughout the core, while in the surface 0–8 cm layers, the Ni adsorption on amorphous Fe-Mn oxyhydroxides plays a noticeable role (to 25% of total content).

Cobalt From our data, Co is a more labile heavy metal compared to Cr and Ni: about 33% on of total Co content was accumulated in sediments due to adsorption processes (sum of forms Co-1 and Co-2) and binding to organic matter and/or sulfides (form Co-3). Similar to Mn, Fe, and Mo, the Co labile forms have a significant proportion (48% on average) in the upper 0–6 cm layers; the main part belongs to adsorption on the amorphous Fe-Mn oxyhydroxides. The thickness of 0–6 cm was formed over the last 50–75 years [47]; thus we may conclude that the recorded Co-2 form's peaks reflected a contribution of anthropogenic

components in the accumulation of Co. Namely, in this time period, the industry related to Co mining was developed.

Copper Contribution of the Cu labile forms (Cu-1, Cu-2, and Cu-3) exceeded 50% on average throughout the core, i.e., a little more than that for Co. A distinctive feature of Cu was its tendency to be bound to the organic matter: about 25% on average throughout the column while in the surface layer – up to 40% (Fig. 12b). In oxidation processes of organic carbon followed by strengthening of reducing conditions down the core, the form Cu-3 could possibly be composed not only of organic matter but both of the Cu adsorption complex on sulfides. About 10–20% of total Cu content was accumulated in sediments due to adsorption on amorphous Fe-Mn oxyhydroxides. In the surface layers (up to 10 cm), percentage of the Cu labile forms was elevated similarly to Fe, Mn, Mo, and Ni. Peaks of total Cu content were detected in the horizon 9 cm that formed within 100 years, possibly due to an anthropogenic factor.

Cadmium and Lead From our data, these toxic heavy metals are characterized by increased contribution of adsorption processes to their accumulation in sediments. In the Cd accumulation, the two types of adsorption have approximately an equal contribution amounting to 35% of total content: on amorphous Fe-Mn oxyhydroxides (form Cd-2) and on clays (form Cd-1) (Fig. 13a).

As to processes that control the Pb accumulation, the adsorption on amorphous Fe-Mn oxyhydroxides dominated (form Pb-2) absolutely reaching up to 60% of labile forms' sum. The proportion of these geochemically labile form exceeded the lithogenous form in most layers, especially in the surface layers (to 9 cm), where

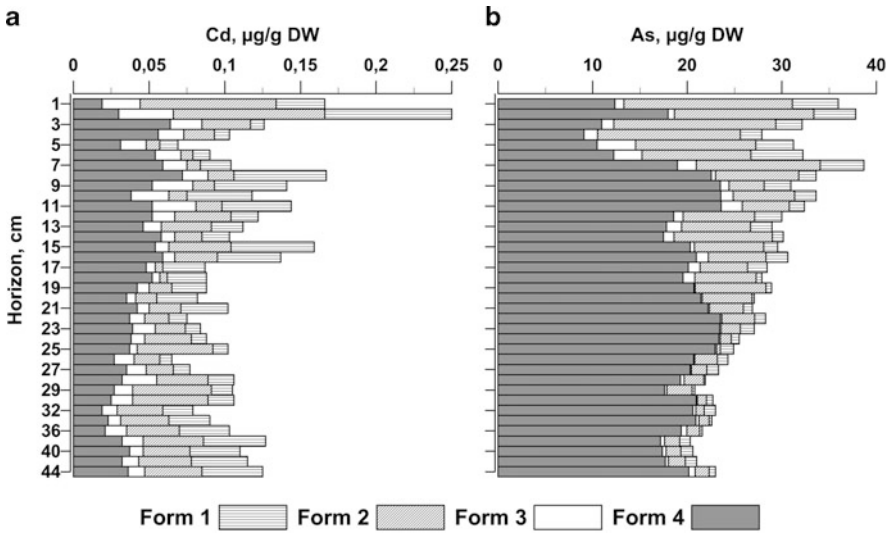

Fig. 13 Partition of the Cd (**a**) and As (**b**) occurrence forms in sediment core at Station 1404. Legend: see at Fig. 1

the processes of Cu and Pb binding with organic matter (forms Cd-3 and Pb-3) are important. Lithogenous forms (Cd-4 and Pb-4) have a minimal contribution in the surface layers, displaying a tendency to slight increase down the core. As a whole, the accumulation of Cd and Pb in the vertical profile of the sediment core has resulted from hydrogenous processes, and only to 30–40% it was related to terrigenous processes.

Arsenic According to our data, two different types of accumulation of metalloid As have been revealed in the sediment core. In the surface layers (0–10 cm), As was accumulated due to mainly (50% of total content) adsorption on amorphous Fe-Mn oxyhydroxides (form As-2) and to a lesser extent (15%) adsorption on clay minerals (form As-1). Down the core, the role of both these geochemical-mobile forms was significantly decreased, and below the 23 cm horizon, the lithogenous form As-4 was dominant (Fig. 13b). Along with this, the As total content was also considerably reduced from the upper layers to the lower ones: from 36 to 22 μg g^{-1} dry w. It should be noted that the elevated As concentration (>30 μg g^{-1} dry w.), as well as large percentage of the labile forms in the nearshore marine sediments of the Mediterranean Sea, testified on their pollution [32]. So we can propose that the high enough As content in uppermost layers (0–7 cm) resulted from anthropogenic influence over recent 100 years, while elevated As content in deeper part of the core was due to geochemical transformations in the processes of early diagenesis.

Based on the average sedimentation rate in the White Sea, being equal to 1–1.5 mm/year [47], and assuming that this rate did not considerably vary, the high-resolution analysis of the bottom sedimentary core (with 1–2 cm discreteness) allows us to estimate short-term (10–15 years) variations in the heavy metals accumulation. A 10-cm-thick layer was deposited over span of 120 years when the anthropogenic load increased because of progress in the local mining industry. This fact likely correlates to peaks of Cd concentration in the 1–2 cm horizon of sediments accumulated 10–30 years ago, as well as to peaks of Cu, Pb, Ni, Cr, and Co in the 7–8 cm horizon which was formed approximately 70–100 years ago.

5 Conclusions

For the first time, based on the analysis of physicochemical forms of metals, the main processes that control accumulation of heavy metals (Mn, Fe, Mo, Cr, Ni, Co, Cu, Pb, Cd, As), in the Holocene bottom sediments of the White Sea, have been quantified.

In the oxidized surface bottom sediments of the White Sea, lithogenous form that reflects a contribution of terrigenous material predominated for rock-forming elements Al and Fe (98% and 79% of the total on average, respectively), for Cr (79%) and Ni (68%) which are fixed in the crystal structure of accessory minerals, as well as for metalloid As (75%). This confirms the major contribution of terrigenous processes in the White Sea sedimentation. On the other hand, some for certain

elements, the geochemical properties of elements are of importance in their occurrence forms' partition. The Mn which is known to be the most redox sensitive metal demonstrated the greatest contribution of geochemical labile forms (on average 85% of its total content). The major Mn occurrence forms were the amorphous oxyhydroxides and associated with carbonate minerals. For the other heavy metals (Cd, Pb, Co, and Cu), the labile forms also predominated (>65% of total content of each metal). Among heavy metals studied, Cu and Mo showed a tendency to be essentially accumulated in association with organic matter (35–40% of total), whereas adsorption processes on amorphous Fe-Mn oxyhydroxides contributed the largest proportion of Pb (60% of total content) and that on clay minerals – of Cd (55% of total content).

The increased contents of geochemical labile forms of metals were found mostly in the fine-grained pelitic sediments which have high adsorption capabilities. Decreased total metal contents were generally recorded in shallow water (depth less than 40 m) bottom sediments of the Gulf of Onega where silty-sandy fractions dominated as usual in the grain-size composition. An increasing order of the average percentage of the elements' labile forms in the surface bottom sediments was as follows: Al < Fe, Cr < As < Ni < Co < Cu < Pb < Cd < Mn.

Based on the total heavy metal content, we may consider the White Sea bottom sediments as uncontaminated ones due to low anthropogenic activity in its basin. The exception was As whose average content was found to lay in an intermediate position between the strongly polluted sediments of some ports and the clean bays of the Mediterranean Sea.

In the White Sea, the behavior of trace elements in the processes of early diagenesis was in fact unknown up to date. We were the first to apply a modified method of sequential chemical leaching to recognize differences in the trace metal behavior during early diagenesis of the Holocene bottom sediments based on the high-resolution analysis (1–2 cm scale). A detailed record of the Fe, Mn, Al, Cr, Co, Mo, Ni, Cd, Cu, Pb, and As behavior within the 44 cm sediment core was documented by their occurrence forms. In most cases, there was a significant increase in the proportion of geochemical labile metal forms in the 0–6 cm layer. There, we have detected the maximum content of Fe and Mn in the two labile (absorbed/carbonate and authigenic Mn-Fe oxyhydroxides) forms. The Mn/Fe ratio in these forms has been strongly changed during early diagenesis. Values of the Mn/Fe ratio (sum of the two labile forms) were the highest in the 1–2 cm upper oxidized sedimentary layer, decreasing sharply in the 6–7 cm horizon, and remained constantly low in deeper sedimentary layers. We suppose Mn/Fe ratio to be applied as a proxy of the early diagenesis of the bottom sediments.

Throughout the 44 cm sediment core, lithogenous form of Al, Cr, and Ni accounted 97, 86, and 68% on average of total content of each metal correspondingly. The sum of three labile forms of Cu, Cd, Pb, and Co (adsorbed on clays/carbonates, authigenic Fe-Mn oxyhydroxides, and bound to organic matter) and their inert (lithogenous) forms contributes approximately equal portions into accumulation of these metals in the bottom sediments. Mn and Mo were found to be the most labile metals: only till 10% of their total content occurred in lithogenous form

in the upper 0–6 cm layer, while down the core portion of this form increased progressively. A diagenetic alteration of most elements (except Al, Cr, and Ni) took place in the uppermost sediment horizons.

Acknowledgments This chapter was prepared on base of bottom sediments sampling and analytical processing in accordance with the state task, the Russian Academy of Sciences for 2017–2018, theme No 0149-2018-0016; the authors thank the Russian Scientific Foundation (Project No 14-27-00114-П) for the financial support over the period of generalization of the data obtained.

References

1. Chester R, Massina-Hanna KG (1970) Trace element partition patterns in Northern Atlantic deep-sea sediments. Geochim Cosmochim Acta 34(10):1121–1128
2. Gibbs RI (1977) Transport phases in the Amazon and Yukon Rivers. Geol Soc Am Bull 88(6):829–843
3. Demina LL, Gordeev VV, Fomina LS (1978) Forms of iron, manganese, zinc and copper in river water and their changes in the mixing zone of river and sea waters (by an example of the rivers of the Black, Azov and Caspian Seas basins). Geochem Int 8:1211–1229
4. Chudaeva VA, Gordeev VV, Fomina LS (1982) Phase state of the elements in suspended matter of some rivers of the Japan Sea basin. Geochem Int 4:585–596
5. Lukashin VN (1983) Forms of elements in sediments. In: Lisitsyn AP (ed) Biogeochemistry of the ocean. Nauka, Moscow, pp 312–344. (in Russian)
6. Demina LL, Shumilin EV, Tambiev SB (1984) Trace metal speciation in suspended matter of the Indian Ocean of surface water. Geochem Int 4:565–576
7. Raiswell R, Canfield DE (1998) Sources of iron for pyrite formation in marine sediments. Am J Sci 298:219–245
8. Raiswell R, Canfield DE (2012) The iron biogeochemical cycle: past and present. Geochem Perspect 1(1):6–221
9. Poulton SW, Raiswell R (2002) The low-temperature geochemical cycle of iron: from continental fluxes to marine sediment deposition. Am J Sci 302:774–805
10. Lisitsyn AP, Novigatsky AN, Shevchenko VP, Kluvitkin AA, Filippov AS, Kravchishina MD, Politova NV (2014) Dispersed forms of sedimentary matter in the ocean and seas on the example of the White Sea (results of 12 years of research). Dokl Earth Sci 456(3):355–359
11. Lisitsyn AP (2014) Current views on the sedimentation in the ocean and seas: the ocean as a natural recorder of the geosphere's interaction. In: Nigmatulin RI, Libkovsky LI (eds) The World Ocean, vol 2. Nauchnyi Mir, Moscow, pp 331–553. (in Russian)
12. Kukina SE, Sadovnokova LK, Kalafat-Frau A, Palerod R, Hummel K (1999) Occurrence forms of metals in bottom sediments of selected estuaries of the White and Barents Seas. Geochem Int 12:1324–1329
13. Demina LL, Levitan MA, Politova NV (2006) About occurrence forms of heavy metals in bottom sediments of the Ob and Yenisei Rivers estuaries (the Kara Sea). Geochem Int 2:212–226
14. Nevessky EN, Medvedev VS, Kalinenko VV (1977) The White Sea: sediment formation and development history in Holocene. Nauka, Moscow. 236 pp (in Russian)
15. Lisitsyn AP, Nemirovskaya IA (eds) (2012) The White Sea system. Vol II Water column and interacting with it atmosphere, cryosphere, river runoff and biosphere. Scientific World, Moscow. 783 pp (in Russian)
16. Lisitsyn AP, Nemirovskaya IA (eds) (2013) The White Sea System. Vol III Dispersed sedimentary matter in hydrosphere, microbial processes and water pollution. Scientific World, Moscow. 665 pp (in Russian)

17. Lisitsyn AP, Nemirovskaya IA (eds) (2017) White Sea System. Vol IV The processes of sedimentation, geology and history. Scientific World, Moscow. 1028 pp (in Russian)
18. Novigatsky AN, Lisitsyn AP, Shevchenko VP, Kluvitkin AA, Kravchishina MD, Filippov AS, Politova NV (2013) Study of vertical fluxes of sedimentary matter by use of automatic deep-sea sediment observatories in the White Sea. In: Sedimentary basins, sedimentation and post-sedimentation processes in geological history. Proceedings of VII All-Russian lithological conference, Novosibirsk, 28–31 Oct 2013, vol 2. SB RAS, Novosibirsk, pp 317–321. (in Russian)
19. Lisitsyn AP, Lukashin VN, Novigatsky AN, Ambrosimov AK, Klyvitkin AA, Filippov AS (2014) Deep-sea observatories at the axial transect in the Caspian Sea and continuous investigations of the dispersed sedimentary matter's fluxes. Dokl Earth Sci 456(4):485–489
20. Yudovich YE, Ketris MP (2011) Geochemical indicators of lithogenesis (lithological geochemistry). Geoprint, Syktyvkar. 741 pp (in Russian)
21. Petelin VP (1967) Grain-size analysis of the marine bottom sediments. Nauka, Moscow. 128 pp
22. Luoma SN, Bryan GW (1981) A statistical assessment of the trace metals forms in oxidized estuarine sediments employing chemical extractants. Sci Total Environ 17:165–196
23. Chester R, Hughes MJ (1967) A chemical technique for separation of ferromanganese minerals and adsorbed trace metals from pelagic sediments. Chem Geol 3:249–262
24. Kitano Y, Fujiyoshi R (1980) Selective chemical leaching of Cd, Cu, Mn and Fe in marine sediments. Geochem J 14:122–128
25. Mamochkina AI, Dara OM (2015) Distribution of fine-dispersed fraction fragmented minerals in the surface sediments of the White Sea. In: Evolution of sedimentary processes in the Earth's history. Proceedings of the VIII Russian lithological conference, vol 1. Gubkin Russian State University of Oil and Gas, Moscow, pp 112–114. (in Russian)
26. Gordeev VV, Shevchenko VP (2012) Forms of occurrence of some metals in the suspended matter of Northern Dvina River. Oceanology 52(2):282–291
27. Belyaev NA (2015) Organic matter and hydrocarbon markers of the White Sea. Abstract PhD thesis, IO RAS, Moscow, 25 pp
28. Rozanov AG, Volkov II, Kokryatskaya NM, Yudin MV (2006) Manganese and iron in the White Sea: sedimentation and diagenesis. Lithol Miner Resour 5:539–558
29. Gusakova AI (2015) Mineral composition of modern bottom sediments of the White Sea. Oceanology 53(2):249–258
30. Demina LL, Fomina LS (1982) On occurrence forms of iron, manganese, zinc and copper in surface suspended particulate matter of the Pacific. Geochem Int 11:1710–1726
31. Demina LL, Nemirovskaya IA (2007) Spatial distribution of trace elements in seston of the White Sea. Oceanology 47(3):390–402
32. AMAP (2005) Assessment of heavy metals in the Arctic. AMAP, Oslo. 265 pp
33. Mamindy-Pajany Y, Hurel C, Geret F, Galgani F, Bataglia-Brunet F, Marmier N, Romeo M (2013) Arsenic in marine sediments from French Mediterranean ports: geochemical partitioning, bioavailability and ecotoxicology. Chemosphere 90(11):2730–2736
34. Beldowski J, Szubska M, Emelyanov E, Gargana G, Drzewinska A, Beldowska M, Vannien P, Ostin P, Fabisiak J (2015) Arsenic concentrations in the Baltic Sea sediments close to chemical munitions dumpsites. Deep-Sea Res II. https://doi.org/10.1016/j.dsr2.2015.03.001
35. Strakhov NM (1960) Basic theory of lithogenesis, vol 2. Nauka, Moscow. 574 pp (in Russian)
36. Savvichev AS, Rusanov II, Zakharova EE (2008) Microbial processes of carbon and sulfur cycle in the White Sea. Microbiology 77(6):823–838
37. Gursky YN (2005) Features of chemical composition of pore waters of the White Sea. Oceanology 45(2):224–239
38. Rozanov AG, Volkov II (2009) Bottom sediments of Kandalaksha Bay in the White Sea: the phenomenon of Mn. Oceanology 47(10):1067–1086
39. Kokryatskaya NM (2004) Sulfur compounds in water and bottom sediments of the White Sea and the Northern Dvina River mouth. Abstract of PhD thesis, IO RAS, Moscow, 24 pp (in Russian)

40. Bezrukov PL, Lisitsyn AP (1960) Classification of marine sediments of modern seas. In: Geological studies in the Far-Eastern Seas Proc of Institute Oceanology XXXII, pp 117–124 (in Russian)
41. Astakhov AS, Rozan V, Crane K, Ivanov MV, Gao A (2013) Lithochemical classification of the depositional environments of the Arctic Chukchi Sea by multicomponent statistical analysis. Geochem Int 4:303–325
42. Schoster F, Behrends M, Müller C, Stein R, Wahsner M (2000) Modern river discharge and pathways of supplied material in the Eurasian Arctic Ocean: evidence from mineral assemblages and major and minor element distribution. Int J Earth Sci 89:486–495
43. Sundby B, Lecroart P, Anschutz P, Katsev S, Mucci A (2015) When deep diagenesis in Arctic Ocean sediments compromises manganese-based geochronology. Mar Geol 366:62–68
44. März C, Stratmann A, Matthiessen J, Meinhardt A-K, Eckert S, Schnetger B, Vogt C, Stein R, Brumsack H-J (2011) Manganese-rich brown layers in Arctic Ocean sediments: composition, formation mechanisms, and diagenetic overprint. Geochim Cosmochim Acta 75:7668–7687
45. Naeher S, Gilli A, North RP, Hamann Y, Schubert CJ (2013) Tracing bottom water oxygenation with sedimentary Mn/Fe ratios in Lake Zurich, Switzerland. Chem Geol 352:125–133
46. Pilipchuck MF, Volkov II (1974) Behavior of molybdenum in processes of sediment formation and diagenesis. In: Degens ET, Ross DA (eds) The Black Sea: geology, chemistry and biology. American Association of Petroleum Geologists, Tulsa, pp 542–552
47. Aliev RA, Bobrov VA, Kalmykov SN, Melgunov MS, Vlasova IE, Shevchenko VP, Novigatsky AN, Lisitsyn AP (2007) Natural and artificial radionuclides as a tool for sedimentation studies in Arctic. J Radioanal Nucl Chem 274(2):315–321

Oil Compounds in the Bottom Sediments of the White Sea

Inna A. Nemirovskaya

Contents

Abstract The content and composition of aliphatic and polycyclic aromatic hydrocarbons in bottom sediments of different areas of the White Sea were studied during low and high waters to estimate the contribution of oil components. It was shown that hydrocarbon (HC) distribution on the border of the Northern Dvina River – Dvina Bay is influenced by the processes that take place in the marginal filter (the riverine-seawater mixing zone) and cause the precipitation of major part of pollutants. With the increase of particles' grain-size, the HC adsorption capability of sediments rose to a lesser extent comparing to the C_{org} adsorption. Therefore, the sandy sediments were more enriched in hydrocarbons than the silty ones. The rapid transformation of petroleum low-molecular hydrocarbons leads to the fact that most resistant terrigenous alkanes dominate in the bottom sediments. The separating lakes of the Rugozerskaya Bay were good examples to show that natural processes can form high levels of hydrocarbons in sediments, while their concentrations in the composition of C_{org} did not exceed 1%.

Keywords Aliphatic hydrocarbons, Low and high waters, Marginal filters of rivers, Oil, Polycyclic aromatic hydrocarbons, White Sea

I. A. Nemirovskaya (✉)
Shirshov Institute of Oceanology, Russian Academy of Sciences ("IO RAS"), Moscow, Russia
e-mail: nemir44@mail.ru

A. P. Lisitsyn and L. L. Demina (eds.), *Sedimentation Processes in the White Sea: The White Sea Environment Part II*, Hdb Env Chem (2018) 82: 271–294,
DOI 10.1007/698_2018_342, © Springer International Publishing AG, part of Springer Nature 2018,
Published online: 20 June 2018

1 Introduction

Oil and its components are among the most common pollutants in the marine environment, whose integrated research is in the focus of attention in many countries and on the international level [1–3]. Environmental risks and oil transference problems have been known for a long time, and such operations would probably never be completely safe.

Due to hydrophobic properties, crude oil (especially its heavy fractions) is easily adsorbed by suspended particulate matter and, together with it, is deposited to the bottom. As some studies show [2–4], similar processes are typical for a narrow coastal zone and shallow water with a high content of suspended matter, especially clay minerals. In these conditions, the concentration of oil in the clay fraction can reach 120–300 μg/g of suspended matter [4], while in river and estuarine waters, it can reach up to a several percent of the suspended matter weight. As the temperature decreases, the accumulation of oil in suspended matter increases [5]. In conditions of permanent oil pollution, the ratio of dissolved to suspended forms of oil in the marine environment varies in an extremely wide range (from 0.1 to 10 times), depending on the particular combination of environmental factors, the content of suspended matter, and also the composition and properties of oil.

Immersion, i.e., removal of heavy aggregated oil from the surface layer of the sea into bottom sediments, takes place when oil drops interact with suspended matter. This happens in two situations [2, 6]: immediately after a heavy oil spill, if its initial density was higher than the sea water density, and some time after the spill of heavy oil, the initial density of which was slightly less than 1, but then increased as a result of weathering or by injection of sand particles into liquid oil, carried to reference zone from the sandy beach.

Another mechanism of the oil and suspended matter's interaction in seawater is the flocculation of mineral (mostly clay) particles of micron size on the surface of water-dispersed oil drops [7].The resulting stable water-oil-mineral complexes (such as flocculated emulsions) limit the coalescence of oil drops, prevent them from floating to the water surface, slow down the oil weathering processes, increase the rate of its biodegradation, and promote sedimentation of oil to the bottom [8]. Experimental work and field observations after oil spills (especially during the accident of the Exxon Valdez tanker) have shown that oil flocculation processes contribute to its accumulation in the littoral [7]. As follows from the world statistics, such scenarios are observed quite often (about 20% of the episodes) under conditions of heavy oil and oil product spills [2, 9]. Cases of precipitation of oil of the average density in the water column due to its emulsification are known, but in these cases, oil remained in a flooded state and did not reach the bottom [10].

Model calculations have revealed [11] that oil can persist for a relatively long period of time on condition that it remains under a snow-ice cover, or under layers of bottom sediments brought by winds and/or water currents, or if it penetrates deeply into bottom sediments, or that it forms bituminous layer. The depth of oil penetration depends on the particle grain-size and its viscosity. Viscous oil and

mousse (water-oil emulsion) usually penetrate not as deeply as low-viscosity oil (in particular, diesel fuel). The oil penetration through muddy sediments occurs more intensively than through sandy deposits. Another mechanism is also possible: the supply of organic compounds (OC) from muddy sediments to bottom water (secondary pollution). Therefore, even in the deep waters of the central part of the White Sea and the Throat, the content of the OC near the bottom may be higher than that on the surface [12]. The most rapid increase of OC concentrations was observed in water samples with an undisturbed sediment layers taken from the Neimisto tube: up to 906 μg/L for hydrocarbons in suspended matter. The increase of the OC in the near-bottom layer is considered as a result of bottom erosion and resuspension. The OC content is affected by the sediment dispersion. Apparently, the secondary migration of the OC is a fairly common process, since in those cases when the bathometer touched the bottom, a significant increase in the content of particulate HCs was observed in the samples [13].

In the White Sea, future environmental deterioration of the marine ecosystem is associated with the industrialization of the coast. In particular, the throughput capacity of the Arkhangelsk terminals increased [14]. The marine traffic also increased, especially the reloading of oil and petroleum products that may cause an increase in the flow of anthropogenic hydrocarbons in the sea area. In addition, a significant part of pollutants in the White Sea comes from the river inflow from self-contained paper mills, fuel and energetic development, the river and marine traffic, and others [15].

2 Sampling and Analyses

Bottom sediments were sampled by the "Ocean" bottom grab sampler. HCs were extracted by methylene chloride previously dried at 50°C bottom sediments by use of the "Sapfir" ultrasonic bath. Before extraction, a 0.25–0.5 mm size fraction was separated by sieving. The concentrations of HCs were analyzed after column chromatography on silica gel. HCs were extracted by hexane, while PAHs were extracted by a mixture of hexane and benzene (3:2) [16]. The concentrations of HC were measured by IR spectroscopy using of wavelength of 2,930 cm^{-1} in a mixture of 37.5% isooctane, 37.5% hexadecane, and 25% benzene [17] on an IRAffinity-1 (Shimadzu). The organic carbon in the particulate matter samples was determined by dry combustion with an AH 7560 analyzer. The concentrations of HCs in sediments and C_{org} were calculated using the coefficient 0.86 [3].

The composition of alkanes was analyzed by the capillary gas-liquid chromatography (column 30 cm long, liquid phase ZB-5) on an Intersmat GS 121-1 chromatograph equipped with a flame-ionization detector at a programmed temperature rise from 100 to 320°C with a rate of 8^0/min. The content and composition of PAHs were analyzed by highly efficient liquid chromatography on an LC-20 Prominence (Shimadzu) chromatograph with the EnviroSep PP column thermostat at 40°C in a gradient mode (from 50 vol % of acetonitrile to 90%) and a rate of eluent flow of

1 cm^3/min. Individual PAHs were determined using RF-20A fluorescent detector with programmed wavelength absorption and extinction. Calculations were performed using LC Solution software. The instrument was calibrated using individual PAHs and mixtures were produced by Supelco.

3 Results and Discussion

Bottom sediments of the White Sea by grain-size composition are commonly referred to pelitic and aleurite-pelitic fractions. The content of pelitic fraction in sediments ranged from 65 to 80% with a maximum content in the deepwater part of the basin. The highest content of sands was found in the Northern Dvina avandelta. All bottom sediments contain a significant amount of aleuritic particles [18].

3.1 Low Water Period

The concentrations of OC in bottom sediments varied in a wide range, and for the surface layer in 2006, they amounted C_{org}, from 0.028 to 1.906%; aliphatic hydrocarbons (HCs), from 20.8 to 116.6 μg/g (Fig. 1); and polycyclic aromatic hydrocarbons (PAHs), from 12.4 to 236.4 ng/g.

The main OC sedimentation reservoir is muddy bottom sediments. In 2006, during the summer low water, a higher HC content was detected in the middle part of the Dvina Bay in the zone of avalanche sedimentation (Fig. 2).

HC concentrations were also increased at the station, which was influenced by waters coming from the Dvina Bay to the Throat area (62.5 μg/g), as well as in the Solovetsky Islands area (80.2 μg/g). The content of HCs in the composition of C_{org} was maximal in the sandy sediments from the Dvina Gulf – 6.4% – which may be due to the passive adsorption of anthropogenic HCs by bottom sediments at shallow depth. On the contrary, in the sediments of the basin, the content of HCs in the composition of C_{org} was lowered (0.29–0.44%). Therefore a degree of anthropogenic pollution of coarse-grained coastal sediments was higher than that of muddy deposits. In the surface layer of bottom sediments, correlation coefficient was calculated between the moisture content (M) in sediments and C_{org}: R(M–C_{org}) = 0.91. Correlation coefficient between moisture and HCs was less significant, as well as between C_{org} and HCs: R(M–HCs) = 0.53; R(C_{org}–HCs) = 0.56. These relationships may indicate either the close origin of the studied compounds or, more likely, the transformation of HCs.

HC concentrations decreased in 2010 due to the fact that in 2010 an oxidized sediment layer of 0–4 cm was selected and, in 2006, an oxidized layer of 0–0.5 cm (Fig. 2). The HC content usually decreases during the transition from oxidized to reduced sediments [3]. The highest HC content, as well as C_{org}, was confined to muddy sediments of the Rugozerskaya and Eremeevskaya Bays (up to 96 μg/g and

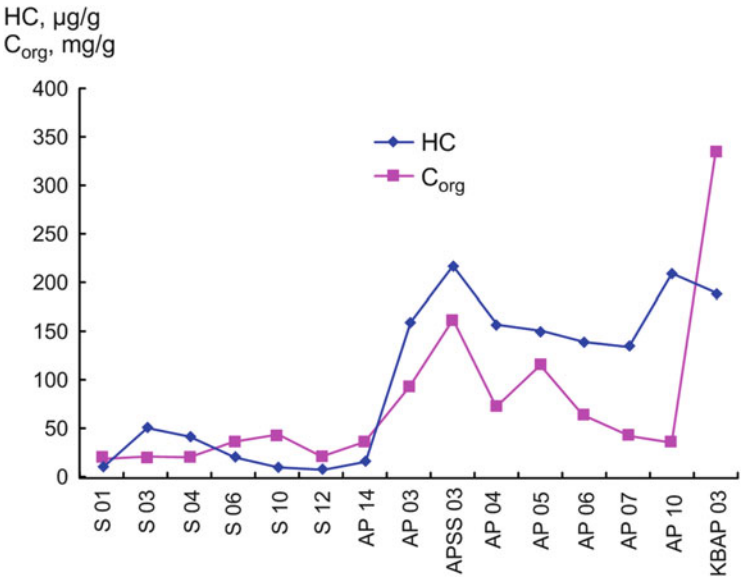

Fig. 1 Distribution of concentrations of C_{org} and HCs in the surface bottom sediments of different grain-size fractions' type of the White Sea during the low water period. *S* sandy, *AP* aleurite-pelitic, *KBAP* Kandalaksha Bay aleurite-pelitic sediments, *APSS* Arkhangelsk Port sandy-silty sediments, *01, 03* . . . years of research

1.06%, respectively). In the open sea areas, their concentrations decreased. In the composition of C_{org}, the HC content varied from 0.08 to 1.06% for muddy sediments and from 0.08 to 0.32% for sandy sediments. At the periphery of the Dvina Gulf and in the straits of Solovetsky Salma, the content of HCs in the composition of C_{org} rose to 0.32%.

The content of alkanes in open areas of the White Sea did not exceed 2.43 μg/g (2–8% of ΣHCs) in sandy bottom sediments that corresponded to their concentrations in sediments in the other Arctic regions [19]. High-molecular uneven compounds predominated in all samples: the ratio $\Sigma(C_{15}–C_{22})/\Sigma(C_{23}–C_{40})$ varied in the range of 0.20–0.54, and the CPI (the ratio of odd to even homologues in the high-molecular part) was in the range of 1.7–4.7. Uneven homologues of $C_{25}–C_{31}$ dominated, reaching up to 23–39% of the total amount of alkanes. Long-chain high-molecular-weight hydrocarbons have a good ability of hydrophobic binding at the water-sediment interface, in comparison with short-chain ones. This group of alkanes is genetically related to higher herbaceous terrestrial plants and water macrophytes.

According to the model proposed by A. P. Lisitzin, the riverine and seawater mixing zone (so-called a marginal filter [20]) consists of three principal zones basically different in their functions: gravitational, physicochemical, and biological ones. In the gravitational zone, because of the damming of the riverine waters by the seawater, sedimentation of sandy-silty fractions occurs; this area is characterized by

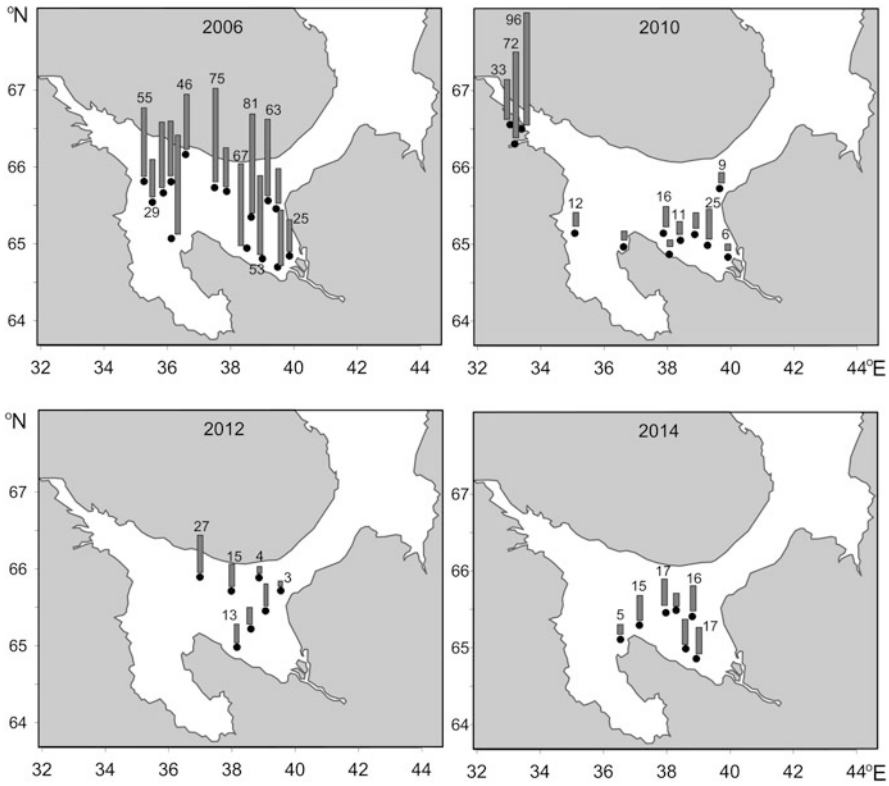

Fig. 2 Changes in the concentrations of HCs (μg/g) in the bottom sediments of the White Sea in different years of study during the low water period

high water turbidity and hindered photosynthesis. In the physicochemical zone, colloids and dissolved compounds are captured (the zone of flocculation and coagulation). After sedimentation of various compounds, water becomes more clear, phytoplankton develops, and biological zone appears (the assimilation and transformation of dissolved substances of mineral and organic composition). In the apex part of the Dvina Bay, oil hydrocarbon content increased in the sediments of the Northern Dvina River estuary region (gravitational zone of the marginal filter) where in the bottom sediments, odd C_{25}–C_{31} homologues amounted only to 15% of the sum of alkanes (Fig. 3).

In the physicochemical zone of the marginal filter, both in the Dvina Bay and in open sea areas, the distribution of alkanes indicated a predominantly biogenic allochthonous HC genesis. In aleurite-pelitic silt in the Throat area, the alkane distribution was bimodal in the surface layer: the content of microbial autochthonous homologues of n-C_{22}–C_{23} was increased in the low-molecular part. The microbial effect on pelitic sediments was higher than on sandy and aleuritic sediments. However, terrigenous alkanes dominated (CPI = 1.7) in the high-molecular domain here as well.

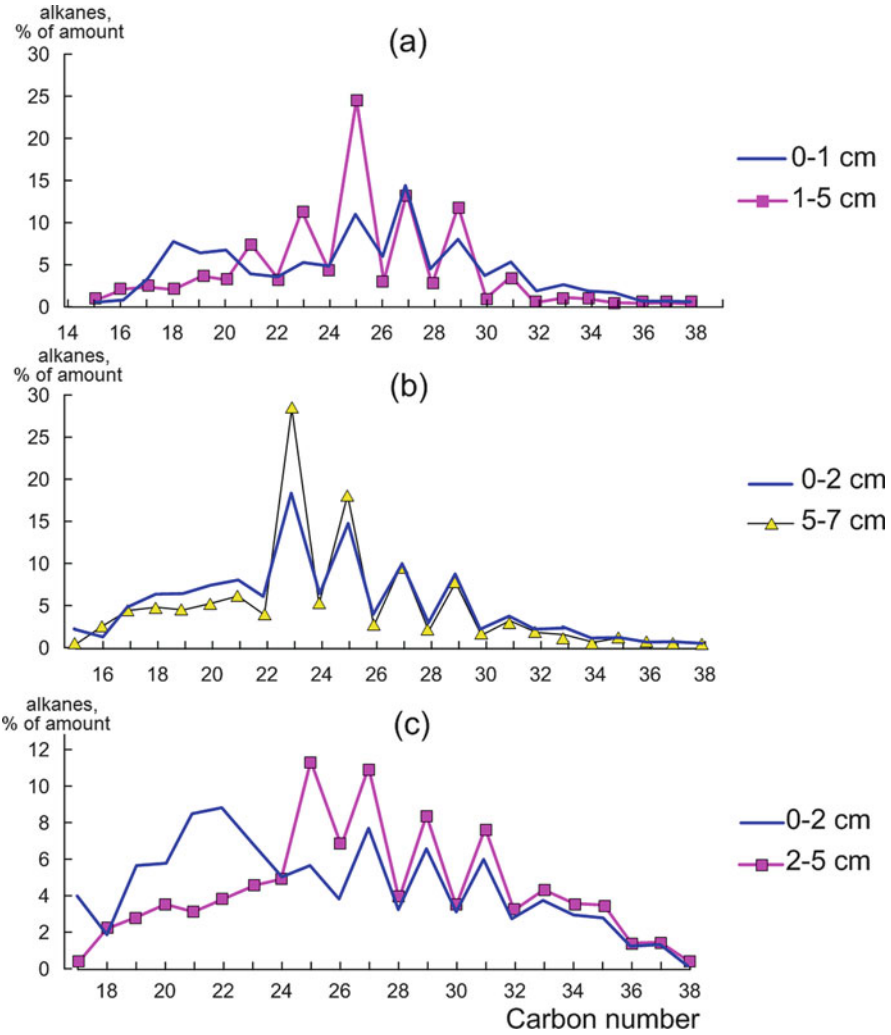

Fig. 3 The composition of the alkanes in the bottom sediments of the Northern Dvina River marginal filter: gravitational (**a**), physicochemical (**b**), and biological (**c**) zones

According to the PAH content in the surface layer, the sediments can be attributed to slightly contaminated, since the sum of 3–6-ringed polyarenes was generally <100 ng/g [21]. The average concentrations in the muddy bottom sediments were 97.4 and in sandy sediments – 30 ng/g. In the composition of the surface layer of bottom sediments, the average content of individual polyarenes decreased as follows: P (pyrene, 22.9%) > FL (fluoranthene, 20.3) > PH (phenanthrene, 16.1) > PL (perylene, 13.0) >CHR (chrysene, 9.6) > BKFL (bens(*k*)fluoranthene, 8.9) >N (naphthalene, 4.6) > BP (bens(*a*)pyrene, 2.2) = AN (anthracene, 2.2%).

The influence of oil PAHs outside the gravitational part of the marginal filter of the Northern Dvina is insignificant, since in all sediments, the ratio of naphthalene/phenanthrene was <1. Low concentrations of naphthalene may also be due to its decomposition at elevated summer temperatures. The rate of photochemical transformation of polyarenes is comparable to the rate of microbiological oxidation of nonaromatic hydrocarbons [22]. At the same time, according to available data, the PAH content in the sediment of the Kandalaksha Bay (the sum of 27 individual polyarenes) reached 2,925 ng/g, and pyrogenic compounds prevailed in their composition [23]. Oil components to a greater extent were recorded in the sediments of the Dvina Gulf.

The bottom sediments of the central part of the Dvina Gulf were contaminated to a lesser degree, since the ratio FL/(FL + P) was ≈1. The amount of pyrogenic compounds along with terrigenous ones in the sediments is quite high, which was proved by the variability in the ratio of P/PL (0.09–3.01). Perylene in considerable quantities was found in bottom sediments enriched with terrigenous plant material. In case of diagenetic origin, the proportion of PL is >10% [21]; in the studied bottom sediments, the perylene percentage averaged to 13%.

Subsequent studies of PAHs in the sediments of the White Sea have established that elevated concentrations in the surface layer during the summer low water were associated with the apex parts of Kandalaksha (2,087 ng/g) and Dvina (230 ng/g) Bays [23]. The benzo(a)pyrene contents according to the classification correspond to the II class, as an insignificant contamination (<420 ng/g), while the concentrations of benz-fluoranthene, indopyrene, and benzoperylene in some cases corresponded to the IV class – hazardous contamination (700–4,800 ng/g). The content of other PAHs corresponded to I and II classes, except for the benzoperylene in the sediments of the Dvina Bay. According to the general picture, PAH levels in the sediments showed mainly moderate contamination [24].

Significant variability in the OC concentrations was observed in the 0–45 cm layer of bottom sediments of the White Sea (Fig. 4). This phenomenon was associated with changes in the rates of hydrolysis and oxidation-reduction processes in the sediments [25]. In the bottom sediments of the Dvina Bay, peaks in the distribution of HCs were more significant at st. 6042 (physicochemical part of the marginal filter) and at st. 6052 (the biological part of the marginal filter) than at st. 6056 (located in the basin area) in 2006. Apparently, intermediate zones with reduced microbiological consumption and resynthesis were formed with the rapid burial of freshly formed organic matter (OM). As a result, there were microfacies with a “fresh” HC composition without visible changes of the initially deposited OM. Aerobic oxidation processes are most intense in slightly transformed sediments in contact with the oxygen of the bottom water [25]. Therefore, HC transformation processes also proceed intensively in the subsurface layers of bottom sediments, along with the boundary layer of the water bottom, generally leading to a decrease in their concentrations and in the alkanes to low-molecular homologues (Fig. 3). This is due to the passive accumulation of the most polymerized and insoluble OM. In the field of anoxic diagenesis, up to 90% of the initial amount of HCs was consumed in bottom sediments under consideration.

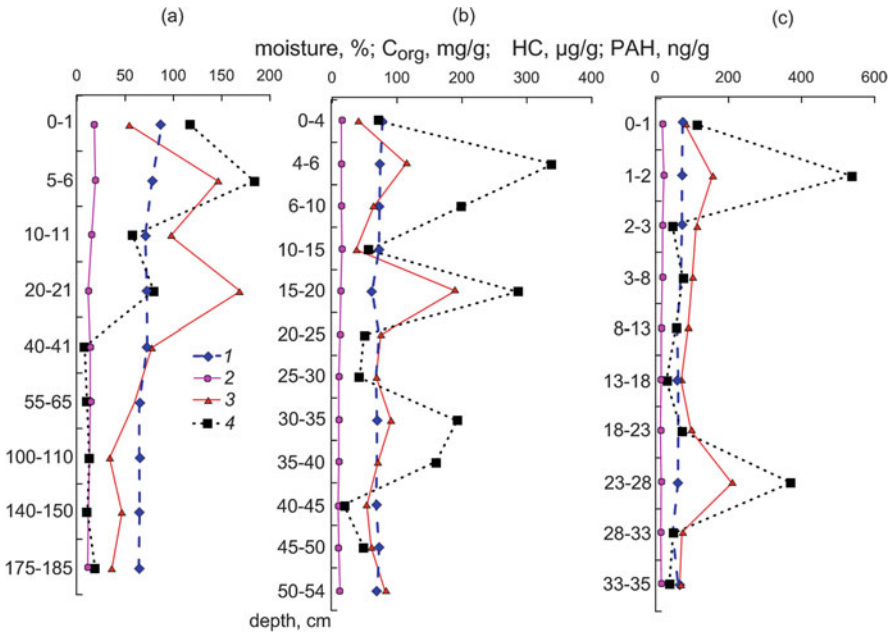

Fig. 4 Distribution of natural moisture (1), C_{org} (2), HCs (3), PAHs (4) in the sediment cores in 2006 at stations 6042 (**a**), 6052 (**b**), 6056 (**c**) (the location of the stations is explained in the text)

Higher concentrations of PAHs in the subsurface layer of bottom sediments can also be attributed to their increased emissions in the 50th of twentieth century [26]. This conclusion is confirmed by a decrease in the ratio of FL/(FL + P) to 0.32 and an increase in the ratio (P + BP)/(PH + CHR) on the station 6042 at the horizon 1–2 cm. The increase in the polyarene content in the subsurface layer of bottom sediments is most typical for the geochemical barrier of the river sea [3, 27, 28]. Perhaps, therefore a maximum in the HC distribution was observed at all stations in the subsurface layer of sediments. In the deep layer (>45 cm), there was a decrease in the content of both HCs and PAHs at the station 6056.

Similar data were obtained in the analysis of the bottom sediment core (21 samples), taken with the help of the Neimisto tube in July 2011 at a station in the Dvina Bay. Collected sediments were represented by oxidized silt from the tan color in the surface layers to light gray and gray colors with black hydrotroilite pieces in the 20–25 cm layer. The concentration of OC changed unevenly down the core, the material composition, and redox conditions of the sediment. HC content varied from 17.44 to 65.45 μg/g; PAHs, from 0.1 to 5.6 ng/g; and C_{org}, from 1.04 to 3.125%. Moreover, if the distribution of HCs and PAHs in the general case coincided and a correlation was observed between their concentrations, R(HCs–PAHs) = 0.7, there was no correlation dependence between the C_{org} and HC distribution. The C_{org} content most intensively changed in the upper 3 cm layer, and the HC and PAH concentrations varied throughout the sediment core to a

25 cm horizon. Consequently, under anaerobic conditions, the HC transformation proceeds intensively as well. Obviously, different groups of native anaerobic microorganisms (sulfate-reducing, oil-oxidizing, fermenting, and denitrifying agents) participate in their transformation even in reducing conditions [29]. The maximum concentration of HCs was confined to the 4.5–5 cm layer (66.45 μg/g), and their formation was due to OC degradation, as the C_{org} content decreased here. The depletion of HCs in the surface layer of sediments, in comparison with the lower horizons, can also occur due to sediment redeposition at high sedimentation rates. This phenomenon is associated with changes in the rates of hydrolysis and redox processes in the sedimentary core [29]. Here, OM undergoes aerobic-anaerobic oxidation, since in the subsurface layer, both aerobic and anaerobic oxidations of OM occur with a limited diffusive penetration of oxygen from the bottom water.

In 2015 the highest concentrations of HCs are found in the bottom sediments of the separated lakes of the Kandalaksha Bay (Rugozerskaya Bay) (Fig. 5, Table 1). On the periphery of the Kandalaksha Bay, the coastline is highly indented, along the banks there are a lot of islands, and for the bottom the interchange of basins and rapids is characteristic. Therefore, there was a gradual separation of small water basins from the sea with a weak freshwater supply [30, 31]. The studied water bodies in order of separation from the sea are as follows. The Ermolinskaya Bay has free water exchange with the sea. The lake on the Green Cape is in the initial stage of

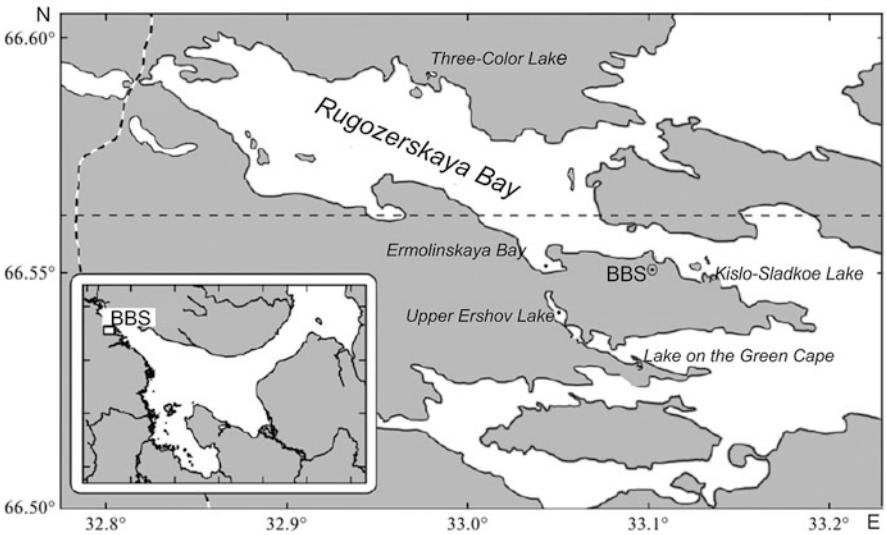

Fig. 5 Location scheme of the separating lakes in the Rugozerskaya Bay (WSBS – White Sea biological station)

Table 1 Content of organic compounds in bottom sediments of Rugozerskaya and Kandalaksha Bays, White Sea, 2015

The location of the sampling	Moisture, %	HCs, μg/L	C_{org}, %	HC content, % in the composition of C_{org}
Three-Color Lake	90.46	73	7.348	0.086
Upper Ershov Lake	78.11	44	4.948	0.077
Lake on the Green Cape	88.57	97	6.982	0.19
Kislo-Sladkoe Lake	89.1	151	8.698	0.149
Ermolinskaya Bay	59.91	9	2.467	0.032
WSBS pier	54.97	15	1.402	0.090

separation, it has a constant tidal water exchange with the sea, and tidal fluctuations of the level are about 10 cm. The Kislo-Sladkoe Lake is deprived of constant water exchange; seawater penetrates into it only occasionally, but the rapid's height does not interfere with free outflowing surface water. The Three-Color Lake is considered to be completely detached from the sea, as indicated by surface's two-meter layer of freshwater and the lower saline layer, the characteristics of which have not changed for several years (a typical feature of a meromictic reservoir). Water of the upper Ershov Lake is completely fresh [30].

In sediments of the separating lakes of the Rugozerskaya Bay, the composition of alkanes had a bimodal distribution of homologues (Fig. 6). In the low-molecular-weight part, autochthonous biogenic alkanes, n-C_{17}, which has a planktonic origin, and even homologues n-C_{14}-C_{18} indicate intensive microbial processes. In the high-molecular part, the concentration of odd allochthonous alkanes n-C_{25}-C_{31} was increased. Therefore, CPI values were high (9.6–11.9), which indicates the terrigenous HCs genesis, associated with waxes of higher terrestrial plants [21].

It should be noticed that the values of CPI in the alkanes of Kandalaksha Bay sediments did not exceed 3.06, and the Dvina Bay, 1.98 [32], i.e., the contribution of terrigenous homologues in the sediments of the bays is evident to a lesser degree than in the sediments of the separating lakes.

3.2 High Water Period

The content and composition of HCs during the high water period changed sharply, where studies were carried out mainly in the spill-streams of the Northern Dvina River (sampling sites are shown in Fig. 7).

Bottom sediments were mainly composed of medium-grained (>100 μm) sand, where percentage of sandy fraction reached up to 80–99% [33], and moisture was <50%. In the exterior part of the delta, sands are characterized by a better particle sorting than in the spill-streams. During the flood, the sandy-aleuritic fraction of the river suspended matter is deposited in the spill-streams and channels of the delta in the gravitational part of the marginal filter, and main part of the fine-grained

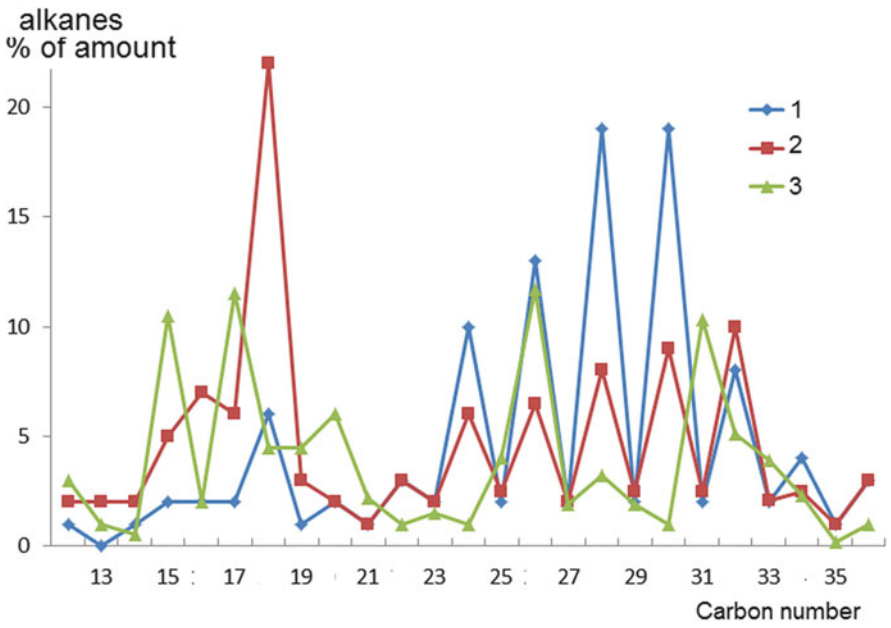

Fig. 6 Composition of alkanes in the lake bottom sediments: Kislo-Sladskoe Lake (1), lake on the Green Cape (2), Three-Color Lake (3)

(<10 μm) pelitic material enters the White Sea. A sharp decrease of flow velocity caused by morphological features of the riverbed led to a rapid deposition of suspended matter containing the hydrocarbons. This was, most likely, due to the wide variety of the OC supply sources and the intensity of the flood. In 2006, the concentrations of C_{org} in bottom sediments varied from 0.005 to 2.640% (mean 0.59%, $\sigma = 0.69$) and HCs from 13.1 to 329.4 μg/g (mean 105.7 μg/g, $\sigma = 73.4$). The concentrations of C_{org} decreased in 1.7 times in comparison with May 2005 (0.015–3.31%, average 1.02, $\sigma = 2.98\%$) and HCs in 3.2 times (12.9–531 μg/g, average 336, $\sigma = 436$ μg/g) (Table 2).

When HC concentrations were ≥50 μg/g for silty and ≥10 μg/g for sandy sediments, they can be considered contaminated [3, 15, 21]. The highest content of HCs was found in the areas of potential input of oil HCs: in case of draining, the sewage of PPP effluent discharge area, Chizhovskii roadstead, Ekonomiya Port (>150 μg/g, Table 2). In these regions, the content of HCs in the composition of C_{org} was also sharply increased (up to a maximum of 35.89%).

An increased HC content in the composition of C_{org} was also found in the Nikolskii Arm at station 33, 25.71%, and in the apex part of Dvina Bay at the exit from the Murmansk Arm on the station 42 – 15.79%. Low HC content was confined to sediments of st. 41 in the area of Kumbich Lake, 0.42%, in the inflow of the Lai River, 0.81%, as well as at st. 10 in the Pinega River, 0.60%. In marine sediments, the HC fraction in the composition of C_{org} did not usually exceed 1%, and HC mean

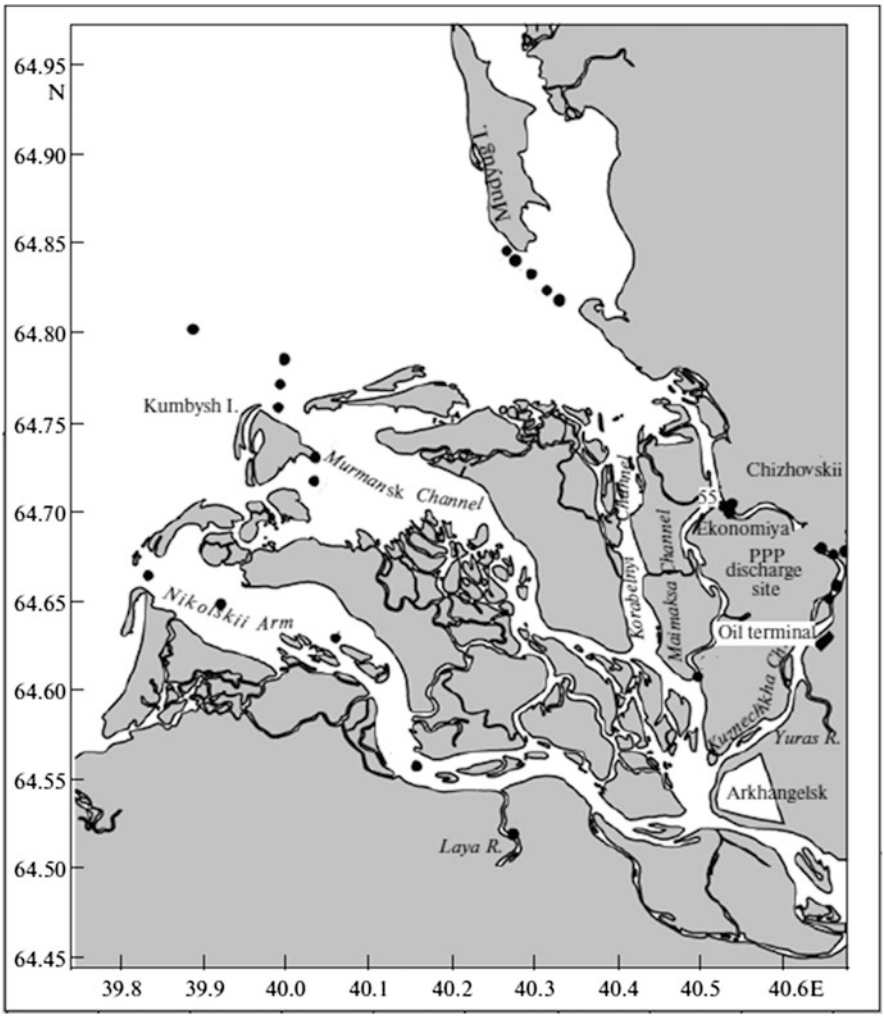

Fig. 7 Location of sampling stations (except stations of the Pinega River)

values in biological objects were even lower: 0.14% in the C_{org} of plankton, 0.048% in the phytobenthos, and up to 0.01% in the higher terrestrial plants (tree leaves) [3].

Increase in the HC content in the composition of C_{org} in bottom sediments of the Northern Dvina River mouth may indirectly indicate the influence of oil HCs, since in the areas contaminated with oil, the percentage of HCs increases. For the entire data, the grain-size composition has a major effect in the OC distribution during the flood, as the correlation coefficient was calculated between the values of C_{org}, natural sediment moisture (M), and HCs in sediments: $R(M–C_{org}) = 0.84$, $R(M–HCs) = 0.78$, and $R(C_{org}–HCs) = 0.81$. This may also indicate the same supply

routes of natural and anthropogenic compounds into bottom sediments, as well as the rapid transformation of the petroleum HCs. However, such strong correlation coefficients were absent in the spill-streams of the Northern Dvina River, where the input of contaminants increased. In particular, in the Kuznechikha Channel, R(M–HCs) = 0.28, and R(C_{org}-HCs) = 0.19. In the area of the pulp and paper plant (PPP) effluent discharge, HC concentrations decreased with an increase in C_{org} (Fig. 8). Here, obviously, the other OCs were also supplied in addition to HCs. A similar picture was observed in the Chizhovskii roadstead area. In May 2005, concentrations of HCs increased with decrease in C_{org} in this area.

In the area of intensive sedimentation nearby the Mudyug Island, effect of grain-size composition decreased, and concentration of HCs at stations 52 and 14 was almost twice as much (63.4 and 121.7 μg/g, respectively), while sediments at these stations have a similar grain-size composition and close C_{org} content (0.714 and 0.688%, respectively). On the contrary, in the area of the Ekonomiya Port, the HC content in sediments of st. 16 and 54 with different grain-size composition was rather similar (311.3 and 329.4 μg/g, respectively), while C_{org} concentrations at these sites differed in 1.6 times (1.645 and 2.638%, respectively). Such type of distribution of HCs when their contents are not controlled by particles' size is probably caused by local input of the oil HCs into bottom sediments. The growth of HC concentrations in water due to passive adsorption by suspended particulate water possibly has led to higher HC content in sandy sediments. Therefore, the HC percentage in C_{org} composition of coarse-grained is higher than that in the clay sediments. Maximum HC content was found at st. 20; however it was rather low – 30 μg/g – if to calculate on dry weight. However, toward the Mudyug Island in the physicochemical zone of marginal filter, the sediments also have a rather high HC content (on average, 106 μg/g, Table 2).

The HC concentrations in the Northern Dvina River's delta were comparable with that from areas exposed to continuous oil input. As an example, in sandy sediments with admixtures of shell detritus and algae, of the northern shelf of the Caspian Sea, where C_{org} content was rather low (0.197–0.582%), the HC contents varied from 70 to 4,557 μg/g [17]. At the western coast of the Taiwan Island, in the delta of the rivers Kaoping and Tungkam, the HC contents were even higher (869–10,300 μg/g) [34]. Meanwhile, in the estuarine regions of the northwestern part of the Black Sea, the HC content was lower and varied from 5 to 402 μg/g; in the Danube River's mouth, it varied within the limits of 49–220 μg/g [35].

The concentrations of alkanes in the bottom sediments during the high water period in 2006 were lower than those reported in May 2005 (Table 3). The terrigenous HC components dominated in the composition of high-molecular-weight fractions, as they are the most stable (Fig. 9). A minimum CPI (odd/even ratio of high-molecular-weight alkanes) value of 1.29 was reported near the pulp and paper plant (PPP) discharge area, where high-molecular-weight homologues also dominated, as the ratio of light and heavy alkanes amounted to 0.62 (Table 3). Some samples from the Nikolskii Arm and Maimaksa Channel have CPI values >2. The low-temperature chromatogram part illustrates the role of evaporation and biodegradation of oil alkanes. Their microbial origin could be responsible for the slight

Table 2 Contents of organic compounds in the surface layer of bottom sediments in high water period

Location	n[a]	Moisture content, %		C_{org}, %		HC, μg/g		HC, % of C_{org} (average)	PAH		
										ng/g	
		Range	Average	Range	Average	Range	Average		n	Range	Average
Gravitational zone of the marginal filter											
Kuznechikha Channel Roadstead of Chizhovskii	3	30.9–50.3	37.9	0.83–2.64	1.70	174–329	272	1.34	3	98–768	350
PPM oil terminal	7	18.3–42.9	31.0	0.40–1.54	0.81	30–293	163	7.54	6	130–1,213	422
Nikolskii Arm	4	17.5–22.0	18.9	0.02–0.16	0.09	34–95	67	10.4	4	195–422	357
Murmansk Arm	3	18.5–51.9	30.7	0.13–2.26	0.88	28–114	74.2	1.67	2	164–168	166
Maimaksa Channel	1	–	18.5	–	0.239	–	48	1.68	1	–	161
Pinega River	9	0.3–37.0	14.6	0.06–1.06	0.27	13–75	40	1.42	9	4–474	74
Physicochemical zone of the marginal filter, Dvina Bay											
Mudyug Island area	5	22.6–36.3	26.7	0.36–1.43	0.68	63–153	106	1.65	3	134–1,785	600
Apex part	4	18.9–34.0	24.6	0.02–1.23	0.43	36–210	86	6.3	2	93–168	131
Zimnii coast	3	16.4–26.1	20.2	0.03–0.46	0.18	23–62	41	4.6	3	30–434	189

[a]Amount of samples

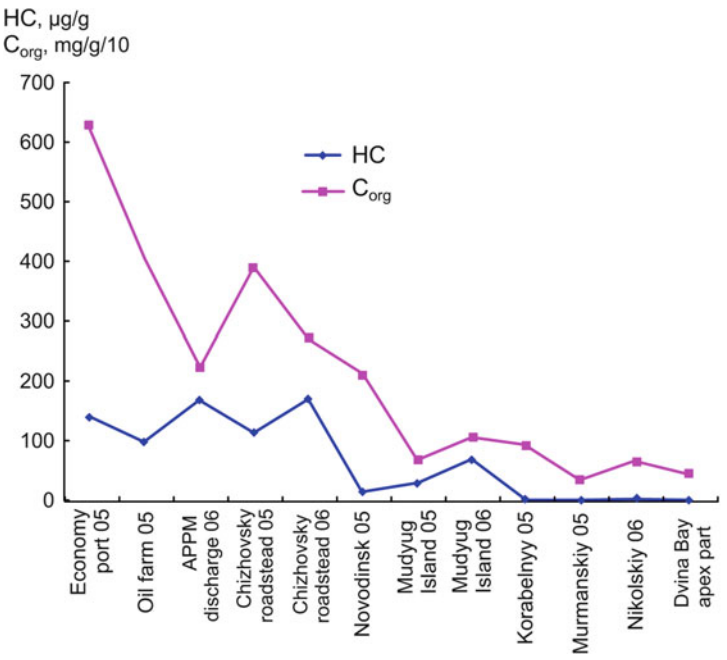

Fig. 8 Distribution of the concentrations of C_{org} (1) and HCs (2) in the bottom sediments of the Northern Dvina River delta at different sampling sites (Ekonomiya Port, oil terminal, etc.); 05 and 06 are May 2005 and May 2006, respectively

predominance of n-C_{19}–C_{23} homologues (Fig. 9b). Oil HCs could influence the intensity of biochemical processes. This may cause an increase in the concentrations of autochthonous alkanes in oil-contaminated sediments [3]. In spite of the generally high HC content in sandy sediments in this area (70–4,557 μg/g, 3.55–62.65% of C_{org}), the biomarkers indicate the predominance of terrigenous biogenic alkanes (CPI values ranged from 3.05 to 6.97).

Thus, in regions with oil hydrocarbon inflow and low temperatures, alkanes are so rapidly degraded that their composition does not correspond to oil. This is due to the fact that even in winter the activity of oil-oxidizing microorganisms can reach quite high values, 57 ng L/h and in the summer 80 ng L/h [36]. Therefore, even after the oil spill (the area of the Baffin Island in Arctic), it turned out that biogenic homologues dominated in the composition of alkanes of coastal sediments, since the pristane/phytane (i-C_{19}/i-C_{20}) ratio varied from 5 to 15 and CPI from 3 to 11 [37].

Concentrations of PAHs, by contrast to HCs, selected in May 2006 (565.8 on average, interval 3.8–2,410.3 σ = 635 ng/g; Fig. 10a), were higher in sediments during high water period than in May 2005 (average, 56.8; interval, 3.4–216; σ = 57.6 ng/g; Fig. 10b). This was due most likely to the different genesis of these hydrocarbon classes. HCs are mainly products of OC biosynthesis, as well as biogeochemical or geochemical transformation of various non-carbon compounds

Table 3 Content of organic compounds in the bottom sediments in high water period

May 2006, zone, station, location										
Compound	Gravitational zone								Physicochemical zone	
	16	54	55	19	32	36	53	51	45	67
	Roadstead of Chizhovskii			PPP discharge site	Nikolskii Arm		Maimaksa Channel		Dvina Bay	
C_{org}, %	1.645	2.64	0.83	1.141	0.149	1.49	0.83	1.43	0.24	0.46
HC, μg/g	311.15	329.37	174.16	212.78	91.82	142.82	117.32	153.03	80.16	210.23
Alkanes, μg/g	15.94	18.90	12.45	23.00	7.04	15.80	12.66	14.29	6.34	10.29
$i\text{-}C_{19}/i\text{-}C_{20}$	0.40	0.27	0.32	0.13	0.17	0.21	0.16	0.13	0.10	0.50
$i\text{-}C_{19}/n\text{-}C_{17}$	0.93	0.79	0.67	0.84	0.58	0.67	0.62	0.86	0.82	1.35
$i\text{-}C_{20}/n\text{-}C_{18}$	2.46	5.06	2.73	3.82	2.63	5.85	4.74	6.30	4.89	1.12
CPI	1.64	1.79	1.53	1.29	1.71	2.67	1.75	2.69	1.91	1.58
$\Sigma(C_{14} + C_{22})/\Sigma(C_{23} + C_{40})$	1.01	0.28	0.29	0.62	0.33	0.16	0.26	0.14	0.28	0.23
May 2005, location										
	Gravitational zone								Physicochemical zone	
	Roadstead of Chizhovskii		Oil terminal	Murmansk Channel	Northern Dvina	Nikolskii Arm	Maimaksa Channel		Dvina Bay	
C_{org}, %	2.184	1.364	0.945	0.015	0.131	0.053	0.087	0.009	0.213	0.182
HC, μg/g	1,348.8	491.2	108.4	16.7	18.2	34.6	17.7	55.7	67.2	453.9
Alkanes, μmg/g	93.0	100.1	11.4	25.7	80.1	90.1	48.6	50.1	38.9	40.0
$i\text{-}C_{19}/i\text{-}C_{20}$	0.86	1.56	5	1.62	1.50	1.36	1.78	1.16	4.50	0.32
$i\text{-}C_{19}/n\text{-}C_{17}$	0.86	0.89	1.92	3	4.20	2.71	4.00	1.01	1.13	1.56
$i\text{-}C_{20}/n\text{-}C_{18}$	1.80	0.83	0.42	1.44	2.00	2.00	1.00	1.08	0.11	0.87
CPI	1.1	1.31	1.63	1.24	1.04	1.11	1.10	1.04	1.04	0.98
Naphthenes, μg/g	790.0	354.9	88.2	14.2	16.1	30.1	15.2	33.7	48.3	64.4
Naphthene/n-alkane	8.5	3.5	7.7	0.6	0.2	0.3	0.3	0.7	1.3	1.6

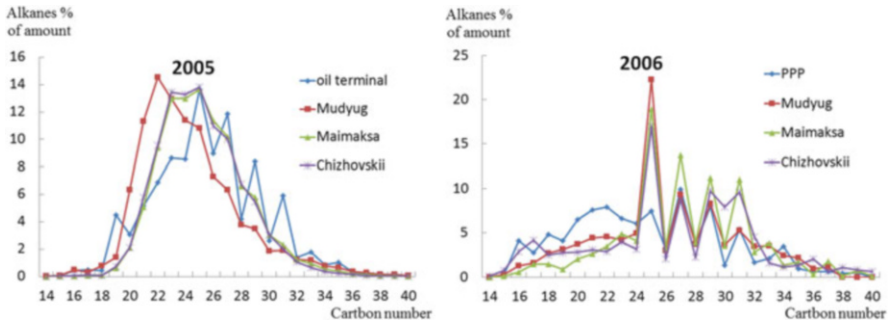

Fig. 9 Composition of n-alkanes in bottom sediments from different estuarine sites of the Northern Dvina River

that constituent dead organisms' biomass in soil, water, and bottom sediments [1, 26].

The PAH concentrations in oils were low and ranged from 10^{-3} to 10^{-1}%. Since PAHs are produced by pyrolysis of organic fuels, they enter the marine environment mainly by the deposition of atmospheric aerosols [1, 21, 38]. Elevated PAH concentrations in terrestrial plants may also be caused by their deposition from polluted air [1]. Since the PAH levels tend to increase during the winter season due to higher atmospheric contamination, the intensity of flooding could influence the concentrations of PAHs in bottom sediments to a lesser degree compared with aliphatic HCs.

In the study area, the average PAH concentrations in bottom sediments decreased in the next order (ng/g): Mudyug Island (600) > pulp and paper plant discharge site (422) > Nikolskii Arm (357) > Zimnii coast (357) > roadstead of Chizhovskii (350) > apex part of the Dvina Bay (131) > Pinega River (74). Despite their different sources, the highest concentrations of both PAHs and aliphatic HCs were detected in bottom sediments around the pulp and paper plant effluent discharge area (station 19). In these samples, the distribution of molecular markers in the PAH composition indicated mixed (petrogenic + pyrogenic) genesis. The naphthalene to phenanthrene ratio (N/PH), which at a value >1 indicates oil polyarenes [3, 21], varied in this area from 4.01 to 6.57. During the summer low water season, naphthalene is a minor component of PAHs [21], because it is the most volatile arene easily decomposing in water. During winter and spring, the degradation of naphthalene is probably depressed by low temperatures.

Elevated pyrene concentrations (up to 151 ng/g,) in this area may indicate a supply of pyrogenic PAHs to bottom sediments. The relatively high levels of perylene (up to 30.5 ng/g) in these sediments can probably be attributed to the accumulation of decomposing wood wastes in the Dvina Bay sediments [23]. Therefore, the pyrene/perylene (P/PL) ratio in this area ranged from 3.07 to 5.48 and averaged 7.45 in Arkhangelsk City. It should be noted that outside the city limits, the concentrations of perylene increased up to 4.3% of total PAHs in sediments from the Pinega River, and pyrene concentrations in the majority of samples from this area

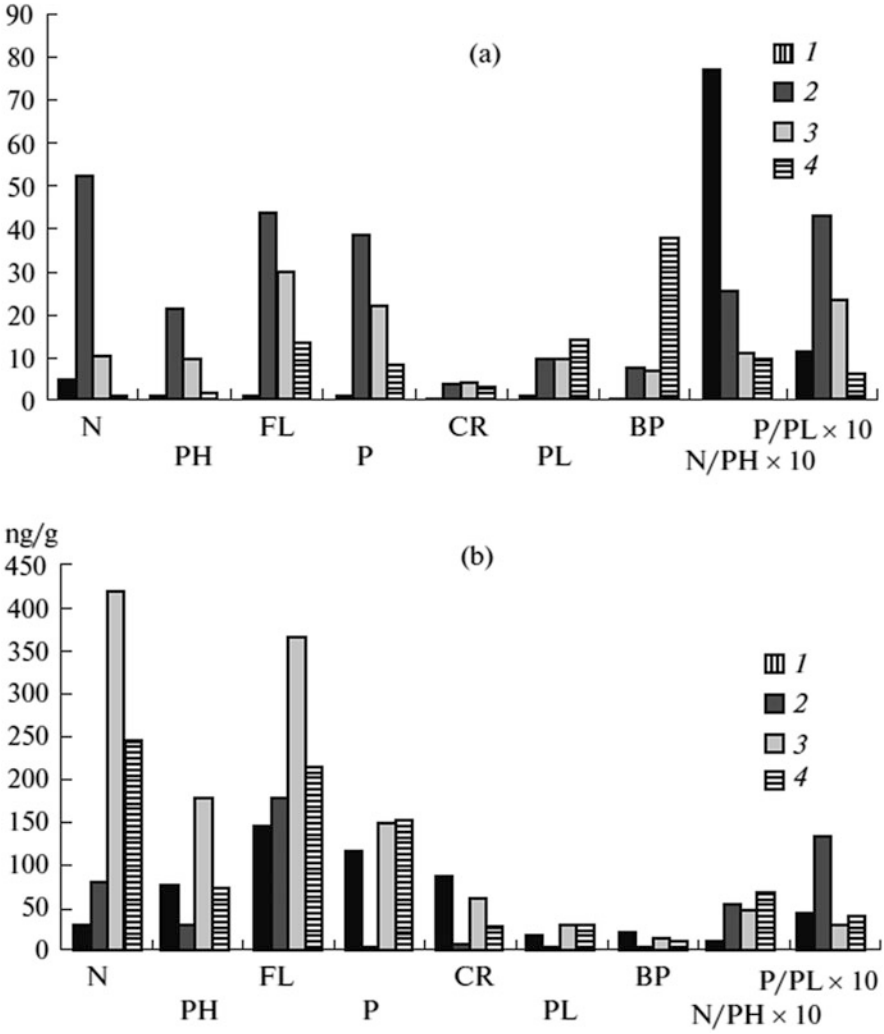

Fig. 10 Compositions of PAHs from bottom sediments in the Northern Dvina River delta: (**a**) 2005 – Mudyug Island (1); Ekonomiya Port (2); oil terminal (3); roadstead of Chizhovskii (4). (**b**) 2006 – st. 13, Mudyug Island (1); st. 19, pulp and paper plant effluent discharge site (2); Laya River (3); st. 55, roadstead of Chizhovskii (4)

were generally very low (close to detection limit). The highest P/PL ratio (17.6–39.7) was measured in sediments from the Nikolskii Arm area within the city limits (Table 3). Phenanthrene is another dominant PAH compound, averaging 22.4% and decreasing within the city limits to 10.3% of total PAHs. It is believed that phenanthrene is most likely a natural arene [26, 39] produced in low-polluted environment by diagenetic transformation of organic matter in humus-rich sediments (indicator of humus accumulation) or through dehydration of steroids by

microorganisms [26, 35]. This could be the reason why phenanthrene accounted for 32.1% of total PAHs, on average, in sediments from the Pinega River.

High concentrations of fluoranthene and pyrene in sediments may be due to supply of combustion products with aerosol particles [23, 38]. Fluoranthene, the most stable polyarene, was found to dominate in many aquatic objects, even at stations remote from pollution sources [13]. Therefore, elevated fluoranthene concentrations may reflect high transformation degree for pyrogenic polyarenes. In soils near combustion sources, the concentrations of pyrene are usually higher than those of fluoranthene, and the molecular ratio of PAHы is preserved in case of precipitation of anthropogenic aerosols close to combustion sources [38].

The content of benzo(a)pyrene (BP), the most toxic of the identified PAHs, was much lower than that of other polyarenes, with an average of 6.7 ng/g (1.8% of total PAHs). However, in sediments at stations 14 and 51 (seaward the Mudyug Island), its concentrations (20.7 and 60.0 ng/g) were comparable or higher than the MPC (что значит эта аббревиатура?) values for soils (20 ng/g). In 2005, benzo(a)pyrene concentrations exceeded the MPC value only in sediments near the Chizhovskii roadstead (37.4 ng/g). Except these sites, the levels of benzo(a)pyrene in sediment samples measured in 2006 and 2005 were, on average, close to each other: 3.4 and 2.7 ng/g, respectively [3]. This is also consistent with previous data. For example, the BP contents in bottom sediments of the Northern Dvina River delta ranged 0.2–4.2 in 1993 [40], 0.2–2.5 in 1994 [23], 0–16 (average 2.5) in 2003 [3], and 0–19.2 (2.8) ng/g in August 2006 [3]. The dominance of anthropogenic polyarenes over natural ones is also influenced by the relatively low proportion of perylene (2.1%) in urban areas in the Northern Dvina sediments, which usually marks terrigenous OM. In case of natural formation in the bottom sediments, the proportion of perylene is >10% [21].

In addition to bottom sediments from the Northern Dvina River, elevated PAH concentrations were detected in sediment samples from the physicochemical zone of the marginal filter, in the areas of avalanche-type sedimentation (the Mudyug Island, apex part of the Dvina Bay). The increase in anthropogenic PAH concentrations (especially pyrogenic high-molecular-weight PAHs) in this area was previously observed during the summer low water season [3]. In the central part of the Dvina Bay, the biomarker distribution indicated natural sources, although the PAH levels were high (>100 ng/g). This suggested that the river-sea geochemical barrier could prevent the supply of anthropogenic polyarenes into the open sea environment.

The HC content varied according to the flood phase. The data obtained on 26.04 and 13.05 in 2017 were indicative (Fig. 11). With the increase of the flood in May, concentrations of all compounds increased in suspended matter by 1.5–4.9 times.

The C_{org} (0.30–0.13%) and HC (12.6–12.3 μg/g) contents differed insignificantly around the Ekonomiya Port and the Mudyug Island, where sediments have similar lithological composition. The coarse-grained fraction increased in sediments near the passenger pier that has led to an increase in the C_{org} concentrations (up to 1.35%) and HCs, to 468 μg/g (up to 3% in the composition of C_{org}), as well. However, the composition of alkanes was close and in all samples where high-molecular uneven terrigenous homologues dominated (Fig. 12). The ratio of low- to high-molecular alkanes varied from 0.16 to 0.28, and the CPI value varied in the interval 2.76–3.99.

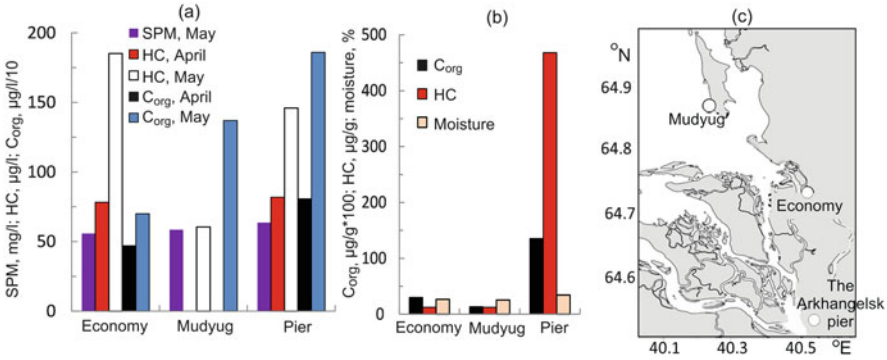

Fig. 11 Variability of organic compounds and suspended matter in various phases of flood – in surface waters (**a**), in bottom sediments (**b**), location of sampling stations (**c**)

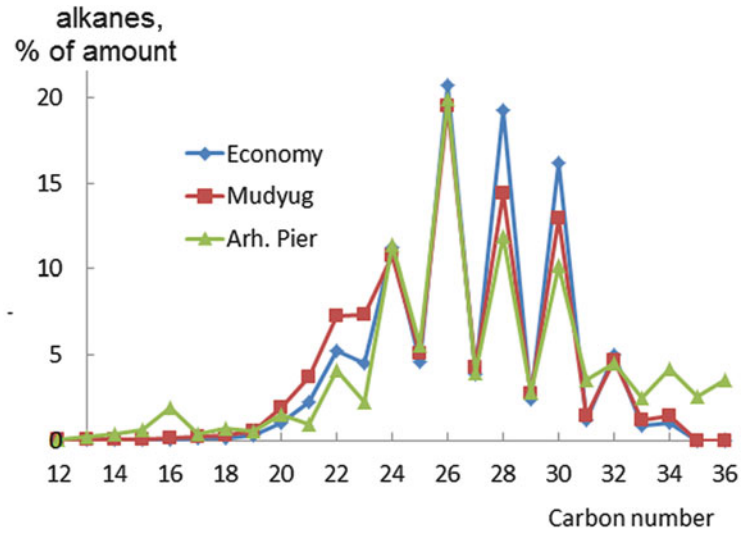

Fig. 12 Compositions of n-alkanes in bottom sediments from different estuarine sites

4 Conclusions

In marginal filters of rivers, where river and sea waters mix, the change in hydrological and biological characteristics determines the peculiarity of sedimentation processes and the variability of the content and composition of both aliphatic hydrocarbons and PAHs in bottom sediments. These processes depend on the season (low water, high water) and the lunar cycle (high and low tides).

Active processes of HC transformation, both in the water column and at the near-bottom water-seabed boundary, led to predominance of components in the

composition of alkanes in bottom sediments. It was evident due to the fact that, despite the low temperatures, the oxidation rates of the OCs in the Arctic seas are comparable with that in temperate and tropical latitudes [25]. Therefore, the composition of HCs and PAHs was mainly presented by natural HCs. High concentrations of C_{org} and HCs in the sediments of the separating lakes of Rugozerskaya Bay were probably caused by natural processes but not pollution.

The incoming oil compounds increase the level of HCs in the sediments, thereby creating a modern HC background level. The same results were obtained during the monitoring of pollutants (the most persistent organic pollutants – PAHs, pesticides, biphenyls, dioxins, furans, as well as some heavy metals) in the White, Barents, and Pechora Seas [24]. Their level in the sediments was estimated as insignificant one.

Acknowledgments This research performed in the framework of the state assignment of FASO Russia (theme No. 0149-2018-0016), and analytical data were processed with support of the RSF grant (Project No. 14-27-00114-p).

References

1. AMAP (Arctic Monitoring and Assessment Programme) (2007) Sources, inputs and concentrations of petroleum hydrocarbons, polycyclic aromatic hydrocarbons, and other contaminants related to oil and gas activities in the Arctic. AMAP Assessment 2007. AMAP, Oslo, p 87
2. NAS (National Academy of Sciences) (2003) Oil in the sea III: inputs, fates, and effects. National Academies Press, Washington, p 265
3. Nemirovskaya IA (2013) Oil in the ocean (pollution and natural flows). Scientific World, Moscow, 432 pp (in Russian)
4. API (American Petroleum Institute) (1999) Fate of spilled oil in marine waters. An information booklet for decision-makers. Health and Environmental Sciences Department, US Department Publication, 42 pp
5. Patin SA (2017) Oil and continental shelf ecology. VNIRO, Moscow, 345 pp (in Russian)
6. Michel J, Galt J (1995) Conditions under which floating slicks can sink on marine settings. In: Proceedings of the 1995 international oil spill conference, API, Washington, pp 573–576
7. Braggs JR, Owens EH (1995) Shoreline cleansing by international between oil and fine material particles. In: Proceedings of the 1995 international oil feel conference, API, Washington, pp 216–227
8. Lee K, Stoffin-Egli P (2001) Characterization of oil-mineral aggregates. In: Proceedings of the 2001 inter oil spill conference, API, Washington, pp 991–995
9. Ansell DV, Dicks B, Guenette CC, Moller TN, Santner RS, White IC (2001) A review of the problems posed by spills of heavy fuel oils. In: Proceedings of the 2001 inter oil spill conference, Tampa, 16 pp
10. Baker JM, Clark RB, Kingston PF, Jenkins RH (1990) Natural recovery of cold water marine environment after an oil spill. Presented at the thirteenth annual Arctic and marine oil spill program technical seminar, June, 111 pp
11. Nemirovskaya IA, Trubkin IP (2013) Anthropogenic and natural hydrocarbons in water and suspended arctic seas. In: Lisitsyn AP (ed) The White Sea system, vol 3. Scientific World, Moscow, pp 438–470 (in Russian)
12. Nemirovskaya IA, Leonov AV (2011) Petroleum hydrocarbons in the waters of major tributaries of the White Sea and its water areas: a review of available information. Water Resour 38 (3):324–351

13. Nemirovskaya IA (2004) Hydrocarbons in the ocean: snow–ice–water–suspension–bottom sediments. Scientific World, Moscow, 328 pp (in Russian)
14. Bambulyak A, Franzen B (2009) Oil transport from the Russian Barents Sea in January 2009 Akvaplan–Niva, Tromsø, 97 pp (in Russian)
15. Quality of marine waters by hydrochemical indicators (2014) Nauka, Moscow, 156 pp (in Russian)
16. Venkatesan MJ, Kaplan IR (1982) Distribution and transport of hydrocarbons in surface sediments of the Alaskan outer continental shelf. Geochim Cosmochim Acta 46:2135–2149
17. Oradovsky SG (ed) (1993) Guidance on methods of analysis of sea water. Gidrometeoizdat, St. Petersburg, 264 pp (in Russian)
18. Rybalko AE, Zhyravlev LR, Semenova LR, Tokarev MY (2017) Quaternary sediments of the White Sea and history of the development of the modern White Sea basin in the late Pleistocene–Holocene. In: Lisitzyn AP, Nemirovskaya IA (eds) The White Sea system, vol 4. Scientific World, Moscow, pp 84–127 (in Russian)
19. Fernandes MB, Sicre MA (2000) The importance of terrestrial organic carbon inputs on Kara Sea shelves as revealed by n-alkanes, OC and $\delta^{13}C$ values. Org Geochem 31:363–374
20. Lisitzin AP (2014) Modern concepts of sedimentation in the oceans and seas. The ocean as a natural recorder for the interaction of Earth's geospheres. In: Nigmatulin RI (ed) World Ocean, vol 2. Scientific World, Moscow, pp 331–571 (in Russian)
21. Tolosa I, Mora S, Sheikholeslami MR, Villeneuve J, Bartocci J, Cattini C (2004) Aliphatic and aromatic hydrocarbons in coastal Caspian Sea sediments. Mar Pollut Bull 48:44–60
22. Izrael YA, Tsyban AV (2009) Anthropogenic ecology of the ocean. Nauka, Moscow, 532 pp (in Russian)
23. Savinov VM, Savinova TM, Carrol J et al (2000) Polycyclic aromatic hydrocarbons (PAHs) in sediments of the White Sea, Russia. Mar Pollut Bull 40(10):807–818
24. Savinov V, Larsen L-H, Green N, Korneev O, Rybalko A, Kochetkov A (2011) Monitoring of hazardous substances in the White Sea and Pechora Sea: harmonisation with OSPAR's Coordinated Environmental Monitoring Programme (CEMP). Akvaplan–niva, Tromsø, 71 pp
25. Agatova AI, Lapina NM, Torgunova NI (2012) Organic substance of the White Sea. In: Lisitzyn AP, Nemirovskaya IA (eds) The White Sea system, vol 2. Scientific World, Moscow, pp 492–548 (in Russian)
26. Rovinsky FY, Teplitskaya TA, Alekseeva TA (1988) Background monitoring of polycyclic aromatic hydrocarbons. Gidrometeoizdat, Leningrad, 224 pp (in Russian)
27. Wakeham SG (1996) Aliphatic and polycyclic aromatic hydrocarbons in Black Sea. Mar Chem 53(2):187–205
28. Wu Y, Zhang IG, Tie-Zhu M, Bin L (2001) Occurrence of n-alkanes and polycyclic aromatic hydrocarbons in the core sediments of Yellow Sea. Mar Chem 76(1–2):1–15
29. Savvichev AS, Rusanov II, Yusupov SK, Pimenov NV, Lein AY (2005) Microbial processes of transformation of organic matter in the White Sea. Oceanology 45(5):689–702 (in Russian)
30. Lisitzin AP, Vasilchuk YK, Shevchenko VP et al (2013) Isotope-oxygen composition of water and snow-ice cover of separated water bodies at different stages of isolation from the White Sea. Doklady Earth Sci 449(2):406–412 (in Russian)
31. Pantyulin AN, Krasnova ED (2011) Separating reservoirs of the White Sea: a new object for interdisciplinary research. In: Proceedings of the international conference on geology of oceans and seas, vol 3, GEOS, Moscow, pp 241–245 (in Russian)
32. Belyaev NA (2015) Organic matter and hydrocarbon markers of the White Sea. Abstract PhD thesis, IO RAS, Moscow, 25 pp (in Russian)
33. Kravchishina MD (2009) Suspended particles of the White Sea and their grain-size composition. Scientific World, Moscow, 264 pp (in Russian)
34. Jeng WL (2006) Higher plant *n*-alkane average chain length as an indicator of petrogenic hydrocarbons contamination in marine sediments. Mar Chem 102(3–4):242–251
35. Readman JW, Fillmann G, Tolosa I (2002) Petroleum and PAH contamination of the Black Sea. Mar Pollut Bull 44:48–62

36. Ilyinsky VV, Semenenko MN (2001) Abundance and activity of the hydrocarbon-oxidizing bacteria in the Kara and White seas. In: Lisitsyn AP (ed) Systematic oceanological studies in the Arctic. Scientific World, Moscow, pp 364–375 (in Russian)
37. Wang Z, Fingas MF (2003) Development of oil hydrocarbon fingerprinting and identification techniques. Mar Pollut Bull 47(3):423–452
38. Page DS, Boehm PD, Douglas GS et al (1999) Pyrogenic polycyclic aromatic hydrocarbons in sediment human activity: a case study in Prince William Sound. Mar Pollut Bull 38(4):247–260
39. Dahle S, Savinov V, Matishov GG et al (2003) Polycyclic aromatic hydrocarbons (PAHs) in bottom sediments of the Kara Sea shelf, gulf of Ob and Yenisei Bay. Sci Environ 36:57–71
40. Moseeva DP, Troyanskaya AF, Bogdanovich LM (1996) Ecological problems of the European North. URO RAS, Yekaterinburg, pp 130–146 (in Russian)

Conclusions

Liudmila L. Demina and Alexander P. Lisitsyn

Contents

Abstract Part II contains the data obtained over continuous 15-year research of modern sedimentation in the White Sea. New data on sedimentation processes, starting from the surface water layer to the bottom sediments, have been obtained. These processes are studied from the viewpoints of the Earth Science's specialists. Geologists and geophysicists have described the Holocene development history and revealed a three-member structure of the Quaternary cover. Sedimentologists evidenced a major contribution of dispersed sedimentary matter in the form of suspended particulate matter, sediment-laden sea ice and snow, and vertical fluxes of settling particles into the formation of sedimentary cover. Biostratigraphs have revealed a relationship between environmental parameters and abundance and species composition of microalgae associations. Mineralogists have investigated the main mineral phases of sedimentary matter at different stages of sediment formation. Geochemists have cleared out the specific character of diagenetic processes; accumulation of heavy metal, including mercury; as well as aliphatic and polycyclic aromatic hydrocarbons in sediments of such subarctic sea as the White Sea is.

Keywords Biogeochemistry, Bottom sediments, Development history, Particle fluxes, Suspended particulate matter, White Sea

In the early 2000s, the White Sea has become a ground for the study of sedimentation processes in the Russian Arctic seas. Since that time, a large database was obtained in different fields of marine geology and geochemistry. Our long-term research program was implemented on the White Sea, one of the Arctic seas. The main aim was to

L. L. Demina (✉) and A. P. Lisitsyn
Shirshov Institute of Oceanology of Russian Academy of Sciences, Moscow, Russia
e-mail: l_demina@mail.ru; lisitzin@ocean.ru

A. P. Lisitsyn and L. L. Demina (eds.), *Sedimentation Processes in the White Sea: The White Sea Environment Part II*, Hdb Env Chem (2018) 82: 295–306,
DOI 10.1007/698_2018_357, © Springer International Publishing AG, part of Springer Nature 2018,
Published online: 15 July 2018

develop a new methodology and devices to solve complex problems, which arose in marine geology in the twenty-first century, based on the development of new research tools in geophysics, geochemistry, mineralogy, biogeochemistry, and sedimentology. As a result, a new sedimentological rather than lithological approach of operations in cruises in the seas has been developed based on the application of new devices, methods, and approaches [1–3].

Part II of the collective monograph "The White Sea Environment" summarizes the results of the research of Russian scientific community for the period from 2001 to 2016.

In accordance with the climatic zoning, contribution of sedimentary matter of each of the geospheres is different. In the ice (polar) zones, contribution of the sediment-laden sea ice and snow dominates, while dry deposition is negligible. The White Sea is a typical basin with the ice type of sedimentation [4]. Arid zones on continents correspond to ocean "deserts," i.e., areas with very low primary production, and there, the main sediment supply is associated with dust storms. These two new real genetic types of sediment formation in the oceans [4–7] were denied by theoretical lithologists in the previous years.

It is well known that the major source of formation of sedimentary material is a suspended particulate matter (SPM), which, in recent time, has been investigated in details in the White Sea. We have managed not only to perform a complex study of different constituents of SPM but to determine sedimentary fluxes at the different horizons of the water column. In addition, a comparative analysis of sediment sources from the cryosphere (ice and snow cover) with SPM taken from different depths of the White Sea was fulfilled. These studies in the White Sea and in its catchment area were carried out in winter being accompanied with direct determinations of the SPM concentration and vertical flows of settling particles [8, 9].

In the water column, sedimentary material delivered by terrigenous processes is mixed in different proportions with the dispersed sedimentary matter produced by biota followed by the formation of biogenous matter; these processes have been under consideration of V.I. Vernadsky about 90 years ago [10]. In the course of our investigations, it was possible to determine the influence of biota on the sedimentary process; it proved to be more diverse and essential than was previously thought. Direct determination of living organisms' influence (microorganisms, plankton, benthos) on sedimentation processes is one of the most important achievements of the expeditions held in 2001–2016 in the White Sea. Biological researches were conducted using the isotope methods, both in expeditions and in stationary laboratories.

Based on a great number ($n10^3$) of measurements of suspended matter concentration, an average mass value of SPM being equal to 1 mg/L was established (or in case of volume concentration, about 1 mm^3/L) [11]. A spatial distribution of SPM concentrations over the surface waters has revealed a close relation with the Severnaya Dvina River runoff: SPM decreased exponentially in the area of the marginal filter (at the first stage of the riverine and seawater mixing), and then it reduced in several times seaward. It was confirmed that the main factor which controls SPM concentration and composition in this area is the water salinity.

Lithogenous particles of river runoff and marine phytoplankton as well as its detritus have been identified as the primary sources of SPM in the White Sea [12]. From our calculations, proportion of phytoplanktonic particles in total SPM varied in dependence of sampling site's location relatively the main source (river runoff): from 27% in the inner part of the Dvina Bay to 65% in the open part of the Kandalaksha Bay (almost no river runoff). The major factor that controlled the vertical distribution of SPM in water column is a water stratification, namely, a pycnocline which is related to the halo- and thermocline. The vertical SPM distribution is characterized by a three-layer pattern: (1) the surface mixed and photic layer, (2) the clear intermediate water layer, and (3) the bottom nepheloid layer which is usually registered in most of the near-bottom waters [13].

The long-term investigations in a small Arctic sea, as the White Sea is, have revealed new regularities of sedimentation processes in the subarctic and Arctic zones. The direct study of micro- and nano-sized particles in different geospheres let us, for the first time, to estimate the contribution of sedimentary matter over different time scales: over months, seasons, years, and decades. For the first time, in situ sedimentation processes in the White Sea, including vertical sedimentary matter fluxes, were studied with the autonomous deepwater observatories of sedimentation (AGOS). Dispersed sedimentary matter (DSM) sampling has been performed automatically, at different depths and with different exposures. When several observatories were operating in the same area, a synchronized sampling was carried out. Methods of measurement of the vertical sedimentary matter's fluxes by the use of AGOS provide us with data on currents' velocities at given depths and another oceanographic parameters, which are crucial for sedimentology. At the same time, for the uppermost water layer, remote-sensing methods were used (satellite observations) continuously and throughout the year. They were accompanied by verification of data obtained at discrete sampling stations, where SPM and chlorophyll-a concentrations were measured, and the hydro-optical determinations (transparency, turbidity, etc.) have been carried out [14, 15]. Quantitative and qualitative analyses were performed simultaneously; there were no such opportunities before.

The total vertical sediment fluxes (mg m^{-2} $year^{-1}$), mineral and chemical composition, as well as properties of dispersed sedimentary matter have been studied in details for the White Sea [16].

It should be concluded that seasonal and even monthly variations not only in the total values of vertical fluxes but in their chemical and mineral composition, as well as in lithological properties, have been revealed [17]. The maximal values of the SPM concentrations (mg L^{-1}) which correspond to high values of vertical fluxes (mg m^{-2} day^{-1}) were characteristic for the ice-free spring-summer period, while the minimal ones are for the winter time. In winter, the White Sea and its catchment areas, feeding the basin with sedimentary matter, are capped by snow-ice cover, while contribution of the river runoff and aeolian sources are very small. Seasonal changes in vertical flux values are caused by hydrometeorological regime changes; the melted sediment-laden sea ice and snow discharge in April, as well as phytoplankton bloom and flooded conditions in May, lead to increase of the fluxes' values. Besides, it was shown that biogenic constituents of vertical flux as a rule decreased

by an order of magnitude during the transformation from the dispersed forms to concentrated ones (bottom sediments), i.e., at the near-bottom water-seafloor interface [16].

Among other important new approaches mentioned above, there is an in situ determination of the particle size distribution by the use of the Coulter counter. From our data, the most common grain-size type of the SPM was a silty-pelitic one [18]. The SPM has a predominant pelitic grain size in June (after spring flood). In the stratified water column, the percentage of pelitic fractions changed slightly. These fine particles are unable to reach the seafloor themselves due to their physical properties caused by their little size and small mass. They can descend just in a transformed form, i.e., captured by fecal pellets and/or aggregates of "marine snow." These are the coarser and heavier aggregates which form the vertical fluxes of dispersed sedimentary matter [19]. The SPM grain-size composition and major constituents in the White Sea are influenced by the two main sources – lithogenous and biogenic – which operate in complicated spatial and temporal interactions. From our data on change of the volume SPM concentration (1 mm^3/L, on average), it was concluded that volume concentration could be considered as reliable proxy for biogenic (phytoplanktonic) particles in the photic layer. Another proxy for the phytoplanktonic particles has proved to be the Chl-a concentration, whose distribution pattern corresponds to that of primary production [20, 21].

An important change in the SPM composition occurs in a very thin fluffy layer (about 0.5–1 cm). This layer operates as a transition zone between the two types of sedimentary matter: a dispersed particulate matter and consolidated ones (bottom sediment). In this layer, the basic processes of SPM transformation into sediment occur, which later undergo early diagenesis processes as well as bioturbation, resuspension, redeposition, etc.

One of the main biogeochemical processes of the early diagenesis is a decay of organic matter (OM) which results to generation of reduced gases (CO_2, NH_3, H_2S, CH_4, etc.), as well as water-soluble compounds and more stable solid compounds. The latter are preserved in a solid phase of sediments, while oxygen is exhausted. These processes lead to change in the pore waters' composition when sulfate concentration gradually decreases down the sediment core. At the same time, value of total alkalinity as well as concentrations of Fe^{2+}, Mn^{2+}, and SiO_3^{2-}, increases. In the White Sea sediments, spatial distribution of C_{org} was studied based on analyses of 202 samples; elevated concentrations were recorded in pelitic sediments of deep-sea areas (Fig. 1) [22]. The C_{org} content varied from 0.5 to 6%, averaging to 0.86%. The values of the C/N ratios and the n-alkanes' composition evidenced a dominance of terrigenous OM [22].

Terrigenous OM is not very suitable for the anaerobic microorganisms' functioning, which leads to the increase in duration of the early diagenetic processes and their incompleteness [23, 24]. The latter was evidenced by finds of authigenic iron sulfides (FeS_{n-1}) represented by X-ray amorphous "hydrotroilite," as well as by the absence of authigenic carbonates.

Over the last decades in the Arctic seas' sediments, another important process has been revealed, namely, an anaerobic oxidation of methane: CH_4 is partially oxidized

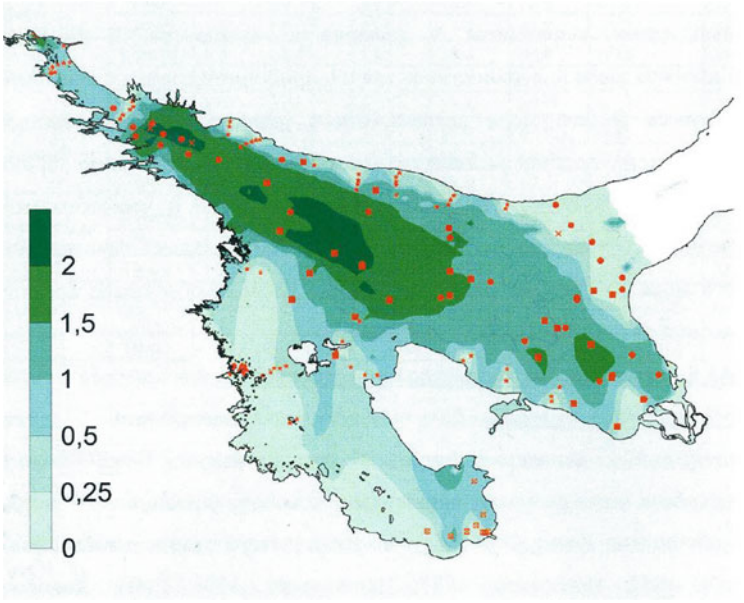

Fig. 1 Content of organic carbon (mass %) in surface layer (0–5 cm) of bottom sediments of the White Sea [22]

under anaerobic conditions followed by a fresh organic matter (OM) formation in the form of biomass of microorganisms and their metabolism's products [24, 25]. This newly formed OM activates diagenetic processes which have been weakened by this time, as it was shown earlier for the Black Sea sediments [26]. Experiments with radioisotopes, which let us to evaluate rates of the basic microbial diagenetic processes, confirm the decreased sulfate reduction rates in the White Sea sediments in comparison with sediments of midland seas of the humid and humid-arid zones. In polar marine basins, only in the caldera of the mud volcano Haakon Mosby (Norwegian Sea), the similar processes were found [27]. Generally, a decrease in rates of diagenesis in the White Sea could be explained by the low primary production, while discharge of terrigenous organic matter is very high. Low temperatures of the microorganisms' habitat are of a secondary importance.

The latest geophysical methods, such as seismic-acoustic surveys and multichannel high-frequency tools, improved our understanding of geological setting and stratigraphic positions in such an inner glacial basin as the White Sea is. There, a wide occurrence of gravity deposits related to neotectonic movements were studied [28]. Based on the seismic profiling, the two new Holocene lithofacies were discovered: the nepheloid sediments deposited in a ridge-dam environment and silt fans in the south Gorlo Strait. The new data make it possible to study in detail the sedimentation process over the Holocene not only in the White Sea basin but in the Kola Peninsula, in Karelia, and in the Arkhangelsk region [29]. The data obtained let us to conclude about predominance of land rise, which may characterize the White

Sea as a regressive basin, at least within the Baltic crystalline shield. This conclusion is of great importance for predicting placers in shallow sediments of the White Sea. These placers, over the entire Holocene, have been subjected to weathering that has led to their gradual enrichment in heavy minerals, including commercial ore minerals. Our studies nearby the Severodvinsk port showed that now the outer delta is subjected to an active destruction which is caused by an anthropogenic impact to the environment leading to a reduced sediment runoff and water shortage in the Severnaya Dvina River [30].

The mineral composition of the fine-grained (<10 and <1 μm) fractions has been studied in both dispersed (aerosols and suspended particulate matter) and consolidated (bottom sediments) forms of sedimentary matter in the White Sea. Based on the data of X-ray powder diffractometry and scanning electron microscopy, an important fact was discovered about mineral composition of pelitic fraction [31]. Unlike traditional views, pelitic fraction (<10 μm) of the White Sea bottom sediments consists mostly of fine-grained *clastic* terrigenous minerals (63%, on average), rather than only of *clay* minerals. Among minerals of pelitic fraction, quartz and feldspars (albite, anorthite, andesine, microcline, orthoclase) dominate. The most common clay minerals in the White Sea sediments are illite and chlorite, which are also predominant in other areas of the Arctic Ocean. From the group of smectite, montmorillonite is the main mineral in the bottom sediments of the White Sea.

In the sediment-laden sea ice and snow, quartz (45–52%) and clay minerals (25–35%) were major mineral phases. The aerosol material of the above-water layer of the White Sea contains albite in considerable amount (16–20%), while in the Northern Atlantic aerosols, another group of feldspars, such as andesine, anorthite, and orthoclase, were mostly recorded. This difference in prevailing minerals may be used as mineral proxies of Aeolian (atmospheric) source from the certain areas. The quartz/feldspars ratio in aerosols varied from 3.4 to 8.7; it is an important characteristic of the feeding provinces [32]. This ratio depends on the intensity of weathering processes, where quartz is the most proof against destruction, while feldspars are primarily and rather easily destructed.

Distribution pattern of diatoms and aquatic palynomorphs in surface sediments of the bays of the White Sea reflects processes of a consistent mixing of sedimentary materials delivered into the bays from the mouths of rivers [33, 34]. At the same time, an increase in the water salinity has specific regional features. Differences in the quantitative and species composition of the microalgae associations are caused by the change in the volume of river inflow, the depths of the bays, and the intensity of the tidal currents. However, at different stages of the marginal filter (MF) of the rivers, an identical sequence of changes in species composition is established [35]. At the MF gravitational stage I, almost exclusively freshwater species of diatoms were encountered. At the MF coagulation-adsorption stage II, percentage of freshwater diatoms and green algae entering the sea from river flow sharply decreased in the number and was observed in the bush area of the bays. At the MF stage III, a normal vegetation of marine plankton species proceeds, which is reflected in the composition of microalgae tanatocenoses in the bottom sediments.

The total diatom content in the surface sediments from MF in the Dvina and Onega bays varies widely, remaining mainly low. It resulted from the high turbidity of water, which prevents vegetation of algae, and the intensity of tidal currents. In the species composition of the group of marine diatoms in the assemblages from the surface sediments, euryhaline species are the most diverse. The dinocysts' assemblages are dominated by heterotrophic species.

The various aspects of the most toxic heavy metal mercury's behavior in bottom sediments of the White Sea and estuaries of inflowing rivers have been studied [36]. Background content of total Hg was determined as 0.03 μg g^{-1} d.w. The highest Hg concentrations – 0.095 μg g^{-1} d.w. – were detected in the 1.5–2.0 cm horizon of the Severnaya Dvina River estuary. This sediment layer was formed in the 1970s–1980s' years of the last century when the pulp and paper industry developed intensively [8, 37]. The major source of Hg for the White Sea is a river runoff. Marginal filter "the Severnaya Dvina River-the White Sea" operates as a geochemical barrier which decreased the Hg input into the open part of the White Sea. When passing a geochemical barrier, an active removal of Hg happens from the aqueous solution due to Hg adsorption on the suspended matter followed by its sedimentation [38–41]. At the same time, Mudyugsky Island acts as a mechanical barrier for river waters' inflow. Here, the current rate sharply decreases, and the finely dispersed suspended material is precipitated, which is the most enriched with Hg [42–44]. Another important source is proved to be an atmospheric input. Percentage of anthropogenic Hg was very high (85–94% from total content) in the Northern Dvina River estuary and delta stations. A range of total Hg concentrations in bottom sediments of the Severnaya Dvina River was comparable to that of other rivers of the European territory of Russia, Europe, Asia, Australia, and North America, as well as the Amur River basin in the Far East region, i.e., in areas of chronic anthropogenic impact.

The main processes that control accumulation of Al, Fe, Mn, and some trace metals (Mo, Cr, Ni, Co, Cu, Pb, Cd, As) in the bottom sediments of the White Sea have been quantified based on the method of selective chemical extraction [45, 46]. The trace metal spatial distribution in the surface (0–5 cm) layer is characterized by increased contents of geochemical labile forms of metals in the deepwater areas with predominance of fine-grained pelitic sediments with high adsorption capabilities [47]. In shallow-water (depth less than 40 m) bottom sediments of the Gulf of Onega where silty-sandy fractions dominated, decreased total metal contents were generally recorded. The rock-forming elements such as Al and Fe, as well as Cr and Ni, were predominantly found (98–68% of the total on average) in lithogenous form. This confirms the major contribution of terrigenous processes in the White Sea sedimentation. On the other hand, geochemical properties of Mn, Cu, Mo, Cd, and Pb are of importance in their occurrence forms' partition. An increasing order of the average percentage of the elements' labile forms in the surface bottom sediments was as follows: Al < Fe, Cr < As < Ni < Co < Cu < Pb < Cd < Mn. High-resolution analysis of sediment core (1 cm scale) let us to reveal changes in mobility of most elements (except Al) during early diagenesis of the bottom sediments. The Mn and Mo were found to be the most labile metals: only till 10% of their

total content occurs in the lithogenous form in the upper 0–6 cm layer [48]. The Mn/Fe ratio reflects changes in partition of labile forms, so it may be applied as a proxy of the early diagenesis of the bottom sediments. Based on the total heavy metal content, we may consider the White Sea bottom sediments as uncontaminated ones due to low anthropogenic activity in its basin; the exception was As whose average content was in intermediate position between the strongly polluted sediments of some ports and the relatively clean bays of the Mediterranean Sea.

For estimating changes in aliphatic and polycyclic aromatic hydrocarbons (HCs) in bottom sediments of different areas of the White Sea, their content and composition were studied during low and high waters [49]. In marginal filters of rivers, where the riverine and seawaters mix, sedimentation processes are controlled by the change in hydrological and biological characteristics, which in turn are depended on the season (low water, high water) and the lunar cycle (high and low tides). Active processes of aliphatic and polycyclic aromatic hydrocarbons' transformation, both in the water column and at the water-seabed boundary, led to predominance of components in the composition of alkanes in bottom sediments [50, 51]. It was evidently due to the fact that, despite the low temperatures, the oxidation rates of the organic matter in the Arctic seas are comparable with that in temperate and tropical latitudes [52]. Therefore, the composition of aliphatic and polycyclic aromatic hydrocarbons was mainly presented by their natural rather than anthropogenic compounds [53]. High concentrations of C_{org} and HCs in the sediments of the separating lakes of Rugozerskaya Bay were probably caused by natural processes rather than pollution.

The incoming oil compounds increase the level of HCs in the sediments, thereby creating a modern HC background level. The same results were obtained during the monitoring surveys of pollutants (the most persistent organic pollutants – PAHs, pesticides, biphenyls, dioxins, furans, as well as some heavy metals) in the White, Barents, and Pechora seas [53]. Their level in the sediments was estimated as insignificant one.

Acknowledgments The research results of Part II were obtained in the framework of the *state assignment* of *FASO* Russia (theme No. 0149-2018-0016). Proceedings of data obtained earlier were summarized with support of Russian Scientific Foundation, project No. 14-27-00114-P.

References

1. Lisitsyn AP, Nemirovskaya IA (eds) (2012) The White Sea system. Vol II. Water column and interacting with it atmosphere, cryosphere, river runoff and biosphere. Scientific World, Moscow, 783 pp (in Russian)
2. Lisitsyn AP, Nemirovskaya IA (eds) (2013) The White Sea system. Vol III. Dispersed sedimentary matter in hydrosphere, microbial processes and water pollution. Scientific World, Moscow, 665 pp (in Russian)
3. Lisitsyn AP, Nemirovskaya IA (eds) (2017) White Sea system. Vol IV. The processes of sedimentation, geology and history. Scientific World, Moscow, 1028 pp (in Russian)

4. Lisitzin AP (2002) Sea-ice and iceberg sedimentation in the ocean: recent and past. Springer, Berlin, 543 pp
5. Lisitsyn AP (1994) The marginal filter of the ocean. Oceanology 34(5):671–682
6. Lisitsyn AP (2014) Modern conceptions of sediment formation in the oceans and seas. Ocean as a natural recorder of geospheres' interaction. In: Lobkovsky LI, Nigmatulin RI (eds) World Ocean: physics, chemistry and biology of the ocean, vol 2. Scientific World, Moscow, pp 331–571 (in Russian)
7. Lisitsyn AP (1996) Oceanic sedimentation: lithology and geochemistry. American Geophys Union, Washington, DC 390 pp
8. Shevchenko VP (2003) The influence of aerosols on the oceanic sedimentation and environmental conditions in the Arctic. Berichte zur Polar- und Meeresfor 464:1–149
9. Lisitsyn AP, Novigatsky AN, Klyuvitkin AA (2015) Seasonal variation of fluxes of dispersed sedimentary matter in the White Sea (Arctic ocean basin). Dokl Earth Sci 465(1):1182–1186
10. Vernadsky VI (1923) The living matter and marine chemistry. Sci Chem Technol Publ, Saint-Petersburg, 241 pp (in Russian)
11. Kravchishina MD (2009) Suspended particulate matter of the White Sea and its grain-size. Scientific World, Moscow, 263 pp (in Russian)
12. Kravchishina M, Klyuvitkin A, Filippov A, Novigatsky A, Politova N, Shevchenko V, Lisitsyn A (2014) Suspended particulate matter in the White Sea: the results of long-term interdisciplinary research. Complex interfaces under change: sea – river – groundwater – lake. IAHS Publ. 365, pp 35–41
13. Lisitsyn AP, Kravchishina MD, Kopelevich OV, Burenkov VI, Shevchenko VP, Vazyulya SV, Klyuvitkin AA, Novigatskii AN, Politova NV, Filippov AS, Sheberstov SV (2013) Spatial and temporal variability in suspended particulate matter concentration within the active layer of the White Sea. Dokl Earth Sci 453(2):1228–1233
14. Burenkov VI, Vazyulya SV, Kopelevich OV, Shebertov SV (2011) Space-time variability of suspended matter in the White Sea derived from satellite ocean color data. Proceedings of VI international conference current problems in optics of natural waters. Nauka, St. Petersburg, pp 143–146
15. Kopelevich OV, Vazyulya SV, Saling IV, Sheberstov SV, Burenkov VI (2015) Electronic atlas "biooptical characteristics of the Russian seas from satellite ocean color data of 1998–2014". Mod Probl Rem Sens Earth Space 12(6):99–110 (in Russian)
16. Novigatsky AN, Lisitsyn AP, Shevchenko VP, Kluvitkin AA, Kravchishina MD, Filippov AS, Politova NV (2013) Study of vertical fluxes of sedimentary matter by use of automatic deep-sea sediment observatories in the White Sea. In: sedimentary basins, sedimentation and post-sedimentation processes in geological history. Proceedings of VII all-Russian lithological conference (Novosibirsk, 28–31 October 2013), vol II. SB RAS, Novosibirsk, pp 317–321 (in Russian)
17. Novigatsky AN, Klyuvitkin AA, Lisitsyn AP (2018) Vertical fluxes of dispersed sedimentary matter, absolute masses of the bottom sediments, and rates of modern sedimentation. In: Lisitsyn AP, Demina LL (eds) Sedimentation processes in the White Sea: the White Sea environment part II, Hdb Env Chem, Springer, doi: https://doi.org/10.1007/698_2018_278
18. Kravchishina MD, Lisitzin AP (2011) Grain-size composition of the suspended particulate matter in the marginal filter of the Severnaya Dvina River. Oceanology 51(1):89–104
19. Lisitsyn AP, Vinogradov ME (1983) Global regularities of living matter and biogeochemistry of particulate matter and bottom sediments in the ocean. In: Lisitsyn AP, Monin AS (eds) Biogeochemistry of the ocean. Nauka, Moscow, pp 112–126 (in Russian)
20. Kravchishina M, Burenkov VI, Kopelevich OV, Sheberstov SV, Vazyulya SV, Lisitsyn AP (2013) New data on the spatial and temporal variability of the chlorophyll *a* concentration in the White Sea. Dokl Earth Sci 448(1):120–125
21. Kravchishina MD, Mitzkevich IN, Veslopolova AF, Shevchenko VP, Lisitsyn AP (2008) Relationship between the suspended particulate matter and microorganisms in the White Sea waters. Oceanology 48(6):837–854

22. Belyaev NA (2015) Organic matter and hydrocarbon markers of the White Sea. Abstract PhD thesis, IO RAS, Moscow, 25 pp (in Russian)
23. Savvichev AS, Rusanov II, Zakharova EE, Veslopolova EF, Mitskevich IN, Kravchishina MD, Ivanov MV (2008) Microbial processes of the carbon and sulfur cycles in the White Sea. Microbiology 77(6):823–838
24. Lein AY, Novichkova YA, Rybalko AY, Ivanov MV (2013) Carbon isotope composition of organic matter in Holocene sediments of the White Sea as one of the indicators of sedimentation conditions. Dokl Eart Sci 452(2):1056–1061
25. Savvichev AS, Rusanov II, Yusupov SK, Pimenov NV, Lein AY, Ivanov MV (2004) The biogeochemical cycle of methane in the coastal zone and littoral of the Kandalaksha Bay of the White Sea. Microbiology 73(4):540–552
26. Lein AY, Ivanov MV (2009) Biogeochemical cycle of methane in the ocean. Nauka, Moscow, 464 pp (in Russian)
27. Lein AY, Vogt P, Crane K, Egorov AV, Pimenov NV, Savvichev AS, Ivanov MV (1998) Geochemical features of gas-bearing (CH_4) deposits of a submarine mud volcano in the Norwegian Sea. Geochem Int 36(3):190–208
28. Rybalko AYe, Lisitsin AP, Shevchenko VP, Zhuravlyov VA, Varlamova AA, Nikitin MA (2009) New data on geology of the White Sea quaternary. In: GG Matishov (ed) Geology, geography, and ecology of the oceans. Publ House UNSC RAS, Rostov-on-Don, 186 pp (in Russian)
29. Rybalko AYe, Spiridonov MA, Spiridonova, YeA, Moskalenko PE (1987) Quarternary deposits of Onega Bay and main features of its paleogeography in the Pleistocene and Holocene. In: Spiridonov MA, Moskalenko PE (eds) Integral marine G&G studies in the glacial shelf interior seas. Publ House VSEGEI, Leningrad, pp 38–52 (in Russian)
30. Rybalko AY, Fyodorova NK, Nikonov KA, Klimov AI (2007) Current state and evolution of the shoreface of Yagry Island (in the Severnaya Dvina delta) in connection with the shoreline reinforcement. In: Geology of the seas and oceans. Materials of the XVII Int. Scientific conference, vol 2. GEOS, Moscow, pp 282–283 (in Russian)
31. Dara OM, Mamochkina AI (2017) Clay minerals in bottom sediments of the Eurasian Arctic Seas. In: Lisitsyn AP, Nemirovskaya IA (eds) White Sea system. Vol IV. The processes of sedimentation, geology and history. Scientific World, Moscow, pp 394–432 (in Russian)
32. Mamochkina AI, Dara OM (2017) Mineral composition of bottom sediments of the White Sea. In: Lisitsyn AP, Nemirovskaya IA (eds) White Sea system. Vol IV. The processes of sedimentation, geology and history. Scientific World, Moscow, pp 365–393 (in Russian)
33. Novichkova EA, Polyakova YI (2007) Dinoflagellate cysts in the surface sediments of the White Sea. Oceanology 47(5):660–670
34. Novichkova EA (2008) Postglacial history of the White Sea based on aquatic and terrestrial palynomorph investigations. PhD thesis. MSU, 262 pp (in Russian)
35. Polyakova YI, Novichkova YA, Klyuvitkina TS (2017) Diatoms and palynomorphs in surface sediments of the Arctic seas and their significance for paleooceanological studies at high latitudes. In: Lisitsyn AP, Shevchenko VP, Vorontsova VG (eds) The White Sea system. Vol IV. The processes of sedimentation, geology and history. Scientific World, Moscow, pp 796–859 (in Russian)
36. Fedorov YA, Ovsepyan AE, Korobov VB (2010) Peculiarities of Hg distribution, migration, and transformation in the estuarine area of the Severnaya Dvina River. Russ Meteorol Hydrol 35(4):289–294. https://doi.org/10.3103/S1068373910040072
37. Fitzgerald WF, Lamborg CH (2003) Treatise on geochemistry. The crust, vol 3. Elsevier, Amsterdam, NY, pp 107–148
38. Fedorov YA, Ovsepyan AE (2006) Hg and it's connection with physicochemical water parameters (on the example of the rivers of the northern ETR). Univ News North-Caucasian Region Nat Sci Ser 2:82–89 (in Russian)

39. Fedorov YA, Garkusha DN, Ovsepyan AE et al (2005) Main results of expeditionary research on the Severnaya Dvina and the Dvina Bay of the White Sea. University news. North-Caucasian region. Nat Sci Ser 3:95–100 (in Russian)
40. Ovsepyan AE, Fedorov YA (2011) Hg in the mouth area of the northern Dvina River. ZAO Rostizdat, Rostov-on-Don 198 pp (in Russian)
41. Skibinskii LE (2005) The role of geochemical barriers and geochemical barrier zones in forming of the hydrochemical regime of coastal waters of Arctic Seas. In: Proceedings of the XII congress of Russian Geographical Society, vol 5. pp 148–155 (in Russian)
42. Fedorov YA, Ovsepyan AE, Korobov VB et al (2010) Bottom sediments and their role in surface water pollution with Hg (with a special reference to the Severnaya Dvina River mouth and the Dvina Bay of the White Sea). Russ Meteorol Hydrol 35(9):611–618. https://doi.org/10.3103/S1068373910090050
43. Fedorov YA, Ovsepyan AE, Lisitzin AP et al (2011) Patterns of Hg distribution in bottom sediments along the Severnaya Dvina–White Sea section. Dokl Earth Sci 436(1):51–54. https://doi.org/10.1134/S1028334X11010041
44. Fedorov YA, Ovsepyan AE (2013) Hg and its connection with physicochemical water parameters (case study of the rivers of the northern European territory of Russia). Hg: sources, applications and health impacts. Nova Science, New York, pp 155–172
45. Demina LL, Levitan MA, Politova NV (2006) On occurrence forms of heavy metals in bottom sediments of the Ob and Yenisei rivers estuaries (the Kara Sea). Geochem Int 2:212–226
46. Demina LL, Budko DF, Lisitsyn AP, Novigatsky AN (2018) The first data on geochemical fractions of heavy metals in vertical fluxes of dispersed sedimentary matter in the White Sea. Doklady Earth Sci 480(Part 1):689–693
47. Demina LL, Budko DF, Alekseeva TN, Novigatsky AN et al (2017) Features of the distribution of trace elements in the early diagenesis of the White Sea sediments. Geochem Int 55(1): 144–149
48. Budko DF, Demina LL, Lisitsyn AP et al (2017) Occurrence forms heavy metals in modern bottom sediments of the White and Barents Seas. Doklady Earth Sci 474(Part 1):552–556
49. Nemirovskaya IA, Leonov AV (2011) Petroleum hydrocarbons in the waters of major tributaries of the White Sea and its water areas: a review of available information. Water Resour 38(3):324–351
50. Nemirovskaya IA, Trubkin IP (2013) Anthropogenic and natural hydrocarbons in water and suspended arctic seas. In: Lisitsyn AP (ed) The White Sea system, vol 3, Scientific World, Moscow, pp 438–470 (in Russian)
51. Nemirovskaya IA (2013) Oil in the ocean (pollution and natural flows), Scientific World, Moscow, 432 pp (in Russian)
52. Agatova AI, Lapina NM, Torgunova NI (2012) Organic substance of the White Sea. In: Lisitzyn AP, Nemirovskaya IA (eds) The White Sea system, vol 2. Scientific World, Moscow, pp 492–548 (in Russian)
53. Savinov V, Evenset A (eds) (2011) Monitoring of hazardous substances in the White Sea and Pechora Sea: harmonization with OSPAR's Coordinated Environmental Monitoring Programme (CEMP). Akvaplan–Niva, Tromsø, 71 pp

Index

A. P. Lisitsyn and L. L. Demina (eds.), *Sedimentation Processes in the White Sea: The White Sea Environment Part II,* Hdb Env Chem (2018) 82: 307–312,
https://doi.org/10.1007/978-3-030-05111-2,